

PLANE SHOCK AND DETONATION WAVES

by

Stewart Paterson

A Thesis Submitted to the University of Glasgow in Support of an
Application for the Degree of D. Sc.

MAY, 1950

ProQuest Number: 13850820

All rights reserved

INFORMATION TO ALL USERS

The quality of this reproduction is dependent upon the quality of the copy submitted.

In the unlikely event that the author did not send a complete manuscript and there are missing pages, these will be noted. Also, if material had to be removed, a note will indicate the deletion.



ProQuest 13850820

Published by ProQuest LLC (2019). Copyright of the Dissertation is held by the Author.

All rights reserved.

This work is protected against unauthorized copying under Title 17, United States Code
Microform Edition © ProQuest LLC.

ProQuest LLC.
789 East Eisenhower Parkway
P.O. Box 1346
Ann Arbor, MI 48106 – 1346

PREFACE

In submitting the present Thesis in support of an application for the degree of D. Sc., I should like to explain the circumstances in which it came to be written.

After graduating in 1936, I carried out research work for three years on gaseous ignition in the Natural Philosophy Department of Glasgow University under the supervision of Professor E. Taylor Jones, with a view to presentation of a Thesis for Ph.D. Part of this work was published at the time in the form of three papers in the Philosophical Magazine, copies of which are attached; and the Thesis would normally have been submitted in the autumn of 1939.

However, in June of that year, I was appointed to the Research Department of the Nobel Explosives Company, Ltd., where research on problems of ignition in gases was being actively pursued. I was given the prospect of continuing my studies in this field. In view of this, Professor Jones, who considered that I had already more than sufficient material to support an application for the degree of Ph. D., was kind enough to suggest that this be reserved for a year or two with a view to supplementing it from my continued work, and extending the application to one for D. Sc. Since opportunities rather seldom arise in industrial research of pursuing a single line of enquiry for a sufficient length of time to form the basis for a D. Sc. Thesis, I was glad to accept Professor Jones' advice.

The development of the war brought to a standstill many programmes of long-term research, among these the one referred to, and my project had to be abandoned. In 1945, however, I was given the opportunity of working on theoretical problems of detonation and of carrying out experimental studies in the same field. The present Thesis is based upon research

conducted under this programme from 1945 to 1949. It consists of two parts, the first dealing with plane adiabatic flow and shock waves in non-reactive media, and the second with shock waves in reactive materials, that is, with detonation waves.

In the first part, as explained in the Summary (§1), I have endeavoured not only to describe my own contributions but also to present a connected and sufficiently detailed account of the subject, within the limitations implied by the title. I have made a point of providing extensive numerical data both for reference and illustration at all stages.

With regard to the second part, the position is slightly different. The opening sections, which describe the classical development of the hydrodynamic theory of detonation and its application to gaseous explosives, have been made as complete as possible. The remaining sections, however, which form the latter half of the thesis, and deal with detonation in condensed explosives, are devoted almost exclusively to a record of my own calculations and experiments in this field. Although a large amount of work is known to have been done on the subject during the war, only a small part appears to have been published, and it would seem premature to attempt any evaluation at the moment. In general, therefore, the sections on condensed explosives should be regarded as covering material available up to the summer of 1949. An exception is, of course, made in regard to work carried out in the I.C.I. laboratories, which though only recently, or in some cases not yet, openly published, was known to me at the time of writing.

Much of the original work described below has already appeared in the form of papers, references to which will be found in §21. Other parts

are in the course of preparation for publication in this form. Part of the text has been taken from a chapter of some 50,000 words on the theory of detonation which I wrote in 1948 at the request of the Editor, Professor C.E.H. Bawn, Liverpool University, and of the Publishers, Messrs. Butterworths, for a book on "The Science of Explosives", shortly to be printed. Other sections form part of three chapters which I contributed to a forthcoming Oxford Monograph on Explosives.

The summary (§1) indicates in general terms those parts of the Thesis for which originality is claimed. To make the matter as clear as possible, however, a red rosette () has been attached to the heading of such sections as are entirely or almost entirely novel, and also to original equations, tables, etc. in sections based primarily on work by others. The figures are, with a few obvious exceptions, all original.

Acknowledgment of assistance received from my colleagues in I.C.I. will be found in §1.3.

In further support of my application I submit herewith copies of the following additional papers, lying outwith the scope of this Thesis:

- (1) The ignition of inflammable gases by hot moving particles.
(Phil. Mag. 28, 1 (1940)).
- (2) The ignition of inflammable gases by hot moving particles II.
(Phil. Mag. 30, 437 (1940)).
- (3) The conduction of heat in a medium generating or absorbing heat.
(Phil. Mag. 32, 384 (1941)).
- (4) Heating or cooling of a sphere in a well-stirred fluid.
(Proc. Phys. Soc. 59, 50 (1947)).

- (5) Conduction of heat from local sources in a medium generating or absorbing heat. (Unpublished).
- (6) On certain types of solution of the equation of heat conduction. (Unpublished).
- (7) Propagation of a boundary of fusion. (Unpublished).
- (8) Rapidly convergent series for $\sum_{n=1}^{\infty} n^{2r} e^{-n^2 x}$ (Unpublished).
- (9) Series expansion of a class of integrals (Unpublished).
- (10) Flow behind a steady plane detonation (Research, 3, 99 (1950)).

Neither the whole nor any part of this Thesis nor of the additional papers has been submitted previously by me for a higher degree of any University.

PLANE SHOCK AND DETONATION WAVES

Contents

§1. Introduction and Summary.

- §1.1 Numbering of sections, equations, tables and figures.
- §1.2 List of principal symbols.
- §1.3 Acknowledgments.

PART I PLANE ADIABATIC FLOW AND SHOCK WAVES

§2. Physical approach to the theory of shock waves.

§3. Mathematical approach to the theory of shock waves.

- §3.1 Flow from a region of constant entropy.
- §3.2 Coördinates of point of onset of shock.
- §3.3 Compression wave produced by a continuously accelerated piston.
- §3.4 Condition for simultaneous steepening of the entire wave.
- §3.5 Development of the condition for simultaneous steepening.
 - §3.51 Unique solutions.
- §3.6 Rarefaction waves produced by a moving piston.

§4. Adiabatic waves in an ideal gas with constant specific heats.

- §4.01 Sonic velocity in a rarefaction from rest.
- §4.1 Compression by a continuously accelerated piston.
 - §4.11 Condition for simultaneous steepening.
 - §4.12 Example of equation 3.5(1).
- §4.2 Compression produced by a piston moving with constant acceleration.
- §4.3 Rarefactions produced by a moving piston.
 - §4.31 Piston withdrawn at constant speed.
 - §4.32 Escape into a vacuum.
 - §4.33 Piston acceleration constant.
 - §4.34 General conditions for existence of a "sonic point".

§4.4 Expansion against an unsupported massive piston.

§4.5 Expansion against a supported massive piston.

§5. The role of dissipative processes in a shock wave.

§5.1 Entropy considerations.

§5.2 General formulation for a real fluid.

§5.3 The stationary plane shock.

§5.4 Structure of the stationary plane shock.

§5.5 Thickness of the shock-front in gases.

§6. The large-scale properties of the steady plane shock.

§6.1 The Rankine-Hugoniot equation.

§6.2 Shock waves in an ideal gas with constant specific heats: independent variable ρ_1 .

§6.21 Relative magnitudes of $D, W_1, a_1, W_1 + a_1$.

§6.22 Approximations for $\pi - 1 \ll 1$.

§6.23 Approximations for $\pi \gg 1$.

§6.24 Approximations for $\gamma - 1 \ll 1$.

§6.25 Development of a shock wave from an adiabatic compression wave.

§6.26 Independent variable v_1 .

§6.27 Independent variable D .

§6.28 Independent variable W_1, E_1, a_1 or T_1 .

§6.29 Numerical values for $\gamma = 1.4$.

§6.3 Shock waves in real gases: air.

§ 6.4 Shock waves in fluids obeying the Tammann equation of state:

ethyl ether.

§ 6.41 Shock waves in water.

§ 6.42 Shock-front thickness in liquids.

§ 6.5 Shock waves in solids.

§ 6.51 The Grüneisen-Debye equation of state.

§ 6.511 Shock waves in fluids, satisfying a
simplified Grüneisen-Debye equation of state.

§ 6.52 The Born-Bradburn equation of state.

§ 6.53 Shock waves in fluids satisfying a simplified
Born-Bradburn equation of state.

§ 6.54 Adiabatic waves for the same state equation.

§ 6.55 Shock and adiabatic waves in lead.

§ 6.56 Shock and adiabatic waves in iron.

§ 6.57 Shock and adiabatic waves in copper and aluminium.

§ 6.58 Shock and adiabatic waves in sodium chloride.

§ 7. Normal reflexion of steady plane shocks at material boundaries.

§ 7.01 Criterion for a reflected shock.

§ 7.1 Normal reflexions in an ideal gas.

§ 7.11 Free surface.

§ 7.111 A lemma.

§ 7.12 Rigid boundary.

§ 7.121 Comparison of $p_2 - p_0$ with Rudenberg's
"Impulsstromdichte".

§ 7.13 Compression of an ideal gas between a rigid wall and a
piston moving with constant velocity.

§ 7.14 Normal reflexion of steady plane shocks at the interface between two ideal gases.

§ 7.141 Estimation of γ for butane vapour.

§ 7.142 Approximate solutions for weak reflexion.

§ 7.2 Shock-waves produced by the sudden release of high-pressure gas.

§ 7.3 Reflexion of gaseous shocks at liquid and solid boundaries.

§ 7.4 Reflexion of shock waves in liquids at gaseous, liquid and solid boundaries.

§ 7.5 Reflexion of shock waves in solids at gaseous, liquid and solid boundaries.

§§ 7.6, 7.61 An experimental method for determining the large-scale shock wave properties in any medium.

PART II STEADY PLANE DETONATION WAVES

§ 8. Historical Introduction.

§ 9. Elementary theory of the stable plane detonation wave.

§ 9.1 The Rankine-Hugoniot equation and the Chapman-Jouguet stability condition.

§ 9.2 The variation of entropy along the RH-curve.

§ 9.3 Jouguet's rule.

§ 9.4 Further consideration of the CJ-condition.

§ 9.5 Summary of basis for computation in the CJ-plane.

§ 9.51 Evaluation of $E - E_o$.

§ 9.52 The CJ-condition.

§ 9.53 Equations of state.

§ 9.54 Equilibrium conditions.

§ 10. Detonation in ideal gases.

§ 11. Detonation in real gases.

§ 11.1 Carbon monoxide/oxygen mixtures.

§ 11.2 Detonation in dust-clouds.

§12. Detonation in low-density condensed explosives.

§12.1 Calculations and experiments on a low-density nitrocotton.

§13. Detonation in condensed explosives of normal bulk density:

introduction.

§13.1 Absolute calculations for condensed explosives of normal density.

§13.2 Analysis of the product equilibria.

§13.21 Approximate solution for $2x + \frac{y}{2} > z > x + \frac{y}{2}$:
oxygen concentration assumed negligible.

§13.22 Approximate solution for $2x + \frac{y}{2} > z > x + \frac{y}{2}$:
hydrogen concentration assumed negligible.

§13.23 Approximate solution for $z < x + \frac{y}{2}$:
pressure extremely high.

§13.24 Approximate solution for $z < x + \frac{y}{2}$:
hydrogen, oxygen and methane concentrations assumed negligible.

§13.25 Formation of NO.

§13.3 The equation of state.

§13.4 The RH-equation.

§13.5 The CJ-condition and formal solution.

§13.6 Theory of real equilibrium.

§14. Method of calculation for an explosive yielding entirely gaseous products.

§14.1 Nitroglycerine.

§14.2 Other oxygen-positive single compounds.

§14.21 NO-formation.

§14.3 Pentaerythritol tetranitrate.

§14.31 Final cycles in full calculations for PETN at
1.5 and 0.75 g/cm³.

- §14.4 Liquid methyl nitrate.
 - §14.5 Nitroguanidine.
 - §14.6 Propellant powders as detonating explosives.
- §15. Explosives whose products contain a condensed phase: introduction.
- §15.1 Formulation.
 - §15.11 Approximate representations of Bridgman's isotherms.
 - §15.2 Markedly oxygen-negative single explosive compounds.
 - §15.21 HCN-formation in the products of TNT and tetryl.
 - §15.3 Cyclotrimethylenetrinitramine.
 - §15.4 Liquid ethylene.
- §16. Calculations for commercial blasting explosives.
- §16.1 Powders and semi-gelatines based on nitroglycerine.
 - §16.2 Gelatinous explosives based on nitroglycerine.
 - §16.3 Powders based on TNT.
 - §16.4 Discussion of the results for commercial blasting explosives.
 - §16.5 Specific volume of condensed phase in thermal equilibrium with the product gases.
- §17. Experimental determination of maximum detonation velocities for commercial explosives: introduction.
- §17.01 The Dautriche method of measuring velocity of detonation.
 - §17.02 Modifications of the Dautriche method.
- §17.1 Experimental determination of the maximum detonation velocities in powders and semi-gelatines based on nitroglycerine.
- §17.2 Experimental determination of the maximum detonation velocities in gelatines based on nitroglycerine.
- §17.21 The spontaneous change from low to high velocity in Blasting Gelatine.
- §17.22 Stability of low velocity in Blasting Gelatine.

§17.3 Experimental determination of the maximum detonation velocities in powders based on trinitrotoluene.

§18. Mixtures of explosive and inert material.

§18.1 Diluent entrained, but absorbing no heat from the reaction products.

§18.2 Diluent entrained, and in thermal equilibrium with the reaction products.

§18.3 Diluent in thermal equilibrium with the products, but not entrained.

§18.4 Diluent neither entrained nor heated.

§18.5 PETN/NaCl mixtures.

§18.6 Nitroglycerine/kieselguhr mixtures.

§18.7 Nitroglycerine/NaCl mixtures.

§18.8 Energy absorbed in compressing inert diluents.

§18.81 Theoretical estimates of heat-transfer to inert diluents.

§18.9 The design of explosives with ultra-low velocities of detonation.

§19. Structure of the reaction zone in a steady plane detonation wave: introduction.

§19.1 Döring's solution for an ideal gaseous explosive.

§19.2 Time- and distance-profiles for an ideal gaseous explosive.

§19.3 Structure of the reaction zone in a condensed explosive.

§19.4 Application to PETN.

§19.5 The source of the light recorded in photographs of detonating explosives.

§19.6 The mechanism of propagation in condensed explosives.

§19.7 The effect on the detonation wave of varying the initial hydrostatic pressure.

§20. Normal incidence of a plane detonation wave upon the boundary of an adjoining medium.

§ 20.01 Condition for forward movement of the rear of a reflected rarefaction.

§20.1 Reflected waves in the products of commercial blasting explosives: products entirely gaseous.

§20.2 Reflected waves in the products of commercial blasting explosives: products partly condensed.

§20.3 The "brisance" of a detonating explosive.

§20.4 Contact transmission of detonation.

§ 21. References.

THE THEORY OF PLANE SHOCK AND DETONATION WAVES

§1. Introduction and Summary

The dynamics of compressional and dilatational waves of finite amplitude, and the formation of "shock waves", were first studied theoretically by Earnshaw and by Riemann about the year 1860. The theory was later developed by Rankine, Hugoniot, Rayleigh, Taylor and others.

When Earnshaw and Riemann published their researches, detonating explosives had already been known for more than ten years. However, it was left to Schuster, in 1880, to suggest a connection between shock and detonation waves. Schuster's suggestion was first applied by Chapman (1899) and by Jouguet (1901). The modern theory of detonation represents a development of the ideas of these writers.

It is therefore logical, in any study of detonation, to provide first some account of the theory of finite compressional waves and shock waves in non-reactive media. For the purposes of a thesis concerned primarily with the detonation process itself, this account might have been made rather brief. However, since no full and connected presentation of the theory of such non-reactive waves appeared to have been published, it was decided to enlarge the scope of the present work by discussing it at some length. Part I therefore contains a redevelopment of this part of the subject. It is restricted to problems of one-dimensional flow adjoining a region of constant entropy, and only steady shock waves are discussed.

Within these limitations, however, it is much more detailed than any prior treatment known to the writer*.

§§2 and 3 contain a general discussion of finite adiabatic waves and the development of shock waves in a fluid with arbitrary equation of state. Although the fundamental concepts are well-known, many of the particular relations derived are believed to be new. For example, §§ 3.2 - 5 represent a generalisation of results given by Rayleigh.

In §4, the theory is applied to ideal gases. Here again, the basic ideas are familiar, but they are developed in more detail than previously, and new matter has been added throughout. §§ 4.01, 4.12, 4.3, 4.34 and 4.5 are wholly new.

§5 presents the fundamental equations for the propagation and structure of steady plane shocks in an arbitrary fluid. It is based, for the most part, on an analysis by Becker, and novelty is claimed only in matters of detail.

*Since Part I was written, an American text has been published (R. Courant and K. Friedrichs, "Supersonic Flow and Shock Waves", New York /¹⁹⁴⁸ /), in which the subject of non-reactive waves of finite amplitude is discussed in great generality. However, as the scope of this work is much wider than that of Part I of the present thesis, so its manner of treatment is much less detailed. Numerical applications are also entirely omitted. In consequence, there is very little overlapping between the two texts.

The large-scale properties of steady plane shock-waves are discussed in § 6. The treatment in § 6.1 of the Rankine-Hugoniot equation is more systematic and rigorous than that given by Becker. In §§ 6.2 - 6.28, the important special case of an ideal gas has been investigated in much greater detail than previously, and a large number of new relations noted. §§ 6.3 - 6.42 include, for completeness, a summary of calculations by other writers on the properties of shock-waves in air, ethyl ether and water. §§ 6.5-6, 19.3 discuss the propagation of intense shocks in solids and heterogeneous media: these ten sections are entirely original.

The normal reflexion of plane shocks at material interfaces is dealt with in § 7. The fundamental theory of "matching" is not new, but it is presented in a more general form, and in much more detail than previously. The contents of §§ 7.01, 7.11, 7.111, 7.13, 7.14, 7.141, 7.142, 7.3, 7.5 and 7.6 are entirely original, and many of those of the remaining sections. A large number of numerical applications have been made.

Part II is concerned with the theory of detonation in gaseous, liquid and solid explosives. After a review of the history of the subject (§ 8), a rather detailed account is given (§§ 9 - 9.4) of the fundamental large-scale theory of the steady plane detonation wave in an arbitrary explosive. In preparing this, we have made use of the work of Jouguet, Becker and Döring, with certain refinements in detail. In §§ 9.5 - 9.54 the theory is developed in a form suitable for practical calculation with any appropriate equation of state. The presentation here is much more general than any known to the writer.

Application to ideal gaseous explosives is made in § 10; the treatment is fundamentally that of Jouguet and Crussard, but it has been improved in point of rigour. In addition, a considerable number of new relations are given.

§11 reviews critically the calculations made by various workers on real gaseous detonations. An original set of detailed calculations for carbon-monoxide - oxygen mixtures is included (§11.1), based on the most recent thermochemical data. The treatment is extended to dust clouds (§11.2) and a numerical application given.

Detonation in low-density condensed explosives is the subject of §12, where the equations of Taffanel and Dautriche are derived and their limitations discussed. The equations are applied to a low-density gun-cotton, and confirmatory experiments reported. Additional theoretical relations are again given.

§§13 and 13.1 contain a general discussion of the most important practical field of application of the Chapman-Jouguet theory, that of solid and liquid explosives at normal loading densities. After a detailed analysis of the relevant chemical equilibria (§§13.2 - 13.25), a product gas equation of state is proposed, sufficiently simple in form to permit wide application without prohibitive labour, while at the same time sufficiently general to serve as a first approximation to the behaviour of gases at detonation pressures and temperatures (§13.3).

The RH-equation, CJ-condition and formal solution are developed in terms of this equation of state in §§13.4, 13.5 and its consequences in the theory of real equilibria analysed in §13.6.

§§14 - 14.6 describe practical applications to typical condensed explosives yielding entirely gaseous products. Detailed numerical calculations are presented, which show that the theoretical wave velocities for the model explosive agree very closely with those actually measured on the real material, not only at a single loading density but over the entire practical range.

5

§15 contains a detailed discussion of the additional problems raised by the presence of a condensed phase in the products. The theory is reformulated for such explosives (§15.1) and applied in §§15.2, 15.3 to the important cases of TNT, tetryl, picric acid and cyclotrimethylenetrinitramine, whose products may include free carbon. Close agreement between theory and practice is again found. §15.4 contains calculations for liquid ethylene, which recent experience has suggested may be capable of detonation.

The application of the theory is extended in §§16 - 16.5 to a large number of commercial blasting explosives representative of the entire range of contemporary British manufacture.

§§17 - 17.3 are concerned primarily with an experimental test of the calculations for commercial explosives reported in §§16 - 16.5. §17 presents, as basis for these experiments, a general qualitative discussion of the stable detonation wave under imperfect lateral confinement; while §§17.01, 17.02 describe certain innovations in the technique of velocity measurement. §§17.1 - 3 then record experimental determinations of the maximum wave velocities. Very good agreement is found with the theoretical predictions of §§16.1 - 16.3.

§18 returns to the question of explosive/inert mixtures. Approximate analyses are given, based upon various alternative assumptions regarding the behaviour of the inert diluent, and experimental and theoretical studies designed to arbitrate between these are described (§§18.1 - 18.8). The bearing of this work upon the design of explosives with ultra-low velocities of detonation is discussed in §18.9.

Novelty is claimed for the whole of §§13 - 18, except in a few instances where acknowledgment is expressed in the text.

§§19, 19.1 contain an analysis of the reaction-zone structure in plane gaseous detonation, based on work by Döring. This theory is extended in §19.2, by inclusion also of the reaction-kinetic equations, to determine the space- and time-profiles of the reaction-zone. A new theory of the reaction-zone structure in condensed explosives is developed in §19.3 and applied (§19.4) to the case of PETN at various cartridge densities. Experimental evidence in support of the theory is reported in §19.5. §19.6 contains a general discussion of the mechanism of propagation in condensed explosives, with particular reference to the dual-velocity effect: a theory of mechanism is then put forward, based on the structural analysis of §19.3, and supported by the effect of hydrostatic pressure upon the detonation wave. §19.7 develops the theory of this effect.

In conclusion, §§20-20.4 deal with the effects of the steady plane detonation wave upon its environment. After a general analysis of normal reflexion, parallel to that given for non-reactive shocks in §7, the theory is developed (§20) in considerable detail for the case of ideal gaseous products. With a few exceptions, the relations derived are new, and various numerical applications are given. A corresponding development is then made for condensed explosives whose products satisfy the Abel equation of state, or alternatively the polytrope $p v^n = \text{const.}$; with numerical examples as before. These paragraphs are also new. §20 concludes with the results of original detailed calculations for normal reflexion, at various liquid and solid boundaries, of plane detonation waves in typical commercial blasting explosives. The necessary theory of reflected shock and rarefaction waves in the products of such explosives is presented in §20.1, §20.2, with numerical applications. §20.3 discusses measures of "brisance".

Finally §20.4 considers the modifications necessary in the fundamental theory of transmission when the target material is itself a detonating explosive,

and formulates a theory of transfer of detonation from one explosive to another.

Literature references are collected in §21.

and the first two are the most important. The first is the "Kāvyaśāstra" of
Bhāskaradeva, which is a very good book, though it is not so well known as
the other. It contains a great deal of information about the Kāvyaśāstra, and
is written in a clear and concise style. The second is the "Kāvyaśāstra" of
Vālmīki, which is also a very good book, though it is not so well known as
the other. It contains a great deal of information about the Kāvyaśāstra, and
is written in a clear and concise style. The third is the "Kāvyaśāstra" of
Bhāskaradeva, which is a very good book, though it is not so well known as
the other. It contains a great deal of information about the Kāvyaśāstra, and
is written in a clear and concise style. The fourth is the "Kāvyaśāstra" of
Vālmīki, which is also a very good book, though it is not so well known as
the other. It contains a great deal of information about the Kāvyaśāstra, and
is written in a clear and concise style. The fifth is the "Kāvyaśāstra" of
Bhāskaradeva, which is a very good book, though it is not so well known as
the other. It contains a great deal of information about the Kāvyaśāstra, and
is written in a clear and concise style. The sixth is the "Kāvyaśāstra" of
Vālmīki, which is also a very good book, though it is not so well known as
the other. It contains a great deal of information about the Kāvyaśāstra, and
is written in a clear and concise style. The seventh is the "Kāvyaśāstra" of
Bhāskaradeva, which is a very good book, though it is not so well known as
the other. It contains a great deal of information about the Kāvyaśāstra, and
is written in a clear and concise style. The eighth is the "Kāvyaśāstra" of
Vālmīki, which is also a very good book, though it is not so well known as
the other. It contains a great deal of information about the Kāvyaśāstra, and
is written in a clear and concise style. The ninth is the "Kāvyaśāstra" of
Bhāskaradeva, which is a very good book, though it is not so well known as
the other. It contains a great deal of information about the Kāvyaśāstra, and
is written in a clear and concise style. The tenth is the "Kāvyaśāstra" of
Vālmīki, which is also a very good book, though it is not so well known as
the other. It contains a great deal of information about the Kāvyaśāstra, and
is written in a clear and concise style.

The following lists summarize only those activities which were in

（三）在於此，我們希望能夠在一個較為廣泛的範圍內，將這些問題，提出來討論，並希望得到各方面的意見。

卷之三十一

卷之三

§1.1 Numbering of sections, equations, tables and figures

The sections are numbered on the decimal system. For the most part, it has been possible to combine this with a logical subdivision of the argument. Equations, tables and figures are numbered afresh in each section. In cross-references, equations are distinguished by enclosing the equation number in plain brackets (), preceded by the appropriate section number, except when the equation belongs to the current section. The word "equation" is generally omitted in such references. In the case of tables and figures, the plain brackets are replaced by a colon: thus table 7.142:4 is the fourth table of section 7.142. The word "Table" or "Figure", and the section number are always expressly stated in references. External references are collected at the end (§21), and indicated in the text by a handwritten figure in blue ink (or in red, when the reference is to the writer's own publication) above the line of text.

§1.2 List of symbols

The following list contains only those symbols which are in frequent use throughout the text, and are not, therefore, as a rule redefined in each section. A few of the symbols listed are used to represent other quantities in particular sections.

x	distance coordinate
t	time coordinate
p	pressure
p_i	partial pressure
\tilde{p}, \tilde{p}_i	fugacity
T	absolute temperature
u, w	particle velocity

W	particle velocity with respect to material ahead of wave.
d	wave velocity
D	wave velocity with respect to material ahead of wave
a, A	sonic velocity
v	specific volume
V	volume
ρ, Δ	density
E	internal energy/mass
S	entropy/mass
n	gaseous moles/mass
N	gaseous moles.
α	covolume/mass
α, β, \dots	moles of CO_2, CO , ----- per total mass.
b, B, B_i	high-temperature second virial coefficient
Q	reaction energy/mass
c_v, c_p, c	true specific heats
\bar{c}	mean specific heat at constant volume
γ	ratio of specific heats
λ	$(\gamma+1)/(\gamma-1)$; also thermal diffusivity
μ	chemical potential; also viscosity
π	pressure ratio; also \dot{p}/N
φ	volume ratio; also specific volume of condensed phase
m	proportion of explosive ingredient/mass
R	gas constant/mole
k	$1 + \frac{nR}{C_v} - \frac{d\alpha}{dv}$

K ideal equilibrium constant

T real equilibrium constant

Subscripts

o condition ahead of wave

$/$ condition behind shock wave, or at CJ-layer
of detonation wave

s condition behind shock-front of detonation
wave

2 condition behind reflected wave

3 condition behind transmitted wave

Superscripts

quantities referred to unit mass of gaseous
phase alone

* standard state

§1.3 Acknowledgments

I wish to express my thanks to Messrs. Imperial Chemical Industries, Ltd. Nobel Division, who have given me the opportunity to pursue the investigations described below, and to write this thesis.

I am especially indebted to Dr. J. Taylor, Research Director of the Nobel Division of I.C.I., who introduced me to the subject and advocated the present studies, for constant encouragement and stimulating criticism at all stages of the work. Dr. Taylor's wide knowledge and experience of explosives have been of great advantage to me throughout.

I have been greatly assisted by extensive thermochemical tables and references compiled by my colleague Dr. H. Thomas.

I wish also to record my appreciation of the skilled assistance of

Miss P.H. Ford (now Mrs. H.P. Stout) and of Miss. J.M. Davidson, who have carried out much of the detailed numerical calculation in Part II.

Finally, it is a pleasure to express my thanks to other colleagues who have helped, at one time or another, in the experimental part of the work.

PLATES CONTAINING EIGHT ADDITIONAL PAGES

PART I

PLANE ADIABATIC FLOW AND SHOCK WAVES

[156, 54]

§2. Physical approach to the theory of shock waves

We imagine a column of fluid to be confined at rest in a rigid cylindrical tube, impervious to heat and closed by a rigid impervious piston. A velocity, small compared with that of sound in the undisturbed fluid, is given to the piston. A compression wave of infinitesimal amplitude will then proceed through the fluid with the velocity of sound. The fluid behind the wave front shares the (small) velocity of the piston, and is also slightly compressed and heated. After an arbitrary interval of time, the piston velocity is increased by a further small amount. A second sound wave then pursues the first, and, since it proceeds through fluid which is moving forward and is also slightly heated, will in general tend to overtake the previous wave. If this process of stepwise acceleration of the piston is continued, a series of small waves will therefore be generated, each tending to overtake its predecessor. It is evident that an arbitrary continuous acceleration of the piston may be considered as the limit of such a discontinuous or stepwise process, and that the continuous compression wave which is formed in front of the piston may correspondingly be regarded as the limit of an infinite sequence of small compression waves, each overtaking those which precede it. Finite compression waves so generated and maintained must therefore necessarily become more steeply fronted as they proceed, and in the absence of dissipative processes end by becoming infinitely steep. Moreover, it may be judged that from the instant when the second infinitesimal wave overtakes the first an acceleration will occur in the wave front itself, whose velocity will accordingly increase as the pressure immediately behind it rises.

We may pursue the argument a little further. If the piston, after an initial period of acceleration, maintains a steady finite speed, the process

of intensification and acceleration of the wave front will continue.

Ultimately, (after certain processes discussed in more detail below), a steady state will be established, in which the pressure and velocity are constant throughout the steadily expanding region between piston and wave front. If a subsequent further acceleration of the piston were to occur, a second steeply-fronted wave would of course pursue the first, and ultimately overtake it. If, on the other hand, the piston decelerates, a rarefaction wave is produced, and this must in the end overtake the wave front and reduce its intensity. Whether steady conditions are resumed at a lower level, or the degeneration proceeds indefinitely depends upon whether the piston velocity again becomes constant or falls to zero.

Moreover, to conclude, it is apparent that if the piston is supposed from the outset to withdraw from the tube rather than to advance into it, so that a finite rarefaction rather than compression wave is produced, each successive elementary wave must travel through fluid which is cooled and set in retrograde motion by its predecessor, and must accordingly fall further and further behind it. Finite rarefaction waves so generated and maintained must therefore necessarily become less steeply fronted as they proceed, and the velocity of the wave front cannot exceed that of sound in the undisturbed fluid. Of course, if the piston, after a period of accelerated withdrawal, maintains a steady velocity, conditions at the piston remain thereafter constant, and the wave merely becomes less and less steep with time. A steady state is never realised, though over any finite length of fluid conditions approach more closely to such a state. If, on the other hand, the piston decelerates, compression waves advance through the rarefied gas and must build up in the manner originally described. Whether conditions near the piston quiesce to zero, or become once more

steady at some intermediate level of rarefaction depends upon whether the piston decelerates indefinitely or only to a prescribed extent.

Compression or rarefaction waves whose front is infinitely steep are described as shock waves. From the above argument we therefore conclude

- (a) that every finite compression wave, if suitably maintained, must become more steep with time, and sooner or later give rise to a shock wave, and
- (b) that every finite rarefaction wave must become less steep with time, and, over a continually greater portion of its length, degenerate into a sound wave.

It is clear, however, that the above conclusions depend on the assumption that the algebraic sum of sound and fluid velocities behind a small compression wave exceeds that of the wave itself. Otherwise, the opposite conclusions must hold, every compressional wave degenerating with time and every rarefaction wave developing into a rarefaction shock; while in the critical case where the sum of sound and fluid velocities is exactly equal to the wave velocity, shocks of neither kind will develop, finite compression or rarefaction waves of arbitrary profile propagating without change.

§3. Mathematical approach [5]

The one-dimensional or linear flow of an ideal compressible fluid, that is, one which exhibits neither viscosity nor thermal conduction, is described in the absence of body-forces by the following three equations, apart from the equations of state:

Equation of Continuity
(Conservation of Mass)

$$\frac{\partial v}{\partial t} + u \frac{\partial v}{\partial x} - v \frac{\partial u}{\partial x} = 0 \quad (1)$$

Equation of Motion
(Conservation of Momentum)

$$\frac{\partial u}{\partial t} + u \frac{\partial u}{\partial x} + v \frac{\partial p}{\partial x} = 0 \quad (2)$$

First Thermodynamic Law
(Conservation of Energy)

$$\frac{\partial E}{\partial t} + p \frac{\partial v}{\partial t} + u \left(\frac{\partial E}{\partial x} + p \frac{\partial v}{\partial x} \right) = 0. \quad (3)$$

Here u is the velocity, in the direction of the axis Ox , of the fluid at position x at time t , $v = 1/\rho$ its specific volume, p its pressure, and E its internal energy per unit mass.

If we represent the time-rate of change of any property for a chosen element of fluid by $\frac{d}{dt} = \frac{\partial}{\partial t} + u \frac{\partial}{\partial x}$, and introduce the entropy S per unit mass defined by $TdS = dE + pdv$, where T is the absolute temperature, equations (1-3) may be written alternatively

$$\frac{dp}{dt} + p \frac{\partial u}{\partial x} = 0 \quad (4)$$

$$\frac{du}{dt} + \frac{1}{\rho} \frac{\partial p}{\partial x} = 0 \quad (5)$$

$$\frac{dS}{dt} = 0. \quad (6)$$

The entropy of any chosen element of fluid thus remains constant, though it may vary from one element to another.

In addition, two relations will exist between E (or S), p , ρ and T . These may be written:-

"Thermal" Equation
of State

$$p = p(\rho, T) \quad (7)$$

"Caloric" Equation
of State

$$E = E(\rho, T) \quad (8)$$

$$S = S(\rho, T). \quad (9)$$

In practice, of course, the place of (8) is normally taken by the equation

$$C_v = C_v(\rho, T) \quad (10)$$

which defines one specific heat, say that at constant volume (C_v), in terms of ρ and T . (8) is then derived by integration of the thermodynamic relation:

$$dE = C_v dT + (\dot{p} - T \frac{\partial p}{\partial T}) \frac{dp}{\rho^2}, \quad (11)$$

using (7). From (7) and (9), we may deduce

$$S = S(\rho, \dot{p}), \quad (12)$$

whereupon the four dependent variables \dot{p} , ρ , u , S are to be determined by the four equations (4,5,6,12) as functions of x , t . u can therefore be regarded in general as a function of ρ and \dot{p} , this function involving the boundary conditions.

[54,141]

§3.1 Flow from a region of constant entropy

In the particular case, however, where S is initially uniform throughout the fluid and therefore constant over all elements at all subsequent times,

3(12) enables us to write

$$\dot{p} = \dot{p}(\rho) \quad (1)$$

and so also

$$u = u(\rho), \quad (2)$$

these relations again involving the boundary conditions. Then 3(4) and 3(5) become

$$\frac{dp}{dt} + \rho \frac{du}{dp} \frac{\partial p}{\partial x} = 0 \quad (3)$$

$$\frac{du}{dp} \frac{dp}{dt} + \frac{1}{\rho} \left(\frac{dp}{dp} \right)_S \frac{\partial p}{\partial x} = 0 \quad (4)$$

whence

$$\left(\frac{du}{dp} \right)^2 = \frac{1}{\rho^2} \left(\frac{dp}{dp} \right)_S. \quad (5)$$

However, if u is small, 3(1,2) give approximately

$$\frac{\partial p}{\partial t} = -\rho \frac{\partial u}{\partial x} \quad \text{and} \quad \frac{\partial u}{\partial t} = -\frac{1}{\rho} \left(\frac{dp}{dp} \right)_S \frac{\partial p}{\partial x},$$

so that to a first approximation

$$\frac{\partial^2 p}{\partial t^2} = \left(\frac{dp}{dp} \right)_S \frac{\partial^2 p}{\partial x^2} \quad \text{and} \quad \frac{\partial^2 u}{\partial t^2} = \left(\frac{dp}{dp} \right)_S \frac{\partial^2 u}{\partial x^2}.$$

Thus

$$\left(\frac{dp}{dp} \right)_S = a^2, \quad (6)$$

where $a(\rho)$ is the speed of propagation of infinitesimal compressions, that

is, the velocity of sound.

(5) therefore yields

$$u - u_0 = \pm \int_{\rho_0}^{\rho} ad\rho/\rho, \quad (7)$$

u_0 being the velocity of the fluid where its density is ρ_0 . Then by (3) or (4)

$$\left. \begin{aligned} \frac{\partial p}{\partial t} + (u \pm a) \frac{\partial p}{\partial x} &= 0 \\ \frac{\partial p}{\partial t} + (u \pm a) \frac{\partial p}{\partial x} &= 0 \\ \frac{\partial u}{\partial t} + (u \pm a) \frac{\partial u}{\partial x} &= 0 \end{aligned} \right\}, \quad (8)$$

so that p , \dot{p} and u are propagated at a speed $u \pm a$. If we now choose the + sign in (7) and (8), corresponding to the propagation of a compression or rarefaction wave in the positive x -direction, we can see immediately that those parts of the wave profile where ρ is greatest advance most rapidly, provided always that $u+a$ increases with ρ , in other words that $a/\rho + da/d\rho$ is positive. By (6), this condition becomes

$$(d^2p/dx^2)_S > 0 \quad (9)$$

Subject then to (9), density gradients in the direction of u become more negative with time. Thus a steeply-fronted compression wave advancing along Ox will become more steep, while if the density falls off behind the wave it will fall off less rapidly as the wave proceeds. On the other hand, if

$$(d^2p/dx^2)_S < 0, \quad , \text{ the opposite conclusions must follow.}$$

Again, choosing the - sign in (7) and (8), corresponding to the propagation of a wave along $-Ox$, we conclude that those parts of the wave profile where ρ is greatest retreat most rapidly, provided that $u-a$ decreases as ρ increases, in other words that (9) holds good as before.

In conclusion, therefore, subject to (9) compression waves in ideal fluids must become more steeply fronted, and rarefaction waves less steeply fronted, as they proceed. Only in a material for which

$(d^2p/dv^2)_S = 0$, that is, in which the (p, v) -adiabatics are straight lines $p = Av + B$, will finite elastic waves propagate [§4] without change of form. This condition is not normally fulfilled by any known substance. In all normal cases (9) applies, though unusual conditions may perhaps exist under which $(d^2p/dv^2)_S$ is < 0 .

In that event, only rarefaction, and not compression, shocks would be possible.

§3.2 Coordinates of point of onset of shock

It remains to show that density gradients which increase by the above process become infinite within a finite time. We proceed from 3.1(8) with the + sign and $\partial p/\partial x < 0$, and examine the variation of $\partial p/\partial x$ with t , when ρ itself remains constant. Regarding ρ, t as independent variables we have

$$\frac{\partial}{\partial t_p} \frac{\partial p}{\partial x} = \frac{\partial^2 p}{\partial x \partial t} + \frac{\partial^2 p}{\partial x^2} \frac{\partial x}{\partial t_p}$$

But

$$0 = \frac{\partial p}{\partial x} \frac{\partial x}{\partial t_p} + \frac{\partial p}{\partial t}$$

Hence

$$\begin{aligned} \frac{\partial}{\partial t_p} \frac{\partial p}{\partial x} &= \frac{\partial^2 p}{\partial x \partial t} + (u+a) \frac{\partial^2 p}{\partial x^2} \\ &= -\left(\frac{\partial p}{\partial x}\right)^2 \frac{d}{dp}(u+a) \end{aligned} \quad (1)$$

By 3.1(9), the right side is < 0 , which confirms that the wave does steepen. Moreover, integration of (1) gives

$$\frac{\partial p}{\partial x} = \frac{(\partial p/\partial x)_{t=0}}{1 + \left(\frac{\partial p}{\partial x}\right)_{t=0} \cdot \frac{d}{dp}(u+a) \cdot t}, \quad (2)$$

whence it appears at once that $\partial p/\partial x$ becomes infinite when

$$t = t_c = \frac{1}{\left(-\frac{\partial p}{\partial x}\right)_{t=0} \cdot \frac{d}{dp}(u+a)},$$

$$\text{i.e. } t_c = \frac{1}{(1 + \frac{\rho}{a} \cdot \frac{da}{dp})(-\frac{\partial u}{\partial x})_{t=0}}, \quad (3)$$

in other words (since the denominator is positive) after a positive finite time. The corresponding distance traversed is of course at_c .

§3.3 Compression wave produced by a continuously accelerated piston

We may, for example, apply the above analysis to the fluid (initially at rest) ahead of a plane piston, which commences to move along Ox from $x = 0$ at $t = 0$. Let $\xi(\tau)$ be the x -coordinate of the piston at time τ , and suppose that $\dot{\xi}_0 = 0$ and $\ddot{\xi} > 0$. Then by 3.1(8), u is constant and equal to $\dot{\xi}$ when x and t are related by [40]

$$x - \xi = (\dot{\xi} + \alpha)(t - \tau), \quad t > \tau, \quad (1)$$

where α is the value of a at (ξ, τ) . However, α is determined by

3.1(1,6,7) as a function of $\dot{\xi}$, so that, $\xi(\tau)$ being prescribed, (1) is an algebraic equation from which $\dot{\xi}$ (and thus u) may be evaluated as a function of x and t . ρ and p then follow. The procedure is legitimate provided (1) yields a unique solution for u . This will cease to be so, however, at (t_c, x_c) when two neighbouring lines of the set (1) corresponding to adjacent values of τ , intersect. The condition for this to happen is that (1) should be consistent at (x_c, t_c) with its τ -derivative, namely

$$-\dot{\xi} = (\ddot{\xi} + \dot{\alpha})(t - \tau) - (\dot{\xi} + \alpha),$$

in other words, that

$$t_c = \tau + \frac{\alpha}{\ddot{\xi} + \dot{\alpha}}, \quad (2)$$

whereupon

$$x_c = \xi + \frac{\alpha(\dot{\xi} + \alpha)}{\ddot{\xi} + \dot{\alpha}}. \quad (3)$$

For example, let $\tau = 0$, so that $\xi = \dot{\xi} = 0$.

$$\text{Then } t_c = \alpha_0 / (\ddot{\xi}_0 + \dot{\alpha}_0), \quad x_c = \alpha_0^2 / (\ddot{\xi}_0 + \dot{\alpha}_0) = \alpha_0 t_c \quad (4)$$

represents the limit beyond which a single valued solution is impossible at the nose of the wave. Beyond t_c , therefore, the gradients of u, ρ, p become infinite at the nose. Since $\alpha_0 \equiv a_0$, the velocity of sound in the undisturbed fluid, and $\dot{\alpha}_0 = \frac{P_0}{a_0} \frac{da_0}{dp_0} \ddot{\xi}_0$, (4) may be written

$$x_c = a_0 t_c = \frac{a_0^2}{\ddot{\xi}_0 \left[1 + \frac{P_0}{a_0} \frac{da_0}{dp_0} \right]}, \quad (5)$$

which is clearly in agreement with 3.2(3), since $\ddot{\xi}_o = -a_o \left(\frac{\partial u}{\partial x} \right)_{t=0}$
by 3.1(8).

§3.4 Condition for simultaneous steepening of the entire wave

It is not, however, necessary that multiple-valued solutions should first appear at the nose. The condition for this is that $dt_c/d\tau > 0$ for all τ . On the other hand, if $dt_c/d\tau = 0$ for every τ , infinite gradients appear only at the nose, and the entire wave front becomes vertical simultaneously. From 3.3(2) we can deduce the manner in which the piston must move for this to occur at t_c . Thus

$$\tau + \frac{\alpha}{\dot{\xi} + \alpha} = t_c = \text{constant} \quad (1)$$

and since α is a known function of $\dot{\xi}$, (1) constitutes a differential equation for $\dot{\xi}$. The solution is completed below for the particular case of an ideal gas with constant specific heats. Of course, if the piston accelerates only up to $\tau = \tau' < t_c$ in the manner prescribed by (1), thereafter moving a constant speed, only the part of the wave generated before $\tau = \tau'$ will become vertical at $t = t_c$; the part generated subsequent to τ' will be characterised by uniform fluid velocity and will thus remain flat up to $t = t_c$. If, however, the piston maintains its acceleration according to (1) up to t_c , the fluid originally occupying the region $0 < x < a_o t_c$ must be compressed to infinite density at $t = t_c$.

From 3.3(4) it is clear that when $\ddot{\xi}_o = \infty$, $t_c = 0 = x_c$; so that in an ideal fluid a discontinuity is instantly generated by a piston which commences to move inward with finite velocity.

§3.5 Development of the condition for simultaneous steepening.

The condition 3.4(1) can be developed as follows.

By 3.1(7), if α and ρ apply at the piston at time τ ,

$$\dot{\xi} = \int_{\rho_0}^{\rho} \alpha d\rho / \rho .$$

Hence

$$\frac{\ddot{\xi}}{\alpha} = \frac{d}{dt} \ln \rho .$$

3.4(1) may therefore be written

$$\frac{d}{dt} \ln \{ \rho \alpha (t_c - \tau) \} = 0$$

In other words

$$\rho \alpha |t_c - \tau| = \text{constant.} \quad (1)$$

An example of this relation will be found in §4.12 below.

§3.5/ Unique solutions

If on 3.1(7) we superimpose any other relation between, say u and a , we define a unique solution. For example, if the flow velocity is sonic, both u and a , together with $/$ etc., are determined in terms of ρ_0, p_0 . (Cf. §4.01 below).

§3.6 Rarefaction waves Produced by a Moving Piston [Generalisation of Rayleigh, 140]

Equation 3.3(1) is equally applicable when $\dot{\xi}$ is negative, and allows the general nature of the motion to be understood. Thus, for $\tau < 0$ we suppose the piston at rest, so that $\dot{\xi} = 0 = \ddot{\xi}$, $\alpha = a_0$. Consequently $x > a_0 t$ corresponds to $u = \dot{\xi} = 0$.

The nose of the wave therefore advances at speed a_0 .

Again if $t > \tau > 0$, $\dot{\xi}(t) < \dot{\xi}(\tau) < 0$, and so

$$\dot{\xi}(t) < x < [\dot{\xi}_0 + \alpha_0] t \quad (1)$$

where $\alpha_0 \equiv \alpha(\dot{\xi}_0) \neq a_0$ unless $\dot{\xi}_0 = 0$. In general $\alpha(\dot{\xi}_0) < a_0$ since $\dot{\xi}_0 < 0$. Between the piston at $\dot{\xi}(t)$, therefore, and a point which moves with constant speed $\dot{\xi}_0 + \alpha_0$, $u = \dot{\xi}(t)$ is determined by 3.3(1) in the manner described above. This leaves only the region $(\dot{\xi}_0 + \alpha_0)t < x < a_0 t$ to be accounted for. Within this region,

which corresponds to $\xi = 0 = \tau$, the relation between $x_c t$ and u is given by 3.3(1) as:

$$x = [u + \alpha(u)]t. \quad (2)$$

u is therefore linear in x within this region, provided α is linear in u , a condition which it is shown below requires the adiabatic 3.1(1) to have the form

$$\dot{p} = \text{const. } p^{\text{const.}} + \text{const.} \quad (3)$$

The condition is fulfilled by an ideal gas.

Of course, if $\dot{\xi}_o = 0$, so that the piston accelerates smoothly from rest, $\alpha_o = a_o$ and the region in question disappears.

A further complication may be introduced if $\dot{p}(u') = 0$ for a finite negative value u' of u . In this event the gas cannot follow the piston at speeds beyond u' ; if $-\dot{\xi} > -u'$ for $\tau > \tau'$, the motion is identical with that which would take place if $\dot{\xi} = u'$ for $\tau > \tau'$. If $-\dot{\xi} \geq -u'$ from the outset, the motion is thus equivalent to expansion into a vacuum. In this case, again, α_o will in general be $= 0$, so that the region (1) vanishes and (2) fills the entire field $u't < x_c < a_o t$.

§4. Adiabatic waves in an ideal gas with constant specific heats [140]

The important example of an ideal gas with constant specific heats serves to illustrate the above more general analysis, and permits algebraic solution in certain cases. 3(7) becomes

$$\dot{p} = nR\rho T, \quad (1)$$

where n is the number of moles per unit mass and R is the gas constant per mole. 3(10, 11) reduce to

$$c_v = \text{constant} \quad (2)$$

$$dE = c_v dT \quad (3)$$

and so 3(8) is

$$E = c_v T + \text{const.} = \frac{p}{(\gamma-1)\rho} + \text{const.}, \quad (4)$$

where $\gamma \equiv 1 + nR/c_v$ is the ratio of specific heats.

3(9) and 3(12) become

$$S = C_v \ln(\tau \rho^{1-\gamma}) + \text{constant} \quad (5)$$

$$S = C_v \ln(\tau \rho^{-\gamma}) + \text{constant}, \quad (6)$$

and 3.1(1) is therefore

$$\tau = (\rho_0 \rho^{-\gamma}) \rho^\gamma, \quad (7)$$

ρ_0 being the pressure where the density is ρ_0 .

3.1(6) is then

$$a^2 = \gamma n R T = \gamma \tau / \rho = \gamma (\rho_0 \rho^{-\gamma}) \cdot \rho^{\gamma-1} = a_0^2 (\rho / \rho_0)^{\gamma-1}, \quad (8)$$

and 3.1(7) accordingly

$$u - u_0 = \pm \frac{2a_0}{\gamma-1} \left[\left(\frac{\rho}{\rho_0} \right)^{\frac{\gamma-1}{2}} - 1 \right] = \pm \frac{2a_0}{\gamma-1} \left[\left(\frac{\rho}{\rho_0} \right)^{\frac{\gamma-1}{2}} - 1 \right] = \pm \frac{2}{\gamma-1} (a - a_0). \quad (9)$$

For propagation along $(+)\partial_x$, with $u_0 = 0$, the differential equations

3.1(8) then take the form:

$$\begin{aligned} \partial u / \partial t + (a_0 + \frac{\gamma+1}{2} u) \partial u / \partial x &= 0 \\ \text{or} \quad \partial a / \partial t + (\frac{\gamma+1}{\gamma-1} a - \frac{2a_0}{\gamma-1}) \partial a / \partial x &= 0. \end{aligned} \quad \left. \right\} \quad (10)$$

Equation 3.1(9) becomes

$$\gamma(\gamma+1) \tau \rho^2 > 0,$$

which is certainly satisfied. Thus rarefaction waves will degenerate, but compressional waves will develop into shock waves. The process of steepening at a chosen level ρ, u, τ, a is represented by

$$\frac{\partial \rho}{\partial x} = \frac{(\partial \rho / \partial x)_0}{1 + \frac{\gamma+1}{2} \frac{a}{\rho} (\partial \rho / \partial x)_0 \cdot t}, \quad (11)$$

so that the gradients at this level become infinite after a time.

$$t_c = \frac{2\rho}{(\gamma+1)a(-\partial \rho / \partial x)_0} = 2 / (\gamma+1)(-\partial u / \partial x)_0. \quad (12)$$

\circlearrowleft 4.0/ Sonic velocity in a rarefaction from rest.

If in 4(9), we choose the + sign and set $u_0 = 0$, $u + a = 0$, we easily deduce

$$u = - \frac{2a_0}{\gamma+1}, \quad (1)$$

whence $\tau / \tau_0 = \left(\frac{2}{\gamma+1} \right)^{\frac{2\gamma}{\gamma-1}}. \quad (2)$

Thus, in any rarefaction starting from rest, the pressure has a constant value defined by (2) wherever the velocity is sonic. (2) is analogous to Reynolds' well-known relation for the minimum throat pressure in a nozzle. Reynolds' pressure-ratio is, however, the square root of that defined by (2).

§4.1 Compression by a continuously accelerated piston.

[40]

As an example of §4, if the suffix \circ refers to conditions at $t = 0 = \tau$ in the gas at rest in front of a piston which advances according to $\xi = \xi(\tau)$, the gas velocity u will be $= \dot{\xi}(\tau)$ at a point x at time t determined by the algebraic equation

$$x - \xi(\tau) = [a_0 + \frac{\gamma+1}{2} \dot{\xi}(\tau)](t - \tau) . \quad (1)$$

The corresponding pressure p is defined by 4(9), which becomes

$$p = p_0 \left[\frac{(\gamma-1) \dot{\xi}(\tau)}{2a_0} + 1 \right]^{\frac{2\gamma}{\gamma-1}} . \quad (2)$$

This solution will not be valid at the level $u = \dot{\xi}(\tau)$ beyond (t_c, x_c) where

$$t_c = \tau + \frac{2a_0 + (\gamma-1)\dot{\xi}(\tau)}{(\gamma+1)\ddot{\xi}(\tau)} \quad (3)$$

$$x_c = \xi(\tau) + \frac{[2a_0 + (\gamma-1)\dot{\xi}(\tau)][2a_0 + (\gamma+1)\dot{\xi}(\tau)]}{2(\gamma+1)\ddot{\xi}(\tau)} . \quad (4)$$

In particular, the conditions at the nose of a wave produced by a piston accelerating smoothly from rest at $\tau=0$ are found by setting $\tau = \xi = \dot{\xi} = 0$. Then (1) becomes $x = a_0 t$,

the equation of a sound wave, and (3) and (4) give:-

$$x_c = a_0 t_c = 2a_0^2 / (\gamma+1) \ddot{\xi}_0 , \quad [40] \quad [5] \quad (5)$$

a generalisation of a formula given by Rayleigh and Becker for the particular case $\dot{\xi} = \frac{1}{2} g \tau^2$. The process of steepening at the nose for $t < t_c$ is represented by, for example,

$$\begin{aligned} \frac{\partial u}{\partial x} &= \frac{(\partial u / \partial x)_0}{1 + \frac{\gamma+1}{2} \left(\frac{\partial u}{\partial x} \right)_0 \cdot t} \\ &= \frac{2 \ddot{\xi}_0}{(\gamma+1) \ddot{\xi}_0 t - 2a_0} , \end{aligned} \quad (6)$$

with similar equations for $\frac{\partial p}{\partial x}$ and $\frac{\partial \rho}{\partial x}$.

35

From (3), $\frac{dt_c}{d\tau} > 0$ for all τ provided

$$2\gamma \dot{\xi}^2 > [2a_0 + (\gamma-1) \dot{\xi}] \ddot{\xi}. \quad (7)$$

This will certainly be true if $\ddot{\xi} \leq 0$, that is, if the acceleration of the piston does not increase with time. Infinite gradients then appear first at the nose.

§4.11 Condition for simultaneous steepening.

Finally, we may enquire, as in §3.4, in what manner the piston must move, so that the entire wave become precipitous at $t = t_c$.

This clearly requires, by 4.1(3),

$$\tau + \frac{2a_0 + (\gamma-1) \dot{\xi}(\tau)}{(\gamma+1) \ddot{\xi}(\tau)} = t_c \quad \text{for all } \tau,$$

the solution of which is found to be

$$\dot{\xi}(\tau) = \frac{2a_0}{\gamma-1} \left[\left(1 - \tau/t_c\right)^{\frac{1-\gamma}{\gamma+1}} - 1 \right] \quad (1)$$

$$\xi(\tau) = a_0 t_c + \frac{2a_0 t_c}{\gamma-1} \left[\left(1 - \frac{\tau}{t_c}\right) - \frac{\gamma+1}{2} \left(1 - \frac{\tau}{t_c}\right)^{\frac{2}{\gamma+1}} \right], \quad (2)$$

whereupon $x_c = a_0 t_c$, as would be expected.

Elimination of ξ and τ between (1), (2) and 4.1(1) gives [40]

$$u = \dot{\xi} = \frac{2}{\gamma+1} \frac{a_0 t - x}{t_c - t}, \quad (3)$$

so that, for $t < t_c$, u must be linear in x ; which is otherwise obvious from 4.1(1), since, when t_c and x_c are common to all parts of the wave, 4.1(1) gives in general

$$x_c - x = (a_0 + \frac{\gamma+1}{2} u)(t_c - t),$$

where t_c, x_c are now independent of u , and in particular

$$x_c = a_0 t_c,$$

whence (3) follows at once.

The necessity for a linear (u, x) -relation forms in fact the starting point for Rayleigh's derivation of (2). A linear relation between u and x cannot, however, be taken in general as a criterion for the entire wave-front to become vertical simultaneously. In general, we must use 3.4(1). The linear $u(x)$ -relationship is appropriate only for fluids for which u is linear in a , as it is for example in an ideal

gas with constant γ (equation 3.1(9)). But by 3.1(7) this requires $\frac{dp}{da} = \text{const.}$ whereupon $a = \text{const.} \times p^{\frac{1}{\gamma-1}}$, so that the adiabatic relation 3.1(1) must be of the form

$$p = \text{const. } p^{\frac{1}{\gamma-1}} + \text{const.}, \quad (4)$$

as remarked by Rayleigh and mentioned in §3.6 above.

§4.12 Example of Equation 3.5(1).

The analogue of 3.5(1) for an ideal gas with constant γ is easily found to be $p^{\frac{1}{2\gamma}} |t_c - \tau| = \text{constant}$, (1)

p being the pressure on the piston. $p^{\frac{1}{2\gamma}}$ is therefore linear in τ .

This is confirmed by the above analysis, since when 4.1(1) applies 4.1(2) becomes

$$p = p_0 (1 - \tau/t_c)^{\frac{-2\gamma}{\gamma+1}}. \quad (2)$$

§4.2 Compression produced by a piston moving with constant acceleration.

In order to solve 4.1(1) explicitly for $u = \xi$ in terms of x and t , we require first to solve it as an algebraic equation in τ . This will not in general be possible analytically, so that 4.1(1) has to be treated numerically. In this event, it is more convenient to proceed in the opposite direction by drawing the straight lines 4.1(1) in the (x,t) -plane for successive values of τ , whereupon a value of τ (and so of u) can be assigned to each point (x,t) . In the special case $\xi = \frac{1}{2}ft^2$, however, the analytical solution is possible. For then

$$\xi = u^2/2f, \quad \tau = u/f \quad \text{so that}$$

4.1(1) becomes

$$x - u^2/2f = (a_0 + \frac{\gamma+1}{2}u)(t - u/f) \quad (1)$$

Writing $t_c = 2a_0/(\gamma+1)f$, we get

$$\gamma u = -a_0(1 - t/t_c) \pm \sqrt{a_0^2(1 - t/t_c)^2 + 2fy(a_0t - x)} \quad (2)$$

It is clear that this provides a single positive root only when $x < a_0t$; but that under this condition it does so for all t . When $x = a_0t$,

however, that is, at the nose, $\partial u / \partial x_c$ becomes infinite at $t = t_c$. When $x > a_0 t$ and $t < t_c$, the roots are both negative (or complex); when $x > a_0 t$ and $t > t_c$, however, they are both positive (or complex). This exemplifies the appearance of many-valued solutions after the onset of shock, and is a clear indication that the equations for an ideal fluid are inapplicable across the shock front.

The pressure $p(x, t)$ follows from 4.2(2) and 4.1(2) with $\dot{\xi}(\tau) = u$.

The pressure at the piston is

$$p(\xi, \tau) = p_0 \left[1 + \frac{\gamma-1}{2a_0} f\tau \right]^{\frac{2\gamma}{\gamma-1}}, \quad (3)$$

so that $[p(\xi, \tau)]^{\frac{\gamma-1}{2\gamma}}$ rises linearly with τ . (3) may be compared with 4.12(2).

§4.3 Rarefactions produced by a moving piston.

The general conclusions expressed in §3.6 become, for an ideal gas with constant γ

$$x > a_0 t : u = 0$$

$$\xi(t) < x < (a_0 + \frac{\gamma+1}{2} \dot{\xi}_0) t : u \text{ determined}$$

$$\text{by } u = \dot{\xi}(\tau) \text{ in 4.1(1)}$$

$$(a_0 + \frac{\gamma+1}{2} \dot{\xi}_0) t < x < a_0 t : u \text{ determined}$$

$$\text{by } x = (a_0 + \frac{\gamma+1}{2} u) t,$$

$$\text{i.e. } u = -\frac{2}{\gamma+1} \cdot \frac{a_0 t - x}{t}. \quad (1)$$

Again, by 4(9), $p = 0$ when $u = -\frac{2a_0}{\gamma-1} \equiv u'$, say.

The gas cannot therefore follow the piston at speeds greater (numerically) than u' . [54]

* After t_c , $x = a_0 t$ will no longer be the nose.

 §4.3/ Piston withdrawn at constant speed

The case of a piston withdrawn at constant speed $-V$, where $V < |u'|$, follows immediately from the above. It is perhaps made clearer by considering first the case of continuous acceleration defined by

$$\dot{\xi} = \frac{-V\tau}{\tau + \epsilon} \quad (1)$$

which passes on to the former when ϵ vanishes. We eliminate τ and from $\dot{\xi}$ and 4.1(1) and (1). Thus, from (1)

$$\tau = \frac{-\epsilon\xi}{\dot{\xi} + V} \quad (2)$$

$$\text{and } \xi/V = \epsilon \ln \frac{\dot{\xi} + V}{\epsilon} - \tau \quad (3)$$

$$= \epsilon \left\{ \frac{\dot{\xi}}{\dot{\xi} + V} + \ln \frac{V}{\dot{\xi} + V} \right\}, \text{ by (2)} \quad (4)$$

4.1(1) then becomes, with $\dot{\xi}$ replaced by u ,

$$x/a_0 t = \frac{V}{a_0 t} \left[\frac{z}{1+z} - \ln(1+z) \right] + \left(1 + \frac{V}{2} \frac{V}{a_0} z \right) \left(1 + \frac{\epsilon}{t} \cdot \frac{z}{1+z} \right), \quad (5)$$

where $z \equiv u/V$.

The position of the piston at time t is $\xi(t)$ where

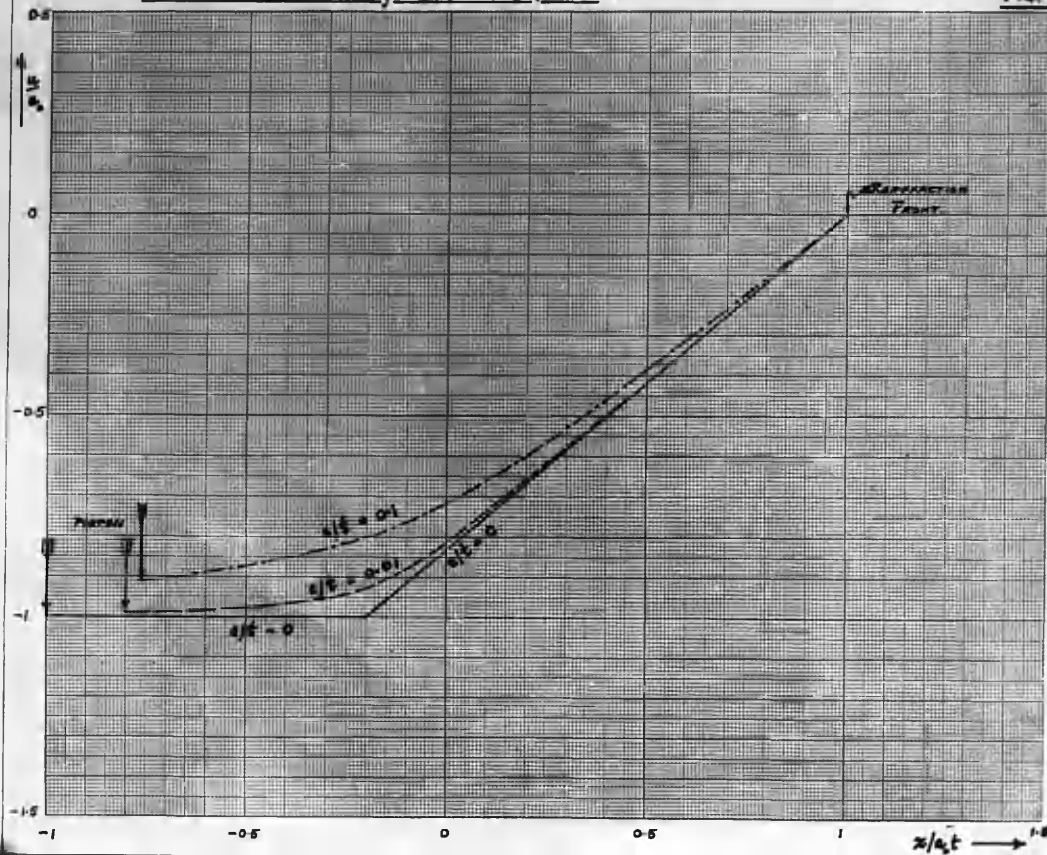
$$\xi(t)/a_0 t = \frac{V}{a_0} \left\{ \frac{\epsilon}{t} \ln \frac{1 + \epsilon/t}{\epsilon/t} - 1 \right\}, \text{ by (3); its}$$

velocity $\dot{\xi}(t) = -V/(1 + \epsilon/t)$, by (1). The nose of the wave corresponds to

$\tau = 0$, in other words $u = \dot{\xi} = 0$ and $x = a_0 t$. (5, therefore applies in the region $-1/(1 + \epsilon/t) < z < 0$ of z or

$$\frac{V}{a_0} \left\{ \frac{\epsilon}{t} \ln \frac{1 + \epsilon/t}{\epsilon/t} - 1 \right\} < \frac{x}{a_0 t} < 1 \text{ of } x/a_0 t. \quad (6)$$

A graph of z against $x/a_0 t$ constructed from (5) between the limits (6) for any chosen values of V/a_0 and ϵ/t shows the velocity profile of the wave at time t . This is illustrated in Fig. 4.31/1 for $\epsilon/t = 0.1, 0.01, 0.0$, and $V/a_0 = 1$ for convenience. The relationship between the profiles for continuous and stepwise acceleration is clear from the figure.

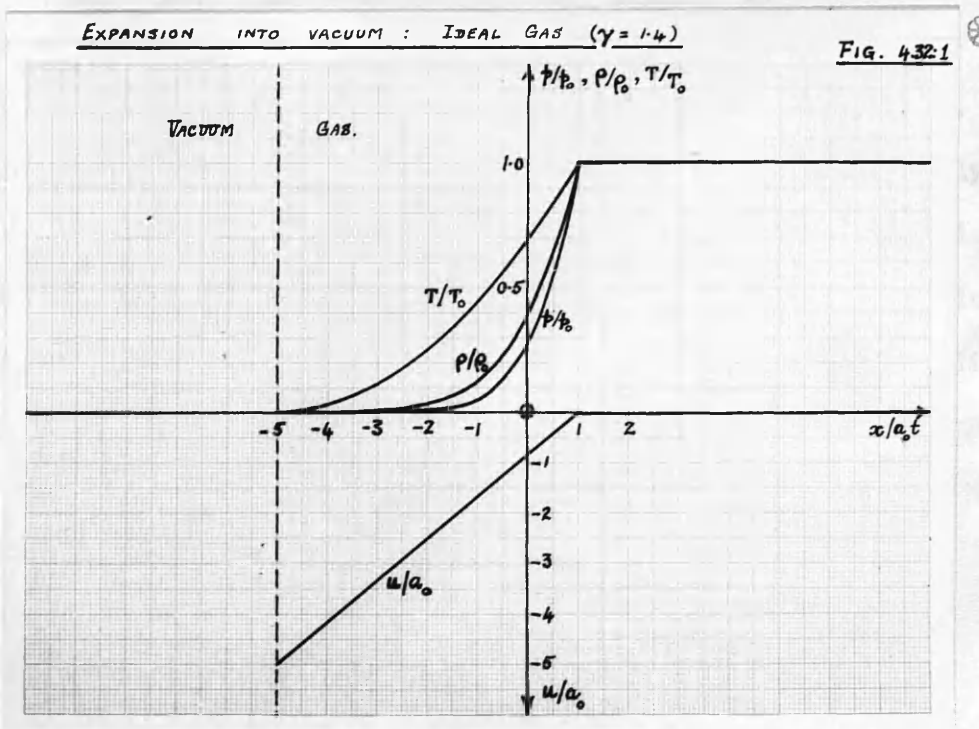


§4.32 Escape into a vacuum [140]

The case of expansion from rest into a vacuum has been already mentioned. If $\xi(\tau)$ represents the fluid surface at time τ , 4(9) shows that $\dot{\xi} = -2a_0/(\gamma-1)$, whereupon the solution is

$$\left. \begin{aligned} x > a_0 t : \quad u &= 0 \\ -2a_0 t/(\gamma-1) < x < a_0 t : \quad u &= \frac{2}{\gamma+1} \cdot \frac{x - a_0 t}{t} \end{aligned} \right\} \quad (1)$$

The velocity-profile is therefore linear throughout. It is illustrated in Fig. 4.32:1 for $\gamma = 1.4$.



Also shown are p/p_0 , ρ/ρ_0 , T/T_0 , calculated from

$$(T/T_0)^{\frac{y}{y-1}} = (\rho/\rho_0)^y = p/p_0 = \left[\frac{2}{\gamma+1} + \frac{\gamma-1}{\gamma+1} \cdot \frac{x}{a_0 t} \right]^{\frac{2y}{\gamma-1}}. \quad (2)$$

The temperature profile is parabolic for any γ .

At $x=0$, $u = -2a_0/(\gamma+1)$, and so $a = 2a_0/(\gamma+1)$.

It follows, therefore, that $u+a=0$ at $x=0$.

The velocity is therefore constant and equal to the local sound velocity at the plane originally bounding the gas. Moreover in this plane, by (2)

$$p/p_0 = \left[2/(\gamma+1) \right]^{\frac{2y}{\gamma-1}}, \quad (3)$$

exemplifying 4.01(2).

§ 4.33 Piston acceleration constant

The case

$$\ddot{\xi} = -f, \quad f > 0 \quad \text{and constant}, \quad (1)$$

is of interest by analogy with that discussed in § 4.2.

Here $\tau = -u/f$, $\xi = -u^2/2f$, and 4.1(1) therefore becomes [140]

$$x + \frac{1}{2}u^2/f = (a_0 + \frac{\gamma+1}{2}u)(t + u/f). \quad (2)$$

Accordingly, if we write t_c for $-2a_0/(\gamma+1)f$,

$$\gamma u = -a_0(1 - t/t_c) \pm \sqrt{a_0^2(1 - t/t_c)^2 - 2f\gamma(a_0 t - x)}, \quad (3)$$

which corresponds to 4.2(2), and applies at first for $-\frac{1}{2}ft^2 < x < a_0 t$.

In this range, (3) has two real negative roots, of which, however, only the (numerically) smaller is admissible. This can be seen most easily from a graph in the (x,t) -plane, as illustrated in Fig. 4.33:1. In this graph the motion of the piston is represented by $OABC'D$, whose equation is $x = -\frac{1}{2}ft^2$ or $\xi = -\frac{1}{2}f\tau^2$, if as usual we distinguish the coordinates of the piston by (ξ, τ) .

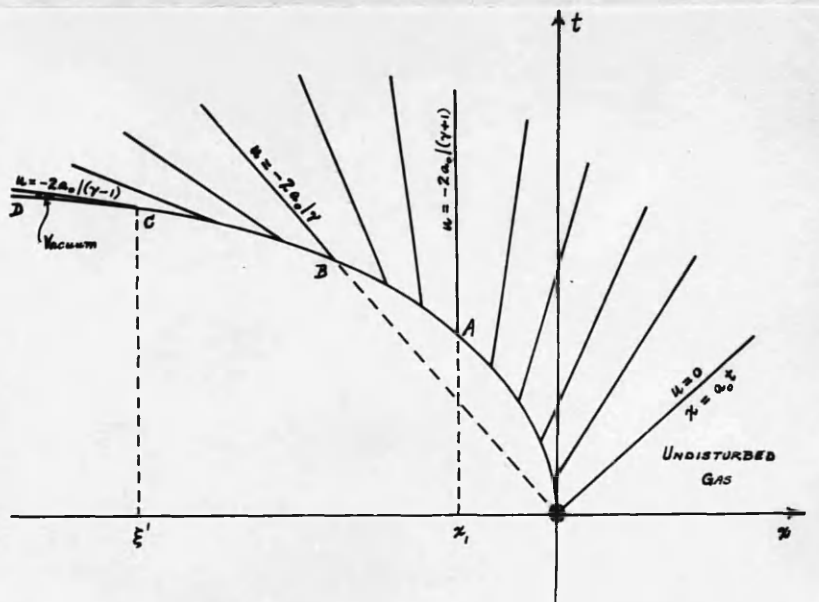


Fig. 4.33:1 RAREFACTION PRODUCED IN AN IDEAL GAS

BY A PISTON WITHDRAWN WITH CONSTANT ACCELERATION.

(Diagrammatic)

From each point (ξ, τ) we draw the straight line (2), along which u is constant and equal to $-f\tau$. This one-parameter family of lines is bounded on the one hand by the line $u=0$, i.e. $x=a_0 t$. As u decreases (algebraically), the slope dt/dx continually increases, passing (at A) when $u=u_1 \equiv -\frac{2a_0}{\gamma+1}$ though infinite values, corresponding to $u_1+a_0=0$, i.e. to a condition where sound waves are propagated neither forward nor backward. This condition and the velocity u_1 , therefore apply permanently in the plane

$$x = x_1 \equiv -\frac{2a_0^2}{(\gamma+1)^2} f$$

For still more negative values of u , dt/dx is negative: small waves are propagated only backward. When $u < -2a_0/\gamma$ (beyond B), the line when extended

downward passes again above $(0,0)$, giving rise to the spurious, numerically larger, solution of (3). Finally, when $u = -2a_0/(\gamma-1)$ (at c), the line touches $x = -\frac{1}{2}ft^2$, and for still more negative u passes below it. No solution can therefore be found for $u < u' \equiv -2a_0/(\gamma-1)$. This limiting velocity, u' , reached when $\tau = \tau' \equiv 2a_0/(\gamma-1)f$ and $\xi = \xi' \equiv -2a_0^2/(\gamma-1)^2f$, corresponds by 4(9) to $p_\xi = 0$; the piston thereafter separates from the gas, whose surface continues to move at u' into a vacuum.

The range of application of (3) is therefore modified as follows:-

$$\left. \begin{array}{l} -\frac{1}{2}ft^2 < x < a_0t, \text{ if } t < \tau' \\ -f\tau'(t - \frac{\xi'}{2}) < x < a_0t, \text{ if } t > \tau'. \end{array} \right\} \quad (4)$$

As an example, let $a_0 = 3.3 \times 10^4$ cm./sec., $f = 10^8$ cm./sec.², $\gamma = 1.4$.

Then

$$\begin{aligned} \tau' &= 1.65 \times 10^{-3} \text{ sec.}, \quad \xi' = -1.36 \times 10^2 \text{ cm.}, \quad u' = -16.5 \times 10^4 \text{ cm/sec.}, \\ \tau_1 &= 0.275 \times 10^{-3} \text{ sec.}, \quad x_1 = \xi_1 = -3.78 \text{ cm.}, \quad u_1 = -2.75 \times 10^4 \text{ cm/sec.} \end{aligned}$$

The velocity distributions at $t = 1.0 \times 10^{-3}$, 1.5×10^{-3} ($< \tau'$), 1.65×10^{-3} ($= \tau'$) and 2.0×10^{-3} ($> \tau'$) are shown in Fig. 4.33:2.

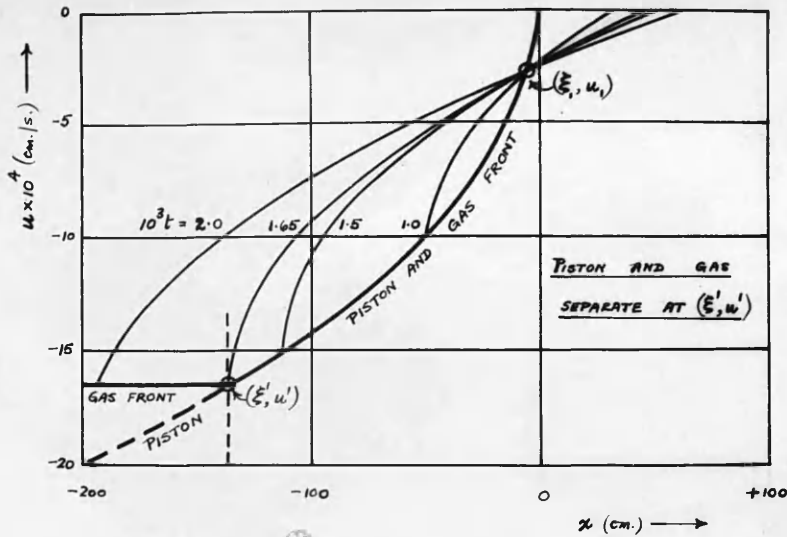


FIG. 4.33:2. RAREFACTION IN IDEAL GAS ($\gamma = 1.4$,
 $a_0 = 3.3 \times 10^4 \text{ cm/s}$) BEHIND PISTON ACCELERATED AT 10^8 cm/s^2 .

§4.34 General conditions for existence of a "Sonic point"

The existence of a point x_1 at which the velocity remains constant and equal in magnitude to the local velocity of sound is not confined to the present case of a uniformly accelerated piston, nor even to ideal gases, but may hold in any case of a piston continuously withdrawn, always provided that its velocity rises beyond a certain point. For by equation 3.3(1),

$$x = \xi(\tau) \text{ when } \dot{\xi}(\tau) + \alpha(\tau) = 0 \quad (1)$$

If (1) has a root τ_1 , then the velocity at $x_1 = \xi(\tau_1)$ is $\dot{\xi}(\tau_1)$ and is numerically equal to $\alpha(\tau_1)$ the local velocity of sound. Clearly, this situation arises only when $\dot{\xi} < 0$, i.e. in rarefactions, and again only provided $|\dot{\xi}|$ rises sufficiently high for (1) to have a root.

In an ideal gas, (1) becomes

$$\dot{\xi}(\tau) = -2a_0/(\gamma+1). \quad (2)$$

For example, suppose $\ddot{\xi} = -f\tau$, so that $\dot{\xi} = -\frac{1}{2}f\tau^2$, $\xi = -\frac{1}{6}f\tau^3$, if acceleration takes place from rest. Then $\tau_1 = 2\sqrt{\frac{a_0}{\gamma+1}}$, and $x_1 = \xi(\tau_1) = -\frac{4}{3}f \left(\frac{a_0}{\gamma+1}\right)^{3/2}$, $u_1 = -2fa_0/(\gamma+1)$.

Thus, although the complete solution — dependent upon a cubic in τ — would

be laborious, we can see at once that the gas velocity is constant and equal to u_1 , in the plane $x = x_1$.

§ 4.4 Expansion against an unsupported massive piston

As a slightly more difficult problem, we may consider the motion of a fluid expanding from rest at a pressure p_0 against a piston, whose mass per unit area is m , the external pressure being zero.

In this case, if $\dot{p}(\xi)$ is the pressure at the piston,

$$m\ddot{\xi} = -\dot{p}(\xi) = -p_0 \left(\frac{\gamma-1}{2a_0} \dot{\xi} + 1 \right)^{\frac{2\gamma}{\gamma-1}} \quad (1)$$

by 4(9).

Integration of (1) with respect to τ gives

$$\dot{\xi} = \frac{2a_0}{\gamma-1} \left[1 + \frac{\gamma+1}{2a_0 m} \cdot \frac{p_0}{m} \tau \right]^{-\frac{\gamma-1}{\gamma+1}} - \frac{2a_0}{\gamma-1}, \quad (2)$$

since $\dot{\xi} = 0$ when $\tau = 0$.

Integration of (1) with respect to ξ gives

$$(\gamma+1) \left(\frac{\gamma-1}{2a_0} \dot{\xi} + 1 \right)^{\frac{-2}{\gamma-1}} - 2 \left(\frac{\gamma-1}{2a_0} \dot{\xi} + 1 \right)^{\frac{-\gamma+1}{\gamma-1}} = (\gamma-1) \left[1 + \frac{\gamma+1}{2a_0^2 m} \cdot \frac{p_0}{m} \xi \right], \quad (3)$$

since $\dot{\xi} = 0$ when $\xi = 0$.

If we eliminate ξ and τ from 4.1(1) by means of (2) and (3), and replace $\dot{\xi}$ by u , there results after reduction

$$u = - \frac{2}{\gamma+1} \cdot \frac{a_0 t - x}{t + 2a_0 m / (\gamma+1) p_0}, \quad (4)$$

showing that u is linear in x throughout the wave.

The motion of the piston is determined by (2), which on integration gives

$$\xi = - \frac{2a_0}{\gamma-1} \tau - \frac{2a_0^2 m}{(\gamma-1)p_0} \left\{ 1 - \left[1 + \frac{\gamma+1}{2a_0 m} \cdot \frac{p_0}{m} \tau \right]^{\frac{2}{\gamma-1}} \right\}. \quad (5)$$

ξ increases without limit, but by (2) $\dot{\xi}$ approaches the velocity $-2a_0 / (\gamma-1)$ of escape into a vacuum.

The pressure $p(x, t)$ is then given immediately by (4) and 4(9). In particular, the pressure on the piston by (1) and (2) is

$$\dot{p}(\xi, \tau) = p_0 \left[1 + \frac{\gamma+1}{2a_0 m} \cdot \frac{p_0}{m} \tau \right]^{-\frac{2\gamma}{\gamma-1}}, \quad (6)$$

so that $[\dot{p}(\xi, \tau)]^{-\frac{\gamma+1}{2\gamma}}$ increases linearly with τ .

Comparison of (5) with 4.11 (2) shows that the two equations are identical if

$$t_c = \frac{-2a_0 m}{(\gamma+1) p_0} \quad (7)$$

This identity is, of course, also reflected in the linear relations (4) and 4.11 (3). It follows, therefore, that the analogue for $\dot{\xi}$ and $t_c < 0$ of the motion discussed in § 4.11 above is that of a fluid expanding against a massive unsupported piston. This can in fact be deduced at once from 4.1 (2) and 4.1(3), for by differentiation of 4.1(3)

$$0 = 1 + \frac{\gamma-1}{\gamma+1} - \frac{2a_0 + (\gamma-1)\dot{\xi}}{\gamma+1} \cdot \frac{\ddot{\xi}}{\dot{\xi}^2},$$

whence $\ddot{\xi}/\dot{\xi} = 2\gamma\ddot{\xi}/(2a_0 + (\gamma-1)\dot{\xi})$. (Cf. 4.1 (7))

Integrating again, we get:-

$$\ddot{\xi} = \text{const.} \left(1 + \frac{\gamma-1}{2a_0} \dot{\xi}\right)^{\frac{2\gamma}{\gamma-1}}, \quad (8)$$

the constant having the same sign as $\ddot{\xi}$.

Hence by 4.1 (2)

$$-m\ddot{\xi} = p(\dot{\xi}) \quad \text{if } \dot{\xi} < 0 \quad (9)(a)$$

$$m\ddot{\xi} = p(\dot{\xi}) \quad \text{if } \dot{\xi} > 0, \quad (9)(b)$$

the constant m being positive in each case. The boundary condition (9a) clearly corresponds to the present problem of expansion against a massive unsupported piston of mass m per unit area.

(9b) corresponds to the motion considered in § 4.11 above, which would, therefore, be realised if the piston were driven in by an external pressure at all times proportional to, and greater than, that exerted by the gas on its inner surface.

§4.5 Expansion against a supported massive piston

If the outward motion of the piston is opposed by a force P per unit area, 4.4 (1) becomes

$$m\ddot{\xi} = P - p_0 \left[\frac{\gamma-1}{2a_0} \dot{\xi} + 1 \right]^{\frac{2\gamma}{\gamma-1}}. \quad (1)$$

If P is prescribed as a function of $\tau, \xi, \dot{\xi}$ etc., the complete solution of the problem depends only on the determination of $\xi(\tau)$ from the differential

equation (1), and the subsequent application of 4.1(1). These operations can always be carried out numerically, but as a rule algebraic solution will not be possible. For example, let P be constant, - say the gravitational force on the piston.

$$\text{Then } \frac{m d\sigma}{P - p_0 \sigma^{2\gamma/(\gamma-1)}} = \frac{\gamma-1}{2a_0} d\tau ; \quad \frac{m(\sigma-1) d\sigma}{P - p_0 \sigma^{2\gamma/(\gamma-1)}} = \left(\frac{\gamma-1}{2a_0}\right)^2 d\xi , \quad (2)$$

where $\sigma \equiv 1 + \frac{\gamma-1}{2a_0} \dot{\xi}$. But (2) cannot in general be integrated in finite terms.

When P is not constant, the difficulties are increased. One important problem under this head arises when the piston separates two gases initially at rest and at different pressures: P_0, p_0 ($P_0 < p_0$). Reserving capital letters for the low-pressure gas, which lies towards ξ negative, we have:-

$$m \ddot{\xi} = P_0 \left[1 - \frac{\Gamma-1}{2A_0} \dot{\xi} \right]^{\frac{2\Gamma}{\Gamma-1}} - p_0 \left[1 + \frac{\gamma-1}{2a_0} \dot{\xi} \right]^{\frac{2\gamma}{\gamma-1}} . \quad (3)$$

Analytical solution appears difficult, even when $\Gamma = \gamma$ (and so $A_0 = a_0$). (3) may, however, be integrated numerically, and the solution for both gases completed by means of 4.1(1).

A shock must ultimately develop in the second gas, and as it is clear on physical grounds, or from (3), that $\ddot{\xi} < 0$, 4.1(7) shows that the shock will first arise at the nose of the compression wave. In fact, since $\dot{\xi}_0 = 0$ and $\ddot{\xi}_0 = - \frac{p_0 - P_0}{m}$, this happens at (t_c, x_c) , where

$$-x_c = A_0 t_c = \frac{2mA_0^2}{(\Gamma+1)(t_c - P_0)} \quad (4)$$

For example, suppose $A_0 = 3 \times 10^4$ cm./sec., $\Gamma = 1.4$, $m = 1$ g./cm.³.

Then

$p_0 - P_0$ (dyne/cm ²)	10^6	10^7	10^8	10^9
t_c (millisec.)	25	2.5	0.25	0.025
$-x_c$ (cm.)	750	75	7.5	0.75

When $m = 0$, $t_c = 0$, so that a shock wave is generated instantly on release, corresponding to the fact that $\ddot{\xi}_0$ is now infinite and $\dot{\xi}_0$ no longer zero. The problem is then intractable by the above analysis, and must be

deferred until after consideration of the propagation of shock waves. (§ 7.2)

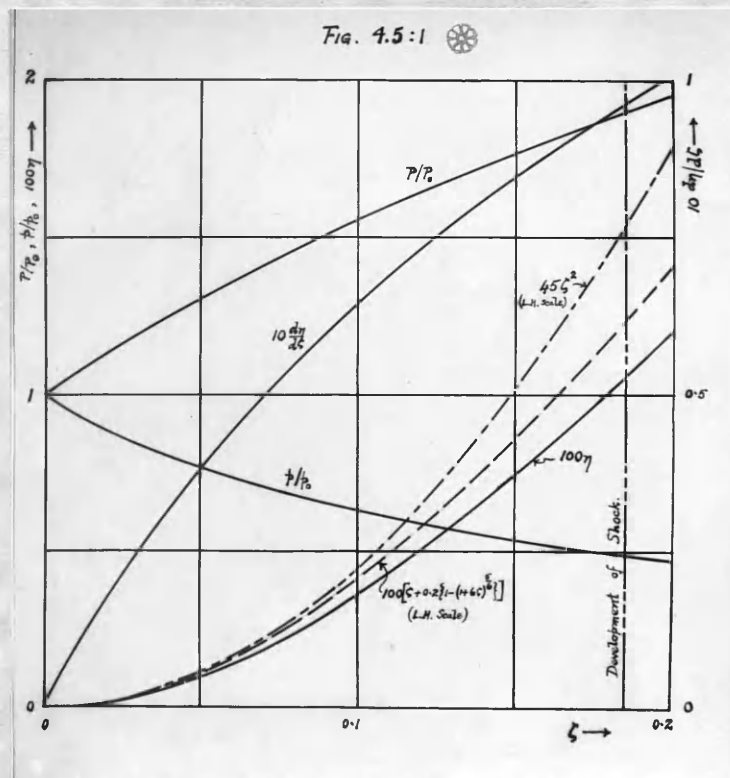
If $\Gamma = \gamma$, (and so $A_0 = a_0$), and if

$$\frac{P_0(\gamma-1)^2 \xi}{4ma_0^2} \equiv -\eta, \quad (\gamma-1)\frac{P_0 T}{2ma_0} \equiv \zeta, \quad \frac{P_0}{P_0} \equiv C, \quad \text{equation (3)}$$

becomes:-

$$\frac{d\eta}{d\xi^2} = (1 - d\eta/d\xi)^{\frac{2\gamma}{\gamma-1}} - C(1 + d\eta/d\xi)^{\frac{2\gamma}{\gamma-1}}. \quad (5)$$

This has been integrated numerically with respect to $d\eta/d\xi$ for $C = 0.1$, $\gamma = 1.4$, and the resultant value of $d\eta/d\xi$ integrated again with respect to ζ . The results are shown in Fig. 4.5:1 which thus represents the motion of a rigid massive piston released between air at, say, 1 atm. and 10 atm.



The solution holds up to $\tau = t_c$, i.e. $\zeta = \frac{\gamma-1}{(\gamma+1)(1-C)} = 0.1852$.

If the compression and rarefaction waves were ignored, the solution would be simply

$$\eta = \frac{1}{2}(1-C)\zeta^2. \quad (6)$$

Comparison shows that the error in (6) becomes appreciable when $\zeta > 3 \times 10^{-2}$ ($\eta > 3.8 \times 10^{-4}$).

Also graphed in Fig. 4.5:1 is equation 4.4(5), which is the limiting form of the integral of (5) when $C \rightarrow 0$, and is represented in terms of (η, ζ) by the equation

$$\eta = \zeta + \frac{\gamma-1}{2} \left\{ 1 - \left[1 + \frac{\gamma+1}{\gamma-1} \zeta \right]^{\frac{2}{\gamma+1}} \right\}. \quad (7)$$

It can be seen that (7) lies between (6) and the integral of (5) for finite C , - as would be expected.

§ 5 The role of dissipative processes in a shock wave

We have seen that compressional waves in an ideal compressible fluid become more steeply-fronted as they advance, and that infinite gradients of fluid velocity, pressure, density (and so also in general temperature) must arise by this process within a finite time. The appearance of infinite velocity and temperature gradients depends, however, upon the ideal nature of the fluid, in other words, upon the assumption that energy transferred by viscosity or thermal conduction across any material layer normal to the motion is negligibly small. In any real fluid, the quantities of energy so transferred must, according to classical laws, increase with the velocity and temperature gradients, the relation between energy transfer and the appropriate gradient being described by a "coefficient" of viscosity or thermal conduction. Accordingly, no matter how small these coefficients may be, the corresponding energy transfer must ultimately become important when the gradients are supposed to increase without limit. This supposition is, therefore, seen to contradict the assumptions on which it is based: velocity and temperature distributions in real fluids cannot in fact become discontinuous by the appearance of infinite gradients. Rather we may expect a stage to be reached in the development of the wave at which these gradients become so steep that the corresponding viscous and conductive transfer, negligible under less extreme conditions, are sufficiently large to prevent further intensification. A balance is thus in the end struck between the inherent tendency towards discontinuity and the enhanced dissipation of energy which it involves.

On the other hand, it is clear that the relevant gradients at

[37, 140]

equilibrium will be greater, and the effective thickness of the shock front therefore less, the smaller the coefficients of viscosity and heat conduction. For normal fluids, in which these coefficients are small, we may thus expect the front to be thin. An estimate of the order of magnitude of its thickness (ℓ) is in fact easily made if we assume the gradient of, say, velocity to have a constant value $\partial u / \partial x$ throughout the front. For the rate of viscous transfer is then $\frac{4}{3} \eta u^2 / \ell$, where η is the ordinary coefficient of "dynamical" viscosity, and u the fluid velocity behind the shock front relative to that ahead. This rate of transfer must be comparable with $\frac{1}{2} \rho u^3$ and $u \Delta p$, if Δp is the pressure difference across the front, so that $\ell \sim \frac{8\eta}{3} / \sqrt{2\rho \Delta p}$, or for air

$$\ell \sim 10^{-5} / \sqrt{\Delta p}, \quad (1)$$

if Δp is in atmospheres. This gives

Δp (atm.)	2	20	100	1000
ℓ (cm. $\times 10^{-7}$)	70	22	10	3

If heat conduction participates to a like degree these estimates of ℓ may perhaps be doubled. More precise estimates of ℓ are reviewed below; but it is already apparent that the shock front, at least in gases, is extremely thin. The conclusion can be extended to liquids of low viscosity, such as ethyl ether, for which $\eta / \sqrt{\rho}$ (and therefore ℓ) is of the same order as in air. Even water should have a shock front only ten to twenty times thicker.

§ 5.1 Entropy considerations [137, 140]

It is apparent from the above discussion that transfer of energy by the dissipative processes of viscous and thermal diffusion, so far from being negligible within the shock front where rapid changes of velocity,

pressure etc. take place, plays a critical or determining role in this region. It follows, therefore, that the entropy of an element of fluid does not remain constant when the element passes through the shock front. This circumstance distinguishes the shock wave fundamentally from the adiabatic waves out of which it develops. In these waves, the gradients of velocity and temperature, though they may be appreciable, are too small to involve a significant level of dissipation: the entropy is therefore effectively constant along each stream-line. If, however, the consequence of continued propagation is a steepening of the wave (which we have seen, on mechanical grounds, to be the case for compressional waves suitably supported by a piston or the like), the importance of the irreversible dissipative processes must continually increase as the wave advances, until in the end these processes become sufficiently important to prevent further steepening. When this stage has been reached, the entropy change experienced by any element of fluid in traversing the shock wave must be significant. Equation 3.1(1) then takes the more general form 3(12), i.e.

$$\phi = \phi(\rho, S), \quad (1)$$

and the previous analysis, which depends upon the simplification $S = \text{constant}$, ceases to apply. It is then necessary to return to the fundamental equations 3(1, 2, 3) and to extend these by the inclusion of terms dependent upon viscous and thermal transfer.

§ 5.2 General formulation for a real fluid

The linear flow of a real fluid, in which viscosity and thermal conduction are appreciable, is described by the following general

equations:

$$\begin{array}{l} \text{Equation of continuity} \\ (\text{Conservation of mass}) \end{array} \quad \frac{\partial v}{\partial t} + u \frac{\partial v}{\partial x} - v \frac{\partial u}{\partial x} = 0 \quad (1)$$

$$\begin{array}{l} \text{Equation of motion} \\ (\text{Conservation of momentum}) \end{array} \quad \frac{\partial u}{\partial t} + u \frac{\partial u}{\partial x} + v \frac{\partial p}{\partial x} = -v \frac{\partial}{\partial x} \left(\mu \frac{\partial u}{\partial x} \right) \quad (2)$$

$$\begin{array}{l} \text{First thermodynamic law} \\ (\text{Conservation of energy}) \end{array} \quad \frac{\partial E}{\partial t} + p \frac{\partial v}{\partial t} + u \left(\frac{\partial E}{\partial x} + p \frac{\partial v}{\partial x} \right) = v \frac{\partial}{\partial x} \left(\lambda \frac{\partial T}{\partial x} \right) + v \mu \left(\frac{\partial u}{\partial x} \right)^2 \quad (3)$$

where λ is the coefficient of thermal diffusion, and μ a coefficient of viscosity related to the "ordinary" coefficient η by

$$\mu = \frac{4}{3} \eta \quad (4)$$

These equations may be written

$$\frac{dp}{dt} + p \frac{\partial u}{\partial x} = 0 \quad (5)$$

$$\frac{du}{dt} + \frac{1}{p} \frac{\partial p}{\partial x} = \frac{1}{p} \frac{\partial}{\partial x} \left(\mu \frac{\partial u}{\partial x} \right) \quad (6)$$

$$pT \frac{dS}{dt} = \frac{\partial}{\partial x} \left(\lambda \frac{\partial T}{\partial x} \right) + \mu \left(\frac{\partial u}{\partial x} \right)^2 \quad (7)$$

The equation of continuity is identical with 3(4). The other two equations are distinguished by the terms in λ and μ from equations 3(5, 6), to which they reduce when $\lambda = 0 = \mu$.

In addition, we have equations 3(7, 8, 9, 10, 11, 12) as before, from which we may deduce

$$T = T(p, \rho) \quad (8)$$

The independent variables p, ρ, u, S are then to be determined as functions of x, t by (5, 6, 7, 8), together with 3(12) and appropriate boundary conditions.

Since S cannot now be regarded as a constant, p and u are no

longer functions of ρ alone. We are therefore unable to take advantage of equations 3.1(1) and 3.1(2), and the complete solution of the variable-state equations would present very great difficulty, even in the simplest cases. In certain circumstances, however, it is reasonable to expect that this complete solution, if it could be obtained, would tend with time towards a steady state, in which the independent variables ϕ, ρ, u, S (and so also E and T) would be functions of a single independent variable $x - Dt$, where D is a constant. Thus, let us consider again the motion of a fluid, initially at rest and at pressure, density etc. indicated by suffix 0, into which a piston advances with a velocity which at first increases but after a certain time becomes steady at a value W . A shock wave will form in the fluid after a finite time and at a finite distance from the piston. The shock front is, as we have seen, a region in which the gradient of velocity (for example) is very high. Behind this region of rapid transition the velocity will change in a much less abrupt manner to its value at the piston. Even the most gentle velocity gradient, however, must rise with time until its further increase is limited by dissipative transfer. It follows therefore that, at some period after the piston speed has become steady, appreciable velocity gradients should be concentrated within a narrow region. In advance of this region, the fluid is effectively at rest; behind, the velocity will remain effectively constant up to the piston surface with a value equal to that of the piston velocity itself. But under such circumstances it is clear that the shock front will advance with *entire motion will be steady from the* constant speed, D let us say, and that the point of view of an observer

who travels with the front. In this event, the wave velocity D , together with the steady pressure, density etc. in the region behind will depend only on the initial state of the fluid, and the velocity W , of the piston. Alternatively, if we regard the wave itself as at rest, in which case the undisturbed fluid passes into it with velocity $-D$, we are led to expect a solution of the general equations in which ϕ, u, ρ etc. are functions only of x , and change within a narrow range of x from initial values $\phi_0, -D, \rho_0$ etc. to final values $\phi_1, u_1 = W, D, \rho_1$ etc.

§ 5.3 The stationary plane shock [140, 5]

In accordance with the above argument we examine the fundamental equations 5.2(1, 2, 3) for stationary solutions of the type described.

Integration of 5.2(1) gives immediately

$$u/v = \text{const.} \equiv A, \text{ say}, \quad (1)$$

whereupon we deduce from 5.2(2)

$$\frac{u^2}{v} + \phi - \mu \frac{du}{dx} = \text{const.} \equiv B. \quad (2)$$

Equation 5.2(3) becomes

$$\frac{dE}{dx} + \frac{d(\rho v)}{dx} - v \frac{d\phi}{dx} = \frac{v}{u} \frac{d}{dx} (\lambda \frac{dT}{dx}) + \frac{v}{u} \mu \left(\frac{du}{dx} \right)^2,$$

and by means of (1) and 5.2(2) we can integrate this to give

$$E + \rho v + \frac{1}{2} u^2 - \mu v \frac{du}{dx} - \lambda \frac{v}{u} \frac{dT}{dx} = \text{const.} \equiv C. \quad (3)$$

(1, 2, 3) may be rearranged as follows

$$u = Av \quad (4)$$

$$A^2 v + \phi - B = \mu A \frac{dv}{dx} \quad (5)$$

$$E + Bv - \frac{1}{2} A^2 v^2 - C = \frac{\lambda}{A} \frac{dT}{dx} \quad (6)$$

Since E and ϕ are supposed known functions of T and v , (5, 6)

constitute two differential equations to determine T, v as functions of x . Their integration is described below. For the moment, we note that when $\lambda = \sigma = \mu$, the only continuous solution of the problem is the trivial one:

$$T = \text{const.}, \quad v = \text{const.}, \quad \text{etc.}$$

that is, $T_1 = T_0, v_1 = v_0, \text{etc.}$

If, when λ and μ differ from zero, a continuous solution is possible of the type proposed, in which u, v etc. change from one set of x -independent values u_0, v_0 etc. to another such set u_1, v_1 etc., it follows from (1, 2, 3) that these must be connected by the three relations:

$$\frac{u_1}{v_1} = \frac{u_0}{v_0} \quad (7)$$

$$\frac{u_1^2}{v_1} + p_1 = \frac{u_0^2}{v_0} + p_0 \quad (8)$$

$$E_1 + p_1 v_1 + \frac{1}{2} v_1^2 = E_0 + p_0 v_0 + \frac{1}{2} v_0^2 \quad (9)$$

Of course, if the possibility of a steady plane wave leading from one uniform region (suffix 0) to another (suffix 1) is assumed, these equations can be written down from the laws of conservation. Since E is supposed a known function of p, v , equations (7, 8, 9) will in general determine (at least) one solution u, v, p , when u_0, v_0, p_0 are prescribed. This solution is formally independent of λ and μ . However, in the complete absence of viscosity and heat conduction, and without the participation of extraneous forces, no such solution is physically possible.^[140] For by (5) this would involve an isentropic relation of the form

$$p = B - A^2 v, \quad (10)$$

which does not apply to any known substance, and indeed is scarcely conceivable since it requires that v should fall to zero at the finite pressure $p = B$. Since (7) and (8) must nevertheless be satisfied by any steady wave of the present type, it follows that the flow cannot in fact be isentropic. In fact, equation (9) results from the integration, with 5.2(1,2), net of $dE = -pdv$ (though this would lead to the same equation) but rather of 5.2(3), i.e. $dE = -pdv + TdS$, where $\int_{S_0}^{S_1} TdS = 0$, although $S_1 \neq S_0$.

§ 5.4 Structure of the stationary plane shock.

Integration of 5.3(4, 5, 6) requires first the specification of $E(T, v)$ and $p(T, v)$. For example, let $\frac{p}{v} = \frac{nR\tau}{v}$ and $E = C_v T = p v / (\gamma - 1)$ where nR , C_v and $\gamma = 1 + nR/C_v$ are constant: (ideal gas with constant specific heats). The integration has been studied in this special case by Rankine,^[37] Prandtl^[36] (ignoring μ),^[68] Hemel (ignoring λ),^[40] Rayleigh,^[40] Taylor and Becker^[59] (taking both λ and μ into account). In the main we follow Becker. For convenience, change to the dimensionless independent variables

$$v' \equiv \frac{A^2}{B} v, \quad p' \equiv \frac{1}{B} p, \quad \tau' \equiv \frac{A^2 n R}{B^2} \tau.$$

Then $p'v' = \tau'$ and 5.3(5, 6) become

$$v'^2 - v' + \tau' = \frac{\mu}{A} v' \frac{dv'}{dx} \quad (1)$$

$$\tau' - \frac{\gamma-1}{2} \left[v'^2 - 2v' + \frac{2CA^2}{B^2} \right] = \frac{\lambda}{AC_v} \frac{dT'}{dx}. \quad (2)$$

It is already clear that if λ and μ alter in the same ratio, the x -scale of the entire wave also alters in this ratio (Taylor).

T' and dT'/dx can be eliminated from (1, 2), yielding

$$-\frac{\lambda\mu}{Av'}w \frac{dw}{dv'} + (2\lambda + \mu c_v)w - \lambda \frac{w}{v'} = \frac{Ac_v}{2} Q(v') , \quad (3)$$

where

$$w \equiv v' dv'/dx ,$$

and

$$Q(v') \equiv (\gamma+1)v'^2 - 2\gamma v' + 2(\gamma-1)\frac{CA^2}{B^2} ;$$

but (3) does not appear easily integrable in the general case.

Alternatively, we may eliminate T' alone from (1, 2), obtaining

$$\mu c_v v' \frac{dv'}{dx} - \lambda \frac{dT'}{dx} = \frac{Ac_v}{2} Q(v') . \quad (4)$$

It is apparent from (4) that v'_0 and v'_1 are the roots of $Q(v') = 0$, so that

$$Q(v') = -(\gamma+1)(v'_0 - v')(v' - v'_1) \quad (5)$$

When $\lambda = 0$, therefore, (4) can be integrated at once to give

$$\frac{(\gamma+1)A}{2\mu} x = \frac{v'_0 \ln |v'_0 - v'| - v'_1 \ln |v' - v'_1|}{v'_0 - v'_1} . \quad (6)$$

As would be expected, this necessarily represents a wave of compression. For, supposing $A > 0$, v' approaches v'_0 at $x = -\infty$ and v'_1 at $x = +\infty$. But when $A > 0$, the fluid velocity is in the positive x -direction. Hence as the fluid passes through the wave its density increases. Similarly if $A < 0$.

It is clear that since, by (4) with $\lambda = 0$, dv'/dx is always finite, the density transition (and so also therefore by (2) the temperature transition) is necessarily continuous. The presence of viscosity thus prevents the appearance of temperature discontinuities, even in the entire absence of heat conduction.⁽¹⁴⁰⁾

When $\mu = 0$ (1) and (2), (or 3), give

$$\frac{dT'}{dx} = (1 - 2v') \frac{dv'}{dx} = \frac{Ac_v}{2\lambda} (\gamma+1) (v_o' - v') (v' - v_i') , \quad (7)$$

whence

$$\frac{(\gamma+1)Ac_v}{2\lambda} \cdot x = \frac{(1 - 2v') \ln |v' - v_i'| + (2v_o' - 1) \ln |v_o' - v'|}{v_o' - v'} \quad (8)$$

In this case, however, a continuous density transition is not guaranteed.

For, if $v_o' > \frac{1}{2} > v_i'$, dv'/dx evidently becomes infinite when $v' = \frac{1}{2}$.

In fact, (8) cannot hold even down to $v' = \frac{1}{2}$, for when $v' = 1 - v_i' (> \frac{1}{2})$, we have

$$(v')^2 - v' = (v_i')^2 - v_i' , \quad \text{and so}$$

$$T' = T_i' .$$

If, then, T rises further for $v' < 1 - v_i'$, it must thereafter fall again.

But, by (7), $\frac{dT'}{dx}$ is positive for $v_o' > v' > v_i'$. Hence T must remain constant beyond $v' = 1 - v_i'$, whereupon v' must also be constant and equal to v_i' beyond this point. At $v' = 1 - v_i'$, therefore, v must change discontinuously from $1 - v_i'$, to v_i' . The temperature changes continuously, though its gradient is discontinuous at T_i' . The fluid velocity and pressure also suffer abrupt changes.

[40,136]

It appears, therefore, that the presence of heat conduction, though sufficient always to prevent temperature discontinuities, may not prevent discontinuities in density, pressure and fluid velocity, when viscous forces are entirely absent. The condition for such discontinuities to appear is evidently

$$2v_o' > 1 > 2v_i' ,$$

which is satisfied provided

$$\frac{CA^2}{B^2} < \frac{3\gamma-1}{8(\gamma-1)} . \quad (9)$$

But by 5.3(7, 8, 9)

$$\frac{CA^2}{B^2} = \frac{\gamma^2}{2(\gamma-1)} \cdot \frac{2 + (\gamma-1)M_o^2}{(1 + \gamma M_o^2)^2}, \quad (10)$$

where $M_o \equiv u_o/a_o$ is Mach's number in the region 0. (9) therefore becomes

$$[\gamma(3-\gamma)M_o^2 - (3\gamma-1)] [\gamma M_o^2 - 1] > 0.$$

Hence, either $M_o^2 < \frac{1}{\gamma}$, which may be rejected on physical grounds, since $M_o \geq 1$, or

$$M_o^2 > (3\gamma-1)/\gamma(3-\gamma). \quad (11)$$

For $1 < M_o^2 < \frac{3\gamma-1}{\gamma(3-\gamma)}$, therefore, thermal conduction alone ensures continuity of all the variables. For $M_o^2 > \frac{3\gamma-1}{\gamma(3-\gamma)}$, on the other hand, only the temperature remains continuous.

Since, as will be shown below, $u_o^2/a_o^2 = [(\gamma+1)\frac{p_1}{p_0} + \gamma-1]/2\gamma$, the criterion for appearance of discontinuities may be written [cf. 140]

$$\frac{p_1}{p_0} > \frac{\gamma+1}{3-\gamma}. \quad (12)$$

$$\gamma = 1.0 \quad 1.1 \quad 1.2 \quad 1.4 \quad 1.6 \quad 1.8$$

$$M_o > 1.0 \quad 1.1 \quad 1.204 \quad 1.43 \quad 1.7 \quad 2.06$$

$$\frac{p_1}{p_0} > 1.0 \quad 1.105 \quad 1.223 \quad 1.5 \quad 1.86 \quad 2.35$$

Only rather weak waves preserve complete continuity.

The integration of (1, 2) cannot readily be effected in the general case when λ and μ have arbitrary values. A solution was however discovered by Becker [5] for the special case where $\lambda = \gamma\mu c_v$. Thus if we try $\omega = aQ(v')$, where a is a constant, as the solution of

(3), we require

$$2a^2 \frac{\lambda\mu}{A} (\gamma+1) - a(2\lambda + \mu c_v) + \frac{Ac_v}{2} = \frac{a\lambda}{v} \left\{ 1 - \frac{2\mu\gamma}{A} \right\},$$

whence $\lambda = 0$ and so $a = \frac{A}{2\mu\gamma}$, leading to the solution (6); or
 $a = A/2\mu\gamma$ and

$$2a^2 \frac{\lambda\mu}{A} (\gamma+1) - a(2\lambda + \mu c_v) + \frac{Ac_v}{2} = 0,$$

and so

$$\lambda = \gamma\mu c_v. \quad (13)$$

The solution is then given by

$$v' \frac{dv'}{dx} \equiv w = \frac{A}{2\mu\gamma} Q(v') = - \frac{A(\gamma+1)}{2\mu\gamma} (v'_0 - v')(v - v'), \quad (14)$$

and so is

$$\frac{\gamma+1}{2\gamma} \cdot \frac{A}{\mu} \cdot x = \frac{v'_0 \ln |v'_0 - v'| - v' \ln |v - v'|}{v'_0 - v'}. \quad (15)$$

The shape of the density profile is therefore identical with that (given by (6)) for a non-conducting but viscous fluid, but with the scale of x increased in the ratio $\gamma:1$, that is, $\lambda/\mu c_v : 1$. Although the equations cannot be integrated in corresponding fashion for values of $\lambda/\mu c_v$ other than γ , it is then reasonable to assume that the profile will in such other cases be again similar to (6), but extended approximately in the ratio $\lambda/\mu c_v : 1$.

The temperature distribution corresponding to (14) is

$$T' = \frac{\gamma-1}{2\gamma} \left(\frac{2CA^2}{B^2} - v'^2 \right) \quad (16)$$

No discontinuities appear, and, as in the case $\lambda = 0$, (15) necessarily represents a wave of compression.

Since for diatomic gases $\gamma\mu c_v/\lambda$ is theoretically equal to $7/6$, the special case $\gamma\mu c_v/\lambda = 1$ corresponds closely to that of a

diatomic gas.

The above analysis establishes the possibility of stable compressional waves in a viscous medium with or without the participation of heat transfer, and justifies the application of 5.3(7, 8, 9) to the steady states on either side of such a wave.

§ 5.5 Thickness of the wave front in gases

According to 5.4(6) and 5.4(14), v' becomes equal to v'_o or v'_i only when $\kappa = \pm \infty$. v' departs appreciably from these values, however, only within a very narrow range of κ . ^[5.5] Thus, let ℓ be the range of κ within which v' changes from

$$v'_o - \frac{1}{m} (v'_o - v'_i) \text{ to } v'_i + \frac{1}{m} (v'_i - v'_o)$$

where $1/m$ is a suitably small fraction, e.g. $1/10$.

Then by 5.4(6)

$$\ell = \frac{2\mu}{(\gamma+1)A} \cdot \frac{v'_o + v'_i}{v'_o - v'_i} \cdot \ln(m-1), \quad (1)$$

and by 5.4(14)

$$\ell = \frac{2\gamma\mu}{(\gamma+1)A} \cdot \frac{v'_o + v'_i}{v'_o - v'_i} \cdot \ln(m-1). \quad (2)$$

However, $\frac{v'_o + v'_i}{v'_o - v'_i} = \gamma \frac{\pi+1}{\pi-1}$, where $\pi \equiv p_i/p_o$,

and $A = \sqrt{\frac{p_o}{2v_o} [(\gamma+1)\pi + \gamma-1]}$ (See § 6.2 below)

Hence, in the case of (2),

$$\ell = \frac{2\gamma^2\mu \ln(m-1)}{\gamma+1} \sqrt{\frac{2v_o}{p_o}} \cdot \frac{\pi+1}{(\pi-1)\sqrt{(\gamma+1)\pi + \gamma-1}} \quad (3)$$

If $\mu = 2.3 \times 10^{-4}$ gm./cm. sec., $v_o = 772$ cm.³/gm., $p_o = 1.013 \times 10^6$ gm./cm. sec.², $\gamma = 1.4$, values appropriate to air at 1 atm. and 273°K, and if we take $m = 10$, (3) gives

π	2	5	10	100	1000	2000
$\ell \times 10^7$ (cm)	425	138	73	21.3	6.6	4.7,

in general agreement with the approximate estimates of § 5.

The front thickness may alternatively be defined (Prandtl, Becker) [136] [5] as the x -projection of the intercept cut by the asymptotes $v' = v'_0$ and $v' = v'_i$ from the tangent at the point of inflection. By 5.4 (14), this point corresponds to $v' = \sqrt{v'_0 v'_i}$, and the slope of the tangent there is

$$-\frac{A(\gamma+1)}{2\mu\gamma} \left(\sqrt{v'_0} - \sqrt{v'_i} \right)^2.$$

The thickness ℓ is accordingly

$$\ell = \frac{2\mu\gamma}{A(\gamma+1)} \cdot \frac{\sqrt{v'_0} + \sqrt{v'_i}}{\sqrt{v'_0} - \sqrt{v'_i}}, \quad (4)$$

which in terms of π becomes

$$\ell = \frac{2\mu\gamma}{\gamma+1} \cdot \frac{\sqrt{\frac{v_0}{p_0}} \cdot \sqrt{\frac{2}{(\gamma+1)\pi + \gamma-1}}}{\sqrt{\frac{v'_0}{p'_0}}} \cdot \frac{\gamma(\pi+1) + \sqrt{\gamma^2(\pi+1)^2 - (\pi-1)^2}}{\pi-1} \quad (5)$$

This expression gives almost the same values for air as (3) above with $m = 10$, so that it may be taken in practice to represent the thickness of the region in which some 8/10 of the transition is accomplished.

At the higher pressures, the wave-front thickness thus calculated [56, 136, 5] falls below the appropriate mean intermolecular distance, so that the use of continuum physics, as expressed in the Navier-Stokes hydrodynamic equations 5.2(1,2,3), is no longer strictly legitimate. Thomas, indeed, has recently [7a] pointed out that if allowance is made for the temperature variation of viscosity and thermal diffusivity, this objection is avoided. However, it is clear in any event that the shock front is for practical purposes ideally thin. A similar conclusion applies to liquids (§ 6.42).

§6. The large-scale properties of the steady plane shock.

The above analysis establishes the possibility of steady plane compressional waves, in which the fluid velocity, specific volume, etc. change within an extremely narrow thickness from uniform values u_0, v_0 , etc. in front of the wave to uniform values u, v , etc.

behind it. These uniform values are related by equations 5.3(7,8,9), from which we deduce at once:-

$$\frac{u_0}{v_0} = \frac{u_1}{v_1} = \sqrt{\frac{p_1 - p_0}{v_0 - v_1}} \quad (1)$$

$$E_1 - E_0 = \frac{1}{2}(p_0 + p_1)(v_0 - v_1) \quad (2)$$

From (1), it also follows that

$$u_0(u_0 - u_1) = v_0(p_1 - p_0), \quad (3)$$

since $v_0 > v_1$, and

$$u_0^2 - u_1^2 = (p_1 - p_0)(v_0 + v_1). \quad (4)$$

It is generally more convenient to regard the fluid in front of the wave, rather than the wave itself, as at rest. If the wave velocity is then D , and the fluid velocity behind it (in the same sense) W_1 , we have from (1)

$$D = v_0 \sqrt{(p_1 - p_0)/(v_0 - v_1)} \quad (5)$$

$$W_1 = \sqrt{(p_1 - p_0)(v_0 - v_1)}, \quad (6)$$

whence

$$\frac{W_1}{D} = 1 - \frac{v_1}{v_0} = 1 - \rho_0/\rho_1 \quad (7)$$

$$W_1 D = (p_1 - p_0)v_0, \text{ i.e. } (p_1 - p_0) = D \rho_1 \rho_0 \quad (8)$$

and

$$D^2 - (D - W_1)^2 = (p_1 - p_0)(v_0 + v_1). \quad (9)$$

Equation (2) remains unchanged. It is already evident that, for compression shocks ($v_0 > v_1$), $p_1 > p_0$, $E_1 > E_0$ and $W_1 > 0$. The fluid behind the wave has therefore a higher pressure and internal energy than that in front, and is moving forward in the same sense as the wave.

Equation (2) was discovered by Rankine and Hugoniot, and named by Hugoniot the "dynamic adiabatic", to stress its analogy, but also its contrast, with the ordinary adiabatic, which would apply to isentropic flow. Since, however, Hugoniot expressly discounted viscous and thermal transfer, his derivation of (2) is not fundamentally acceptable. As we have seen, and as was realised by Rankine, and later stressed by Rayleigh, this equation depends in fact upon the presence of dissipative forces, and therefore contradicts the assumption

of constant entropy implied in Hugoniot's approach. The contradiction is clear from the form of (2), which for isentropic processes would require to become the integral of

$$dE = -pdv. \quad (10)$$

If the wave is weak, however, that is, if $v_0/v_1 - 1$, $p_1/p_0 - 1$ etc. are small, (2) evidently approximates to (10), and the flow becomes almost isentropic. At the same time, by (6, 5), H_1 falls to zero, and D approaches $v_0 \sqrt{-(\partial p_0 / \partial v_0)_s}$, the velocity a_0 of sound in the undisturbed fluid.

§6.1 The Rankine-Hugoniot equation [5]

Since E_1 is supposed a known function of p_1 and v_1 , 6(2) constitutes an equation which must be satisfied by v_1, p_1 . 6(2,5, and 6) thus provide three relations between p_1, v_1, H_1 , and D , so that any three of these quantities are determined in terms of the remaining one. For example, if the wave velocity is measured, the pressure, density and fluid velocity behind the wave may be calculated.

Equation 6(2), expressed in terms of v_1, p_1 , defines a curve in the (v, p) -plane on which the terminal point (v_1, p_1) must lie. This Rankine-Hugoniot (R.H.) curve passes through the initial point (v_0, p_0) , at which it touches the appropriate "ordinary" or equal-entropy adiabatic, since for $0 < p_1/p_0 - 1 \ll 1$, 6(2) reduces to 6(10). The further discussion of the R.H.-curve, for materials which obey a simple equation of state, can be made explicit. For ideal gases it is presented in detail below.

In the general case, where the form of $E(v, p)$ remains unspecified, it is difficult to offer a correspondingly simple and rigorous treatment. Most or all of the known presentations fall short in this respect. However, with the aid of a small number of unrestrictive assumptions, which are certainly fulfilled in the very great majority of real instances, we may make the argument reasonably simple and conclusive.

Let $B(v, p)$ (where for convenience we omit the suffix $,$) be any point, other than $A(v_0, p_0)$ on the R.H.-curve; and let θ, φ, ψ be the angles, measured clockwise, from the negative v -axis to the secant AB , the tangent at B to the ordinary adiabatic through B , and the tangent to the R.H.-curve at B , respectively. For convenience, write $\Theta \equiv \tan \theta$, $\Phi \equiv \tan \varphi$, $\Psi \equiv \tan \psi$. Here we make the first assumption, namely

(a) that no two adiabatic curves intersect.

Then

$$\Theta = \frac{p - p_0}{v_0 - v} \quad (1)$$

$$\Phi = -\left(\frac{\partial p}{\partial v}\right)_S = \frac{\partial E/\partial v + p}{\partial E/\partial p}, \text{ by } 6(10), \quad (2)$$

$$\Psi = -\left(\frac{\partial p}{\partial v}\right)_{RH} = \frac{\partial E/\partial v + p - \frac{1}{2}(p - p_0)}{\partial E/\partial p - \frac{1}{2}(v - v_0)}, \text{ by } 6(2), \quad (3)$$

the suffix R.H. denoting differentiation along the R.H.-curve. Then

$$\frac{\Psi - \Phi}{v_0 - v} = \frac{\Phi - \Theta}{2\partial E/\partial p - (v_0 - v)} = \frac{\Psi - \Theta}{2\partial E/\partial p}. \quad (4)$$

Further

$$\begin{aligned} T\left(\frac{ds}{dv}\right)_{RH} &= \left(\frac{dE}{dv}\right)_{RH} + p = -\frac{1}{2}(v_0 - v)\Psi + \frac{1}{2}(p - p_0) \\ &= \frac{1}{2}(v_0 - v)(\Theta - \Psi) = \frac{\Theta - \Phi}{2 - (v_0 - v)/\partial E/\partial p}. \end{aligned} \quad (5)$$

Then, when $|v_0 - v|$ is sufficiently small, $T\left(\frac{ds}{dv}\right)_{RH}$ has the sign of $\theta - \varphi$.

We now make the second assumption:

(b) that $(\partial^2 p / \partial v^2)_S$ does not change sign.

Then geometrical considerations show at once that $\theta - \varphi$ has the opposite sign to $(\partial^2 p / \partial v^2)_S$. Consequently, near (v_0, p_0) ,

$$\begin{aligned} \text{if } (\partial^2 p / \partial v^2)_S > 0, \quad (ds/dv)_{RH} &\leq 0 & ; \\ \text{if } (\partial^2 p / \partial v^2)_S < 0, \quad (ds/dv)_{RH} &\geq 0 & ; \end{aligned} \quad \} \quad (6)$$

the signs of equality applying when $\theta = \varphi$, i.e. at (v_0, p_0) .

In the first case, compressional waves must correspond to an increase in entropy, and are therefore permitted on thermodynamic grounds; while

rarefaction waves involve a spontaneous fall in entropy, and are therefore thermodynamically impossible. In the second case, the position is reversed. These conclusions are identical with those deduced earlier from dynamical arguments. Moreover, it is clear that the RH-curve crosses the adiabatic through (v_0, p_0) at that point. The two curves therefore have contact of at least the second order at (v_0, p_0) , as can be verified at once from (5), since $v_0 - v$ and $\theta - \psi$ are separately zero there. That the contact is in fact of the second order may be confirmed as follows.

By successive differentiation of (5) along the RH-curve, we have

$$\begin{aligned} T \frac{d^2S}{dv^2} + \frac{dT}{dv} \frac{dS}{dv} &= -\frac{1}{2} \bar{\Psi} + \frac{1}{2}(v_0 - v) \frac{d\bar{\Psi}}{dv} + \frac{1}{2} \bar{\Psi} \\ &= \frac{1}{2}(v_0 - v) d\bar{\Psi}/dv. \end{aligned} \quad (7)$$

$$T \frac{d^3S}{dv^3} + 2 \frac{dT}{dv} \frac{d^2S}{dv^2} + \frac{d^2T}{dv^2} \frac{dS}{dv} = \frac{1}{2}(v_0 - v) \frac{d^2\bar{\Psi}}{dv^2} - \frac{1}{2} \frac{d\bar{\Psi}}{dv}. \quad (8)$$

At (v_0, p_0) , therefore, by (5, 7, 8),

$$(dS/dv)_{RH} = 0 = (d^2S/dv^2)_{RH}, \quad (9)$$

$$(d^3S/dv^3)_{RH} = -\frac{1}{2} d\bar{\Psi}/dv. \quad (10)$$

But, by (4), when $v = v_0$, $\psi = \varphi = \theta$, we have

$$(d\bar{\Psi}/dv)_{RH} = (d\bar{\Phi}/dv)_{RH} = (\partial\bar{\Phi}/\partial v)_S = -(\partial^2\bar{\Psi}/\partial v^2)_S \quad (11)$$

Hence, at (v_0, p_0) ,

$$(d^3S/dv^3)_{RH} = \frac{1}{2} (\partial^2\bar{\Psi}/\partial v^2)_S \quad (12)$$

The RH-curve therefore makes double contact at (v_0, p_0) with the appropriate adiabatic, and crosses over it.

The above argument holds from (v_0, p_0) , up to the point, if any, where $2\partial E/\partial p = v_0 - v$. $\bar{\Psi}$ then becomes infinite, and the subsequent course of the RH-curve cannot be analysed in the general case without excessive complication, which obscures rather than clarifies the question.

We have not as yet specified the signs of $(\partial p/\partial v)_S$ or $(\partial E/\partial p)_v$, which are not material to the preceding discussion. As a rule, however, $(\partial E/\partial p)_v = T(\partial S/\partial p)_v$ will be > 0 , and $(\partial p/\partial v)_S$ will be < 0 .

These conditions are equivalent to $\frac{\partial S}{\partial p} > 0$, $\frac{\partial S}{\partial v} > 0$.

Also, $(\frac{\partial^2 p}{\partial v^2})_S$ will be positive; this is equivalent, in view of the former conditions, to $S_{pv}^2 < S_{pp} \cdot S_{vv}$. The adiabatics have then the familiar form, concave upward and rising in p as v decreases; and the corresponding entropy increases along any radius from the origin. The RH-curve is then also concave upward, and rises (at every point save (v_0, p_0)) more steeply than the adiabatics.

S decreases along the entire curve, with increasing v . This is the case illustrated in Fig. 6.1:1.

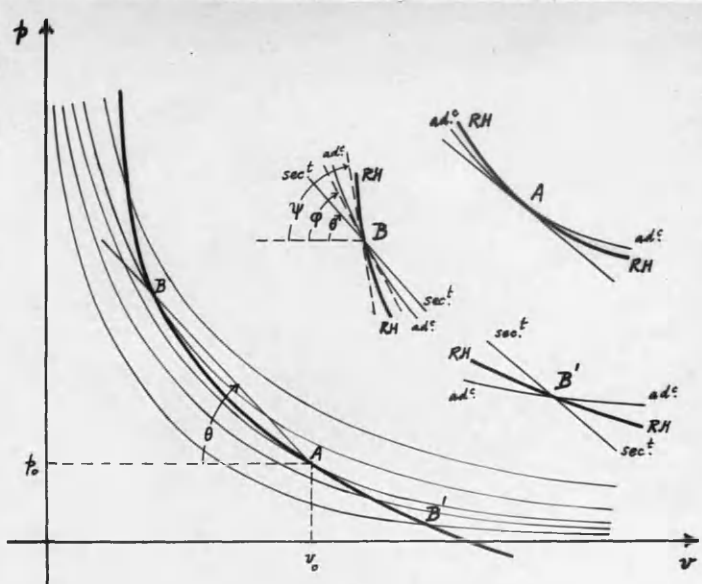


FIG. 6.1:1 RANKINE-HUGONIOT CURVE AND

ORDINARY ADIABATICS, when $(\frac{\partial p}{\partial v})_S < 0$, $(\frac{\partial^2 p}{\partial v^2})_S > 0$, $(\frac{\partial S}{\partial p})_S > 0$.

In this case, by 6(5,6),

$$D - W_i = v_i \sqrt{\Phi} \leq v_i \sqrt{\Psi} \equiv a_i \quad (13)$$

according as $v_i \leq v_0$, a_i being the velocity of sound behind the wave.

Thus,

$$a_i + W_i \gtrsim D \text{ , as } v_i \leq v_0 , \quad (14)$$

so that infinitesimal waves, either of compression or rarefaction, can

Since for an ideal gas, $E = \frac{Pv}{\gamma-1} + \text{const.}$, the RH-equation

becomes

$$\frac{v_1}{v_0} = \frac{\pi+\lambda}{\lambda\pi+1}, \quad (1)$$

where we have written π for p_1/p_0 and λ for $(\gamma+1)/(\gamma-1)$.

Accordingly,

$$\frac{E_1}{E_0} = \frac{T_1}{T_0} = \frac{a_1^2}{a_0^2} = \pi \cdot \frac{\pi+\lambda}{\lambda\pi+1}, \quad (2)$$

and by 6(5,6)

$$\frac{D}{a_0} = \sqrt{\frac{\lambda\pi+1}{\lambda+1}}, \quad (3)$$

$$\frac{W_1}{a_0} = \frac{(\lambda-1)(\pi-1)}{\sqrt{(\lambda+1)(\lambda\pi+1)}}, \quad (4)$$

whereupon also

$$\frac{D-W_1}{a_0} = \frac{\pi+\lambda}{\sqrt{(\lambda+1)(\lambda\pi+1)}}, \quad (5)$$

and

$$\frac{u_0^2 - u_1^2}{a_0^2} = \frac{D^2 - (D-W_1)^2}{a_0^2} = \frac{(\lambda-1)(\pi^2-1)}{\lambda\pi+1}. \quad (6)$$

The entropy change $S_1 - S_0$ is obtained by integrating

$$dS = (dE + Pdv)/T = c_v (\gamma \frac{dv}{v} + \frac{dp}{P}):$$

$$\frac{S_1 - S_0}{c_v} = \gamma \ln \frac{\pi+\lambda}{\lambda\pi+1} + \ln \pi. \quad (7)$$

[140] Since from (7)

$$\frac{d}{d\pi} (S_1 - S_0) = \frac{c_v \lambda (\pi-1)^2}{\pi(\pi+\lambda)(\lambda\pi+1)} > 0 \quad (8)$$

it is clear once again that $S_1 > S_0$. The double contact of RH-curve and adiabatic at $\pi=1$ is apparent from (8), and the fact that the curves cross there can easily be established by verifying that $d^2S/d\pi^2 = 0$, $d^3S/d\pi^3 > 0$ when $\pi = 1$.

Approximate forms of the above equations for weak, strong and nearly isothermal waves respectively are given in §§ 6.22, 6.23, 6.24.

§6.21 Relative magnitudes of D, W_1, a_1, W_1+a_1

From 6.2(3), $D > a_1$, and D rises without limit as π is increased.

Again from 6.2(2,5)

$$\frac{D-W_1}{a_1} = \sqrt{\frac{\pi+\lambda}{(\lambda+1)\pi}} < 1. \quad (1)$$

Thus $W_1+a_1 > D$, in accordance with §§ 2,6.1.

As to W_1 and a_1 separately, it is clear that $W_1 < D$; but the relative magnitudes of a_1 and D are less obvious. By 6.2(2,3)

$$\frac{D}{a_1} = \frac{\lambda\pi+1}{\sqrt{(\lambda+1)\pi(\pi+\lambda)}}, \quad (2)$$

so that

$$\frac{D^2 - a_1^2}{D^2} = \frac{(\pi-1)[\pi\lambda(\lambda-1)-1]}{(\lambda\pi+1)^2}. \quad (3)$$

Thus $D \gtrless a_1$, according as $\pi \lessgtr 1/\lambda(\lambda-1) = (\gamma-1)^2/2(\gamma+1)$.

But $1/\lambda(\lambda-1) = 1$ when $\lambda = \frac{1}{2}(1 + \sqrt{5}) = 1.62\dots$

(i.e. when $\gamma = 4.23$). For $\lambda < 1.62$, $1/\lambda(\lambda-1) > 1$, and vice versa.

Hence, for $\gamma < 4.23$, $D > a_1$, for all $\pi (> 1)$

for $\gamma > 4.23$, ($> a_1$, for $\pi > 1/\lambda(\lambda-1)$
 $D (= a_1, " \pi = 1/\lambda(\lambda-1)$
 $< a_1, " \pi < 1/\lambda(\lambda-1)$)

It is clear that $D > a_1$ always in ideal gases. For media which follow an adiabatic $\rho v^\gamma = \text{constant}$, with $\gamma > 4.23$, however, it is possible for a_1 to exceed D up to a pressure defined by

$$\pi = (\gamma-1)^2/2(\gamma+1). \quad (4)$$

Again, from 6.2(2,4),

$$\frac{W_1}{a_1} = \frac{(\lambda-1)(\pi-1)}{\sqrt{(\lambda+1)\pi(\pi+\lambda)}}. \quad (5)$$

The post-shock flow is thus subsonic or supersonic according as $f(\pi, \lambda) \leq 0$, where

$$f \equiv \pi^2 \lambda(\lambda-3) - \pi(3\lambda^2 - 3\lambda + 2) + (\lambda-1)^2. \quad (6)$$

It can be readily shown that, if $\lambda > 3$, (i.e. $\gamma < 2$), $f = 0$ has always two positive real roots, one of which is < 1 , and one > 1 . The flow is then subsonic for π less than this larger root, but supersonic thereafter. If, however, $\lambda < 3$ ($\gamma > 2$), the flow is always subsonic.

The critical pressure ratio, π_c , varies with γ as follows.

Table 6.21:1

γ	1.0	1.1	1.2	1.4	5/3	2
λ	∞	21	11	6	4	3
π_c	2.62	2.98	3.44	4.82	9.26	∞

§ 6.22 Approximations for $\pi - 1 < 1$. [Cf. 53]

Equations 6.2(1-7) express the various characteristics of the wave in terms of π , and lead at once to the following series, suitable when $\pi - 1 < 1$.

$$\frac{v_1}{v_0} = 1 - \frac{1}{\gamma}(\pi - 1) + \frac{\gamma+1}{2\gamma^2}(\pi - 1)^2 - \frac{(\gamma+1)^2}{4\gamma^3}(\pi - 1)^3 + \dots \quad (1)$$

$$\frac{E_1}{E_0} = \frac{T_1}{T_0} = \frac{a_1^2}{a_0^2} = 1 + \frac{\gamma-1}{\gamma}(\pi - 1) - \frac{\gamma-1}{2\gamma^2}(\pi - 1)^2 + \frac{(\gamma-1)(\gamma+1)}{8\gamma^3}(\pi - 1)^3 - \dots \quad (2)$$

$$\frac{D}{a_0} = 1 + \frac{\gamma+1}{4\gamma}(\pi - 1) - \frac{(\gamma+1)^2}{32\gamma^2}(\pi - 1)^2 + \frac{(\gamma+1)^3}{128\gamma^3}(\pi - 1)^3 - \dots \quad (3)$$

$$\frac{W_1}{a_0} = \frac{1}{\gamma}(\pi - 1) - \frac{\gamma+1}{4\gamma^2}(\pi - 1)^2 + \frac{3(\gamma+1)^2}{32\gamma^3}(\pi - 1)^3 - \dots \quad (4)$$

$$\frac{W_1 - D}{a_0} = -1 + \frac{3-\gamma}{4\gamma}(\pi - 1) - \frac{7-\gamma}{32\gamma^2}(\gamma+1)(\pi - 1)^2 + \dots \quad (5)$$

$$\frac{u_0^2 - u_1^2}{a_0^2} = \frac{D^2 - (D-W_1)}{a_0^2} = \frac{2}{\gamma}(\pi - 1) - \frac{1}{\gamma^2}(\pi - 1)^2 + \frac{\gamma+1}{2\gamma^3}(\pi - 1)^3 - \dots \quad (6)$$

$$\frac{s_1 - s_0}{c_v} = \frac{\gamma^2 - 1}{12\gamma^2}(\pi - 1)^3 - \frac{\gamma^2 - 1}{8\gamma^2}(\pi - 1)^4 + \dots \quad (7)$$

For comparison, the specific volume, temperature, etc. behind an adiabatic compression wave, across which the pressure ratio is again π , are given by:

$$\frac{v_1}{v_0} = \pi^{-\frac{1}{\gamma}} = 1 - \frac{1}{\gamma}(\pi - 1) + \frac{\gamma+1}{2\gamma^2}(\pi - 1)^2 - \frac{(\gamma+1)(2\gamma+1)}{6\gamma^3}(\pi - 1)^3 + \dots \quad (8)$$

$$\frac{E_1}{E_0} = \frac{T_1}{T_0} = \frac{a_1^2}{a_0^2} = \pi^{\frac{\gamma-1}{\gamma}} = 1 + \frac{\gamma-1}{\gamma}(\pi - 1) - \frac{\gamma-1}{2\gamma^2}(\pi - 1)^2 + \frac{\gamma^2 - 1}{6\gamma^3}(\pi - 1)^3 - \dots \quad (9)$$

$$\frac{D}{a_0} = 1 + \frac{\gamma+1}{\gamma-1} \left[\pi^{\frac{\gamma-1}{2\gamma}} - 1 \right] = 1 + \frac{\gamma+1}{2\gamma}(\pi - 1) - \frac{(\gamma+1)^2}{8\gamma^2}(\pi - 1)^2 + \frac{(\gamma+1)^2(3\gamma+1)}{48\gamma^3}(\pi - 1)^3 - \dots \quad (10)$$

$$\frac{W_1}{a_0} = \frac{2}{\gamma-1} \left[\pi^{\frac{\gamma-1}{2\gamma}} - 1 \right] = \frac{1}{\gamma}(\pi - 1) - \frac{\gamma+1}{4\gamma^2}(\pi - 1)^2 + \frac{(\gamma+1)(3\gamma+1)}{24\gamma^3}(\pi - 1)^3 - \dots \quad (11)$$

$$\frac{W_1 - a_0}{a_0} = -1 + \frac{1}{\gamma} (\pi - 1) - \frac{\gamma + 1}{4\gamma^2} (\pi - 1)^2 + \frac{(\gamma + 1)(3\gamma + 1)}{24\gamma^3} (\pi - 1)^3 - \dots \quad (12)$$

$$\frac{u_0^2 - u_1^2}{a_0^2} = \frac{a_0^2 - (a_0 - W_1)^2}{a_0^2} = \frac{2}{\gamma} (\pi - 1) - \frac{\gamma + 3}{2\gamma^2} (\pi - 1)^2 + \frac{(\gamma + 1)(3\gamma + 7)}{12\gamma^3} - \dots \quad (13)$$

$$S_1 - S_0 = 0 \quad (14)$$

The quantity $W_1 - a_0$ in (12) represents the fluid velocity at the rear of the wave (where $\frac{t}{t_0} = \pi$), from the point of view of an observer travelling with the wave front (i.e. at a_0). It therefore corresponds to $W_1 - D$ in (5). Similarly, the quantity $a_0^2 - (a_0 - W_1)^2$ in (13) represents the decrease in kinetic energy of a fluid particle in passing through the wave, from the standpoint of the same observer; it thus corresponds to $D^2 - (D - W_1)^2$ in (6).

If $\pi - 1$ is sufficiently small to justify retention only of terms in $\pi - 1$, and if $\Delta p \equiv p_1 - p_0$, etc. these equations give

Shock Wave	<u>Adiabatic</u> Compression Wave
$-\frac{\Delta v}{v_0} = \frac{\Delta p}{p_0}$	$\frac{1}{\gamma} (\Delta p/p_0)$

(15)

$$\frac{\Delta E}{E_0} = \frac{\Delta T}{T_0} = \frac{2\Delta a}{a_0} \quad \frac{\gamma - 1}{\gamma} (\Delta p/p_0) \quad \frac{\gamma - 1}{\gamma} (\Delta p/p_0) \quad (16)$$

$$-\frac{1}{2} \frac{\Delta u^2}{u_0^2} = -\frac{\Delta u}{u_0} = \frac{W_1}{a_0} \quad \frac{1}{\gamma} (\Delta p/p_0) \quad \frac{1}{\gamma} (\Delta p/p_0) \quad (17)$$

$$\frac{D - a_0}{a_0} \quad \frac{\gamma + 1}{4\gamma} (\Delta p/p_0) \quad \frac{\gamma + 1}{2\gamma} (\Delta p/p_0) \quad (18)$$

$$\frac{\Delta S}{c_v} \quad 0 \left[\frac{\gamma^2 - 1}{12\gamma^2} (\Delta p/p_0)^3 \right] \quad 0 \quad (19)$$

With the exception of D , the differences between shock and adiabatic waves are of the order of $(\pi - 1)^3$ or $(\Delta p/p_0)^3$. The difference in D is, however, of order $\pi - 1$. For small $\pi - 1$, v_1 , T_1 , and W_1 are larger in the shock wave than in the adiabatic wave of equal pressure ratio, but D is smaller.

§ 6.23 Approximations for $\pi \gg 1$. [cf. 53]

$$\frac{v_1}{v_0} = \frac{1}{\lambda} + \frac{\lambda^2 - 1}{\lambda^2 \pi} - \frac{\lambda^2 - 1}{\lambda^3 \pi^2} + \frac{\lambda^2 - 1}{\lambda^4 \pi^3} - \dots \quad (1)$$

$$\frac{E_1}{E_0} = \frac{T_1}{T_0} = \frac{a_1^2}{a_0^2} = \frac{\pi}{\lambda} + \frac{\lambda^2 - 1}{\lambda^2} - \frac{\lambda^2 - 1}{\lambda^3 \pi} + \dots \quad (2)$$

$$\frac{D}{a_0} = \sqrt{\frac{\lambda\pi}{\lambda+1}} \left(1 + \frac{1}{2\lambda\pi} - \frac{1}{8\lambda^2\pi^2} + \dots \right) \quad (3)$$

$$\frac{W_i}{a_0} = (\lambda-1) \sqrt{\frac{\pi}{\lambda(\lambda+1)}} \left(1 - \frac{1}{2\lambda\pi} + \frac{3}{8\lambda^2\pi^2} - \dots \right) \quad (4)$$

$$\frac{W_i - D}{a_0} = - \sqrt{\frac{\pi}{\lambda(\lambda+1)}} \left(1 - \frac{2\lambda^2-1}{2\lambda\pi} - \frac{4\lambda^2-3}{8\lambda^2\pi^2} + \dots \right) \quad (5)$$

$$\frac{u_e^2 - u_i^2}{a_0^2} = \frac{\lambda-1}{\lambda} \pi - \frac{\lambda-1}{\lambda^2} - \frac{(\lambda-1)(\lambda^2-1)}{\lambda^3\pi} + \dots \quad (6)$$

$$\frac{S_i - S_o}{c_v} = \ln \pi - \gamma \ln \lambda + (\lambda+1)^2 \left(\frac{1}{\lambda\pi} - \frac{1}{2\lambda^2\pi^2} + \dots \right). \quad (7)$$

For very intense waves, therefore

$$\frac{v_i}{v_o} \sim \frac{1}{\lambda} = \frac{\gamma-1}{\gamma+1} \quad (8)$$

$$\frac{E_i}{E_o} = \frac{T_i}{T_o} = \frac{a_i^2}{a_o^2} \sim \frac{\pi}{\lambda} = \frac{\gamma-1}{\gamma+1} \cdot \pi \quad (9)$$

$$\frac{D}{a_0} \sim \sqrt{\frac{\lambda\pi}{\lambda+1}} = \sqrt{\frac{\gamma+1}{2\gamma} \cdot \pi} \quad (10)$$

$$\frac{W_i}{a_0} \sim (\lambda-1) \sqrt{\frac{\pi}{\lambda(\lambda+1)}} = \sqrt{\frac{2\pi}{\gamma(\gamma+1)}} \quad (11)$$

$$\frac{W_i - D}{a_0} \sim - \sqrt{\frac{\pi}{\lambda(\lambda+1)}} = - (\gamma-1) \sqrt{\frac{\pi}{2\gamma(\gamma+1)}} \quad (12)$$

$$\frac{u_e^2 - u_i^2}{a_0^2} \sim \frac{\lambda-1}{\lambda} \pi = \frac{2\pi}{\gamma+1} \quad (13)$$

$$\frac{S_i - S_o}{c_v} \sim \ln \pi \quad (14)$$

Comparison with 6.22(8-14) shows that, for large π , all the above quantities (including D/a_0) are larger than in the adiabatic wave of equal pressure ratio. From these comparisons it appears that an adiabatic compression wave cannot in general turn simply into a shock wave of equal pressure ratio, without for example a change in the velocity behind the wave, in other words, a reflection of some kind. This circumstance, noticed by Stokes and Rayleigh, is discussed further in § 6.25 below.

Most significant is the fact that v_i cannot be reduced indefinitely in a single shock wave, however intense, but only down to a limit equal to v_o/λ . This limited compression, which is in sharp contrast to the behaviour of adiabatic waves, is a consequence of the entropy rise, and may be described as due to "superadiabatic" heating. The volume can of course be further reduced by ensuing shock waves.

The wave and fluid velocities and the temperature and entropy rise without limit as π is increased.

§6.24 Approximations for $\gamma-1 \ll 1$

When γ is close to 1, as will be the case with complex molecules, the adiabatic conditions approach the isothermal, and we have the following:-

<u>Shock wave</u>	<u>Adiabatic Wave</u>	
-------------------	-----------------------	--

$$\frac{v_i}{v_o} \sim \frac{1}{\pi} \quad \frac{1}{\pi} \quad (1)$$

$$\frac{E_i}{E_o} = \frac{T_i}{T_o} = \frac{a_i^2}{a_o^2} \sim 1 \quad 1 \quad (2)$$

$$\frac{D}{a_o} \sim \sqrt{\pi} \quad 1 + \ln \pi \quad (3)$$

$$\frac{W_i}{a_o} \sim \sqrt{\pi} - \frac{1}{\sqrt{\pi}} \quad \ln \pi \quad (4)$$

$$\frac{D-W_i}{a_o} \sim \frac{1}{\sqrt{\pi}} \quad 1 \quad (5)$$

$$\frac{u_o^2 - u_i^2}{a_o^2} \sim \pi - \frac{1}{\pi} \quad \ln \pi (2 - \ln \pi) \quad (6)$$

$$\frac{s_i - s_o}{c_v} \sim 0 \quad 0 \quad (7)$$

§6.25 Development of a shock from an adiabatic compression wave

It was pointed out in § 6.23 that a shock could not in general develop out of an adiabatic wave without some species of reflexion. In other words, the process of intensification of the shock not only represents a consequence of the steepening of the adiabatic wave, but in turn reacts upon and modifies this wave.

For example, let us suppose that a piston accelerates smoothly from rest to a velocity W in an ideal gas, a shock wave not yet having formed. Then if $\pi \equiv p/p_0$, where p_0 is the original gas pressure and $p(W)$ the pressure at the piston

$$\frac{W}{a_0} = (\lambda - 1) \left[\pi^{\frac{1}{\lambda+1}} - 1 \right]. \quad (1)$$

Let the piston continue to move with velocity W . The ultimate position will be one in which a steady shock precedes the piston, conditions being steady with velocity W' and pressure p' , say, between the piston and shock.

If $\pi' \equiv p'/p_0$, then

$$\frac{W}{a_0} = \frac{(\lambda - 1)(\pi' - 1)}{\sqrt{(\lambda + 1)(\lambda \pi' + 1)}}. \quad (2)$$

The values of W given by (1) and (2) are clearly not in general equal.

To decide which is the greater, consider the two functions

$$y = x^{\frac{1}{\lambda+1}} - 1, \quad (3)$$

$$y' = \frac{x-1}{\sqrt{(\lambda+1)(\lambda x+1)}}. \quad (4)$$

Evidently, since $\lambda > 1$, $y' > y$ for sufficiently large x . On the other hand, when $x-1 < 1$, if $\mu \equiv 1/(\lambda+1)$,

$$y = \mu(x-1) - \frac{\mu(1-\mu)}{12}(x-1)^2 + \frac{\mu(1-\mu)(2-\mu)}{13}(x-1)^3 - \dots \quad (5)$$

$$y' = \mu(x-1) - \frac{\mu(1-\mu)}{12}(x-1)^2 + \frac{3\mu(1-\mu)^2}{412}(x-1)^3 - \dots, \quad (6)$$

so that, near $x = 1$, $y' < y$ if

$$\frac{3(1-\mu)}{4} < \frac{2-\mu}{3},$$

i.e. if $\mu > \frac{1}{5}$, $\lambda < 4$, $y' > y$.

Provided, then, that $y' > y$ for $\pi < \pi_c$, there will be a value π_c , such that $y' < y$ for all $\pi > \pi_c$, while we may conclude (though by something short of a rigorous proof) that $y' > y$ for all $\pi < \pi_c$. Similarly, if $y' < y$ for both small and large π and therefore presumably for all π ; if $y' = y$, the same conclusion applies, from consideration of the fourth-order terms in (5,6).

But γ and γ' are both monotonically increasing functions of x .

Reverting then to equations (1) and (2), we find that (a) if $\gamma \leq 5/3$, then $\pi' < \pi$, the difference between π' and π increasing with W ; while (b) if $\gamma > 5/3$, π' is again less than π provided W exceeds a certain critical value, $W_c(\gamma)$ say; but (c) if $W < W_c$, then $\pi' > \pi$. Cases (a) and (b) imply a reflected rarefaction, case (c) a reflected compression. In the very special case $W = W_c$, there is apparently no reflexion, and the shock develops without reacting upon the parent wave; but this case cannot arise in true ideal gases, for which γ is always $\leq 5/3$.

The variation of W_c with γ is indicated by Table 6.25:1

Table 6.25:1

γ	λ	π_c	W_c/a_0
5/3	4	1	0
2	3	2.73	0.570
3	2	20.5	1.728
5	3/2	239.8	3.978
∞	1	∞	∞

§6.26 Independent variable v_i

In terms of the independent variable $\varphi \equiv v_i/v_{i_0}$, the shock-wave equations become

$$\pi \equiv p_i/p_{i_0} = \frac{\lambda - \varphi}{\lambda \varphi - 1} \quad (1)$$

$$\frac{E_i}{E_{i_0}} = \frac{T_i}{T_{i_0}} = \frac{a_i^2}{a_{i_0}^2} = \varphi \cdot \frac{\lambda - \varphi}{\lambda \varphi - 1} \quad (2)$$

$$\frac{D}{a_{i_0}} = \sqrt{\frac{\lambda - 1}{\lambda \varphi - 1}} \quad (3)$$

$$\frac{W_i}{a_{i_0}} = (1 - \varphi) \sqrt{\frac{\lambda - 1}{\lambda \varphi - 1}} \quad (4)$$

$$\frac{D - W_i}{a_{i_0}} = \varphi \sqrt{\frac{\lambda - 1}{\lambda \varphi - 1}} \quad (5)$$

$$\frac{u_{i_0}^2 - u_i^2}{a_{i_0}^2} = \frac{(\lambda - 1)(1 - \varphi^2)}{\lambda \varphi - 1} \quad (6)$$

$$\frac{S_i - S_{i_0}}{c_v} = \gamma \ln \varphi + \ln \frac{\lambda - \varphi}{\lambda \varphi - 1} \quad (7)$$

§6.27 Independent variable D

In some respects D , being the most easily measured of the large-scale shock-wave characteristics, is the most convenient independent variable.

In terms of $\delta \equiv D^2/a_0^2$, the principal equations become:-

$$\pi \equiv p_1/p_0 = \frac{(\lambda+1)\delta-1}{\lambda} \quad (1)$$

$$v_1/v_0 = \frac{\delta+\lambda-1}{\lambda\delta} \quad (2)$$

$$\frac{E_1}{E_0} = \frac{T_1}{T_0} = \frac{a_1^2}{a_0^2} = \frac{[(\lambda+1)\delta-1][\delta+\lambda-1]}{\lambda^2\delta} \quad (3)$$

$$\frac{W_1}{a_0} = \frac{\lambda-1}{\lambda} \left(\sqrt{\delta} - \frac{1}{\sqrt{\delta}} \right). \quad (4)$$

§6.28 Independent variable W_1 , E_1 , a_1 , or T_1

The expressions in terms of W_1 , E_1 , a_1 , or T_1 , though easily derived, are less simple in form, and are probably of no great practical advantage.

§6.29 Numerical values for $\gamma = 1.4$

The relatively simple form of the equations of §§6.2 - 6.28 make numerical evaluation straightforward. Table 6.29:1 is therefore added merely as an illustration.

It will be seen that the post-shock flow becomes supersonic for $\pi > \pi_c \sim 4.8$ in agreement with Table 6.21:1. The narrow limits of variation of $(W_1+a_1)/D$ are rather remarkable: the maximum at $\pi \sim 10$ is authentic, as can be verified algebraically.

Table 6.29:1

Large scale properties of shock waves in an ideal gas with $\gamma = 1.4$

$\frac{P_1}{P_0} \equiv \pi$	ρ_1/ρ_0	T_1/T_0	a_1/a_0	W_1/a_0	D/a_0	W_1/a_1	D/a_1	$\frac{W_1 + a_1}{D}$	$\frac{S_1 - S_0}{c_v}$
1	1	1	1	0	1	0	1	1	0
2	1.625	1.23	1.11	0.525	1.36	0.473	1.23	1.20	0.012
3	2.11	1.42	1.19	0.867	1.65	0.738	1.39	1.25	0.053
4	2.50	1.60	1.27	1.135	1.89	0.894	1.49	1.27	0.103
5	2.82	1.77	1.33	1.36	2.11	1.02	1.59	1.275	0.159
10	3.81	2.62	1.62	2.18	2.95	1.35	1.82	1.29	0.430
20	4.65	4.30	2.07	3.27	4.16	1.56	2.01	1.25	0.845
50	5.37	9.30	3.05	5.33	6.56	1.75	2.15	1.28	1.56
100	5.67	17.6	4.20	7.62	9.27	1.81	2.21	1.275	2.18
200	5.83	34.3	5.86	10.83	13.11	1.85	2.24	1.275	2.83
500	5.93	84.2	9.18	17.2	20.7	1.87	2.25	1.275	3.73
1000	5.965	168	12.95	24.4	29.3	1.895	2.265	1.275	4.41
∞	6	∞	∞	∞	∞	$\frac{1.890}{11}$	2.268	1.275	∞
						$(5/\sqrt{7})$	$(6/\sqrt{7})$	$(\frac{5+\sqrt{7}}{6})$	

§6.3 Shock waves in real gases : air

Since even the most intense shock waves involve only a moderate compression, the ideal gas equation

$$pv = nRT \quad (1)$$

may be applied without significant error to real gases, provided v has normal values, and T is well above the critical temperature. The assumptions of § 6.2 become inadequate, however, because even at low temperatures c_v rises rapidly with T , and at higher temperatures dissociation and finally ionisation become important, and the internal energy depends on density. The number n in (1) likewise ceases to be constant.

For completeness, we summarise in this section the results of various calculations for air at NTP, in which account is taken of the above factors to a greater or less degree.

[5]

a) Becker: Dissociation and ionisation ignored. An experimental equation for \bar{c}_v due to Pier and Siegel leads to

$$\frac{1}{n} (E - E_{273}) = 4.78 + 0.45 \times 10^{-3} T \text{ cal/mol.}^{\circ}\text{K} , \quad (2)$$

when $T \neq 3000^{\circ}\text{K}$.

[53]

b) Burkhardt: As above, but allowance made for dissociation and ionisation. Pressure range up to 4000 atm.

[47]

c) Davies: As in (b).

[9]

d) Bethe: As in (b).

[60]

e) Fuchs, Kynch and Peierls: As in (b), but extended up to 5×10^6 atm., and extrapolated from there to infinity.

The RH-curves, graphed for convenience on a (p, ρ) -diagram, are collected in Fig. 6.3:1. Considering the nature of the problem, they show very good agreement, and the general behaviour is probably not in doubt. A mean curve has been superimposed, and the corresponding shock properties summarised in Fig. 6.3:2. Up to $p \sim 600$ atm., Becker's

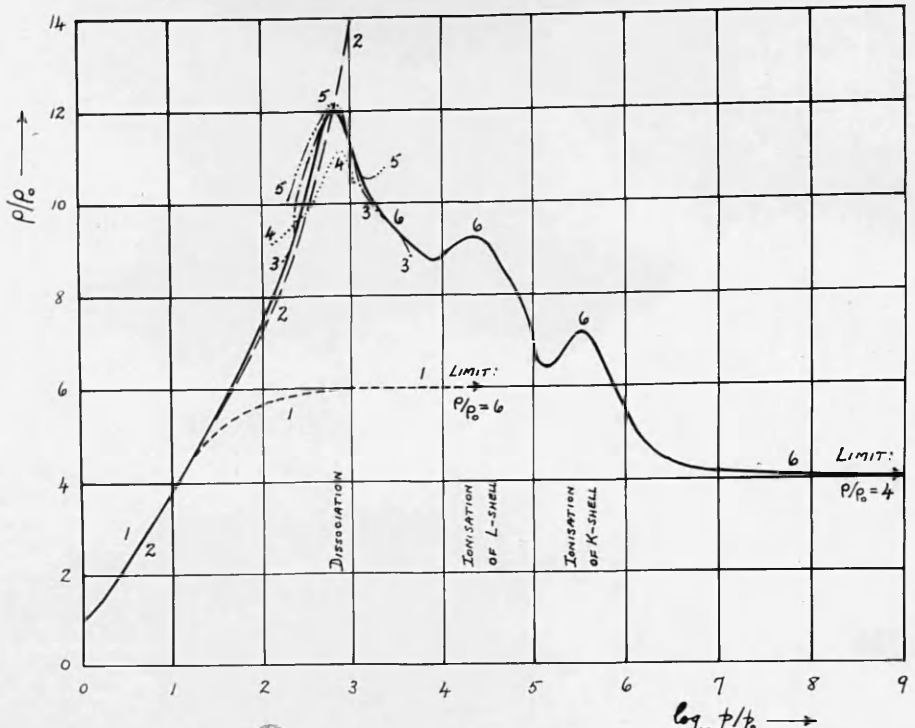
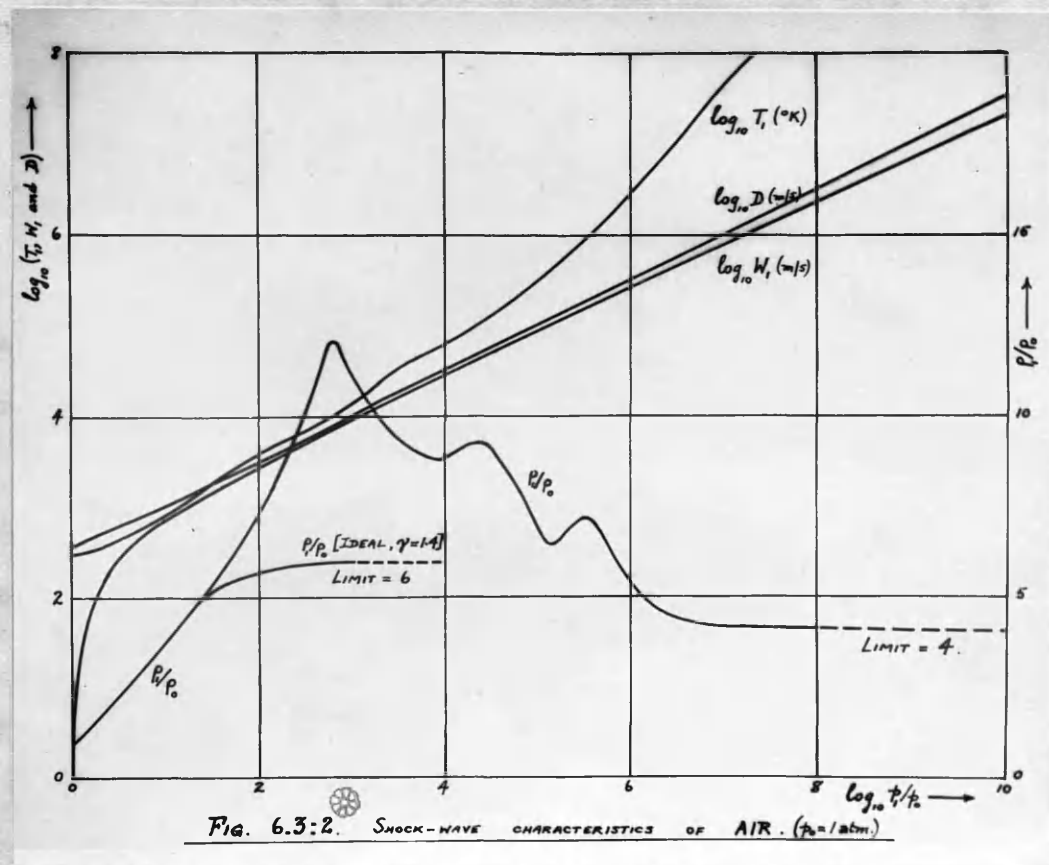


FIG. 6.3:1 SHOCK WAVES IN AIR. 1. IDEAL, $\gamma = 1.4$, 2. Becker,
 3. Burkhardt, 4 Davies, 5. Bethe, 6. Fuchs,
 Lynch and Peierls. ————— Fairied mean curve.

calculations are useful, although T_1 is becoming seriously overestimated, due to neglect of dissociation. Between 500 and 2000 atm., dissociation becomes paramount, and has the remarkable effect of causing the density to decrease with rising pressure. The slope of the curve regains its normal positive sign at $p_1 \sim 10,000$ atm., but is again reversed by ionisation of the L-shell and once more by ionisation of the K-shell. Above $p_1 \sim 10^6$ atm., the curve approaches $P = 4P_0$ asymptotically.

Although dissociation and ionisation lower the shock temperatures, these still rise to a very high level when P_1 exceeds 500 atm.



§6.4 Shock waves in a fluid obeying the Tamman equation of state : ethyl ether

The behaviour of gases over a range of density in which the ideal gas equation becomes inaccurate, can often be closely described by the van der Waals equation

$$(p+a)(v-b) = nRT, \quad (1)$$

where a and b are, in the first place at least, constants for the particular gas in question. A similar equation [58]

$$(p+a)(v-b) = KT, \quad (2)$$

with constant a , b , K , represents the behaviour of certain liquids, e.g. ethyl ether and carbon tetrachloride, up to relatively high pressures.

The solution for these cases is therefore of interest, and follows easily (Becker): ^[5] Here $c_p - c_v = T \frac{\partial p}{\partial T \partial v} = K$, and

$$dE = c_v dT + \left(T \frac{\partial p}{\partial T} - p \right) dv = c_v dT + adv, \quad (3)$$

so that

$$E = c_v T + av + \text{const.}, \quad (4)$$

if c_v is regarded as constant.

The RH-equation is then

$$\left[\frac{c_v}{K} (p+a)(v-b) + av \right]_o' = \frac{1}{2} (p_i + p_o)(v_o - v_i). \quad (5)$$

If we write $P \equiv p+a$, $V \equiv v-b$, (5) reduces to

$$\frac{c_v}{K} (P_i V_i - P_o V_o) = \frac{1}{2} (P_i + P_o)(V_o - V_i), \quad (6)$$

whereupon, as before:

$$\frac{V_i}{V_o} = \frac{\Pi + \Lambda}{\Lambda \Pi + 1}, \quad (7)$$

where $\Pi \equiv P_i/P_o$, $\Lambda \equiv (\Gamma+1)/(\Gamma-1) = 2 \frac{c_v}{K} + 1 = 2 \frac{c_b}{K} - 1$,
 $\Gamma \equiv 1 + K/c_v$.

Moreover, the adiabatics are

$$PV^{\gamma} = \text{const.}, \quad (8)$$

so that

$$a = \nu \sqrt{\frac{rP}{V}}. \quad (9)$$

Hence, corresponding to 6.2(2), we have

$$\frac{T_1}{T_0} = \left(\frac{\nu_0 V_1}{\nu_1 V_0} \right)^2 \cdot \frac{a_1^2}{a_0^2} = \pi \cdot \frac{\pi + 1}{\lambda \pi + 1}. \quad (10)$$

Also, by 6(5),

$$\frac{D}{a_0} = \sqrt{\frac{\lambda \pi + 1}{\lambda + 1}}, \quad (11)$$

$$\frac{W_1}{a_0} = \frac{(\lambda - 1)(\pi - 1)}{\sqrt{(\lambda + 1)(\lambda \pi + 1)}}, \quad (12)$$

and equations formally identical with 6.2(5-8) follow easily.

The Tamman equation (2) applies to ethyl ether up to a few thousand atmospheres, and the shock wave properties were calculated by Becker using the above theory over a much wider pressure range. His results are corrected and summarised in Table 6.4:1. At the higher pressures they must be considered as qualitative only.

Table 6.4:1/

Table 6.4:1

Shock waves in ethyl ether with $p_0 = 1 \text{ atm.}$, $T_0 = 273^\circ\text{K}$.

In equation (2), $a = 2792 \text{ atm.}$, $b = 0.94 \text{ cm.}^3/\text{g.}$,

$K = 0.1001 \text{ cal./g.}^\circ\text{K}$; also mean $c_p = 0.564 \text{ cal./g.}^\circ\text{K}$,

so that $\Gamma = 1.215$, $A = 10.28$

$p,$ atm.	$v,$ $\text{cm.}^3/\text{g.}$	$T, - 273$ °	$T_{ad}, - 273$ °	$W,$ m/s.	D m/s.	$a,$ m/s.
1	1.36	0	0	0	1230	1230
100	1.35	1.7	1.5	10.8	1260	
1,000	1.27	16	15.1	96.5	1420	1520
10,000	1.07	114	84	539	2540	
20,000	1.03	211	123	820	3340	5600
60,000	1.00	593	200	1470	5590	
100,000	0.995	974	244	1920	7140	15000

The flow behind even intense shocks is markedly subsonic.

6.41 Shock waves in water

Water does not follow the Tamman equation, and no equation of state of simple algebraic form seems to be available. Extensive (p, v, T) -data have, however, been measured and tabulated by Bridgeman, and the shock-wave properties may be evaluated from these by numerical methods. For this purpose, we use the general thermodynamic relation [7, 8]

$$dE = (c_p - p \frac{\partial v}{\partial T}) dT - (T \frac{\partial v}{\partial T} - p \frac{\partial v}{\partial p}) dp. \quad (1)$$

Since $c_p(T)$ is known at $p = p_0 = 1 \text{ atm.}$, we integrate along the following path:

a) $p = p_0, \quad T = T_0 \text{ to } T = T_1,$

b) $T = T_1, \quad p = p_0 \text{ to } p = p_1.$

This gives

$$E_i - E_o = \int_{T_o}^{T_i} (c_p)_{p=p_o} dT + \int_{p_o}^{p_i} (v - T_i \frac{\partial v}{\partial T})_{T=T_i} dp - (p_i v_i - p_o v_o), \quad (2)$$

so that the RH- equation is

$$\int c_p dT + \int (v - T_i \frac{\partial v}{\partial T}) dp = \frac{1}{2} (p_i - p_o)(v_o + v_i). \quad (3)$$

This can be solved numerically with the aid of Bridgman's tables, which [53]
extend to 80°C and 12,000 Kg./cm.². Results obtained by Döring in this
way are shown in Table 6.41:1, which also includes an extrapolation due to
[53]
Burkhardt.

Table 6.41:1 [53]

Shock waves in water. $p_o = 1 \text{ atm.}$, $T_o = 288^\circ\text{K}$, $v_o = 1.007 \text{ cm.}^3/\text{g.}$
Supercooling assumed above $p_i = 27,000 \text{ Kg./cm.}^2$.

p_i Kg/cm ²	$T_i - T_o$ °	$v_o - v_i$ cm. ³ /g.	W_i m/s.	D m/s.
1.03	0	0	0	1440
1,000	1.57	0.0387	62	1592
2,000	4.04	0.0683	116	1700
5,000	13.9	0.1272	250	1963
10,000	35.3	0.1818	423	2325
12,000	44.9	0.1964	483	2461
18,000	68	0.221	630	2850
30,000	112	0.243	850	3500
56,700	212	0.261	1220	4630
86,900	340	0.281	1560	5510
97,600	405	0.291	1690	5740

A curious situation arises when \dot{p} exceeds 27,000 Kg./cm.². Beyond this pressure, $T(\dot{p})$ lies below the freezing-point at \dot{p}_f , as measured by [19] Bridgman. In a state of equilibrium, therefore, the water behind such a shock would be partially solidified. Döring has extended his calculations to cover this possibility. The wave velocities are not greatly different from those of Table 6.41:1, which presume supercooling. In any case, it is doubtful whether there is time in practice for freezing to take place, though certain observations of Schardin on water, and also on carbon tetrachloride, appear to confirm the effect. [146]

Independent calculations by Kirkwood, using the same data and procedure, agree very closely with those of Table 6.41:1. More recently, a set of [131] calculations by Penney and Dasgupta up to 50,000 Kg./cm.² have been published, and are shown for comparison in Table 6.41:2. dE was integrated along a slightly different path from that used by Döring and Kirkwood, namely,

- the adiabatic from (v_0, \dot{p}_0) to $\dot{p} = \dot{p}_f$,
- thence to (v, \dot{p}_f) at constant \dot{p} .

This method is advantageous since the adiabatics can be closely represented by equations of the form

$$(\dot{p} + a)v^n = \text{const.}, \quad (4)$$

where $n \sim 7$. Penney's results differ significantly from Döring's only in the range of extrapolation ($\dot{p} > 12,000$ Kg./cm.²).

Table 6.41:2/

[31]
Table 6.41:2

Shock waves in water. $P_0 = 1 \text{ atm.}$, $T_0 = 293^\circ\text{K.}$

P , Kg./cm. ²	$T, - T_0$ °	$T_{ad} - T_0$ °	$v_0 - v$, cm. ³ /g.	W , m/s.	a , m/s.	D , m/s.
1,000	1.84	1.81	0.0389	62	1655	1591
4,000	11.1	10.2	0.1101	208	2106	1891
6,000	18.2	16.5	0.1403	288	2347	2052
10,000	34.5	29.7	0.1822	423	2750	2324
20,000	84	65	0.240	688	3517	2850
30,000	172	135	0.277	893	4109	3266
50,000	380	305	0.317	1229	5040	3493

§6.42 Shock-front thickness in liquids

It was shown in §5, by an approximate argument, that the region of pressure rise in a gaseous or liquid shock was extremely thin; and this conclusion was later verified in detail for gases (§5.5). The use of the Tamman equation 6.4(2) allows the analysis to be extended in an obvious way to liquids, though here, because of the relatively greater importance of viscosity, equation 5.5(1) is more suitable than 5.5(2). The following results, due to Becker,^[5] confirm that the shock-front thickness (ℓ) in ethyl ether is negligible; and this will evidently remain true for all liquids of normal viscosity

P , (atm.)	100	1,000	10,000	100,000
$10^7 \times \ell$ (cm.)	52	5.3	0.65	0.14

The remarks at the end of §5.5 are relevant here also.

§6.5 Shock waves in solids

The theoretical study of shock waves in solids is complicated not only by the difficulty of formulating a reliable equation of state, but also by

18

the existence at moderate pressures of a finite resistance to shear and the consequent appearance of distortional as well as compressional waves. Below the yield point, in fact, the state of the solid, even when this is isotropic, cannot be described in terms of two variables only such as (v, T) . On the other hand, the pressures prevailing in practice in shock waves through solids are frequently so high as to justify neglect of the yield stress. In effect we then regard the solid as a fluid.

Even when this is not legitimate, an approximation can be made, at least in the case of one-dimensional waves, by means of the following argument. Let e_1, e_2, e_3 be the small extensions, parallel to rectangular axes $O(x, y, z)$, of an element in the (isotropic) solid, and X the normal traction over the yz -plane through that element. Then

$$X - p_0 = \lambda(e_1 + e_2 + e_3) + 2\mu e_1, \quad \text{etc.} \quad (1)$$

where p_0 is the initial hydrostatic pressure, and λ, μ are Lame's coefficients. If motion occurs only parallel to Ox , the tangential tractions, together with e_2, e_3 , are zero, and so

$$(X - p_0, Y - p_0, Z - p_0) = (\lambda + 2\mu, \lambda, \lambda)e_1. \quad (2)$$

Accordingly, since then $e_1 = (v_0 - v)/v_0$, where v_0 and v are the specific volumes before and after straining,

$$X - p_0 = \frac{v_0 - v}{v_0} (\lambda + 2\mu). \quad (3)$$

On the other hand, for simple compression under hydrostatic pressure P to the same final specific volume v , $e_1 = e_2 = e_3 = (v_0 - v)/3v_0$, so that

$$P - p_0 = \frac{v_0 - v}{v_0} \left(\lambda + \frac{2\mu}{3} \right). \quad (4)$$

Thus
$$\frac{P - p_0}{X - p_0} = \frac{3\lambda + 2\mu}{3\lambda + 6\mu} = \frac{1 + \sigma}{3(1 - \sigma)} \sim \begin{cases} 5/9 & \text{if } \sigma = \frac{1}{4} \\ 2/3 & \text{if } \sigma = \frac{1}{3} \\ 1 & \text{if } \sigma = \frac{1}{2} \end{cases}, \quad (5)$$

$(\sigma \equiv \text{Poisson's ratio}).$

So far, therefore, as the total volume change is concerned, the rise in axial stress behind a mild plane shock wave in an isotropic solid may be identified with a hydrostatic pressure rise $(1+\sigma)/3(1-\sigma)$ times as great. In other words, since ρ_0 is negligible, and the quantity denoted by ρ_1 in the fundamental theory corresponds to the axial stress X , we may regard the compression $v_0 - v_1$ as approximately equal to that which would be produced, under otherwise similar circumstances, by a hydrostatic pressure $P \equiv \rho_1(1+\sigma)/3(1-\sigma)$. Since $0 < \sigma < \frac{1}{2}$, this equivalent pressure P lies between $\frac{1}{3}\rho_1$ and ρ_1 . It may be expected to approach most closely to ρ_1 in the case of soft materials like lead, and to be smallest for metals such as copper or iron.

In fact, of course, the stress is not isotropic under the conditions envisaged, and cannot be fully described by a hydrostatic pressure P : the solid does not satisfy a two-parameter equation of state. The above treatment is therefore a crude one. However, we shall not be further concerned with it, since the pressures of greatest interest are far above the normal yield point, and may be regarded as hydrostatic.

§6.51 The Gruneisen-Debye equation of state

Shock wave pressures in solids may easily rise, in consequence of the small compressibility, to the level of 10^5 atm. or higher. Information regarding the pressure-volume-temperature relations at this level is at present far from complete. Although extensive studies on compressibility [6] have been made for many solids up to 10-12,000 atm., and for a smaller number up to 50,000 and 100,000 atm., these provide as a rule only a single isotherm at $T_0 = 288^\circ\text{K}$; but for a complete discussion a series of such isotherms would be necessary. However, it may be expected that even

intense shocks will involve only moderate temperature changes, at least in the less compressible solids, so that the prospect arises of extrapolation from a single isotherm by means of a suitable theoretical form of equation of state.

For this purpose, the Debye model should serve as a reasonable approximation, according to which the internal energy $E(v, T)$ is given by

$$E = F(v) + 3nRT \mathcal{D}[\Theta(v)/T], \quad (1)$$

where $F(v)$ is the potential energy referred to 0K and zero pressure, $\Theta(v)$ is the Debye characteristic temperature, and

$$\mathcal{D}(x) \equiv \frac{3}{x^3} \int_0^x \frac{\xi^3 d\xi}{e^{\xi} - 1} \quad (2)$$

is Debye's transcendent.

From (1), writing x for $\Theta(v)/T$, we have

$$\begin{aligned} C_v &= \frac{\partial E}{\partial T} = 3nR \left[\mathcal{D} - x \mathcal{D}' \right] \\ &= 3nR \left[4\mathcal{D} - \frac{3x}{e^x - 1} \right]. \end{aligned} \quad (3)$$

The corresponding equation of state is

$$\dot{P} = -F'(v) - 3nRT \frac{\Theta'(v)}{\Theta(v)} \mathcal{D}[\Theta(v)/T]. \quad (4)$$

When x is small,

$$\mathcal{D}(x) = 1 - \frac{3x}{8} + \frac{x^2}{20} + O(x^4), \quad (5)$$

$$\frac{C_v}{n} = 5.955 \left[1 - \frac{x^2}{20} + O(x^4) \right]. \quad (6)$$

Table 6.51:1 indicates the course of $\mathcal{D}(x)$ and c_v/n , with $R = 1.987$ cal./mol. $^{\circ}$ K.

[48]
Table 6.51:1

$\frac{\Theta}{T} \equiv x$	$\mathcal{D}(x)$	c_v/n (cal./mol. $^{\circ}$ K)	$\frac{\Theta}{T} \equiv x$	$\mathcal{D}(x)$	c_v/n (cal./mol. $^{\circ}$ K)
0.0	1.000	5.955	1.0	0.67	5.67
0.1	0.965	5.95	2.0	0.44	4.92
0.2	0.933	5.94	3.0	0.28	3.95
0.4	0.86	5.91	4.0	0.18	3.00
0.6	0.79	5.85	5.0	0.12	2.20
0.8	0.73	5.77			

Typical values of Θ at 1 atmosphere are shown in Table 6.51:2

[49]
Table 6.51:2

Solid	Θ ($^{\circ}$ K)	Solid	Θ ($^{\circ}$ K)
Fe	453	Ag	215
Al	398	Pb	88
Cu	315	NaCl	281
Zn	235	KCl	230

It is clear that, at normal temperatures and 1 atm. pressure, x varies from 0.3 (Pb) to 1.6 (Fe) but is usually of the order of 1. Over the range $0 < x < 1.6$, \mathcal{D} is varying quite rapidly. The variation in $c_v/n = 3R \frac{\partial}{\partial T}(\mathcal{D})$ for $T > 273^{\circ}$ K, is, however, much smaller, not more than 10% even for iron, and generally well below this for the other materials. Despite the pronounced variation in \mathcal{D} , therefore, it is a fair approximation to regard $\mathcal{D}T$ as linear in T , with slope unity, i.e. to assume

$$\beta_n R \partial T = A(v) + \beta_n R T, \quad (7)$$

where A is independent of temperature. Then (4) becomes

$$pv = f(v) - \beta_n R T v \frac{\Theta'(v)}{\Theta(v)}, \quad (8)$$

the T -independent terms being collected in $f(v)$. The approximate constancy of ∂T at high pressures depends on the further assumption that $\Theta(v)$ does not become too great. It is clear from (4), according to which

$$c_v \frac{\Theta'}{\Theta} = - \frac{\partial p}{\partial T} = - \frac{3\alpha}{K}, \quad (9)$$

where α is the coefficient of linear expansion and K the compressibility, that $\Theta' < 0$, so that Θ rises as the solid is compressed. The probable extent of this rise may be gauged from (9), taking into account the order of magnitude of $3\alpha v_0 / K c_v$ which for the substances listed above varies only between 1.8 and 2.8 at $288^\circ K$ and 1 atm. Thus,

$$\frac{d\Theta}{\Theta} \sim - 2 \frac{dv}{v}.$$

But under isothermal conditions $dv/v \sim 0.2$ at 10^5 atm. for NaCl and ~ 0.05 for Cu and Fe, the other materials showing intermediate values. Hence Θ will probably not increase by more than about 40% for NaCl, or more than 10% for Cu or Fe, at 10^5 atm. and $288^\circ K$. This increase is not sufficient to invalidate the argument, and in a shock wave of corresponding pressure the volume decrease must be rather less than the above, and the temperature greater than $288^\circ K$, so that the effect upon the approximate linearity of ∂T should on the whole be smaller than we have allowed for here.

Equation (8) is of the general form:

$$pv = f(v) + g(v).T , \quad (10)$$

where $f(v)$ and $g(v)$ are as yet undetermined. If, indeed, more than one isotherm have been extensively studied, the equation of state may be tested, and the functions f and g evaluated. Thus, if $p_1(v)$, $p_2(v)$ and $p_3(v)$ are the isotherms at T_1 , T_2 and T_3 , we must have [6]

$$\frac{p_1 - p_2}{p_2 - p_3} = \frac{T_1 - T_2}{T_2 - T_3} = \text{const.} , \quad (11)$$

and then [6]

$$\frac{1}{v} f(v) = \frac{T_1 p_2 - T_2 p_1}{T_1 - T_2} , \quad (12)$$

$$\frac{1}{v} g(v) = \frac{p_1 - p_2}{T_1 - T_2} \quad (13)$$

However, if only one isotherm is known, assumptions must be made concerning the form of f or g . In view of the comparative constancy of $v\alpha'/\alpha$ among various solids, the most reasonable procedure is to take g as constant. This is equivalent to assuming that $3\alpha/\kappa$ is independent of volume, and since both α and κ must decrease with v the assumption is rather plausible. The equation of state may then be written

$$pv = f(v) + KT , \quad (14)$$

or more conveniently, since f is disposable,

$$pv = f(v) + K(T - T_0) . \quad (15)$$

Before proceeding to apply this equation, we note that in the general case given by (1) and (4),

$$E = F(v) - \frac{\Theta}{\Theta}, (\dot{p} + F'), \quad (16)$$

and the RH-equation therefore becomes:

$$\begin{aligned} F(v_i) - F(v_o) + [\dot{p}_o + F'(v_o)] \frac{\Theta(v_o)}{\Theta'(v_o)} - [\dot{p}_i + F'(v_i)] \frac{\Theta(v_i)}{\Theta'(v_i)} \\ = \frac{1}{2} (\dot{p}_i + \dot{p}_o)(v_o - v_i). \end{aligned} \quad (17)$$

§6.5II Shock waves in fluids satisfying a simplified Grüneisen-Debye equation of state

As we have seen, over a moderate range of temperature the Grüneisen-Debye equation of state for crystalline solids may be taken in the form:

$$\dot{p}v = K(T-T_o) + f(v), \quad (1)$$

where K is a constant, to be evaluated in terms of the specific volume (v_o), linear expansion coefficient (α_o) and compressibility (κ_o) under normal atmospheric conditions ($\dot{p} = 1$ atm., $v = v_o$, $T = T_o$) by

$$K = v_o \left(\frac{\partial \dot{p}}{\partial T} \right)_o = \frac{3v_o \alpha_o}{\kappa_o}. \quad (2)$$

If (1) applies, $f(v)$ may be determined by measurements of specific volume over the required range of pressure at any convenient single temperature, say at T_o . Measurements of this kind have been made for a large number of solids up to pressures of 10-12,000 atm., and for a smaller number up to 50,000 and 100,000 atm. It is therefore of value to derive the RH-equation corresponding to (1).

From the general thermodynamic relation

$$dE = C_v dT + \left(T \frac{\partial p}{\partial T} - p \right) dv ,$$

we have, using (1),

$$dE = C_v dT + [KT_o - f(v)] \frac{dv}{v} , \quad (3)$$

whence $E = \frac{C_v}{K} [pv - f(v)] + KT_o \ln v - \int f(v) \frac{dv}{v} + \text{const.} \quad (4)$

The RH equation, relating p , to v , is therefore

$$\frac{C_v}{K} [pv - f(v)] - KT_o \ln \frac{v_o}{v_i} + \int_{v_i}^{v_o} f(v) \frac{dv}{v} = \frac{1}{2} (p_i + p_o)(v_o - v_i) , \quad (5)$$

which is at once explicitly soluble for p . $f(v)$ is obtained from the isotherm at T_o , viz.

$$p = f(v)/v . \quad (6)$$

$\int_{v_o}^{v_i} f(v) dv/v$ may then in general be evaluated numerically or graphically, or an empirical function suitable for extrapolation and analytical integration may be fitted to $f(v)/v$. Thus, for example, the isotherms for many solids can be closely represented over the experimental range by the form:

$$v = v_o \cdot \frac{p - p_o + B}{A(p - p_o) + B} , \quad (7)$$

where A, B are constants. Then

$$f(v)/v = p_o + \frac{B(v_o - v)}{Av - v_o} , \quad (8)$$

the equation of state is accordingly :

$$(p - p_0)v = K(T - T_0) + \frac{Bv(v_o - v)}{Av - v_o}, \quad (9)$$

and the RH-equation :

$$\begin{aligned} \left[\frac{C_v}{K} - \frac{1}{2}(x-1) \right] (p - p_0) &= \\ &= \frac{KT_o}{v_o} x \ln x - \frac{(A-1)B}{A^2} x \ln \frac{(A-1)x}{A-x} \\ &\quad + \left[\frac{C_v B}{K(A-x)} + \frac{B}{A} \right] (x-1), \end{aligned} \quad (10)$$

where $x \equiv v_o/v$.

Also

$$K = \frac{3B\alpha_o v_o}{A-1}. \quad (11)$$

§6.52 The Born-Bradburn Equation of State

The Debye theory rests upon an approximation involved in replacing the natural frequencies of the atomic lattice by a continuous spectrum. Attempts have been made by Born and co-workers to refine the theory by considering the actual modes of vibration. In particular, Born and [2] [5] Bradburn and Bradburn have recently succeeded in developing an equation of state for cubic crystals, based upon the assumption of interatomic attractive and repulsive forces proportional respectively to inverse powers (m, n) of the interatomic distance, as in the treatment by [64] Lennard-Jones and others of the virial coefficients of gases. Bradburn's equation, which is strictly applicable only above the Debye temperature, takes the form

$$pv = F(\xi) + nRG(\xi) \cdot T, \quad (1)$$

where

$$\xi \equiv (v/v_{\infty})^{-\frac{n-m}{3}} - 1, \quad (2)$$

v_{∞} being the specific volume at zero pressure and temperature. $F(\xi)$ and $G(\xi)$ are defined in terms of the sublimation energy (Λ), together with the force-law exponents (m, n) and certain lattice sums (S_q°) which have been tabulated by Born and Misra. [13] In fact,

$$F(\xi) = \Lambda \frac{mn}{3(n-m)} \left\{ \left(\frac{\nu}{v_{\infty}} \right)^{-\frac{n}{3}} - \left(\frac{\nu}{v_{\infty}} \right)^{-\frac{m}{3}} \right\}, \quad (3)$$

$$G(\xi) = C + B \cdot \frac{1+\xi}{1+K\xi} , \quad (4)$$

where

$$A \equiv \frac{mn}{6(n-m)} \cdot \frac{(S_m^\circ)^{\frac{n}{n-m}}}{(S_n^\circ)^{\frac{m}{n-m}}} , \quad (5)$$

$$B \equiv \frac{Ks}{2} , \quad C \equiv \frac{m}{2} + 1 , \quad (6)$$

and

$$K^{-1} \equiv 1 - \frac{(m-1) S_n^\circ S_{m+2}^\circ}{(n-1) S_m^\circ S_{m+2}^\circ} . \quad (7)$$

From our remarks on the Debye equation it may be expected that $G(\xi)$ will vary little with ξ . To confirm this, we have calculated $G(\xi)$ for the following elements: Fe, Ni, Al, Cu, Zn, Cd, C, Pb, Sn, Na, using the values of m, n deduced by Fürth, [61] and extrapolating S_q°, K where necessary from the tabulated data of Born and Misra. The conclusion is that G will vary by less than 10% provided ν varies by less than

30% for Fe, Ni, Al, Cu, C

15% for Zn.

In the case of Pb, Sn and Na, the permissible variation of v is very much greater, $G(\epsilon)$ being effectively constant. For Cd, G varies quite rapidly, but this metal is of less practical interest. These calculations are probably of small fundamental significance, since the values of m, n are ill-defined; but they indicate that G may be regarded as constant without serious error over a range of v corresponding to extreme pressure changes (several hundred thousand atmospheres).

Bradburn's equation then takes the form:

$$\rho v = \frac{a}{v^b} - \frac{c}{v^d} + eT \quad (8)$$

where a, b, c, d, e are constants defined in terms of m, n and A . It would now be possible to evaluate these constants, as Fürth has done, by comparison with the experimental data at low temperatures and pressures. Since, however, we propose to apply equation (8) specifically at high pressures, it seems preferable to depart at this point from the strictly theoretical approach, and (using (8) merely as a guide) to determine a, b, c, d, e by reference chiefly to such information as is available regarding behaviour in the high pressure region. By doing so, of course, we relinquish immediate contact with the dynamical theory on which (8) is based. On the other hand, the inverse power laws of force can hardly be regarded as more than a convenient approximation, so that the exponents m, n have in any case no fundamental significance; and the procedure suggested ensures at least that our equation of state will approximate to the truth in the region of greatest immediate interest. First, however, we may simplify the position, by taking advantage of Fürth's conclusion [61] that $m \sim 3$ to set $d = 1$. Then (8) becomes

$$\frac{\rho}{P} = a\rho^b - c\rho + eT. \quad (9)$$

e is determined at once by the equation

$$e = -v \frac{\partial p}{\partial T} = \frac{3\alpha_0 v_0}{\kappa_0}. \quad (10)$$

It is important to notice here that the equation has not been made to fit α_0 and κ_0 separately, but only their ratio. Subsequent agreement with either α_0 or κ_0 may therefore be taken as confirmation of the reliability of the equation. a, b, c are now to be determined by fitting (9) for example to three points on an isotherm. It is natural to place one of these points at atmospheric pressure, and another at the highest experimental pressure; the third may be at any convenient intermediate pressure, but it is particularly advantageous to choose this third pressure so that the corresponding density is a geometric mean to the former two; for then a and b may be at once eliminated together from the three equations, leaving a linear equation in e . This method is illustrated below for the case of lead. Meantime, we proceed to derive the RH-equation corresponding to (9).

§6.53 Shock waves in a fluid satisfying a simplified Born-Bradburn equation of state

Since, by 6.52(9),

$$dE = C_v dT + \left(\frac{C_v}{v^2} - \frac{a}{v^{a+1}} \right) dv, \quad (1)$$

where C_v is regarded as constant, the RH-equation 6(2) is:

$$\frac{C_v}{e} (p_v - p_{v_0}) + a \left(\frac{1}{v} - \frac{C_v}{e} \right) \left(\frac{1}{v} - \frac{1}{v_0} \right) + c \left(\frac{C_v}{e} - 1 \right) \left(\frac{1}{v} - \frac{1}{v_0} \right) = \frac{1}{2} (p_v + p_{v_0}) (v_0 - v), \quad (2)$$

which can easily be generalised if $d \neq 1$, and is at once soluble for p . Neglecting p_0 , and writing G for e/C_v (Grüneisen's constant), we get

$$\frac{p_i}{\rho_i} [v_i - \frac{G}{2}(v_o - v_i)] = c(G-1)(\frac{1}{v_i} - \frac{1}{v_o}) - a(\frac{G}{t} - 1)(\frac{1}{v_i} - \frac{1}{v_o}) . \quad (3)$$

G is dimensionless and of the order of 2.

If p_i is the pressure which would produce the same volume v_i at T_0 , we have (neglecting p_0)

$$a(\frac{1}{v_i} - \frac{1}{v_o}) = p_i v_i + c(\frac{1}{v_i} - \frac{1}{v_o}) . \quad (4)$$

Substitution in (3) gives then

$$\frac{p_i}{\rho_i} [v_i - \frac{G}{2}(v_o - v_i)] = Gc(1 - \frac{1}{t})(\frac{1}{v_i} - \frac{1}{v_o}) - (\frac{G}{t} - 1)p_i v_i . \quad (5)$$

Since p_i is a known function of v_i , this equation gives p_i rather more easily than the former. Another form, advantageous when $p_i - p_i$ is small, is

$$\begin{aligned} (p_i - p_i) \left[\frac{v_i}{G} - \frac{1}{2}(v_o - v_i) \right] &= \\ &= \frac{c}{2} (3 - \frac{v_o}{v_i}) (\frac{1}{v_i} - \frac{1}{v_o}) - a \left[\frac{1}{t} - \frac{1}{2} \cdot \frac{v_o - v_i}{v_i} \right] \left(\frac{1}{v_i} - \frac{1}{v_o} \right) \end{aligned} \quad (6)$$

From (5) it is clear that the maximum density attainable in a single plane shock is

$$\rho_{i(\max)} = \rho_o (1 + \frac{2}{G}) \sim 2\rho_o . \quad (7)$$

$\rho_{i(\max)}$ would be realised only in a shock wave of infinite pressure ratio. The temperature rise in any shock is given conveniently by:

$$p_i v_i = a v_i^{-t} - c v_i^{-1} + e T_i ,$$

$$p_i v_i = a v_i^{-t} - c v_i^{-1} + e T_0 ,$$

so that

$$T_i - T_0 = (\dot{p}_i - \dot{p}_0) v_i / e . \quad (8)$$

Before $P_{i(\max)}$ were reached, therefore, the temperature would already have risen to values at which the equation of state could no longer be expected to apply.

D , H_i , and $E_i - E_0$ follow at once in the usual manner.

The entropy change $S_i - S_0$ is obtained from

$$TdS = dE + pdv ,$$

whence, by (1) and 6.52(8)

$$dS = C_v \frac{dT}{T} + e \frac{dv}{v} , \quad (9)$$

so that

$$S_i - S_0 = C_v \ln \left[\frac{T}{T_0} \cdot \left(\frac{v}{v_0} \right)^G \right] , \quad (10)$$

and is independent of a , b , c , d .

§6.54 Adiabatic waves for the same state equation

The adiabatic differential relation is, by 6.53(9),

$$\frac{dT}{T} = - G \frac{dv}{v} , \quad (1)$$

whence

$$Tv^G = \text{constant} \quad (2)$$

Substituting for T from 6.52(9), we get

$$\dot{p}/p = e f p^G + a p^f - c p , \quad (3)$$

where f is the constant in (2). The (\dot{p}, T) -relation follows at once from (2,3).

From (3), the velocity of sound A is given by

$$A^2 = (\partial p / \partial \rho)_S = (\ell + 1) \frac{P}{\rho} + (\ell - 1) c\rho + (G - \ell) eT. \quad (4)$$

The streaming velocity w in an adiabatic wave is then

$$w = w^* \pm \int_{\rho^*}^{\rho} Ad\rho / \rho, \quad (5)$$

w^* being the velocity where $\rho = \rho^*$.

§6.55 Shock and Adiabatic Waves in Lead

Equation of State

The theory of §§ 6.52, 6.53 will be illustrated in some detail for the case of lead.

At $T_0 = 288^\circ\text{K}$, we take

$$\alpha_0 = 2.9 \times 10^{-5} \text{ } ^\circ\text{K}^{-1}$$

$$K_0 = 2.37 \times 10^{-12} \text{ cm.}^2/\text{dyne} = 2.32 \times 10^{-6} \text{ cm.}^2/\text{Kg.wt.} \quad (1)$$

$$\rho_0 = 11.37 \text{ g./cm.}^3$$

$$\text{Then } e = 3.23 \times 10^6 \text{ erg/g. } ^\circ\text{K} = 3.29 \frac{\text{Kg.wt.cm.}}{\text{g. } ^\circ\text{K}}$$

$$= 0.07718 \text{ cal./g. } ^\circ\text{K.}$$

[21] Bridgman has determined the isotherm at 288°K up to $\rho_i = 10^5 \text{ Kg.wt/cm.}^2$, where $\rho = 13.30 \text{ g./cm.}^3$. We therefore fit the constants a , b , c , in 6.52(9) to Bridgman's data at $\rho = 11.37, 13.30$ and $12.297 = \sqrt{11.37 \times 13.30} \text{ g./cm.}^3$. At the latter density, $\rho_i = 40,000 \text{ Kg.wt./cm.}^2$. Accordingly,

ρ	ρ_i	$\frac{p}{\rho^2} - \frac{288e}{\rho}$
11.37	1.03	-83.28
12.297	40,000	+187.50
13.30	100,000	+494.12

whence

$$(c + 187.50)^2 = (c - 83.28)(c + 494.12),$$

yielding

$$c = 2129.0 \frac{\text{Kg.wt.cm.}^4}{\text{g.}^2}$$

Then $b = 2.5858$

$$a = 43.32 \frac{\text{Kg.wt.cm.}^{3b}}{\text{g.}^b}$$

The equation of state deduced for lead above its yield point and Debye temperature is therefore:

$$pv = 43.32 v^{-2.5858} - 2129.0 v^{-1} + 3.29T, \quad (2)$$

in units of Kg.wt./cm.^2 , $\text{cm.}^3/\text{g}$ and $^\circ\text{K}$.

This equation is found, in fact, to fit the Bridgman isotherm very closely throughout its entire range. In particular, it gives, at 288°K and 1 atm.,

$$\kappa_o = 2.45 \times 10^6 \text{ cm.}^2/\text{Kg.wt.}$$

which shows satisfactory agreement with the value assumed at the outset, especially when it is considered that the equation is not strictly applicable at NTP and is not intended for use there. The agreement in κ_o (and so also in α_o) is an indication that the form of the equation of state 6.52(9) is suitable, and that it may therefore now be used to extrapolate Bridgman's isotherm up to, say 10^6 Kg./cm.^2 .

The results are shown in Table 6.55:1 and Fig. 6.55:1.

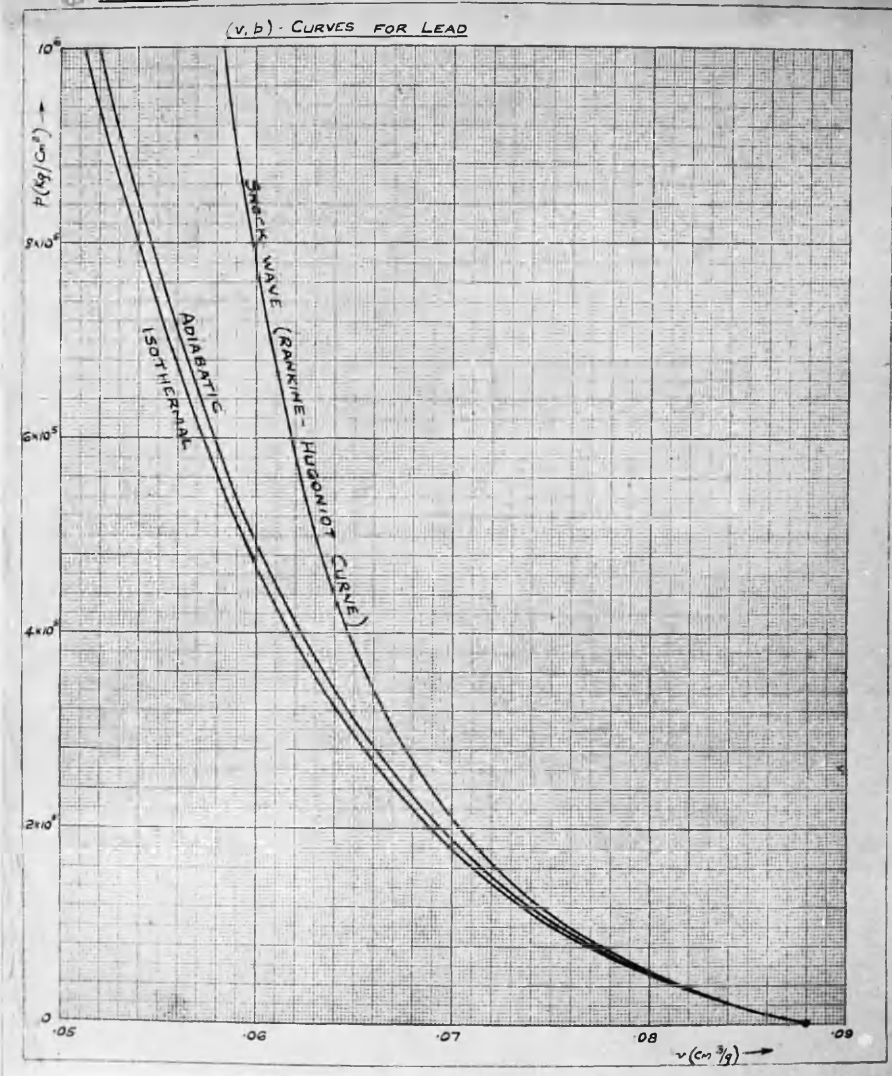
Table 6.55:1.

Isothermal, adiabatic and shock relations for lead, with $T_0 = 288^{\circ}\text{K}$, $P_0 = 1 \text{ atm}$. $v_1, \rho_1, p_1, w_1, A_1, E_1$, S_1 are the specific volume, density, pressure, streaming velocity, sound velocity, internal energy and entropy behind the shock wave. D is the wave velocity, p_i is the pressure required to produce v_1 isothermally at T_0 . P_{ad} , T_{ad} correspond to v_1 along the adiabatic through (T_0, P_0).

v_1 $\text{cm}^3/\text{gm.}$	ρ_1 $\text{gm}/\text{cm}^3.$	p_i $\text{kg}/\text{cm}^2.$	p_1 $\text{kg}/\text{cm}^2.$	P_{ad} $\text{kg}/\text{cm}^2.$	$T_1 - 288$	$T_{\text{ad}} - 288$	D	w_1 m./s.	A_1 m./s.	$E_1 - E_0$ cal/gm.	$S_1 - S_0$ $\text{cal/gm.}^{\circ}\text{K}$
0.08795	11.37	1.03	1.03	0	0	0	1,940	0	1,940	0	0
0.08695	11.50	4,824	5,160	5,160	8.9	8.9	1,979	22.4	1,990	0.06	1×10^{-5}
0.08333	12.00	25,758	27,566	27,554	45.8	45	2,123	112	2,180	1.50	1.2×10^{-4}
0.08132	12.30	40,000	43,200	43,136	79	68	2,225	168	2,300	3.35	9.7×10^{-4}
0.07788	12.84	70,000	76,800	74,328	161	111	2,410	276	2,520	9.05	4.81×10^{-3}
0.07519	13.30	100,000	111,600	106,773	265	150	2,580	374	2,710	17.0	6.79×10^{-2}
0.07143	14.00	153,900	178,500	163,620	535	213	2,860	538	3,015	34.5	1.43×10^{-2}
0.066667	15.00	249,700	317,000	265,230	1,360	316	3,370	815	3,520	79.0	2.91×10^{-2}
0.06250	16.00	370,800	539,000	393,370	3,210	428	4,015	1,161	4,150	160.5	4.60×10^{-2}
0.05882	17.00	520,000	933,000	550,790	7,390	553	4,940	1,635	5,000	318	0.253
0.05556	18.00	700,000	1,765,000	741,220	18,000	694	6,450	2,370	6,380	670	0.501
0.05000	20.00	1,171,340	-*	1,237,800	-	1,012	-	-	-	-	-

* p_1 becomes infinite when $\rho_1 = 19.9 \text{ gm}/\text{cm}^3$. (see equation 6.53(7)).

FIG. 6.55:1 /ISOTHERMAL, ADIABATIC AND SHOCK-WAVE

RH-equation

Adopting a value of $C_v = 6.0 \text{ cal./mol.}^\circ\text{K} = 1.235 \text{ Kg.cm./g.}^\circ\text{K}$, we have $G = 2.665$, and can now evaluate 6.53(3 and 5), obtaining

$$P_i(v, -0.05025) = \frac{1520}{v_i} - \frac{0.5642}{v_i^{2.5858}} - 16,965 \quad (3)$$

and

$$P_i(v, -0.05025) = \frac{1492}{v_i} - 0.01302 P_i v_i - 16,965 \quad (4)$$

in units of Kg.wt./cm.^2 and $\text{cm.}^3/\text{g.}$ Fig. 6.55:1 allows a comparison to be made between the isothermal and RH pressure-volume relations.

All the shock parameters may now be computed, and are set out in Table 6.55:1. The calculations extend up to $\rho_{1(\max)}$, though the major temperature rises at the highest pressures show that in this region the results must be treated with reserve.

The (ρ, v) -relation, which is of particular importance in studying reflexions, is drawn in Fig. 7.3:1.

Adiabatic Waves

6.54(2,3) become, for lead:

$$T v^{2.665} = \text{const.}, \text{ i.e. } v T^{0.3753} = \text{const.}, \quad (5)$$

and

$$\frac{\rho}{v} = \text{const.} \times \rho^{2.665} + 43.32 \rho^{2.5858} - 2129.0 \rho. \quad (6)$$

For example, the adiabatic through $T = 288^{\circ}\text{K}$, $\rho = 11.37 \text{ gm./cm.}^3$ is

$$v T^{0.3753} = 0.7349 \quad \text{or} \quad T v^{2.665} = 0.4424, \quad (7)$$

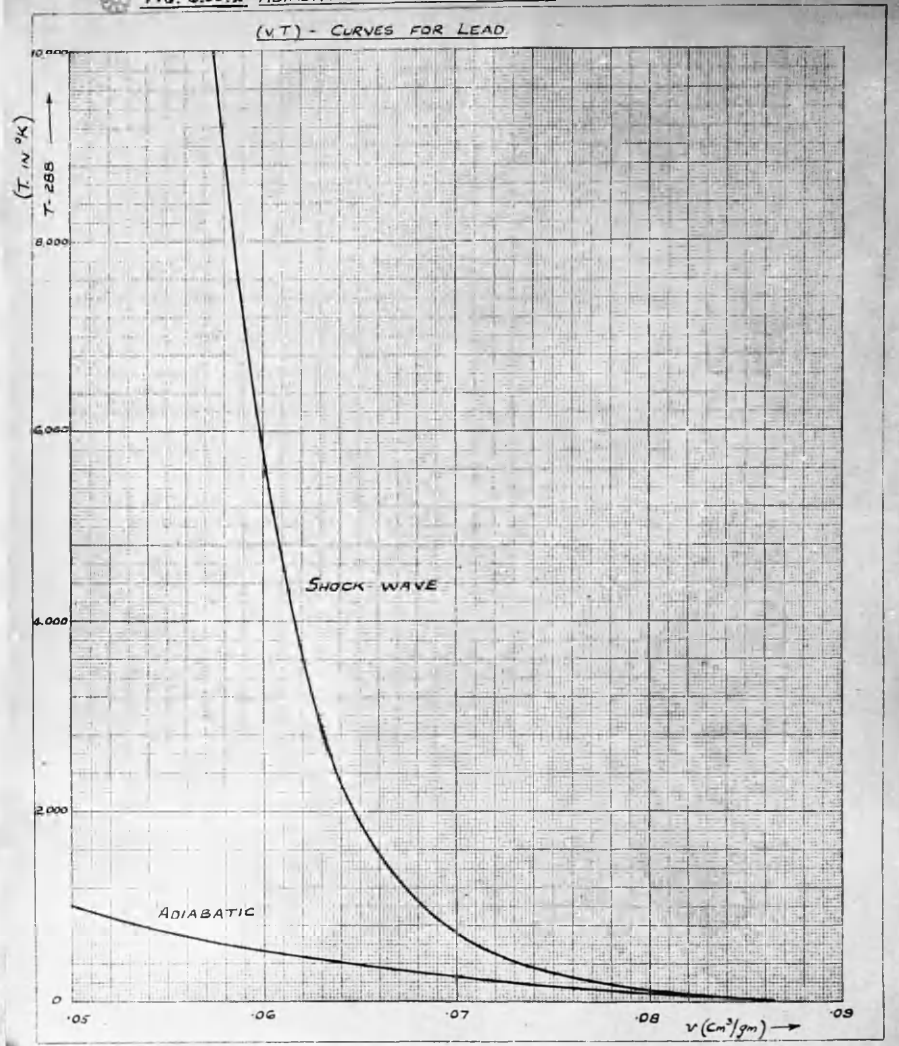
or

$$\frac{\rho}{v} = 1.456 \rho^{2.665} + 43.32 \rho^{2.5858} - 2129.0 \rho. \quad (8)$$

This adiabatic is drawn in Fig. 6.55:1 for comparison with the isothermal and RH-curve through the same initial point. As would be expected, the adiabatic lies between the other two curves. The relative temperature changes under adiabatic and shock conditions are shown in Fig. 6.55:2.

The velocity of sound A in metre/sec. is given by:

$$A^2 = 351.63 \rho v + 331080/v + 25.649 T. \quad (9)$$



By means of (5) and (6) we can easily express A^2 in terms of ρ alone, but since A/ρ cannot in general be integrated analytically, this offers no particular advantage. In determining the properties of an adiabatic wave with end conditions ρ^* , p^* , T^* , w^* , we rather proceed as follows, taking ρ as independent variable:

- 1) Calculate T from (5).
- 2) Calculate p from (6) or (2).
- 3) Calculate A from (9)
- 4) Calculate w from 6.54(5) by numerical integration.

An example of this procedure, as applied to rarefaction waves reflected through a slab of lead will be found in § 7.5 below.

§6.56 Shock and adiabatic waves in iron

Calculations similar to those made for lead have been carried out for iron. Here, $\alpha_0 = 1.16 \times 10^{-5} \text{ }^{\circ}\text{K}^{-1}$, $\kappa_0 = 5.826 \times 10^{-7} \text{ cm.}^2/\text{Kg.}$, $\rho_0 = 7.88 \text{ g./cm.}^3$, at $T_0 = 288^{\circ}\text{K}$. Then $e = 7.58 \text{ Kg.cm./g.}^{\circ}\text{K}$. The 288°K isotherm is known only to $30,000 \text{ Kg./cm.}^2$, where $\rho = 8.014 \text{ g./cm.}^3$.^[6] The following equation of state gives a good fit over this range.

$$\rho v = 3509.8v^{-2} - 27,935v^{-1} + 7.58T \quad (1)$$

(Kg./cm.^2 , $\text{cm.}^3/\text{g.}$, $^{\circ}\text{K}$). It yields, at 288°K and 1 atm.,

$$\kappa_0 = 5.883 \times 10^{-7} \text{ cm.}^2/\text{Kg.}$$

which agrees well with the value assumed. Bridgman's isotherm may now be extrapolated to, say, 10^6 Kg./cm.^2 . (Table 6.56:1).

We take $C_v = 5.3 \text{ cal./mol.}^{\circ}\text{K} = 4.05 \text{ Kg.cm./g.}^{\circ}\text{K}$, so that $G = 1.874$. The RH(ρ, v) - equation is then (Kg./cm.^2 and $\text{cm.}^3/\text{g.}$):

$$\rho_v(v, -0.06138) = \frac{12604}{v} + \frac{114.1}{v^2} - 106,400, \quad (2)$$

from which the shock parameters can be determined (Table 6.56:1, Fig. 7.3:1).

The adiabatics are

$$Tv^{1.874} = \text{const.} \quad (3)$$

$$\frac{\rho}{\rho} = \text{const.} \times \rho^{1.874} + 3509.8\rho^2 - 27,935\rho, \quad (4)$$

from which A and ω can be deduced, as in the case of lead. For example, the adiabatic through (1 atm., 288°K) has the constant in (4) equal to 45.763, and the velocity of sound at NTP would be 4660 m/s. if the equation were strictly applicable at such low pressures.

Table 6.56:1

Isothermal and shock relations for iron, with $T_0 = 288^{\circ}\text{K}$, $P_0 = 1 \text{ atm.}$ The symbols are explained in Table 6.55:1

γ_1	ρ_1 $\text{gm/cm}^3.$	p_1 $\text{kg/cm}^2.$	p_1 $\text{kg/cm}^2.$	$T_1 - 288$	D	w_1 m./s.	$E_1 - E_0$ cal/gm.
0.127	7.88	1.03	1.03	0	4,660	0	0
0.1265	7.9	4,290	4,422	2.2	4,670	11.8	0.017
0.125	8.0	26,663	27,195	8.8	4,755	68.8	0.605
0.1212	8.25	87,526	89,350	29.0	4,981	223.9	5.965
0.1177	8.5	154,773	159,440	72.4	5,217	380.5	17.274
0.1142	8.75	231,719	238,665	104.7	5,467	543.5	35.46
0.1111	9.0	315,165	327,050	173.9	5,720	711.8	60.18
0.1053	9.5	508,757	538,660	415.3	6,271	1,069	136.54
0.1000	10.0	738,150	803,977	868.4	6,887	1,457	253.4
0.0976	10.25	866,337	961,078	1,219.3	7,194	1,664	330.3
0.0952	10.5	1,021,653	1,138,962	1,473.8	7,539	1,881	422.5

The properties of rarefaction or shock waves reflected through a slab of iron when the shock waves of Table 6.56:1 fall upon an interface, will be found in § 7.5 below.

§6.57 Shock and adiabatic waves in copper and aluminium

Equations of state of the form 6.52(9) have also been developed for copper and aluminium, metals of some importance in connection with detonating explosives since they form the materials of detonator tubes. The relevant constants are collected in Table 6.57:1, which permits the theory to be fully applied to Cu and Al whenever required. Detailed shock and adiabatic wave calculations have not, however, as yet been made for these metals.

Table 6.57:1

[20,23]

Physical constants and coefficients in the state equation for copper and aluminium

(Kg./cm.², g./cm.³, °K)

:	:	:	:	e	:	a	b	c	:
Metal :	α_0	κ_0	ρ_0						
:	:	:	:	:	:	:	:	:	:
Copper:	1.67×10^{-5}	7.18×10^{-7}	8.9	7.84	929.18	2.2325	$13,978$		
Alu-	2.55×10^{-5}	13.45×10^{-7}	2.7	21.1	$88,074$	1.7145	$181,380$		
minium:									

§6.58 Shock and adiabatic waves in sodium chloride

As an example of a non-metallic cubic crystalline solid, which may serve to illustrate the theory for mineral substances, we have chosen NaCl. At 288°K , $\alpha_0 = 3.73 \times 10^{-5} \text{ }^{\circ}\text{K}^{-1}$, $\kappa_0 = 4.124 \times 10^{-6} \text{ cm.}^2/\text{Kg.}$, $\rho_0 = 2.17 \text{ g./cm.}^3$, so that $e = 12.514 \text{ Kg.cm./g. }^{\circ}\text{K}$. The isotherm [21] is known to $100,000 \text{ Kg./cm.}^2$, and fits the state equation

$$\frac{1}{\rho v} = 49,238 v^{-1.6529} - 83,320 v^{-1} + 12.514 T. \quad (1)$$

This gives $\kappa_o = 4.29 \times 10^{-6} \text{ cm.}^2/\text{Kg.}$, in reasonable agreement with the value assumed.

Table 6.58:1 contains the calculated shock variables; the $RH(p, w)$ -relation in particular is shown in Fig. 7.3:1. The adiabatic equations could be evaluated exactly as for lead or iron, if required, from the above data.

Table 6.58:1

Isothermal and shock relations for sodium chloride, with $T_0 = 288^{\circ}\text{K}$ and $P_0 = 1 \text{ atm}$. The symbols are explained in Table 6.55:1

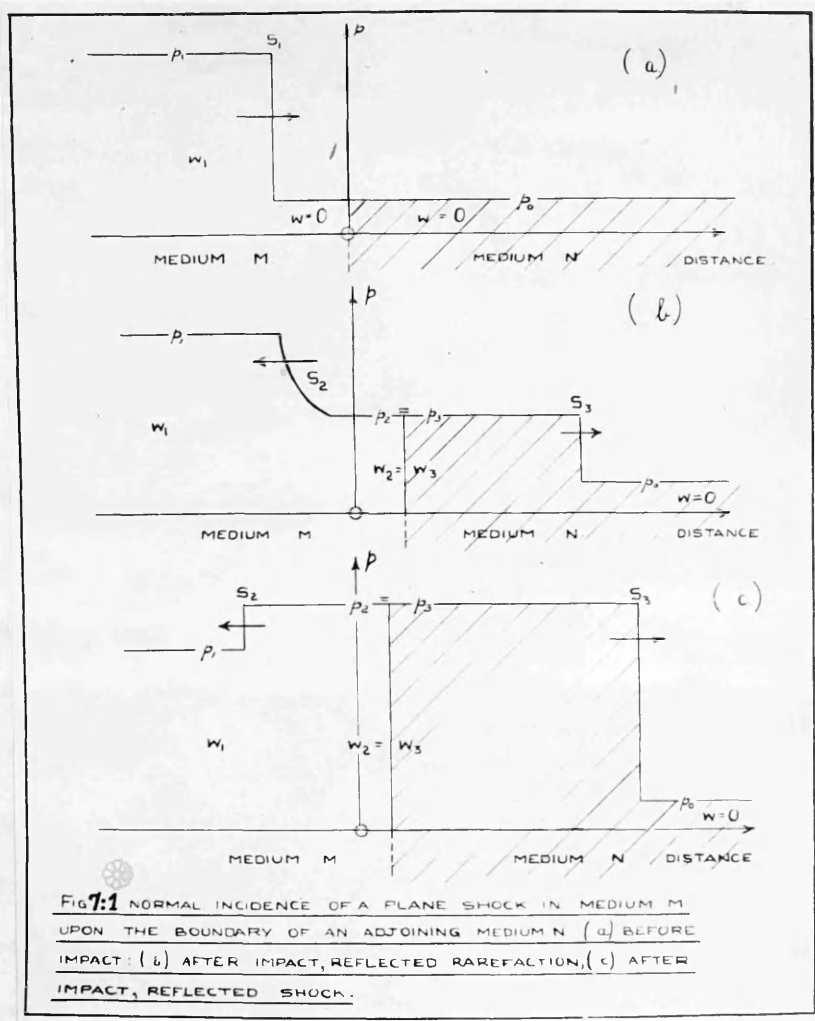
v_1 $\text{cm}^3/\text{gm.}$	ρ_1 $\text{gm}/\text{cm}^3.$	p_1 $\text{kg}/\text{cm}^2.$	$T_1 - 288$	D	w_1 m./s.	$E_1 - E_0$ cal/gm.
0.46183	2.17	1.03	0	3,310	0	0
0.44444	2.25	9,526	10,616	38.7	3,577	134.5
0.42551	2.35	23,345	26,089	93.3	3,878	304.8
0.40958	2.44415	37,800	42,860	165.6	4,134	468.7
0.36406	2.7468	100,000	125,613	745	5,173	1,098
0.35714	2.8	112,850	146,880	971	5,419	1,228
0.34482	2.9	139,470	194,600	1,519	5,900	1,495
0.33333	3.0	168,750	258,860	2,400	6,590	1,830
0.30769	3.25	254,480	563,350	7,591	8,728	2,919
0.28572	3.5	358,310	2,292,750	44,166	15,127	5,781
0.26667	3.75	482,800	- *	-	-	-

* p_1 is infinite when $\rho_1 = 3.613 \text{ gm}/\text{cm}^3$. (See equation 6.53(7))

§ 7 Normal reflexion of steady plane shocks at material boundaries

When a plane shock wave (S_1) passes through a medium (M) and falls normally upon the interface between M and a second medium (N), a disturbance (S_3) will be transmitted through N, and a further disturbance (S_2) reflected through M. It is clear on physical grounds that S_3 must be a wave of compression, and, moreover, by the arguments of § 3.2 since the interface moves impulsively, that S_3 will from the outset be a shock wave. S_2 , on the other hand, may be either a shock wave or a rarefaction wave, depending upon the physical properties of M, N and in the most general case also upon the intensity of S_1 .

Shortly before the arrival of S_1 at the interface, conditions are as indicated in Fig. 7:1a. In medium N, and also in the thin undisturbed layer of M, the velocity is zero and the other variables have values distinguished as usual by suffix 0. Behind S_1 , conditions are again constant, and represented by suffix 1. Figs. 7:1b and 1c represent the position shortly after arrival at the interface. A steady shock has developed in N and a shock or rarefaction has returned a little way into M. Conditions in N behind S_3 are distinguished by suffix 3, and are constant up to the interface, which must itself therefore move forward with velocity w_3 . Immediately beyond the interface, the conditions in M are distinguished by suffix 2. In a reflected shock (Fig. 7:1c) these values are maintained up to S_2 , where they change abruptly to p_1 , w_1 , etc. Otherwise (Fig. 7:1b) the values p_2 , w_2 , etc. persist back only to a point which moves relative to M with sonic speed $-a_2$; thereafter they change smoothly to p_1 , w_1 , etc. at the nose of the reflected rarefaction, which moves with velocity $-a_1 + w_1$. This is



negative for $\pi_i = p_i/p_0$ small, but may be positive for π_i large. For example in an ideal gas, there is, in fact, a definite value π_c of π_i , defined by §6.21 as the larger root of

$$\lambda(\lambda-3)\pi_c^2 - (3\lambda^2 - 3\lambda + 2)\pi_c + (\lambda-1)^2 = 0, \quad (1)$$

for which $w_1 = a_1$. If π_i has this value, the nose of the rarefaction is stationary in space in the plane originally occupied by the free surface. The variation of π_c with λ is shown in Table 6.21:1. In any case, the gradients in the rarefaction decrease with time. If S_2 is a shock, $p_2 > p_1$ and $w_2 < w_1$; if a rarefaction, $p_2 < p_1$ and $w_2 > w_1$.

By the usual shock wave equations, and the equation of state for N, we can now prescribe a relation between w_3 and p_3 : this may be referred to as the RH(pw)-relation* for the transmitted shock. Similarly, by means either of the shock equations or the adiabatic wave equations together with the state equation for M, a relation is prescribed between $w_2 - w_1$ and p_2 : this may be called the RH(pw)-relation or the R(pw)-relation** for the reflected wave, according to the nature of the wave. The former applies in the range $p_2 > p_1$, $w_2 < w_1$; the latter in the range $p_2 < p_1$, $w_2 > w_1$. Together, they form a composite relation, which will be referred to as the RHR(pw)-relation for reflected waves. However, continuity at the interface requires that

$$p_3 = p_2 \quad (2)$$

and

$$w_3 = w_2 \quad (3)$$

Two equations are therefore available to determine p_2 and w_2 , whereupon the problem may be completely solved.

* Rankine-Hugoniot

** Riemann

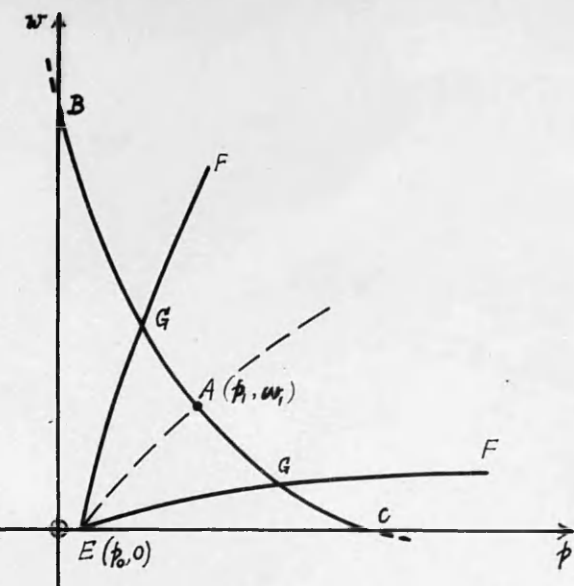


FIG. 7:2. (p, w) -DIAGRAM FOR NORMAL

INCIDENCE . BA : REFLECTED RAREFACTIONS
AC : REFLECTED SHOCKS . EF, EF' : TRANSMITTED
SHOCKS.

The analysis is best illustrated graphically. Thus, in Fig. 7:2, let EA represent the RH(p, w)-relation for shocks in M, and $A(p_1, w_1)$ the state (supposed constant in space) behind S_1 . Then the state 2 is defined by some point on BAC, of which the branch BA (where $p_2 < p_1, w_2 > w_1$) represents rarefactions in M with initial state A, while AC (where $p_2 > p_1, w_2 < w_1$) represents shocks in M under the same initial conditions. BA is defined by

$$w_2 - w_1 = \int_{v_1}^{v_2} adv/v \quad (4)$$

in conjunction with the adiabatic (p, v)-relation:

$$dE = -pdw \quad (5)$$

AC is defined by

$$w_2 - w_1 = -\sqrt{(\rho_2 - \rho_1)(v_1 - v_2)} \quad (6)$$

in conjunction with the RH(p, v)-relation

$$E_2 - E_1 = \frac{1}{2}(\rho_2 + \rho_1)(v_1 - v_2). \quad (7)$$

The composite curve BAC, which may be called the RHR-curve through A, though defined by entirely different analytical equations above and below A, is continuous together with its slope (and curvature) at A, as can be seen by reference to § 6.1; the RH- and R-curves have in fact double contact and cross at A.

On the other hand, conditions (p_3, w_3) behind S_3 are necessarily represented by some point on the curve EF, the RH(p, w)-curve for shocks in N. This curve may lie entirely above or entirely below EA, or may even (in exceptional cases - see § 7.14 below) cross over EA. In virtue of equations (2,3), conditions between S_2 and S_3 are therefore defined by the point of intersection G of curves BAC and EF. It is clear that while S_3 is necessarily a shock (since rarefactions in N are represented by the adiabatic continuation of FE below the pressure axis) S_2 may be of either type, according as G lies above or below A.

Evidently, the RHR-curve BAC, in conjunction with a series of RH-curves EF for various media N, is sufficient to solve all problems relating to the normal reflection of a shock of intensity p_1 in M. In order now to cover incident waves of arbitrary strength, it is necessary only to supplement BAC by a family of such curves, passing through the various points A on EA. The intersection of these RHR curves with the w-axis represents conditions at a free surface, i.e. when N is a vacuum; their intersection with the p-axis conditions at a rigid boundary, i.e. when N is incompressible. Passage from a liquid or solid to a gas and vice versa correspond very approximately to these extreme cases.

§ 7.01 Criterion for a reflected shock

The condition that S_2 should be a shock wave is that $p_2 > p_1$ ($w_2 < w_1$).

This condition is, so far, of an a posteriori nature. In solving an actual problem, we must base our choice of equations 7(4) or 7(6) upon an assumption regarding the nature of S_2 ; if the conclusions contradict this assumption, the alternative equation is to be used. Since the adiabatic and RH-relations involve the energy function E , it is not possible to express the condition for, say, a reflected shock explicitly in terms of the initial conditions alone, unless indeed $E(p, v)$ is specified. The criterion must therefore remain in general a posteriori. However, in practice there is usually little difficulty in deciding the character of S_2 , and in doubtful cases it may be expected that p_2 will be close to p_1 , so that the solution may be carried out equally well with either equation, since the two overlapping curves BA and AC are almost coincident. If, indeed, the curves are monotonic as in Fig. 7:2 (which will usually and perhaps always be the case in practice), the criterion for a reflected shock may be expressed directly. For then the condition that S_2 be a shock is evidently that EF intersect the ordinate through A at a point lower than A itself, in other words that:

$$w_3(p_1) < w_1. \quad (1)$$

The condition for a reflected rarefaction is, similarly,

$$w_3(p_1) > w_1. \quad (2)$$

If $w_3(p_1) = w_1$ (3)

no reflected wave arises, and S_3 has the same pressure ratio as S_1 . This will rarely happen in practice with two different media, but a case where it does so is discussed below. (§7.14) In such cases, unless

indeed curves EA and EF coincide throughout their length (which cannot be expected ever to happen in practice) they must cross at A, and the reflected wave then changes type as p_1 passes through the value defined by equation (3).

It is also clear that when the curves are monotonic the relations between M and N are inverse: if a shock wave in M of intensity p_1 is reflected as a shock by N, then a shock of intensity p_1 in M is reflected as a rarefaction by N.

§ 7.1 Normal reflexions in an ideal gas

The RH(p_w)-equation for the incident shock S_1 is here given by 6.2(4), or, since $w_i = W_i$, by

$$\omega_i = \sqrt{(\lambda-1)v_o} \cdot \frac{p_i - p_o}{\sqrt{\lambda p_i + p_o}} . \quad (1)$$

The RHR(p_w)-relation for S_2 is derived at once from 6.2(4) and 4(9) in the form:

$$\omega_2 - \omega_i = \begin{cases} -\sqrt{(\lambda-1)v_i} \cdot \frac{p_2 - p_i}{\sqrt{\lambda p_2 + p_i}} , & \text{if } p_2 > p_i \\ +\sqrt{(\lambda^2-1)p_i v_i} \left[1 - \left(\frac{p_2}{p_i} \right)^{\frac{1}{\lambda+1}} \right] , & \text{if } p_2 < p_i . \end{cases} \quad (2a)$$

(Velocities w are measured in the direction of propagation of S_1).

From (1) and (2) we may draw the RH-curve for S_1 and the family of RHR-curves for S_2 . The properties of reflected and transmitted waves are then determined by the intersection of (2) with the RH-curve for the adjoining medium. The incident RH-relation and representative members of the RHR-family are set out in Tables 7.1:1-4, and drawn in Figs. 7.1:1-4 for each of the following gases, assumed ideal, and initially at 1 atm. and 288°K: He, Ar, O₂, CO₂, and for $p_1 = 2, 5, 10, 20, 50, 100, 150, 200, 300, 400, 600, 800, 1000$ atm. The results are,

of course, only approximate at the higher pressures, in view of the changes in specific heats and the effects of dissociation and ionisation which must in fact accompany such high shock wave temperatures.

The RHR equation (2) represents w_2 as a monotonic function of p_2 , which decreases continuously from $w_1 + \sqrt{(\lambda^2-1)p_1 v_1}$ when $p_2 = 0$ through w_1 when $p_2 = p_1$ to 0 when p_2 satisfies $w_1 = (p_2 - p_1) \sqrt{\frac{(\lambda-1)v_1}{\lambda p_2 + p_1}}$.

The monotonic nature of w_2 and the continuity of its slope at $p_2 = p_1$ are easily established, and the latter property is in any case implied in the fundamental theory (see §§6.1 and 7).

Table 7.1:1

$\text{RR}(P_2, w_2)$ -relations for reflexions in Helium ($\gamma = \frac{5}{3}$, $\lambda = 4$), $P_1 = 1 \text{ atm}$, $T_1 = 288^\circ\text{K}$.
 Units: atm. and w/s. Figures in [brackets] give the $\text{RR}(P_1, w_1)$ -relation for incident shocks.

$P_1 = 1$		$P_1 = 2$		$P_1 = 5$		$P_1 = 10$		$P_1 = 20$	
P_2	w_2	P_2	w_2	P_2	w_2	P_2	w_2	P_2	w_2
0	3,906	0	5,580	0	7,450	0	10,160	0	10,160
0.2	1,721	0.5	2,800	1	3,936	2	5,440	2	5,440
0.4	1,396	1	2,384	2	5,416	4	4,850	4	4,850
0.8	1,024	2	1,908	4	2,818	8	4,066	8	4,066
1.2	784	3	1,594	6	2,429	12	3,551	12	3,551
1.6	597	4	1,363	8	2,132	16	3,160	16	3,160
2.0	[446]	[5]	[1,170]	[10]	[1,890]	[20]	[2,840]	[20]	[2,840]
3	152	7.5	793	15	1,419	30	2,219	30	2,219
4	(-69)	10	513	20	1,065	40	1,750	40	1,750
		15	76	30	513	60	1,020	60	1,020
		20	(-266)	40	92	80	460	80	460
				50	(-590)	100	(-10)	100	(-10)

(cont.)

Table 7.1:1 (Contd.)

P ₁ = 50		P ₁ = 100		P ₁ = 150		P ₁ = 200		P ₁ = 300	
P ₂	w ₂	P ₂	w ₂	P ₂	w ₂	P ₂	w ₂	P ₂	w ₂
0	15,640	0	22,170	0	26,750	0	30,860	0	37,650
10	7,670	10	12,360	15	15,010	20	17,340	30	21,180
20	6,480	20	10,900	30	15,270	40	15,330	60	18,730
30	5,710	40	9,220	60	11,270	80	15,020	120	15,920
40	5,120	60	8,130	90	9,960	120	11,510	180	14,090
[50]	[4,640]	80	7,300	120	8,960	160	10,366	240	12,690
75	3,705	[100]	[6,620]	[150]	[8,150]	[200]	[9,450]	[300]	[11,550]
100	3,000	150	5,300	225	6,570	300	7,610	450	9,330
150	1,910	200	4,300	300	5,380	400	6,240	600	7,660
200	1,060	300	2,760	450	3,540	600	4,110	900	5,120
250	340	400	1,560	600	2,100	800	2,450	1,200	3,050
300	(-280)	500	570	750	900	1,000	1,080	1,500	1,350
		600	(-350)	900	(-160)	1,200	(-140)	1,800	(-120)
P ₁ = 400		P ₁ = 600		P ₁ = 300		P ₁ = 1,000		P ₁ = 2,000	
P ₂	w ₂	P ₂	w ₂	P ₂	w ₂	P ₂	w ₂	P ₂	w ₂
0	45,500	0	55,300	0	61,300	0	68,700	0	68,700
10	24,500	60	30,000	80	34,500	100	38,740	200	34,280
20	21,680	120	26,510	160	30,500	200	34,280		
30	18,470	240	22,575	320	25,920	400	29,150		
40	16,320	360	19,980	480	22,930	600	25,820		
50	14,715	480	18,010	640	20,660	800	23,280		
[60]	[13,400]	[600]	[16,400]	[300]	[18,800]	[400]	[21,200]		
60	10,340	900	15,250	1,200	15,190	1,500	17,160		
80	8,920	1,200	10,870	1,600	12,470	2,000	14,120		
100	5,940	1,800	7,200	2,400	8,240	3,000	9,420		
120	3,610	3,000	4,400	5,200	4,940	4,000	5,740		
140	1,660	5,600	1,920	4,000	2,200	5,000	2,700		
160	(-50)	(-50)	(-60)	(-60)	(-60)	(-200)	6,000	0	

Table 7.1:2 RH(p_2, w_2)-relations for reflexions in argon ($\gamma = 5/3, \lambda = 4$) $p_0 = 1$ atm. $T_0 = 288^\circ K$. Units: atm. and m/s. Figures in brackets give RH(p_1, w_1)-relation for incident shocks.

$p_1 = 1$	$p_1 = 2$	$p_1 = 5$	$p_1 = 10$	$p_1 = 20$
p_2	w_2	p_2	w_2	p_2
0	1,232	0	1,765	0
0.2	543	0.5	884	1
0.4	441	1	753	2
0.8	324	2	604	4
1.2	247	3	506	6
1.6	189	4	431	8
[2]	[141.4]	[5]	[370]	[10]
3	48.6	7.5	251	15
4	(-22)	10	162	20
		15	24	30
		20	(-58)	40
				50
				(-87)
				100

(cont.)



Table 7.1:2 (Contd.)

$p_1 = 50$		$p_1 = 100$		$p_1 = 150$		$p_1 = 200$		$p_1 = 300$	
p_2	w_2	p_2	w_2	p_2	w_2	p_2	w_2	p_2	w_2
0	4,950	0	7,015	0	8,460	0	9,760	0	11,890
10	2,427	20	3,442	30	4,200	40	4,846	60	5,920
20	2,052	40	2,913	60	3,564	80	4,116	120	5,030
30	1,808	60	2,568	90	3,152	120	3,640	180	4,451
40	1,622	80	2,305	120	2,857	160	3,276	240	4,010
[50]	[1,470]	[100]	[2,090]	[150]	[2,580]	[200]	[2,980]	[300]	[3,650]
75	1,174	150	1,672	225	2,080	300	2,404	450	2,950
100	952	200	1,357	300	1,705	400	1,970	600	2,420
150	607	300	870	450	1,122	600	1,300	900	1,624
200	337	400	488	600	667	800	774	1,200	970
250	113	500	170	750	290	1,000	340	1,500	430
300	(-85)	600	(-110)	900	(-45)	1,200	(-50)	1,800	(-30)
$p_1 = 400$		$p_1 = 600$		$p_1 = 800$		$p_1 = 1,000$			
p_2	w_2	p_2	w_2	p_2	w_2	p_2	w_2	p_2	w_2
0	13,790	0	16,820	0	19,370	0	21,700		
80	6,866	60	9,470	80	10,880	100	12,230		
160	5,840	120	8,380	160	9,625	200	10,820		
240	5,168	240	7,120	320	8,180	400	9,210		
320	4,657	360	6,317	480	7,243	600	8,165		
[400]	[4,240]	[480]	[5,688]	[640]	[6,517]	[800]	[7,355]		
600	3,430	[600]	[5,180]	[800]	[5,930]	[1,000]	[6,700]		
800	2,820	900	4,191	1,200	4,790	1,500	5,420		
1,200	1,870	1,200	3,445	1,600	3,930	2,000	4,460		
1,600	1,130	1,800	2,290	2,400	2,590	3,000	2,980		
2,000	520	2,400	1,390	3,200	1,550	4,000	1,820		
2,400	(-20)	3,000	645	4,000	680	5,000	850		
		3,600	(-80)	4,800	(-70)	6,000	0		



Table 7.1.3

KHR($p_2 w_2$)-relations for reflexions in oxygen ($\gamma = 7/5$, $\lambda = 6$) $p_o = 1$ atm. $T_o = 288^\circ K$.
 Units: atm. and m/s. Figures in [brackets] give RHR($p_1 w_1$)-relation for incident shocks

$p_1 = 1$	p_2	w_2	$p_1 = 2$	p_2	w_2	$p_1 = 5$	p_2	w_2	$p_1 = 10$	p_2	w_2	$p_1 = 20$	p_2	w_2
[1.0]	[0.0]		0	1,965	0	2,590	0	3,335	0	4,416				
			0.2	674	0.5	1,043	1	1,442	2	1,998				
			0.4	538	1	882	2	1,244	4	1,746				
			0.8	390	2	703	4	1,027	8	1,467				
			1.2	296	3	591	6	890	12	1,293				
			1.6	226	4	507	8	787	16	1,161				
			2.0	[170]	[5]	[440]	[10]	[705]	[20]	[1,056]				
			3	62.7	7.5	312	15	548	30	855				
			4	(-18.5)	10	214	20	429	40	703				
						67	30	250	60	474				
						(-47)	40	110	80	296				
						50	(-8)	(-8)	100	144				
									120	13				
									140	(-106)				

(cont.)

Table 7.1:3 (Contd.)

P ₁ = 50		P ₁ = 100		P ₁ = 150		P ₁ = 200		P ₁ = 300	
P ₂	w ₂	P ₂	w ₂	P ₂	w ₂	P ₂	w ₂	P ₂	w ₂
0	6,670	0	9,260	0	11,290	0	13,010	0	15,850
5	3,118	10	4,380	15	5,360	20	6,180	30	7,550
10	2,746	20	3,886	30	4,735	40	5,464	60	6,680
20	2,336	40	3,302	60	4,050	80	4,675	120	5,724
30	2,078	60	2,948	90	3,620	120	4,179	180	5,122
40	1,884	80	2,682	120	3,297	160	3,806	240	4,670
[50]		[100]		[150]		[200]		[300]	
75	1,434	150	2,064	225	2,547	300	2,942	450	3,620
100	1,211	200	1,757	300	2,175	400	2,513	600	3,097
150	873	300	1,293	450	1,610	600	1,862	900	2,305
200	610	400	930	600	1,170	800	1,360	1,200	1,690
250	387	500	626	750	800	1,000	930	1,500	1,170
300	194	600	360	900	480	1,200	560	1,800	720
350	20	700	120	1,050	190	1,400	225	2,100	310
400	(-137)	800	(-95)	1,200	(-80)	1,600	(-75)	2,400	(-60)
P ₁ = 400		P ₁ = 600		P ₁ = 800		P ₁ = 1,000		P ₁ = 1,200	
P ₂	w ₂	P ₂	w ₂	P ₂	w ₂	P ₂	w ₂	P ₂	w ₂
0	18,280	0	22,370	0	25,750	0	28,850	0	32,850
40	8,710	60	10,680	80	12,300	100	13,780	120	15,200
80	7,710	120	9,460	160	10,890	200	12,200	140	14,470
160	6,610	240	8,110	320	9,340	400	10,470	160	12,375
240	5,916	360	7,266	480	8,370	600	9,375	180	10,554
320	5,395	480	6,627	640	7,634	800	8,554	200	9,790
[400]		[600]		[6,120]		[800]		[1,000]	
600	4,205	900	5,149	1,200	5,931	1,500	6,649	1,700	7,700
800	3,584	1,200	4,414	1,600	5,086	2,000	4,270	1,800	5,150
1,200	2,673	1,800	3,300	2,400	3,810	3,000	4,210	2,200	5,000
1,600	1,970	2,400	2,440	3,200	2,800	4,000	4,400	2,400	5,650
2,000	1,370	3,000	1,710	4,000	1,960	5,000	5,210	2,800	6,000
2,400	850	3,600	1,070	4,800	1,230	6,000	6,400	3,200	6,600
2,800	380	4,200	500	5,600	570	7,000	7,400	3,600	8,000
3,200	(-45)	4,800	(-30)	6,400	(-20)	8,000	(-10)	4,000	8,600

Table 7.1:4

RHR($p_2 w_2$)-relations for reflexions in carbon dioxide ($\gamma = 1.30$, $\lambda = 7.67$). $p_0 = 1$ atm.
 $T_0 = 288^{\circ}\text{K}$. Units: atm. and m/s. Figures in [brackets] give RHR($p_1 w_1$)-relation for
incident shocks

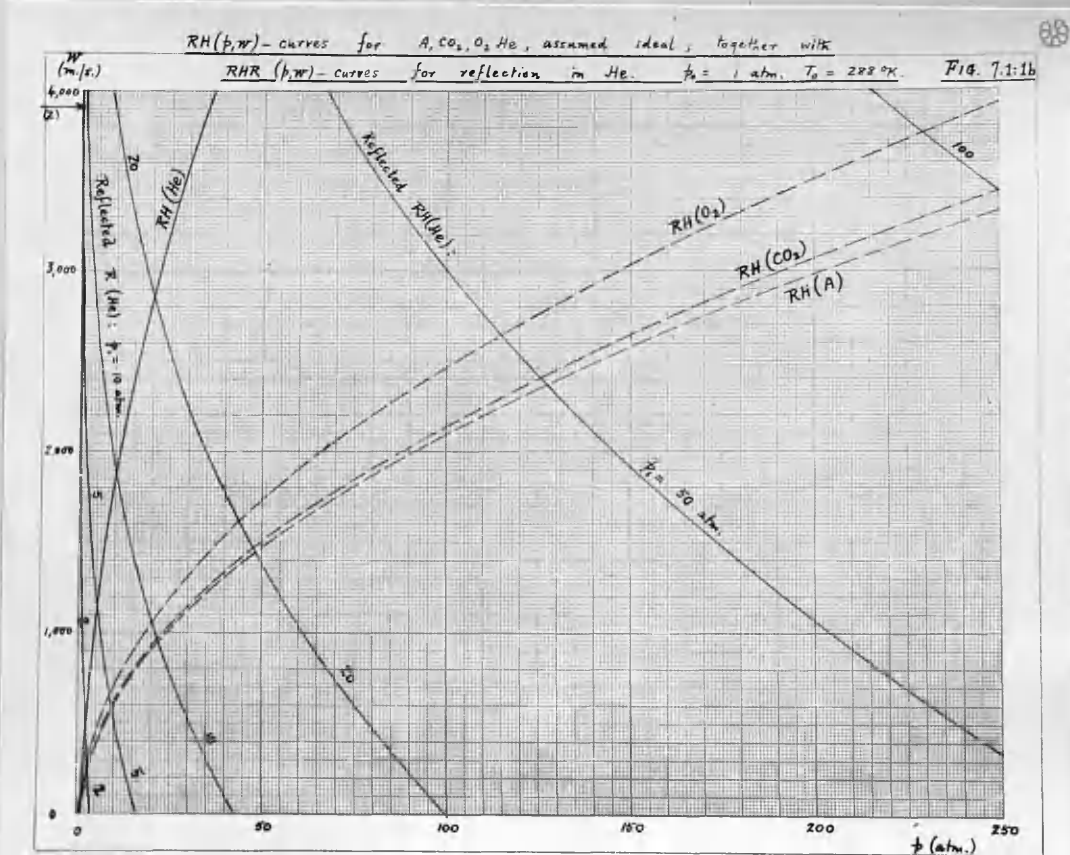
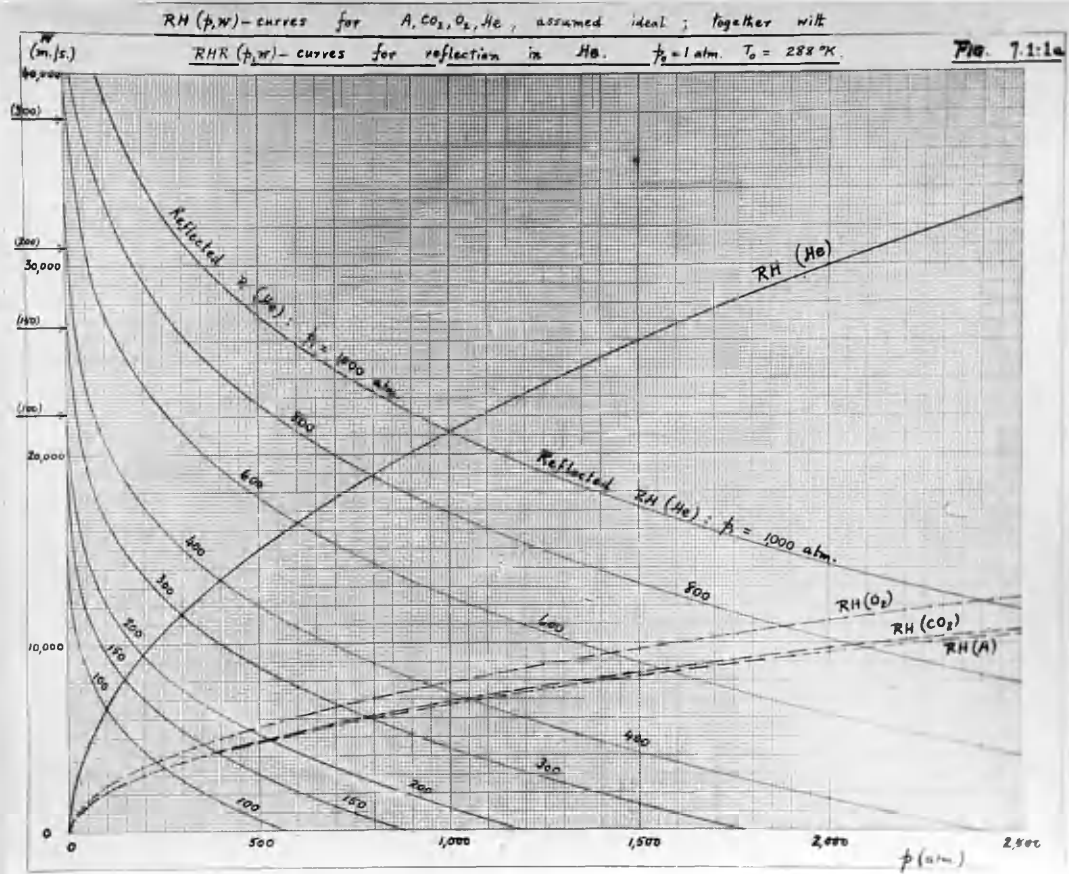
$p_1 = 1$		$p_1 = 2$		$p_1 = 5$		$p_1 = 10$		$p_1 = 20$	
p_2	w_2	p_2	w_2	p_2	w_2	p_2	w_2	p_2	w_2
[1.0]	[0.0]	0	2,079	0	2,656	0	3,275	0	4,271
		0.2	599	0.5	914	1	1,236	2	1,701
		0.4	476	1	769	2	1,066	4	1,488
		0.8	343	2	612	4	882	8	1,257
		1.2	260	3	514	6	768	12	1,113
		1.6	198	4	442	8	683	16	1,006
		[2.0]	[149.2]	[5]	[384]	[10]	[615]	[20]	[921]
		3	56.5	7.5	275	15	487	30	760
		4	(-14)	10	193	20	391	40	639
				15	69	30	245	60	456
				20	(-28)	40	132	80	313
						50	37	100	194
						60	(-45)	120	91
									(-4)

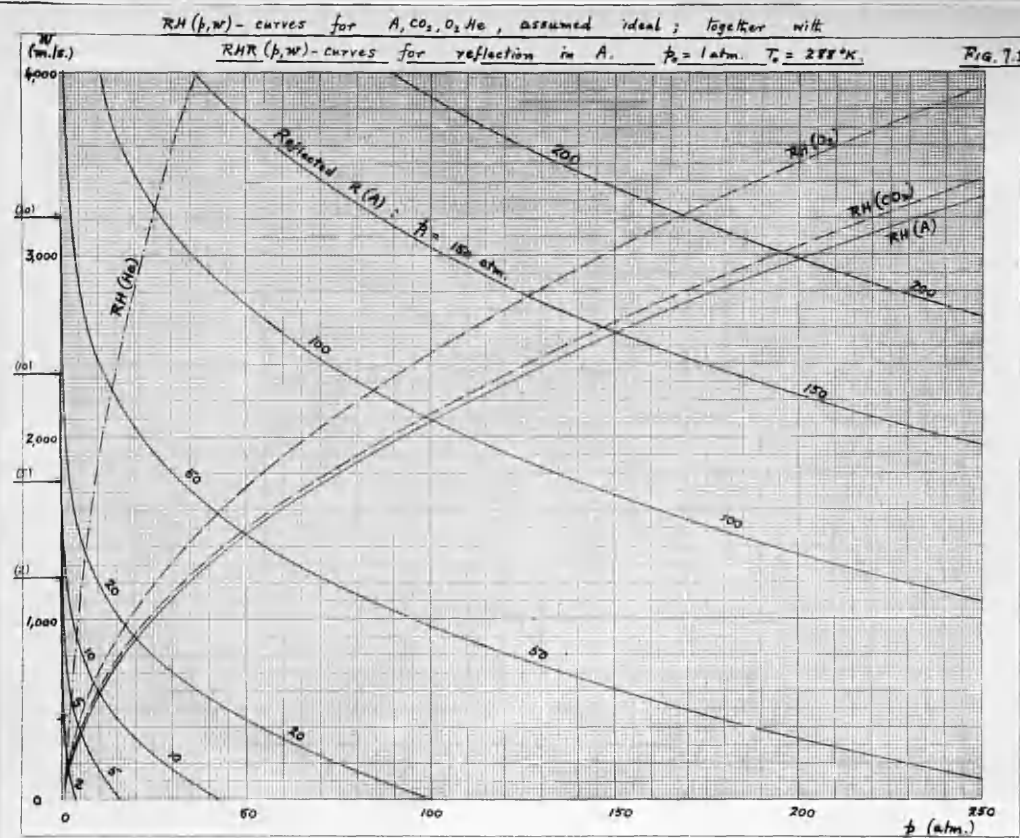
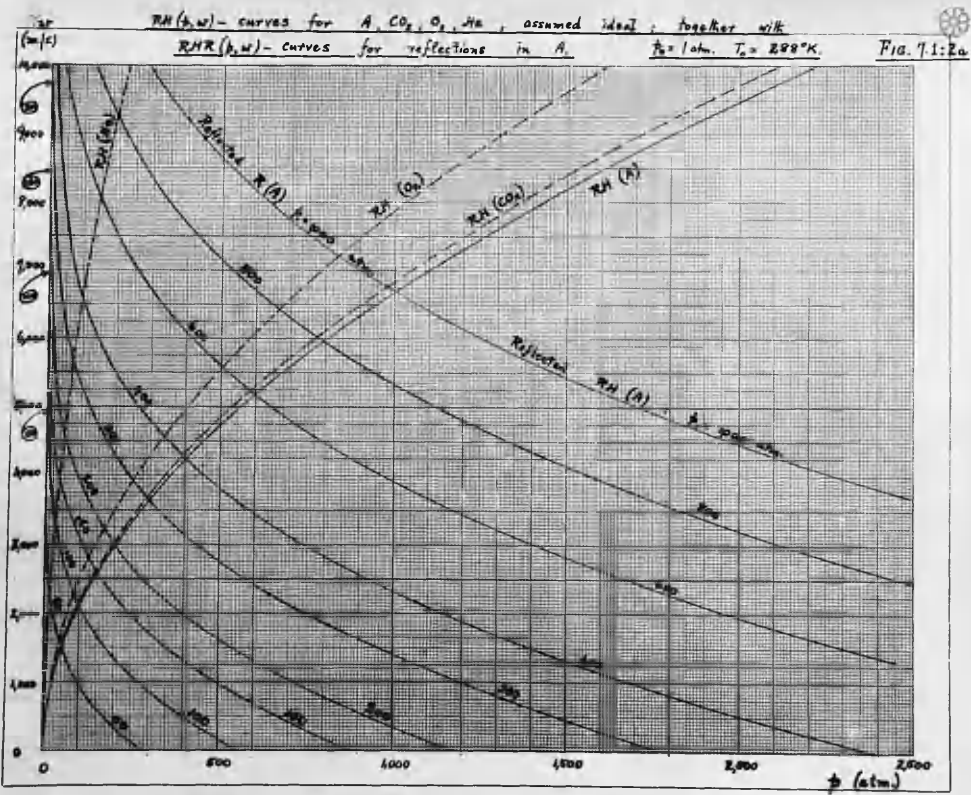
(cont.)

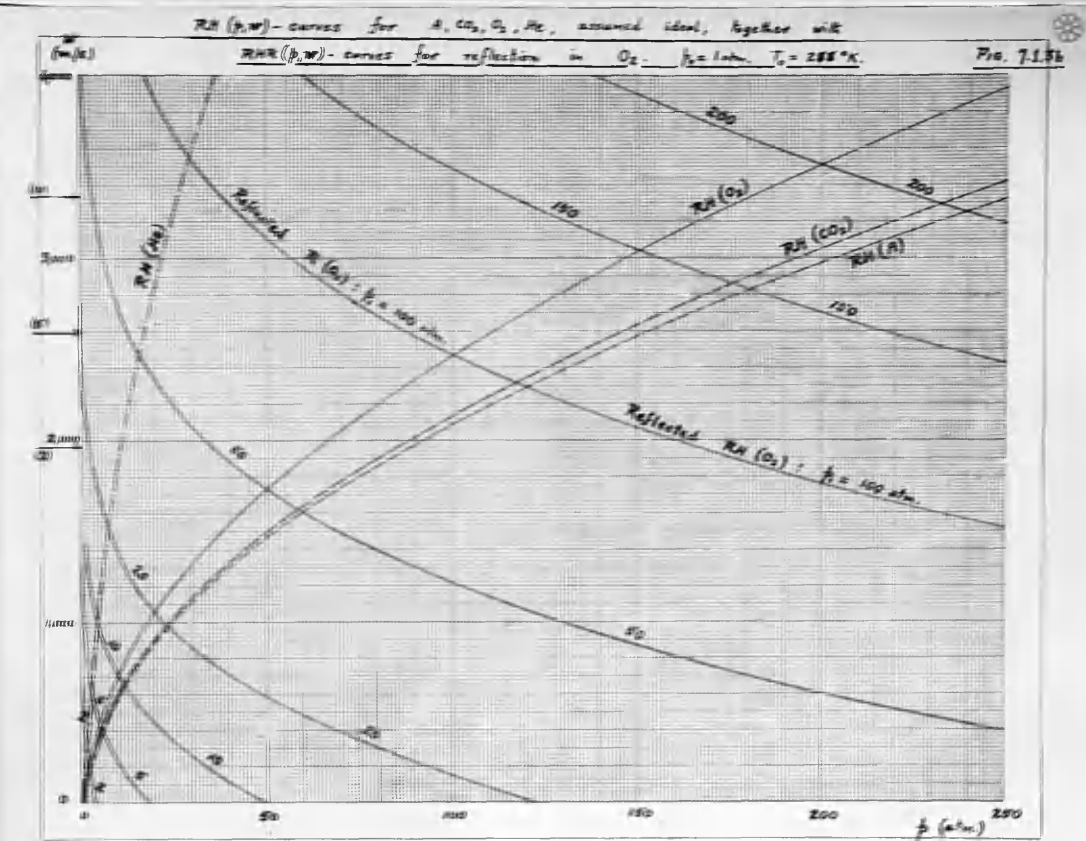
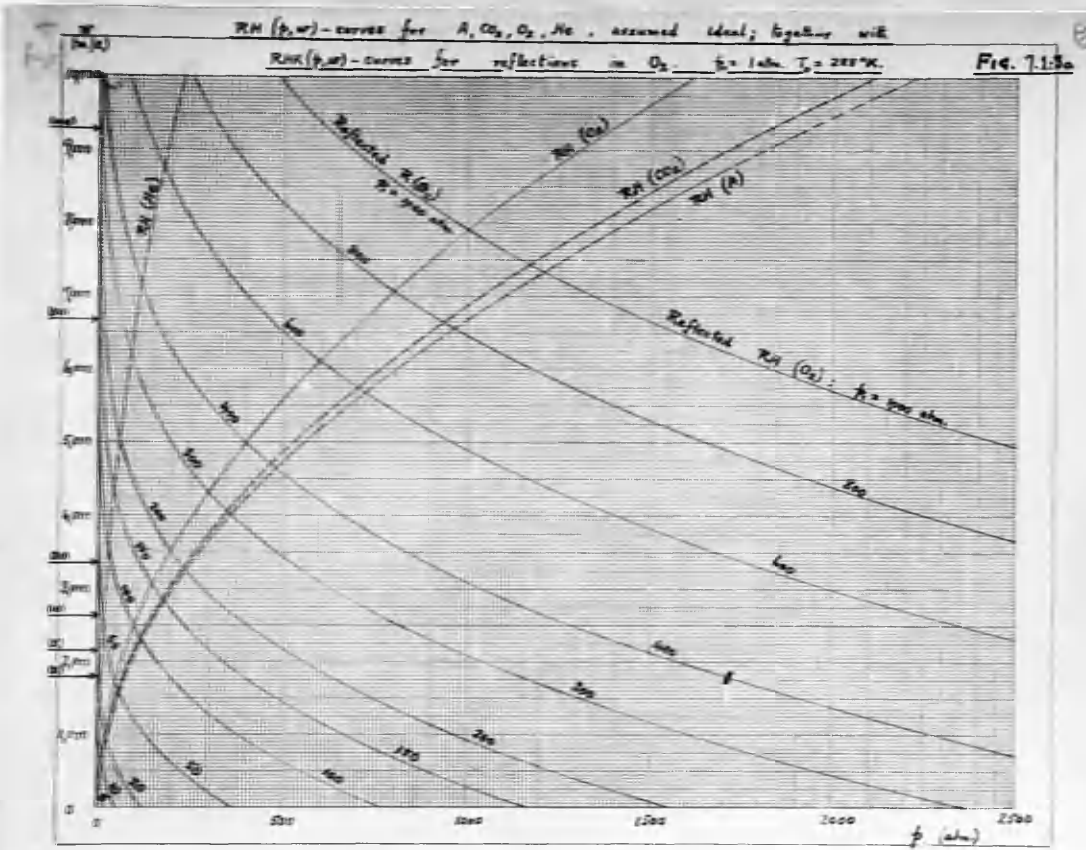
Table 7.1:4 (Contd.)

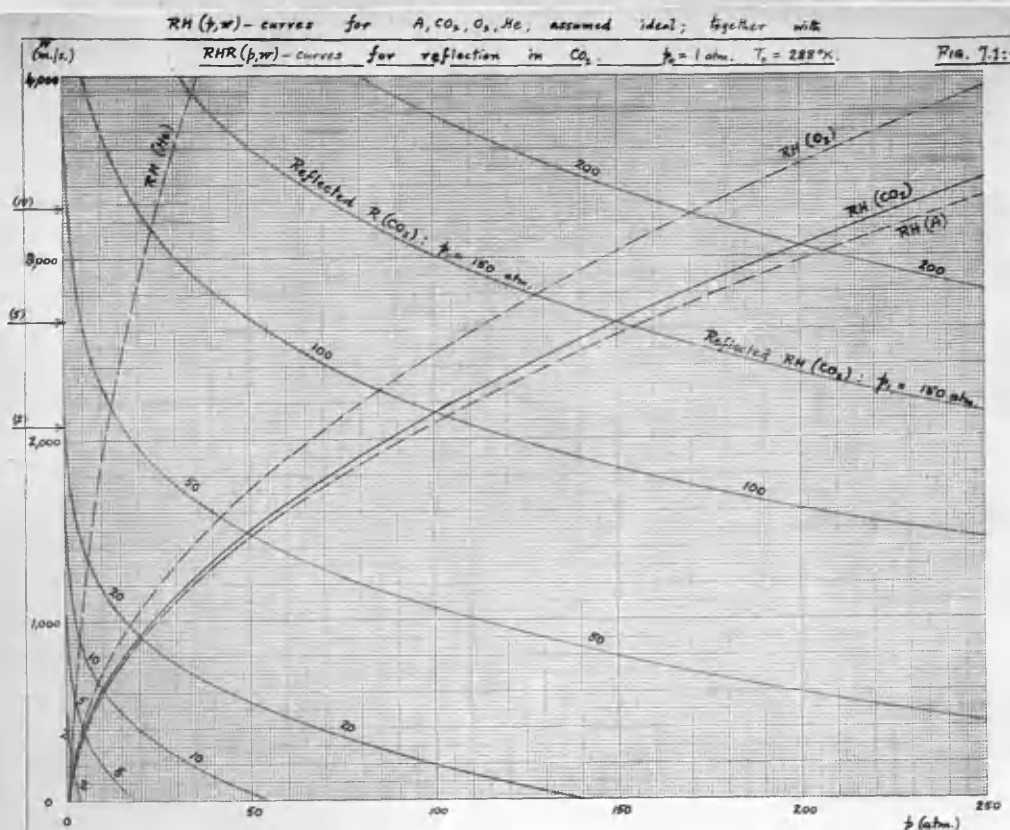
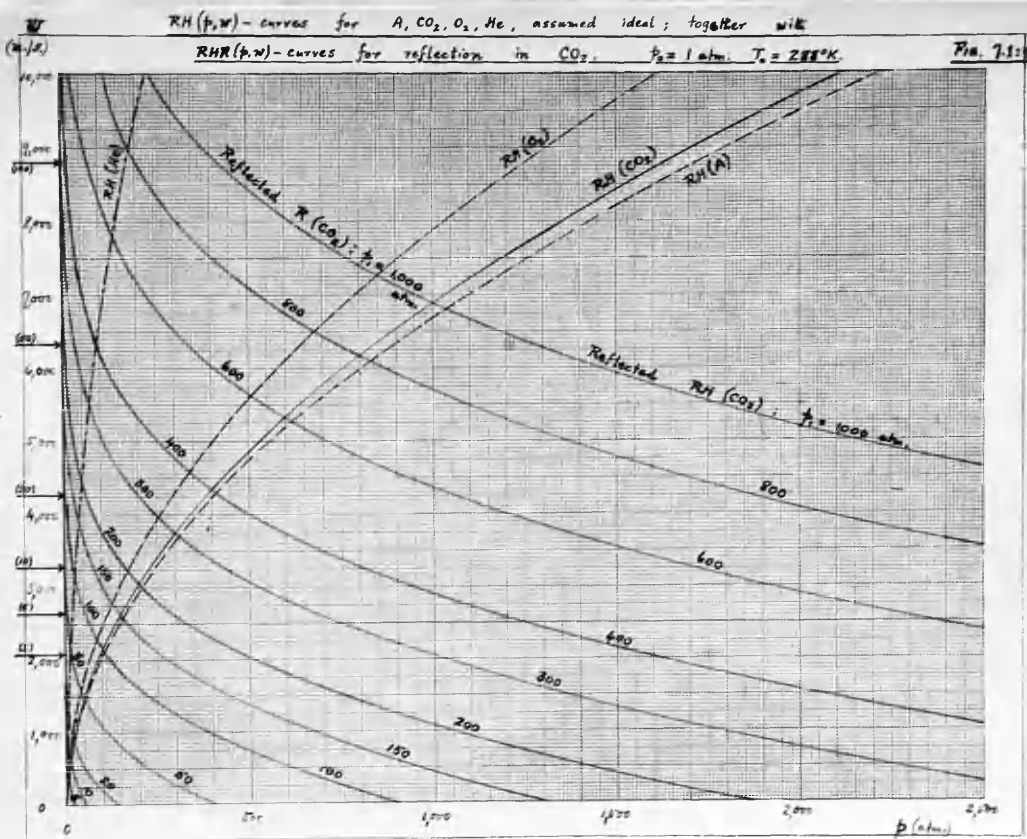
11 10

$p_1 = 50$		$p_1 = 100$		$p_1 = 150$		$p_1 = 200$		$p_1 = 300$	
p_2	w_2	p_2	w_2	p_2	w_2	p_2	w_2	p_2	w_2
0	6,337	0	8,785	0	10,930	0	12,340	0	15,030
5	2,609	10	3,701	15	4,567	20	5,230	30	6,388
10	2,300	20	3,279	30	4,038	40	4,640	60	5,670
20	1,964	40	2,820	60	3,463	80	4,000	120	4,890
30	1,755	60	2,535	90	3,105	120	3,600	180	4,404
40	1,601	80	2,324	120	2,842	160	3,306	240	4,057
[50]	[1,477]	[100]	[2,155]	[150]	[2,630]	[200]	[3,070]	[300]	[3,760]
75	1,237	150	1,837	225	2,232	300	2,625	450	3,220
100	1,061	200	1,603	300	1,944	400	2,290	600	2,813
150	796	300	1,235	450	1,480	600	1,785	900	2,197
200	590	400	955	600	1,128	800	1,408	1,200	1,720
250	417	600	514	900	580	1,200	780	1,800	970
300	274	800	155	1,200	130	1,600	280	2,400	370
350	130	1,000	(-145)	1,500	(-250)	2,000	(-140)	3,000	(-140)
400	4								
$p_1 = 400$		$p_1 = 600$		$p_1 = 800$		$p_1 = 1,000$			
p_2	w_2	p_2	w_2	p_2	w_2	p_2	w_2	p_2	w_2
0	17,310	0	21,120	0	24,380	0	27,290		
40	7,370	60	9,004	80	10,400	100	11,640		
80	6,540	120	7,997	160	9,240	200	10,350		
160	5,650	240	6,904	320	7,980	400	8,935		
240	5,090	360	6,223	480	7,191	600	8,057		
320	4,680	480	5,723	640	6,615	800	7,410		
[400]	[4,350]	[600]	[5,320]	[800]	[6,150]	[1,000]	[6,890]		
600	3,729	900	4,561	1,200	5,275	1,500	5,910		
800	3,260	1,200	3,990	1,600	4,625	2,000	5,172		
1,200	2,555	1,800	3,130	2,400	3,622	3,000	4,060		
1,600	2,010	2,400	2,460	3,200	2,850	4,000	3,200		
2,400	1,150	3,600	1,410	4,800	1,640	6,000	1,840		
3,200	450	4,800	560	6,400	660	8,000	740		
4,000	(-130)	6,000	(-155)	8,000	(-160)	10,000	(-170)		









§ 7.11 Free surface [cf 145]

7.1(2) becomes with $p_2 = 0$

$$\omega_2 = \omega_1 + (\lambda - 1)a_1 = \omega_1 + \frac{2a_1}{\gamma - 1}. \quad (1)$$

The subsequent motion is therefore identical with escape from pressure p_1 into a vacuum, save that a velocity w_1 is superimposed.

Since, by 6.2(2,4), if $\pi_i \equiv p_i/p_0$,

$$\frac{(\lambda - 1)a_1}{w_1} = \frac{\sqrt{(\lambda + 1)\pi_i(\pi_i + \lambda)}}{\pi_i - 1}, \quad (2)$$

and it can be shown (§ 7.111) that the right side of (2) is necessarily greater than unity, it follows that $w_2 > 2w_1$, as compared with the acoustic case, where $w_2 = 2w_1$.

Since the nose of the rarefaction spreads backward with velocity $-a_1 + w_1$, the overall length of the rarefaction increases at constant rate λa_1 . The velocity and other profiles have been described in § 4.7.

§ 7.111 Proof that $\sqrt{(\lambda + 1)\pi_i(\pi_i + \lambda)} / (\pi_i - 1) > 1$.

The proposition holds provided

$$\lambda\pi_i^2 + (\lambda^2 + \lambda + 2)\pi_i - 1 > 0,$$

which is true, unless π_i lies between

$$\frac{1}{2\lambda} \left\{ -(\lambda^2 + \lambda + 2) \pm \sqrt{(\lambda^2 + \lambda + 2)^2 + 4\lambda} \right\}.$$

Since $\pi_i > 1$, the proposition fails, therefore, only if

$$(\lambda^2 + \lambda + 2)^2 + 4\lambda > (\lambda^2 + 3\lambda + 2)^2,$$

i.e. if

$$\lambda(\lambda^2 + 2\lambda + 1) < 0,$$

which is evidently impossible since $\lambda > 0$.

§ 7.12 Rigid boundary [Cf. 145, 160, 132, 71, 123, 124]

When $w_2 = 0$, 7.1(1,2), together with 6.2(2) give:

$$\frac{\pi_2 - 1}{\sqrt{\lambda \pi_2 + 1}} \cdot \sqrt{\frac{\pi_i(\pi_i + \lambda)}{\lambda \pi_i + 1}} = \frac{\pi_i - 1}{\sqrt{\lambda \pi_i + 1}}, \quad (1)$$

where $\pi_2 \equiv p_2/p_1$.

On simplification, (1) leads to

$$\pi_2 = \frac{(\lambda+2)\pi_i - 1}{\pi_i + \lambda}. \quad (2)$$

If we write $\pi_n' \equiv \pi_n - 1$, (2) may be exhibited in the symmetrical form:

$$\frac{1}{\pi_2'} = \frac{1}{\pi_i'} + \frac{1}{\lambda + 1}. \quad (3)$$

But, by 6.2(1)

$$\varphi_i \equiv \frac{v_i}{v_o} = \frac{\pi_i + \lambda}{\lambda \pi_i + 1} \quad \text{and} \quad \varphi_2 \equiv \frac{v_2}{v_i} = \frac{\pi_2 + \lambda}{\lambda \pi_2 + 1}$$

Hence, by (2)

$$\varphi_2 = \frac{2\pi_i + \lambda - 1}{(\lambda + 1)\pi_i}, \quad (4)$$

so that

$$\frac{v_2}{v_o} = \frac{(\pi_i + \lambda)(2\pi_i + \lambda - 1)}{(\lambda + 1)\pi_i(\lambda \pi_i + 1)}. \quad (5)$$

Also, eliminating π_i from (4),

$$\varphi_2 = \frac{(\lambda+2)\varphi_i + 1}{\lambda - \varphi_i}, \quad (6)$$

which, if $\varphi_n' \equiv 1 - \varphi_n$, can be exhibited in the symmetrical form:

$$\frac{1}{\varphi_2'} = \frac{1}{\varphi_i'} + \frac{1}{\lambda - 1}. \quad (7)$$

Again

$$\tau_2 \equiv \frac{a_2^2}{a_i^2} = \frac{T_2}{T_i} = \pi_2 \varphi_2 = \frac{[(\lambda+2)\pi_i - 1][2\pi_i + \lambda - 1]}{(\lambda + 1)\pi_i(\pi_i + \lambda)}, \quad (8)$$

so that

$$\frac{a_2^2}{a_o^2} = \frac{T_2}{T_o} = \frac{[(\lambda+2)\pi_i - 1][2\pi_i + \lambda - 1]}{(\lambda + 1)(\lambda \pi_i + 1)}, \quad (9)$$

Also, by 6.2(3)

$$\delta_1 \equiv \frac{D_1^2}{a_0^2} = \frac{\lambda\pi_1+1}{\lambda+1} \quad \text{and} \quad \delta_2 \equiv \frac{D_2^2}{a_0^2} = \frac{\lambda\pi_2+1}{\lambda+1},$$

where D denotes the algebraic velocity of a wave relative to the gas ahead of it.

Hence

$$\delta_2 = \frac{(\lambda+1)\pi_1}{\pi_1+\lambda}, \quad (10)$$

so that

$$\frac{D_2^2}{a_0^2} = \delta_2 \tau_1 = (\lambda+1) \frac{\pi_1^2}{\lambda\pi_1+1}, \quad (11)$$

and

$$\delta_2 = \frac{(\lambda+1)\delta_1-1}{\delta_1+\lambda-1}. \quad (12)$$

If $\delta_n' \equiv \delta_{n-1}$, (12) can be exhibited more symmetrically as:

$$\frac{1}{\delta_2'} = \frac{1}{\delta_1'} + \frac{1}{\lambda}. \quad (13)$$

For the wave velocity d_2 relative to the boundary, measured in the sense of d_1 , we have

$$\frac{d_2}{a_1} = \frac{w_1 + D_2}{a_1} = - \frac{2\pi_1 + \lambda - 1}{\sqrt{(\lambda+1)\pi_1(\pi_1+\lambda)}}, \quad (14)$$

by 6.2(2,3,4).

Consequently

$$-\frac{d_2}{a_0} = \frac{2\pi_1 + \lambda - 1}{\sqrt{(\lambda+1)(\lambda\pi_1+1)}}, \quad (15)$$

and

$$-\frac{d_2}{D_1} = \frac{2\pi_1 + \lambda - 1}{\lambda\pi_1+1}. \quad (16)$$

$-d_2/a_0$ has a minimum equal to $\frac{2}{\lambda} \sqrt{2(\lambda-2)}$ [0.9428]*

when $\pi_1 = (\lambda^2 - \lambda - 4)/2\lambda$ [2.17].

A further quantity of some interest is

$$\Delta E_2 \equiv E_2 - E_1 = c_v(\tau_2 - \tau_1).$$

By 6.2(2) and equation (8), it is easily shown that

$$\frac{\Delta E_2}{\Delta E_1} = \frac{(\lambda+3)\pi_1 + \lambda - 1}{(\lambda+1)(\pi_1+1)}. \quad (17)$$

* The [bracketed] figures correspond to $\gamma = 1.4$

Various useful conclusions can be drawn from the above results. Thus by equation (2), as $\pi_1 \rightarrow 1$, $\pi_2 \rightarrow 1$ also; and

$$\frac{\pi_2 - p_1}{p_1 - p_0} = \pi_1 \cdot \frac{\pi_2 - 1}{\pi_1 - 1} = \frac{(\lambda+1)\pi_1}{\pi_1 + \lambda} \rightarrow 1. \quad (18)$$

The intensity of weak waves is therefore doubled on reflexion.

However, as $\pi_1 \rightarrow \infty$, $\pi_2 \rightarrow \lambda+2$ [8]; the intensity of strong waves thus increases many-fold. On the other hand,

$$\pi_2 - \pi_1 = - \frac{(\pi_1 - 1)^2}{\pi_1 + \lambda} < 0 ; \text{ i.e. } \pi_2 > \pi_1 > 1. \quad (19)$$

Similarly, as $\pi_1 \rightarrow 1$, $\varphi_2 \rightarrow 1$, $\frac{v_2 - v_1}{v_0 - v_1} \rightarrow 1$; and as $\pi_1 \rightarrow \infty$,

$$\varphi_2 \rightarrow \frac{2}{\lambda+1} \quad \left[\frac{2}{7} \right], \text{ and so } \frac{v_2}{v_0} \rightarrow \frac{2}{\lambda(\lambda+1)} \quad \left[\frac{1}{21} \right]; \text{ while } 1 > \varphi_2 > \varphi_1.$$

Again, as $\pi_1 \rightarrow 1$, $\tau_2 \rightarrow 1$, $\frac{\tau_2 - \tau_1}{\tau_1 - \tau_0} \rightarrow 1$; and as $\pi_1 \rightarrow \infty$,

$$\tau_2 \rightarrow \frac{2(\lambda+2)}{\lambda+1} \quad \left[\frac{16}{7} \right]; \text{ while } 1 < \tau_2 < \tau_1. \quad \text{The temperature rise}$$

in the incident wave is thus approximately doubled for any π_1 . Again,

as $\pi_1 \rightarrow 1$, $\delta_2 \rightarrow 1$, and $-D_2 \rightarrow a_0$; while as $\pi_1 \rightarrow \infty$, $\delta_2 \rightarrow \lambda+1$ [7]

and $-D_2/a_0$ and $-d_2/a_0$ increase without limit as $\sqrt{\frac{\lambda+1}{\lambda} \cdot \pi_1}$. $\left[\sqrt{\frac{\pi_1}{6}} \right]$

and $\frac{2\sqrt{\pi_1}}{\sqrt{\lambda(\lambda+1)}} \quad \left[2\sqrt{\frac{\pi_1}{42}} \right]$ respectively, though $-\frac{d_2}{d_1} \rightarrow \frac{2}{\lambda} \quad \left[\frac{1}{3} \right]$.

The meaning of these results is more readily appreciated from a selection of numerical values, such as are given in Table 7.12:1 for $\lambda = 6$ ($\gamma = 1.4$).

Table 7.12:

Rigid reflexion of plane shock waves in an ideal gas with constant $\gamma = 1.4$. For symbols see § 7.12

$\frac{P}{P_0}$	$\frac{P_1}{P_0}$	T_1/T_0	ω_1/a_0	d_1/a_0	P_2/P_0	T_2/T_0	τ_2/τ_0	$-d_2/a_0$	$-d_2/d_1$
1	1	1	0	1	1	1	1	1	1
1.2	1.14	1.05	0.132	1.08	1.195	1.434	1.137	1.296	1.05
1.5	1.33	1.13	0.299	1.20	1.47	2.21	1.31	1.74	1.12
2	1.63	1.23	0.525	1.36	1.88	3.76	1.56	2.54	1.21
3	2.11	1.42	0.867	1.65	2.56	7.68	1.91	4.03	1.34
4	2.50	1.60	1.133	1.89	3.10	12.4	2.15	5.37	1.44
5	2.82	1.77	1.36	2.10	3.54	17.7	2.33	6.57	1.52
10	3.82	2.62	2.18	2.95	4.94	49.4	2.80	10.70	1.76
20	4.65	4.31	3.26	4.16	6.12	122.4	3.11	14.46	1.97
50	5.38	9.31	5.34	6.55	7.12	356	3.33	17.9	2.14
100	5.67	17.6	7.64	9.27	7.53	753	3.42	19.4	2.20
200	5.83	34.4	10.85	13.10	7.77	1554	3.46	20.2	2.25
500	5.93	84.3	17.25	20.7	7.90	3950	3.48	20.6	2.27
1000	5.97	168	24.37	29.3	7.95	7950	3.49	20.8	2.28
∞	6	∞	∞	∞	8	∞	3.5	21	2.29
							∞	∞	∞
									0.333

§ 7.121 Comparison of $p_s - p_0$ with Rudenberg's "Impulsstromdichte"

The expression $p_s - p_0$, where

$$p_s \equiv p_i + \rho_i \omega_i^2 \quad (1)$$

^[144, 147]
was proposed by Rudenberg as a measure of the effect on a plane obstacle of a shock wave behind which the pressure, density and fluid velocity were p_i , ρ_i , ω_i . The correct representation is $p_2 - p_0$ as defined in §7.
^[53]
For an ideal gas and a rigid obstacle, however, as Döring has pointed out, the two pressures are closely related. Thus by (1) and 6.2(1,5),

$$\frac{p_s - p_0}{p_i} = \frac{(\lambda \pi_{i+1})(\pi_{i-1})}{\pi_i(\lambda + \pi_i)}, \quad (2)$$

while, by 7.12(2)

$$\frac{p_2 - p_0}{p_i} = \frac{[(\lambda + 2)\pi_i + \lambda](\pi_{i-1})}{\pi_i(\lambda + \pi_i)}. \quad (3)$$

Hence

$$\frac{p_s - p_0}{p_2 - p_0} = \frac{\lambda \pi_{i+1}}{(\lambda + 2)\pi_i + \lambda}. \quad (4)$$

When $\pi_{i-1} \ll 1$, this approaches $\frac{1}{2}$.

When $\pi_i \gg 1$, it approaches $\frac{1}{\lambda + 2} = \begin{cases} 1 & \text{for } \gamma = 1 \\ 2/3 & \text{for } \gamma = 5/3 \end{cases}$

When $\lambda = 2$ ($\gamma = 3$), the ratio is $1/2$, irrespective of π_i .

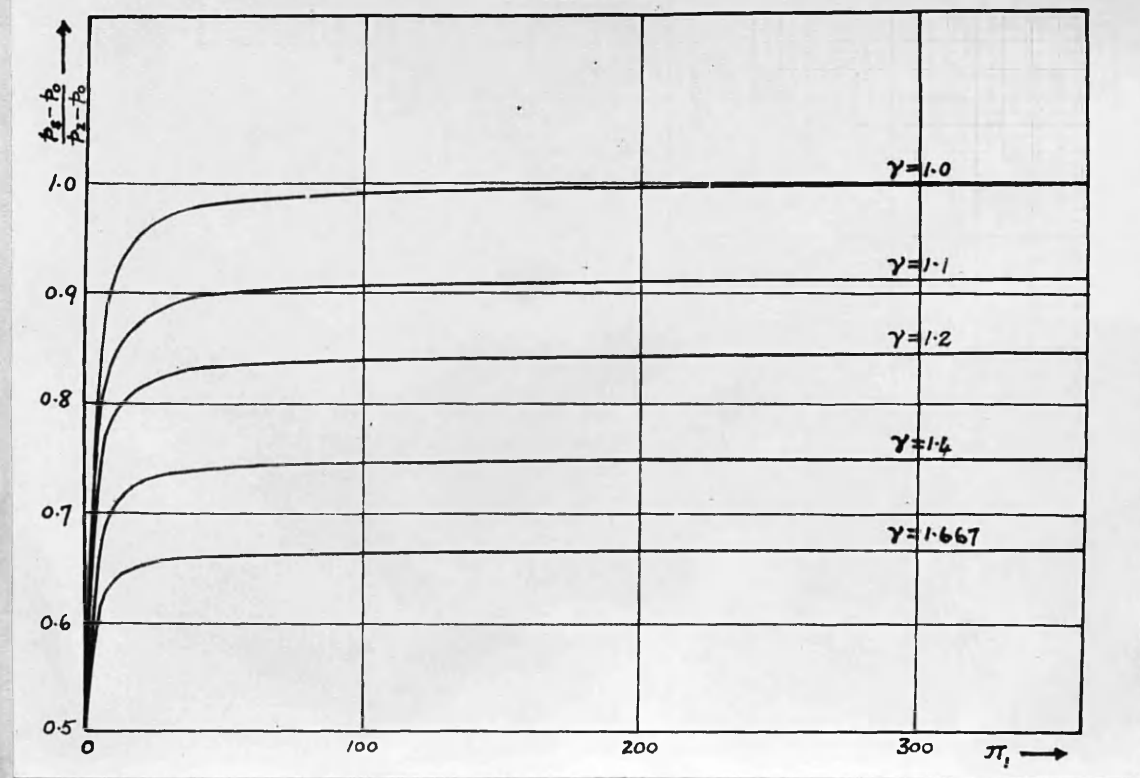
The ratio is shown in Table 7.121:1 and Fig. 7.121:1 for typical values of γ . It can be seen that the Rudenberg expression gives a correct qualitative account of the effect, though seriously underestimating it, except for small γ and large π_i .

Table 7.121:1

$(P_s - P_0) / (P_2 - P_0)$ as a function of π_i and γ

π_i	γ	1.0	1.1	1.2	1.4	1.667
:	:	:	:	:	:	:
:	1	0.5	0.5	0.5	0.5	0.5
:	1.2	0.545	0.540	0.534	0.526	0.518
:	1.5	0.6	0.585	0.574	0.556	0.538
:	2	0.667	0.642	0.622	0.591	0.562
:	3	0.75	0.712	0.680	0.633	0.591
:	4	0.8	0.752	0.714	0.658	0.607
:	5	0.833	0.780	0.737	0.674	0.618
:	10	0.909	0.840	0.787	0.710	0.640
:	20	0.953	0.875	0.815	0.729	0.653
:	50	0.98	0.898	0.834	0.742	0.661
:	100	0.99	0.905	0.840	0.745	0.663
:	200	0.995	0.910	0.843	0.748	0.665
:	500	0.998	0.912	0.845	0.749	0.666
:	1000	0.999	0.913	0.846	0.750	0.667
:	∞	1	0.913	0.847	0.750	0.667
:	:	:	:	:	:	:

FIG 7.121:1.



§ 7.13 Compression of an ideal gas between a rigid wall and a piston moving with constant velocity [123, 124]

The form of equations 7.12(3, 7, 13) enables us to extend the analysis of § 7.12 to the problem of repeated reflections in an ideal gas compressed against a rigid wall by a rigid piston which moves with constant velocity U . As usual, let suffix o refer to conditions before the piston commences to move. When the velocity U is suddenly communicated to the piston, a shock wave (S_1) traverses the gas, to be reflected in turn from wall and piston as successive shock waves $S_2, S_3, \dots, S_n, \dots$. Let D_n, W_n be the algebraic velocities of S_n and of the gas behind it, respectively, relative to the gas ahead; d_n, w_n the corresponding velocities relative to the fixed wall. p_n, v_n etc. denote quantities behind S_n . Further, for convenience, let $\pi_n \equiv p_n/p_{n-1}$, $\varphi_n \equiv v_n/v_{n-1}$, $\tau_n \equiv T_n/T_{n-1} = a_n^2/a_{n-1}^2$, $\delta_n \equiv D_n^2/a_{n-1}^2$, $\psi_n \equiv W_n^2/a_{n-1}^2$.

Then, by the equations of § 6.2,

$$\varphi_n = \frac{\pi_n + \lambda}{\lambda \pi_n + 1}, \quad (1)$$

$$\psi_n = \frac{(\lambda - 1)^2 (\pi_n - 1)^2}{(\lambda + 1)(\lambda \pi_n + 1)}, \quad (2)$$

$$\delta_n = \frac{\lambda \pi_n + 1}{\lambda + 1}, \quad (3)$$

$$\tau_n = \varphi_n \pi_n = \pi_n \cdot \frac{\pi_n + \lambda}{\lambda \pi_n + 1}. \quad (4)$$

However, we have also

$$d_{2n+1} = D_{2n+1}, \quad n = 0, 1, 2, \dots \quad (5)$$

$$d_{2n} = D_{2n} + U, \quad n = 1, 2, \dots \quad (6)$$

$$w_{2n+1} = U, \quad n = 0, 1, 2, \dots \quad (7)$$

$$w_{2n} = 0, \quad n = 1, 2, \dots \quad (8)$$

$$W_n = w_n - w_{n-1} = (-1)^{n+1} U, \quad n = 1, 2, \dots \quad (9)$$

From (9),

$$\psi_{n-1} = \psi_n \tau_{n-1},$$

and so, by (2) and (4),

$$\frac{(\pi_{n-1}-1)^2}{\pi_{n-1}(\pi_{n-1}+\lambda)} = \frac{(\pi_{n-1})^2}{\lambda\pi_n+1},$$

whence

$$\pi_n = \frac{(\lambda+1)\pi_{n-1}-1}{\pi_{n-1}+\lambda}. \quad (10)$$

Equation (10), therefore, which is exactly analogous to 7.12(2), applies not only to the first, but also (as a recurrence formula) to all subsequent reflexions. As in § 7.12, we deduce:

$$\varphi_n = \frac{(\lambda-1)\varphi_{n-1}+1}{\lambda-\varphi_{n-1}}, \quad (11)$$

$$\delta_n = \frac{(\lambda+1)\delta_{n-1}-1}{\delta_{n-1}+\lambda-1}. \quad (12)$$

The bilinear recurrence formulae (10, 11, 12) can be written:

$$\frac{1}{\pi'_n} = \frac{1}{\pi'_{n-1}} + \frac{1}{\lambda+1}, \quad (13)$$

$$\frac{1}{\varphi'_n} = \frac{1}{\varphi'_{n-1}} + \frac{1}{\lambda-1}, \quad (14)$$

$$\frac{1}{\delta'_n} = \frac{1}{\delta'_{n-1}} + \frac{1}{\lambda}, \quad (15)$$

where $\pi'_n \equiv \pi_{n-1}$, $\varphi'_n \equiv 1-\varphi_n$, $\delta'_n \equiv \delta_{n-1}$.

Hence

$$\pi'_{n+1} = \frac{(\lambda+1)\pi'_n}{\lambda+1+n\pi'_n}, \quad (16)$$

$$\varphi'_{n+1} = \frac{(\lambda-1)\varphi'_n}{\lambda-1+n\varphi'_n} = \frac{(\lambda-1)\pi'_n}{\lambda+1+n\pi'_n}, \quad \text{by (1)} \quad (17)$$

$$\delta'_{n+1} = \frac{\lambda\delta'_n}{\lambda+n\delta'_n} = \frac{\lambda\pi'_n}{\lambda+1+n\pi'_n}, \quad \text{by (3)}. \quad (18)$$

As examples of the use of (16, 17, 18) we may write down the values of π , φ and δ for the first few reflected waves:

$$\begin{aligned}\pi_2 &= \frac{(\lambda+2)\pi_i - 1}{\pi_i + \lambda} = \frac{(3\gamma-1)\pi_i - (\gamma-1)}{(\gamma-1)\pi_i + \gamma + 1} \\ \pi_3 &= \frac{(\lambda+3)\pi_i - 2}{2\pi_i + \lambda - 1} = \frac{(2\gamma-1)\pi_i - (\gamma-1)}{(\gamma-1)\pi_i + 1} \\ \pi_4 &= \frac{(\lambda+4)\pi_i - 3}{3\pi_i + \lambda - 2} = \frac{(5\gamma-3)\pi_i - 3(\gamma-1)}{3(\gamma-1)\pi_i + 3 - \gamma}\end{aligned}\quad (19)$$

etc.

$$\begin{aligned}\varphi_2 &= \frac{(\gamma-1)\pi_i + 1}{\gamma\pi_i} \\ \varphi_3 &= \frac{3(\gamma-1)\pi_i + 3 - \gamma}{(3\gamma-1)\pi_i - (\gamma-1)} \\ \varphi_4 &= \frac{2(\gamma-1)\pi_i + 2 - \gamma}{(2\gamma-1)\pi_i - (\gamma-1)}\end{aligned}\quad (20)$$

etc.

$$\begin{aligned}\delta_2 &= \frac{2\gamma\pi_i}{\gamma + 1 + (\gamma-1)\pi_i} \\ \delta_3 &= \frac{(3\gamma-1)\pi_i - (\gamma-1)}{2[(\gamma-1)\pi_i + 1]} \\ \delta_4 &= \frac{2[(2\gamma-1)\pi_i - (\gamma-1)]}{3(\gamma-1)\pi_i + 3 - \gamma}\end{aligned}\quad (21)$$

etc.

Expressions for ψ_{n+1} , τ_{n+1} , etc. can be derived as follows from (2, 9, 16).

$$\frac{a_n^2}{U^2} = \frac{1}{\psi_{n+1}} = \frac{[\lambda + i + n\pi_i'][\lambda + i + (n+\lambda)\pi_i']}{(\lambda - 1)^2(\pi_i')^2}, \quad (22)$$

and so

$$\tau_{n+1} = \psi_{n+1}/\psi_{n+2} = \frac{[\lambda + i + (n+1)\pi_i'][\lambda + i + (\lambda + n+1)\pi_i']}{[\lambda + i + n\pi_i'][\lambda + i + (\lambda + n)\pi_i']}, \quad (23)$$

and

$$\frac{T_n}{T_0} = \frac{a_n^2}{a_0^2} = \frac{\psi_i}{\psi_{n+1}} = \frac{[\lambda_{+1} + n\pi_i'] [\lambda_{+1} + (\lambda+n)\pi_i']}{(\lambda_{+1})(\lambda\pi_i' + \lambda_{+1})}. \quad (24)$$

A recurrence formula not involving π_i can also be obtained for τ_n :

it is, however, much less elegant and useful than (13, 14, 15):

$$\tau_n = \frac{2(\lambda^2 - 2)}{\lambda^2 - 1} - \frac{\lambda_{+1}}{(\lambda^2 - 1)\tau_{n-1}} + \frac{2\sqrt{\{\lambda^2(\tau_{n-1})^2 + 4\tau_{n-1}\}}}{(\lambda^2 - 1)\tau_{n-1}}. \quad (25)$$

D_{n+1} and d_{n+1} are now evaluated as follows:

$$(-1)^n \frac{D_{n+1}}{U} = \sqrt{(\delta_{n+1}/\psi_{n+1})} = \frac{\lambda_{+1} + (\lambda+n)\pi_i'}{(\lambda_{-1})\pi_i'}, \quad \text{by (18) and (22)}, \quad (26)$$

whence

$$(-1)^n \frac{D_{n+1}}{a_0} = \frac{(\lambda+n)\pi_i' - (n-1)}{\sqrt{(\lambda_{+1})(\lambda\pi_i' + 1)}}, \quad (27)$$

$$\frac{d_{2n+1}}{U} = \frac{(\lambda_{+1}) + (\lambda+2n)\pi_i'}{(\lambda_{-1})\pi_i'}, \quad (28)$$

$$\frac{d_{2n+1}}{a_0} = \frac{(\lambda+2n)\pi_i' - (2n-1)}{\sqrt{(\lambda_{+1})(\lambda\pi_i' + 1)}}, \quad (29)$$

$$-\frac{d_{2n}}{U} = \frac{\lambda_{+1} + 2n\pi_i'}{(\lambda_{-1})\pi_i'}, \quad (30)$$

$$-\frac{d_{2n}}{a_0} = \frac{2n\pi_i' + \lambda_{+1} - 2n}{\sqrt{(\lambda_{+1})(\lambda\pi_i' + 1)}}. \quad (31)$$

The following relations are readily deduced:

$$\left. \begin{array}{ll} 1 < \pi_{n+1} < \pi_n & \text{and} \quad \pi_n \rightarrow 1 \quad \text{as} \quad n \rightarrow \infty \\ 1 > \varphi_{n+1} > \varphi_n & \text{and} \quad \varphi_n \rightarrow 1 \quad \text{as} \quad n \rightarrow \infty \\ 1 < \delta_{n+1} < \delta_n & \text{and} \quad \delta_n \rightarrow 1 \quad \text{as} \quad n \rightarrow \infty \\ 1 < \tau_n < \tau_{n+1} & \text{and} \quad \tau_n \rightarrow 1 \quad \text{as} \quad n \rightarrow \infty \end{array} \right\} \quad (32)$$

Also, by (27)

$$|D_{n+1}| > |D_n| > a_0, \quad (33)$$

and by (28,30)

$$d_{2n+1} + d_{2n} = \frac{\lambda U}{\lambda - 1} > 0 ;$$

and

$$d_{2n} + d_{2n-1} = \frac{(\lambda-2)U}{\lambda - 1}.$$

Thus $|d_{2n+1}| > |d_{2n}|$, and (unless indeed $\gamma > 3$)

$$|d_{2n}| < |d_{2n-1}|.$$

Also,

$$d_{n+1} - d_{n-1} = (-1)^n \frac{2U}{\lambda - 1}.$$

The absolute velocity of successive waves in any one direction therefore increases by $2U/(\lambda - 1)$; but while reflexion at the piston enhances d , reflexion at the wall reduces it (unless $\gamma > 3$).

The $p_n - v_n - T_n$ relationship

From (16), we have

$$\frac{p_n}{p_0} = \frac{\Gamma(x) \Gamma(x + \lambda + 1 + n)}{\Gamma(x + \lambda + 1) \Gamma(x + n)}, \quad (34)$$

and from (17)

$$\frac{v_n}{v_0} = \frac{\Gamma(x + \lambda) \Gamma(x + n + 1)}{\Gamma(x + 1) \Gamma(x + \lambda + n)} \quad (35)$$

where $\Gamma(x)$ is the gamma function, and for convenience we have written x for $(\lambda + 1)/\pi'$. (34) and (35), with (24), define the $p-v-T$ relations for the compression. Thus, the n -eliminants of these equations, two at a time, replace the ordinary adiabatic

$$t = (\frac{p_n}{p_0}) (\frac{v_n}{v_0})^\gamma = (\frac{p_n}{p_0})^{\gamma-1} (\frac{T_n}{T_0})^{-\gamma} = (\frac{v_n}{v_0})^{\gamma-1} (\frac{T_n}{T_0}), \quad (36)$$

and might be called the "dynamic adiabatic" for the compression.

n cannot be eliminated explicitly; however, if U/a_0 , and so π' , are

small, then $\frac{\lambda+1}{\pi'_i}$ and $\frac{\lambda+1}{\pi'_i} + n$ are both large, irrespective of the value of n . Hence, by the asymptotic formula for $\Gamma(x)$,

$$\Gamma(x+\lambda+1+n) \sim (x+n)^{\lambda+1} \Gamma(x+n)$$

$$\Gamma(x+\lambda+1) \sim x^{\lambda+1} \Gamma(x),$$

so that

$$\frac{p_n}{p_0} \sim \left(1 + \frac{n}{x}\right)^{\lambda+1}. \quad (37)$$

Similarly,

$$\frac{v_n}{v_0} \sim \left(1 + \frac{n}{x}\right)^{1-\lambda}. \quad (38)$$

Then

$$p_n v_n^\gamma \sim p_0 v_0^\gamma. \quad (39)$$

That is, the ordinary adiabatic is closely followed throughout the compression.

If n is also small, from (37, 38)

$$p_n/p_0 \sim 1 + n\pi'_i$$

$$v_n/v_0 \sim 1 - \frac{\lambda-1}{\lambda+1} n\pi'_i \sim 1 - n\phi'_i$$

Hence

$$p_n - p_0 \sim n(p_i - p_0) \quad (40)$$

$$v_0 - v_n \sim n(v_0 - v_i), \quad (41)$$

and so also

$$T_n - T_0 \sim n(T_i - T_0). \quad (42)$$

That is, the pressure, volume and temperature changes produced by the first wave are approximately doubled in the second, trebled in the third, and so on.

When π'_i is not small, p_n and v_n are not connected by the ordinary adiabatic relation (39). The changes in p , v , T in successive waves can be deduced at once from (16, 17, 23, 24, 27, 29, 31).

Thus,

$$\pi_{n+1} \sim \frac{\lambda+n+1}{n} \quad (43)$$

$$\varphi_{n+1} \sim \frac{n+1}{\lambda+n} \quad (44)$$

$$\tau_{n+1} \sim \frac{(n+1)(\lambda+n+1)}{n(\lambda+n)} \quad (45)$$

$$T_n/T_0 \sim \frac{n(\lambda+n)}{\lambda(\lambda+1)} \cdot \pi_i \quad (46)$$

$$D_{n+1} \sim (-1)^n \frac{\lambda+n}{\lambda-1} U \sim (-1)^n \frac{(\lambda+n)a_0}{\sqrt{\lambda(\lambda+1)}} \cdot \sqrt{\pi_i} \quad (47)$$

$$d_{2n+1} \sim \frac{\lambda+2n}{\lambda-1} U \sim \frac{(\lambda+2n)a_0}{\sqrt{\lambda(\lambda+1)}} \cdot \sqrt{\pi_i} \quad (48)$$

$$d_{2n} \sim -\frac{2n}{\lambda-1} U \sim \frac{2na_0}{\sqrt{\lambda(\lambda+1)}} \cdot \sqrt{\pi_i} \quad (49)$$

When n is large, however, a further application of the asymptotic formula for the Γ -function gives:

$$\frac{p_n}{p_0} \sim \frac{n^{\lambda+1} \Gamma(x)}{\Gamma(x+\lambda+1)} , \quad (50)$$

$$\frac{v_n}{v_0} \sim \frac{n^{1-\lambda} \Gamma(x+\lambda)}{\Gamma(x+1)} , \quad (51)$$

x having the same meaning as before (i.e. $\frac{\lambda+1}{\pi_i}$).

Hence

$$p_n v_n^\gamma \sim A p_0 v_0^\gamma , \quad (52)$$

where

$$A \equiv \frac{1}{x(\lambda+x)} \left[\frac{\Gamma(x+\lambda)}{\Gamma(x+1)} \right]^{\gamma-1} . \quad (53)$$

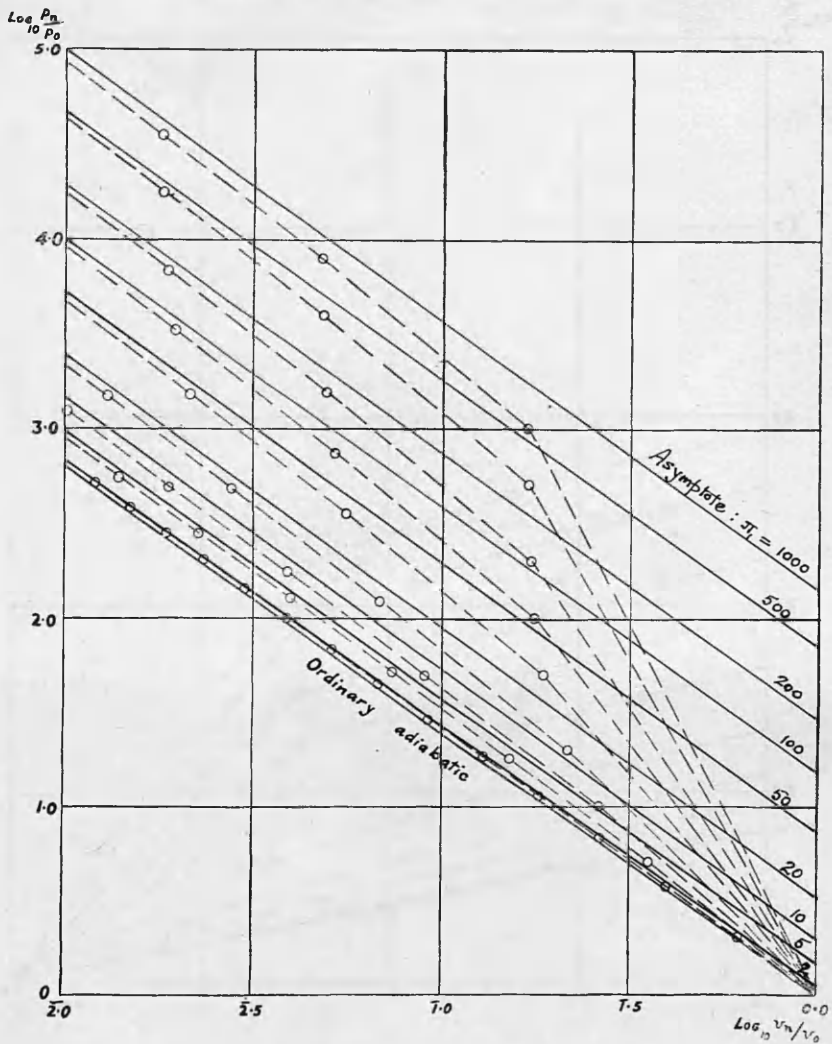
(v_n, p_n) thus ultimately follows an ordinary adiabatic, though not that through (v_0, p_0) . It is indeed natural that this should be so, since each succeeding shock wave has a smaller pressure ratio than its predecessor, and therefore causes a smaller entropy change (equation 6.2(7)). This entropy change becomes in fact vanishingly small as the order of the wave increases: hence the "dynamic adiabatic" must in the end become indistinguishable from an isentropic. From a hydrodynamic standpoint, equation (18) shows that $\delta_n \rightarrow 1$ as $n \rightarrow \infty$, irrespective of the value of π_i . The shock waves, though travelling with higher and higher velocities as their order rises, degenerate simultaneously into sound waves in the medium through which they are propagated*.

A few values of A for $\gamma = 1.4$ are given in Table 7.13:1. As π_i' becomes larger, A approaches $[\Gamma(\lambda)]^{\gamma-1} \cdot \pi_i' / \lambda(\lambda+1)$. The relation between t_n , v_n and T_n is shown for the same values of π_i in Figs. 7.13:1, 2 together with the isentropic asymptotes.

Table 7.13:1

U/a_0	π_i	A	U/a_0	π_i	A
0.0	1	1.0	5.34	50	8.73
0.524	2	1.08	7.63	100	16.85
1.36	5	1.59	10.75	200	33.0
2.18	10	2.31	17.2	500	81.3
3.27	20	3.91	24.4	1000	162.5

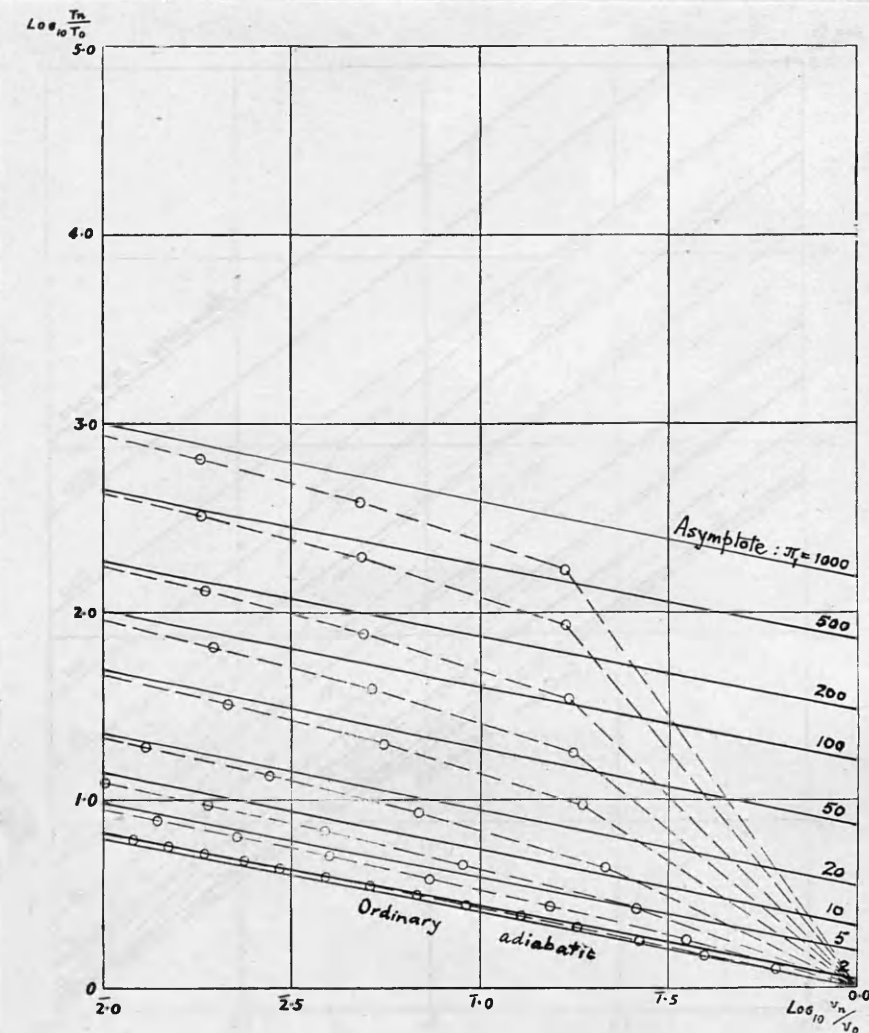
* I am indebted to Sir Geoffrey Taylor for pointing out to me this explanation of (52).



Repeated reflection of shock-waves in an ideal gas with γ constant and equal to 1.4.

The broken curves, reading down, correspond to $\pi_1 = 1000, 500, 200, 100, 50, 20, 10, 5, 2$. The points on each, reading from right to left, represent conditions behind the first, second, etc., waves. The full curve is the ordinary adiabatic.

FIG. 7.13:1



Repeated reflection of shock-waves in an ideal gas with γ constant and equal to 1.4.

The broken curves, reading down, correspond to $\pi_1 = 1000, 500, 200, 100, 50, 20, 10, 5, 2$. The points on each, reading from right to left, represent conditions behind the first, second, etc., waves. The full curve is the ordinary adiabatic.

FIG. 7.13: 2

§ 7.14 Normal reflexion of steady plane shocks at the interface between two ideal gases [28]

Referring to §7.1, let us suppose that the adjoining medium is a second ideal gas, initially at the same pressure (p_0) and temperature (T_0) as the first. Its specific volume at the outset is v_0' and its ratio of specific heats γ' . Equation 7.1(2) is then to be taken in conjunction with the RH(p, w)-relation for the second gas, namely:

$$\omega_3 = \sqrt{\lambda' - 1} v_0' \cdot \frac{p_3 - p_0}{\sqrt{\lambda' p_3 + p_0}}. \quad (1)$$

This equation presents ω_3 as a monotonic function of p_3 , which increases from 0 when $p_3 = p_0$. It is therefore clear that 7.1(2) and equation (1) are bound to provide a single solution (p, ω) , with $p > p_0$, $\omega > 0$, when we set $p_3 = p_2 \equiv p$ and $\omega_3 = \omega_2 \equiv \omega$. This solution can be obtained without difficulty in practice with the aid of a graph, or by a process of successive approximation, though not analytically. The type of wave reflected depends upon whether p , obtained in this way, is $>$ or $< p_1$; or in other words whether ω is $<$ or $> \omega_1$. In view, however, of the monotonic nature of ω_2 and ω_3 , this criterion can be transformed, as indicated in §7.01. The condition for a reflected shock is then, by 7.01(1) and 7.1(1),

$$\sqrt{\lambda' - 1} v_0' \cdot \frac{p_1 - p_0}{\sqrt{\lambda' p_1 + p_0}} < \sqrt{\lambda - 1} v_0 \cdot \frac{p_1 - p_0}{\sqrt{\lambda p_1 + p_0}}, \quad (2)$$

that is,

$$\frac{(\lambda - 1)v_0}{\lambda \pi_1 + 1} > \frac{(\lambda' - 1)v_0'}{\lambda' \pi_1 + 1}, \quad (3)$$

which may be written

$$(\pi_1 - 1) [(\gamma + 1)p_0 - (\gamma' + 1)p_0'] < 2 [\gamma p_0' - \gamma p_0]. \quad (4)$$

Four alternatives then arise:

$$(a) \quad \gamma p_o < \gamma' p'_o \quad \text{and} \quad (\gamma+1)p_o < (\gamma'+1)p'_o.$$

Then (4) is satisfied irrespective of $\pi_i (> 1)$, and the reflected wave is always a shock.

$$(b) \quad \gamma p_o > \gamma' p'_o \quad \text{and} \quad (\gamma+1)p_o > (\gamma'+1)p'_o.$$

Then (4) cannot be satisfied for any π_i , and the reflected wave is always a rarefaction.

$$(c) \quad \gamma p_o < \gamma' p'_o \quad \text{but} \quad (\gamma+1)p_o > (\gamma'+1)p'_o$$

Then (4) is satisfied for $\pi_i < \pi_{i_0}$, but not for $\pi_i > \pi_{i_0}$, where

$$\pi_{i_0} = \frac{(\gamma'-1)p'_o - (\gamma-1)p_o}{(\gamma+1)p_o - (\gamma'+1)p'_o}. \quad (5)$$

Thus for $\pi_i < \pi_{i_0}$, S_2 is a shock wave, but for $\pi_i > \pi_{i_0}$, S_2 is a rarefaction.

$$(d) \quad \gamma p_o > \gamma' p'_o \quad \text{but} \quad (\gamma+1)p_o < (\gamma'+1)p'_o$$

Then for $\pi_i < \pi_{i_0}$, S_2 is a rarefaction, but for $\pi_i > \pi_{i_0}$, S_2 is a shock.

Cases (a) and (b) are evidently reciprocal. Thus, they show that if shock waves in the first gas are always reflected as shock waves by the second, shock waves in the second will always be reflected as rarefaction waves by the first; which is physically reasonable. Cases (c) and (d) are reciprocal in a similar sense, but the existence of a critical incident pressure ratio (π_{i_0}), at which the reflexion changes type, is somewhat surprising. It remains to enquire whether this effect should be expected with actual gases. The necessary condition for its appearance may be conveniently written:

$$\gamma m \leq \gamma' m' \quad \text{and} \quad (\gamma+1)m \geq (\gamma'+1)m', \quad (6)$$

where m, m' denote molecular weights, and the two upper or the two lower signs are to be taken together. Examination of tabulated constants shows that (6) is not usually satisfied, so that cases (a) and (b) form the rule.

However, the possibility of satisfying (6) is not excluded, if γ and γ' differ sufficiently. Suppose, for example, that $\gamma = 1.1$ and $\gamma' = 1.667$. Then (6) requires that $1.27m' < m < 1.515m'$. It appears in fact that (6) is satisfied by the following pairs of gases:

neon with acetylene

argon with butane vapour or methyl chloride vapour,

for which approximate constants at 1 atm. and 273°K and corresponding values of π_{c} , are given in Table 7.14:1.

Table 7.14:1

Gas	γ	ρ	$\gamma\rho$	$(\gamma+1)\rho$	π_{c}
Neon	1.642	0.966	1.586	2.553	
Acetylene	1.28	1.190	1.52	2.71	1.78 (with Ne)
Argon	1.667	1.781	2.964	4.750	
Butane vapour	1.11	2.599	2.88	5.48	1.51 (with A)
Methyl chloride vapour	1.279	2.238	2.862	5.10	1.60 (with A)

Calculations for the vapours are rather unreliable, in view of the high critical temperatures and correspondingly large deviations from the ideal gas laws. For neon and acetylene, however, the effect is probably authentic, and could perhaps be detected in Schlieren photographs by the reversal in sign of $p_2/p_1 - 1$ at π_{c} : the wave and mass velocities do not, of course, change sign, though the reflected wave intensity vanishes at the critical incident intensity. The properties of transmitted and reflected waves in this system up to $\pi_c = 2.5$ are shown in Fig. 7.14:1

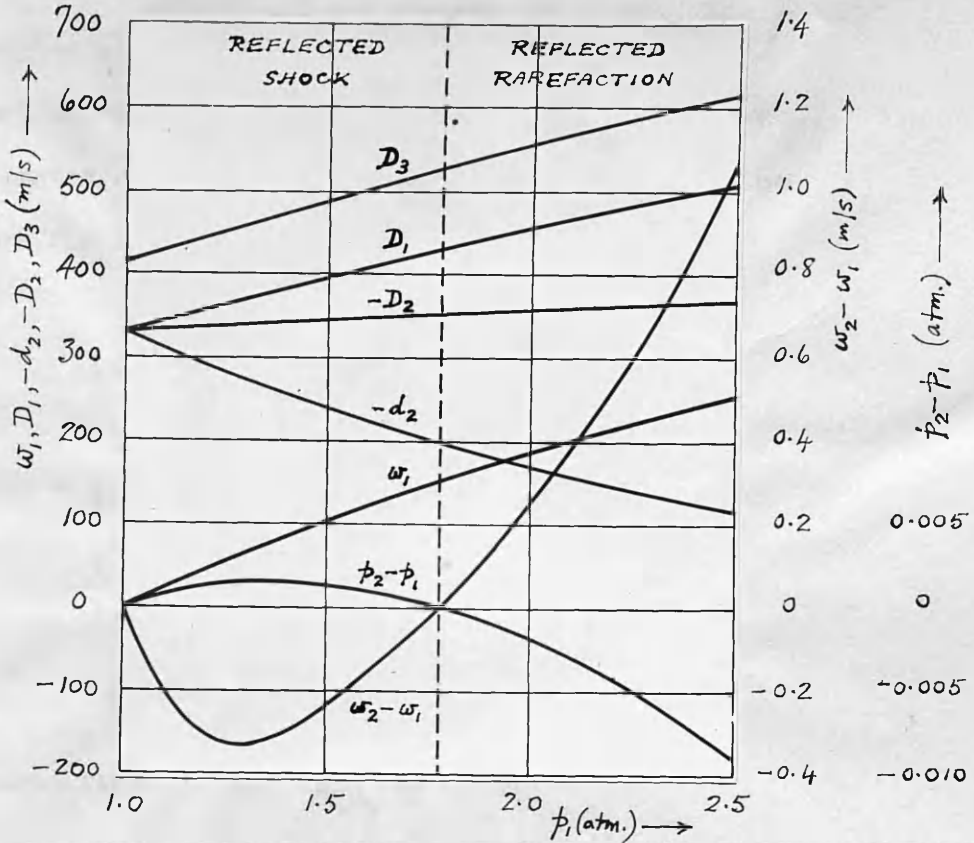


FIG 7.14.1 REFLEXION OF WEAK SHOCKS IN ACETYLENE BY NEON.

$P_0 = 1 \text{ atm.}, T_0 = 273^\circ\text{K}$. Symbols as in text.

For the great majority of gaseous systems (6) fails, and the condition for a reflected shock is then simply

$$\gamma_m < \gamma'm' , \quad (7)$$

which may also be written:

$$a_{0m} < a_{0'm'} , \quad (8)$$

or

$$|(\partial v_0 / \partial p_0)_S| > |(\partial v'_0 / \partial p_0)_S| \quad (9)$$

For such systems the character of the reflected wave is independent of the incident shock pressure.

The condition that the type of reflexion should change at π_{r0} is evidently that the RH-curves for the two gases should cross at π_{r0} . (§7.01)

§ 7.141 Estimation of γ for butane vapour

γ does not appear to have been measured for butane vapour.

However, Partington and Shilling give for other members of the homologous paraffin series:

		γ
Methane	(CH ₄)	1.310
Ethane	(C ₂ H ₆)	1.220
Propane	(C ₃ H ₈)	-
Butane	(C ₄ H ₁₀)	-
Pentane	(C ₅ H ₁₂)	1.086
Hexane	(C ₆ H ₁₄)	1.080

whence by interpolation

$$\gamma_{C_3H_8} \doteq 1.155$$

$$\underline{\gamma_{C_4H_{10}} \doteq 1.110}$$

This estimate may be confirmed as follows. According to Berthelot's equation, which should provide ample accuracy for our purpose,

$$\gamma^{-1} = \frac{R}{C_v} \left[1 + \frac{27}{16} \frac{p}{p_c} \cdot \left(\frac{T_c}{T} \right)^3 \right], \quad (1)$$

Where p_c , T_c are the critical pressure and temperature. The boiling point is 273°K and we may take T_c to be about 1.65 x 273°K. If $T = 273^{\circ}\text{K}$, then $(T_c/T)^3 \sim 4.5$. p/p_c may be assumed to be of the order of 1/30. Then, taking $C_v = 22.7 \text{ cal./mol } ^{\circ}\text{K}$, we have $\gamma \doteq 1.11$ as before.

7.14

§ 7.142 Approximate solutions for weak reflexion

Having determined the nature of the reflected wave in advance by 7.14(2), we are in a position to choose the correct equation from 7.1(2) and with 7.14(1) to solve for $\omega_2 = \omega_3$ and $\phi_2 = \phi_3$. In general, the solution is carried out numerically or graphically; but, if $\pi_2 \equiv \phi_2/\phi_1$ is close to 1, an approximate explicit solution can be used. Thus, let $\pi_2 - 1 \equiv x \ll 1$. Then, by 7.14(1), with $\omega_3 = \omega_2$, $\phi_3 = \phi_2$,

$$\omega_2 = \sqrt{(\lambda'^{-1})\phi_0 v'_0} \cdot \frac{\pi_i \pi_2 - 1}{\sqrt{\lambda' \pi_i \pi_2 + 1}}$$

$$\text{i.e. } \omega_2 \doteq \sqrt{\frac{(\lambda'^{-1})\phi_0 v'_0}{\lambda' \pi_i + 1}} \left[\pi_i - 1 + \frac{\lambda'(\pi_i + 1) + 2}{2(\lambda' \pi_i + 1)} \pi_i \cdot x \right], \quad (1)$$

while by 7.1(2)

$$\omega_2 = \omega_i - \sqrt{(\lambda^{-1})\phi_i v_i} \cdot \frac{\pi_2 - 1}{\sqrt{\lambda \pi_2 + 1}}, \quad \text{if } \pi_2 > 1$$

$$\text{i.e. } \omega_2 \doteq \omega_i - \sqrt{\frac{(\lambda^{-1})\phi_i v_i}{\lambda + 1}} \cdot x \quad (x > 0). \quad (2)$$

Equating (1) and (2) gives x at once.

If $\pi_2 < 1$, 7.1(2) gives

$$\omega_2 = \omega_i + \sqrt{(\lambda^2 - 1)\phi_i v_i} \left[1 - \frac{1}{\pi_2 \lambda + 1} \right]$$

$$\text{i.e. } \omega_2 \doteq \omega_i - \sqrt{\frac{(\lambda - 1)\phi_i v_i}{\lambda + 1}} \cdot x \quad (x < 0),$$

so that, as expected, (2) holds for any weak reflected wave, of whichever sort.

As an example, we consider a shock wave behind which the pressure is 2 atm. proceeding through oxygen at NTP ($v_o = 699.8 \text{ cm}^3/\text{g.}$, $\gamma = 7/5$, $\lambda = 6$) and falling normally upon argon at NTP ($v'_o = 561.5 \text{ cm}^3/\text{g.}$, $\gamma' = 5/3$, $\lambda' = 4$) 7.14(2) shows that the reflected wave is a shock. However, for illustration, we have calculated both parts of the RHR-curve for reflexions through the oxygen, as well as the RH-curve for transmission through the argon. Table 7.142:1 summarises the results which are shown also in Fig. 7.142:1. It is clear from the graph that the reflected and transmitted waves are both shocks, and that the gas velocity and pressure between them are approximately 150 m./s. and 2.12 atm. Equations (1) and (2) give, in fact, $\pi_2 - 1 \equiv x = +0.059$, whence $p_2 = p_3 = 2.118 \text{ atm.}$ If the 2 atm. incident wave proceeds from argon to oxygen, the RH and RHR-relations are as given in Table 7.142.2 and Fig. 7.142.2 The reflected wave is now a rarefaction, and (1,2) give, in fact, $\pi_2 - 1 \equiv x = -0.059$, so that $p_2 = p_3 = 1.882 \text{ atm.}$, in agreement with Fig. 7.142:1. $w_2 = w_3 = 149 \text{ m./s.}$

The wave-velocities, densities and temperatures are easily evaluated when $p_2 = p_3$ has been determined. Table 7.142:3 presents a complete picture of the incident, reflected and transmitted waves. In (b) D_2 and d_2 refer to the nose of the reflected wave.

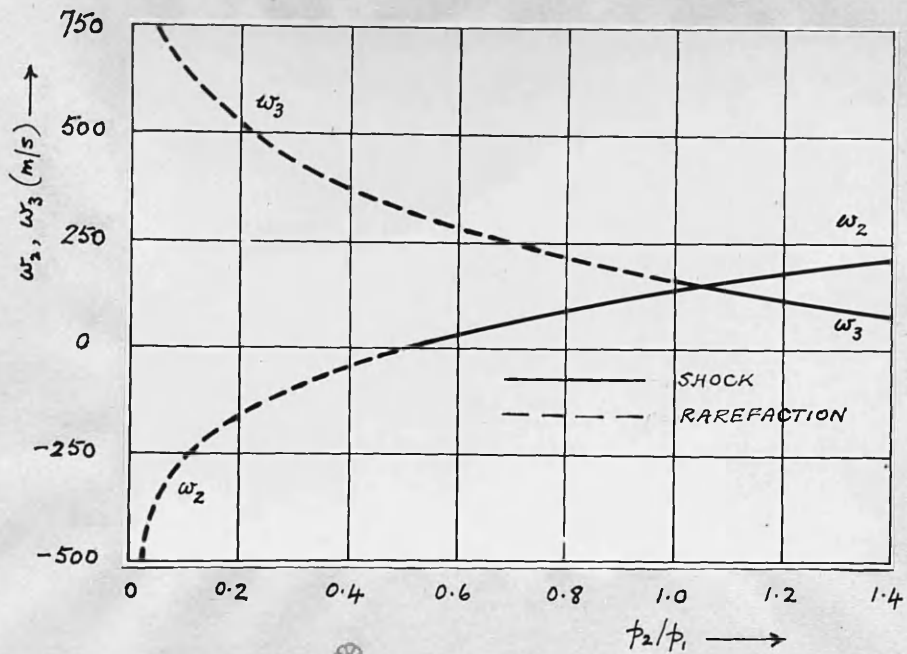


FIG. 7.142:1 2-atm. SHOCK IN OXYGEN

REFLECTED BY ARGON. $p_0 = 1 \text{ atm.}$, $T_0 = 273^\circ\text{K.}$

Table 7.142:1

2 atm. shock in oxygen reflected by argon. RH- and RHR(p, w)-relations for transmitted (3) and reflected (2) waves. $p_0 = 1 \text{ atm.}$ $T_0 = 273^\circ\text{K.}$

$p_2 = p_3$ (atm.)	w_2 (m./s.)	w_3 (m./s.)	$p_2 = p_3$ (atm.)	w_2 (m./s.)	w_3 (m./s.)
1.0	330	0	2.4	119	177
1.2	288	34.3	2.8	79	212
1.4	251	64.2	3.2	44	244
1.6	220	90.8	3.6	12	273
1.8	191	115	4.0	(-17.5)	300
2.0	165	138			

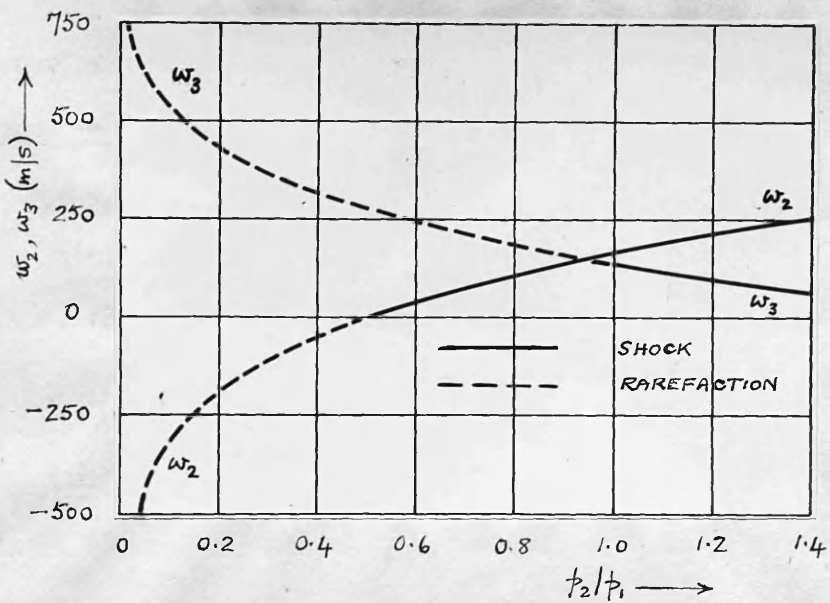


Fig. 7.142:2 2-atm SHOCK IN ARGON

REFLECTED BY OXYGEN. $p_0 = 1 \text{ atm.}$, $T_0 = 273^\circ\text{K}$

Table 7.142:2

As in Table 7.142:1, but incident wave in argon, reflected by oxygen.
 $p_0 = 1 \text{ atm.}$ $T_0 = 273^\circ\text{K}$.

$p_2 = p_3$ (atm.)	w_2 (m./s.)	w_3 (m./s.)	$p_2 = p_3$ (atm.)	w_2 (m./s.)	w_3 (m./s.)
1.0	275	0	2.4	98	212
1.2	240	41.5	2.8	63	254
1.6	184	110	3.2	32	291
2.0	137	165	3.6	4	325
			4.0	(-21)	356

Table 7.142:3

Reflexion of a 2 atm. shock at oxygen-argon interface.

(a) Oxygen → argon (Reflected shock)

p_1 (atm.)	$p_2 = p_3$ (atm.)	v_1 ($\text{cm}^3/\text{g.}$)	v_2 ($\text{cm}^3/\text{g.}$)	v_3 ($\text{cm}^3/\text{g.}$)	T_1 ($^\circ\text{K}$)	T_2 ($^\circ\text{K}$)	T_3 ($^\circ\text{K}$)
2.0	2.118	431	413	356	336	342	374
$W_1 = w_1$ (m./s.)	$-W_2$ (m./s.)	$W_3 = w_3 = w_2$ (m./s.)	$D_1 = d_1$ (m./s.)	$-D_2$ (m./s.)	$-d_2$ (m./s.)	$D_3 = d_3$ (m./s.)	
165	15	150	428	357	192		421

(b) Argon → oxygen (Reflected rarefaction)

p_1 2.0	$p_2 = p_3$ 1.882	v_1 374	v_2 258	v_3 450	T_1 364	T_2 236	T_3 330
$W_1 = w_1$ 137	W_2 12	$W_3 = w_3 = w_2$ 149	$D_1 = d_1$ 413	$-D_2$ 355	$-d_2$ 218	$D_3 = d_3$ 417	

The properties of reflected and transmitted waves may be evaluated over a wide range (up to $p_1 = 1000$ atm.) for the four typical gases He, A, O₂, CO₂, regarded as ideal, by means of the graphs of Figs. 7.1:1-4. For this purpose all four RH-curves have been drawn on each figure, and the approximate values shown in Table 7.142:4 derived from their intersections with the RHR-family.

Table 7.142:4

Pressure and gas velocity after reflection in ideal gases. $p_0 = 1 \text{ atm.}$
 $T_0 = 288^\circ\text{K.}$ (Units atm. and m./s.)

<u>Incident wave in Helium</u>	<u>Transmitted wave in</u>				<u>Argon</u>	
	Oxygen	<u>CO₂</u>				
p_1	p_2	w_2	p_2	w_2	p_2	w_2
1,000	2,400	12,200	2,600	11,100	2,640	10,900
800	1,880	10,800	2,060	9,900	2,090	9,700
600	1,420	9,400	1,560	8,600	1,580	8,400
400	950	7,700	1,040	7,000	1,060	6,900
300	710	6,600	780	6,100	790	6,000
200	480	5,400	520	5,000	530	4,900
150	350	4,600	390	4,200	400	4,100
100	229	3,760	250	3,440	255	3,360
50	115	2,640	126	2,400	127	2,370
20	44	1,610	48	1,470	48	1,440
10	20	1,060	22	970	22	950
5	9	650	9.2	600	9.2	580
2	3	270	3	260	3	250
<u>Oxygen</u>	<u>Helium</u>		<u>CO₂</u>	<u>Argon</u>		
1,000	289	11,320	1,170	7,450	1,207	7,340
800	230	10,130	934	6,650	965	6,550
600	175	8,760	700	5,750	721	5,670
400	116	7,150	467	4,700	480	4,640
300	89	6,220	350	4,050	359	4,010
200	59	5,020	232	3,290	238	3,250
150	44	4,340	178	2,860	182	2,820
100	29	3,550	118	2,340	120	2,300
50	16	2,470	59	1,600	61	1,570
20	7.3	1,530	23	990	23.5	980
10	4.2	1,010	11.4	665	11.9	650
5	2.7	620	5.5	410	5.8	395
2	1.2	300	1.8	200	2	185

Table 7.142:4 (Contd.)

<u>Incident wave in CO_2</u>	<u>Helium</u>		<u>Transmitted wave in Oxygen</u>		<u>Argon</u>	
	P_2	w_2	P_2	w_2	P_2	w_2
P ₁						
1,000	232	10,050	850	7,260	1,040	6,800
800	180	8,970	680	6,500	830	6,080
600	140	7,800	507	5,620	616	5,260
400	90	6,300	340	4,600	412	4,300
300	70	5,500	256	3,970	310	3,700
200	48	4,450	170	3,240	207	3,020
150	35	3,910	128	2,790	155	2,590
100	24	3,160	85	2,270	104	2,120
50	13	2,180	42	1,580	52	1,460
20	6	1,340	17	980	21	900
10	3.8	900	8.7	660	10.4	605
5	2.4	570	4.4	410	5.2	380
2	1	260	1.8	200	2	148
<u>Argon</u>	<u>Helium</u>		<u>Oxygen</u>		<u>CO_2</u>	
1,000	243	10,400	836	7,210	980	6,760
800	194	9,260	667	6,430	775	6,020
600	158	8,070	502	5,570	584	5,230
400	98	6,600	340	4,570	393	4,290
300	72	5,660	250	3,930	290	3,680
200	50	4,600	168	3,220	195	3,010
150	37	3,990	127	2,800	147	2,600
100	26	3,250	84	2,260	98	2,100
50	14	2,260	42	1,580	49	1,480
20	11.5	1,360	17	960	19.5	910
10	4.0	900	8.8	640	9.7	600
5	2.5	550	4.2	410	4.9	390
2	1	250	1.7	200	2	147

[cf. 145]

§ 7.2 Shock waves produced by the sudden release of high-pressure gas

A problem closely analogous to that of reflexion of gaseous shock waves arises when a weightless diaphragm separating two gases at different pressures becomes suddenly free to move. The case of a massive diaphragm was analysed in § 4.5, where it was seen that a shock developed in the low-pressure gas after a time proportional to the mass of the diaphragm. When this mass vanishes, the shock must form immediately on release, and the problem then differs from that of § 7.14 only in the absence of an incident streaming velocity w_1 . The solution is therefore determined by equations 7.1(2b) with $w_1 = 0$, and 7.14(1), together with the matching conditions 7(2,3). In the (p, w) -plane, we intersect the RH-curve for shocks in the second gas with the R-curve for rarefactions in the first, drawn through the point $(p_1, 0)$ representing initial conditions on the high-pressure side.

Let suffices 0, 1 apply to the initial states of the two gases, and p be the interfacial pressure after release. If λ, λ' have the same meaning as in § 7.14, and $\pi_i \equiv p_i/p_0$, $\pi \equiv p/p_0$, then

$$\frac{\pi - 1}{\sqrt{\lambda' \pi + 1}} = A^{\frac{1}{2}} \left[1 - \left(\frac{\pi}{\pi_i} \right)^{\frac{1}{\lambda' + 1}} \right], \quad (1)$$

where $A \equiv (\lambda'^{-1}) p_i v / (\lambda^{-1}) p_0 v_0$. Evidently, when $\pi_i \rightarrow \infty$, π cannot become infinite also, but must rather approach a limit, which is therefore defined by

$$\frac{(\pi - 1)^2}{\lambda' \pi + 1} = A, \quad (2)$$

that is, if $z \equiv \pi - 1$, by

$$z^2 - A \lambda' z - A(\lambda' + 1) = 0. \quad (3)$$

The discriminant is positive, the sum of the roots positive, and their

product negative. Both are therefore real, and one and only one positive.

Thus, (2) defines a single upper limit

$$\pi_{\max} = 1 + \frac{1}{2} [A\lambda' + \sqrt{A^2\lambda'^2 + 4A\lambda' + 4A}] . \quad (4)$$

Shock waves with an intensity greater than this cannot be produced in the second gas by release of the first, no matter how high its initial pressure. The limiting intensity is frequently of a rather modest order, as Table 7.2:1 will show.

Table 7.2:1

Maximum shock pressures produced in air by release of various compressed gases. $p_0 = 1$ atm. $T_0 = T_1$.

Gas:	Argon	Air	CO_2	Helium	Hydrogen
π_{\max} :	15.2	45.1	48.5	133	615

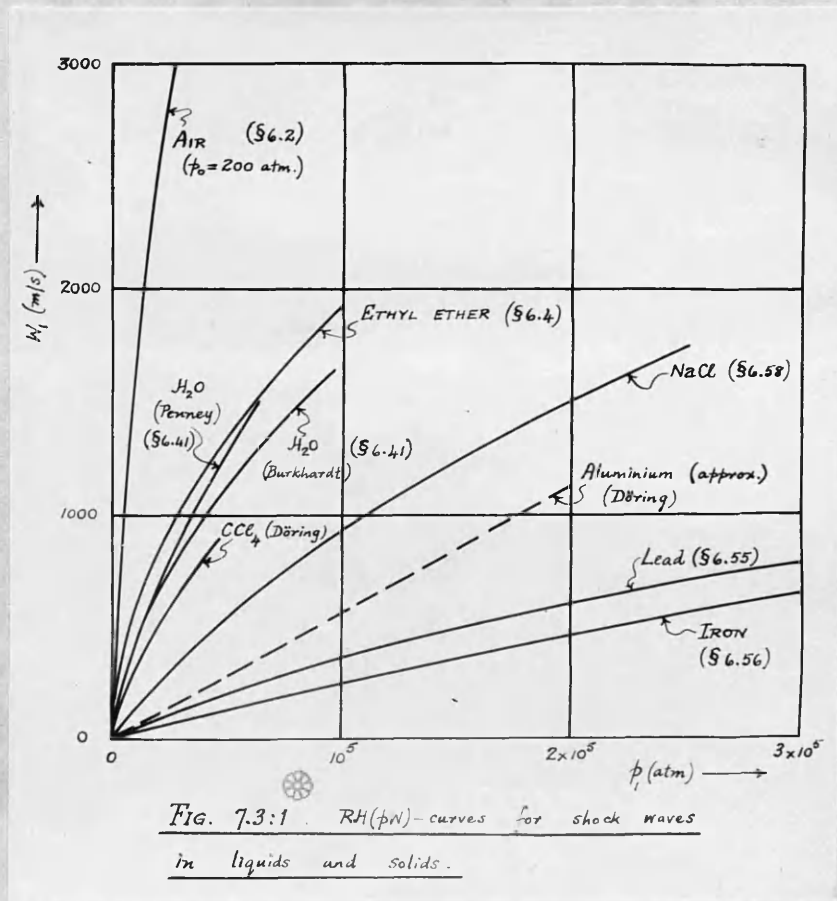
A brief theoretical treatment of the present problem has been given [^[29]] by Taylor, and shown to explain satisfactorily Payman's "shock-tube" [^[29]] experiments.

The theory also provides an explanation of the ignitions which sometimes occur when combustible gas under high pressure is suddenly released into the atmosphere. Since the gas must be cooled by expansion, this effect appears at first sight rather difficult to understand. However, very high temperatures may be produced in the atmospheric shock which arises at the instant of release, and these may well be sufficient to ignite the escaping gas by thermal diffusion. For example, consider the fracture of a cylinder containing hydrogen at 100 atm. and 0°C . According to (1), an air shock is developed of about 25 atm. pressure. The corresponding temperature, by 6.2(2), is almost 1100°C , whereas the hydrogen is cooled in the adiabatic expansion only to about -90°C .

§ 7.3 Reflexion of gaseous shock waves at liquid and solid boundaries

Problems of this type are solved by intersecting the RHR(pw)-curve for reflected gas waves with the RH(pw)-curve for transmitted shocks.

Examples of the former have been shown in Figs. 7.1:1-4, and of the latter are collected in Fig. 7.3:1.



From these figures it is clear that solid surfaces are effectively rigid to gaseous shocks, even of hundreds of atmospheres in intensity. The pressure p_2 after reflexion may thus be estimated by the method of § 7.12, and the properties of the transmitted shock, including the (small) interfacial velocity w_2 , then determined. A similar approximate procedure is adequate for liquid targets, if the incident wave is not too intense;

Table 7.3:1

Reflexion of shock waves in oxygen at liquid and solid surfaces
(Units atm. and m./s.)

otherwise the general method must be used. Table 7.3:1 illustrates the reflexion of waves in oxygen at liquid and solid surfaces.

Ethyl ether				Water				NaCl				Pb				Fe			
P_1	P_2	w_2																	
1	1	0	1	0	1	0	1	0	1	0	1	0	1	0	1	0			
2	3.7	0.4	3.7	0.2	3.72	0.047	3.75	0.016	3.76	0.010									
5	17.6	1.9	17.6	1.1	17.6	0.22	17.6	0.076	17.7	0.047									
10	49	5.3	49	30	49	0.62	49.2	0.21	49.3	0.14									
20	121	13.2	121	7.7	122	1.55	122	0.53	122.2	0.33									
50	350	34	352	22	354	4.5	355	1.5	356	0.95									
100	730	70	740	48	747	9.5	751	3.3	752	2.0									
200	1,460	140	1,500	90	1,540	19.5	1,550	6.7	1,552	4.2									
500	3,680	280	3,750	198	3,910	50	3,940	17.1	3,945	10.6									
1,000	7,350	445	7,500	350	7,830	99	7,900	34.2	7,920	21.1									

§ 7.4 Reflexion of shock waves in liquids at gaseous, liquid and solid boundaries

Conditions after transmission of a shock wave from a liquid to a gaseous or condensed medium are determined in the usual way, that is, by intersecting the RH(p, w)-curve for the target medium with the appropriate RHR-curve for the liquid. From the point of view of the liquid, an interface with a gas at normal pressure may be treated as a free surface, the properties of the transmitted shock being subsequently determined from the velocity w_2 of the interface. At liquid-liquid and liquid-solid boundaries, the reaction of the second medium upon the first would require to be taken into account from the outset.

We have made no original detailed calculations of RHR-curves for liquids. However, for comparison purposes, Table 7.4:1 is included showing the results of certain calculations by Döring on reflexion at liquid-gas boundaries.

[53]
Table 7.4:1

Reflexion of shocks in ethyl ether and water at an interface with air
(Units atm., m./s. and °C)

P_1	Ethyl ether			Water		
	P_2	w_2	$T_2 - T_o$	P_2	w_2	$T_2 - T_o$
1,000	2.10	192	0.1	1.63	124	0.0
2,000	3.52	344	0.8	2.42	232	0.1
5,000	8.73	679	6.8	5.53	497	1.4
10,000	18.6	1,062	22.6	12.1	834	4.6
20,000	39.3	1,600	61.	26.7	1,300	19.
50,000	107	2,680	186.	:	:	:
100,000	238	3,950	390.	:	:	:

§ 7.5 Reflexion of shock waves in solids at gaseous, liquid and solid boundaries.

Solution of problems under this head depends upon knowledge of the RHR(p, w)-curve for the solid (M), whose initial state is defined by conditions (p_1, w_1) behind the incident shock.

When the reflected wave is a rarefaction, as will normally be the case with a gaseous or liquid target, the (p, w) -relation is obtained from 6.54(3,5), as indicated in § 6.55.

For reflected shocks, the RH-equation 7(7) is treated in exactly the same way as the RH-equation for the incident shock, except that the "initial pressure" is now p_1 and is no longer negligible. The labour of calculation may, however, be very materially reduced by taking advantage of the form of 6.53(2). For 7(7), on evaluation of $E_2 - E_1$ by means of the equation of state, becomes identical with 6.53(2), except that the suffices 0, 1 are replaced by 1, 2 throughout. Let us call this new equation (α) . Again, if P is the pressure corresponding to v_2 along the original RH-curve 6.53(2), equation 6.53(2) also holds with v_1 replaced by v_2 and p_1 by P . Call this equation (β) . Then adding 6.53(2) and (α) , and subtracting (β) , we obtain the simple result (\neq negligible):

$$p_2 \left[v_2 - \frac{G}{2} (v_1 - v_2) \right] = P v_2 - \frac{G}{2} (P - p_1) (v_0 - v_2), \quad (1)$$

from which p_2 may be quickly calculated in terms of v_2 since $P(v_2)$ is already known by equation (β) .

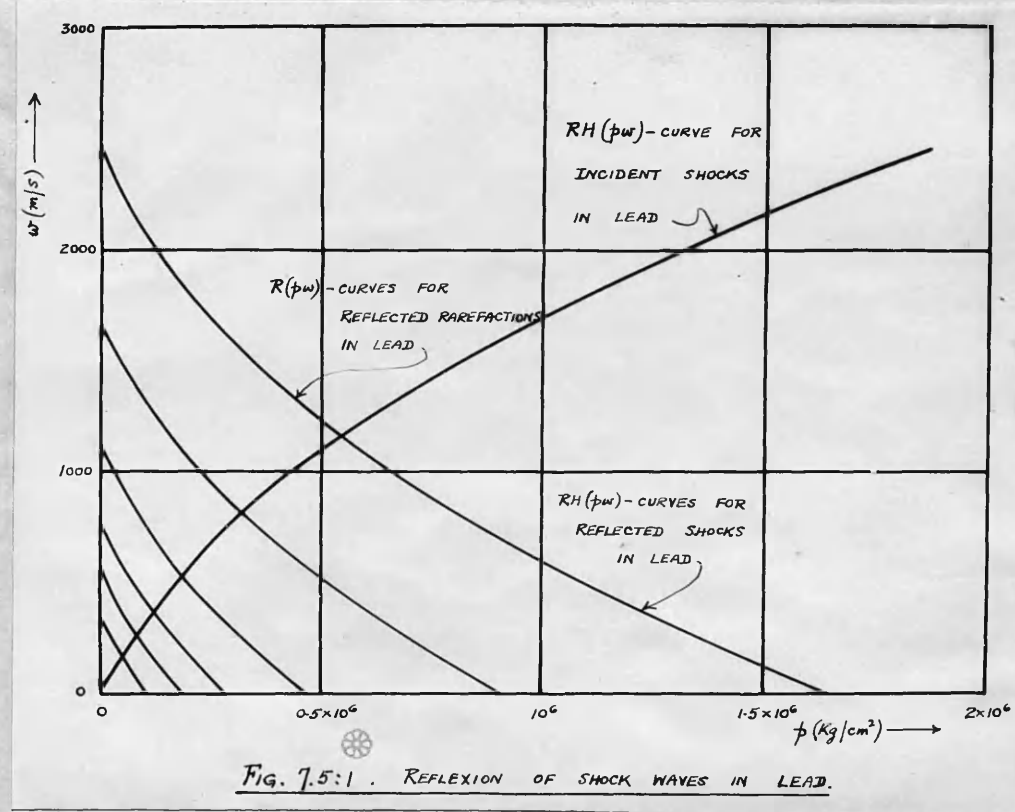
According to (1), p_2 becomes infinite when

$$p_2 = p_1 \left(1 + \frac{2}{G} \right), \quad (2)$$

which has exactly the same significance as 6.53(7): the density increases by at most a factor $(1 + 2/G)$ in each of a sequence of

shock waves. It follows, of course, that P will pass through an infinite value before ρ_2 reaches the limit defined by (2). However, the right side of (1) remains finite, and since P may still be formally calculated beyond this point (though it takes negative values), (1) can be used throughout, except in practice close to $\rho_2 = \rho_{1(\max)} \equiv \rho_0(1 + \frac{2}{G})$.

Applying the above methods, we have determined the RHR-curves for the waves reflected through a slab of lead, when the plane shock waves of Table 6.55:1 pass through the slab and fall normally upon a target material. The composite curves are shown in Fig. 7.5:1 and can be seen to join smoothly on the incident (p, w)-curve, as required by the fundamental theory.



The intersection of these curves with the w -axis represents conditions at a free surface (a gas at normal pressure provides a very close approximation to this case), their intersections with the p -axis

conditions at a rigid boundary (for example in the head-on collision of two identical waves). The states of the lead after reflexion in these two extreme cases are summarised in Table 7.5:1.

As an intermediate case, we may consider a $317,000 \text{ Kg./cm}^2$ shock in lead, emerging upon water. By means of Figs. 7.5:1 and 7.3:1 it can be deduced that a $71,000 \text{ Kg./cm}^2$ shock advances into the water, and that the interfacial velocity is $1,390 \text{ m./s.}$ The surface density of the lead is 12.37 g./cm^3 and its temperature is 990°K. The temperature of the water, according to Table 6.41:1, if supercooling is assumed, will be about 560°K. , so that the lead will subsequently undergo a further (relatively slow) fall in temperature by conduction to the water.

Exactly similar calculations for iron are summarised in Fig. 7.5:2 and corresponding diagrams could be constructed if required for Cu, Al or NaCl by use of the data of §§ 6.57 and 6.58.

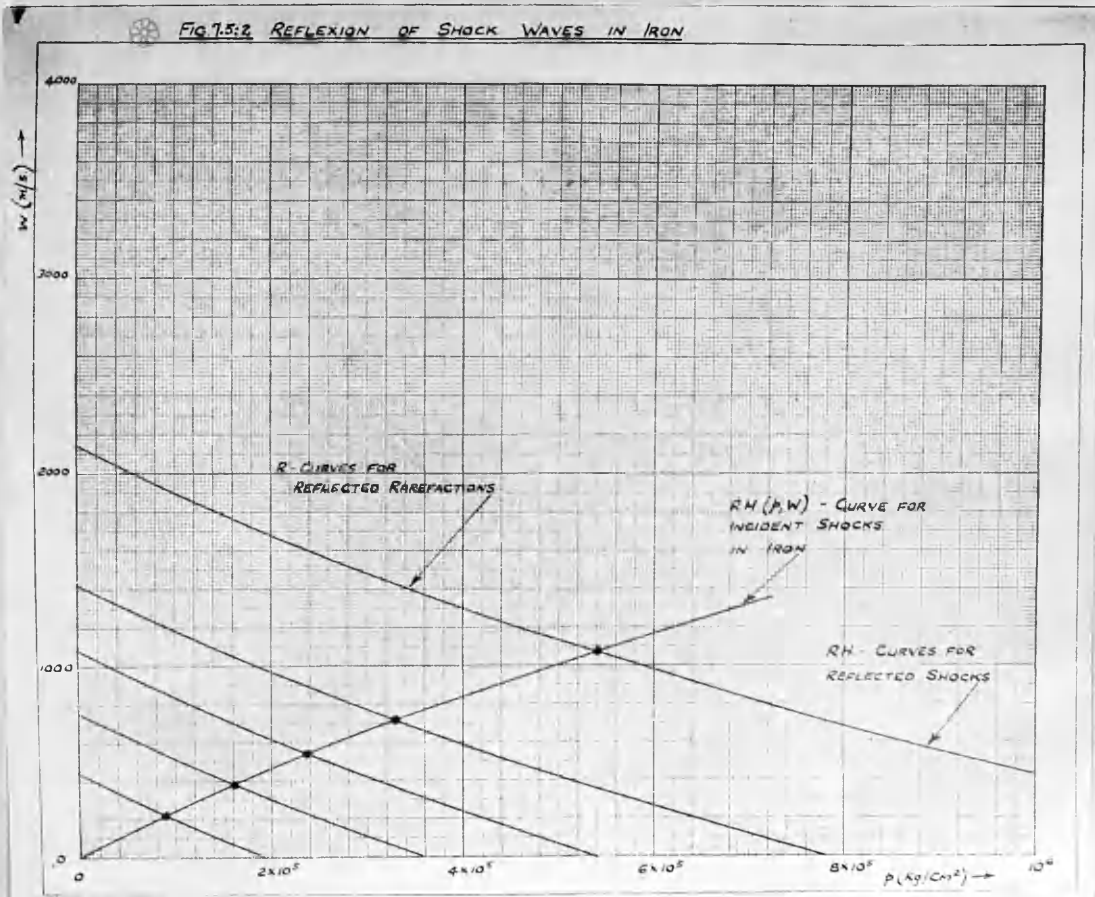


Table 7.5:1

Incidence of shock waves in lead upon a free surface or a rigid obstacle

Incident wave	Free surface ($p_2 = 0$)						Surface condition after reflection					
	ρ_1	p_1	T_1-288	w_1	ρ_2	T_2-288	w_2	$\frac{w_2}{w_1}$	$\frac{T_2-288}{T_1-288}$	ρ_2	p_2	T_2-288
12.30	43,200	79	168	11.36	10	336	2.00	0.127	13.16	97,000	152	2.25
12.84	76,800	161	276	11.33	40	554	2.01	0.249	14.20	183,000	268	2.41
13.30	111,600	265	374	11.29	76	753	2.01	0.287	15.01	278,000	572	2.49
14.00	178,500	535	538	11.18	170	1,090	2.03	0.318	16.29	471,000	1,132	2.64
15.00	317,000	1,360	815	10.90	418	1,662	2.04	0.307	18.14	905,000	2,982	2.86
16.00	539,000	3,210	1,161	10.41	823	2,408	2.08	0.256	20.00	1,630,000	6,982	3.02

§7.6 An experimental method for determining the large-scale shock wave properties in any medium

Provided the thermal and caloric equations of state of the fluid are known, and one large-scale property of the shock wave, for example its velocity, can be measured, equations 6(2,5,6) enable us to calculate the remaining properties. If the equations of state are unknown, it is still possible to deduce the values of pressure (p_1), density (ρ_1) internal energy (E_1) and material velocity (W_1) behind the wave, together with the wave velocity (D) itself, provided any two of these can be measured. In practice, the wave and material velocities (D, W_1) are the only properties at all readily susceptible of direct measurement. Thus, if the medium is transparent, D may be measured by Schlieren photography on a moving film; while if the medium is opaque, it may still be possible to record the time $\frac{x}{D}$ taken to traverse a known thickness x by direct shadow photography, or by means of a high-speed chronograph connected to suitable electrical contacts. W_1 might also in favourable cases be measured by a shadow or Schlieren photograph either of the near surface of the medium, if the pressure there is suitably maintained, or of indicator particles suspended in the medium itself. The prospects of measuring W_1 are probably most favourable when the shock is produced by transmission from an adjoining medium. A reflected wave will then proceed through this medium, and (until rarefaction waves arrive from the boundaries of the system) the pressure will remain constant at the interface, which will move forward with a velocity equal to that of the material behind the transmitted shock. If D and W_1 are measured in some such manner, then we have at once

$$\dot{P}_1 = \dot{P}_0 + DW, \rho_0 \quad (1)$$

$$\rho_1 = \frac{\rho_0 D}{D - W} \quad (2)$$

$$E_1 = E_0 + \frac{1}{2} W^2 + \frac{\dot{P}_0 W}{D \rho_0} \quad (3)$$

Moreover, if W, D can be measured for a series of shocks of varying intensity traversing the same material in the same initial state (\dot{P}_0, ρ_0), (1) and (2) enable us to determine the RH-curve corresponding to that state, and (3) then specifies the value of $E_1 - E_0$ along the curve. Finally, let us suppose that the above series of measurements can be made for each of a number of states (\dot{P}_0, ρ_0). For example, ρ_0 might be kept constant, and \dot{P}_0 varied by adjusting the temperature T_0 . Then it would be possible to evaluate $E_1 - E_0$ as a function of (\dot{P}, v) for an entire region of the (\dot{P}, v) -plane (in the above example, for $v_\infty < v < v_0$, where v_∞ is the smallest volume attainable in a single shock wave compression). The fundamental equations thus provide a powerful means of studying the internal energy of any material in a range of pressure difficult of access by other methods.

Experiments along these lines do not appear as yet to have been made.

§7.61

The necessity for direct measurement of W , can be avoided if we take advantage of the equations for reflection at an interface. Thus, let D_1, W_1 etc. refer to the wave (S_1) under study, moving in a medium (M) whose initial density is ρ_0 . Let S_1 fall normally upon the interface between M and a second medium N , so chosen that the reflected wave (S_2) is a shock. A shock wave (S_3) also proceeds into N , whose initial density is ρ'_0 . Then, if D_n, W_n denote the (algebraic) velocities of S_n ($n=1, 2, 3$), and of the material behind it, respectively, relative to the material ahead, and d_n, w_n the corresponding velocities relative to

the undisturbed media M , N , (the sign of D , being positive) and if p_n , ρ_n are the pressure and density behind S_n , we have at once, since $p_3 = p_2$,

$$p_i - p_o = D_i W_i \rho_o \quad (1)$$

$$p_2 - p_o = D_3 W_3 \rho'_o \quad (2)$$

$$p_2 - p_i = D_2 W_2 \rho_i \quad (3)$$

Eliminating p_o , p_i , p_2 and noting that $W_3 = w_3 = w_2 = W_1 + W_2$, $D_2 = d_2 - W_1$, $D_{1,3} = d_{1,3}$ /we get

$$(W_1 - d_2)(W_1 - w_2)p_i = d_3 w_2 \rho'_o - d_1 W_1 \rho_o \quad (4)$$

However,

$$\frac{p_i}{\rho_o} = \frac{d_1}{d_1 - W_1} \quad .$$

Hence (4) becomes

$$\frac{W_1}{d_1} = \frac{w_2(d_3 \rho'_o - d_2 \rho_o)}{\rho_o d_1 (d_1 - d_2 - w_2) + \rho'_o d_3 w_2} \quad , \quad (5)$$

which can also be written:

$$\frac{d_1}{W_1} - 1 = \frac{(d_1 - w_2)(d_1 - d_2)\rho_o}{w_2(d_3 \rho'_o - d_2 \rho_o)} \quad . \quad (6)$$

W_1 may thus be calculated without knowledge of the equations of state, provided that d_1 , d_2 , d_3 and w_2 can be measured. The three wave velocities should in certain cases be measurable by the same method, for example Schlieren photography in the case of transparent media. w_2 is the velocity of the interface and may be measurable by a shadow or Schlieren method. Under favourable circumstances it should evidently be possible to determine all four velocities from a single photograph on moving film.

The trace to be expected is of the type shown in Fig. 7.61:1.

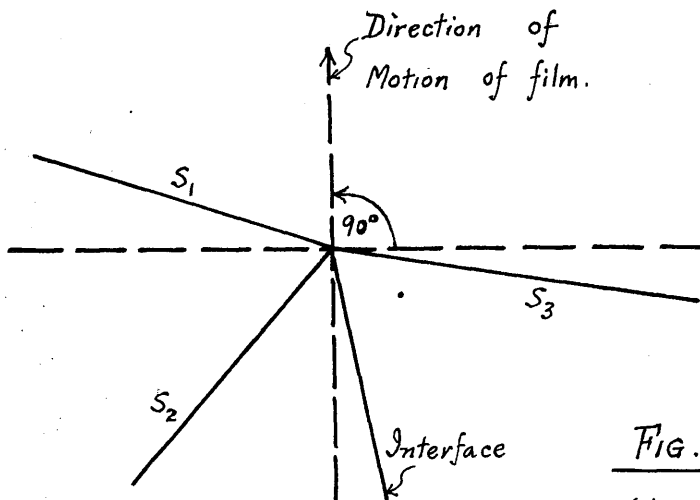


FIG. 7.61:1
(diagrammatic)

The present method offers little advantage in the study of non-reactive shocks, whose stability requires that W should be constant in space behind the wave front, and therefore equal to the velocity of the rear surface of the medium. It will clearly be simpler to measure this velocity, together with d_1 , rather than to measure d_1 , d_2 , d_3 and w_2 . The present method would still, of course, be useful for confirmation. In the case of reactive shocks, e.g. detonation waves, however, the conditions behind the wave front are entirely different. Here the material velocity W does not theoretically require to remain constant in space up to the rear surface of the medium behind the wave, and in normal practice will never do so. On the contrary, W , so far from remaining constant, decreases through W , as we retreat from the wave front, and eventually changes sign at a point between the front and the rear surface. The velocity of this surface therefore does not normally correspond to W : only when the wave is artificially maintained at a velocity greater than its stable value will these velocities coincide. Accordingly, the method proposed above should be of value in the experimental measurement of W (etc.) for detonation waves.

Expressions for ρ_1 , ρ , and E , corresponding to (6) may easily be deduced. They are

$$\rho_1 = \rho_0 + \frac{d_1^2 w_2 (d_3 \rho_0' - d_2 \rho_0)}{\rho_0 d_1 (d_1 - d_2 - w_2) + \rho_0' d_3 w_2} \quad (7)$$

$$\rho_1 = \frac{\rho_0 d_1 (d_1 - d_2 - w_2) + \rho_0' d_3 w_2}{(d_1 - w_2)(d_1 - d_2)} \quad (8)$$

$$E_1 = E_0 + \frac{1}{2} \frac{w_2^2 d_1^2 (d_3 \rho_0' - d_2 \rho_0)^2}{[\rho_0 d_1 (d_1 - d_2 - w_2) + \rho_0' d_3 w_2]^2} + \frac{\rho_0 w_2 (d_3 \rho_0' - d_2 \rho_0)}{\rho_0 [\rho_0 d_1 (d_1 - d_2 - w_2) + \rho_0' d_3 w_2]} \quad (9)$$

The pressure, densities and energies behind the transmitted and reflected waves can also be at once deduced from the same four measurements, which thus provide information not only with regard to the detonation wave and the shock or adiabatic relation for the detonation products, but also with regard to the shock wave in the target material.

There seems little doubt that the method could be successfully applied to determine the detonation pressure in gaseous explosives. It appears well worth investigation for liquids and solids also. Although the difficulties in this case would be much greater, the advantages of a reliable measurement of pressure can hardly be exaggerated.

PART II

STEADY PLANE DETONATION WAVES

§8 Historical introduction [122a]

The first detonating explosive was probably produced by Berthollet, when in 1788 he attempted to increase the strength of gunpowder by replacing the saltpetre with potassium chlorate. The history of detonation may however in practice be regarded as commencing in 1846, with the discovery of guncotton by Schönbein and Böttger, and of nitroglycerine by Sobrero. The unprecedented power and violence ("brisance") of decomposition in nitroglycerine, far surpassing those of the traditional blackpowder, induced Nobel to devote many years to the problem of its control. Meanwhile attention was being turned to the design of other explosives with comparable performance, and by the end of the century detonating compositions of many different types were in widespread use.

The reasons for the superiority of these new explosives were not at once fully understood, though it soon appeared that they must be sought in something more fundamental than a mere increase in the heat of reaction [155] and the volume of gas produced. The experience of Sprengel, who prepared detonating mixtures from oxidising and combustible substances which were separately incapable of detonation, demonstrated likewise that their behaviour did not depend essentially upon the presence of an unstable molecule; and though guncotton and nitroglycerine are themselves extremely sensitive, instability is not in fact a characteristic feature of high explosives. Many such substances can be safely melted, and some even distilled, without decomposition.

The first real insight into the mechanism of detonation was provided [6] by the experiments of Berthelot and Vieille and of Mallard and le Chatelier [11] on explosion in gases. It was found that explosive gaseous mixtures,

which had hitherto been considered to propagate steady reaction only by a quiet flame, travelling with a velocity of at most a few metres per second, were capable of decomposing in an alternative and very different manner.

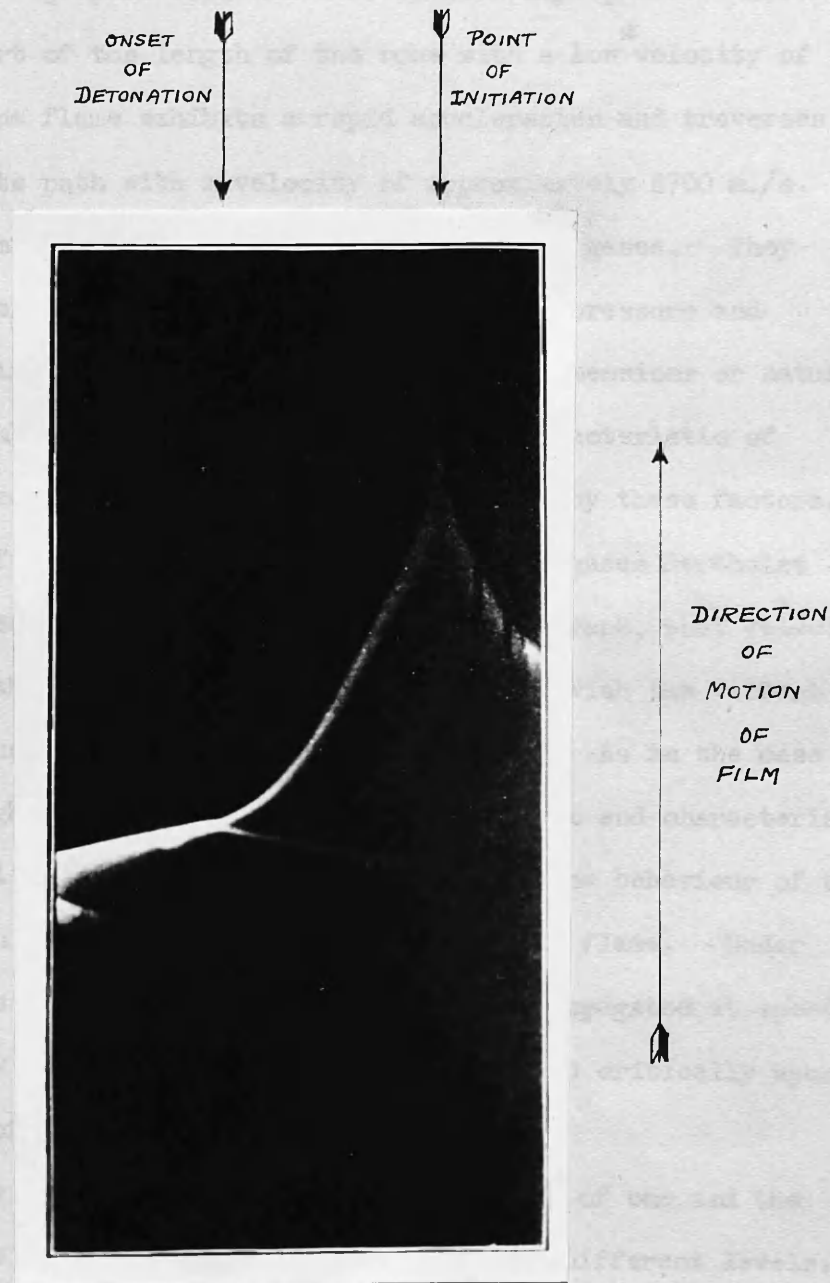


FIG. 8:1 MOVING-FILM RECORD OF

THE DEVELOPMENT OF DETONATION IN

A COLUMN OF $C_2N_2 + O_2$.

(DIXON, PHIL. TRANS. (A) 200, 315 (1903))

[51]

Figure 8:1 which is taken from a later paper of Dixon, represents for example the explosion of a cyanogen-oxygen mixture ignited near the open end of a glass tube. The passage of the flame to left and right is recorded upon a photographic film which moves steadily upward. After running through part of the length of the tube with a low velocity of about 300 m./s., the flame exhibits a rapid acceleration and traverses the remainder of its path with a velocity of approximately 2700 m./s. Velocities of a similar order were recorded with other gases. They proved to be insensitive to variations in the initial pressure and temperature, the circumstances of ignition, and the dimensions or nature of the confining tube, whereas the low velocities characteristic of ordinary flames were notoriously subject to influence by these factors.

A few years after the discovery of detonation in gases Berthelot [8] demonstrated, by measurements with an electric chronograph, that velocities of propagation of the same high order were associated with the violent decomposition of the new solid and liquid explosives. As in the case of gases, these high velocities appeared to be constant and characteristic for each individual explosive, in marked contrast to the behaviour of the same explosive when set alight by the application of a flame. Under such conditions, as with blackpowder, decomposition propagated at speeds which were not only of a much lower order, but depended critically upon the circumstances of test.

It thus became clear that explosive decomposition of one and the same material might proceed at either of two entirely different levels. The first process, usually described as "deflagration", was characterised by relatively low flame speed, correspondingly slow pressure development

(* This velocity is exceptionally high for an ordinary flame : it is, however, "low" by comparison with those of detonation.)

with moderate or slight brisance, and marked sensitivity to environmental conditions. The second process, which we shall term "detonation", involved high speed of propagation, shattering development of pressure, and relative independence of external conditions. Most gaseous, liquid and solid explosives with the important exception of gunpowder, were found, in fact, to be capable of either mode of decomposition.

The first attempts to account quantitatively for the process of
[7]

detonation in gases were made by Berthelot, who compared the wave velocity [50] with the mean molecular velocity in the explosion products; and by Dixon, who identified it with the velocity of sound in the products. The observed velocities of detonation were, of course, much greater than either molecular or sound velocities at normal temperature; and it was realised that the appropriate values would be those calculated at the theoretical temperatures of explosion. Velocities estimated in this way were of the correct order, and often remarkably close to those observed. However, this close agreement was largely fortuitous. According to the presently accepted theory, which is explained in detail below and has withstood many searching tests, the velocity of detonation must necessarily exceed that of sound in the reaction products, which was in general overestimated by Dixon through failure to allow for dissociation at the high prevailing temperatures. One important aspect of Berthelot's and Dixon's theories nevertheless deserves notice. In each case, attention is focussed upon the products, rather than upon the undetonated gas. It is the physical properties of the products which determine how fast the wave can be supplied with energy and therefore at how high a velocity it may proceed. This aspect, though not explicitly emphasised by either investigator, is implicit in the work of each, and is fundamental to the modern theory of detonation.

The first and essential step towards this theory was taken by Schuster in a note contributed to Dixon's paper. Schuster suggested an analogy between detonation waves and the shock waves studied theoretically by Riemann, [41] Earnshaw, [54] Rankine [37] and Hugoniot, [78,79] and observed [69] by Mach and others. An account of the theory of these waves has been given in Part I, where it was shown that compressional waves of finite amplitude, if suitably maintained in any normal fluid, must suffer a progressive increase of pressure and velocity gradients in the wave front, and in the absence of thermal and viscous transfer, soon become infinitely steep. The resultant discontinuity or "shock" differs in many important respects from the generating adiabatic wave. In particular, it travels at supersonic speed and raises the entropy of each element of fluid in passing over it. It is not, however, stable, and in the absence of support must degenerate into a sound wave.

If the medium is non-reactive, such support can come only from some external agency, for example a piston moving behind the wave. In a reactive medium support might conceivably be provided by release of chemical energy within the wave itself. Schuster's suggestion assumes in effect that this is possible. It was first exploited by Chapman, [30] who found, however, that a straightforward application of the Rankine-Hugoniot theory was insufficient to determine a unique detonation velocity, such as was observed in practice, though it did set a lower limit to the value which the velocity might have. Thermodynamic considerations led Chapman to select this minimum as the theoretically stable value, and although it has since appeared that his argument was at fault, there is now no doubt regarding the conclusion, which was reached independently and by an illuminating hydromechanical argument by

[86, §1]
Jouguet, and is associated with the names of both workers. The Chapman-Jouguet theory is in essence that accepted today, and depicts the steady detonation wave as a "stable reactive shock", that is, as a shock wave of the Rankine-Hugoniot type, continuously initiating the undetonated explosive into which it proceeds, and itself continuously sustained by the chemical energy thus set free.

Perhaps the most immediately striking aspect of the new theory was the fact that it made provision also for a second mode of flame propagation characterised by much lower velocity and distinguished in several fundamental respects from the first. At one stroke, therefore, the theory was able to resolve the central problem presented by the discoveries of 1881, and to assign a definite and quantitative meaning to the terms deflagration and detonation. The precise nature of the shortcomings in Dixon's treatment were also illustrated in an unusually clear way. Thus, Jouguet's formulation of the stability condition identifies the wave velocity with the velocity of sound in the products, but with respect to an observer at rest in the undetonated explosive. It is, however, a parallel conclusion that the products themselves possess a well-defined forward velocity. The slight yet important difference from Dixon's conjecture is apparent.

The Chapman-Jouguet theory permits in principle the absolute calculation of detonation velocities, pressures, etc., subject only to a knowledge of the relevant equations of state and thermodynamic functions. The imperfect state of knowledge of these functions in 1899, however, prevented Chapman from attempting such absolute calculations. Instead he made use of the observed wave velocities for a few selected gas

mixtures, in conjunction with his theoretical relations, to evaluate the specific heats at detonation temperatures, subsequently employing the values thus deduced to compute the wave velocities for other mixtures. The agreement was in most cases remarkably close, when we remember that, in the absence of reliable information regarding high temperature equilibrium constants, nothing approaching an exact thermochemical analysis was then possible. Similar success attended [87] the numerical applications made by Jouguet, who also developed and [92] consolidated the fundamental aspects in a series of important papers.

When the use of quantum mechanical methods opened the way to an accurate determination of thermodynamic functions for ideal gases at high temperatures, it became possible to carry out a rigorous test of the Chapman-Jouguet theory, and to employ it for absolute calculations of the detonation parameters. This was performed in 1930 by Lewis [97] and Friauf, whose results will be exemplified in a later section. The agreement between theoretical and measured velocities was for the most part within 1%. In a calculation which makes no reference at any point to direct observation of explosive performance, and in which no adjustable constants whatsoever are available, this level of agreement must be regarded as providing very fine confirmation of the theory for gaseous explosives.

There is nothing in the theory which restricts its application to gaseous explosives, or indeed refers at all either to the physical state of the undetonated material or to the kinetics of the chemical reaction. On the contrary, as we have seen, emphasis is laid essentially on the physical properties of the products. The fundamental equations may thus be immediately applied to condensed explosives. In practice, however, two separate difficulties arise.

(1) The theory in its simple form refers to a one-dimensional process, and assumes therefore that the wave front is plane and that no lateral motion of the products can occur. This will be true in practice if the cylindrical cartridge is confined in a rigid tube, or if its diameter is sufficiently large. The first condition is rather easily fulfilled in gaseous explosions, where the detonation pressures are only a few tens of atmospheres; but no material envelope can provide rigid confinement for solid and liquid explosives. The elementary theory then applies only to cartridges of large diameter, and allowance must be made in other cases for the depression of velocity by lateral expansion.

(2) The very much higher densities associated with condensed explosives, and the consequent difficulty in determining the thermodynamic functions for the detonation products, raise serious practical problems in numerical calculation, even for a well-confined cartridge.

It is only in recent years that a noteworthy advance has been made [2,5] in these directions. Early numerical studies by Becker of the propagation of the plane wave were restricted to expressing the wave velocity, pressure etc. in terms of an assumed detonation temperature, on the basis [3] of a semi-empirical equation of state designed for nitrogen. An inverse procedure was used by Schmidt, and subsequently by several other workers. [4,9] In view of the difficulty in formulating the equation of state, and the relative ease of measuring the wave velocity, Schmidt employed the experimental velocities to estimate the properties of the products, and thence to predict the behaviour of other explosives. His approach provided very valuable information of a general character, and also

underlined the possibility of using the detonating cartridge as a laboratory in which to study matter at combinations of pressure and temperature probably accessible by no other means. In the last few years, more elaborate attacks have been made on the problem by the inverse method. However, this method (which was already proposed by Becker) in its most general form requires much more extensive data than are yet available. In the present work, we use purely theoretical equations of state for gases at high densities to attempt absolute calculations for large diameter cartridges of condensed explosive. The results of such calculations are sufficiently encouraging to warrant faith in the general soundness of the approach.

The theory permits estimates not merely of the velocity of detonation, but also of the translational velocity of the products, and of their temperature, pressure, density, energy and composition. Of these quantities, only the wave velocity can be easily measured, but attempts have recently been made to evaluate the others, either directly as in the case of product velocity and temperature, or with the aid of auxiliary theory which relates the properties of the wave to the effects produced [28, 85, 172, 40, 58, 1, 32] in its environment. The results of such studies agree in order of magnitude with the various theoretical estimates, though they are not yet sufficiently precise or concordant to make adjudication possible between these. There is, however, every reason to believe that the theory provides a fundamentally correct picture of the physical processes in a detonating cartridge, and that the behaviour of such cartridges, provided their diameter is sufficiently large, can be not only explained but quantitatively predicted.

The imperfectly confined cartridge is beyond the scope of this thesis.

[82,51]

Some theoretical advance has, however, been made very recently with this problem and will be referred to in connection with the experimental study of maximum detonation velocities.

Finally, attention has been given to the microscopic structure of the detonation wave, and the mechanism whereby reaction is initiated and transferred from one layer of explosive to the next. We have seen that the large-scale properties of the stable plane wave, may be successfully described without reference to such questions, which are therefore best elucidated by study of the behaviour of the explosive under conditions where a steady plane wave does not develop, or at least has not yet developed.

§9 Elementary theory of the stable plane detonation wave

Shock waves in chemically inert materials are unstable; that is to say, they tend to degenerate into sound waves. This experimental observation is also a fundamental consequence of the Riemann theory described in Part I, for according to that theory the development of a shock depends upon the fact that each of a succession of small compression waves, generated in a normal fluid, tends to overtake its predecessors. It follows that any rarefaction arising behind the resultant shock will also in due course encroach upon the wavefront and so reduce its speed. Shock waves in inert materials cannot therefore remain steady unless supported by some such external agency as a piston which pursues the wave at appropriate speed, and prevents the development of rarefactions.

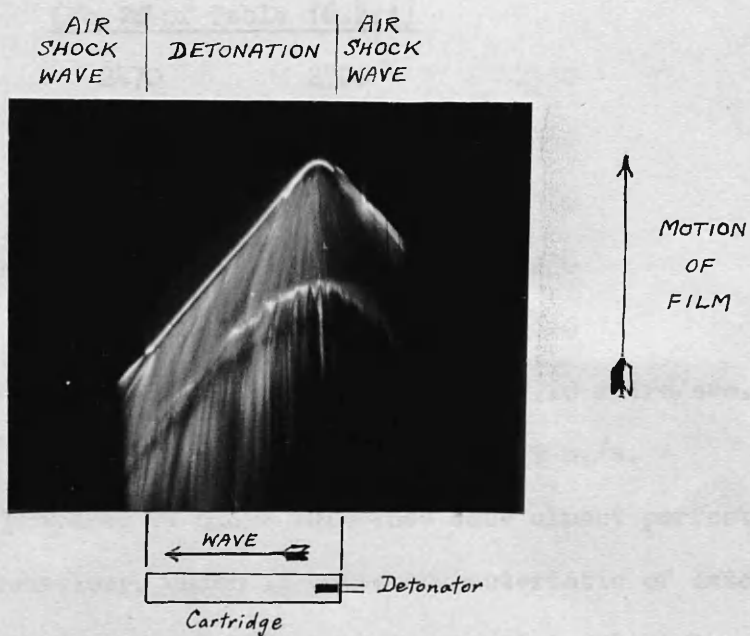


FIG 9:1 A TYPICAL ROTATING-DRUM

CAMERA RECORD OF DETONATION IN A

CARTRIDGE OF SOLID EXPLOSIVE.

177

In a detonating explosive, conditions are evidently otherwise. Figure 9:1 is a photographic record, obtained with a rotating-drum camera, of the progress of detonation along a cartridge of a commercial blasting explosive. The velocity of the wave is inversely proportional to the slope of the trace, and can be seen to reach a steady value almost immediately and to retain that value without detectable variation throughout its subsequent course. A second similar cartridge of the same material will show very closely the same velocity as the first; Table 9:1 illustrates the level of consistency found in practice with cartridges taken from normal manufacture.

Table 9:1

Velocities of detonation measured on a sample of 24 cartridges selected at random from manufacture of a commercial blasting explosive

(No. 26 of Table 16.2:1)

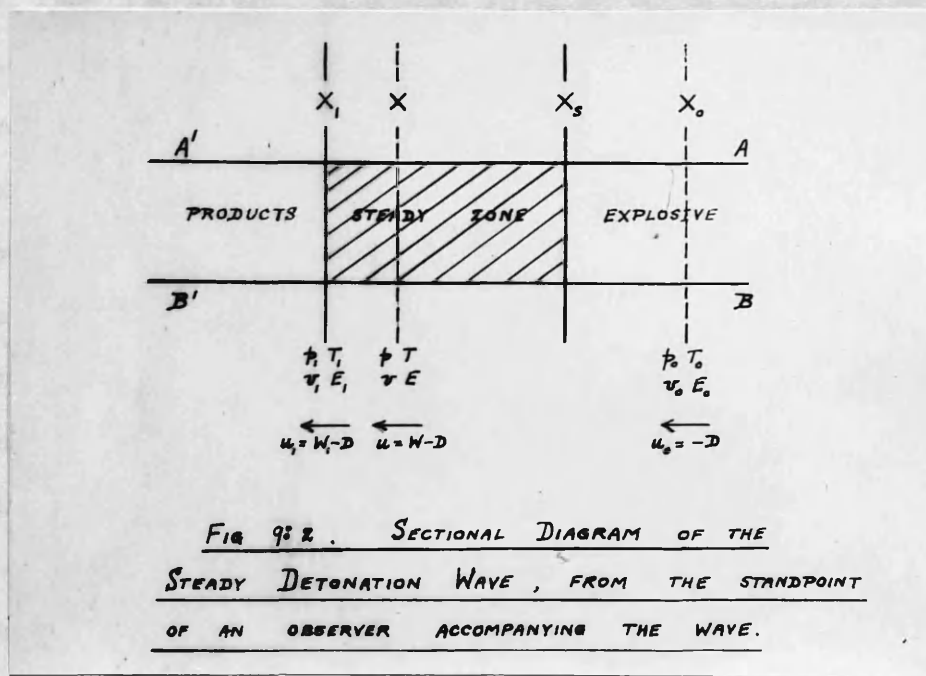
2320	2470	2500	2550
2370	2480	2510	2550
2420	2480	2530	2580
2420	2480	2540	2630
2450	2490	2540	2660
2470	2490	2540	2720 metre/sec.

Mean: 2508 m./s. Standard Deviation: 89 m./s.

Cartridges specially prepared to close tolerance show almost perfect consistency. This behaviour, which is quite characteristic of detonating explosives, makes it clear that stable waves in reactive material can and do regularly arise, despite the fact that no supporting piston is present and rarefactions must always form in the reaction products. We are

therefore led to examine theoretically the properties of such a stable wave, once established, and to conjecture that the release of chemical energy will in some way enable us to avoid the conclusion that rarefactions arising in the products must necessarily overtake the wave-front.

We suppose a plane detonation wave to advance normal to itself with constant velocity D relative to the unconsumed explosive. Figure 9:2 represents conditions in the neighbourhood of such a wave from the standpoint of an observer who moves with it.



X_s is part of the section of the shock front at any instant. The region to the right of X_s is occupied by undetonated explosive, which flows into the wave front with constant velocity $u_o = -D$. We shall use the subscript $_o$ to indicate conditions in this region; thus p_o is the pressure (frequently 1 atm.), T_o the temperature (as a rule 273°K or some neighbouring value), v_o the specific volume (so that $v_o = \frac{1}{p_o} = \frac{1}{\Delta}$),

where ρ_0 or Δ is the cartridge density), and E_0 the total internal energy. E_0 comprises both extramolecular (that is, kinetic and intermolecular potential) and intramolecular (including "chemical") energy. To the left of X_s , reaction proceeds, and the values of pressure, temperature etc. will in general vary with the distance from X_s . The wave is further supposed to be steady from X_s up to some parallel section X_1 . That is to say, conditions between X_s and any section X_1 drawn through the undetonated explosive, while not constant in space, remain absolutely unaltered in time from the point of view of the moving observer. We use the unqualified symbols p, T , etc. to denote values at an arbitrary section X between X_s and X_1 . Conditions in the plane X_1 itself are distinguished by a subscript 1 . Beyond X_1 , we do not assume the wave to be steady. Finally, let AA', BB' represent the boundaries of a stream-tube of unit cross-sectional area which traverses the wave.

Then we may apply the laws of conservation of mass, momentum and energy in integral form to the volumes bounded by the stream-tube and the control surfaces, X_0, X . This leads directly to the following three equations

$$\frac{u}{v} = \frac{u_0}{v_0} \quad (1)$$

$$\frac{u^2}{v} + p = \frac{u_0^2}{v_0} + p_0 \quad (2)$$

$$E + \frac{1}{2}u^2 + pv = E_0 + \frac{1}{2}u_0^2 + p_0v_0. \quad (3)$$

In deriving the last two equations, it is assumed that the rate of transfer of energy by viscosity and heat conduction across the control surfaces X_0, X is negligible. It is to be noted that this assumption does not require viscous and thermal effects to vanish throughout the region between X_0 and X , but only that they should do so at these sections. Since the rates of transfer increase with the space-derivatives of velocity and temperature and since conditions are not only steady but also space-independent to the right of X_s , there is certainly no viscous or thermal transfer across X_0 . Equations (2) and (3) may thus be applied at any section X at which the gradients of velocity and temperature are sufficiently small. It will be shown below that this is probably true at all parts of the steady zone except within the actual thickness of the shock front, and that it is certainly true in particular at the bounding section X_1 . Equation (1) applies, of course, without reservation at any section in the steady zone, since this equation is exact even in the presence of viscous and thermal effects.

(1), (2) and (3) may easily be transformed into the following

$$u_0 = -v_0 \sqrt{\frac{p-p_0}{v_0-v}} \quad (4)$$

$$u = -v \sqrt{\frac{p-p_0}{v_0-v}} \quad (5)$$

$$E - E_0 = \frac{1}{2}(p+p_0)(v_0-v). \quad (6)$$

Equations (4)-(6) are of course identical in form with those for non-reactive shocks derived in Part I. Equation (6) is the Rankine-Hugoniot (RH) equation,

named "dynamic adiabatic" by Hugoniot, who believed that no transfer of heat occurred in the wave. As a matter of fact, it is only the participation of dissipative processes such as viscous and thermal diffusion within the shock front that makes a relation of the form (6) possible; in the entire absence of such processes, (6) would require to be replaced by the true adiabatic relationship

$$dE = -pdv. \quad (7)$$

From (4) and (5), we have also, eliminating v ,

$$u_o(u_o - u) = (p - p_o)v_o, \quad (8)$$

and eliminating p ,

$$\frac{u_o - u}{u_o} = 1 - \frac{v}{v_o} = 1 - \frac{p_o}{p}. \quad (9)$$

Moreover

$$\frac{1}{2}(u_o^2 - u^2) = \frac{1}{2}(p - p_o)(v_o + v). \quad (10)$$

It is frequently convenient to use a system of reference at rest in the undetonated explosive rather than one which moves with the wave. Since these two systems are in constant relative motion, only the velocities are changed in transforming from one to the other. Let W be the translational velocity, measured algebraically in the direction of advance of the wave, with regard to the new system. Then $u_o = -D$, $u = W - D$, and so (4), (5), (8), (9) become

$$D = v_o \sqrt{\frac{p - p_o}{v_o - v}} \quad (11)$$

$$W = (v_o - v) \sqrt{\frac{p - p_o}{v_o - v}} \quad (12)$$

$$DW = (p - p_o)v_o \quad (13)$$

$$\frac{W}{D} = 1 - \frac{v}{v_o} \quad (14)$$

Equation (6) is unaffected.

Although the undetonated explosive is not in thermodynamic equilibrium, reaction is restrained by the low temperature and substantial activation energy, until the arrival of the shock front X_s . Between X_s and some later section Y , reaction proceeds, reaching equilibrium only in the plane Y . In the region $X_s Y$, which we shall call the reaction zone, the material passes through a series of non-equilibrium states, in a manner which will depend upon the reaction-kinetic equations. At Y , and subsequently, the state variables must satisfy the conditions for thermodynamic equilibrium. There is nothing at the outset to indicate whether or not Y will fall within $X_s X_1$, in other words whether reaction is complete within the steady zone, but we assume, on the basis of arguments to be developed later, that Y coincides with X_1 , so that the reaction and steady zones also coincide. We must note, however, that this is not obvious a priori, and that it need not necessarily remain true outwith the present context of steady plane waves.

Postponing discussion of the course of events within $X_s X_1$, consider now the plane X_1 , which separates the steady and non-steady regions, and in which chemical equilibrium is attained. The values of the variables W_1, p_1, v_1, E_1 at X_1 , together with D , satisfy equations (6), (11), (12). Since D appears only in (11) and W_1 only in (12), we may set these equations aside, leaving (6), which involves p_1, v_1, E_1 . E_1 depends, of course, on the chemical composition and state-variables at X_1 . However, the composition is itself expressible by the thermodynamic equilibrium conditions, in terms of the state-variables. Equation (6) may thus be regarded as involving p_1 and v_1 alone, and so defining a relation between the values of these two quantities in the plane X_1 . However, it evidently

cannot lead to a unique solution, such as experiment suggests should exist. For this it is necessary to introduce other considerations than those implied by the conservation laws. In the light of what has been said above, it is not difficult to foresee the nature of these considerations. Thus, if the sum of fluid and sound velocities at X_1 exceeds the wave velocity D , rarefactions which in practice must always arise behind the wave will overtake and encroach upon it; under such circumstances the wave cannot be steady. If, on the other hand, the sum of fluid and sound velocities at X_1 falls short of D , this must be true also for some distance at least into the steady zone. The energy released in this part of the zone cannot then be available to support the wave, which will in consequence be unable to maintain its assumed velocity. From such considerations, it would appear that in a stable wave the sum of sound and fluid velocities at the end of the steady zone must equal the wave-speed itself. The condition for stability was first formulated in this way by [§7] Jouguet, and shown to be identical in effect with the condition proposed [§6] earlier by Chapman, which rested on arguments of a different kind. Since the Chapman-Jouguet condition occupies a central position in the theory, and since we have not yet offered any but indirect reasons for believing that it can in fact be fulfilled, we must proceed to examine in somewhat greater detail the conditions at the end of the steady zone. The presentation in § 9.1 is largely due to Jouguet and Becker. [§2] [§5]

§9.1 The Rankine-Hugoniot equation and the Chapman-Jouguet stability condition

In order to avoid unnecessary complication, we shall in the present section assume that

$$\left(\frac{\partial p}{\partial v}\right)_S < 0, \quad \left(\frac{\partial^2 p}{\partial v^2}\right)_S > 0, \quad \left(\frac{\partial S}{\partial v}\right)_P > 0. \quad (1)$$

These conditions are unrestrictive and should almost always be fulfilled in practice. The adiabatics, $S = \text{constant}$, then form in the (v, p) -plane a non-intersecting family of curves of the familiar type, sloping downward with increasing v , and concave towards positive p . The entropy S rises along any radius through $(0, 0)$.

The RH-equation, as we have seen, also defines a relation between p , and v , which can again be represented by a curve in the (v, p) -plane. This curve is normally of the same general shape as the adiabatics, that is

$$\left(\frac{\partial p}{\partial v}\right)_{RH} < 0, \quad \left(\frac{\partial^2 p}{\partial v^2}\right)_{RH} > 0, \quad (2)$$

the suffix RH denoting differentiation along the curve; we shall in fact assume (2) to hold for the present discussion. However, the RH-curve, represented diagrammatically by CGFH in Figure 9.1:1, does not in general approach the p -axis and it may intersect the v -axis at a finite value of v .

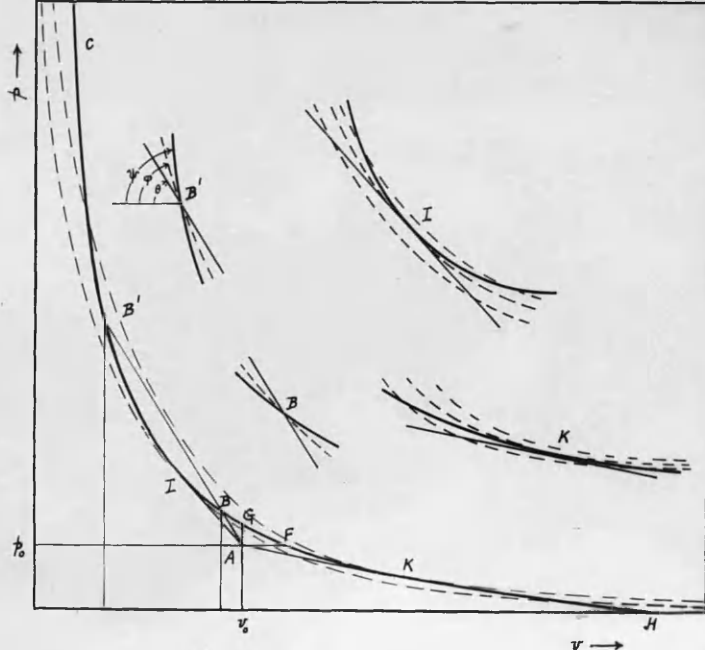


FIG. 9.1:1. THE RANKINE-HUGONIOT CURVE (DIAGRAMMATIC):
ORDINARY ADIABATICS REPRESENTED BY BROKEN LINES.

The point $A(v_0, p_0)$, representing the undetonated explosive, lies not on the curve, as in the case of a non-reactive shock, but beneath it. This becomes clear when we reflect that in a reaction at constant volume, leading from A to G, the pressure must normally increase. Similarly, a reaction at constant pressure, leading from A to F, must normally involve an increase in volume. It is, of course, assumed that we are dealing only with exothermic changes.

According to the RH-equation, the state of the products, in equilibrium at the end of the steady zone, is represented by some point on CGFH, but the equation itself tells us no more than this. However, by 9.(11), the velocity of a steady wave with end state (v_1, p_1) is

$$D = v_0 \sqrt{\tan \theta}, \quad (3)$$

where θ is the angle between the negative v -axis and the secant from A through (v_1, p_1) . It is clear, therefore, that no steady wave is possible with end-state defined by a point on FG. On the other hand, points on either CG or FH may conceivably represent steady waves; but evidently of very different kinds. If the terminal point lies on FH, the wave is one of rarefaction; if on CG, of compression and indeed involves pressures greater than those produced by reaction at constant volume. Moreover, the wave velocity will clearly be much larger in the latter case than in the former. At the outset, therefore, the theory makes provision, in a very simple manner, for two fundamentally different types of reaction wave, with properties, moreover, which closely reproduce those observed in detonation and deflagration respectively. It is evident that the branch CG must correspond to detonation, and by 9.(12) the reaction products have a translational

velocity in the same sense as the wave; similarly the branch FH must represent deflagration, and it appears that the products move in the opposite sense. Summarising these results:

Detonation

$$p_1 > p_0, v_1 < v_0, W_1 > 0$$

D large

Deflagration

$$p_1 < p_0, v_1 > v_0, W_1 < 0$$

D small

We now restrict our attention to CG. Let ABB' be any secant through A, B(v, p), and B'(v', p'), where $v_1 > v_1'$, and let AI be the upward tangent from A. By the Rankine-Hugoniot equation,

$$E_1 - E_0 = \frac{1}{2}(p_1 + p_0)(v_0 - v_1) \quad (4)$$

$$E'_1 - E_0 = \frac{1}{2}(p'_1 + p_0)(v_0 - v'_1) , \quad (5)$$

and so

$$E'_1 - E_1 = \frac{1}{2}(p'_1 + p_1)(v_1 - v'_1) . \quad (6)$$

But every point on the RH-curve represents by assumption a thermodynamically stable equilibrium state of the material. In particular, B and B' represent two such states, (as compared with A which does not). The RH-relation (6) corresponds therefore to a non-reactive shock in material whose initial state is defined by B. This means, since $p'_1 > p_1$, that $s'_1 > s_1$. Moreover, if we suppose the change represented by the straight line BB' to be executed reversibly, then in such a change, by (6)

$$\int_{BB'} T ds = \int_{BB'} (dE + pdv) = 0 . \quad (7)$$

in
It follows, /the first place, that if the secant ABB' is supposed to swing round until it coincides with the tangent AI, then

ultimately by (6) or (7).

$$TdS = dE + pdv = 0, \quad (8)$$

so that the RH-curve touches at I the adiabatic through that point.

Secondly, by (7), dS must again be zero at some point on the chord BB' , which therefore touches a member of the adiabatic family between B and B' . In view of our assumption regarding the shape of the adiabatic curves we conclude that the adiabatic through B' rises more steeply than the chord BB' , while the adiabatic through B rises less steeply. Thus if φ is the angle between the negative v -axis and the adiabatic at any point on CG , above I we have $\varphi > \theta$, and below I $\varphi < \theta$, while at I itself $\varphi = \theta$. Since, however,

$$D - W_i = v_i \sqrt{\tan \theta}, \quad (9)$$

and

$$a_i = v_i \sqrt{\tan \varphi}, \quad (10)$$

where a_i is the velocity of sound in the plane X_i , the above conclusion may be written:

$$\text{On } CI, \quad a_i + W_i > D \quad (11)$$

$$\text{On } IG, \quad a_i + W_i < D \quad (12)$$

$$\text{At } I, \quad a_i + W_i = D. \quad (13)$$

But (13) is precisely the condition which we have seen to be required on mechanical grounds in a steady wave, and the previous arguments can now be applied. Thus, if the end-state were represented by any point on CI , rarefactions arising behind the wave would overtake and weaken it, so that the terminal point would fall towards I . If on the other hand the terminal point lay on IG , not all the energy liberated at equilibrium would be available to support the wave which

would accordingly lose speed; in this process, the terminal point would rise towards I . If, however, the end-state is represented by the point I itself, there is no reason to expect any change. It appears, therefore, that liberation of chemical energy does in fact enable the condition for mechanical stability to be fulfilled.

The above argument further shows that the condition for a steady wave may be expressed by any of the following four equivalent equations:

$$a_1 + W_1 = D \quad (14)$$

$$-\left(\frac{dp_1}{dv_1}\right)_{RH} = \frac{p_1 - p_0}{v_0 - v_1} \quad (15)$$

$$\left(\frac{dp_1}{dv_1}\right)_{RH} = \left(\frac{\partial p_1}{\partial v_1}\right)_S \quad (16)$$

$$-\left(\frac{\partial p_1}{\partial v_1}\right)_S = \frac{p_1 - p_0}{v_0 - v_1} \quad (17)$$

(14-17) will be referred to as the Chapman-Jouguet (CJ) stability condition, and the plane X_1 (terminating the steady zone) at which they apply the CJ-plane. Of the four equations, (15) and (17) are the most useful in actual computations.

§ 9.2 The variation of entropy along the RH-curve

We have seen that the adiabatics rise more steeply than the secant ABD' at points B' above I , and less steeply at points B below I . The same is obviously true of the RH-curve itself, assuming its general form to be that shown in Figure 9.1:1. The argument does not indicate the relative slopes of the RH-curve and adiabatics. Since, however, for any secant ASS' through $A, S > S'$, it is clear that the adiabatic is either always steeper than the RH-curve above I and less steep below I ; or vice versa. In the former case, S must have a maximum at I , in the

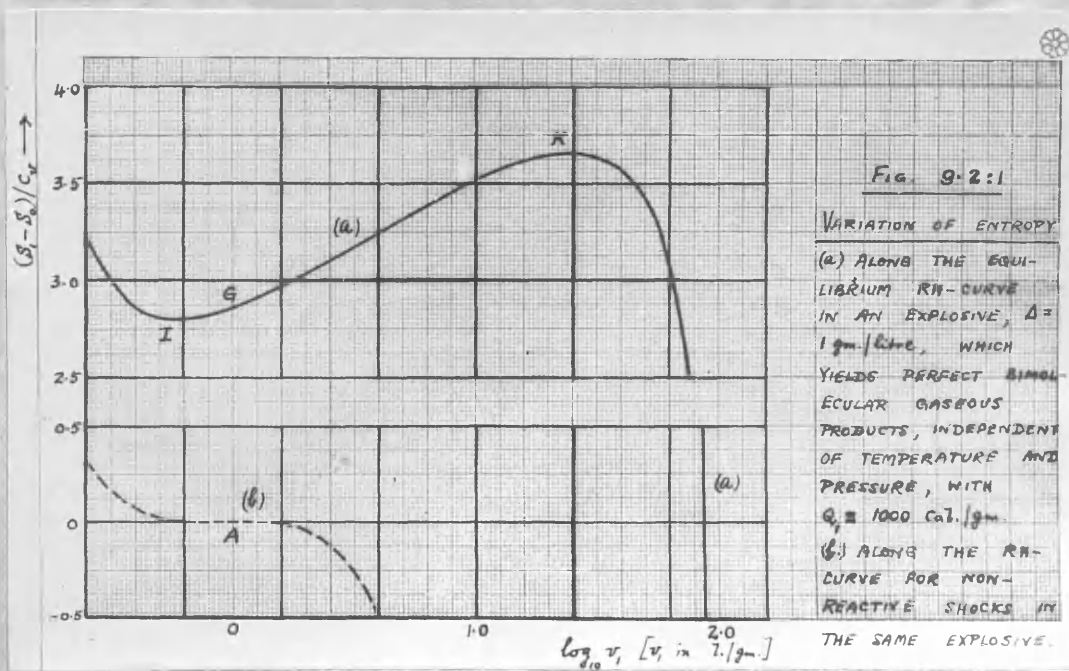
[30]

latter a minimum, as we pass along CG . Chapman based his choice of the point I to determine stability partly on the fact that this point corresponds to a minimum value of D , and partly on an argument intended to prove that S has a maximum at I . The turning value is, however, [5] in fact a minimum, as the following considerations will show. Along the RH-curve by 9.(6)

$$TdS = dE + pdv = \frac{1}{2}(v_0 - v) \left[\frac{p - p_0}{v_0 - v} - \left(-\frac{dp}{dv} \right)_{RH} \right] dv \quad (1)$$

As we descend the arc CG , $v_0 - v$ and dv are both positive; dS has therefore the sign of $\theta - \psi$, where ψ is the angle between the negative v -axis and the RH-curve. dS is thus negative above I , but positive below I , so that this point corresponds to an entropy minimum.

Equation (1) also shows at once that S has a maximum at the lower point of tangency K on the deflagration branch FH , where $v_0 - v < 0$. The changes in S along the RH-curve are illustrated by Figure 9.2:1 which applies to the case of a gaseous explosive, $A = 1$ gm./litre, yielding ideal bimolecular gaseous products, independent of temperature and pressure, with a "heat of reaction" $Q_r = 1000$ cal/gm.



In the (v, p) -diagram these conclusions can be expressed as follows:

Above I and below K, the RH-curve rises more steeply at each point than the appropriate adiabatic. Between K and I it rises less steeply. The adiabatic, which touches the curve at I, lies beneath it on either side of I, but intersects it again below K. Similarly, the adiabatic which has contact at K lies above the curve on either side of K, but cuts it at a point above I. Figure 9.1:1 illustrates these relations.

If the heat of reaction is supposed to become vanishingly small, I, K and A approach each other and finally coincide on the RH curve. (The curve changes position also, of course). The only stable wave is then the sound wave whose velocity is defined by the common slope of RH-curve and adiabatic at A. The two tangent adiabatics in the limit also coincide; it is therefore clear that in a non-reactive shock the adiabatic through A touches and crosses the RH curve there, lying below the curve to the left of A and above it to the right. The variation of S with v along the curve is then as shown by the broken line in Figure 9.2:1. An analytical proof of these relations may be supplied without difficulty.

§ 9.3 Jouguet's rule

The conclusion expressed by 9.1 (11, 12) can be more simply stated in a reference system moving with the wave-front X_s . In such a system, the velocity of flow ahead of the wave is $-D$; in the plane X_1 , it is $W_s - D \equiv u_1$. Then

$$\text{on } CI, \quad |u_1| < a_1 \quad (1)$$

$$IG, \quad |u_1| > a_1. \quad (2)$$

By a precisely similar argument, it can be shown that

$$\text{on } FK, \quad |u_1| < a_1, \quad (3)$$

$$KH, \quad |u_1| > a_1. \quad (4)$$

Waves whose terminal points lie beyond I or K have been termed "strong"; those corresponding to IG or FK "weak". Equations (1) - (4) can therefore be expressed by saying that the flow is subsonic behind a strong detonation or weak deflagration, but supersonic behind a weak detonation or strong deflagration. As to the wave velocity D , it is clear that, under our assumptions regarding the adiabatic family

$$D > a_0 \quad \text{in detonation} \quad (5)$$

$$D < a_0 \quad \text{in deflagration.} \quad (6)$$

In the moving reference system, therefore, the flow ahead of the wave-front is supersonic in every detonation and subsonic in every deflagration.

[90] These relations are due in the first place to Jouguet.

§ 9.4 Further consideration of the Chapman-Jouguet condition

We have seen that points B' above I on the RH-curve cannot represent the end-state behind a steady wave. Such points are excluded because, in terms of Jouguet's rule, the flow at X_1 relative to the wave front, is then subsonic, and rarefactions arising behind the steady zone will penetrate into it. Of course if we imagine the wave to be supported by a piston which moves with the velocity W' , defined by B' and so prevents the formation of rarefactions, metastable waves corresponding

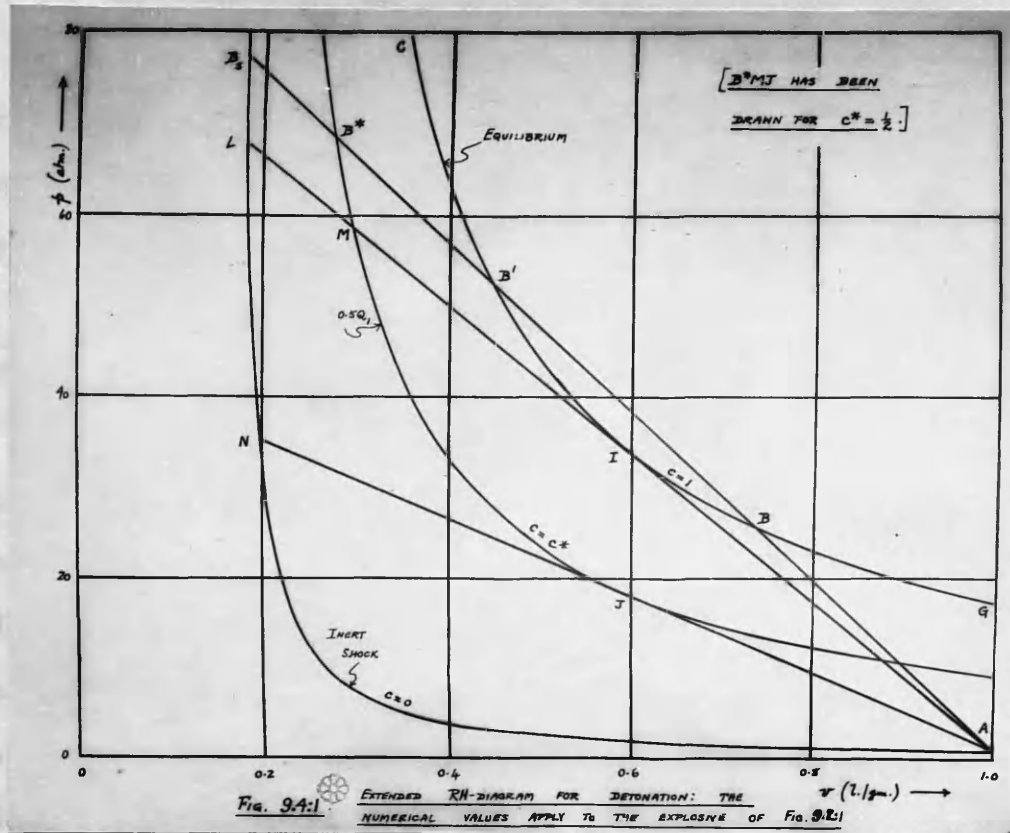
to points above I, with velocities greater than the stable value, can be realised; but such hypothetical waves are of little practical interest.

Points B below I have also been rejected, but on entirely different grounds. At such points, the flow at X, relative to the wave front, is supersonic. Rarefactions cannot then overtake the steady zone; but for the same reason the reaction energy cannot all be made available to support the wave-front. The above argument for excluding B appears [84] [5] to have been first advanced by Jost. Becker rejected B on the thermodynamic grounds; since $S' > S$, the point B' represents a more probable state than B. More elaborate thermodynamic reasons for the rejection of both B and B' and the selection of I have since been [52] offered by Scorah. Such arguments, however, as Jost pointed out, fail to explain convincingly why a wave whose end-state is perturbed from I along IG should tend to return towards the condition represented by I. From this point of view, Jost's own reasoning is to be preferred.

The following more detailed discussion, which is based upon a treatment given by Döring, provides further grounds for excluding the branch IG and for selecting I, and in addition casts considerable light on the structure of the steady zone. As has already been indicated, we regard the detonation wave as a shock followed by chemical reaction. The shock advances into the undetonated material, raising this to a high pressure and temperature and so precipitating reaction; the chemical energy thus released serves to maintain the shock, which because of the essentially subsonic nature of the relative flow behind it would otherwise rapidly degenerate into a sound wave. According to this view, the shock and attendant reaction are complementary and

[140, 159, 5, 170]

inseparable aspects of the detonation wave. It has been shown, however, (§§ 5.5, 6.42) that the region of pressure rise in an intense shock in gases or liquids is extremely thin - of the same order as the interatomic distance; [57] and this conclusion appears also to hold good for solids. Within the time necessary for the wave to traverse this distance only a few molecular collisions can occur, whereas a large number of such collisions will certainly be required to decompose the average molecule in a solid or liquid explosive, even if we suppose the reaction completely homogeneous. In other words, the length of the reaction zone must greatly exceed the shock front thickness, within which no significant chemical change will take place. The steady zone then consists of a non-reactive shock of negligible thickness, advancing into the virgin explosive with velocity D , and changing the state-variables in an effectively discontinuous manner from their initial values p_0, v_0, \dots to p_s, v_s, \dots ; followed by a zone of chemical reaction in which these variables change continuously from p_s, \dots to their equilibrium values p_e, \dots . Since the entire zone is steady, equations 9.1 (1-14) are satisfied, not only by p_e, \dots but also by p_s, \dots and likewise by the values p_s, \dots at any intermediate plane X . Equation 9.1(6) with subscript s defines an RH(v, p)-curve on which the state-point (v_s, p_s) must lie. Since the shock is non-reactive, this curve, represented by $B_s LNA$ in Figure 9.4:1, passes through A. Equation 9.1(6) with subscript 1 defines the usual RH (v, p)-curve CIG for chemical equilibrium. This curve does not pass through A but lies above it. Let us suppose that steady detonation proceeds with a velocity D defined by the secant ABB'_s .



Then by equation 9.1(11), since the wave is steady, each point (v, p) representing a state of incomplete reaction, and in particular the point (v_s, p_s) , must lie on the straight line ABB'_s . In the leading shock, therefore, the state point is carried "discontinuously" from A to B_s , thereafter subsiding along $B_s B'$ to B' , where equilibrium is reached. The state point cannot proceed continuously within the steady zone to points lying on the secant between B' and B , since such points do not correspond to states of thermodynamic equilibrium. The only conceivable further change is a discontinuous one from B' to B . However, it has been shown that the states B', B stand in the same relation to each other as the final and initial states in a non-reactive compressional shock. It follows that B would represent the final state in a non-reactive rarefaction shock leading from B' . In order that the state-point should move from B' to B , therefore, a rarefaction shock must intervene.

Alternatively we might suppose that, after reaction had proceeded some way, and the representative point had traversed part of the step B_sB' , a rarefaction shock carried the point to a position on AB, from which B might be reached by renewed compression. But without the intervention of a rarefaction shock, B cannot be reached in a steady wave. Since rarefaction shocks are normally impossible on both mechanical and thermodynamic grounds, we are justified in disqualifying terminal points B below I.

No stable wave, therefore, can have a velocity greater than that [52] defined by I. Döring has extended the treatment to exclude also the possibility of a steady wave with velocity less than the value at I. In order to take advantage of this argument, we shall assume that the chemical composition at any stage during reaction can be defined by a single parameter c . This will not, of course, in general be possible, but it will be the case if the combustion process involves only one elementary reaction, for example $\alpha\beta \rightarrow \alpha+\beta$, or alternatively if all other parallel reactions proceed at a relatively much faster speed, so that they reach effective equilibrium at every stage of the process. In this event, we may suppose all the state variables, including those defining the composition, to be expressed in terms of v, p and c . The RH-equation then determines a one-parameter family of RH-curves, with parameter c . If c represents the fraction of an initial reactant decomposed, then the RH-curve $c=0$ coincides with B_sLA , the shock-wave curve in the undetonated explosive. If we further assume that the concentration of this reactant is negligibly small in any practicable equilibrium state, the curve $c=1$ coincides with cIG , the RH-curve for equilibrium. Between these two extreme curves will lie the rest of

the RH-family, corresponding to values of c between 0 and 1. One member, B^*MJ , defined by $c=c^*$, is drawn in Figure 9.4:1. Let us postulate a steady wave with velocity defined by the upward tangent AJ to this curve, and therefore less than the value at I. The state-point must then be carried in the leading shock from A over to N, thereafter subsiding along NJ to J. The fraction of the principal reactant decomposed has now risen to C^* . Values of c larger than c^* , however, cannot be reached along NJA; in other words the wave cannot be steady beyond the point at which $c=c^*$. The subsequent course of the reaction then takes place in a part of the wave which changes with time. We cannot, however, immediately dismiss the possibility that the first part of the wave, corresponding to NJ, may be capable of independent steady propagation. For by precisely the same argument as was used above we can show that the Chapman-Jouguet relation $W+a=D$ applies, not only at I, but also at every point of tangency J on the intermediate curves. This follows from our assumption that the rate-determining process is relatively slow, so that a state of quasi-equilibrium applies at each value of c . Rarefactions arising behind the steady part of the wave are therefore unable to penetrate it. However, reaction will, in fact, proceed in the non-steady zone, giving rise ultimately to a second wave of compression which must develop into a second shock. This shock, which moves with supersonic velocity relative to the products will be able, unlike the rarefactions, to overtake and penetrate the steady zone. Moreover, it follows also from the argument that the sum of streaming and sound velocities exceeds the wave-velocity at every point on an intermediate RH-curve above the appropriate point of tangency; but all points along NJ are such upper

points on the corresponding RH-curves. Hence the secondary shock will not only penetrate into the steady zone but will propagate through to the leading shock, whose velocity will be thereby increased until ultimately the terminal point reaches I. The present analysis therefore demonstrates the impossibility, under the conditions assumed, of steady waves with velocities smaller than that defined by I, and provides justification also for our assumption, made at the outset, that the end of the steady zone should coincide with the plane in which chemical equilibrium is realised. It is clear too that we may now complete the discussion of waves defined by such secants as ABB' . Since $W+a > D$ not only at B' but also throughout BB'_s , the rarefaction which was shown to overtake the wave at B' will in fact penetrate to its head. Finally, we may satisfy ourselves that at I the wave is stable; for although at I, $a+W=D$, throughout IML $a+W>D$. Rarefactions cannot, therefore, penetrate the wave, whose energy may nevertheless all be made available to sustain the shock-front.

The above discussion is naturally rather idealised. However, it is not unreasonable to assume that the reaction rate in a condensed explosive is determined principally by the initial decomposition of the explosive molecule, and in many cases even by a heterogeneous process confined to the surface of grains, and that the subsequent reorganisation of the gaseous decomposition products is achieved at a much more rapid rate. Again the implicit assumption that the RH-family do not intersect or possess an envelope is probably well justified in practice. It must, however, be emphasised that the argument whereby velocities less than normal are excluded depends entirely on the absence of lateral expansion behind X_s . If such expansion occurs, as in practice

it always will do unless the cartridge diameter is exceptionally large, lateral rarefactions will spread into the reaction zone. In this case, shock waves are not bound to develop in the non-steady part of the reaction zone, and a stable wave may be established with velocity smaller than that defined by Al. However, the motion is no longer strictly one-dimensional, and its determination becomes much more complex. (See § 17).

We shall also defer until § 19 further consideration of the wave profile in a well-confined cartridge, that is, of the variation in pressure, density etc. throughout the steady zone. The general nature of this variation, however, is already clear. The pressure, density, mass velocity and temperature increase abruptly in the leading non-reactive shock; thereafter, as reaction proceeds, towards equilibrium, the pressure and density decrease again to their values $\bar{p}, \bar{\rho}$, in the CJ-plane. The mass-velocity W , by equation 9(13) proportional to the pressure, must then also decrease throughout $X_s X_p$. The temperature, on the other hand, is determined (at least for a homogeneous explosive of low or moderate density) principally by release of chemical energy, and should, therefore, continue to rise beyond T_s in the reaction zone.

§ 9.5 Summary of basis for computation in the CJ-plane

In order to determine conditions in the CJ-plane, we require to solve (a) the three conservation equations, together with (b) the CJ-condition, (c) the equations of state and (d) the thermodynamic equilibrium conditions for the products.

§ 9.51 Evaluation of $E_i - E_o$.

The equations expressing conservation of mass and momentum are purely mechanical and require no further comment. In the RH-equation, however,

$E_i - E_o$ must be evaluated in terms of the state-variables. For this purpose, we write

$$E_i - E_o = (E_i - E_i^*) - (E_o - E_o^*) - (E_o^* - E_i^*). \quad (1)$$

The suffix i refers throughout to the actual CJ product composition, the suffix o to the reactants. The star (*) is used to denote a chosen standard state of pressure and temperature, typically (1 atm., 273°K) or (1 atm., 298°K). The third bracket in (1) thus represents the internal energy change which would occur if the explosive were supposed to pass at (p^*, T^*) into the actual CJ-products. In other words, $E_o^* - E_i^*$ is the difference in internal energy of formation (heat of formation at constant volume) of reactants and CJ-products at T^* , and is considered positive if heat is evolved in the reaction. For convenience, we write Q_i for this quantity, so that

$$Q_i = E_o^* - E_i^* = (E_o^* - E_{el}^*) - (E_i^* - E_{el}^*), \quad (2)$$

where E_{el}^* is the internal energy of the constituent elements in the state *. Representative values of E_{el}^* , when * = (1 atm., 273°K), are collected in Table 9.51:1.

The first bracket in (1) represents the increase in energy of the CJ-products in a hypothetical non-reactive change from the state * to the state (p_i, T_i, v_i) . However along such a path,

$$dE = C_v dT + (T \frac{\partial p}{\partial T} - p) dv. \quad (3)$$

Hence

$$E_i - E_i^* = \int_*^{T_i, v_i} [C_v dT + (T \frac{\partial p}{\partial T} - p) dv], \quad (4)$$

and similarly

$$E_o - E_o^* = \int_*^{T_o, v_o} [C_v dT + (T \frac{\partial p}{\partial T} - p) dv]_o. \quad (5)$$

Table 9.51:1

Energies of formation $E^* - E_{el}^*$ from the elements at 273°K (K.cal./mol.)

Substance	$E^* - E_{el}^*$	Ref.	Substance	$E^* - E_{el}^*$	Ref.
CO ₂	-94.02	142	C ₂ H ₂	+54.48	134
CO	-26.73	142	H	+51.94	72
H ₂ O(gas)	-57.47	142	O	+58.88	72
CH ₄	-17.16	134	N	+85.37	72
NO	+21.52	106	H ₂ , O ₂ , N ₂ , C	0	
<hr/>					
Nitroglycerine (C ₃ H ₅ O ₉ N ₃)	-84.6	167	Trinitrotoluene (C ₇ H ₅ O ₆ N ₃)	-10.3	148
Nitroglycol (C ₂ H ₆ O ₂ N ₂)	-54.9	148	Tetryl (C ₇ H ₅ O ₈ N ₅)	+12.1	148
Erythritol (C ₄ H ₁₀ N ₄)	-112.0	148	Ammonium nitrate (NH ₄ NO ₃)	-84.7	10
Tetranitrate (C ₄ H ₁₂ N ₄)	-150.2	148	Sodium nitrate (NaNO ₃)	-110.6	10
Mannitol	-4.6	148	Potassium nitrate (KNO ₃)	-117.6	10
Hexanitrate (C ₆ H ₈ O ₁₈ N ₆)	-121.2	148	Cellulose (C ₆ H ₁₀ O ₅)	-223.6	148
Tetranitromethane (CO ₈ N ₄)					
Pentaerythritol					
Tetranitrate (C ₅ H ₈ O ₁₂ N ₄)					

Let 1 gm. of the CJ-products contain $n_{(1)}$ moles of the first molecular species, $n_{(2)}$ of the second, etc. Then (4) can be evaluated, if this composition is known, and also the equations of state of these products, viz.

$$f_1(p, v, T; n_{(1)}, n_{(2)}, \dots) = 0 \quad (6)$$

$$f_2(c_v, v, T; n_{(1)}, n_{(2)}, \dots) = 0, \quad (7)$$

between * and (T_1, v_1) . If * coincides with (p_0, T_0) , (5) is zero; otherwise its evaluation requires a knowledge of the equations of state of the explosive between * and (p_0, T_0) .

If the products satisfy an equation of state for which $T \frac{\partial b}{\partial T} - p \equiv 0$, (4) becomes

$$E_i - E_i^* = \int_{T^*}^{T_1} c_v dT = \bar{c}_v (T_1 - T^*), \quad (8)$$

where \bar{c}_v is the mean specific heat from T^* to T_1 ; if also * coincides with (p_0, T_0) the RH-equation is then

$$E_i - E_0 = \bar{c}_v (T_1 - T_0) - Q_1 = \frac{1}{2} (p_1 + p_0)(v_0 - v_1). \quad (9)$$

Whether this is true or not, however, the gaseous phase in the products will be ideal at *, since p^* in practice is almost always 1 atm. This circumstance permits a convenient transformation of (4). Thus in place of (3) we can write

$$dE = [c_v + \frac{\partial v}{\partial T} (T \frac{\partial b}{\partial T} - p)] dT - [T \frac{\partial v}{\partial T} + p \frac{\partial v}{\partial p}] dp. \quad (10)$$

We integrate (a) from T^* to T_1 , with $p = p^*$, and thereafter (b) from p^* to p_1 , with $T = T_1$. Since the product gases are ideal over (a),

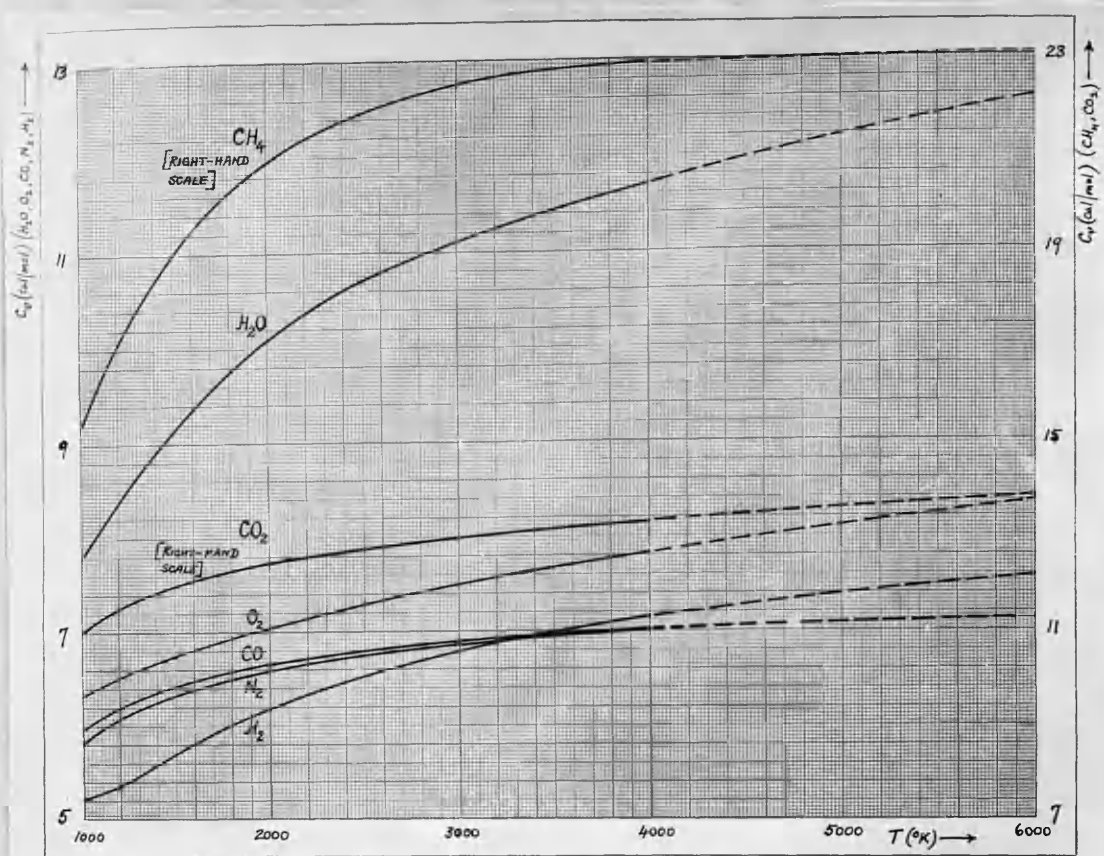


FIG. 9.51:1 TRUE SPECIFIC HEAT AT CONSTANT VOLUME

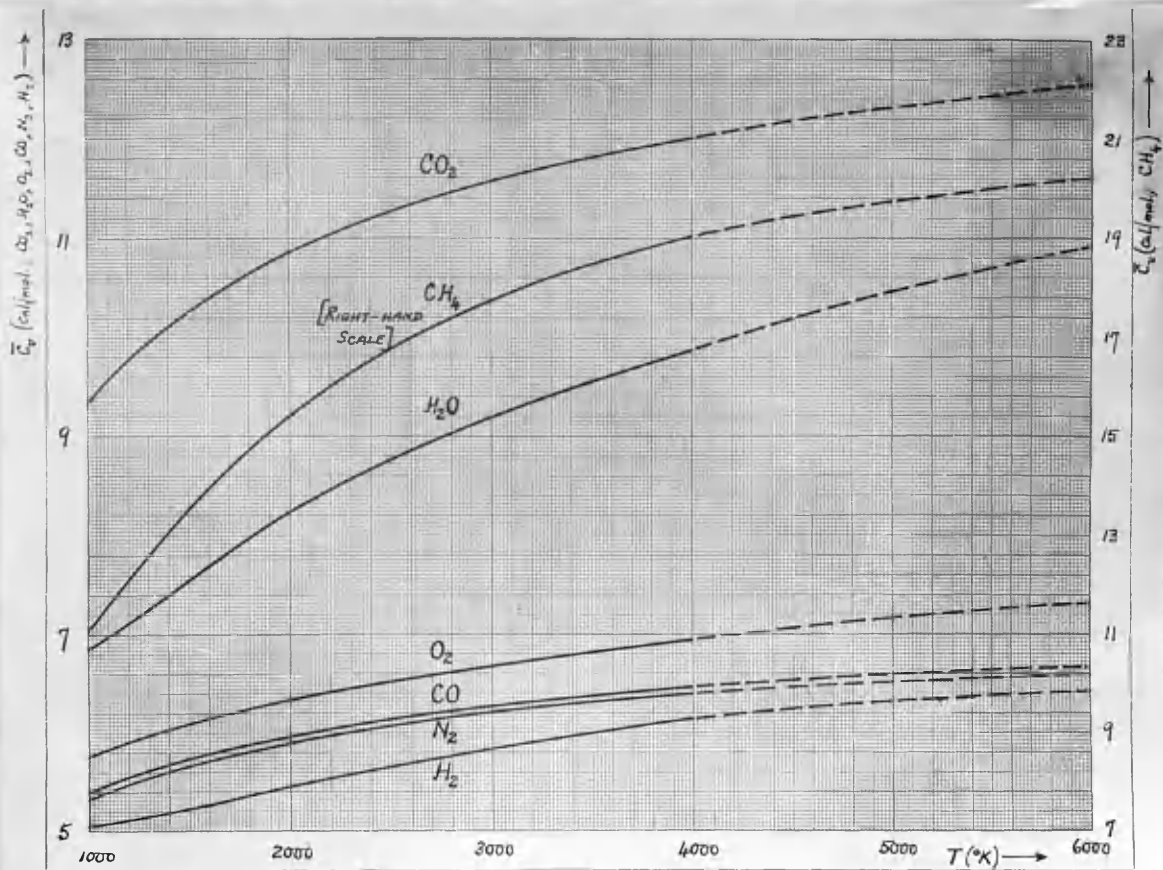


FIG. 9.51:2 MEAN SPECIFIC HEAT AT CONSTANT VOLUME BETWEEN 273°K AND T°K.

this yields, for purely gaseous products

$$E_i - E_i^* = \left[\int_{T^*}^{T_1} c_v dT \right]_{p=p^*} - \left[\int_{p^*}^{p_1} (T \frac{\partial v}{\partial T} + p \frac{\partial v}{\partial p}) dp \right]_{T=T_1}. \quad (11)$$

The first integral is the change in energy from * to 1 in the ideal gas state, and may be written $\Delta E^{(o)}$. If the products are not entirely gaseous, (11) may still be applied to the gaseous phase.

$c_v(T)$ and $\bar{c}_v(T)$ are shown graphically for the principal detonation product species in Figs. 9.51:1, 2.

§ 9.52 The Chapman-Jouguet condition

The CJ-condition is expressed by any one of the four equations 9.1(14-17). In applying 9.1(16 or 17), $(\partial p_i / \partial v_i)_s$ should properly be calculated with reference to the most general isentropic change, that is, one in which the chemical composition does not remain constant [88] but varies in equilibrium with the changing state-variables. However, it may be expected that the effect upon $(\partial p_i / \partial v_i)_s$ of the adjustment in equilibrium will be small provided that the equilibrium itself is not unduly sensitive to changes in pressure and temperature. $(\partial p_i / \partial v_i)_s$ may then in many cases be evaluated as an algebraic function of the state-variables, thus permitting an analytic statement of the CJ-condition (by means of equation 9.1(17)), and so allowing the CJ-state to be identified directly. This is equivalent to determining the point of tangency I (Fig. 9.1:1) without prior calculation of the RH-curve. Examples of this procedure, which is usually justified in practice, will be found below. Otherwise, it is best, as a rule, to determine a portion of the RH-curve near to the CJ point, which is then selected graphically by drawing the upward tangent from (v_0, p_0) .

§ 9.53 Equations of state

These are expressed by 9.51(6,7), and must be suitably formulated for each type of explosive.

§ 9.54 Equilibrium conditions

The product composition is defined as a function of pressure and temperature by (I) a set of material balance equations, expressing conservation of mass in a chemical change, and equal in number to the atomic species involved, together with (II) a complementary set of equilibrium equations expressing the stationary property of the Gibbs free energy in an equilibrium change at the given temperature and pressure.

The detonation products may contain solid or liquid as well as gaseous phases. Consider, therefore, an arbitrary representative mass of the total products, occupying a volume $V = V_g + V_c$ where V_g, V_c are the volumes of gaseous and condensed phases respectively. Let V_g contain N_i moles of the i^{th} molecular species L_i present, where $N_g \equiv \sum_{i=1}^s N_i$ and let V_c contain in all N_c moles. We are not normally concerned with equilibria in the condensed phase. Then, the state of the gases will be completely described by their uniform temperature T and pressure p together with N_i ; and if $G_g \equiv E_g + pV_g - TS_g$ [65] is the appropriate Gibbs free energy, we have

$$dG_g = -S_g dT + V_g dp + \sum_i \mu_i dN_i. \quad (1)$$

where

$$\mu_i \equiv \left(\frac{\partial G_g}{\partial N_i} \right)_{T, p, N_j \neq i}. \quad (2)$$

μ_i may therefore be called a "partial molar Gibbs free energy", but is more commonly known as a (partial) chemical potential.

The condition for thermodynamic equilibrium at prescribed temperature T and pressure p is that, in any infinitesimal change in which T, p remain constant and consequently only the N_i vary,

$$dG_g = 0. \quad (3)$$

By by (1) this implies

$$\sum \mu_i dN_i = 0. \quad (4)$$

Between the s gaseous species there will exist, say, r reactions which are represented by linearly independent chemical equations.

Let one of these equations be

$$\sum \ell_i L_i = 0, \quad (5)$$

where L_i denotes one mole of the i^{th} species, and ℓ_i the number of moles of this species participating in the chosen reaction; some of the ℓ_i may of course be zero. Then in any small change at constant T, p in which only the species involved in the reaction (5) are affected, we have

$$\frac{dN_i}{\ell_i} = \frac{dN_j}{\ell_j} = \text{etc.} \quad (6)$$

For such a change, therefore, (4) becomes

$$\sum \mu_i \ell_i = 0, \quad (7)$$

and a similar equation will hold for each of the other $r-1$ independent reactions.

However, by (1),

$$\left(\frac{\partial \mu_i}{\partial p} \right)_{T, N_i} = \left(\frac{\partial V_g}{\partial N_i} \right)_{T, p, N_j \neq i}. \quad (8)$$

In a single perfect gas L_i ,

$$pV_g = N_i RT, \quad (9)$$

so that

$$\frac{\partial \mu_i}{\partial p} = \frac{RT}{p}, \quad (10)$$

and consequently [65]

$$\mu_i = \mu_i^\circ(T) + RT \ln \frac{p}{p_0}, \quad (11)$$

where μ_i° is a function of T alone.

A perfect gas mixture is then defined as one in which the partial potential μ_i of each species is given by [65]

$$\mu_i = \mu_i^\circ(T) + RT \ln \frac{p_i}{p_0}, \quad (12)$$

where $p_i \equiv p N_i / N_g$, and μ_i° is the same function as in (11). For such an ideal mixture, therefore, the equilibrium condition (7) becomes

$$RT \sum \ell_i \ln \frac{p_i}{p_0} = \sum \ell_i \mu_i^\circ, \quad (13)$$

or

$$\prod (p_i)^{\ell_i} = K(T) \equiv e^{\sum \ell_i \mu_i^\circ / RT},$$

where the function $K(T)$ is called the equilibrium constant for the reaction (5). (13) may evidently be written

$$\prod (N_i)^{\ell_i} = (N_g/p)^{\sum \ell_i} \cdot K(T), \quad (14)$$

which depends on p , unless indeed $\sum \ell_i = 0$.

In deriving (13), (14), we have assumed that all the species participating in (5) are present in the gaseous phase. If, however, certain of these species are present also in the condensed phase, their vapour pressures will frequently be small by comparison with the total pressure, and will also be almost independent of this pressure. Species present in the condensed phase are, therefore, understood to be disregarded in performing the operations denoted by \prod and \sum in (13) and (14).

The equilibrium constants with which we shall be concerned are given in Table 9.54:1. Linear interpolation may be carried out on a graph of $\log K$ against $\frac{1}{T}$.

All gas mixtures may be assumed to become perfect at sufficiently low pressure, and will then satisfy equation (12) and its consequences. In the general case of an imperfect mixture, (12) does not apply.

However, for such a mixture, we define a function \tilde{f} by the equation [65]

$$\mu_i^o = \mu_i^o(T) + RT \ln \tilde{f}, \quad (15)$$

where μ_i^o is the same function of T as before. \tilde{f} is called the fugacity of the i^{th} species in the mixture, and (13) must evidently now be replaced by

$$\prod (\tilde{f}_i)^{\ell_i} = K(T). \quad (16)$$

We cannot, of course, write $\tilde{f}_i = \frac{p N_i}{N_g}$, but we may express the equilibrium condition (16) as

$$\prod (N_i)^{\ell_i} = I \cdot \left(\frac{N_g}{p} \right)^{\sum \ell_i} K(T), \quad (17)$$

where

$$I \equiv \prod \left(\frac{p_i}{\tilde{f}_i} \right)^{\ell_i} \quad (18)$$

In applying these equations, it is again understood that species present also in the condensed phase are disregarded.

It remains only to identify the fugacities \tilde{f}_i or the corresponding activity coefficients $A_i \equiv \tilde{f}_i / p_i$. This can be done if the equation of state is known. Thus, by (8) and (15)

$$\left(\frac{\partial \ln \tilde{f}_i}{\partial p} \right)_{T, N_i} = \frac{1}{RT} \left(\frac{\partial V_g}{\partial N_i} \right)_{T, p, N_j}. \quad (19)$$

But

$$\left(\frac{\partial \ln p_i}{\partial p} \right)_{T, N_i} = \frac{1}{p}. \quad (20)$$

Hence

$$\left(\frac{\partial \ln A_i}{\partial p} \right)_{T, N_i} = \frac{1}{RT} \frac{\partial V_g}{\partial N_i} - \frac{1}{p}. \quad (21)$$

Moreover, since the mixture becomes perfect for small ϕ ,

$$A_i \rightarrow 1 \quad \text{as} \quad \phi \rightarrow 0. \quad (22)$$

Consequently

$$\ln A_i = \int_0^\phi \left(\frac{1}{RT} \frac{\partial V_g}{\partial N_i} - \frac{1}{\phi} \right) d\phi. \quad (23)$$

An alternative expression for A_i is sometimes advantageous. It is obtained by introducing the Helmholtz free energy $F_g \equiv G_g - \phi V_g$, for which by (1)

$$dF_g = -S_g dT - \phi dV_g + \sum \mu_i dN_i, \quad (24)$$

so that

$$\left(\frac{\partial \mu_i}{\partial V_g} \right)_{T, N_i} = - \left(\frac{\partial \phi}{\partial N_i} \right)_{T, V_g, N_j}. \quad (25)$$

Using (15) as before, we then have

$$\frac{\partial \ln A_i}{\partial T} = - \frac{1}{RT} \frac{\partial \phi}{\partial N_i} - \frac{1}{\phi} \frac{\partial \phi}{\partial V_g}, \quad (26)$$

whence

$$\ln A_i = \int_{V_g}^{\infty} \left(\frac{1}{RT} \frac{\partial \phi}{\partial N_i} + \frac{1}{\phi} \frac{\partial \phi}{\partial V_g} \right) dV_g. \quad (27)$$

The integrations in (23) and (27) are to be performed at constant temperature and composition. Since

$$0 \equiv \left(\frac{\partial V_g}{\partial N_i} \right)_{T, \phi, N_j} + \left(\frac{\partial V_g}{\partial \phi} \right)_{T, N_i} \cdot \left(\frac{\partial \phi}{\partial N_i} \right)_{T, V_g, N_j},$$

it can be seen at once that the two integrals are equivalent.

To evaluate (23) or (27), a knowledge of the equation of state for the gaseous phase is necessary. If this can be written in the form

$$\phi = \phi(T, V_g, N_g), \quad (28)$$

we have

$$\frac{\partial V_g}{\partial N_i} = \frac{\partial V_g}{\partial N_g} ; \quad \frac{\partial p}{\partial N_i} = \frac{\partial p}{\partial N_g}, \quad (29)$$

so that A_i has the same value, say A , for all the species. If $A \equiv \frac{p}{f}$, (17) then becomes

$$\pi(N_i)^{\ell_i} = \left(\frac{N_g}{f}\right)^{\sum \ell_i} \cdot K(T). \quad (30)$$

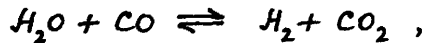
Moreover, in such a case we may assume that

$$\frac{\partial V_g}{\partial N_g} = V_g/N_g, \quad (31)$$

the derivative representing physically a simple increase in the total quantity of gas, at constant T, f . Then by (23)

$$\ln A = \int_0^f \left(\frac{V_g}{N_g R T} - \frac{1}{f} \right) df. \quad (32)$$

It is to be noted that if in addition to (28) we have also $\sum \ell_i = 0$, as for example in the important watergas reaction



(30) and (14) become identical. The mixture thus behaves ideally so far as such reactions are concerned.

In general, it cannot be assumed at the outset that N_i will vanish explicitly from the equation of state, as required by (28). The fugacity of each species must then be evaluated separately by (23) or (27).

Equations (17), together with the material balance equations representing conservation of mass, provide the requisite information for determining the equilibrium composition at any prescribed temperature and pressure.

Table 9.54:1

Short table of equilibrium constants

T (°K)	$\log_{10} K_1$	$\log_{10} K_2$	$\log_{10} K_3$	$\log_{10} K_4$	$\log_{10} K_5$	$\log_{10} K_6$	$\log_{10} K_7$
2500	0.8089	2.5779	3.8651	7.1308	2.1910	2.7766	2.9865
3000	0.8798	1.5285	4.1845	7.5702	1.0785	1.0900	1.4130
3500	0.9193	0.1964	4.4127	7.8996	1.7132	1.3133	1.7119
4000	0.9421	0.6917	4.5912	6.1656	0.1905	1.4791	1.9205
4500	0.9519	1.0694	4.7408	6.3872	0.5618	1.6060	0.0767
5000	0.9548	1.3676	4.8618	6.5800	0.8607	1.7068	0.1907

[75]

210

$$\begin{aligned}
 K_1 &\equiv p_{CO} \cdot p_{H_2,0} / (p_{CO_2} \cdot p_{H_2}) && (CO_2 + H_2 \rightleftharpoons CO + H_2O) \\
 K_2 &\equiv p_{CO} \cdot p_{O_2}^{1/2} / p_{CO_2} && (CO_2 \rightleftharpoons CO + \frac{1}{2} O_2) \\
 K_3 &\equiv p_{H_2}^2 / p_{CH_4} && (CH_4 \rightleftharpoons C + 2H_2) \\
 K_4 &\equiv p_{O_2}^{1/2} / p_{CO} && (CO \rightleftharpoons C + \frac{1}{2} O_2) \\
 K_5 &\equiv p_O / p_{O_2}^{1/2} && (\frac{1}{2} O_2 \rightleftharpoons O) \\
 K_6 &\equiv p_{NO} / p_{O_2}^{1/2} \cdot p_{N_2}^{1/2} && (\frac{1}{2} O_2 + \frac{1}{2} N_2 \rightleftharpoons NO) \\
 K_7 &\equiv p_{HCN} / p_{H_2}^{1/2} \cdot p_{N_2}^{1/2} && (C + \frac{1}{2} H_2 + \frac{1}{2} N_2 \rightleftharpoons HCN).
 \end{aligned}$$

§10 Detonation in ideal gases [42,91]

The fundamental theory has a particularly simple and explicit form when the detonation products are assumed to constitute an ideal gas mixture whose specific heats and chemical equilibrium composition are independent of temperature and pressure. Since density increases during detonation, this will usually imply that the original explosive was also gaseous; but there is no need to assume this: the physical state before detonation is irrelevant, and the theory will also apply, for example, to atmospheric clouds of combustible particles or to explosive foams or emulsions at extremely low bulk density.

For simplicity, we identify (T_0, p_0) with (T^*, p^*) . The product gas equation of state is

$$pv = nRT \quad (1)$$

n being the number of moles per gm. and R the gas constant per mole.

$T \frac{\partial b}{\partial T} - p$ then vanishes identically, and since further C_v is supposed constant = C , say, the RH-equation becomes, by 9.51(9),

$$C_v(T_1 - T_0) = \frac{p_1 v_1 - p_0 v_0'}{\gamma_i - 1} = Q_i + \frac{1}{2} (p_1 + p_0)(v_0 - v_1), \quad (2)$$

where $\gamma_i \equiv 1 + nR/C$, and v_0' is the specific volume which the products would have at (p_0, T_0) . In the convenient notation

$$v_0' \equiv v_0, \quad \pi \equiv p_1/p_0, \quad \varphi \equiv v_1/v_0, \quad B \equiv \frac{Q_i(\gamma_i - 1)}{p_0 v_0} + \gamma_i - 1,$$

(2) reduces to

$$(\pi + \frac{\gamma_i - 1}{\gamma_i + 1})(\varphi - \frac{\gamma_i - 1}{\gamma_i + 1}) = \frac{2}{\gamma_i + 1} (B + \frac{2\gamma_i}{\gamma_i + 1}). \quad (3)$$

The RH-curve is thus a rectangular hyperbola, with asymptotes

$$v_1 = \frac{\gamma_i - 1}{\gamma_i + 1} v_0 \quad ; \quad p_1 = - \frac{\gamma_i - 1}{\gamma_i + 1} p_0. \quad (4)$$

The curve evidently does not approach the p -axis, but cuts the v -axis where

$$\frac{v}{v_0} = 1 + 2 \frac{B + 1}{\gamma_i - 1}. \quad (5)$$

The slope at any point (v_i, p_i) is

$$(dp_i/dv_i)_{RH} = - \frac{(\gamma_i+1)p_i + (\gamma_i-1)p_0}{(\gamma_i+1)v_i - (\gamma_i-1)v_0}, \quad (6)$$

while the slope of the adiabatic at the same point is

$$(dp_i/dv_i)_S = - \frac{\gamma_i p_i}{v_i}, \quad (7)$$

since we assume the equilibrium composition independent of T , and p .

The two curves therefore touch where

$$\frac{(\gamma_i+1)p_i + (\gamma_i-1)p_0}{(\gamma_i+1)v_i - (\gamma_i-1)v_0} = \frac{2\gamma_i p_i}{2v_i} = \frac{p_i - p_0}{v_0 - v_i}, \quad (8)$$

by adding the numerators and denominators. Thus the RH- and adiabatic curves touch at, and only at, the two points of contact of the tangents from (v_0, p_0) . It may now readily be shown that the RH-curve, adiabatic and secant AB through an arbitrary point B have the relative slopes already illustrated in Figure 9.1:1.

By (8), the CJ-condition for stability is

$$\frac{\pi - 1}{1 - \varphi} = \frac{\gamma_i \pi}{\varphi}, \quad (9)$$

whence

$$\pi = \frac{\varphi}{(\gamma_i+1)\varphi - \gamma_i}. \quad (10)$$

Elimination of π from (3) and (10) gives

$$\varphi^2 - \frac{2}{\gamma_i} (B + \gamma_i) \varphi + \frac{2B}{\gamma_i+1} + 1 = 0, \quad (11)$$

from which the values of φ at the points I, K of tangency may be determined. The corresponding values of π follow from (10). They are the roots of:

$$\pi^2 - 2(B+1)\pi + \frac{2B}{\gamma_i+1} + 1 = 0. \quad (11a)$$

Again, by 9(11) and (8), (10)

$$\frac{D^2}{\gamma_i p_0 v_0} = \frac{\pi}{\varphi} = \frac{1}{(\gamma_i+1)\varphi - \gamma_i}, \quad (12)$$

$$\frac{W_i^2}{\gamma_i p_0 v_0} = \frac{\pi}{\varphi} (1-\varphi)^2 = \frac{(1-\varphi)^2}{(\gamma_i+1)\varphi - \gamma_i}. \quad (13)$$

Elimination of π, φ from (12) leads to the following quadratic in $\delta = D^2/\gamma_1 p_0 v_0$:

$$\delta^2 - \frac{2}{\gamma_1} [B(\gamma_1 + 1) + \gamma_1] \delta + 1 = 0. \quad (14)$$

If δ, δ' are the roots of (14), then $\delta \delta' = 1$, from which we conclude that D and D' , the wave-velocities corresponding to I, K, are related by

$$DD' = \gamma_1 p_0 v_0. \quad (15)$$

When the unreacted material is an ideal gas, this relation becomes:

$$DD' = (\gamma_1 / \gamma_0) a_0^2 \quad (16)$$

$$= a_0^2, \text{ if } \gamma_1 = \gamma_0. \quad (17)$$

The velocity of sound in the undetonated gas is then a geometric mean to the minimum velocity of detonation and the maximum velocity of deflagration.

It is also possible to eliminate φ and π from equations (3), (9) and (13), yielding the surprisingly simple result:

$$W_1^2 / \gamma_1 p_0 v_0 = 2B / \gamma_1 (\gamma_1 + 1) \quad (18)$$

The gas velocities behind the waves of slowest detonation and fastest deflagration are therefore equal (numerically).

In practice, B is always large compared with 1; for example if $p_0 = 1 \text{ atm.}$, $v_0 = 1000 \text{ cm}^3/g$, $\gamma_1 = 1.4$, $\nu = 1$ and $Q_1 = 1000 \text{ cal/g}$, then $B \approx 16.5$. The following solution of (11) in descending powers of B is therefore useful:

$$\text{At I, } \frac{v_1}{v_0} = \frac{\gamma_1}{\gamma_1 + 1} \left[1 + \frac{1}{2(\gamma_1 + 1)B} - \frac{\gamma_1}{2(\gamma_1 + 1)B} \right] \quad (19)$$

$$\text{At K, } \frac{v_1}{v_0} = \frac{2B}{\gamma_1} + \frac{1}{\gamma_1 + 1} \left[\gamma_1 + \frac{\gamma_1}{2(\gamma_1 + 1)B} + \frac{\gamma_1}{2(\gamma_1 + 1)B} \right]. \quad (20)$$

The corresponding values of pressure, temperature, mass velocity and wave velocity are

$$\text{At I, } \frac{p_i}{p_0} = 2B \left[1 + \frac{2\gamma+1}{2(\gamma+1)B} - \frac{\gamma^2}{\gamma(\gamma+1)} \right] \quad (21)$$

$$\text{At K, } \frac{p_i}{p_0} = \frac{1}{\gamma+1} \left[1 + \frac{\gamma^2}{2(\gamma+1)B} - \frac{\gamma^2}{\gamma(\gamma+1)} \right] \quad (22)$$

$$\text{At I, } \frac{T_i}{T_0} = \frac{2B\gamma}{\nu(\gamma+1)} \left[1 + \frac{1}{B} - \frac{\gamma^2}{\gamma(\gamma+1)} \right] \quad (23)$$

$$\text{At K, } \frac{T_i}{T_0} = \frac{2B}{\nu\gamma(\gamma+1)} \left[1 + \frac{\gamma}{B} - \frac{\gamma^2}{\gamma(\gamma+1)} \right] \quad (24)$$

$$\text{At or K, } \frac{W_i^2}{\gamma_i p_0 v_0} = \frac{2B}{\gamma_i(\gamma+1)} \quad (\text{exactly}) \quad (25)$$

$$\text{At I, } \frac{D^2}{\gamma_i p_0 v_0} = \frac{2B(\gamma+1)}{\gamma_i} \left[1 + \frac{\gamma}{(\gamma+1)B} - \frac{\gamma^2}{\gamma(\gamma+1)} \right] \quad (26)$$

$$\text{At K, } \frac{D^2}{\gamma_i p_0 v_0} = \frac{\gamma_i}{2B(\gamma+1)} \left[1 - \frac{\gamma}{(\gamma+1)B} + \frac{\gamma^2}{\gamma(\gamma+1)} \right]. \quad (27)$$

To a first approximation, therefore, we have the solution summarised in Table 10:1. The numerical values represent orders of magnitude, when

$p_0 = 1 \text{ atm.}$, $v_0 = 1000 \text{ cm}^3/\text{gm.}$, $T_0 = 300^\circ\text{K}$, $\gamma_i = 1.4$, $Q_i = 1,000 \text{ cal/gm.}$, and $c_i = 0.33 \text{ cal/gm.}^\circ\text{K}$. It can be seen from the Table that the product $D_i \cdot D_K$ is equal to $\gamma_i p_0 v_0$, in agreement with (15); and also that $W_i = -W_K$. Moreover $T_i \approx \gamma_i^2 T_K$.

Table 10:1 [91]

Approximate properties of the stable detonation and fastest deflagration in an explosive whose products form an ideal gas

Steady Detonation		Fastest Deflagration	
$\gamma_i v_0 / (\gamma_i + 1)$	$5 \cdot 10^2 \text{ cm}^3/\text{gm.}$	$2Q_i(\gamma_i - 1) / \gamma_i p_0$	$2 \cdot 10^4 \text{ cm}^3/\text{gm.}$
$2Q_i(\gamma_i - 1) / v_0$	30 atm.	$p_0 / (\gamma_i + 1)$	0.4 atm.
$2Q_i \gamma_i / (\gamma_i + 1) c_i$	3000°K	$2Q_i / \gamma_i (\gamma_i + 1) c_i$	1500°K
$\sqrt{2Q_i(\gamma_i - 1) / (\gamma_i + 1)}$	1000 m/s	$-\sqrt{2Q_i(\gamma_i - 1) / (\gamma_i + 1)}$	-1000 m/s
$\sqrt{2Q_i(\gamma_i^2 - 1)}$	3000 m/s	$\gamma_i p_0 v_0 / \sqrt{2Q_i(\gamma_i^2 - 1)}$	50 m/s

It is also of interest to compare the pressure \dot{p}_1 , and temperature T_1 , reached in the steady detonation wave with the values p_v, T_v attained in explosion at constant volume (that is, at the point G in Figure 9.1:1). Assuming as before that Q_1 is large, we have $T_v \sim \frac{Q_1}{C_1}$, and $\dot{p}_v = n_v R T_v / v_0 \sim (\gamma - 1) Q_1 / v_0$. Hence

$$T_1 \sim \frac{2\gamma_1}{\gamma_1 + 1} T_v \sim 1.1 T_v \quad (28)$$

$$\dot{p}_1 \sim 2\dot{p}_v \quad (29)$$

The detonation pressure is thus approximately twice the constant-volume explosion pressure. The temperature, however, is only about 10% higher than the constant-volume value. The source of this additional temperature rise is evidently to be found in the so-called "Rankine-Hugoniot" energy of compression represented by the term $\frac{1}{2}(\dot{p}_1 + p_0)(v_0 - v_1)$ on the right of equation (2). We shall find that (28) and (29) are not restricted to detonation in ideal gases, but remain approximately true for all explosives.

Equations (12) and (13) may also be written

$$D = \frac{v_0}{v_1} \sqrt{\gamma_1 n_1 R T_1} = \frac{v_0}{v_1} a_1, \quad (30)$$

$$W_1 = \left(\frac{v_0}{v_1} - 1 \right) \sqrt{\gamma_1 n_1 R T_1} = \left(\frac{v_0}{v_1} - 1 \right) a_1, \quad (31)$$

from which the Chapman-Jouguet condition in the form

$$D = W_1 + a_1,$$

is clearly fulfilled. The approximation $\frac{v_0}{v_1} \approx \frac{\gamma_1 + 1}{\gamma_1}$ then gives

$$D \approx (\gamma_1 + 1) \sqrt{\frac{\gamma_1 n_1 R T_1}{\gamma_1}} = \frac{\gamma_1 + 1}{\gamma_1} a_1, \quad (32)$$

$$W_1 \approx \sqrt{\frac{\gamma_1 n_1 R T_1}{\gamma_1}} = \frac{a_1}{\gamma_1}. \quad (33)$$

Another interesting series of relations, expressing φ_i , W_i and D in terms of π_i , can be derived without explicit use of the R-H-equation itself. By (9)

$$(34a) \quad \frac{v_i}{v_0} \equiv \varphi_i = \frac{\gamma_i \pi_i}{(\gamma_i + 1) \pi_i - 1} \quad \begin{array}{c} \text{Detonation} \\ \hline \end{array} \quad \frac{(\gamma_i - 1) \pi_i + \gamma + 1}{(\gamma_i + 1) \pi_i + \gamma - 1} \quad (34b)$$

and so (35a) $W_i^2 = \frac{p_0 v_0 (\pi_i - 1)^2}{(\gamma_i + 1) \pi_i - 1} \quad \begin{array}{c} \text{Detonation} \\ \hline \end{array} \quad \frac{2 p_0 v_0 (\pi_i - 1)^2}{(\gamma_i + 1) \pi_i + \gamma - 1} \quad (35b)$

$$(36a) \quad D^2 = p_0 v_0 [(\gamma_i + 1) \pi_i - 1] \quad \begin{array}{c} \text{Detonation} \\ \hline \end{array} \quad \frac{1}{2} p_0 v_0 [(\gamma_i + 1) \pi_i + \gamma - 1] \quad (36b)$$

$$(37a) \quad a_i^2 = \frac{p_0 v_0 \gamma_i^2 \pi_i^2}{(\gamma_i + 1) \pi_i - 1} \quad \begin{array}{c} \text{Detonation} \\ \hline \end{array} \quad \frac{p_0 v_0 \gamma_i \pi_i [(\gamma_i - 1) \pi_i + \gamma - 1]}{(\gamma_i + 1) \pi_i + \gamma - 1} \quad (37b)$$

The corresponding relations in a non-reactive shock have been set alongside for comparison. If accented symbols refer to the latter case, with $\gamma = \gamma_i$ and $\pi_i \gg 1$, we conclude that, for the same pressure ratio π_i ,

$$\left(\frac{a_i}{a'_i} \right)^2 \sim \frac{\varphi_i}{\varphi'_i} \sim \frac{\gamma}{\gamma - 1} ; \quad \left(\frac{W_i}{W'_i} \right)^2 \sim \frac{1}{2} ; \quad \left(\frac{D}{D'} \right)^2 \sim 2 . \quad (38)$$

Alternatively, for the same wave-velocity D ,

$$\frac{\pi_i}{\pi'_i} \sim \frac{W_i}{W'_i} \sim \frac{1}{2} ; \quad 2 \left(\frac{a_i}{a'_i} \right)^2 \sim \frac{\varphi_i}{\varphi'_i} \sim \frac{\gamma}{\gamma - 1} . \quad (39)$$

§ 11 Detonation in real gases

The solutions of §10 give of course only an approximate account of detonation in real gases, though they indicate the correct orders of magnitude and provide very valuable guidance. Thus, since the temperatures and pressures reached in detonating gases amount only to a few thousands of degrees and a few tens of atmospheres, the products may still safely be regarded as a perfect gas mixture and the ideal gas law 10(3) retained. In numerical calculations for real gases, however, we may no longer regard the specific heats as constant, nor the equilibrium composition as independent of temperature and pressure. Of these two complications, the second is much the more serious. It is a comparatively simple matter to make allowance for the variation of C_v and γ , if we assume a fixed set of products, and the earliest [30] calculations by Chapman were simplified in this way; for example, a balanced hydrogen-oxygen mixture was assumed to react completely to water vapour, whose dissociation was ignored. For such a calculation equations 10(1, 2, 11) may be used at once in a process of successive approximation. Thus, a value is assumed for T_1 , whereupon γ_1 is also known; v_1 may then be evaluated from 10(11) and $\dot{\tau}_1$ by 10(1). A corrected T_1 is calculated from 10(2), and the process repeated until agreement is reached. D and W_1 are finally given by 10(30 and 31). [87] Jouguet's first absolute calculations followed essentially the above procedure, and showed very encouraging agreement with the experimental detonation velocities determined by Dixon. That this close agreement was however, fortuitous, and due in fact to the approximate cancellation of errors arising from the neglect of dissociation on the one hand and the

use of inaccurate specific heats on the other, became clear in [93] subsequent calculations, first by Jouguet himself and later by Lewis and Friauf. In Jouguet's later /calculations, which attempted to make allowance for the dissociation equilibria, but were still obliged to use incorrect thermal data, [107] the agreement was poorer than before; and Lewis and Friauf showed that the use of accurate specific heats based on spectral data did not prevent serious discrepancies between theory and experiment when dissociation was ignored. Comparison of the second and fourth columns of Table 11:1 shows the order of errors arising from this source, which leaves the calculated velocity significantly in excess.

A rigorous test of the theory requires that account should be taken of the actual equilibrium product composition at detonation pressure and temperature. The hydrodynamic equations are not in themselves then sufficient to determine the properties of the stable wave, but must be solved in conjunction with the equations of thermodynamic equilibrium which define the molar concentrations of the various product species as functions of temperature and pressure. It is clear that this complication does not affect the determinacy of the solution, since the molar concentrations represent merely so many auxiliary variables which are defined (§9.54) by an equivalent number of supplementary equations in terms of the state-variables, and so may be in effect eliminated. Moreover ideal equilibrium constants are applicable. It does add very materially, however, to the labour of computation since the parameters Q_1 , $n_i = \nu n_o$, γ_i , and c_v depend on both p , and T , and it is impossible to obtain an equation which does not contain at least one of these parameters. A simple cyclical method of solution cannot therefore be used. An additional difficulty

[88]

arises from the fact that the Chapman-Jouguet condition cannot now strictly be expressed by 10(9), since 10(7) does not hold. However, both Jouguet and Lewis and Friauf found that for the mixtures which they studied 10(7) could be used, without appreciable error. Assuming that this is so, we may proceed as follows. Plausible values of p_i/n_i and T_i are chosen, and the corresponding product composition determined, together with γ_i , \bar{c}_v , n_i , and Q_i . v_i may now be calculated from 10(8) and compared with the value given by 10(1). Retaining T_i unchanged, we now adjust p_i/n_i until agreement in v_i is reached, whereupon T_i is recalculated by 10(2). This process is repeated for several assumed values of T_i and the recalculated values graphed against those assumed. It is then possible by interpolation to assess the true solution. Finally D and H_i are derived, e. g. from 10(30,31). This procedure is illustrated below by an outline calculation for a balanced mixture of carbon monoxide and oxygen.

The most careful calculations which have been published on the basis of the constant-composition adiabatic are those of Lewis and Friauf for a balanced mixture of hydrogen and oxygen diluted with various proportions of excess hydrogen or oxygen, or with inert gas (He, A, N₂). Allowance is made for appearance of the following product species:

H₂O, H₂, OH, O₂, H with He, A or N₂; dissociation of the O₂ and N₂ should be negligible at the prevailing temperatures and pressures.

Table 11:1 allows the velocities so calculated to be compared, on the one hand with experiment, and on the other with theoretical values for undissociated explosion products H₂O, H₂, O₂. The importance of dissociation can be judged from columns 2 and 3. The general agreement between columns 3 and 4 is very good, and for mixtures

Table 11:1

Detonation in gaseous explosives

Calculations by Lewis and Friauf. [107]
 Observations by Lewis and Friauf
 and by Payman and Walls. [130]

Explosive gas	D(calc.) m./s.	D(obs.)	P,	T,	W,	V,
			atm.	°K	m./s.	v.
	Dissociation: ignored	Dissociation: not ignored				
: 2H ₂ + O ₂	: 3278	: 2806	: 2819	: 18.05	: 3583	: 1225 : 0.564 :
: + N ₂	: 2712	: 2378	: 2407	: 17.37	: 3367	: 1040 : 0.562 :
: + 3N ₂	: 2194	: 2033	: 2055	: 15.63	: 3003	: 870 : 0.572 :
: + 5N ₂	: 1927	: 1850	: 1822	: 14.39	: 2685	: 797 : 0.570 :
: + O ₂	: 2630	: 2302	: 2319	: 17.4	: 3390	: 1013 : 0.560 :
: + 3O ₂	: 2092	: 1925	: 1922	: 15.3	: 2970	: 818 : 0.575 :
: + 5O ₂	: 1825	: 1735	: 1700	: 14.13	: 2620	: 747 : 0.570 :
: + 2H ₂	: 3650	: 3354	: 3273	: 17.25	: 3314	: 1465 : 0.564 :
: + 4H ₂	: 3769	: 3627	: 3527	: 15.97	: 2976	: 1590 : 0.562 :
: + 6H ₂	: 3802	: 3749	: 3532	: 14.18	: 2650	: 1595 : 0.575 :
: + 1.5 He:	: 3772	: 3200	: 3010	: 17.60	: 3412	: 1345 : 0.580 :
: + 3 He	: 3990	: 3432	: 3130	: 17.11	: 3265	: 1420 : 0.587 :
: + 5 He	: 4083	: 3613	: 3160	: 16.32	: 3097	: 1465 : 0.594 :
: + 2.82He:)	: 3012	: 2620	: 2390	: 16.68	: 3175	: 1074 : 0.590 :
: + 1.18 A:)						
: + 1.5 He:)						
: + 1.5 A :)	: 2741	: 2356	: 2330	: 17.11	: 3265	: 975 : 0.587 :
: + 1.5 A :	: 2500	: 2117	: 1950	: 17.60	: 3412	: 890 : 0.580 :
: + 3A	: 2210	: 1907	: 1800	: 17.11	: 3265	: 788 : 0.587 :
: + 5A	: 1992	: 1762	: 1700	: 16.32	: 3097	: 715 : 0.594 :

diluted with oxygen or nitrogen might be described as well-nigh perfect. In view of the absolute nature of these calculations, no adjustable constants whatever being available, and no reference made at any stage in the work to parameters defined by reference to explosive performance, this close agreement provides an unusually convincing demonstration, both of the correctness of the Chapman-Jouguet theory, and of the accuracy of the thermal data employed.

When the stoichiometric mixture is diluted with O_2 , N_2 or A , the wave velocity is depressed. This reflects a reduction in both n , and T (see equation 10(30)). Dilution with H_2 or He again involves a drop in temperature, but this is more than compensated by the increase in n ; the wave-velocity is therefore actually enhanced. Particularly significant is the effect of He; that the velocity should rise with addition of chemically inert material, provided only that its molecular weight is small enough, must be regarded as a powerful vindication of the mechanical basis of the theory.

The agreement between calculated and observed velocities is less close in the case of mixtures containing He or A than for those diluted with O_2 or N_2 . The experimental values are due to Lewis and Friauf, who consider that they may require slight revision.

[⁶⁰⁷] Alternatively, Lewis and Friauf suggest that discrepancies of this kind, which are observed also at large dilutions with H_2 (see Table 11:1) and always leave the observed velocity in defect, are due to a decrease in reaction speed which it is claimed will prevent equilibrium being reached "in the wave-front". The failure to attain the full theoretical velocity would then reflect merely the incomplete nature of the effective reaction.

[^{64,65}] Jost has examined the question in some detail, and offers essentially the same explanation, though he rightly lays stress on the fact that reaction

cannot in any case be supposed to reach equilibrium in the wave-front (understood as the region of pressure rise), and that the theory does not require this. To make Jost's position clear we may quote a sentence from his work:

"It is easy to imagine that in certain (gas) mixtures the reaction speed, though still high enough to maintain a shock wave, is no longer high enough to ensure complete reaction in the combustion zone". Consideration will show, however, that this formulation is inconsistent with the Chapman-Jouguet theory sketched in § 9.4, at least if we are discussing a perfectly confined cartridge. For it has been shown that detonation waves with velocities less than that defined by chemical equilibrium cannot be steady in such a cartridge, but must accelerate. The explanation put forward by Lewis and Friauf and by Jost is therefore to be interpreted in this sense, that the conditions of perfect lateral confinement envisaged in the basic theory were not altogether realised in the experiments. This view is taken by Döring, who considers therefore that the full theoretical velocities would be reached in tubes of sufficiently wide diameter; a prediction which does not appear to have been tested experimentally.

[85]

Jost has also put forward an alternative, though similar explanation, based on the finite time required to establish statistical equilibrium between the translational and vibrational degrees of freedom in a polyatomic molecule. Remarking that the reaction energy is in the first place largely absorbed in molecular vibrations, and only distributed in thermal motion after a large number of collisions, Jost suggests that the effective energy release may fall below that corresponding to full statistical equilibrium. It appears that this argument is subject to the same criticism as the preceding, and must accordingly be

interpreted in a similar way. Energy made available by whatever mechanism behind the steady zone will give rise to secondary shocks which will in due course overtake and intensify the primary shock. Only when the confinement is imperfect, so that laterally generated rarefactions invade the products, will this conclusion cease to apply. The processes envisaged by Jost may then well become operative.*

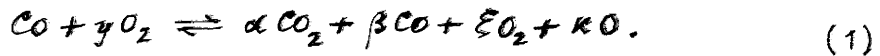
As we have seen, it is not strictly correct to apply the CJ-condition in the form 10(8) when the product composition depends upon pressure and temperature. Equation 9.1(17) is still, of course, valid, but $(\partial p_i / \partial v_i)_S$ must be evaluated under conditions where S alone remains constant, and not both S and the various molar concentrations as in equation 10(7). It is possible to formulate $(\partial p_i / \partial v_i)_S$ under these general conditions; however, it is probably simpler in the present case to determine the RH-curve itself, or at least a small part of it in the neighbourhood of I (Fig. 9.1:1), and thereafter to apply the CJ-condition in the form 9.1(15) rather than 9.1(17), by drawing the upward tangent from (v_0, p_0) . The RH-curve may be traced as follows. (1) Choose a value of p/n ,
 (2) assume a corresponding T , and calculate the appropriate equilibrium^{composition}, whereupon n, p and $E - E_0 = \int_{T_0}^T c_v dT - Q$ may be found. Estimate v from the equation $E - E_0 = \frac{1}{2}(p + p_0)(v_0 - v)$, and recalculate $T = p v / n R$, thereafter repeating the process until agreement is reached.
 (3) Carry out a similar calculation for other values of p/n .

* The reaction may perhaps remain "effectively" incomplete in certain cases, even in a well-confined cartridge, for example if the explosive contains an inert diluent to which heat is lost by thermal conduction (cf. § 17.1, page 336)

§ 11.1 Carbon monoxide/oxygen mixtures

A new set of calculations have been made for dry carbon-monoxide/oxygen mixtures containing various proportions of CO. The unreacted gas is supposed at 25°C and 1 atm.

The first calculations follow the method of the constant-composition adiabatic, as described above. In determining the equilibrium compositions, it is convenient to consider a mass (x gm.) of gas containing one mole (28 gm.) of CO diluted with y moles of O₂, and reacting at (T_1, p_1) according to the equation



For material balance, we require

$$\alpha + \beta = 1 \quad (2)$$

$$2\alpha + \beta + 2\xi + \kappa = 2y + 1. \quad (3)$$

At equilibrium,

$$K_2 \alpha = \pi^{\frac{1}{2}} \beta \xi^{\frac{1}{2}} \quad (4)$$

$$K_5 \xi^{\frac{1}{2}} = \pi^{\frac{1}{2}} \kappa, \quad (5)$$

where $K_2 \equiv p_{CO} \cdot p_{O_2}^{\frac{1}{2}} / p_{CO_2}$ and $K_5 \equiv p_O / p_{O_2}^{\frac{1}{2}}$ are the ideal equilibrium constants of the reactions



and $\pi \equiv p_i / N$, $N \equiv \alpha + \beta + \xi + \kappa$.

K_2 and K_5 will be found tabulated in Table 9.54:1 above.

Algebraic determination of $\alpha, \beta, \xi, \kappa$ from (2) - (5) depends upon the solution of a cubic equation. For example, eliminating β, ξ, κ we have

$$\alpha + \frac{K_2 \alpha}{\pi(1-\alpha)} \left[K_5 + \frac{2K_2 \alpha}{1-\alpha} \right] = 2y. \quad (8)$$

In practice, it is simpler to proceed by a cyclical method of successive approximation. Thus, α is assumed, whereupon β, ξ and κ are computed in turn from (2), (4) and (5), and α recalculated from (3). The calculation is then repeated with an intermediate value of α , until agreement is reached.

Q_1 is determined by

$$-\alpha Q_1 = \alpha (E.F.)_{CO_2} + (\beta-1)(E.F.)_{CO} + \kappa (E.F.)_O, \quad (9)$$

where $(E.F.)_{CO_2}$, etc. are the molar energies of formation of the various species at (T_0, p_0) from the elements in their standard states, also at (T_0, p_0) : these energies are obtained from Table 9.51:1, according to which

$$(E.F.)_{CO_2} = -94.0 \text{ K.cal/mole}, \quad (E.F.)_{CO} = -26.7 \text{ K.Cal/mole},$$

$$(E.F.)_O = +58.9 \text{ K.cal/mole.}$$

Using (2), we have, therefore,

$$\alpha Q_1 = 67.3\alpha - 58.9\kappa \text{ K.cal.} \quad (10)$$

The detailed results of such calculations for $y = 0.25, 0.5, 1, 1.5$, corresponding to 80, $66^2/3$, 50, 40% CO by volume respectively, are collected in Table 11.1:1. For comparison the Table also shows the theoretical wave-properties if dissociation is neglected, so that, for example, $CO + \frac{1}{4}O_2 \rightarrow \frac{1}{2}CO_2 + \frac{1}{2}CO$, and $CO + \frac{3}{2}O_2 \rightarrow CO_2 + O_2$.

[29]

Experimental velocities, due to Campbell, Whitworth and Woodhead, are also included. It can be seen that dissociation produces a marked lowering of temperature, pressure and velocity, and brings the latter into very fair agreement with the experimental values. In particular, the variation with percentage CO is well reproduced.

In order to test the error involved in calculating $(\partial p_i / \partial v_i)_s$ without allowance for chemical change, the more rigorous method described on page 223 has been applied to the balanced mixture $\text{CO} + \frac{1}{2}\text{O}_2$. This involves determination of a small arc of the RH-curve around the point of tangency I (Fig. 9.1:1). The calculation is laborious, since it is necessary to retain five significant figures in order to achieve any accuracy in p_i . The results of this calculation are also shown in Table 11.1:1. It can be seen that the discrepancies are small, particularly in D, T , and the CJ-products. The constant-composition adiabatic appears to provide ample accuracy for calculations of the present type.

Table 11.1:1

Detonation in carbon monoxide/oxygen mixtures.

Method A: constant-composition adiabatic

B: RH-curve

C: dissociation neglected

$T_0 = 273^\circ\text{K}$, $p_0 = 1 \text{ atm.}$

Experimental velocities: Campbell, Whitworth [29]
and Woodhead.

Reactants	$\frac{p_0}{p_{\infty}}$	CO	Products (mol./kg.)			D	n_i	p_i	T_i	v_i/v_o	γ_i	$\frac{D}{(obs.)}$
			CO_2	CO	O_2		$10^3 n_i$	ml./s.	ml./s.			
1CO + O ₂	A:80	:10.82	16.93	1.21	0.63	29.6:1803	790	17.8	3445	0.562	1.217	1770
2CO + O ₂	A:66 ² /3:11.70	11.02	4.80	1.46	29.0:1803	790	17.9	3510	0.562	1.212	1760	
2CO + O ₂	B:66 ² /3:11.75	11.00	4.76	1.46	29.0:1790	805	18.2	3510	0.550	1.212	1760	
CO + O ₂	A:50	11.25	5.41	10.17	1.59	28.4:1756	770	17.6	3405	0.562	1.218	1710
2CO + 3O ₂	A:40	10.39	2.76	14.12	1.30	28.6:1725	740	16.9	3250	0.571	1.214	1680*
1CO + O ₂	C:80	13.89	13.89	-	-	27.8:1945	860	20.8	4250	0.556	1.198	1770
2CO + O ₂	C:66 ² /3:22.73	-	-	-	-	22.7:2150	985	25.6	6100	0.543	1.144	1760
CO + O ₂	C:50	16.67	-	8.34	-	25.0:2000	904	23.1	4940	0.548	1.170	1710
2CO + 3O ₂	C:40	13.16	-	13.16	-	26.3:1875	830	20.4	4180	0.557	1.187	1680*

* Extrapolated.

§ 11.2 Detonation in dust clouds

Since the physical state of the unreacted explosive is irrelevant, the same treatment applies to atmospheric clouds of explosive or combustible dust. It may, of course, be necessary to allow for the presence of a solid or liquid phase in the products. This condensed phase may either arise in the reaction or survive from the dust originally present. In the former case, it will be assumed to have the same temperature and streaming velocity as the product gases: this assumption is rather less reliable in the latter case. The question is considered again in § 15 below. In either event, the volume occupied by the condensed phase should be negligible. With regard to the CJ-condition for a low-density mixture of gas and condensed particles, it is perhaps most correct to regard the two phases as thermally insulated: in other words, the elementary adiabatic change envisaged in the CJ-condition will be one involving the gas alone. This formulation simplifies the analysis and will not as a rule greatly affect the final results.

The differential equation of a constant-composition adiabatic is

$$dE = -pdv. \quad (1)$$

Since, at the low pressures involved, the energy of compression of the condensed phase is negligible, (1) leads to

$$\left(\frac{\partial p}{\partial v}\right)_S = -\frac{p}{v}\left(1 + \frac{nR}{c_v}\right), \quad (2)$$

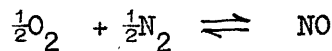
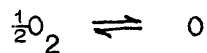
where n is, as usual, the number of moles of gas per gram total products. If the condensed phase is thermally insulated in the adiabatic change, c_v is the heat capacity of the n moles of gas, so that (2) becomes

$$\left(\frac{\partial p}{\partial v}\right)_S = -\frac{rp}{v}, \quad (3)$$

where γ is the ratio of specific heats of the gaseous phase.

Otherwise, c_v refers to the total products and (2) must be used.

As an example, we have carried out calculations for a uniform mixture of 0.2 gm. aluminium dust with 1 litre of air. The Al, which is present in less than balanced proportions, is supposed to react quantitatively to Al_2O_3 which condenses at T_i to small liquid droplets: allowance is made for the presence of O_2 , O, N_2 and NO, according to the equilibria



The equilibria at given (p , T_i) are best computed by an iterative process. Each such computation forms one stage in a general iteration involving the RH- and CJ-equations. The final conclusions are shown in Table 11.2:1. It appears that only minor differences arise from the use of equations (2) or (3).

Reliable experimental velocities and pressures are not available.
[63]

The values of D measured on coal-dust/air mixtures are generally only about one-half as large as those quoted in Table 11.2:1; full velocity will be most nearly attained when the dust is very fine, both because reaction is then completed more quickly with consequent reduction in lateral loss, and also because there is less tendency to segregation.

Table 11.2:1

Detonation of a dust cloud consisting of 200 mg. aluminium dispersed in 1 litre air.
 $(T_0 = 273 \text{ K}; P_0 = 1 \text{ atm.})$

A: equation 11.2(3)
B: equation 11.2(2)

Assumption	Products (mol./kg.)				Wave properties				
	Liquid	Gaseous	D	W	P	T	v/v_0		
AL ₂ O ₃	O ₂	O	N ₂	NO	m/s.	m/s.	atm.	°K	
A : 2.49	: 1.36	1.07	23.03	1.34:1810	765	21.7	3735	0.576	
B : No significant change				: 1815	804	22.7	3780	0.557	

In addition the volume concentration of vapour may also remain constant or at least constant. This will obviously be legitimate provided no violent vaporization, provided it is still small enough. In other words (since $v = n/V_{\text{gas}}$) for vapours which are either out number or less, there are indeed certain concentrated explosive substances, for example nitroalcohols, where sufficient strength makes it possible to handle them at concentrations less than 0.1 g/cm³. The equations developed in this section are clearly applicable to such cases, though the high level of precision permitted by the relatively gentle detonation pressures taken into account. The chief interest in the quantitative calculations

§ 12 Detonation in low-density condensed explosives

When the density of the detonation products exceeds a few gm/litre, they cannot be supposed, even if still entirely gaseous, to follow the ideal gas laws. The development set out in §§ 10, 11 applies therefore only to explosives whose density is of the order of that of a gas, that is, in practice to gaseous mixtures, or at most to extremely dilute suspensions of condensed material, for example dust clouds or foams. In attempting to extend the field of numerical application of the theory to solid and liquid explosives of normal density, it is natural to commence by modifying the ideal gas equation in the manner proposed by van der Waals, to allow for the effect of intermolecular forces. Since, however, the detonation products have not merely a high density but also a high temperature, we may simplify the van der Waals equation to that used by Abel, viz.,

$$P(v-\alpha) = nRT, \quad (1)$$

in which only the volume correction of "covolume" α is retained. We regard α as a constant. This will evidently be legitimate in practice to a first approximation, provided α is still small compared with v , in other words (since $\alpha \sim 1/\text{cm}^3/\text{gm.}$) for explosives whose density is of the order of 0.1 gm/cm³ or less. There are indeed certain condensed explosive substances, for example nitrocottons, whose physical structure makes it possible to cartridge them at densities less than 0.1 gm/cm³. The equations developed in this section would be closely applicable to such cases, though the high level of dissociation permitted by the relatively small detonation pressures makes numerical work involved. The chief interest in the equations attaches, however, less to their literal application than to the useful guidance which they afford when used with suitable precautions as a first approximation in

the practical case of explosives of normal density ($0.5 - 2 \text{ gm./cm}^3$).

The analysis is simplified by the fact that ρ_0 is less than $0.01 p_1$, and can be neglected from the outset. The constant-composition adiabatic is now defined by

$$\begin{aligned}-pdv &= dE \\ &= c_v dT\end{aligned}$$

since by (1) $\left(\frac{\partial E}{\partial v}\right)_T = T \frac{\partial p}{\partial T} - p \equiv 0$. In terms of (1), the adiabatic becomes

$$-\left(\frac{\partial p}{\partial v}\right)_S = \frac{\gamma p}{v-\alpha}, \quad (2)$$

where

$$\gamma \equiv 1 + nR/c_v = c_p/c_v,$$

since $c_p - c_v = -T \left(\frac{\partial v}{\partial T}\right)^2 / \left(\frac{\partial v}{\partial p}\right) = nR$ by (1).

The Chapman-Jouguet condition 9.1(17) is then (ρ_0 being neglected)

$$v_i = \frac{\gamma_i v_o + \alpha}{\gamma_i + 1}, \quad (3)$$

whereupon by equations (1) and (3)

$$p_i = \frac{(\gamma_i + 1)n_i R T_i}{\gamma_i(v_o - \alpha)}, \quad (4)$$

$$D = \frac{\gamma_i + 1}{1 - \alpha D} \sqrt{\frac{n_i R T_i}{\gamma_i}}, \quad (5)$$

$$W_i = \sqrt{\frac{n_i R T_i}{\gamma_i}}, \quad (6)$$

and the EH-equation becomes

$$E_i - E_i^* = \int_{T_0}^{T_i} c_v dT = Q_i + \frac{n_i R T_i}{2\gamma_i}. \quad (7)$$

[157]

Equations (3) - (7) are due to Taffanel and Dautriche.

c_v , n_i , γ_i , Q_i and α naturally depend on the chemical composition,

which is in turn determined by the equilibrium equations in terms of p , and T . Equations (3), (4) and (7) are therefore to be solved, in conjunction with the equilibrium equations, by a process of trial and error; D and H , are then found at once from (5) and (6).

Alternatively, and more correctly, as in the case of gaseous explosives, without assuming the constant composition adiabatic(2) we may evaluate the RH-curve, or a sufficient part of it, point by point, and complete the solution graphically by drawing the upward tangent from (v_0, p_0).

Approximate relations may again be deduced between p , T , and the corresponding values p_v, T_v reached in a constant-volume reaction, if we assume that the chemical composition does not differ greatly in the two processes. Thus, provided T is reasonably close to T_v we may write

$$E_i - E_v \doteq C_i(T_i - T_v) \doteq \frac{n_i R T_i}{2\gamma_i} ,$$

whence

$$\frac{T_i}{T_v} \doteq \frac{2\gamma_i}{\gamma_i + 1} \sim 1.1 , \quad (8)$$

justifying the assumption made.

Then, by (1) and (4)

$$\frac{p_i}{p_v} \doteq \frac{T_i}{T_v} \cdot \frac{\gamma_i + 1}{\gamma_i} \sim 2 . \quad (9)$$

[so3] These equations, which were derived above for gases, therefore

hold approximately also for condensed explosives of moderate density, and indeed it is not difficult to see that they will remain roughly true in all cases. The detonation pressure is thus always about twice the pressure reached in reaction at constant volume, a circumstance which helps to explain the superior brisance of detonating as compared with deflagrating explosives. Again at low densities, where α is negligible, (3) gives

$$v_i \doteq \frac{\gamma_i}{\gamma_i + 1} v_0 \sim \frac{3}{5} v_0 ,$$

while at high densities α and v , must each approach v_0 . A mean value is therefore

$$v_i \sim \frac{3}{4} v_0 , \quad (10)$$

whence, by 9(14)

$$D \sim 4W_i . \quad (11)$$

Finally, we note that while W_i varies only indirectly and to a minor extent with the cartridge density A , D depends explicitly upon A . According to equation (5), the velocity of detonation of a condensed explosive, under perfect lateral confinement, falls with decreasing A but cannot be reduced in this way below a minimum value,

$$D_i = (\gamma + 1) \sqrt{\frac{nRT_i}{\gamma}} , \quad (12)$$

which may be called the "ideal" velocity since it corresponds to densities so low that the products behave like a perfect gas (cf. equation 10(32)). Velocities close to these ideal values have in fact been realised in large-diameter cartridges of solid explosives such as nitrocotton whose physical form makes it possible to cartridge them at extremely low densities (down to 0.02 gm/cm^3), or with liquids, for example nitroglycerine, dispersed as emulsions. As the density is raised, D increases at first slowly and then more rapidly, in agreement with (5). Beyond $A \sim 0.5 \text{ gm/cm}^3$, the experimental velocity-density relationship is found, however, to become almost linear, whereas according to (5) its slope would continuously increase. This reflects merely the limitations of (1) at higher densities; in practice α cannot be expected to remain constant, but must rather decrease, as the pressure rises. Equation (1) nevertheless gives a qualitatively correct explanation of the well-known effect of packing density upon velocity, in

terms of the progressive departure of the products from the ideal
 [649]
 gas state.

The approximate formulae appropriate to ideal gases presented in Table 10:1 admit of simple extension to condensed systems obeying the Abel equation (1). For, if this equation is assumed to hold down to low temperatures and pressures, the equation of state itself, together with the RH-equation and CJ-condition, and their various consequences, save only those involving D , are identical with the equations of § 10, provided v_0, v , are replaced by $v_0 - \alpha$, $v - \alpha$ respectively. We are thus able at once to deduce the approximate relations of Table 12:1.

Table 12:1

Approximate properties of the stable detonation and fastest deflagration in an explosive whose products satisfy

$$p(v-\alpha) = nRT, \alpha \text{ constant}$$

[92]

	<u>Steady Detonation</u>	<u>Fastest Deflagration</u>
v	$\frac{\gamma_1 v_0 + \alpha}{\gamma_1 + 1} \quad 0.8 \text{ cm}^3/\text{gm.}$	$\frac{2Q_1(\gamma_1 - 1)}{\gamma_1 p_0} \quad 2 \times 10^{-4} \text{ cm}^3/\text{gm.}$
p	$\frac{2Q_1(\gamma_1 - 1)}{v_0 - \alpha} \quad 5 \times 10^4 \text{ atm.}$	$\frac{p_0}{\gamma_1 + 1} \quad 0.4 \text{ atm.}$
T	$\frac{2Q_1 \gamma_1}{(\gamma_1 + 1) C_v} \quad 3000^\circ\text{K}$	$\frac{2Q_1}{\gamma_1 (\gamma_1 + 1) C_v} \quad 2000^\circ\text{K}$
W	$\sqrt{2Q_1 \frac{\gamma_1 - 1}{\gamma_1 + 1}} \quad 1000 \text{ m/s.}$	$-\sqrt{2Q_1 \frac{\gamma_1 - 1}{\gamma_1 + 1}} \quad -1000 \text{ m/s.}$
D	$\frac{v_0}{v_0 - \alpha} \sqrt{2Q_1(\gamma_1^2 - 1)} \quad 5500 \text{ m./s.}$	$\frac{\gamma_1 p_0 v_0}{\sqrt{2Q_1(\gamma_1^2 - 1)}} \quad 0.06 \text{ m./s.}$

The numerical values indicate orders of magnitude, corresponding to the following typical constants: $p_0 = 1 \text{ atm.}$, $v_0 = 1 \text{ cm}^3/\text{gm.}$, $T_0 = 300^\circ\text{K}$, $\gamma_1 = 1.25$, $Q_1 = 1000 \text{ cal/gm.}$, $C_v = 0.33 \text{ cal/gm.}^\circ\text{K}$, and $\alpha = 0.6 \text{ cm}^3/\text{gm.}$ It is interesting to note that the maximum

deflagrating velocity is proportional to the initial pressure, a relation reminiscent of the familiar law of burning of propellants, although the burning speeds observed in practice fall very far short of the theoretical maxima.

Equations similar to 10(34-36) can also be readily derived. They are:

$$(13a) \quad \frac{v_i - \alpha}{v_o - \alpha} = \frac{\gamma_i \pi_i}{(\gamma + 1) \pi_i - 1} \quad (13b)$$

$$(14a) \quad W_i^2 = \frac{p_o (v_o - \alpha) (\pi_i - 1)^2}{(\gamma + 1) \pi_i - 1} \quad (14b)$$

$$(15a) \quad D^2 = \frac{v_o}{v_o - \alpha} p_o v_o [(\gamma + 1) \pi_i - 1] \quad \frac{1}{2} \frac{v_o}{v_o - \alpha} p_o v_o [(\gamma + 1) \pi_i + \gamma - 1] \quad (15b)$$

The corresponding relations for non-reactive shocks are again stated for comparison, and lead at once to conclusions similar to 10(38,39).

§ 12.1 Calculations and experiments on a low-density nitrocotton

As an example of the use of equations 12(3-7), we have carried out approximate calculations and experimental measurements on a nitrocotton made by nitrating cotton-wool. With this material, which contained 13.1% nitrogen and 0.87% moisture, and yielded 0.29% ash, it was possible to reach mean cartridge densities as low as 0.02 gm/cm^3 .

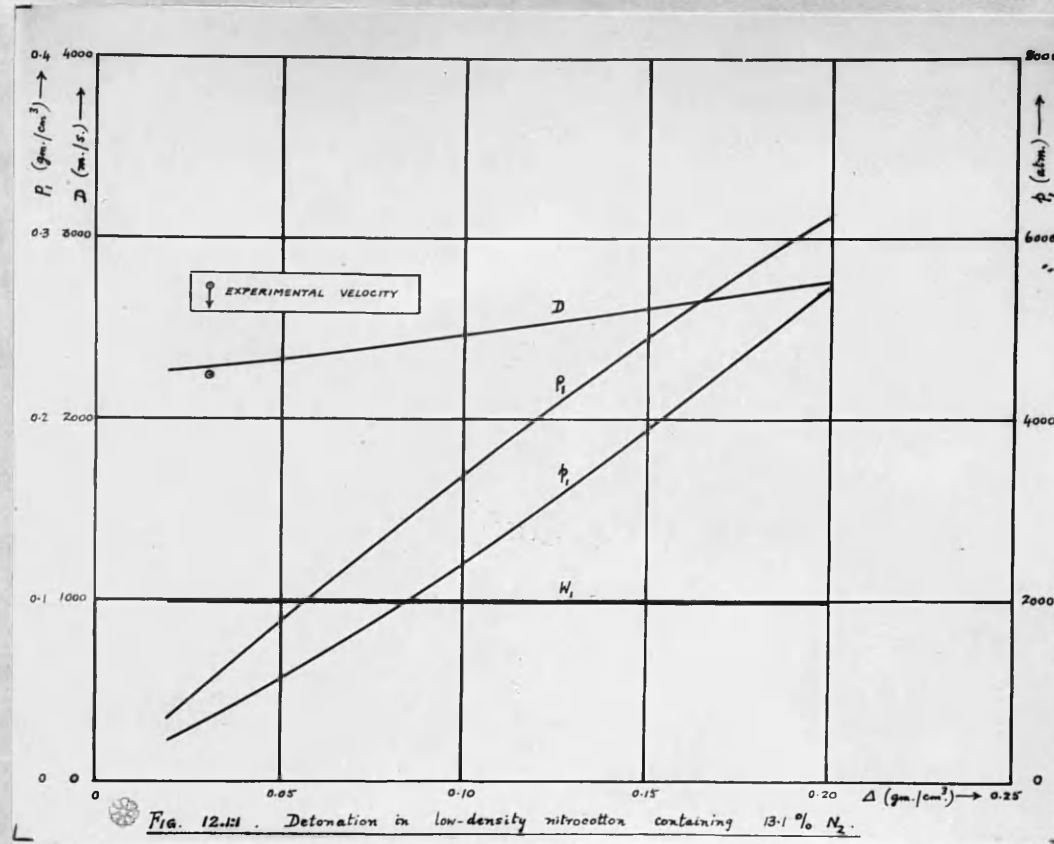
In the calculations, dissociation was neglected, and the equilibrium products computed on the basis of the water-gas reaction alone. The covolume α was given the value $1.01 \text{ cm}^3/\text{gm}$. indicated by manometric bomb experiments; this is in very close agreement also with the values calculated by the method of § 13.3 below. The conclusions are summarised in Table 12.1:1 and Fig. 12.1:1. It can be seen that the ratios T_i/T_v and particularly p_i/p_v are of the expected order, and

that, while W_i is independent of Δ , D and p_i rise as Δ is increased. D_i must be close to 2,200 m./s.

Table 12.1:1

Nitrocotton containing 13.1% nitrogen

Δ (gm/cm ³)	0.02	0.04	0.07	0.10	0.15	0.20
T_v (°K)	3080	3080	3080	3080	3080	3060
T_i (°K)	3730	3730	3730	3730	3725	3725
T_i/T_v	1.21	1.21	1.21	1.21	1.21	1.22
p_v (atm.)	221	452	807	1206	1910	2660
p_i (atm.)	446	914	1650	2400	3875	5440
p_i/p_v	2.02	2.02	2.04	2.00	2.02	2.05
v_i (cm ³ /gm.)	28.0	14.2	8.28	5.96	4.10	3.19
W_i (m./s.)	996	996	996	996	996	996
D (m./s.)	2260	2310	2390	2460	2610	2760



Contemporary photographic experiments with low-density nitrocotton cartridges, mainly 1 inch in diameter, showed velocities down to 1,100 m./s. It was concluded that these "ultra-low" velocities must be due to failure to realise the conditions of perfect lateral confinement envisaged by the theory, and a series of special measurements was therefore undertaken by the same method at larger diameters, with the nitrocotton specified above. A density of $0.03 \text{ gm}/\text{cm}^3$ was chosen, and cartridges made up in cellophane shells (for transparency), with diameters of $1, \frac{3}{16}, \frac{5}{16}, \frac{9}{16}, \frac{7}{16}, 5$ and 8 inches. All the cartridges were 24 inches long, and were initiated by Cordtex fuse*,

* Pentaerythritol tetranitrate in a guttapercha or plastic tube.

a single strand in the lower diameter cartridges, four parallel strands taped to a common detonator and inserted at four symmetrical points in the end of the cartridge being used at the higher diameters to accelerate the development of a plane wave. Photographic measurement of the velocity was made between the 16 and 22 inch marks.

Again, the nitrocotton was cartridged at the same density in $1\frac{1}{8}$ " internal diameter steel tubes of $\frac{1}{4}$ " wall and 38-ton bursting pressure, open at both ends and perforated ^{along} a generator with a series of small holes to permit passage of light. The tubes suffered an expansion of at most one or two thousandths of an inch. Previous tests had shown rupture to occur at $\Delta = 0.25 \text{ gm/cm}^3$, but very little expansion at 0.10 gm/cm^3 . This is in agreement, as far as it goes, with the detonation pressures in Table 12.1:1.

The experimental results are shown in Fig. 12.1:2.

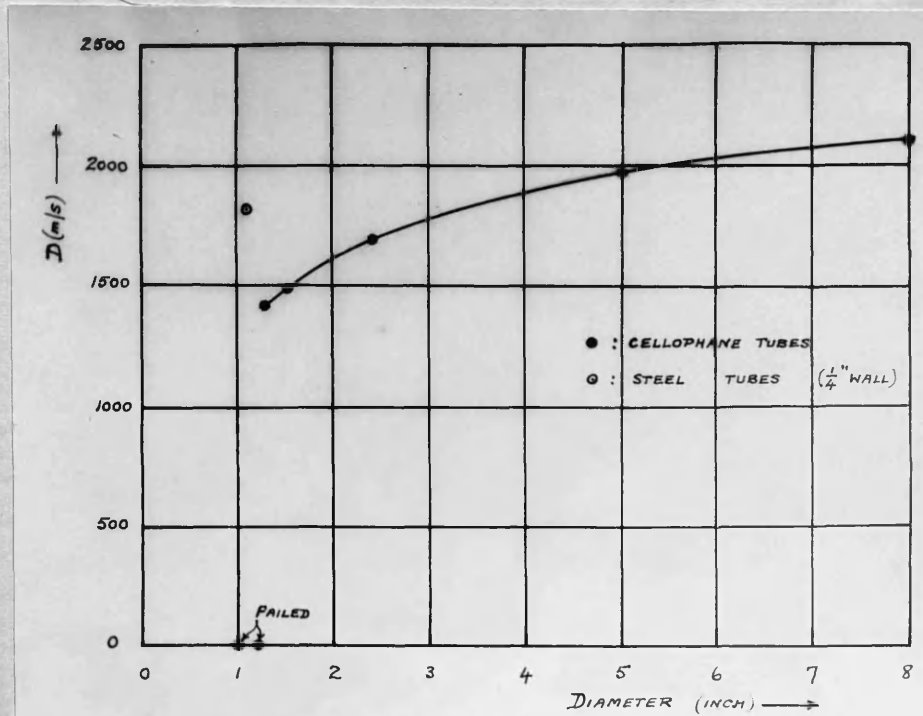


FIG. 12.1:2 EXPERIMENTAL DETONATION

VELOCITIES OF NITROCOTTON (13.1% N), 0.03 g/cm^3 .

Extrapolation of the velocities in lightly wrapped cartridges to infinite diameter yields the limiting velocity marked in Fig. 12.1:1. The agreement is close.

§13. Detonation in condensed explosives of normal bulk density:
introduction

The loading density Δ of explosives for military and civil use falls normally between $0.3\Delta_{cr}$ and Δ_{cr} , where Δ_{cr} is the maximum or crystal density of the explosive material itself. Since in most cases $\Delta_{cr} \sim 1-2 \text{ gm./cm}^3$, Δ lies within the range $0.3 - 2.0 \text{ gm./cm}^3$. (An exception is made, of course, in the case of heavy metal salts, such as mercury fulminate or lead azide).

Table 12:1 permits an estimate of the order of magnitude of density and pressure which we may then expect to arise behind the reaction zone. It is clear that product densities as high as 2 gm./cm^3 and corresponding pressures of the order of 100,000 atm. will not be unusual. The temperatures may reach several thousands of degrees. Numerical applications to normal liquid and solid explosives depend, therefore, on the formulation of equations of state to describe the products in a region of the state variables far outwith that which can be explored by any ordinary experimental method, and in which, moreover, the effect of gas imperfections on the thermodynamic equilibria themselves requires to be considered. It would be remarkable if the Abel equation 12(1) with constant α provided more than a very rough description of the behaviour of gases under such extreme conditions.

Confronted with these serious difficulties, the earlier workers approached the problem in the reverse direction. Renouncing the attempt to calculate the detonation parameters in an absolute fashion, on the basis of an entirely theoretical equation of state, as had been done for gaseous explosives, they proposed rather to determine this equation for the products of selected high-density explosives by means of the observed detonation velocities and their dependence upon cartridge density. The resulting equation of state might then be used to

define, at least approximately, the remaining large-scale properties of the wave, and also to estimate such properties, together with the wave speeds themselves, for other condensed explosives.

It is immediately clear that a rigorous analysis along these lines would be extremely complex, since, although the thermodynamic functions are now known with high precision for ideal gases, even at elevated temperatures (Figs. 9.51:1,2) their correction for gas imperfections under the enormous pressures of detonation depends itself upon a knowledge of the gas equation. This difficulty, however, though serious enough in practice, does not in principle prevent a solution. More serious is the fact that the problem of determining the equation of state from observed velocities for a single explosive is not strictly determinate; for it would require the evaluation of a function of many independent variables, say $v(p, T, n_1, n_2, \dots)$, from experiments in which these variables are allowed to assume only values defined by the velocity-density relation: $D = D(A)$. For a complete solution, even if the state equation were assumed independent of chemical composition (n_1, n_2, \dots) , it would be necessary to provide an additional degree of freedom by permitting either p_0 or T_0 also to vary. Alternatively, the composition of the explosive itself might be continuously varied, but this would introduce fresh computational difficulties.

Short of such expedients, the problem in its inverse form can be made tractable only with the assistance of some simplifying assumption regarding the form of the equation of state. This assumption must have the effect of reducing the unknown function to a function of a single independent variable. Thus, every equation of state for a

two-parameter substance can be expressed in the form

$$\phi(v-\alpha) = nRT \quad (1)$$

by suitable choice of the function α ; but (1) is itself too general for our purpose until some assumption is made concerning α . For example, we may assume that α is independent of chemical composition, and also

$$(\partial\alpha/\partial T)_v \equiv 0, \text{ i.e. } \alpha = \alpha(v) \quad (2)$$

or

$$(\partial\alpha/\partial v)_T \equiv 0, \text{ i.e. } \alpha = \alpha(\phi). \quad (3)$$

The simplest possible assumption is that implied in the original Abel equation, namely,

$$\alpha = \text{constant} \quad (4)$$

It is possible to use the experimental $D(A)$ -curve for any single explosive yielding entirely gaseous products, in conjunction with (2), (3) or (4), to determine α . The disadvantage of all such inverse procedures lies, of course, in the difficulty of judging whether or not the resultant equation of state is in fact authentic. This can be tested in general only by (a) the inherent plausibility of the assumption made, (b) the consistency of the equation of state with those similarly calculated for the products of other explosives, or alternatively the success of the equation in predicting wave velocities for other explosives, and (c) the accuracy or otherwise of estimates, based on the equation, of effects produced in the cartridge environment. In the particular case of assumption (4), however, which was made by Schmidt, and which enables the equations of § 12 to be applied, we have an immediate test in the constancy of the values of α corresponding to different loading densities. The covolumes deduced by Schmidt failed to satisfy this test. Although the values of α extrapolated reasonably well to the

[149]

corresponding van der Waals constants at low density, and also varied rather little from one explosive to another, so that they might be used with fair success for predicting detonation velocities, at least in explosives of similar composition, their rapid decrease with rising gas density was much too large to be reconciled with the assumption of constancy implied in the use of equation 12(2). Disregarding this [43] objection, however, Roth has used Schmidt's results to make calculations for a wide range of explosives. He also took account of the chemical equilibria, so that the method involved successive approximations; but no allowance was made for the modification in the ideal equilibrium constants implied by the equation of state. Roth's work has only recently come to hand.

These calculations are vitiated by the fact that they determine a variable covolume $\alpha(\nu)$ by means of a theory which assumes α to be constant. However, it is not difficult (§ 13.5) to modify the equations of § 12 in such a way as to allow for dependence of α on ν . If $(\partial\alpha/\partial T)_v \equiv 0$, the equations remain valid, provided γ is replaced by k , where

$$k \equiv \gamma - (d\alpha/d\nu)_{\nu=v} \quad (5)$$

It is to be noted, however, that though γ is still equal to $1 + nR/c_v$, this is no longer the same thing as c_p/c_v since $c_p - c_v = nR/(1 - d\alpha/d\nu)$. [37] The above modification has, indeed, been made by Cook, who used it as the basis for inverse calculations of $\alpha(\nu)$ from the observed variation of D with Δ in a number of pure explosive compounds. It will be seen that the system of equations of § 12, when modified as above, contain a differential equation in α , and Cook's method of successive approximation amounts to determining the singular solution of this system. Cook concludes that the function $\alpha(\nu)$ is independent of

product constitution, and states that successful estimates of D have been made for a wide range of explosives. Moreover, since the computed detonation temperatures vary appreciably among the cases studied, the coincidence of $\alpha(v)$ is held to provide a posteriori justification for (2). Cook indeed attempted to confirm this by a more general analysis, in which allowance was to be made for a possible variation with T ; but we have seen that this is impossible, and Cook's argument was in fact fallacious, as appeared from subsequent correspondence on the subject.
 [127, 38]

The problem has been attacked along closely similar lines by Caldirola.
 [27] He concludes that $1/\alpha$ is linear in $1/v$, but not independent of the explosive studied. His estimates of temperature etc. also differ in some cases rather sharply from those of Cook.

§ 13.1 Absolute calculations for condensed explosives of normal density

In the following sections we shall describe the development of methods of calculating the large-scale detonation properties of condensed explosives at normal loading densities. These calculations are absolute, in the sense that they rest on entirely theoretical grounds, and involve neither adjustable constants nor parameters defined by appeal to observation of explosive performance. It is, of course, clear that attempts to solve such a problem must be more than usually tentative, and that effective progress can be made only by considerable simplification of a highly complex system. Thus, in particular, we make use of an equation of state which regards the product gas molecule as a hard inelastic sphere. The picture which we shall develop should therefore be regarded rather as a model than as a rigorous description of the actual processes within a detonating cartridge. Nevertheless, the level of agreement found to exist between the results of such a formulation and experimental facts may suggest that the model

retains to a considerable degree the most important features of its subject.

In §13.2, we present the method of analysis of the chemical product equilibria. §§ 13.3 - 13.6 and §14 are then concerned with detonating explosives whose products are entirely gaseous at the Chapman-Jouguet pressure and temperature. In §13.3, the equation of state is described. §§ 13.4 and 13.5 deal with the RH-equation and CJ-condition, while in § 13.6 the theory of real equilibria is developed, subject in each case to this equation of state. We then proceed to applications (§14). Later sections are devoted to explosives whose products contain condensed material.

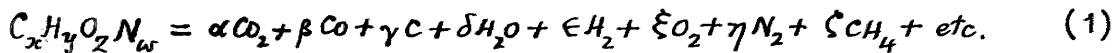
§13.2 Analysis of the product equilibria

Condensed detonating explosives may be single chemical compounds, or mixtures. In the latter case they may contain organic substances, as a rule composed of C, H, O and N only (such as nitroglycerine and cellulose), and inorganic salts, which are either reactive (e.g. nitrates) or non-reactive (chlorides, etc.). More rarely, elementary substances (e.g. aluminium, carbon, liquid oxygen) are introduced. The products will therefore, in general, consist of (a) a solid or liquid phase, formed typically from carbon or lead, together with metallic oxides or carbonates and non-reactive substances surviving from the original mixture; and (b) a gaseous phase, in which the elements C, H, O, N will be present in various combinations.

It will be assumed that reactive metallic salts transform quantitatively into the corresponding oxides or carbonates; equilibria involving such end-products are therefore ignored. All available information concerning these equilibria indicate that the assumption is sound. [17] The analysis is thus reduced, in all but the most exceptional cases, to

a consideration of equilibrium in a gaseous phase containing compounds of C, H, O, N, with the possible co-presence of condensed carbon.

Let $C_x H_y O_z N_w$ represent the atom content of any chosen mass of the gas and condensed carbon, taken together, and supposed to yield the following products* in equilibrium at p and T



Then material balance requires

$$\alpha + \beta + \gamma + \zeta + \dots = x \quad (2)$$

$$2\delta + 2\epsilon + 4\xi + \dots = y \quad (3)$$

$$2\alpha + \beta + \delta + 2\xi + \dots = z \quad (4)$$

$$2\eta + \dots = w, \quad (5)$$

while, at equilibrium,

$$J_1 \alpha \epsilon = \beta \delta \quad (6)$$

$$J_2 \alpha = \pi^{\frac{1}{2}} \beta \xi^{\frac{1}{2}} \quad (7)$$

$$J_3 \zeta = \pi \epsilon^2 \quad (8)$$

$$J_4 \beta \pi^{\frac{1}{2}} = \xi^{\frac{1}{2}}, \quad (9)$$

etc.,

where J_1, J_2 , etc. are the real equilibrium constants ($J = IK$, as in § 9.54 above) of the following reactions

* $\alpha, \beta, \gamma, \text{etc}$ should be distinguished from other quantities represented elsewhere by the same symbols.



etc.,

and $\pi \equiv p/N$, $N \equiv \alpha + \beta + \delta + \dots$ being the total number of gaseous moles.

Besides the equilibria (10) - (13), there will be others involving such species as O, H, N, NO, HCN, NH₃, and so forth. Consideration of the appropriate constants shows, however, that dissociation of O₂, H₂ and N₂ will be negligible even at the temperatures of detonation, because of the high prevailing pressures. Formation of NO from O₂ and N₂ is independent of pressure, at least under ideal conditions, but will be significant only for markedly oxygen-positive explosives, which are rare: the importance of NO is discussed for such cases in § 13.25. Formation of HCN, NH₃, and other polyatomic molecules is promoted by high pressure, but the relevant equilibrium constants indicate that such product species will normally be unimportant, except perhaps at the highest cartridge densities.

Accordingly we proceed by first disregarding all possible products except those mentioned explicitly in (10) - (13). When the major products have been thus determined, we can then test a posteriori that the concentrations of other potential species are in fact negligible. Equations (2) - (9) can be solved in the most general case by throwing them into the form:

$$\eta = \omega/2 , \quad (14)$$

$$\alpha = \frac{J_4 \pi}{J_2} \beta^2 , \quad (15)$$

$$\xi = J_4^2 \pi \beta^2 , \quad (16)$$

$$\delta = z - (2\alpha + \beta + 2\xi) , \quad (17)$$

$$\epsilon = \frac{\beta \delta}{J_1 \alpha} , \quad (18)$$

$$\zeta = \frac{\pi \epsilon^2}{J_3} , \quad (19)$$

together with (2) (3). Assuming a value for β , we calculate α , ξ , δ , ϵ , ζ and check in (3). Finally, by (2),

$$\gamma = x - (\alpha + \beta + \zeta) .$$

If the explosive is "oxygen-positive" with respect to the carbon and hydrogen, that is if

$$z > 2x + y/2 \quad (20)$$

(as in nitroglycerin), this procedure fails, and we have instead the simple solution:

$$\begin{aligned} \alpha &= x , \quad \delta = y/2 , \quad \xi = \frac{z}{2} - x - y/4 , \quad \eta = w/2 , \\ \beta &= \gamma = \epsilon = \zeta = 0 . \end{aligned} \quad (21)$$

The products are thus CO_2 , H_2O , N_2 and excess O_2 , and may be written down at once. (NO-formation remains to be considered).

If the explosive is oxygen-negative, but has sufficient oxygen to transform all the H to H_2O , and all the C to CO , that is if

$$2x + y/2 > z > x + y/2 \quad (22)$$

(as in PETN), the general procedure again fails. We must then omit the carbon-forming reactions (12) and (13), whereupon the major products

are defined by J_1 and J_2 alone. The ideal water-gas constant K_1 is of the order of 9 at detonation temperatures, and the effect of gas imperfections, according to the theory of § 13.6 below, is found to increase this markedly. The proportion ϵ of H_2 is therefore always small, even at low densities. ξ is defined by (7) and thus depends on J_2^2/π . Since the ideal constant K_2 is of the order of 20 - 40, the proportion of O_2 calculated on an ideal basis will not be large, even at low density; the effect of allowance for imperfections is to lower the O_2 still further. The actual calculation is best carried out by a cyclical process, based on (2) - (7), though approximate solutions can be obtained by ignoring either ϵ or ξ , and are given below in §§ 13.21, 13.22.

The great majority of British commercial explosives fall into one or other of the above two categories.

When, as in TNT and a large number of other organic detonating compounds, the explosive is so deficient in oxygen that

$$Z < x + y/2 , \quad (23)$$

we must allow for the possible formation of free carbon. The relatively low detonation temperatures which arise with such explosives oblige us to regard the C as condensed, and so to apply equations (2) - (9). Approximate analytical solutions can be obtained suitable for certain ranges: two of these are derived in §§ 13.23, 13.24. However, such solutions have a restricted validity, and in general it is simpler and safer to use an iterative method based on (14) - (19).

§ 13.21

Approximate solution for $2x + y/2 > z > x + y/2$:

oxygen concentration (ϵ) assumed negligible

The equations of § 13.2 become

$$\alpha + \beta = x \quad (1)$$

$$\delta + \epsilon = y/2 \quad (2)$$

$$2\alpha + \beta + \delta = z \quad (3)$$

$$J_i \alpha \epsilon = \beta \delta, \quad (4)$$

whence

$$\alpha = F(J_i) \quad (5)$$

$$\beta = x - F(J_i) \quad (6)$$

$$\delta = z - x - F(J_i) \quad (7)$$

$$\epsilon = x + y/2 - z + F(J_i) \quad (8)$$

$$N \equiv \alpha + \beta + \delta + \epsilon + \eta = x + \frac{1}{2}(y + w) \quad (9)$$

where

$$F(J_i) \equiv \frac{J_i(z-x-y/2)-z+\sqrt{J_i^2(z-x-y/2)^2-[2(z-x)(z-2x)-yw]J_i+(z-2x)^2}}{2(J_i-1)}. \quad (10)$$

When $J_i \gg 1$, this reduces to

$$\alpha = z - x - y/2, \quad (11)$$

$$\beta \doteq 2x + y_{1/2} - z , \quad (12)$$

$$\delta \doteq y_{1/2} , \quad (13)$$

$$\epsilon \doteq 0 . \quad (14)$$

The smallness of ξ can be verified from equation 13.2(7).

§ 13.22 Approximate solution for $2x + y_{1/2} > z > x + y_{1/2}$:

hydrogen concentration (ϵ) assumed negligible

The equations are

$$\alpha + \beta = x \quad (1)$$

$$\delta = y_{1/2} \quad (2)$$

$$2\alpha + \beta + \delta + 2\xi = z \quad (3)$$

$$J_2 \alpha = \pi^{1/2} \beta \xi^{1/2} , \quad (4)$$

whence

$$(x - \alpha) \sqrt{(z - x - y_{1/2}) - \alpha} = \sqrt{\frac{2}{\pi}} \cdot J_2 \alpha . \quad (5)$$

For any particular values of x, y, z (5) can be most easily solved by graphing J_2 against α . In the case of PETN ($C_5H_8O_12N_4$), the relationship between α and J_2 can be represented very closely for the relevant range ($2 < \alpha < 3$) by

$$\alpha \doteq 3.04 - 0.586 J_2 \quad \text{per mole PETN} , \quad (6)$$

whereupon

$$\beta \doteq 1.96 + 0.586 J_2 , \quad (7)$$

$$\delta \doteq 4 , \quad (8)$$

$$\xi \doteq 0.29 J_2 , \quad (9)$$

and

$$N \equiv \alpha + \beta + \delta + \xi + \eta = 11 + 0.29 J_2 . \quad (10)$$

§ 13.23 Approximate solution for $x < x + y/2$: pressure extremely high

[8]

H. Jones has derived an approximate solution for use at the highest loading densities in TNT, whose products contain free carbon. We shall generalise this solution for the explosive $C_x H_y O_z N_w$, where

$$x < x + y/2 . \quad (1)$$

The products are supposed to be those stated explicitly in 13.2(1). Jones takes $\xi \equiv 0$, but this need not be assumed at the outset. The equations are then 13.2(2-9), from which, eliminating $\alpha, \beta, \gamma,$

δ, ξ, η, ζ , we deduce

$$2\pi\epsilon^2 = \left(\frac{2\pi}{J_3} \epsilon^2 + \epsilon - y/2 \right) \left[\left\{ \frac{4J_2}{J_1^2 J_3 J_4} (J_2 J_4 + 1) - 1 \right\} \pi\epsilon^2 + \left\{ \frac{2J_2}{J_1^2 J_4} (J_2 J_4 + 1) - \frac{J_2}{J_1 J_4} \right\} \epsilon - \frac{J_2 y}{J_1 J_4} (J_2 J_4 + 1) \right] . \quad (2)$$

If π is sufficiently large, the terms in ϵ may be neglected, so that

$$x - \frac{\pi\epsilon^2}{J_3} \doteq \left(2 \cdot \frac{\pi\epsilon^2}{J_3} - y/2 \right) \left[(F-1) \cdot \frac{\pi\epsilon^2}{J_3} - \frac{yF}{4} \right] , \quad (3)$$

where

$$F \equiv \frac{4J_2}{J_1^2 J_3 J_4} (J_2 J_4 + 1) . \quad (4)$$

(3) is a quadratic in $\pi\epsilon^2/J_3$, from which

$$\frac{\pi\epsilon^2}{J_3} = \frac{x - y/2 + yF \pm \sqrt{(x - y/2)^2 + 2yzF}}{4(F-1)} . \quad (5)$$

If we denote this quantity by ψ , then the solution for π very large is:

$$(H_2) \quad \epsilon \doteq \sqrt{\frac{J_3 \psi}{\pi}} \doteq 0 \quad (6)$$

$$(C4_4) \quad \zeta \doteq \frac{\pi \epsilon^2}{J_3} = \psi \quad (7)$$

$$(H_2O) \quad \delta \doteq y_{1/2} - \epsilon - 2\zeta \doteq y_{1/2} - 2\psi \quad (8)$$

$$(Co) \quad \beta \doteq \frac{J_2 \delta}{J_1 J_4 \pi} \doteq \frac{J_2 \left(\frac{y}{2} - 2\psi \right)}{J_1 J_4 \sqrt{J_3 \pi \psi}} \doteq 0. \quad (9)$$

$\xi = J_2 J_4 \alpha$, and so, by 13.2(4),

$$\alpha \doteq \frac{x - \beta - \delta}{2(1 + J_2 J_4)} \doteq \frac{\frac{x}{2} - \frac{y}{4} + \psi}{1 + J_2 J_4} \quad (10)$$

$$\xi \doteq \frac{J_2 J_4 \left(\frac{x}{2} - \frac{y}{4} + \psi \right)}{1 + J_2 J_4} \quad (11)$$

$$\gamma \doteq x - \psi - \frac{\frac{x}{2} - \frac{y}{4} + \psi}{1 + J_2 J_4} \quad (12)$$

Finally, $\eta = \omega/2$, (13)

and

$$N \doteq \alpha + \beta + \delta + \epsilon + \xi + \eta + \zeta \doteq (y + 2x + 2\omega)/4, \quad (14)$$

and is therefore constant.

When ideal constants are used, from the tables of K_1 etc., suitably extrapolated, we have

T ($^{\circ}$ K)	1,000	2,000	3,000	4,000	5,000	6,000
F	1.70	3.35	4.60	5.50	6.18	6.60

so that $F > 1$. With real constants, there is no guarantee that $F > 1$.

When $F > 1$, both roots of (5) are positive, since

$$(z - \gamma_{1/2} + yF)^2 = (z - \gamma_{1/2})^2 + 2yzF + y^2F(F-1)$$

Similarly, when $F < 1$, the - sign in (5) corresponds to a positive root, but the + sign to a negative root. In either case, however, the - sign must be taken. For, by (8)

$$2\delta(F-1) = -(z + \gamma_{1/2}) \mp \sqrt{(z + \gamma_{1/2})^2 + 2yz(F-1)}, \quad (15)$$

and $\delta > 0$ demands the + sign in (15) and so the - sign in (5), if $F > 1$.

Hence ϵ and δ are both positive only when the - sign is used in (5).

ζ and β are then also positive. By a similar argument, it follows that α and ξ are positive. The condition for a solution is then that $\gamma > 0$. It does not appear possible to establish algebraically that this is satisfied, but in practice it has always been found to follow, subject to (1), which applies to a large number of organic explosives, such as TNT, tetryl, picric acid, etc. If ideal constants are used, the products of such explosives can readily be evaluated at any given temperature and at high pressures by means of the above theory. A selection is shown in Table 13.23:1.

Table 13.23:1

The products are expressed in mole/kg.; ψ refers to one mole of the explosive

Explosive	Formula : 3000°K (T = 4.72)						5000°K (T = 6.225)											
	C	H	O	N	ψ	CO ₂	H ₂ O	CH ₄	C	N ₂	ψ	CO ₂	H ₂ O	CH ₄	C	N ₂		
TNT	7	5	6	3	0.666	10.64	5.15	2.95	17.53	6.60	0.717	10.87	4.70	3.16	16.82	6.60		
Tetryl	7	5	8	5	0.598	11.67	4.55	2.08	10.63	8.71	0.653	11.85	4.16	2.27	10.25	8.71		
Picric acid	6	3	7	3	0.306	13.34	3.88	1.34	11.52	6.55	0.341	13.49	3.57	1.49	11.22	6.55		
Ammonium picrate	6	6	7	4	0.807	11.42	5.63	3.28	9.70	8.13	0.868	11.67	5.14	3.53	9.20	8.13		
Trinitrobenzene	6	3	6	3	0.356	12.24	3.70	1.67	14.27	7.04	0.361	12.26	3.65	1.70	14.23	7.04		
Trinitroanthraene	6	4	6	4	0.491	10.92	4.47	2.16	13.24	8.77	0.533	11.12	4.10	2.34	12.88	8.77		
Trinitrocresol	7	5	7	3	0.630	11.86	5.10	2.59	14.37	6.17	0.683	12.07	4.67	2.81	13.93	6.17		
Trinitroresorcinol	6	3	8	3	0.287	14.44	3.78	1.17	8.88	6.12	0.321	14.57	3.50	1.31	8.61	6.12		
Hexanitrodiphenylamine	12	5	12	7	0.504	11.97	3.40	1.15	14.22	7.98	0.560	12.11	3.06	1.28	13.88	7.98		

\S 13.24 Approximate solution for $z < x + y/2$: ϵ, ξ, ζ negligible

The equations reduce to

$$\delta \doteq y/2 \quad (1)$$

$$\alpha + \beta + \gamma \doteq x \quad (2)$$

$$2\alpha + \beta \doteq x - y/2 \quad (3)$$

and $\frac{\pi J_4}{J_2} \beta^2 = \alpha$, (4)

whence

$$\beta \doteq \frac{1}{4A} \left\{ -1 + \sqrt{1 + 8A(x - y/2)} \right\}, \quad (5)$$

where $A \doteq \pi J_4/J_2$. α and γ follow at once. $\gamma = \frac{\pi}{2}$, as usual.

If $A \gg 1$, then

$$\beta \doteq \frac{1}{2} \sqrt{\frac{2x-y}{A}} \doteq 0 \quad (6)$$

$$\alpha \doteq \frac{x}{2} - \frac{y}{4} \quad (7)$$

$$\gamma \doteq x - \frac{x}{2} + \frac{y}{4}. \quad (8)$$

\S 13.25 Formation of NO

The negligible O_2 -content in the products of oxygen-negative explosives ensures that NO-formation will be unimportant. For oxygen-positive explosives, this is not necessarily true. We may, however, obtain a sufficient estimate of the level of NO-formation in such cases by applying the NO-equilibrium:



to the product mixture as determined without reference to NO. If

ξ, η are the numbers of moles of O_2, N_2 already determined in this way, and λ the resultant NO, the above approximate procedure gives:

$$\frac{\lambda}{\sqrt{(\xi - \frac{\lambda}{2})(\eta - \frac{\lambda}{2})}} = \frac{P_{NO}}{P_{O_2}^{\frac{1}{2}} \cdot P_{N_2}^{\frac{1}{2}}} \equiv K_6(T) \quad (2)$$

where K_6 has been tabulated in Table 9.54:1.

Since the reaction is equimolecular, and the covolume very little affected, ideal equilibrium constants may be used. If

$$\Lambda \equiv \lambda/\eta, \quad E \equiv \xi/\eta,$$

(2) yields

$$\Lambda = \frac{K_6 \sqrt{(E+1)K_6^2 + 16E} - (E+1)K_6^2}{4 - K_6^2}. \quad (3)$$

K_6 is less than 1 even at $5,000^{\circ}\text{K}$, and E will scarcely ever rise as high as 1. In general, therefore, $\Lambda < 0.75$, so that at most one third of the nitrogen is oxidised. As a rule, the fraction is much less. The variation of Λ over a wide range of T and E is shown in Table 13.25:1.

Table 13.25:1

$10^3 (NO/N_2)$ as a function of T and O_2/N_2

O_2/N_2	1,400	2,000	2,500	3,000	3,500	4,000	5,000
0.1	0.63	6.28	15.15	35.2	55.3	75.3	111.2
0.2	0.88	8.90	21.6	51.0	81.6	113.6	170
1.0	2.0	20.0	48.9	117	189	267	414
5.0	4.4	44.5	109	256	412	570	890

§13.3 The equation of state

A gas of inelastic spherical molecules obeys the ideal equation

$$pV = nRT \quad (1)$$

when the attractive forces and collisions between molecules are both negligible, that is, at low densities. The effect of allowance for intermolecular attraction and binary collisions is to replace (1) by the equation of van der Waals

$$(p + \frac{a}{v^2})(v - b) = nRT, \quad (2)$$

where a and b are constants, the latter equal to four times the volume of 1 gm. of the spherical molecules. If a/pv^2 is small, (2) reduces to the Abel equation 12(1). Since at moderate pressures a is found to decrease with rising temperature, the Abel equation should be particularly useful at high temperatures and moderate pressures, which explains its success in describing the behaviour of propellant powder gases.

At higher densities, allowance must be made for the effect of collisions [11, 69, 110] between three, four, etc. molecules. When this is done, the equation becomes

$$(p + \frac{a}{v^2})v = nRT \left(1 + \frac{b}{v} + 0.625 \frac{b^2}{v^2} + 0.287 \frac{b^3}{v^3} + \dots\right). \quad (3)$$

The numerical coefficients of powers of b/v are deduced from purely geometrical considerations of the impossibility of overlapping in hard identical spheres, and their calculation has not been extended beyond those [105] shown in (3). On the other hand, Lennard-Jones and Devonshire derive an equation of state for dense gases in the form

$$[p + f(v, T)]v = nRT \left(1 - K \frac{b^3}{v^3}\right)^{-1}. \quad (4)$$

[77,56]

Hirschfelder, Stevenson and Eyring develop an essentially similar equation from geometrical considerations of free volume, identifying $f(v, T)$ with a/v^2 . The constant K is a pure number, whose value depends on the configuration of the closely packed molecules.

(4) may therefore be regarded as the limit towards which (3) approaches, when v is small; it would be expected to apply in the neighbourhood of $b/v = 2$, and the values which we shall calculate for high-density explosives are just of this order. However, the range of validity of the equation is clearly restricted in both directions: it cannot be reliable for small values of b/v such as will occur at lower loading densities, and on the other hand it cannot apply when b/v approaches $K^{-3} (\sim 3)$. Such objections do not arise with equation (3): there is no immediate lower density limit to its application, and v may be indefinitely reduced without leading to any formal absurdity. This suggests that if, by means of a further, fourth-order, correction (3) were made to agree with (4) at or about $b/v = 2$, (3) would be applicable over a wide range of b/v up to, and perhaps even beyond, this value. Hirschfelder et al. propose, in fact, to interpolate between (3) and (4) by adding a fifth series term empirically to (3) and determining the appropriate coefficient in such a way that the two equations agree at $b/v = 2$. The coefficient depends upon K. When $K = 0.7163$ (corresponding to body-centred cubic packing), the resultant equation is, apart from the term a/v^2 ,

$$\phi_v = \pi R T (1 + b/v + 0.625 b^2/v^2 + 0.287 b^3/v^3 + 0.193 b^4/v^4). \quad (5)$$

On the other hand, for $K = 0.6962$ (face-centred cubic packing),

[26]

(3) requires no significant modification, since it then already almost coincides with (4) around $b/v = 2$. In this case, the equation of state becomes, at high temperatures and pressures:

$$\frac{p}{v} = \pi RT \left(1 + b/v + 0.625 b^2/v^2 + 0.287 b^3/v^3 \right). \quad (6)$$

However, equation (5) has been used in our calculations, except where otherwise stated.

Neglect of a/v^2 or $f(v, T)$ brings the equation of state under the form

$$\frac{p}{v} = \pi RT \sigma(b/v). \quad (7)$$

If b is then regarded as independent of T , we have

$$\left(\frac{\partial F}{\partial v} \right)_T = T \left(\frac{\partial p}{\partial T} \right)_v - p \equiv 0, \quad (8)$$

so that no account is taken of the potential energy of intermolecular repulsion. This is almost certainly legitimate for propellant powders ($\Delta \sim 0.5 \text{ g/cm}^3$), and in a blasting explosive cartridge whose density does not exceed 1 g/cm^3 the errors should not be too serious. Even at higher densities, the neglect of repulsive forces will in fact have a minor effect on all the calculated parameters except the temperature, which will tend to be exaggerated. Thus, at $\Delta = 1.5 \text{ gm/cm}^3$, Brinkley [25] estimates an energy absorption of about 7% in intermolecular repulsion, with corresponding reduction in T . Neglect of $f(v, T)$, however, may be partly compensated, if we identify b with the theoretical second virial coefficient

$$b = B(T) = \left[\frac{d(pv/\pi RT)}{d(1/v)} \right]_{v=\infty}, \quad (9)$$

rather than with the van der Waals covolume constant. A similar procedure [76] was adopted by Hirschfelder and Roseveare, who were able thus to reach close agreement with experimental Joule-Thomson coefficients. However, whereas these workers retained the van der Waals b in all terms of higher order than b/v , we shall use $B(T)$ throughout. It is not claimed that this procedure has any rigorous justification, but it

appears more consistent with the Boltzmann model on which our equation (5) is based.

$B(T)$ varies with T , reaching a maximum when $T \sim 3000^{\circ}\text{K}$. However, over a range of $2000 - 5000^{\circ}\text{K}$, the variation is slight, and we take advantage of this to simplify the analysis by adopting a mean molar value B_i for each (i^{th}) product gaseous species. The manner in which these values should be compounded for a mixture of gases raises further problems. Several theoretical rules have been formulated for determining the virial coefficients of mixtures in terms of those of the components. In view of the uncertainties which arise at other points in the theory, it seems sufficient here to adopt the simplest, that is, the linear method of combination. Then

$$\ell = \sum_i n_i B_i , \quad (10)$$

where n_i is the number of moles of the i^{th} species in 1 gm. of the products, and B_i is the high-temperature second virial coefficient for 1 mole of this species. This would lead, if the theory were accurate at all other points, to an exaggeration of α and hence also of the calculated detonation velocity. The values of B_i necessary for our work are collected in Table 13.3:1.

[117]
Table 13.3:1

Second virial coefficients B_i at high temperatures
($\sim 3000^{\circ}\text{K}$)

Gas	B_i cm ³ /mol.	Gas	B_i cm ³ /mol.
: CO ₂ (rotating)	: 63	: H ₂	: 14.0
: CO ₂ (non-rotating)	: 37.0	: O ₂	: 30.5
: CO	: 33.1	: N ₂	: 33.9
: H ₂ O	: 7.9	: CH ₄	: 37.0

In order to facilitate the use of the equations of § 12,

we retain the Abel form

$$\frac{P}{\rho}(v-\alpha) = \pi RT, \quad (11)$$

whereupon

$$\alpha = v \left(1 - \frac{1}{\sigma}\right) \quad (12)$$

and $\frac{d\alpha}{dv} = 1 - \frac{1}{\sigma} - \frac{x}{\sigma^2} \frac{d\sigma}{dx}, \quad (13)$

where

$$x \equiv \frac{\ell}{v} \equiv \frac{\sum n_i B_i}{v}, \quad (14)$$

and $\sigma(x)$ denotes the bracketed series in (5) [or (6)]; that is,

$$\sigma(x) \equiv 1 + x + 0.625x^2 + 0.287x^3 [+ 0.193x^4]. \quad (15)$$

For comparison, the value of α indicated by (4) is $K\ell^{1/3}v^{2/3}$, so that

$$\frac{d\alpha}{dv} = \frac{2}{3}K(\ell/v)^{1/3}. \quad \alpha/\ell \text{ and } d\alpha/dv \text{ are graphed as functions of } v/\ell$$

in Fig. 13.3:1, which illustrates the comparative behaviour of the

three equations of state. $\sigma(x)$ is also shown as a function of x

for (5) and (6) in Fig. 13.3:2.

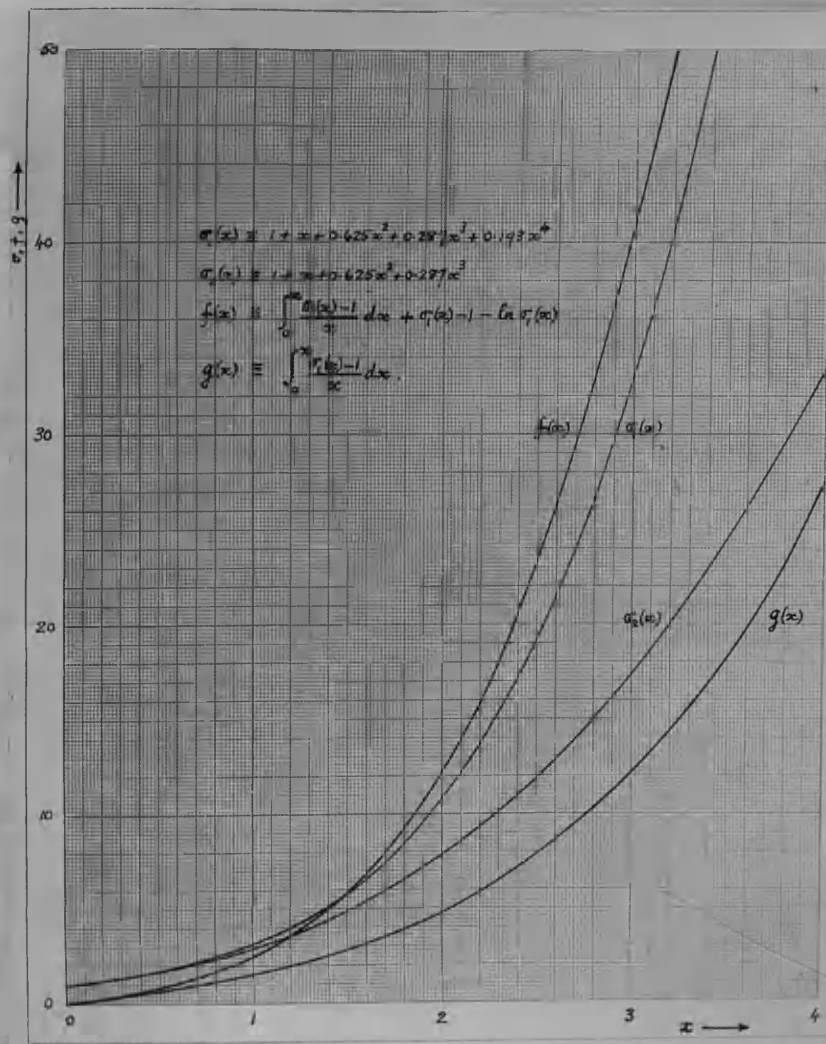
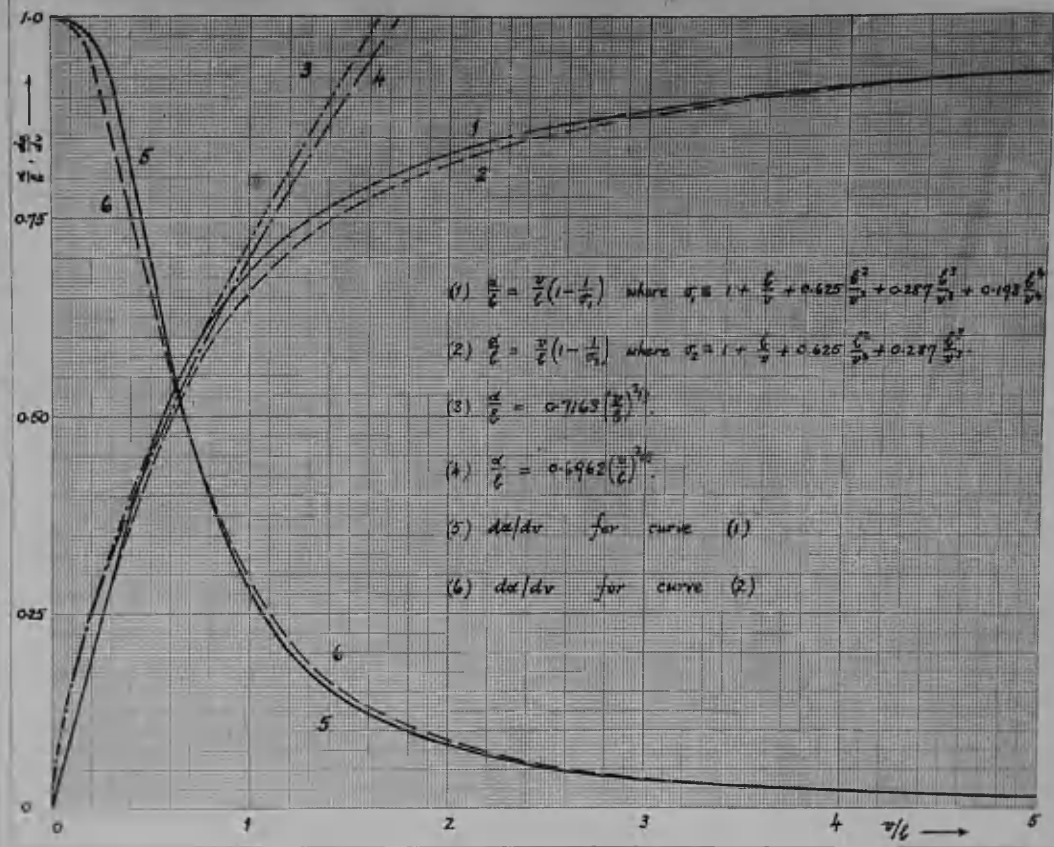


FIG. 13.3:2

§ 13.4 The RH-equation

(

In consequence of 13.3(8), the RH-equation takes the form 9.7(9), which, since \dot{p}_o is negligible, becomes

$$E_i - E_o = \Delta E_i^{(o)} - Q_i = \bar{C}_v(T_i - T_o) - Q_i = \frac{1}{2} p_i(v_o - v_i), \quad (1)$$

where $\Delta E_i^{(o)}$ represents the difference in internal energy of the products in the ideal gas state between T_o and T_i , and Q_i is obtained from the energies of formation, as explained in § 9.7.

§ 13.5 The CJ-condition and formal solution

Since $\alpha = \alpha(v)$, the analysis of § 12 requires to be slightly modified. The constant-composition adiabatic in differential form is now:

$$-pdv = dE = C_v dT = \frac{C_v}{nR} [(v-\alpha)dp + p(1 - \frac{d\alpha}{dv})dv],$$

or

$$-\left(\frac{\partial p}{\partial v}\right)_{S, n_i} = \frac{k_p}{v-\alpha}, \quad (1)$$

where

$$k \equiv 1 + \frac{nR}{C_v} - \frac{d\alpha}{dv}. \quad (2)$$

Equations 12(3-7) therefore continue to apply, provided γ is replaced by k , throughout. Thus:

$$v_i = \frac{k_i v_o + \alpha}{k_i + 1} \quad (3)$$

$$p_i = \frac{(k_i + 1)n_i R T_i}{k_i(v_o - \alpha)} \quad (4)$$

$$D = \frac{k_i + 1}{1 - \alpha D} \sqrt{\frac{n_i R T_i}{k_i}} \quad (5)$$

$$W_i = \sqrt{\frac{n_i R T_i}{k_i}} \quad (6)$$

$$E_i - E_i^* = \bar{c}(T_i - T_0) = Q_i + \frac{n_i R T_i}{2 k_i} \quad (7)$$

§ 13.6 Theory of real equilibrium

In the present section, as in § 9.54, V, N, B refer to an arbitrary mass of the products. The general theory has been presented in § 9.54. According to equations 9.54 (17, 18, 27) equilibrium in the reaction

$$\sum \ell_i L_i = 0 \quad (1)$$

is determined by

$$\prod_i N_i^{\ell_i} = I \cdot \left(\frac{N_g}{P}\right)^{\sum \ell_i} \cdot K(T), \quad (2)$$

where

$$-\ln I \equiv \sum \ell_i \ln A_i \quad (3)$$

and

$$\ln A_i = \int_V^\infty \left(\frac{1}{RT} \frac{\partial P}{\partial N_i} + \frac{1}{P} \frac{\partial P}{\partial V} \right) dV. \quad (4)$$

However,

$$PV = NRT \sigma(x), \quad (5)$$

where σ is defined in 13.3(15) and

$$\chi \equiv \frac{\sum N_i B_i}{V} \equiv \frac{B}{V} \quad (6)$$

From (5), (6),

$$\frac{1}{RT} \frac{\partial P}{\partial N_i} = \frac{\sigma(x)}{V} + N \sigma'(x) \cdot B_i / V^2$$

$$\text{while } \frac{1}{P} \frac{\partial P}{\partial V} + \frac{1}{V} = \frac{1}{\sigma} \frac{d\sigma}{dV}.$$

Hence

$$\ln A_i = \int_0^{\sigma} \frac{\sigma-1}{x} dx - \ln \sigma + \frac{N\beta_i}{B} (\sigma-1). \quad (7)$$

The same expression can be derived, somewhat less conveniently, from 9.54(23).

(7) is independent of the form of $\sigma(x)$. When σ is given by 13.3(15), it becomes

$$\begin{aligned} \ln A_i &= \frac{N\beta_i}{B} (\sigma-1) - \ln \sigma + \\ &+ \frac{\beta}{V} + \frac{5\beta^2}{16V^2} + 0.096 \frac{\beta^3}{V^3} + 0.048 \frac{\beta^4}{V^4}. \end{aligned} \quad (8)$$

If $N\beta_i = B$, which will be true if all the component gases have the same virial coefficient, but may also happen by accident for a particular species, (7) reduces to the activity for a single gas, namely

$$\ln A = \int_0^{\sigma} \frac{\sigma-1}{x} dx - \ln \sigma + \sigma-1; \quad (9)$$

otherwise it does not, the activity of each species being affected by the others present.

The ideal equilibrium constant $K(T)$ thus requires, by (3), to be multiplied by a factor I , where

$$-\ln I = f(\alpha) \sum \ell_i + (\sigma-1) \sum \ell_i \left(\frac{N\beta_i}{B} - 1 \right), \quad (10)$$

and $f(\alpha)$ is the function on the right of (9). The last term of (10) is due entirely to differences between the virial coefficients; the second last, $f(\alpha) \sum \ell_i$ however, survives (except for equimolecular reactions, where $\sum \ell_i = 0$) even when these coefficients are all equal. Both terms vanish of course at low density; otherwise, the ideal constant K can be used only when the reaction is equimolecular and the molar virial coefficients are equal. The function $f(\alpha)$ is shown in Fig. 13.3:2 for the state equation 13.3(5).

It has been assumed that the B_i are all independent of V .

[117]

However, the high-temperature coefficient for CO_2 is believed to change abruptly from 37 to 63 cm^3/mol . as the density falls through a critical value of 0.030 mol/cm^3 . This increase is due to the possibility of molecular rotation at the lower densities.

It is not entirely clear how one should define the critical condition in a gaseous mixture. For want of a better theory, we shall assume that the change occurs when the volume of the mixture as a whole reaches a critical level V' . The integral in equation 9.54(27) must then be evaluated in two parts if $V < V'$, though the result remains immediately expressible in terms of σ and f . Thus, let

$$B_{\text{CO}_2} = B_{\text{CO}_2}^{(1)} \quad \text{and} \quad B = B^{(1)}, \quad V > V'$$

$$B_{\text{CO}_2} = B_{\text{CO}_2}^{(2)} \quad \text{and} \quad B = B^{(2)}, \quad V < V'$$

Then, for $V > V'$,

$$\ln A_i = f\left(\frac{B^{(1)}}{V}\right) + \left(\frac{NB_i}{B^{(1)}} - 1\right) \left[\sigma\left(\frac{B^{(1)}}{V}\right) - 1 \right] \quad (11)$$

where $B_i \equiv B_{\text{CO}_2}^{(1)}$ for CO_2 . Denoting the right side of (11) by $F(B^{(1)}/V, B_i/B^{(1)})$, we then have, for $V < V'$,

$$\ln A_i = F\left(\frac{B^{(2)}}{V}, \frac{B_i}{B^{(2)}}\right) - F\left(\frac{B^{(2)}}{V'}, \frac{B_i}{B^{(2)}}\right) + F\left(\frac{B^{(1)}}{V'}, \frac{B_i}{B^{(1)}}\right), \quad (12)$$

where $B_i \equiv B_{\text{CO}_2}^{(2)}$ for CO_2 . For a single gas, such as CO_2 , (11) and (12) reduce to

$$\ln A = f\left(\frac{B^{(1)}}{V}\right), \quad V > V' \quad (13)$$

$$\ln A = f\left(\frac{B^{(2)}}{V}\right) - f\left(\frac{B^{(2)}}{V'}\right) + f\left(\frac{B^{(1)}}{V'}\right), \quad V < V'. \quad (14)$$

Although the values of $\ln A$ for single gases are not necessary for our purpose, they have been calculated from (9), (13) and (14) and appear in Table 13.6:1.

Table 13.6:1

$$\ln A \equiv \ln \left(\frac{P}{P_0} \right) \text{ for individual imperfect gases}$$

V (in cm ³ /mol.)	$\ln A$					
	CO ₂	CO	H ₂ O	H ₂	O ₂	N ₂
10	87.0	56.0	1.58	4.96	43.1	60.6
11.1	64.5	39.9	1.32	3.94	30.9	43.1
12.5	45.7	27.7	1.09	3.05	21.6	29.6
14.3	33.3	18.8	0.89	2.35	14.9	20.1
16.7	24.1	12.0	0.71	1.75	9.70	13.1
20.0	17.5	7.48	0.55	1.28	6.11	7.97
25.0	13.2	4.40	0.42	0.91	3.65	4.62
33.3	10.5	2.41	0.30	0.60	2.06	2.51
50.0	3.93	1.17	0.19	0.36	1.03	1.21
100	1.08	0.45	0.10	0.17	0.40	0.45

§ 14

Method of calculation for an explosive yielding entirely gaseous products

The method of calculation which we have adopted is as follows.

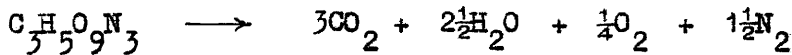
Values of T_1 and p_1/n , are assumed, and by means of the equilibrium equations the corresponding product gas composition is determined, allowing n_i , Q_i , c_i , \bar{c} and α to be estimated. An approximate value of k , is next derived by assuming $v_i = 0.75 v_o$ (Equation 12(10)) and using 13.5(2) and Figure 13.3:1. T_1 and p_1 are then recalculated from equations 13.5(7) and 13.5(4), and compared with the values assumed. If the discrepancy is marked, a second cycle of operations must be carried out. When reasonably close agreement is reached, which with experience will usually be the case after not more than two cycles, v_i , α and k , are estimated more precisely by means of 13.5(2,3) and Figure 13.3:1. This step involves a further process of successive approximation. T_1 is then checked from 13.5(7), with the new value of k . Agreement within sufficient limits will usually be reached at this stage. Similar remarks apply to p_1 , which is recalculated from 13.5(4). A final cycle of operations commencing with adjustment of the equilibrium composition may be carried out, but as a rule this is not necessary. Lastly, when agreement has been reached, D and H , are obtained from 13.5(5,6), or from the fundamental equations.

§ 14.1

Nitroglycerine ($C_3H_5O_9N_3$)

The theory was first applied to nitroglycerine, a liquid explosive with the high natural density of 1.6g/cm^3 . We assume, as in all

subsequent calculations except where otherwise stated that $T_o = 273^{\circ}\text{K}$ and $\bar{P}_o = 1 \text{ atm}$. The slight oxygen excess ($\frac{1}{2}O$ per mole) permits us to use the simple product solution 13.2(21), i.e.



so that $n_1 = 7.25/227 = 0.0319 \text{ mole/gm.}$, and from the relevant heats of formation $Q_1 = 1507 \text{ cal/gm.}$ Also, from Table 13.3:1, $b = 0.832 \text{ cm}^3/\text{gm.}$ Reference to the specific heat data shows that at constant volume (and subject always to our state equation, which discounts intermolecular potential energy) the temperature would reach about 4950°C . Adding 15% to this to allow for the HH-compressional heat, we estimate:

$$T_1 \sim 5700^{\circ}\text{K},$$

whereupon $c_v = 0.3754 \text{ cal./gm.}^{\circ}\text{K}$, $\bar{c} = 0.3350 \text{ cal./gm.}^{\circ}\text{K}$, and so $\gamma_1 = 1.170$. v_1, α and k_1 may now be calculated at once, as follows

v_1 (assd.)	$\frac{v_1}{b}$	da/dv_1 (Fig. 13.3:1)	α/b	α (Equ. 13.5(2))	k_1 (Equ. 13.5(3))	v_1 (Equ. 13.5(3))
0.50	0.602	0.551	0.514	0.428	0.619	0.504
0.505	0.607	0.546	0.517	0.430	0.624	0.505

T_1 , by 13.5(7), is now 5640°K , and the difference of 60° from the assumed value has a quite negligible effect upon γ_1 etc. The product composition, specific volume, and temperature are now all consistent with each other and with the theoretical equations. We may, therefore, calculate P_1 , H_1 and D by 13.5(4-6), obtaining

$$P_1 = 199,000 \text{ atm.}$$

$$H_1 = 1,550 \text{ m./s.}$$

$$D = 8,060 \text{ m./s.}$$

The results are collected in Table 14.1:1.

Table 14.1:1
Oxygen-positive or oxygen-balanced explosive compounds

Explosive	Δ	Products (mol/kg.)	n_i	Q_i	α	$\frac{d\alpha}{d\nu_i}$	R_i	v_i	T_i	P_i	W_i	D	$D(\text{obs.})$
		g./cm ³	H ₂ O	O ₂	N ₂	mol./g.	cm ³ /g.	cm ³ /g.	atm. x 10 ⁴	m.s.	m.s.	m.s.	m.s.
Nitroglycerine C ₃ H ₅ O ₉ N ₃	.60	13.2:1.0:-	1.1	6.6	0.032	1,507	0.430	0.546	0.624	0.505	5,640	19.9	1,550 : 8,060 : 8,000
Nitroglycol C ₂ H ₄ O ₂ N ₂	1.496	3.2:13.2:-	-	6.6	0.033	1,630	0.445	0.500	0.668	0.535	5,730	17.4	1,530 : 7,630 : 8,000
Erythritol tetranitrate C ₄ H ₆ O ₁₂ N ₄	.50	13.3:9.9:1.7	6.6	0.032	1,441	0.453	0.514	0.658	0.538	5,500	6.9	1,480 : 7,670 : -	
Mannitol hexanitrate C ₆ H ₈ O ₁₂ N ₆	.73	13.3:8.9:2.2	6.6	0.031	1,423	0.416	0.608	0.567	0.475	5,670	24.8	1,60 : 8,980 : 8,300	
Tetranitromethane CO ₈ N ₄	1.643	5.1:-	15.3:10.2:	0.031	-	457	0.465	0.666	0.573	0.517	5,000	4.7	1,60 : 7,740 : -
Ammonium nitrate NH ₄ NO ₃	1.00	-	25.0:6.3:12.5:	0.044	-	378	0.535	0.308	0.935	0.759	1,770	2.86	832 : 3,460 : see text
95% NH ₄ NO ₃ /5% H ₂ O	* 1.40	-	26.5:5.9:11.9:	0.044	-	387	0.458	0.448	0.790	0.572	1,980	6.45	967 : 4,810 : -
90% NH ₄ NO ₃ /10% H ₂ O ** 1.40	-	28.1:5.6:1.2:	0.045	-	31.0	0.452	0.433	0.813	0.570	1,680	5.33	882 : 4,340 : -	
Ammonium nitrite NH ₄ NO ₂	1.00	-	31.3:-	15.6:0.047	-	857	0.519	0.290	0.915	0.750	2,910	4.90	1,110 : 4,430 : 3,60 & test

* $T_0 = 435^\circ\text{K}$ ** $T_0 = 413^\circ\text{K}$.

The velocity of detonation of nitroglycerine has been repeatedly measured: its exceptionally high order is responsible for a certain scatter in the experimental results, which however lie about a mean value close to 8,000 m./s. The most accurate determinations are probably [99] those of Khariton and Ratner, according to which

$$D = 7,500 \pm 500 \text{ m./s.}$$

It should be emphasised that the method of calculation makes no use, at any stage, of measurements on explosive performance, and could in fact have been equally well applied in the absence of information as to whether nitroglycerine were capable of detonation or not. There is thus no guarantee whatsoever at the outset that calculated and observed velocities will even be of the same order of magnitude. The fact that they nevertheless are not only of the same order but coincide within experimental error offers strong support to the theory. We shall show that close agreement of this kind is not confined to nitroglycerine, but extends to a very wide range of explosives at all normal loading densities.

In close thermochemical relationship to nitroglycerine itself is Blasting Gelatine, in which the nitroglycerine is gelled, and its oxygen balance simultaneously brought close to zero, by addition of a small proportion of nitrocotton. Blasting Gelatine is discussed in § 16 below, along with other commercial detonating explosives.

§ 14.2 Other oxygen-positive single compounds

The number of familiar oxygen-positive or -balanced detonating compounds is not large, but it includes nitroglycol ($\text{C}_2\text{H}_4\text{O}_2\text{N}_2$), mannitol hexanitrate ($\text{C}_6\text{H}_8\text{O}_{18}\text{N}_6$), erythritol tetrinitrate ($\text{C}_4\text{H}_6\text{O}_{12}\text{N}_4$) and tetranitromethane (CO_3N_4); and measured velocities are available for at least the first two of these. Calculations, carried out at [99, 97] practical loading densities by the same method as for nitroglycerine are again summarised in Table 14.1:1. Agreement is good where comparison can be made.

Ammonium nitrate (NH_4NO_3), which is an extremely important ingredient in mixed explosives, and is oxygen positive, should be included in the present category. Although this substance is not used as an explosive by itself, and was in fact for many years considered so little capable of independent detonation that it was frequently quarried out of large storehouses by means of small blasting charges, there is now abundant evidence of its power to detonate when present in large quantities or under strong confinement. Recent experiments have shown [174] that the velocity at $\Delta = 0.9 \text{ g./cm}^3$. reaches 1,500 m./s. in 9-inch diameter cartridges. The calculated detonation properties under perfect confinement are summarised in Table 14.1:1 for $\Delta = 1 \text{ gm./cm}^3$.

We include also the results for two concentrated aqueous solutions of ammonium nitrate. Such solutions arise in certain industrial operations, and the 95/5 mixture has been found capable of detonation. [34] It will be noted that the temperature and pressure are both higher than for the dry salt at 1 gm./cm^3 . No experimental velocities are available for comparison.

Ammonium nitrite is a less familiar but easily detonated compound. It is oxygen-balanced. The calculated properties are shown in Table 14.1:1. It will be seen that the temperature and pressure are both much higher than for ammonium nitrate which may help to explain the relative ease of detonation of the nitrite. A single experimental velocity of 4,900 m./s. at 0.8 g./cm.³. has been recorded. [13] It must be said that this result is surprisingly high and if authentic would rank the nitrite with PETN as a blasting explosive.

§ 14.21 NO-formation

In §§ 14.1 and 14.2, formation of nitric oxide has been disregarded. The analysis of § 13.25 enables us to test how far this will affect the results. Using a heat of formation of + 21.4 K.cal. (absorbed) for one mole of NO formed from $\frac{1}{2}O_2 + \frac{1}{2}N_2$, we have computed the values shown in Table 14.21:1.

Table 14.21:1

Effect of NO-formation upon D

Explosive	NO/N ₂	100 $\frac{\delta Q}{Q_i}$	100 $\frac{\delta D}{D}$
Nitroglycerine	0.174	-1.50	-0.8
Erythritol tetranitrate	0.282	-2.45	-1.2
Mannitol hexanitrate	0.326	-2.80	-1.4
Tetranitromethane	0.160	-7.02	-3.5
Ammonium nitrate	0.007	-0.50	-0.25

The correction is small, and since it is doubtful whether such a slow reaction reaches equilibrium in the time available, no change appears called for in the solutions already tabulated.

* Pentaerythritol tetranitrate (§ 14.3).

§ 14.3 Pentaerythritol tetranitrate ($\text{C}_5\text{H}_{12}\text{O}_{12}\text{N}_4$)

This important, slightly oxygen-negative, explosive compound, to which the analysis of § 13.2 ($2x + \frac{y}{2} > z > x + \frac{y}{2}$) applies, provides a useful comparison of theory and experiment over a wide range [59] of loading density, since careful measurements of D have been made from $\Delta = 0.241$ to $\Delta = 1.727 \text{ gm./cm.}^3$

In the first calculations, ideal equilibrium constants were used. For this purpose, the product composition was evaluated at four pressures, 20,000, 50,000, 100,000 and 200,000 atm., for each of five temperatures, 3,000, 4,000, 4,500, 5,000 and 5,500°K. The composition appropriate to any point in this region could then be estimated at once by interpolation at each stage of the main calculation.

The final results are shown in detail in Table 14.3:1, together with the accepted experimental wave velocities. Agreement is close: there appears to be no systematic divergence, except at the extreme upper end of the density range, where D is very sensitive to slight changes in α (a variation of only 5% in α producing one of 10% in D). Agreement in this region could indeed be improved by using the state equation 13.3(6) instead of 13.3(5), but the latter provides a closer overall fit.

Considering the absolute nature of the calculation, and the unusual sensitivity of D to changes in α , the agreement indicated by Table 14.3:1 may be regarded as strong presumptive evidence of the general correctness of the approach. However, the use of ideal equilibrium constants is not strictly consistent with the equation of state employed, and it is now necessary to consider how far the results are modified by allowing for gas imperfection in accordance with the state equation.

Table 14.3:1
Pentaerythritol tetranitrate (PETN): ideal equilibrium constants

Δ J / cm^3	Products (mol/kg.)	n_1	Q_1	α	$\frac{dx}{dt}$	k_1	v_1	T_1	P_1	W_1	D	$D(\text{obs.})$
	$\text{CO}_2 : \text{CO} : \text{H}_2\text{O}$	$\text{H}_2\text{O} : \text{O}_2 : \text{N}_2$						$\text{atm.} \times 10^4$	m.s.	m.s.		
1.50	9.45:6.41:11.71	0.89:0.45:6.33	0.0352:	1,341:	0.461: 0.550	0.638:	0.541:	5,160:	18.8:	1,540:	8,200:	7,600
1.25	9.47:6.37:1.75	0.90:0.43:6.33:	0.0352:	1,345:	0.510: 0.458	0.731:	0.633:	5,040:	12.0:	1,420:	6,780:	6,500
1.00	9.33:0.49:11.74	0.91:0.53:6.33:	0.0353:	1,335:	0.566: 0.358	0.832:	0.763:	4,930:	7.30:	1,320:	5,580:	5,550
0.75	9.15:6.68:1.67	0.98:0.71:6.33:	0.0355:	1,319:	0.630: 0.243	0.948:	0.972:	4,800:	4.12:	1,225:	+530:	+650
0.50	8.9:7.0:11.6	1.1:1.0:6.33:	0.0359:	1,300:	0.706: 0.137	1.057:	1.370:	4,700:	2.10:	1,150:	3,660:	3,850

For this purpose, we apply the theory of § 13.6. Proceeding from the solution already obtained, and making use of equations 13.6(10) or 13.6(3,11,12), and of Fig. 13.3:2, we compute the factors I_1, I_2 , by which the ideal water-gas and CO_2 -dissociation constants require to be multiplied. A revised equilibrium composition at the assumed temperature and pressure can then be obtained, leading in turn by the usual methods, in which specific volume and covolume are simultaneously recalculated, to new estimates of temperature and pressure. The entire procedure, commencing with computation of I_1 and I_2 , is then repeated, until a set of self-consistent values is reached, whereupon W and D may be finally determined.

Complete calculations of this kind have been made for two densities, 1.5 and 0.75 gm./cm^3 . The work is laborious, and will not be presented in detail here, though for illustration § 14.31 outlines the final cycle in each case. The virial coefficient of CO_2 was assumed to change from 37 to $63 \text{ cm}^3/\text{mol}$ at $v' = 0.75 \text{ cm}^3/\text{gm}$. (see § 13.6). The result of allowance for gas imperfection is then a marked increase in the water-gas constant J_1 , so that the hydrogen content is negligible and the approximate solution of § 13.2.2 can be used, together with the following relations, which follow from 13.22 (6 - 9):

$$Q_1 = 445.3 - 39.6 J_2 \quad \text{cal./mole PETN} \quad (1)$$

$$B^{(1)} = 355.7 - 8.60 J_2 \quad \text{cm}^3/\text{mole PETN} \quad (2)$$

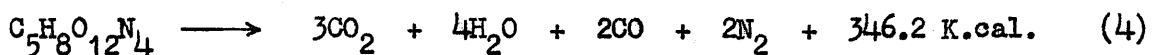
$$B^{(2)} = 276.2 + 6.66 J_2 \quad \text{cm}^3/\text{mole PETN} \quad (3)$$

The final solutions are summarised in Table 14.3:2. It will be seen that the temperature, pressure, density, streaming and wave velocities are affected only to a very minor degree by the refinements introduced. Since the changes are so small, and the assumption regarding v' uncertain,

Table 14.3:2

Δ	Products (mol/kg.)	n_1	Q_1	α	$d\alpha$	k_1	v_1	I_1	ρ_1	W_1	D	$D(\text{obj}_3)$
Δ	CO_2	H_2O	H_2	O_2	N_2	mol/g.	cal/g.	$\text{cm}^3/\text{g.}$	atm.	$\times 10^4$	m./s.	m./s.
1.50	9.5	6.3	12.6	0.05	0.02	6.3	0.0348	1,400	0.458	0.538	0.647	0.540
0.75	7.8	8.0	12.5	0.2	0.9	6.3	0.036	1,276	0.627	0.241	0.954	0.973
											4.740	4.13
											1,200	1,200
											4,480	4,700
											8,140	7,600
											1,550	1,550

it does not appear justified to take particular account of the change in virial coefficient for CO_2 . If we regard the value of $37 \text{ cm}^3/\text{mol}$ as applicable at all densities, we may use equation 13.6(10) and the work is considerably simplified. The result, as would be expected, is to redress the equilibrium in favour of CO_2 , and in fact it now appears that the simple composition defined by



should apply at all practicable densities. This is the composition which would be predicted by the following simple rules:

(a) oxidise all the hydrogen to H_2O

(b) oxidise all the carbon to CO

(c) oxidise the CO as far as possible to CO_2 .

The useful conclusion therefore emerges that the properties of oxygen-positive or moderately oxygen-negative condensed explosives $\text{C}_x\text{H}_y\text{O}_z\text{N}_w$

($z > x + y/2$) may be studied on the basis of these rules alone.

The final results for PETN are collected in Table 14.3:3.

Table 14.3:2

§ 14.31 Final cycles in full calculation for PETN at 1.5 and 0.75 g./cm³.

(1) 1.5 g./cm³.

The previous cycle leads to the set of values given in the first row of Table 14.3:2. The proportions of H₂ and O₂ may be disregarded, whereupon the reaction per mole PETN agrees very closely with equation 14.3(4). Then, per mole PETN,

$$\begin{aligned} B^{(1)} &= 3 \times 63 + 2 \times 33.1 + 4 \times 7.9 + 2 \times 33.9 \\ &= 354.6 \text{ cm}^3. \end{aligned}$$

$$B^{(2)} = 3 \times 37 + \text{etc.} = 276.6 \text{ cm}^3.$$

Also $V_i = 0.540 \times 316 = 171 \text{ cm}^3.$

$$V' = 33 \times 11 = 363 \text{ cm}^3.$$

The values of $\ln A_i$ may now be calculated for each species by equations 13.3(7) and 13.3(12). They are

	CO ₂	CO	H ₂ O	H ₂	O ₂
$\ln A_i$	11.91	9.39	4.37	4.88	8.76

It will be noted that these values differ among themselves much less than the corresponding values indicated by Table 13.6:1 for the species considered separately at the mean molar volume $V_i/N_i = 15.55 \text{ cm}^3/\text{mol.}$: this reflects the allowance made for the effect on each gaseous species of the co-presence of the others. We now have

$$I_1 \equiv \frac{A_{CO_2} \cdot A_{H_2}}{A_{CO} \cdot A_{H_2O}} = 20.7$$

$$I_2 \equiv \frac{A_{CO_2}}{A_{CO} \cdot A_{O_2}^{1/2}} = 0.156$$

At $T_i = 5300^\circ\text{K}$ and $p_i = 188,000 \text{ atm.}$, $K_1 = 8.80$ and $K_2 = 39.3$, while $\pi_i \equiv p_i/N_i = 17,000$. The product composition can now be calculated by the method of § 13.2. It is that given in Table 14.3:2, so that the

entire solution can be taken as self-consistent.

(2) 0.75 g./cm³.

The penultimate cycle yields $\text{CO}_2 = 2.56$, $\text{CO} = 2.144$, $\text{O}_2 = 0.24$, $\text{H}_2\text{O} = 3.96$, $\text{H}_2 = 0.04 \text{ mol/mol PETN}$; $V_i = 307 \text{ cm}^3$, $p_i = 41,000 \text{ atm}$, $T_i = 4750^\circ\text{K}$; which lead to $I_1 = 11.86$, $I_2 = 1.70$, $K_1 = 8.57$, $K_2 = 19.0$, and $\pi_i = 3,650$. The products are now those given in Table 14.3:2, which are very close to the above. Completing the calculation of V_i , p_i and T_i we again find almost identical agreement, and $D_i W_i$ may be evaluated, with the results shown.

§ 14.4 Liquid methyl nitrate ($\text{CH}_3\text{O}_3\text{N}$)

The rules enunciated at the end of § 14.3 may be applied to this compound, which is in the same category as PETN. The results of calculation at the natural density of 1.21 g./cm³ are set out in the last line of Table 14.5:1. Agreement with the experimental [35; also 138] velocity (in $1\frac{1}{4}$ " diameter) is very good.

§ 14.5 Nitroguanidine ($\text{CH}_4\text{O}_2\text{N}_4$)

In view of its marked oxygen deficiency ($Z < \alpha + \gamma/2$), this compound might be expected to fall into the same class as TNT, tetryl and picric acid, which are dealt with in § 15.2 below. However, the carbon/hydrogen ratio is so low that no equilibrium product composition containing free carbon can be found, at least at the low loading densities (0.2 to 0.6 g./cm³.) at which the explosive is usually employed. The products then depend only on the water-gas equilibrium. Results of calculations for the density range in question are collected in Table 14.5:1, together with the available observations on wave velocity. The agreement is good, particularly since the limiting experimental values may well be somewhat higher than those tabulated. [165, 66]

Table 32.5.1
Calculations for nitroguanidine at low densities, in 1 mol/liter methyl nitrate at various liquid density

Explosive	Products (mol./fig.)			α	$\frac{d\alpha}{d\nu}$	κ_1	ν_1	γ'_1	ρ_1	κ'_1	ν'_1	γ''_1	ρ''_1	κ''_1	ν''_1	γ''_1	ρ''_1	D (obs.)	D (m.s.)
	CO_2	H_2	N_2																
C	0.23	0.5:9.1:9.1	10.1:19.2	0.0480	641	1.012	0.058	1.205	2.83	2.620	0.570	933	2.680	2.350					
Nitroguanidine	0.51	0.2:9.4:9.4	9.8:19.2	0.0480	637	0.857	0.200	1.063	1.43	2.650	1.84	998	3.720	3.440					
Ethyl nitrate	0.60	-	9.6:9.6:9.6	9.6:19.2	0.0480	636	0.816	0.253	1.006	1.24	2.670	2.48	1,027	4.340	3,850				
Ethyl nitrate	1.21	6.5:6.5:19.5	-	6.5:0.039	1.575	0.500	0.406	0.779	0.643	5.200	11.72	1,470	6.640	6,400					

◎

§ 14.6 Propellant powders as detonating explosives

Propellant powders are capable of detonating if the grist size is sufficiently fine and the confinement sufficiently good. Table 14.6:2 summarises the results of calculation for four powders at low loading densities. In three of the four, $Z > x + \frac{y}{2}$ and in the fourth $Z = x + \frac{y}{2}$. The water-gas equilibrium was therefore used. Only one experimental velocity is available, but it agrees reasonably with the calculated value: the maximum may well be even closer.

Blackpowder ("gunpowder") is also best classed as a propellant, though its thermochemistry is very different from that of the modern nitroglycerine and nitrocotton powders mentioned above. There is as yet no certain evidence that blackpowder can detonate; however, it will probably do so, if a sufficiently large mass is initiated. An approximate picture of the wave which would then be established in a typical blasting blackpowder is given in Table 14.6:2. The products assumed were those experimentally measured, after cooling, by Noble and Abel. This is, of course, a very crude approximation, but it seems all that the case warrants. The surviving sulphur and KNO_3 are assumed to have absorbed no heat; the other condensed products share the temperature of the gaseous phase. No very reliable thermal data are available for K_2SO_4 and K_2S , and their specific heats were therefore identified with those of K_2CO_3 and KCl . The specific heats of H_2S had also to be extrapolated, and an approximate value used for the molar covolume of this gas.

Table 14.6:1

Weight % compositions of propellant explosives

Explosive	Nitro-glycerine	Nitro-cellulose	Potassium nitrate	Sulphur	Charcoal	Minor ingredients
1	99	0	0	0	0	1
2	99	0	0	0	0	1
3	40	60	0	0	0	0
4	45	52	0	0	0	3
5	0	0	74.7	10.1	14.0	1.2

Table 14.6:2
Results of calculation for propellant explosives [†]

Explosive	Gaseous products (mol./kg.)						Condensed products kg./kg.	n' mol./g. cal./g.	v' $\text{cm}^3/\text{g.}$	T'_K °K	H' ton/in ² .	D lb./s.	D (obs.) lb./s.	
	Δ g./cm ³	CO ₂	CO	H ₂ O	H ₂ S	N ₂	H ₂							
1	0.65	1.8	20.6	11.9	4.6	2.0		0.0409	845	1.132	3,470	182	1,065	4,020
2	0.77	2.4	19.4	12.0	4.7	1.2		.0397	931	.975	3,810	270	1,154	4,640
3	0.77	6.4	12.3	12.5	5.3	0.2		.0367	1,155	.958	4,450	276	1,200	4,580
4	0.193	5.7	13.8	11.4	5.4	2.2		.0385	1,084	3.20	4,080	38	1,050	2,750
5	0.90	5.99	1.89	0.53	0.40	4.20	0.35	.0139	715	.783	3,400	94	640	2,500

* 2½ inch diameter cartridge: private communication from Dr. J. Taylor.

[†] For composition see Table 14.6:1.



§ 15 Explosives whose products contain a condensed phase: introduction

So far, we have considered only explosives whose products form a homogeneous gaseous phase. Non-gaseous components may, however, appear in the products, either because certain species arising out of the reaction exist as solids or liquids at the pressures and temperatures concerned, or because the original explosive contains chemically inert ingredients which may form a condensed phase in the products. Explosives such as TNT whose marked oxygen deficiency leads to the presence of free carbon at the end of the steady zone, fall into the former class. Examples of the latter are found among commercial blasting explosives, in which non-reactive substances are frequently incorporated for various purposes, e.g. to modify the physical state of the mixture, to provide a vehicle for liquid components, to reduce sensitivity to shock, or to increase the margin of safety when the cartridge is fired in an explosive atmosphere. The possibility of such a condensed product phase raises various theoretical questions associated with the process of heat-transfer to it, its entrainment, compression and possible change of state.

The case where non-gaseous components arise out of the reaction appears relatively straightforward. We may, no doubt, assume thermal equilibrium with the gases, and complete entrainment by them. There remains only the problem of compression of the condensed phase.

When the non-gaseous product is present from the outset as an inert diluent, we must first decide to what extent it shares the velocity W , of the gases at the end of the steady zone. It can be seen that the answer to this question may depend to some extent on the grain size of the diluent, when this is granular, and also on its density.

The finer and the less dense the diluent is, the more probable complete entrainment will be. An exact treatment would involve analysis of the mechanics of a polyphase system in which chemical reaction is taking place and the mass-ratios of the various phases vary. Such analysis, particularly at the pressures and temperatures concerned, would be extremely difficult and is not attempted here. Instead, we shall assume in general that complete entrainment occurs: thus the streaming velocity is common to both diluent and reaction products and their relative proportions by weight in any representative element of volume are therefore the same at the CJ-plane as in the undetonated material. This assumption appears reasonable, particularly when (as is usually the case) the densities of the two phases are comparable. The success of our calculations for mixed explosives such as amatols, where the more slowly reacting component is assumed to remain "in step" with the other during reaction, is further warrant for extending the same principle to systems in which certain components remain permanently inert. Some more direct experimental evidence for this view is presented below (§§ 18.5, 18.6).

The degree of energy transfer by thermal conduction from the reacting gases to non-reactive diluent has next to be considered. Here, of course, it is a question, not of the ultimate heat transfer, but of the extent to which it proceeds within the steady zone. Once again, it is clear that the grit size of the diluent, when this is granular in form, will affect the answer to such questions, and indeed approximate calculations (§ 18.81) suggest that the degree of effective heat diffusion within a plausible reaction time may vary appreciably according to the proportion, grit size and thermal conductivity of the diluent. We have obtained certain experimental evidence for this view also (§§ 18.6, 18.7). In many practical

cases, indeed, the proportion of inert material does not exceed 30 per cent, the average radius of the inert particle is not less than 0.1 mm., and the estimated reaction time not greater than $10 \mu\text{sec.}$; in these circumstances, thermal transfer will be unimportant. This conclusion, for which again there is direct evidence (§ 18.5), does not at all contradict the possibility of reaction penetrating within the same period to the centre of a reactive particle of comparable size, since the surface of such a particle is constantly eroded as reaction proceeds. In the calculations described below, however, the consequences of assuming the diluent on the one hand to absorb no heat, and on the other to reach thermal equilibrium with the reaction products, have in most cases been worked out separately.

Finally, we have to consider the compression of the condensed phase, whether diluent or reaction product. This will affect the equations at two points, first directly, through the specific volume of the condensed phase, and also indirectly, in the estimation of the energy content of this phase. The quantity required is, of course, $(E - E^*)_{\text{cond.}}$ in the notation of § 9.5, and may be expressed generally by the integral

$$\int_{(*)}^{(1)} [C_v dT + (T \frac{\partial p}{\partial T} - p) dv]_{\text{cond.}} , \quad (1)$$

if the condensed material is regarded as a two-parameter fluid. In the relatively simple case of a diluent which absorbs no heat by diffusion, and for which shock relations have been determined, the most reliable method of evaluating (1) is to identify it with the energy change in a shock leading from p^* to p . This procedure should give a close approximation to the truth, and is used in § 18.8 below to illustrate the order of magnitude of (1). However, the results of such calculations show

that the energy in question is negligible for all normal cases. It is then sufficiently accurate to regard the compression as isothermal, and to assign a specific volume (φ) to the condensed phase on the basis of low-temperature (p, v)-data such as those of Bridgman. These approximations are a consequence of the low compressibility of solids; for liquid diluents they would be rather less precise. Even in such a case, however, it is only when the pressure and the proportion of inert material present are both high that the exact level of φ will be important.

When the non-gaseous phase is in thermal equilibrium with the gaseous, and especially when it is liquid, the closest approach would no doubt be to regard both phases as following similar equations of state. The distinction could still be drawn by ignoring the partial pressure of the liquid, and excluding its covolume; physically, the free volume of the liquid is then unavailable to the gases, so that the phases remain discrete. For simplicity, however, we have supposed that a condensed phase in thermal equilibrium with the product gases retains its standard density. §16.5 below shows that this is on the whole a reasonable assumption. The volume integral in (1) then vanishes, so that $E_i - E_i^*$ for the total products may be expressed as

$$E_i - E_i^* = \int_{(*)}^{(i)} C_v dT, \quad (2)$$

where C_v includes both phases. Since the entire integral (1) is negligible, for a diluent which absorbs no heat by diffusion, (2) applies in every case, if such diluents are simply regarded as having zero heat capacity.

§ 15.1 Formulation for explosives whose products include a condensed phase

Throughout this and subsequent sections we shall use accented symbols to denote "extensive" properties of the gaseous phase per unit mass of that phase. Thus, ν' is the specific volume of the gases, considered alone, and n' the number of moles of gas in 1 gm. of gas, whereas n , denotes, as hitherto, the number of gaseous moles per gm. of total products. In the same way, α' would denote the gaseous covolume per gm. gas, but since no confusion can arise in this case we shall omit the accent. The equation of state of the product gases is then

$$\frac{P}{T}(\nu' - \alpha) = n'RT, \quad (1)$$

Let 1 gm. of equilibrium products contain a mass m of gas, and a mass $1-m$ of condensed material, of specific volume ϕ , which may be either inert diluent or reaction product. Then

$$\nu = m\nu' + (1-m)\phi, \quad (2)$$

and (1) becomes

$$\frac{P}{T}(\nu - \beta) = nRT, \quad (3)$$

where

$$\beta \equiv m\alpha + (1-m)\phi. \quad (4)$$

The formal solution of § 13.5 then applies, provided only that α is replaced by β throughout. Attention must, however, be drawn to the following points:

- (a) In terms of the argument of § 15, we have disregarded the energy of compression of the condensed phase, thus permitting the equation $dE = c_v dT$ to be carried forward.

- (b) c_v is the heat capacity of 1 gm. of the total products. Components not heated are regarded as having zero heat capacity in forming c_v . n_i , however, as already stated, is the number of gaseous moles only in 1 gm. of products.
- (c) The adoption of equations 13.5(1,2), with α replaced by β , implies that the condensed phase follows the same behaviour in an elementary adiabatic change (such as is envisaged in the physical justification of the Chapman-Jouguet condition - §§ 9.1, 9.4) as it does in the reactive shock change represented by passage through the wave as a whole. In other words, if the condensed phase remains thermally insulated up to the CJ-plane, it continues to be so in any small compression or rarefaction at CJ; and vice versa,. We have referred to this question already in § 11.2.

From equations 13.5(1,2), the CJ-condition becomes

$$\frac{p_i - p_0}{v_0 - v_i} = \frac{k_i p_i}{v_i - \beta}, \quad (5)$$

where

$$k_i \equiv 1 + \frac{n_i R}{c_v} - \frac{d\beta}{dv_i}. \quad (6)$$

It is therefore necessary to evaluate $d\beta/dv_i$. From (2,4) we have

$$\frac{d\beta}{dv_i} = \frac{d\alpha}{dv'_i} + (1-m)\left(1 - \frac{d\alpha}{dv'_i}\right) \frac{d\varphi_i}{dv_i}. \quad (7)$$

In the event of thermal equilibrium, when φ_i has been assumed equal to φ^* , the value at standard temperature and pressure, (7) reduces at once to

$$\frac{d\beta}{dv_i} = \frac{d\alpha}{dv'_i}. \quad (8)$$

Otherwise, we make use of the CJ-condition itself to write

$$\frac{d\varphi_i}{dv_i} = - \frac{p_i}{v_o - v_i} \cdot \frac{d\varphi_i}{dp_i}, \quad (9)$$

and $d\varphi_i/dp_i$ is to be evaluated approximately from the isothermal compression data. Experience proves that the second term on the right of (7) is negligible in all normal cases, so that (8) may safely be used. Under extreme conditions when both p_i and $1-m$ are very high, as for example in a liquid or cast explosive, free from air and loaded with a large proportion of inert material, or when the compressibility of the diluent is very high, it may be necessary to apply (7) and (9), using a cyclical method. However, in such cases, the compressional energy would also become significant. [Cf. 39]

The method of solution is similar to that used for purely gaseous products. Thus, assuming values of T_i and p_i , we make a first estimate of the products, and decide whether non-gaseous components will arise, in addition to any which may survive as inert diluents. An approximate k_i is next obtained by assuming $v_i = 0.75 v_o$ and using (2, 6, 8) with $\varphi_i = \varphi_i^*$. T_i and p_i may then be recalculated. When approximate agreement is reached in this way, we can proceed to improve the estimates of v_i, β and k_i . This is performed as before by a cyclical process. φ_i is first estimated in terms of p_i . Starting then from an assumed v_i , we derive v'_i by (2), read off α and $d\alpha/dv'_i$ from Figure 13.3:1, deduce β from (4) and finally recalculate v_i by 13.5(3) (with β substituted for α). T_i and p_i are then checked, and lastly H_i and D evaluated.

In §15.2, we discuss explosives whose products contain condensed carbon. Commercial blasting explosives, in the products of most of which

a condensed phase occurs, are treated generally in § 16. A more specialised discussion of mixtures of explosive and inert material is given in § 18.

§ 15.11 Approximate representations of Bridgman's isotherms

[16]

Bridgman's isotherms for solid materials may be represented by equations of the type derived in § 6.52. An alternative form, which is [126] convenient for the present purpose is

$$\varphi = \varphi_0 \cdot \frac{P+B}{AP+B} \quad (1)$$

where A and B are constants for each material. φ_0 , A and B are listed in Table 15.11:1 for the room-temperature isotherm in solids commonly encountered as non-gaseous products.

Table 15.11:1

Substance	φ_0 (cm ³ /g.)	A	B (atm.)
NaCl	0.461	1.805	20.1×10^4
KCl	0.503	1.623*	3.47 "
Graphite	0.445	1.204	6.57 "
Sulphur	0.521	1.579	5.67 "
Lead	0.088	1.666	29.2 "

* For pressures greater than 20,000 atm. only.

§ 15.2 Markedly oxygen-negative single explosive compounds

In the present section, we discuss TNT ($C_7H_5O_6N_3$), tetryl ($C_7H_5O_8N_5$) and picric acid ($C_6H_3O_7N_3$) as examples of single explosive compounds $C_xH_yO_zN_w$ for which $\chi < x + y/2$. These explosives are sufficiently oxygen-negative and their carbon/hydrogen ratio is sufficiently high for free carbon to appear in the products. In determining the product compositions, we have regarded the carbon as condensed at the relatively low detonation temperatures to be expected from such explosives, and have therefore (§15) assumed its density to retain the standard value of 2.25 gm./cm^3 .

A series of preliminary calculations were first carried out, in which differences between the virial coefficients B_i for the various product gases were ignored. This simplification permits the use of equation 9.54(30), so that ideal equilibrium constants can be used, provided the pressure p is replaced by a mean fugacity \tilde{p} . 9.54(32) shows that \tilde{p} must always exceed p , and indeed, for large \tilde{p} , \tilde{p}/p reaches very high values, as can be verified from Table 13.6:1. Under these conditions, the equilibrium analysis of § 13.23 can be used, with ideal constants. The products depend only on temperature, and that to a slight extent, as can be seen from Table 13.23:1 or in more detail from Table 15.2:1. Q is effectively constant. These circumstances facilitate the calculations, which result in the values shown in Table 15.2:2.

The agreement is once again good though there is a tendency to exaggerate the velocity at the highest loading densities.

Table 15.2.1

Explosive	T	φ	Products (mol./Kg.)				Q cal./gm.
			CO_2	H_2O	CH_4	C	
TNT $C_7H_5O_6N_3$	3,000	0.669	10.6	5.2	2.95	17.5	6.6
	3,800	0.691	10.8	4.9	3.0	17.1	6.6
	3,900	0.696	10.8	4.9	3.1	17.0	6.6
	5,000	0.718	10.9	4.7	3.16	16.8	6.6
$Tetryl^1$ $C_7H_5O_8N_5$	3,000	0.598	11.67	4.55	2.08	10.63	8.71
	4,500	0.644	11.82	4.22	2.24	10.32	8.71
	4,600	0.646	11.84	4.21	2.25	10.31	8.71
	4,700	0.648	11.85	4.20	2.26	10.30	8.71
	4,800	0.650	11.85	4.18	2.27	10.28	8.71
	5,000	0.653	11.85	4.16	2.27	10.25	8.71
$Picric acid$ $C_6H_3O_7N_3$	3,000	0.306	13.34	3.88	1.34	11.52	6.55
	4,000	0.327	13.44	3.70	1.43	11.34	6.55
	4,200	0.330	13.46	3.67	1.44	11.31	6.55
	4,500	0.334	13.50	3.64	1.46	11.30	6.55
	5,000	0.341	13.50	3.57	1.49	11.22	6.55
	5,500	0.344	13.51	3.55	1.50	11.20	6.55

Table 5.2:2

Explosive	Δ	Products (mol./kg.)	n_i	α	3	$\frac{\partial \beta}{\partial n_i}$	k_i	$\frac{v_i}{cm^3/g.}$	T_i atm. x 10 ⁴	P_i atm. x 10 ⁴	W_i m./s.	D m./s.	D_{obs} m./s.
	R/cm^3	CO_2	H_2O	C	N_2								
TNT	1.50	10.8:4.9:3.1:17.0:6.6	0.254	1.296	0.498	0.487	0.558	0.574	0.552	5,890	12.4	1,196	6,970
$C_7H_5NO_2$	1.00	10.6:5.1:2.9:17.3:6.6	0.0252	1.296	0.625	0.588	0.552	0.798	0.769	3,873	4.42	1,010	4,400
$C_7H_5NO_3$	0.50	10.6:5.1:2.9:17.3:6.6	0.0252	1.296	0.766	0.699	0.17	1.05	1.354	5,873	1.24	894	2,770
Tetryl	1.50	11.9:4.2:2.3:10.2:8.7	0.027	1.396	0.489	0.483	0.576	0.57	0.550	4,790	16.0	1,375	7,850
$C_7H_5NO_5$	1.00	11.8:4.2:2.3:10.3:8.7	0.0270	1.396	0.610	0.590	0.562	0.785	0.770	4,600	5.69	1,150	5,000
$C_7H_5NO_5$	0.50	11.8:4.2:2.2:10.3:8.7	0.0269	1.396	0.758	0.719	0.30	1.017	1.366	4,500	1.56	1,000	3,140
Trinitro Acid	0.50	13.5:3.6:1.5:1.3:6.6	0.0252	1.280	0.478	0.474	0.551	0.593	0.545	4,400	12.7	1,245	6,900
$C_6H_3NO_3$	1.00	13.5:3.7:1.4:11.3:6.6	0.0252	1.280	0.595	0.575	0.342	0.802	0.764	270	4.57	1,055	4,475
$C_6H_3NO_3$	0.50	13.5:3.7:1.4:11.3:6.6	0.0252	1.280	0.730	0.692	0.122	1.022	1.350	4,200	1.33	930	3,130

In the above preliminary discussion of TNT, tetryl and picric acid, the various virial coefficients B_c were assumed identical. This is not strictly consistent with our general theory, and more detailed calculations, parallel for those for PETN (§ 14.3), will now be described, in which due allowance is made for the differences between these coefficients. This involves the use of § 13.6, as described in § 14.3, and proceeds from the solutions already obtained as starting-point. In determining the equilibrium composition at each stage, however, we discard the approximate analysis of § 13.23, which is reliable only at the highest pressures, and employ the general iterative method (§ 13.20), although useful guidance is obtained from § 13.24 at the higher loading densities. One slight simplification has been made, by taking $B_{CO_2} = 37 \text{ cm}^3/\text{mole}$ throughout (Cf. § 14.3).

The work will not be described in detail. It involved considerable labour, three or four complete cycles being necessary in most cases before close agreement was reached. For this reason, we have had to be content with calculations for TNT and tetryl at three loading densities, 0.5, 1.0 and 1.5 gm./cm.³. The final solutions are set out in Table 15.2:3. Comparison with Table 15.2:2 shows considerable change in the product compositions, which, moreover, now vary to a marked degree with cartridge density. Despite this fact, which merely emphasises the extreme uncertainty of equilibrium analysis for such a high negative oxygen balance, the important wave parameters, pressure, velocity and so forth, are relatively little changed. There is no doubt, however, that agreement with the experimental values of D has been materially improved, and must now be considered as very close. The only significant divergence is for TNT at the lowest density, where in any case an error by defect in the observed velocity, due to imperfect confinement, is most likely to occur.

Table 5.2.3
Final calculations for TNT and tetryl

Explosive	Δ	Product: (mol./kg.)	ω'	ω	x	χ^3	χ	k	k'	v_i	v_o	T_i	T_o	ν_i	ν_o	Int. x : 10 ⁴	Int. x : 10 ⁴	D	$D(\text{rhs})$
TNT	1.50	6.3: 3.0:21.6: - :10.9:0.1:6.6: 0.0263:	1.295	0.482	0.072	0.482	0.663	0.55	3.37	1.0	1.40	6.443	6.700	8	8				
$\text{C}_7\text{H}_5\text{NO}_3$	1.00	2.9:11.4:16.5:0.1: 9.3:1.6:6.6: 0.0313:	1.065	0.658	0.599	0.151	0.331	0.73	5.87	5.6	10	5.060	4.900	6	6				
Tetryl	0.50	0.6:23.1: 6.4:0.9: 2.2:7.2:5.6: 0.0405:	7.63	0.910	0.375	0.496	0.047	0.45	3.250	1.89	1.020	3.730	3.200	8	8				
Tetryl	1.50	8.2:2.8: 13.3: - : 3.7: - : 8.7: 0.0284:	1.390	0.480	0.475	0.523	0.64	0.550	4.750	4.8	3.20	7.550	7.300	8	8				
$\text{C}_7\text{H}_5\text{NO}_5$	0.10	3.7:12.7: 7.9: - : 7.7:0.9:8.7: 0.0384:	1.170	0.629	0.611	0.385	0.820	0.786	4.450	7.0	2.40	5.800	5.550	8	8				
	0.50	2.0:18.8: 3.5:0.1: 5.0:3.5:8.7: 0.0384:	0.020	0.830	0.814	0.170	1.067	1.428	1.140	2.3	1.110	3.870	3.850	8	8				

§15.21 HCN-formation in the products of TNT and of tetryl

In the calculations of § 15.2, we have ignored HCN-formation, though the products set out in Table 15.2:3 might be expected, at densities below 1.0 g./cm³, to yield an appreciable proportion of HCN. Reliable values of the equilibrium constants and virial coefficient are lacking, but we have obtained at least an estimate of the probable level of error involved in disregarding HCN for TNT at 0.5 g./cm³, by using the ideal constant (Table 9.54:1) and assuming a covolume

$$B_{HCN} = \frac{1}{2}(B_{H_2} + B_{N_2}) + \varphi_c^* = 28 \text{ cm}^3/\text{mol.}$$

The results of Table 15.2:3 are modified only to a minor degree.

Thus the products are: CO₂ 1.39, CO 19.5, C 7.93, CH₄ 0.56, HCN 1.48, H₂O 4.18, H₂ 4.95, N₂ 5.87; the temperature is about 3,100°K and the velocity about 3,600 m./s.

§15.3 Cyclotrimethylenetrinitramine ($\text{C}_3\text{H}_6\text{O}_6\text{N}_6$) ("CTMTN")

According to oxygen balance, this important [REDACTED] explosive falls into the class of PETN ($2x + \frac{y}{2} > z > x + \frac{y}{2}$), discussed in §14.3. Its oxygen deficiency is however, considerably greater than that of PETN or methyl nitrate, and calculations based on the method of §14.3 (in which the possibility of carbon formation is ignored) lead to theoretical detonation velocities greatly (some 25%) in excess of those observed. On the other hand, when provision is made for the appearance of free carbon, by applying the methods of §15.2, with the equilibrium analysis of §13.20, and the theory of real equilibria developed in §13.6, consistent solutions are obtained, and the velocities agree rather well with observation (Table 15.3:1).

This raises, of course, the question as to whether similar consistent solutions involving free carbon might arise with PETN also. We have therefore applied the same detailed procedure to PETN at 1.5 g/cm³. It appears, in fact, that such a solution does exist, and the results are included in Table 15.3:1. The amount of carbon released is, however, extremely small, and the detonation wave properties are almost identical with those deduced in §14.3. No revision is therefore necessary in the case of PETN.

Table 15.3:1 also includes the result of similar calculations for a cordite which falls into the same thermochemical category as CTMTN. The calculated velocity is confirmed by a measurement reported in the literature.¹⁶ When carbon formation is neglected, the velocity is 9500 m/s.

Table 15.3:1

Explosive:	Δ g/cm ³	Products (Mol/Kg)			n_i	Q_i cal/g	ν_i cm ³ /g	T_i K	P_i atm. [*]	W_i m/s	D m/s	D_{obs}
		CO ₂	CO	C	H ₂ O	H ₂	N ₂		10^4			
CTNTN	1.50	5.91	1.76	5.85	13.48	0.05	13.52	0.0347	1472	0.541	5190	17.4
$C_3H_6O_6N_6$	1.00	2.73	9.32	1.46	12.26	1.26	13.52	0.0391	1303	0.780	4940	8.73
Cordite*	0.50	2.81	10.71	-	10.71	2.81	13.52	0.0406	1260	1.413	4770	2.55
PETN	1.50	10.62	4.13	1.08	12.61	0.10	6.33	0.0338	1445	0.540	5320	17.8
$C_5H_8O_2N_4$												
Cordite*	1.62	10.73	1.53	7.32	13.66	-	5.34	0.0343	1357	0.502	4580	16.2

* Nitroglycerine 45%, nitrocotton 52%, stabiliser 3%.

(5)

§5.4 Liquid ethylene (C_2H_4)

Explosions during polymerisation of this material suggest that it may be capable of detonation. We suppose the ethylene to be initially at 1 atm. pressure, and just beneath its boiling point, $169^{\circ}K$. The density is then 0.566 g./gm.^3 . The RH-equation may be evaluated by aid of 9.51(1). Thus $E_o^* - E_o$ is the sum of the latent heat (L) at the boiling point and the energy integral $\int dE$ for ethylene vapour from 169 to $273^{\circ}K$ at 1 atm. Now the vapour has been found to follow the state-equations [98, 26, 175]

$$\frac{P}{T}[v - b(T)] = nRT, \quad (1)$$

$$C_p = 0.3442 - 1.110 \times 10^{-3} T + 5.539 \times 10^{-6} T^2 - \\ - 5.080 \times 10^{-9} T^3 + \frac{129.6}{T^2} + \frac{2.352 \times 10^6}{T^3} \text{ cal./g.}^{\circ}\text{K}, \quad (2)$$

where

$$b(T) = 121.6 - 7.50 \times 10^4/T - 2.26 \times 10^8/T^3 \text{ cm}^3/\text{g.} \quad (3)$$

From (1) and 9.51(10), we have, in a constant-pressure change,

$$dE = (C_p - nR - P \frac{db}{dT})dT, \quad (4)$$

so that

$$E_o^* - E_o = L + \int_{169}^{273} C_p dT - 104nR - 0.0242[b(273) - b(169)], \quad (5)$$

since 1 atm. = 0.0242 cal./cm^3 . With $L = 115.5 \text{ cal/g.}$, [55]

this yields

$$E_o^* - E_o = 136.3 \text{ cal./g.} \quad (6)$$

Again, $E_o^* - E_o^*$ is the difference in energy of formation of gaseous ethylene and of the detonation products from C and H_2 at

273°K. The energy of formation of ethylene vapour at 298.2°K is [100]

$$12.496 - 2 \times 0.2982 = 11.90 \text{ K.cal/mol}$$
$$= 425 \text{ cal/g}$$

and, deducting 11 cal/g to reduce to 273°K, we get

$$E_o^* - E_i^* = 414 - E_i^* \text{ cal./g.,} \quad (7)$$

where E_i^* represents the energy of formation of the products.

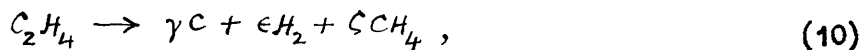
The usual state-equation 13.3(5) is adopted for the products, so that

$$E_i^* - E_i^* = \int_{273}^{T_1} (C_v)_i dT. \quad (8)$$

Hence, from (6, 7, 8) the RH-equation is

$$\frac{1}{2} p_1 (v_o - v_i) = \int_{273}^{T_1} (C_v)_i dT + E_i^* - 278 \text{ cal/g.} \quad (9)$$

Equilibria The possible products are C_2H_2 , CH_4 , CH , H_2 , H , C , of which C_2H_2 , CH and H can be eliminated by reference to the equilibrium constants. Thus,



where

$$\epsilon + 2\zeta = 2 \quad (11)$$

$$\zeta + \gamma = 2 \quad (12)$$

$$\frac{p_1 \epsilon^2}{\zeta(\epsilon + \zeta)} = J_3. \quad (13)$$

J_3 is the constant for the reaction $CH_4 \rightleftharpoons C + 2H_2$, as defined in § 13.2. The solution is

$$\frac{\epsilon}{2} = 1 - \zeta = \gamma - 1 = \sqrt{\frac{1}{1 + 4p_1/J_3}}. \quad (14)$$

$4\dot{p}_1/T_3$ is certainly $\gg 1$, so that a good approximation is

$$\epsilon = 0, \quad \varsigma = \gamma = 1,$$

whereupon $E_i^* = 570$ cal. The calculation is now completed in the normal way, giving $T_i = 1700^\circ K$, $\dot{p}_i = 17,160$ atm., $v_i = 1.11 \text{ cm}^3/\text{g}$. $W_i = 1060 \text{ m/s}$, $D = 2870 \text{ m/s}$.

If we had ignored methane formation, and assumed that $C_2H_4 \rightarrow 2C + 2H_2$, then $E_i^* = 0$, and the solution would be $T_i = 820^\circ K$, $\dot{p}_i = 14,250$ atm., $v_i = 1.41 \text{ cm}^3/\text{g}$. $W_i = 717 \text{ m/s}$, $D = 3540 \text{ m/s}$. The former solution is almost certainly much closer to the truth, but it is noteworthy that even complete neglect of CH_4 leaves \dot{p}_i and D of the same order as before.

§16 Calculations for commercial blasting explosives

The methods of §§ 14, 15 have been systematically applied to a large number of modern commercial blasting explosives. These are rarely, if ever, single compounds, but consist of mixtures, more or less intimate, of various materials. A typical composition will contain (a) an energy-and gas-producing complex, for example fuel + oxygen-carrier, which may or may not be capable of independent detonation, (b) a "sensitiser", that is a sensitive detonating explosive, whose function is to ensure propagation, (c) inert material, added for various direct or indirect reasons. According to the nature and proportions of these constituents, which depend on the purpose to be served, and may not all be present, the explosive falls into one or other of certain rather loosely defined classes. We have carried out calculations for representative members of all the most important classes. When the proportion of inert material present is at all large, and where the high level of cartridge diameter necessary to achieve full velocity suggests a relatively long reaction time, the possibility of thermal equilibrium between diluent and product gases has been allowed, and calculations made both on this basis and on that of zero heat transfer. Otherwise, inert diluents are supposed to absorb no heat by diffusion. Complete entrainment of the diluents is assumed, and their compressional energy neglected (see §§ 15, 18.8). Since the compositions are all close to oxygen balance, the equilibrium analysis may be carried out by the rules derived in § 14.3, and is therefore straightforward.

For convenience, the explosives studied may be grouped in three main categories:

- (a) Nitroglycerine-based powders and semi-gelatines
- (b) Nitroglycerine-based gelatines
- (c) TNT-based powders.

These are dealt with in turn in §§ 16.1, 16.2, 16.3, and the results discussed in § 16.4.

§ 16.1 Powders and semi-gelatines based on nitroglycerine

The compositions are set out in Table 16.1:1 and the results of calculation in Table 16.1:2.

§ 16.2 Gelatinous explosives based on nitroglycerine

The compositions are given in Table 16.2:1 and the results of calculation in Table 16.2:2.

§ 16.3 Powders based on TNT

The compositions are given in Table 16.3:1 and the results of calculation in Table 16.3:2.

Table 16.1:1

Weight - % compositions of nitroglycerine powders and semi-gelatines

	Explosive:Nitro-glycerine	Nitro-cotton:nitrate	Sodium Cellulose:Aluminium:Ammonium:Kieselguhr:Limestone:sulphate:chloride:etc.	China clay	Minor ingredients
1	7.85	0.11	61.64	15.8	12.2
2	9.0	59.0	4.0	26.0	2.4
3	10.0	55.5	10.0	12.0	2.0
4	10.0	80.0	10.0	10.0	0.5
5	10.5	71.25	8.0	9.0	1.25
6	10.5	61	9.15	18.75	0.6
7	11.5	48.4	4.45	35.4	
8	13.0	67.0	6.0	12.5	1.5
9	14.4	0.6	12.2	2.8	
10	15.0	0.35	62.9	5.75	0.8
11	15.0	0.25	78.45	5.5	0.8
12	15.0	0.5	73.8	6.0	0.7
13	15.0	0.25	76.45	4.0	0.5
14	15.9	0.1	7.0	12.0	0.25
15	15.9	0.1	30.0	14.0	0.3
16	17.0	0.5	44.0	5.25	0.5
17	18.0	0.4	65.5	7.4	1.2
18	29.0	0.7	57.3	5.0	
19	29.3	0.7	52.0	18.0	
20	38.6	1.5	40.1	18.7	1.1
21	58.5	1.5	18.0	21.0	1.0
22	75.0			25.0	

Table 16.1.2

Results of calculation for nitrocellulose powders and semi-relatines

(1) diluent (NaCl or Kieselguhr) unheated during the reaction;
 (2) diluent in thermal equilibrium with reaction products

Table 16.2:1

Weight - % compositions of nitro-glycerine gelatines

	Explosive:Nitro-glycerine	Nitro:cotton:nitrate	Ammonium:Sodium:Cellulose:nitrate:etc.	Aluminium:Sodium:chloride	Sulphur	Barium:sulphate:carbonate	Barium:clay	China:clay	Minor:ingredients
23	24.0	1.6	63.6	9.6					1.2
24	26.0	1.1	47.1	16.0	7.0		2.0		0.8
25	27.0	0.75	35.95		5.8	28.0			2.5
26	27.0	0.75	40.45		5.3	24.0			2.5
27	28.0	1.1	47.6	13.8	6.7		2.0		0.8
28	30.3	1.4			5.0			63.3	
29	31.0	1.0		52.3	14.7				1.0
30	32.0	1.0	38.9	18.0	9.4				0.7
31	40.0	2.8	48.6		2.8		5.0		0.8
32	50.0	2.0		32.4	10.0		5.0		0.6
33	50.0	2.3		41.5		5.5			0.7
34		57.5	1.5		27.0	13.4			0.6
35		58.1	3.2		30.8	7.6			0.3
36		69.1	4.0		20.6	5.7			0.6
37		91.2	8.2						0.6

Table 16.2.2

Results of calculation for nitroglycerine solutions.

(1) Diluent [MCl] unchanged during the reaction.

(2) MCl in thermal equilibrium with reaction products.

Explosive	Δ_{rxn}	Gaseous products (mol/Kg.)		n_f	Q_f	α	β	γ	T_f	p_f	D	
		Eq.	%									
		002	00	H ₂ O	O ₂	N ₂						
23	1.47	5.90	2.59	21.48	2.90	0.05	CaO, SiO ₂	{ Al ₂ O ₃	0.012: 0.197: 1056: 0.459: 0.485: 0.705: 0.582: 0.545	3770	54.9	13.0 6660
24	1.45	6.55										2400
25 (1)	1.55	5.9										
(2)		1.4+2	0.3	6.4+								
26 (1)	1.55	5.8		18.9	0.5	7.0						
(2)		1.4+2	0.3	18.1								
27	1.45	6.56		17.24	1.57	8.5						
28	2.48	5.1	2.1	3.5	2.1							
29	1.55	6.9		8.0	2.4	5.3						
30	1.50	7.1		16.2	2.1	8.2						
31	1.51	7.51		18.35	1.19	9.00						
32	1.55	9.15		9.68	0.65	5.32						
33	1.50	9.3		16.4	0.4	8.6						
34	1.47	10.9	0.6	11.5								
35	1.55	9.6		9.5	2.5	5.8						
36	1.47	11.0		10.2	0.8	6.0						
37	1.45	13.6	0.4	11.7								

* These explosives were specially designed to give a high velocity in small diameter.

Table 16.3:1

Weight - % compositions of TNT - powders

Explosive	TNT	Ammonium nitrate	Cellulose	Aluminium	Sodium chloride	Dinitro-naphthalene	Minor ingredients
38	5	86				9	
39	12	68			20		
40	12	70	3		15		
41	12	79		9			
42	15	76		9			
43	15	79.8		5			0.2
44	18	81.8					0.2
45	21.3	78.7					

Table 16.3:2
Results of calculation for TNT powders

(1) diluent (NaCl) unheated during the reaction;
(2) diluent in thermal equilibrium with reaction products;
(3) Al inert and absorbing no heat

Explosive: g/cm ³	Δ mol/Kg.	Gaseous products (mol/Kg.)		Condensed products Kg./Kg.	n_i	α	β	φ_i	v_i	T_f	ρ_f	η_f	D (obs.)	D (routine)									
		CO ₂	CO																				
38	1.10	5.7	23.3	0.3	11.5																		
39 (1)	1.10	3.7	18.3	1.4	9.3	NaCl	0.200	0.0327	635	533	507	296	907	406	940	4060	2400	4300					
(2)									532	517	296	882	461	702	2280	221	840	3660					
40 (1)	0.95	4.9	19.9	0.2	9.5	NaCl	1.50	0.0345	772	548	525	242	951	413	782	3200	233	983	2400				
(2)									547	535	246	933	461	785	2600	189	895	3560					
41	1.20	3.1	0.6	21.0		10.7	:Al ₂ O ₃		169	0.0354	1323	516	471	328	832	250	636	4070	476	1200	5050	3500	4950
42	1.12	2.4	2.2	20.4		10.5	0.2:Al ₂ O ₃		174	0.0357	1298	543	493	307	856	250	678	4030	424	1180	4900	4000	4900
(3)	1.10	5.1	22.7	1.4	11.5	:Al	0.09	0.0407	890	553	532	360	837	323	703	3230	415	1140	5050				
43	1.15	4.6	0.2	21.7		11.0	:Al ₂ O ₃		0.92	0.0375	1191	513	488	331	842	250	663	3860	451	1200	5020	3500	
44	1.15	5.6	22.6	0.8	11.4				0.0404	953	501	501	362	832	-	669	3390	445	1172	5060	3500	5250	
	1.10								510	343	852	-	654	3360	403	1154	4870						
45	0.95	6.6	22.0		11.2				0.0398	1040	537	537	283	907	-	783	3620	321	1150	4500	4500		

§ 16.4 Discussion of the results for commercial blasting explosives

When the above calculations were made, the only available experimental wave velocities were those obtained in routine proof, which is carried out on paper-cased cartridges of small diameter, typically $1\frac{1}{4}$ inch, initiated by an ordinary detonator. Typical values of the velocities in question are entered for comparison in the second-last column of Tables 16.1:2, 16.2:2, 16.3:2. It can be seen at once that the calculated velocity, even on the assumption of thermal equilibrium between product gases and any inert material which may be present, is in almost every case much higher than that normally attributed to the explosive in question.

The only ready explanation of these wide discrepancies, apart from gross error in the theoretical treatment, was to be found in the effect [46, 95, 150, 82] of cartridge diameter upon velocity of detonation. It was known that the velocity of most condensed explosives tended to increase with the cartridge diameter, and an explanation of this effect had been proposed by Schmidt. According to Schmidt's explanation, which has since been formulated [82] quantitatively by Jones, failure to attain full velocity in cartridges of small calibre is due to lateral expansion of the detonation products, which involves a reduction in the Chapman-Jouguet pressure. Confinement of the cartridge, for example in a heavy metal tube, by restricting the freedom of expansion must cause the wave velocity to approximate more closely to its limiting or theoretical value, characteristic of a plane wave. Increase in the cartridge diameter will evidently have a similar effect. If this explanation of the discrepancies noted in Tables 16.1:2, 16.2:2 and 16.3:2 is correct, the theoretical values of D should be approached when the cartridge diameter is made sufficiently large. Experiments designed to

test this conclusion have been made, by measuring the velocity of detonation of a large number of the explosives studied, in unusually large cartridges, up to $8\frac{1}{2}$ inch diameter and of proportionate length. These experiments are described below (§§ 17.1 - 17.3); here it may be stated that they not only confirm the predicted diameter effect but show very satisfactory agreement between the limiting velocities, attained in cartridges of large diameter, and the theoretical values calculated as above. This can be judged from Tables 16.1:2, 16.2:2 and 16.3:2, where the maximum experimental velocities are collected in the final column. (Nos. 1, 12, 16, 26, 28, 31, 32, 33, 41 are taken from subsequent measurements by the writer's colleagues).

Very little detailed comment on the individual results appears necessary. Where inert material is present in moderate proportions, and is of normal grist size, and where the reaction time may be expected to be relatively short (for example, in Nos. 5, 25, 39), experiment seems to favour the assumption of negligible heat transfer. Otherwise the assumption of thermal equilibrium may be closer to the truth: notable examples are Nos. 2, 14. In each of these cases, the low cartridge density may be supposed to prolong the reaction time of the nitrate/cellulose complex, while in No. 14 the high proportion of NaCl and the use of sodium, rather than ammonium, nitrate must improve the prospects of heat transfer. All these features are in accordance with the theoretical expectations of § 15. The only outstanding discrepancy is in No. 1. This explosive is distinguished from all the others for which we have made calculations by the fact that even in cartridges of very large diameter its velocity fell far short of the theoretical maximum. The same explosive, however, was also distinguished by the unusually coarse grist of the solid reactants, which were selected with the express purpose

of limiting the velocity of detonation. We are therefore entitled to regard the results in this instance as standing rather in confirmation than otherwise of the theory. Indeed, if the nitroglycerine alone is assumed to react, and the remaining constituents behave as inert diluents absorbing no heat, the theoretical velocity is approximately 2,000 m./s., which is rather close to the observed value.

§ 16.5 Specific volume of condensed phase in thermal equilibrium with the product gases

As explained in § 15, it has been assumed that a solid or liquid product phase in thermal equilibrium with the gaseous phase retained its normal density appropriate to 1 atm. with 273°K . In other words, the effects of compression and thermal expansion were assumed to cancel. The work on equations of state for condensed material, described in §§ 6.5 - 6.58 enables us to test how far this simplification is permissible. Thus, for sodium chloride, the following equation applicable at high pressures, has been derived

$$\frac{p}{\varphi} = 312.6 \varphi^{-1.653} - 529.0 \varphi^{-1} + 0.07946 T \quad (1)$$

in units of ton/in.²., cm³/g. and $^{\circ}\text{K}$. According to (1), φ remains constant at 0.461 cm³/g. for values of p and T satisfying the linear relation

$$\frac{p}{\varphi} = 0.172 T - 46 \quad (2)$$

It will be found that the points (T , $\frac{p}{\varphi}$) corresponding to the already calculated detonation temperatures and pressures for commercial blasting explosives and oxygen-negative compositions lie almost evenly disposed about the line (2), although there is a considerable spread. If, then, (2) is taken to apply to all condensed products, the assumption of § 15 is on the average not unreasonable. Of course, this argument is

qualitative only, since (1) applies in the first place only to NaCl and is not explicitly designed for high temperatures. Nevertheless, support is given to the procedure followed in our calculations. If appropriate equations of state were available for the actual condensed products in any given case, a more precise treatment would be possible. However, the correction thus introduced would, as we have seen, be on the average small, and more detailed consideration of it appears out of place at the moment.

§ 17 Experimental determination of maximum detonation velocities for commercial explosives: introduction

Reference has already been made in § 6.4 to the experimental fact that velocity of detonation increases with cartridge diameter when other circumstances are constant; and an explanation in general terms was mentioned, according to which at sufficiently large diameters the velocity should approach an upper limit, with which theoretical estimates based on a one-dimensional analysis may be legitimately compared.

It is beyond the scope of this thesis to attempt any quantitative treatment of the imperfectly confined cartridge. However, the two contributions in this direction which have recently been published [82, 57] proceed from entirely different, not to say contradictory, premises, and it does not appear that either can be regarded as complete. A brief qualitative review of the factors involved is, therefore, desirable, before we proceed to describe experimental measurement of the limiting velocities for representative blasting explosives.

The fundamental theory discussed in §§ 9-9.4 refers to an explosive under perfect lateral confinement. It can be seen, however, that the conditions of the theory are satisfied provided no significant lateral expansion occurs within the reaction zone. For the propagation of the wave is controlled entirely by conditions in the layer where the Chapman-Jouguet condition applies. Between shock-front and CJ-layer, $W + a > D$, so that energy can be propagated forward or backward to maintain or reduce the wave. This region accordingly becomes steady. At the CJ-layer, however, $W + a = D$, so that conditions further to the rear can have no effect upon the propagation of the steady zone. It is clear, therefore, that lateral expansion behind the CJ-layer

cannot affect the propagation; on the other hand, if expansion were to occur within the reaction zone, this must reduce the CJ-pressure and so lead to a decrease in the wave-velocity.

Such expansion will also entail a convexity of the wave-front towards the undetonated explosive. Close to the cartridge axis, however, the wave will still be approximately plane, and the reduced velocity of the wave as a whole will equal the velocity of propagation in this axial core when a steady state is again established. This velocity depends on the degree of expansion of the core within the reaction zone, which in turn will depend on (1) the diameter (d) of the cartridge, (2) the nature of the confining envelope, if any and (3) the length of time (τ) required for reaction in any element of explosive to reach effective completion.

Considering, first, bare cartridges of a given explosive at fixed loading density but variable cartridge diameter, we conclude that the full velocity will be realised only in large diameters. As the diameter is reduced, the steady velocity will decrease, at first slowly, afterwards more and more rapidly, until it reaches a level so low that propagation from layer to layer becomes impossible. We are thus led to expect a diameter (d_1) below which detonation cannot persist, and a second, larger and less precisely defined, diameter (d_2) at which maximum steady velocity has been for practical purposes attained. Experiment amply confirms these predictions.

Again, the effect of encasing a cartridge of any chosen diameter between d_1 and d_2 must in general be to increase its velocity towards the maximum; d_1 and d_2 will also be reduced. The graph of velocity against diameter should thus move as a whole (though not necessarily

103

without change of shape) towards the velocity axis. When the case is sufficiently thin for lateral shocks to penetrate it in a time short compared with the reaction time τ , its effect will be predominantly inertial, and should thus depend rather on the density of the [82] case material than on its compressibility: for example, 1 mm. of lead should as a rule prove more effective confinement than the same thickness of steel. The velocity will also increase with the case thickness. However, when this becomes so great that the lateral shock requires a time comparable with τ to penetrate it, the [82] compressibility must play an important role. Under such circumstances, steel will probably be more effective than lead. When the penetration time exceeds τ , the case is equivalent to an infinite block, and further increase in its thickness will have no effect. In consequence of the compressibility of the case, however, full velocity is not yet altogether attained. We, therefore, conclude that the mere addition of metal to a small-diameter cartridge cannot raise the velocity beyond a definite level, which may fall distinctly short of the maximum value realised in large-diameter bare cartridges. Experimental [83] confirmation of these predictions is also available.

Finally, circumstances of diameter and confinement being equal, the maximum velocity will be more nearly approached, the shorter the reaction time τ . This assists us to understand (a) why d_c is small for pure explosive compounds (of the order of 1 cm. or less for nitroglycerine, and 1 inch for cast TNT) whose reaction time must be relatively short, and much larger (in some cases as high as 8-12 inches) for many commercial blasting explosives which consist of mixtures of

oxidants and fuels in coarse grist sizes, and must require a relatively long time to react; (b) why the interval (d_1 , d_2) and the corresponding range of stable velocities are also much greater in the latter case than in the former; and (c) why all granular explosives, but particularly mixtures, show an increase in velocity at any chosen diameter, and a decrease in both d_1 and d_2 , as the grist size of the reactive components is reduced.

A rigorous quantitative treatment of stable detonation in imperfectly confined cartridges would involve the search for steady solutions of the hydrodynamic equations applied in conjunction with suitable equations of state to the reacting material and to the case, together with the reaction-kinetic equations and the second law of thermodynamics. The one-dimensional approach would require to become three-dimensional. Such a treatment would be exceptionally complex, even if all the necessary information were to hand. Attempts to tackle the problem, therefore, depend on simplifications of one kind or another. The theory advanced by Jones, for example, depends upon a number of assumptions, the principal effect of which is to restrict application to cases where the axial expansion is small within the reaction zone, and the velocity, therefore, approaches its maximum value. A more fundamental objection to Jones' theory, however, is that the CJ-plane is assumed to coincide with the end of the reaction zone. When there is no lateral expansion, Döring's analysis (§ 9.4) shows that this is certainly true. However, as was mentioned in § 9.4, it need not remain true under conditions of imperfect confinement.

The CJ-layer cannot, of course, in any circumstances, fall outwith the reaction zone; but it may well fall within it if lateral expansion prevents the formation of secondary shocks in the non-steady part of the reaction. The effect of imperfect confinement is then to divide the course of reaction into two parts, only the first of which is effective in supporting the wave. We may say that, so far as the wave is concerned, reaction is arrested at an intermediate stage, corresponding to only partial release of the total chemical energy. Of course, it is not necessarily implied that reaction fails in the end to complete itself, but merely that it does not do so within the steady zone. Whether the reaction continues behind the steady zone or whether it rapidly fades out, leaving unconsumed explosive, is irrelevant to the propagation of the wave, though it may be of great importance in determining other aspects of performance (See §18.9 below). There is, however, experimental evidence to show that unconsumed explosive does in fact frequently survive detonation in poorly confined charges.

[161,80]

The above argument is stated in its simplest terms, and it must not be taken to mean that the first part of the reaction follows exactly the same course, irrespective of the stage at which it is "interrupted". The effective energy release determines the temperature and pressure at the shock-front, and so the initial reaction speed, on which in turn the rates of subsequent reaction (and expansion) depend. We must suppose that a balance is reached between these various interdependent processes, when, in any given set of circumstances, a steady wave is formed. The principal purpose of this discussion, however, is to stress that the

velocity of a poorly confined cartridge will fall below its maximum value not merely because of the direct mechanical effect of the expansion, as considered in Jones' theory, but also because a smaller proportion of the chemical energy is now available to support the wave.

§ 17.01 The Dautriche method of measuring velocity of detonation

In the normal Dautriche method of measuring detonation velocity,^[45] the cartridge is fired from one end, and the mean velocity measured over a short length at any chosen "run-up" distance from the initiator. This is done by inserting into the cartridge, at the beginning and end of the short length, the two extremities of a length of standard detonating fuse, whose velocity is known. The waves initiated in turn at either end of the fuse, and travelling along it in opposite directions, meet at a point whose position, determined by the sharp cut produced on a lead plate placed under the fuse, allows the required mean velocity to be calculated.

Thus, in Fig. 17.01:1, let AB be the cartridge and EFG the fuse, whose length is $2L$ and whose mid-point is F; and let the wave-meet lie at a distance x from F when EG has length d . Then, if C is the velocity of the fuse and D the mean cartridge velocity over EG,

$$\frac{L+x}{C} = \frac{d}{D} + \frac{L-x}{C}, \quad (1)$$

so that

$$D = dc/2x. \quad (2)$$

This method depends, among other things, on the assumption that

* See p. 442.

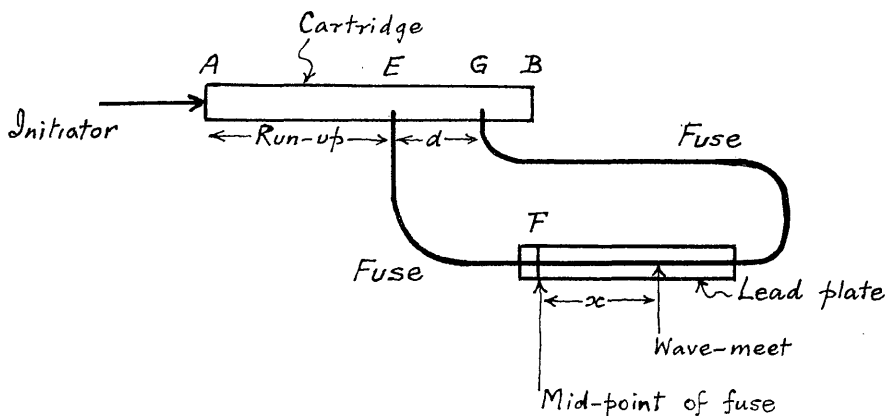


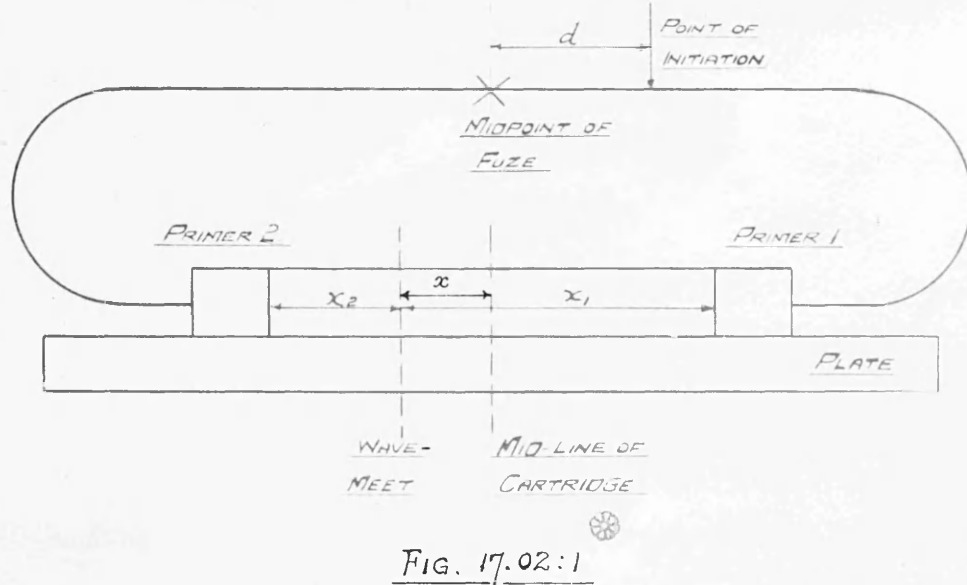
FIG. 17.01:1. DAUTRICHE METHOD
of measuring velocity of detonation.

the conditions of initiation at E and G are identical, so that any time-lag introduced at one of these points is cancelled by an equal lag at the other. While this may be taken for granted when the detonation velocity is steady, it is unlikely to be true when the velocity is either increasing or decreasing over EG. In the former case, D will tend to be overestimated and in the latter underestimated. It is also assumed that detonation proceeds with the constant standard velocity along the two arms of the fuse. Experience shows, however, [31] that the fuse may detonate unsymmetrically (because of the proximity of the detonating cartridge) unless its geometrical disposition is carefully controlled.

§17.02 Modifications of the Dautriche method

(1) Inverse Dautriche method

The difficulties mentioned above should not arise with the method of Fig. 17.02:1. Here, the cartridge is initiated at both ends, but at instants separated by a known time interval: this is done by means



of a length of detonating fuse of known velocity, connected to the two initiators and fired at a chosen distance from its centre. The wave-meet in the cartridge is recorded by a metal plate placed underneath.

It is clear that the cartridge should not react upon the fuse. That pick-up lags should also be eliminated depends on the fact that the detonation wave is headed by a shock. When two such waves of different, but not too dissimilar, intensities meet, it seems reasonable to assume that a metal plate will record the position of the point of collision of the shock-fronts.

If the fuse is initiated at a distance d from its centre, and if the wave-meet lies at x from the cartridge mid-point, it can easily be shown that the mean velocity D over a length $2x$ at the centre

of the cartridge is

$$D = xC/d. \quad (1)$$

The measured distance x is therefore proportional directly to the unknown velocity D , whereas in the normal method it is inversely proportional (equation 17.01(2)). If, therefore, the fuse is initiated at such a distance from its centre that the limit of the recording plate corresponds to the highest velocity to be expected, the wave-meet must necessarily fall on the plate. The method is thus complementary to the normal method, and is particularly suited to the measurement of low velocities.

The method was tested by using it to time six of a batch of twelve cartridges, the remainder being timed by the normal method. The results, which need not be detailed here, were completely satisfactory.

(2) Semi-continuous Dautriche method

In studying the effect of diameter and initiation upon the detonation velocity, under circumstances where this may alter along the cartridge length, it is desirable to have either a continuous record or at least a record sufficiently close to continuous for all major variations in velocity to be detected. For small cartridges, the high-speed camera provides an ideal solution; but for large charges the camera cannot be used without damage. Purely geometrical difficulties of arranging the fuse and metal plates prevent more than a few records being taken by the normal Dautriche method from any single cartridge.

The arrangement of Fig. 17.02:2 was devised to overcome these difficulties. It represents only one, though perhaps the most convenient, of several variants of the same idea. BE is the cartridge under

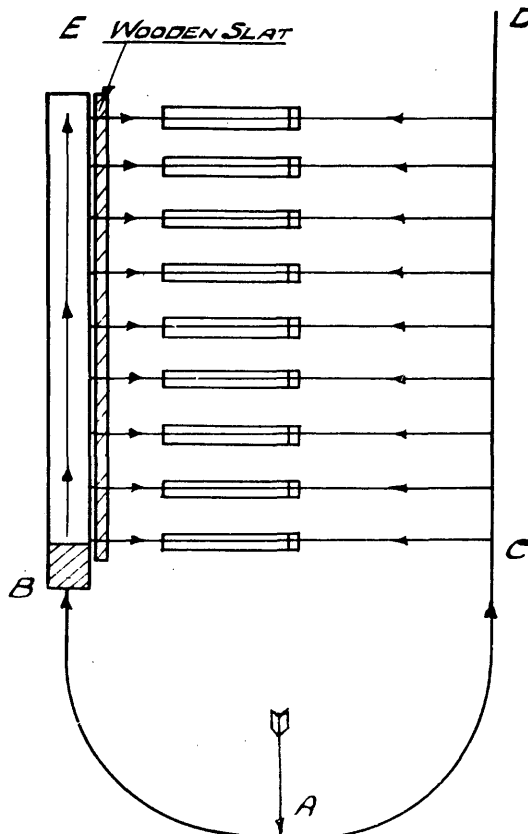


FIG 17.02:2

study: its initiator at B is connected to one end of the detonating fuse strand BACD. Cross strands all of length $2L$, marked at their mid-points and taped to lead plates, pass from chosen points on the cartridge to chosen points on the fuse. The minimum separation of the points of attachment on BE is determined by the distance over which lateral propagation can succeed between the fuse strands; this rarely exceeds half an inch in air. The lead plates may stand on edge if necessary. In selecting the corresponding intervals on CD, we take into account the highest and lowest velocities expected along BE.

BACD is initiated near the mid-point A of BC, though there is no

need for precision in fixing A . Let us suppose that the cut on the n^{th} plate is at a distance x_n from the point originally covered by the mid-point of the n^{th} cross-strand, x_n being positive if measured towards the cartridge. Let t_n be the time, from some arbitrary zero, for the wave in BE to reach the end of the n^{th} strand, and a_n the distance along CD between some arbitrary zero, for example A, and the other end of the same strand. Then, evidently,

$$A_1 + t_n + \frac{L - x_n}{C} = A_2 + \frac{a_n + L - x_n}{C}, \quad (2)$$

where A_1 and A_2 represent time-lags, supposed independent of n .

Consequently,

$$D_n = \frac{d_n}{t_n - t_{n-1}} = \frac{d_n c}{2(x_n - x_{n-1}) + (a_n - a_{n-1})}, \quad (3)$$

where D_n is the mean velocity over the length d_n between the ends of the $(n - 1)^{\text{th}}$ and n^{th} strands.

A test of the method was made with three 15 inch-long cartridges of a coal-mining explosive. One was timed by the present method, over $1\frac{1}{2}$ inch intervals, the other two by a high-speed camera, which provides a continuous record. In one of these last two, conditions in the Dautriche test were simulated by inserting a series of detonators at $1\frac{1}{2}$ -inch intervals down the side of the cartridge. The results were:

Camera; no detonators inserted: mean of 10 velocity measurements over $1\frac{1}{2}$ -inch intervals 1847 m./s. (Standard deviation 86 m./s.)

Camera; detonators inserted: mean of 10 as before 1850 m./s. (S.D. 135 m./s.).

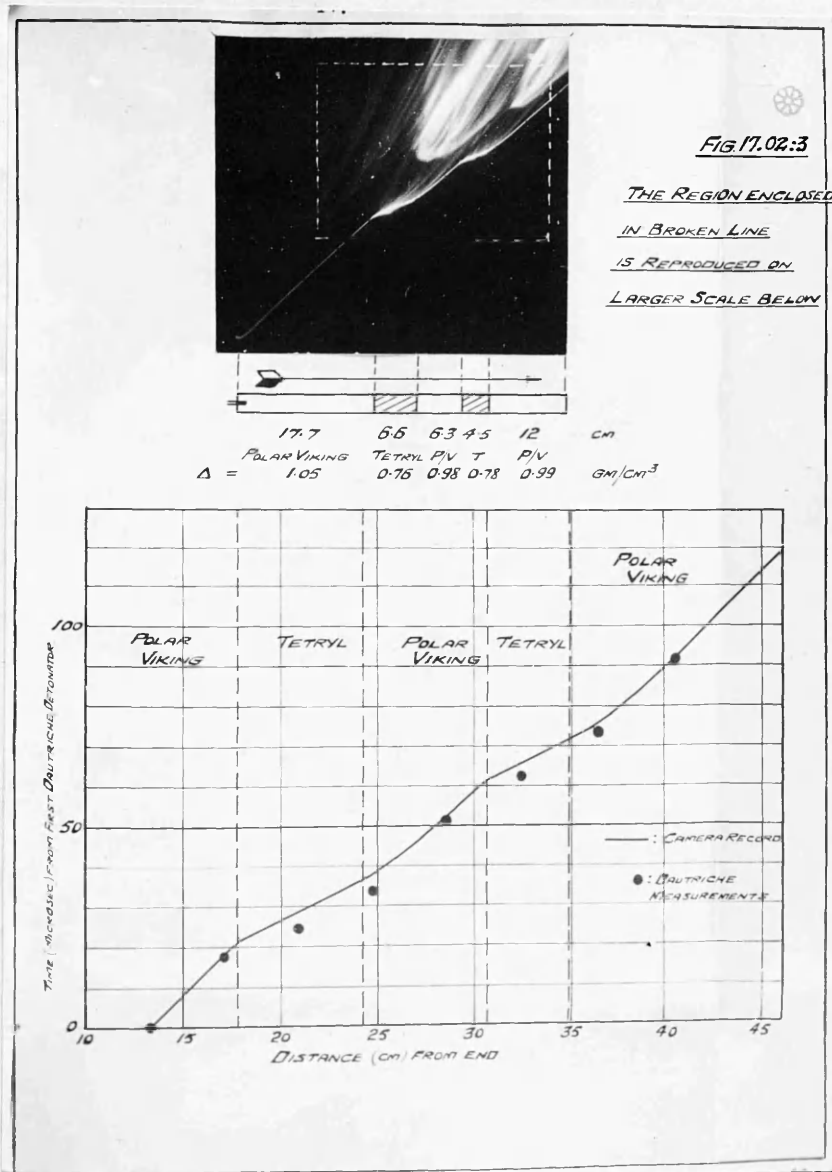
Dautriche: mean of 10 as before 1850 m./s. (S.D. 191 m./s.).

The method is evidently satisfactory. It will be noted also that

the presence of 10 fulminate detonators had no effect at all upon the velocity.

A further, and rather interesting, test was made on a "zebra" charge consisting of alternate layers of tetryl and the explosive ("Polar Viking") used above. This cartridge was timed by both camera and Dautriche method simultaneously. Details and results are shown in Fig. 17.02:3. It will be seen that the Dautriche method provides a very useful picture of the progress of the wave. The small discrepancies that remain are significant. So long as the $(n-1)^{\text{th}}$ and n^{th} cross-strands meet the cartridge at points where the velocities are equal, the Dautriche record is faithful. When the velocity at the end of the n^{th} strand exceeds the other, the time-interval is underestimated: this happens at each passage from Polar Viking to tetryl. Conversely, on passage from tetryl to Polar Viking, with drop in velocity, the interval is overestimated to the same extent. The divergence of the two records is abrupt in the former case, where in fact the velocity change is also abrupt; in the latter case the velocity changes more slowly and the divergence is also cancelled more slowly. These features are explained if we suppose the transfer of detonation from cartridge to fuse to involve a time-lag, which increases as the cartridge velocity falls. If this explanation is correct, the time-lags in question differ by about 4 microseconds in the present case.

Application of the method to study of Blasting Gelatine in large diameters is referred to below (§17.21).



§ 17.1 Experimental determination of the maximum detonation velocity in powders and semi-gelatines based on nitroglycerine:

(a) Explosive 5 (Table 16.1:1) (28 shots fired)

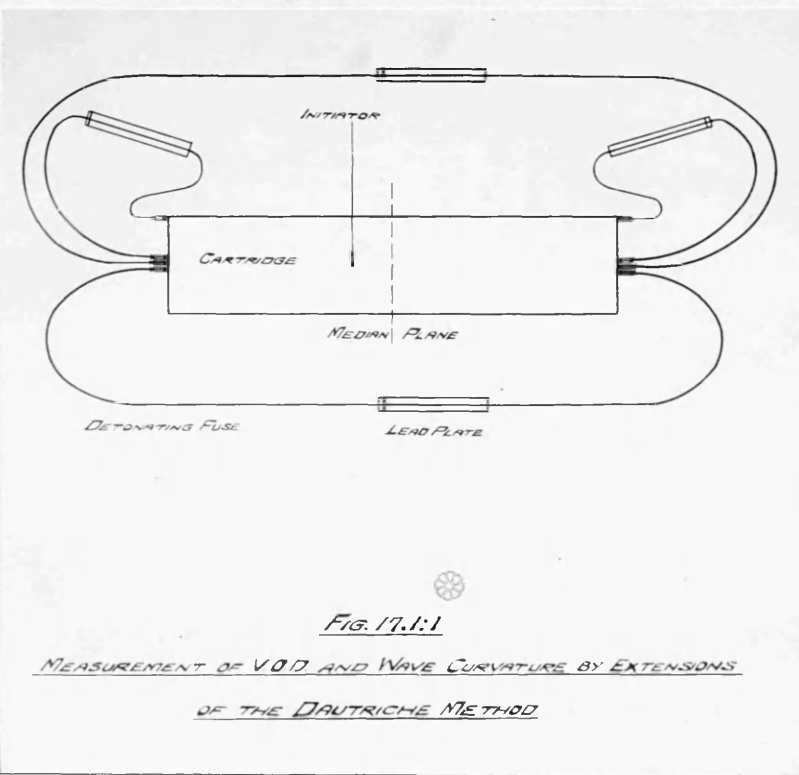
Routine proof of this coal-mining explosive is carried out on $1\frac{1}{4}$ inch diameter cartridges confined only in paper shells, and the velocity then lies between 1,900 and 2,200 m./s. as compared with theoretical values of 3,700 - 4,000 m./s. (Table 16.1:2).

In order to make an immediate test of the suggestion that velocities of the order of those calculated should be realised in large-diameter charges, the explosive was loaded in weighed increments at a density of 0.98 g./cm^3 into four cardboard tubes, each 5 inch diameter by $10\frac{1}{2}$ inch long. These were laid on hard earth and butted end to end. The composite cartridge was initiated by a fulminate detonator inserted axially at one end, and the wave velocity measured by the Dautriche method (see § 17.01), both on the surface and at the axis, at a "run-up" distance of 90 cm. from the detonator. The values recorded, 3750 and 3780 m./s., agree closely and are of precisely the theoretical order.

A shorter cartridge of the same diameter (run-up 28 cm.) gave 3670 m./s.

In confirmation, a further 5-inch diameter shot was fired, made up from six cardboard-cased charges of the sort described. A more certain estimate of the axial velocity was secured by using a modified [66] Dautriche arrangement (Fig. 17.1:1) in which the pick-up detonators were butted against the centres of the cartridge ends, and the charge fired on the axis at a point 7.5 cm. from its centre, and thus 72.0 and 87.0 cm. respectively from the two ends. This arrangement provides a measure

of the mean velocity over the 15 cm. interval from 72 to 87 cm: the result was 3,900 m./s. The curvature of the wave at the two extremities of the cartridge was also measured by attaching auxiliary Dautriche assemblies in the manner shown in Fig. 17.1:1.



At 72 cm. the axis led the periphery by 3.7 microsec., and at 87 cm. by 3.1 microsec; these times correspond to distances, parallel to the axis, of 1.44 and 1.21 cm. On the other hand, a spherical wave [173, 116, 73] spreading from the detonator would have an axial lead of only 0.25 to 0.3 cm., so that the above values must represent a permanent curvature of the wave, due to lateral expansion.

To complete the study, cartridges of $\frac{3}{4}$, 2, 3, 4 and $8\frac{1}{2}$ inch diameter and proportionate length were fired. The mean velocities, together with those already mentioned, are collected in Fig. 17.1:2.

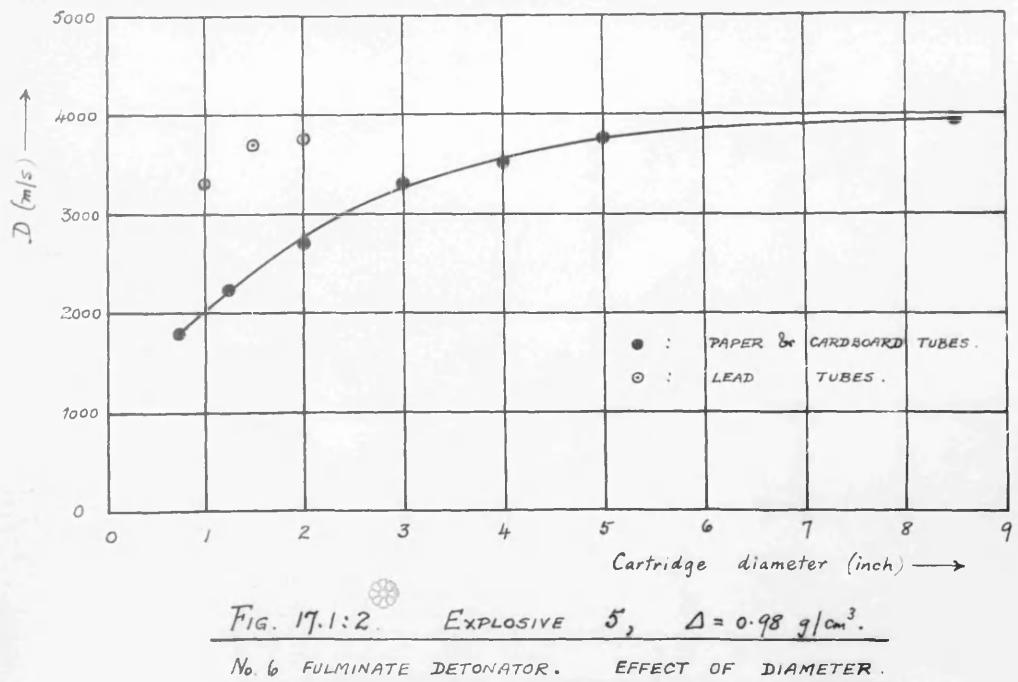


FIG. 17.1:2. EXPLOSIVE 5, $\Delta = 0.98 \text{ g/cm}^3$.

No. 6 FULMINATE DETONATOR. EFFECT OF DIAMETER.

These experiments entitle us to conclude that the velocity of Explosive 5 approaches a value of about 4,000 m./s. in large cartridges. The limiting velocity is thus in good agreement with the theoretical value.

In confirmation of the above work on lightly cased charges, and of

the general theory of confinement, a series of cartridges were prepared by loading the powder directly into lead tubes, 18 inch long and $1, \frac{1}{2}$, 2 inch internal diameter, with $\frac{1}{4}$ -inch thick wall. The Dautriche detonators passed through corks in the tube wall. The mean velocities were 3,300, 3,700 and 3,750 m./s. respectively, from which it again appears that in sufficiently well-confined charges D approaches the theoretical value.

(b) Explosive 6 (Table 16.1:1) (21 shots)

This composition is not greatly different from the last, and it was considered sufficient to measure the velocity in $8\frac{1}{2}$ -inch diameter cardboard tubes and $1\frac{1}{2}$ -inch lead and steel tubes. The large cartridges were erected vertically and fired from the top, four Dautriche assemblies being attached symmetrically round the base. The mean of 16 such results was 3,800 m./s., in close agreement with theory; the lead-cased charges gave a mean of 3,490 (12 shots) and the steel-cased 3,510 (5 shots).

(c) Explosive 3 (Table 16.1:1) (2 shots)

The velocity in $1\frac{1}{4}$ -inch paper shells is usually 1,800 - 1,950 m./s. at the standard ensity of 0.65 g./cm.³. In $8\frac{1}{2}$ -inch diameter cardboard tubes, after a run-up of 87 cm. the velocity was found to be 2,840 m./s. which agrees with theory.

(d) Explosive 14 (Table 16.1:1) (5 shots)

Measurements were made on $1\frac{1}{4}$, 2, $3\frac{1}{2}$ and $5\frac{1}{16}$ -inch diameter cardboard-cased charges of appropriate length. Mean results (of 2 in each case) were 1,725, 1,930, 2,040, 2,070 m./s., indicating a

maximum velocity of about 2,100 m./s., which agrees closely with the value of 2,020 m./s. calculated for thermal equilibrium with the NaCl present, but falls well below the figure of 3,020 m./s. corresponding to zero heat transfer. Of course, the high percentage of salt makes the assumption of thermal transfer more reasonable than usual, for a large inert/explosive ratio involves not only a lower ultimate temperature but also a faster time-rate of heat transfer, so that a larger proportion of the final transfer has taken place within any specified time (See § 18.81 below). Moreover, the sodium nitrate/fuel reaction is less readily initiated than that between fuels and ammonium nitrate, a fact no doubt related to the endothermic nature of the NaNO_3 decomposition itself. It is, therefore, quite possible that the salt has had time to absorb a substantial amount of heat before the nitrate has entered fully into reaction. In that event, we cannot expect to achieve the full theoretical velocity no matter how large a cartridge we use (Cf. footnote to § 11).

(e) Explosive 2 (Table 16.1:1) (2 shots)

Two isolated experiments on $8\frac{1}{2}$ -inch diameter cartridges, one at 1.15 and the other at 1.04 g./ cm^3 , gave 3,300 and 3,000 m./s. respectively. Comparison with the theoretical figures of § 16.1 appears on the whole to favour thermal equilibrium, but the maximum experimental velocity may not have been reached: the proportion of salt is moreover substantial.

(f) Explosive 22 (Table 16.1:1) (12 shots)

This explosive was first loaded in paper and cardboard shells of $1\frac{1}{4}$, $1\frac{1}{2}$ and $2\frac{5}{16}$ -inch diameter, at 1.52 g./ cm^3 , but gave unusually erratic results, although the highest recorded velocity, 6,500 m./s., was of the theoretical order (see Table 16.1:2). A fresh batch of powder

was therefore mixed and filled directly into 1, $1\frac{1}{2}$ and $2\frac{1}{2}$ -inch lead tubes, of $\frac{1}{4}$ -inch wall. Considerable pains were taken by careful measurement of the tubes, and incremental loading, to achieve accurate and constant density (1.55 g./cm^3). Although the velocities measured were no more regular than before, they indicated a maximum between 6,900 and 7,000 m./s., so that the agreement is highly satisfactory. This explosive is ~~w~~awkward to handle, since the heavy pressing necessary to produce the standard density of 1.55 g./cm^3 tends to break down the porous kieselguhr structure and allow the nitroglycerine to soak out.

(g) Explosive 11 (Table 16.1:1) (3 shots)

This composition was loaded at the standard density of 1.23 g./cm^3 into lead tubes of $1\frac{1}{2}$, 2 and $2\frac{1}{2}$ inch diameter, with $\frac{1}{4}$ -inch wall. The velocities were respectively 4,130, 4,550 and 4,790 m./s. A larger number of cartridges, and probably some of larger diameter, would be required for a precise estimate of the limiting velocity, but the present results extrapolate well to the calculated value of 5,150 m./s. (Table 16.1:2).

(h) Explosive 10 (Table 16.1:1) (10 shots)

This explosive was fired at 1.15 g./cm^3 in cardboard tubes of diameters 1, 2, 3, 4 and 6 inch. Only two cartridges of each size were made, but they were very carefully loaded and the pairs of results agreed well. The mean velocities were 1,900, 2,260, 3,260, 4,200 and 4,300 m./s. at the diameters mentioned. The first two values suggest a limit of about 2,500 m./s.; above 2-inch diameter, however, a fresh increase appears to take place, and the limiting velocity in large diameters is estimated to be about 4,400 m./s. in satisfactory agreement with the theoretical figure of 4,450 m./s. This behaviour suggests

that the reaction may occur in two stages, the second of which gives effective support to the wave only in cartridges of more than 2-inch diameter. Alternatively, the process of initiation may change at that level in a way discussed at greater length below (§19.6).

(i) Explosive 7 (Table 16.1:1) (34 shots)

This explosive was fired at the same density and in the same cartridge diameters as the last, and similar precautions were taken to ensure consistency. The general behaviour was very similar to that of Explosive 10, though the velocities, as would be expected, were rather lower. In 1, 2, 3, 4 and 6 inch cartridges they were 1,530, 1750, 2,260, 2,730 and 3,100 m./s. The first two values suggest a limit of about 2,000 m./s., but in larger cartridges the velocity rises well beyond this level, and promises to approach a limit of about 3,650 in perfect confinement. It is clear that more massive charges would require to be fired in order to estimate this limit precisely, but it will evidently fall between the two theoretical limits of Table 16.1:2.

A series of experiments has been made to assess the degree of reactive participation of the various ingredients in small cartridges, and the importance of heat transfer to those which remain inert. The method consisted in varying their grist sizes individually, while keeping the cartridge density and diameter and the composition constant. The results are shown in Table 17.1:1.

Table 17.1:1

Explosive 7. 1½-inch diameter bare cartridges. $\Delta = 1.13 \text{ g./cm.}^3$

Batch number	Grist sizes			Mean m./s.	D	St. Dev. m./s.	:
	Ammonium nitrate	Sodium chloride	Cellulose				
:	:	:	:	:	:	:	:
1	C	C	C	2115	:	4	:
2	C	C	F	2315	:	4	:
3	C	F	C	2015	:	16	:
4	C	F	F	2355	:	12	:
5	F	C	C	2215	:	15	:
6	F	C	F	2570	:	30	:
7	F	F	C	2205	:	15	:
8	F	F	F	2235	:	11	:
:	:	:	:	:	:	:	:

It was unfortunately not possible without greatly increased labour to make the variation in grist size as wide as was desired. The "coarse" materials were caught on a 60 B.S.S. * sieve, the "fine" passed on 80 B.S.S. sieve. The variations in velocity are therefore small. However, there is no doubt that increase in fineness of either nitrate or cellulose separately raises the velocity; when both are made finer simultaneously, the rise is more marked. Reduction in size of the NaCl tends to reduce D. The most outstanding contrast is naturally between batch 3, containing coarse reactants and fine diluent ($D = 2015 \text{ m./s.}$) and batch 6, containing fine reactants and coarse diluent ($D = 2570 \text{ m./s.}$).

If we regard the depression of velocity below the maximum as due entirely to invasion of the reaction zone by the CJ- layer (see §17 above), it would appear that the nitrate/cellulose complex contributes only about one-fifth of its reaction energy to maintain the

* See p. 357.

wave in $1\frac{1}{4}$ -inch bare cartridges. Similar remarks apply to all the explosives studied in this section.

§17.2 Experimental determination of the maximum detonation velocities in gelatines based on nitroglycerine

[34,120,95]

It is well known that nitroglycerine gelatines may detonate at one or other of two distinct levels of velocity ($\sim 2,000$, $\sim 6,000$ m./s. respectively) according to circumstances. In all previous experiments known to the writer, the cartridge diameter was maintained constant and attention focussed upon the effects of the initiator and of the physical state (for example, the degree of aeration) of the explosive in deciding which velocity level was attained. Evidently, theory should be compared with the "high velocity" rather than with the "low", and in two of the four explosives of this class for which we have made measurements the high velocity was expressly selected for study by using a powerful detonator which ensured its development. In the other two cases, however, the effect of initiator was examined over a wide diameter range.

(a) Explosive 30 (Table 16.2:1) (10 shots)

Charges $1\frac{1}{8}$, $1\frac{1}{2}$, 2, 5 and $6\frac{1}{8}$ inch in diameter, loaded in paper and cardboard shells, were fired with a powerful detonator. The mean velocities recorded were 5,300, 5,400, 5,850, 5,750 and 6,020 m./s. respectively. More numerous measurements would be desirable for a precise estimate of D_{max} , but this must evidently be about 6,000 m./s. or slightly higher. For comparison, two charges in $1\frac{1}{2}$ and $2\frac{1}{2}$ -inch diameter lead tubes gave 5,720 and 5,920 m./s. Agreement with theory (Table 16.2:2) is satisfactory.

(b) Explosive 36 (Table 16.2:1) (6 shots)

The velocity was measured in $1\frac{1}{2}$, 2, $2\frac{1}{2}$ -inch diameter lead tubes. Two cartridges of each size were used, one initiated by a detonator of moderate strength, the other by a powerful detonator. This variation in initiator had no significant effect under the good confinement provided by the lead; the means were 5860, 6140, 6360 m./s., with a probable maximum of about 6,600 m./s. The theoretical value was 6,520 m./s. (Table 16.2:2).

(c) Explosive 25 (Table 16.2:1) (75 shots)

A rather comprehensive study was carried out on this [redacted]
[redacted] explosive.

A preliminary experiment was made with a 7-inch diameter cartridge, two days old, cased in cardboard and initiated by a moderate detonator (No.6 fulminate). The velocity was measured at six points, 10, 20, 35, 50, 60 and 85 cm. from the detonator, and was almost constant at 5,700 m./s. which is close to the predicted maximum of 5,850 m./s. At the other end of the diameter range, $\frac{3}{4}$ -inch cartridges, two days old, fired successfully, but $\frac{5}{8}$ -inch cartridges failed to propagate detonation, even with a heavy primer consisting of blasting gelatine fired at high velocity.

Two samples of the explosive, each containing 170 lb. were then drawn from current manufacture and cartridged on two consecutive days. In view of the known tendency for gelatinous explosives to change their behaviour on storage, it was considered essential that all the cartridging be done as nearly as possible at the same time; and similarly for the firing. The effect of small differences in age at the date of firing was minimised by storing the cartridges for three weeks before use.

This programme, however, made it necessary to budget in advance for the experimental requirements. The first sample was used to make a series of cartridges distributed evenly over the diameter range from $\frac{1}{2}$ -inch to 5 inch; the second to provide an auxiliary supply of cartridges around 2-inch and below $\frac{3}{4}$ -inch, where maximum ambiguity was thought likely to develop. As it turned out, this supply met the needs of the experiment very well.

The cartridges were wrapped in waxed paper, and stored in an upright position, each inside a closely fitting cardboard tube to prevent deformation. Before use, the cardboard was removed. The firing occupied four days, and was carried out with (1) a No. 6 fulminate detonator, or (2) a powerful "Briska" detonator, plus Blasting Gelatine.

The results are best summarised graphically (Fig. 17.2:1), and lead to the following conclusions.

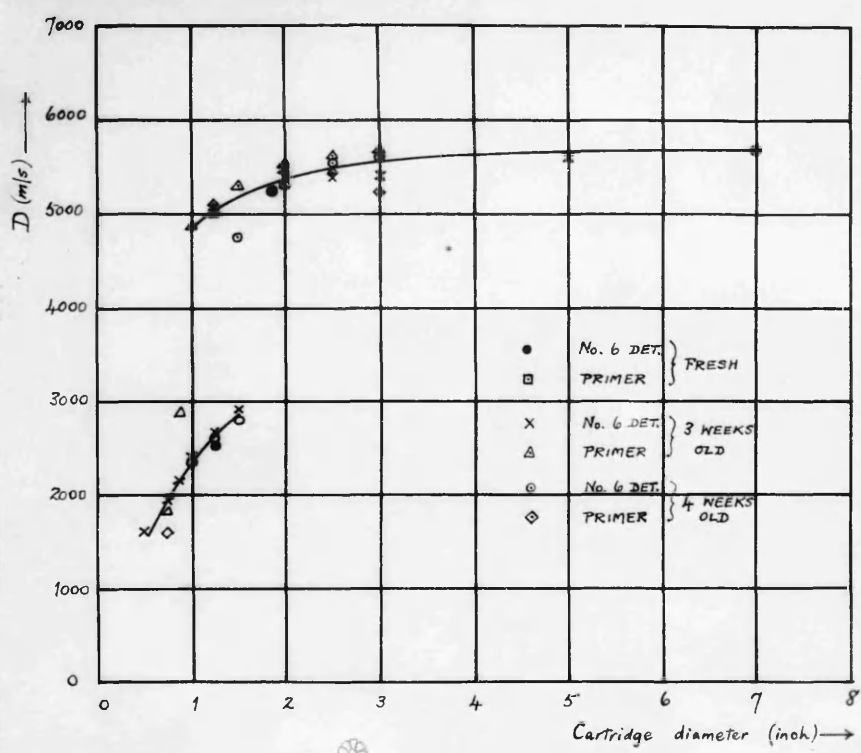


FIG. 17.2:1. EXPLOSIVE 25. EFFECT OF
DIAMETER AND INITIATOR.

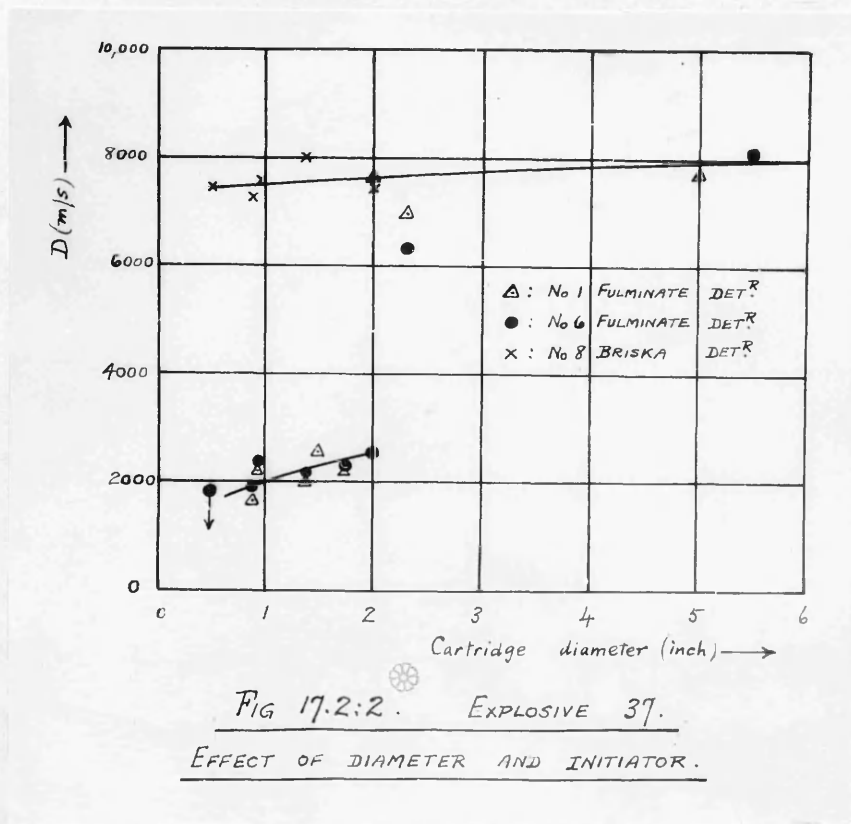
- (1) Below 1 inch diameter, it is difficult to obtain high velocity, and below $\frac{3}{4}$ -inch difficult to produce stable detonation at all.
- (2) From 1 to $1\frac{1}{2}$ -inch, inclusive, low velocity ($\sim 2,500$ m./s.) or high velocity ($\sim 5,000$ m./s.) can be obtained at will, according to the primer used.
- (3) Above $1\frac{1}{2}$ -inch, only the high velocity is stable, and further increase in diameter produces only a moderate further rise in velocity.

Theoretical comment on these features is reserved until § 19.6 below. It is clear, however, that the experimental maximum - about 5,800 m./s. - is in close agreement with the prediction of § 16.2.

(d) Explosive 37 (Table 16.2:1) (44 shots)

The behaviour in normal cartridge sizes of this extremely important explosive ("Blasting Gelatine") was known to be similar to that of the last. The effect of different intensities of priming and of age and [95, etc] aeration had been rather extensively studied, but little if any attention paid to the influence of cartridge diameter. It was, therefore, decided to explore this field along the same lines as for the previous explosive. The experiment was conducted as before, except that the smaller cartridges were studied by means of a moving-film camera, which is more informative than the Dautriche device; the larger charges had to be timed by the Dautriche method, but a cross-check was provided at $1\frac{1}{4}$ -inch diameter, where both methods were applied simultaneously. A wide range of detonators was used, from No.1 fulminate (a very small detonator) to the powerful Briska type.

Figure 17.2:2 summarises the results, and leads to the following conclusions.



- (1) At $\frac{1}{2}$ inch diameter, a steady low velocity cannot be obtained. Attempts in this direction resulted either in a rise to high velocity or (more usually) in failure. Steady high velocity is consistently produced by the Briska detonator.
- (2) From $7/8$ to 2-inch, inclusive, a steady low or high velocity can be produced, according to the detonator used.
- (3) Above 2-inch, only the high velocity is stable; even when as

weak an initiator as a No.1 fulminate detonator is used, the high velocity is attained.

(4) The high velocity varies very little over the entire diameter range, if we except the immediate neighbourhood of 2-inch, where the mechanism of spontaneous transfer from the low to high level is evidently just becoming operative, and where we should, therefore, expect occasional anomalous intermediate results.

The measurements have not been extended below $\frac{1}{2}$ -inch diameter, but an experiment with a plastic "Blasting Gelatine", which detonated at 7,600, 7,480, 7,440 m./s. in $\frac{3}{4}$, $\frac{5}{8}$ and $\frac{1}{4}$ -inch bare charges, and failed only at $\frac{3}{16}$ -inch, suggests that the high velocity is likely to persist down to smaller diameters than $\frac{1}{2}$ inch.

Two further experimental points in connection with Blasting Gelatine are discussed in §17.21, §17.22; and the phenomenon of dual velocity in §19.6. Here we may notice finally that the limiting experimental velocity is about 7,800 m./s., which must be regarded as agreeing well with the theoretical value of 7,370 m./s. Part or all of the difference is in fact probably due to an experimental density somewhat greater than the value of 1.45 g./cm³ assumed in the calculations.

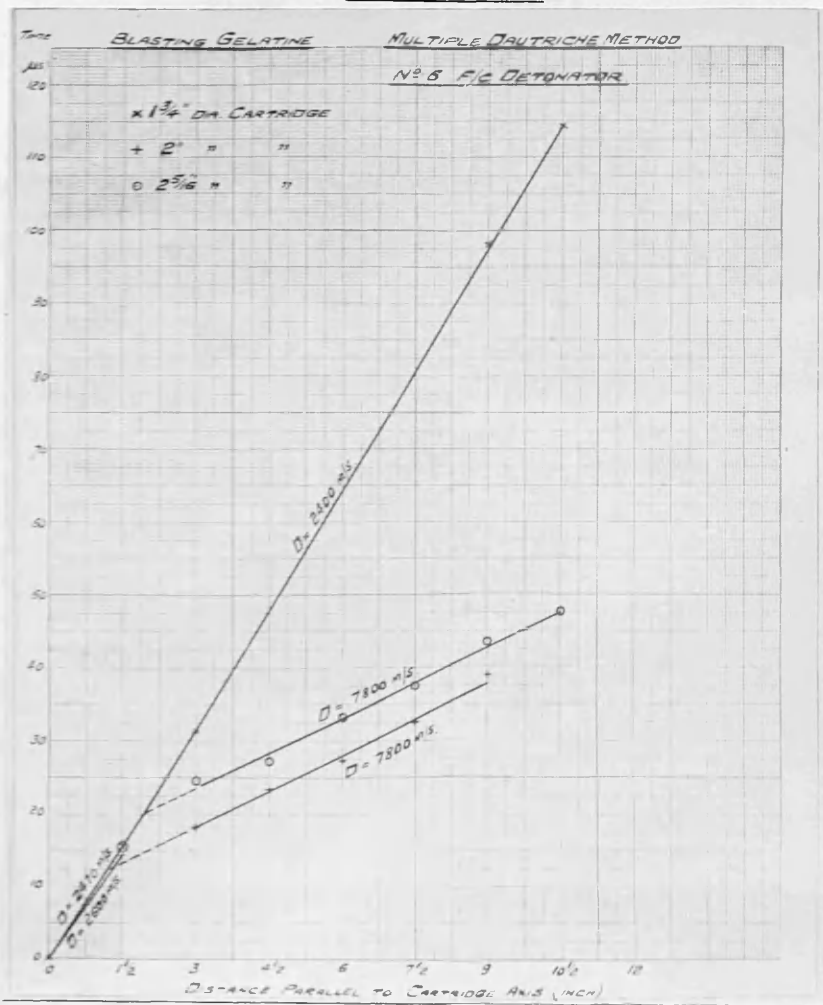
§17.21 The spontaneous change from low to high velocity in Blasting Gelatine

Since it is a reasonable conjecture, confirmed in other similar cases [116] by direct experiment, that the velocity initiated in the immediate neighbourhood of a weak detonator is low in every case, and subsequently rises to the high level only in cartridges above 2-inch in diameter, it becomes of interest to discover whether the change takes place smoothly or abruptly. The question would be more easily answered if cartridges of large diameter and adequate length could be fired in front of the high-speed camera, but this was not possible. Some information, however, is

provided by an extension of the Dautriche method, described above (§ 17.02), which provides a semi-continuous record of the progress of the wave.

The method was applied to three cartridges, of diameters $1\frac{3}{4}$, 2 and $2\frac{5}{16}$ inch, four weeks old and fired by a No. 6 fulminate detonator. The results are shown in Fig. 17.21:1, where the origin corresponds to passage of the wave through a section $2\frac{1}{2}$ -inch from the detonator. It is clear that the transfer took place rather abruptly, certainly within a length of $1\frac{1}{2}$ -inch along the cartridge surface. The $1\frac{3}{4}$ -inch shot maintained low velocity throughout its length, as would be expected from Fig. 17.2:2.

Fig. 17.21:1



§17.22 Stability of the low velocity in Blasting Gelatine

In order to test whether the low velocity in gelatines represents a permanently stable condition, a column of Blasting Gelatine, $1\frac{1}{2}$ -inch in diameter and 18 feet long, was extruded in one piece, and stored for a fortnight. It was laid out on the ground in a straight line and initiated by a No. 1 fulminate detonator at one end. The velocity was measured at $\frac{1}{2}$, $\frac{3}{4}$, $\frac{4}{4}$, $\frac{6}{4}$, 8, $\frac{9}{4}$, $11\frac{1}{2}$, $13\frac{1}{4}$, 15 and 17 feet from the detonator. The results are shown in Table 17.22:1.

Table 17.22:1

Run-up (ft.)	Velocity (m./s.)	Run-up (ft.)	Velocity (m./s.)
$\frac{1}{2}$	2,360	$\frac{9}{4}$	2,390
$\frac{2}{4}$	2,390	$11\frac{1}{2}$	2,310
$\frac{4}{2}$	2,360	$13\frac{1}{4}$	2,360
$\frac{6}{4}$	2,270	15	2,350
8	2,360	17	2,310

These figures appeared to establish the stability of low-velocity detonation in Blasting Gelatine of suitable diameter, etc. It was afterwards suggested, however, that the Dautriche attachments might have maintained and stabilised the detonation. Two further strings of explosive, $1\frac{1}{2}$ inch diameter and $13\frac{1}{2}$ feet long, were fired as before, after 12 days storage. The initial velocity was measured by a few Dautriche assemblies distributed over the first few feet. The velocity at the remote end was measured by an electronic chronoscope.^[24] Since the pick-up used with this instrument is non-explosive, the objection mentioned above can hardly apply to such measurements. In any case, the wave had travelled unsupported for about 10 feet before reaching the point at which this final measurement was made. The results are shown in Table 17.22:2.

Table 17.22:2

<u>Shot</u>	<u>Run-up</u> (ft.)	<u>Method</u>	<u>Velocity</u> (m./s.)
1	1	Dautriche	2,470
	2	"	2,600
	3	"	2,130
	4	"	2,780
	13	Chronoscope	3,370
2	1	Dautriche	2,510
	2	"	2,410
	13	Chronoscope	2,570

Measurements by the chronoscope on $1\frac{1}{2}$ -foot lengths cut from the strings before use gave velocities of 2,460, 2,640 m./s. respectively.

Shot 1 is ^{con}inclusive for the present purpose. The four Dautriche records themselves, however, show irregularity, which is no doubt due to the comparative freshness and rather uneven contour of the charge. Shot 2 proves, as far as this is possible with a single chronoscope measurement, that Blasting Gelatine can under suitable conditions detonate with a steady velocity of around 2,500 m./s. over at least 13 feet of a $1\frac{1}{2}$ inch diameter cartridge.

Theoretical comments on the collected results for Blasting Gelatine are made below in §19.6

§17.3 Experimental determination of the maximum detonation velocity in powders based on trinitrotoluene

(a) Explosive 39 (Table 16.3:1) (12 shots)

In 1, $1\frac{1}{2}$ and $2\frac{1}{2}$ -inch diameter lead tubes this explosive gave 3,760, 4,170, 4,300 m./s. while $8\frac{1}{2}$ -inch diameter cardboard-cased charges detonated at 4,260 m./s. The maximum is evidently just over 4,300 m./s., which compares well with the theoretical value of 4,060 (Table 16.3:2). In $1\frac{1}{4}$ -inch paper shells, the velocity was only 2,400 m./s. In $1\frac{1}{4}$ -inch paper shells, the velocity was only 2,400 m./s.

(b) Explosive 44 (Table 16.3:1) (9shots)

The velocities in 1, $1\frac{1}{2}$, and $2\frac{1}{2}$ -inch lead tubes were 4,450, 4,800, 5,110 m./s. with a probable maximum of about 5,250 m./s. Theory predicts 5,060 m./s. (Table 16.3:2).

(c) Explosive 42 (Table 16.3:1) (16 shots)

This explosive was loaded in $\frac{5}{8}$, $\frac{7}{8}$, $1\frac{1}{4}$, 2, 3-inch paper shells, and in 5-inch cardboard tubes; the two smallest sizes were timed by the camera and the three largest by the Dautriche method. A check was provided by timing half of the $1\frac{1}{4}$ -inch cartridges by one method and half by the other. The results were, in order, 3,780; 4,110; 4,500 (Dautriche), 4,600 (camera); 4,600; 4,840; 4,860 m./s., indicating a maximum of 4,900 m./s., as compared with the theoretical figure of 4,900 m./s. if the aluminium is assumed to react in the steady zone (Table 16.3:2).

(d) Explosive 45 (Table 16.3:1) (45 shots)

This is an oxygen-balanced mixture of ammonium nitrate and TNT. It is an experimental composition, [redacted] rather [redacted] than a commercial TNT powder, [redacted], and was selected for a study of the effect of nitrate grist size upon the velocity in cartridges of small diameter.

TNT powders, such as 44, are prepared by more or less protracted milling together of the ingredients, and the velocity in cartridges of [62] normal diameter then increases with the milling time. In terms of the theory outlined in § 17, this is no doubt due to the enhanced fineness of the nitrate and its more intimate association with the TNT. According to this theory, we should expect the velocity at any chosen diameter to rise towards the theoretical maximum as the grist size is reduced. Moreover, we should expect the velocity to increase with cartridge

diameter towards the same maximum when grist size and intimacy of mixing are maintained constant.

Precise control and assessment of grist are difficult in a milled product. In order to test the theory, we have, therefore, worked with mixtures prepared at a temperature above the melting point of the TNT. Grinding can be largely avoided in this process: the final product consists of nitrate grains coated with TNT, and the grist of the nitrate should be similar to, if not identical with, that of the material originally introduced.

In the first experiment, the coarsest fraction from a nitrate sample was caught on a No.60 British Standard sieve and set aside. The remainder was then ball-milled and the fraction passing a 170 B.S.S. sieve also set aside. The coarse and fine fractions were then mixed separately with TNT at 80°C. Table 17.3:1 summarises the velocities, and shows the remarkable contrast between the two powders, which differ only in nitrate grist size.

Table 17.5:1

21.3 TNT/78.7 ammonium nitrate. $\Delta = 0.95 \text{ g.}/\text{cm}^3$

Effect of nitrate grist size

Diameter (inch)	Detonation Velocity (m./s.)	
	Coarse NH ₄ NO ₃	Fine NH ₄ NO ₃
7/8	1,400	3,800
1	1,700	4,200
1 ¹ / ₄	1,760	4,430
1 ¹ / ₂	1,870	4,360
2	1,975 → 2825	4,500

* See p. 357.

The velocity of the mixture containing fine nitrate clearly approaches a limit of 4,500 - 4,600 m./s. comparing well with the theoretical figure of 4,500 m./s. The velocity of the coarse material in diameters up to $1\frac{1}{2}$ -inch is apparently approaching a limit of about 2,200 m./s., which may be compared with the value of 2,160 m./s. calculated on the assumption that the nitrate remains inert. In the single 2-inch cartridge which it was possible to fire, however, the velocity, commencing at the level of 1,975 m./s. which falls in line with the results for smaller charges, rose rapidly to 2,825 m./s. Although it seems very probable that this behaviour implied two levels of velocity in the coarse mixture, it has not been possible to study the question in greater detail, because of the labour involved in separating a large quantity of coarse nitrate.

In the second experiment, a sample of nitrate was divided into the following fractions "caught on 30", 30-60, 60-85, 85-100, 100-170, 170-200 and "through 200" B.S.S. The fractions were hot-mixed with TNT in the balanced proportions, and three cartridges, $15/16$ -inch diameter, $\Delta = 0.959 \text{ g./cm}^3$, prepared from each, of which one was fired by a small detonator, one by a Briska detonator, and one by a powerful primer. The velocities showed no significant variation with initiator, and we quote only the mean value at each grist, namely

B.S.S.	Caught on 30,	30-60,	60-85,	85-100,	100-170,	170-200	Through 200
D(m./s.)	1345,	1440,	1515,	2330,	3000,	3940	4190

It is clear that velocities approaching the maximum may be reached, even in small cartridges, by sufficient reduction in the nitrate grist size.

§ 18 Mixtures of explosive and inert material

[168, 163, 164]

It is found that when cartridges of coal mining explosives are submitted to a test of their power to ignite firedamp when suspended in a methane-air atmosphere, the incendivity increases with velocity of detonation, other relevant parameters such as the total energy release being maintained constant. This observation may be thought to imply that the shock-wave sent out by a suspended cartridge plays an important part in the mechanism of ignition. In any event, it suggests that enhanced safety will be associated with low detonation velocity. It will be shown below that the most effective method of reducing the velocity is to load the explosive with non-reactive material.

Again, in the same connection, it has long been known that the safety of a detonating explosive is increased by wrapping it in a sheath of finely ground inert powder. We may conjecture that the effect is due to extinction of any incipient flame by the cloud of fine particles developed from the sheath.

The two principles are, in fact, combined in all British "Permitted" explosives by incorporating a substantial proportion (10 - 30%) of common salt in the composition itself, and very recently coal mining explosives whose safety when unsheathed is equivalent to that of a traditional sheathed explosive have been successfully designed by [163, 164, 153] including large quantities of salt in the explosive formula.

Detonating compositions which consist of simple mixtures of reactive and inert material are, therefore, of great practical interest.

The theoretical problems connected with such mixtures have already been discussed in § 15, where it was stated:

- (1) that the compressional energy absorbed by the diluent could be disregarded in all normal cases,
- (2) that the diluent might be assumed to be completely entrained by the explosive products,
- (3) that the diluent should remain effectively cold within reaction times of normal order, provided the proportion present were moderate and its grist size not unusually fine; but that otherwise absorption of heat by the diluent might become important.

Apart from the general success of calculations (§§16.1 - 16.4) based on these premises, evidence for them was postponed and is collected in the present and following sections.

The general methods of calculation used in §16 may, of course, be, and were there, applied in particular to mixtures of explosive and inert material. However, simplified analyses can be developed, which are of advantage in considering the experimental evidence for (2) and (3) above .

§ 18.1 Diluent entrained, but absorbing no heat from the reaction products

In the first place, we shall assume that the diluent is completely entrained, but absorbs neither thermal nor compressional energy within the steady zone. Then a rough estimate of its effect upon the velocity may be obtained by considering that the forward kinetic energy of the reaction products must be reduced in the ratio $m:1$, where m is, as usual, the proportion by weight of explosive present. We should, therefore, expect the velocity to be approximately proportional to \sqrt{m} .

Although this argument is crude, the result is in fact rather well confirmed by the following more detailed approach. In the notation of § 15.1

$$D = \frac{k_i+1}{1-\beta\Delta} \sqrt{\frac{mn'_i RT_i}{k_i}} . \quad (1)$$

Now, let us imagine that the explosive component were cartridges alone, at a loading density Δ_e , say. Using the suffix e to identify the variables for this case, we have

$$D_e = \frac{k_e+1}{1-\alpha_e\Delta_e} \sqrt{\frac{n_e R T_e}{k_e}} . \quad (2)$$

Moreover

$$v_i = \frac{\frac{k_i}{\Delta} + \beta}{k_i+1} , \quad (3)$$

whence, by 15.1(2),

$$v'_i = \frac{\frac{k_i}{m} \left[\frac{1}{\Delta} - (1-m)\varphi_i \right] + \alpha}{k_i+1} . \quad (4)$$

Similarly,

$$v_e = \frac{\frac{k_e}{\Delta_e} + \alpha_e}{k_e+1} . \quad (5)$$

However, $T_e = T_i$, $n_e = n'_i$ to a close approximation, on the conditions assumed. Hence, by 15.1(6, 8), k_e is the same function of α_e as k_i is of α . It follows from (4, 5) that $\alpha = \alpha_e$, $v'_i = v_e$, $k_i = k_e$, provided only that

$$\Delta_e = \frac{m\Delta}{1-(1-m)\Delta\varphi_i} . \quad (6)$$

Subject to (6), we then have

$$D = \frac{D_e \Delta_e}{\Delta \sqrt{m}} , \quad (7)$$

and

$$p_i = p_e . \quad (8)$$

In other words, the CJ-pressure is equal to that of the explosive alone, and the detonation velocity $A_e/\Delta\sqrt{m}$ times that of the explosive alone, cartridged at A_e , where A_e is defined by (6)

Equations (6, 7) were stated (without proof) by H. Jones in an unpublished memoir.^[81] They enable D to be quickly calculated, provided D_e, p_e are known as functions of A_e , and φ_i as a function of p_i . We shall, as usual, assume φ_i to be determined with sufficient accuracy by isothermal compression measurements. $D_e(A_e)$ is usually available from experiment. The only uncertainty then attaches to $p_e(A_e)$, which must be calculated. However, by taking advantage of the basic equation

$$p_e = D_e A_e W_e , \quad (9)$$

and the fact that W_e depends much less than p_e on the equation of state employed, we may minimise the error if we use the experimental values of D_e in (9)

§ 18.2 Diluent entrained, and in thermal equilibrium with reaction products

In this case the diluent causes a depression of the velocity by sharing not only the kinetic energy of the products but also their heat energy. We might, therefore, expect D to be reduced in the ratio $(\sqrt{m})^2 : 1$; in other words that D should be approximately proportional to m .

No worthwhile simplification of the general theory suggests itself in the present case; but calculations carried out by the methods of § 15.1 confirm the above expectation, as will be seen below (§ 18.5).

§ 18.3 Diluents in thermal equilibrium with the products, but not entrained

According to the arguments of §§ 18.1, 18.2, we should expect D in this case to be once more proportional to \sqrt{m} . In other words, the present case should imply a $D(m)$ -relation rather similar to that of § 18.1, and it may be difficult on the basis of velocity measurements alone to arbitrate between the two. However, independent evidence (§§ 18.5, 18.81) gives much more support to the assumptions of § 18.1.

§ 18.4 Diluent neither entrained nor heated

If the diluent remained uncompressed at its original specific volume φ_0 , it would constitute merely an irregular envelope for the explosive component, whose velocity would, therefore, correspond to a loading density

$$\Delta' \equiv \frac{m\Delta}{1-(1-m)\Delta\varphi_0} . \quad (1)$$

As m is decreased, D then falls more slowly than \sqrt{m} , and cannot become less than the "ideal" velocity D_i of the explosive component, corresponding to zero density.

If we allow for compression of the diluent from φ_0 to φ_i , the cross-section available to the explosive or its products increases through the steady zone in the ratio

$$Z \equiv [1 - (1-m)\Delta\varphi_i] / [1 - (1-m)\Delta\varphi_0] . \quad (2)$$

If the basic equations are then written down, it will be found that the problem corresponds exactly to that of the explosive component cartridges at Δ'/Z , in other words at

$$\Delta'' \equiv \frac{m\Delta}{1 - (1-m)\Delta\varphi_i} . \quad (3)$$

Since $\varphi_i < \varphi_0$, D is, therefore, somewhat reduced by compression of the diluent, as would be expected. However D still decreases more

slowly than \sqrt{m} , and is still bounded below by D_i .

It will be shown that experiment decisively rejects the alternatives presented by the present section.

§ 18.5 PETN/NaCl mixtures

A series of calculations were first made by the method of § 18.1 for mixtures of PETN and NaCl, at a loading density of 1.0 g./cm.³, and containing from 1 to 100% PETN by weight. The procedure at each m was to assume a value for φ_i , whereupon D_e was known by 18.1(6) and ρ from 18.1(8,9), in terms of the experimental data for D_e ; φ was then recalculated from Bridgman's isotherm, and the process repeated until consistency was reached. D was finally obtained from 18.1(7).

Table 18.5:1 shows the results.

An experiment was designed to test the theory. A sample of NaCl was divided by means of British Standard Screen Scale (B.S.S.) sieves into five fractions ranging from "30-44 B.S.S." to "passing 200 B.S.S." (the numbers refer to meshes per linear inch). Each fraction was mixed with PETN in five different proportions up to 70% NaCl. (Mixtures containing higher percentages of NaCl failed to propagate). The twentyfive mixtures were cartridge in 1 $\frac{1}{4}$ " diameter paper shells, and as nearly as possible at a standard ensity of 1.00 gm./cm.³; and two cartridges of each tested for velocity with a high-speed camera.

Table 18.5:2 gives the mean velocity for each mix. It will be seen that the densities varied slightly with m , and for comparison purposes, a small correction was applied to bring all the densities to 1.00 g./cm.³. The corrected values are also given in Table 18.5:2.

Inspection shows that D was almost independent of NaCl grist size,

Table 18.5: 1

Calculations for PERN/NaCl mixtures by method of §18.1

($\Delta = 1 \text{ g}_\circ/\text{cm}^3$)

m	P_i atm.	Φ_i $\text{cm}^3/\text{g}_\circ$	Δe_γ gm/cm^3	D_e $\text{m}_\circ/\text{s}_\circ$	D $\text{m}_\circ/\text{s}_\circ$
0.01	600	0.459	0.018	2,420	1,35
0.02	1,200	0.458	0.036	2,450	623
0.03	2,000	0.457	0.054	2,490	776
0.05	3,000	0.455	0.088	2,550	1,005
0.10	6,000	0.451	0.169	2,750	1,470
0.20	12,000	0.441	0.309	3,150	2,180
0.30	18,000	0.431	0.450	3,550	2,790
0.40	25,000	0.424	0.537	3,900	3,310
0.45	28,500	0.419	0.586	4,080	3,570
0.50	32,000	0.415	0.651	4,230	3,780
0.60	40,000	0.407	0.716	4,520	4,180
0.70	48,000	0.399	0.796	4,800	4,570
0.75	52,500	0.396	0.833	4,930	4,750
0.80	56,000	0.393	0.868	5,030	4,880
0.90	65,000	0.385	0.938	5,280	5,210
1.00	73,000	0.379	1.000	5,500	5,500

Table 18.5:2

Experimental velocities of PEG/NaCl mixtures. The bracketed values have been corrected to 1.00 gm./cm.³. The B.S.S. numbers indicate meshes per linear inch.

$100m \equiv$ $\rho \cdot D^2$	B.S.S.			Mean	Maximum by extrapolation: m./s.
	30-44	44-52	52-60	Through 200	m./s.
	$D = 1.04 \text{ g./cm}^3$	1.02	1.01	1.04	1.05
30	2575 m./s. (2455)	2450 (2390)	2550 (2520)	2450 (2330)	1950 (1800) (2300)
45	1.01	1.00	0.99	0.98	1.04
	3425 (3395)	3250 (3250)	3225 (3255)	3125 (3185)	2950 (2830) (3185)
60	0.985	0.98	0.98	0.97	0.98
	3775 (3820)	3825 (3885)	3725 (3785)	3650 (3740)	3775 (3835) (3815)
75	0.97	0.97	0.97	0.97	0.98
	4450 (4540)	4425 (4515)	4375 (4465)	4275 (4365)	4200 (4260) (4430)
90	0.94	0.95	0.95	0.95	0.96
	4750 (4930)	4850 (4900)	4700 (4850)	4625 (4775)	4660 (4780) (4845)

except for a significant drop when the finest size was used in conjunction with a high proportion of diluent. It may, therefore, be inferred that in general no effective thermal transfer to the salt particles occurred, since any such transfer would certainly be sensitive to their total surface area, which varied in this experiment by a factor of at least five to one. The mean velocities over all grists, and also the estimated maxima for coarse NaCl, are graphed in Figure 18.5:1. together with the theoretical values of table 18.5:1, with which they stand in very fair agreement.

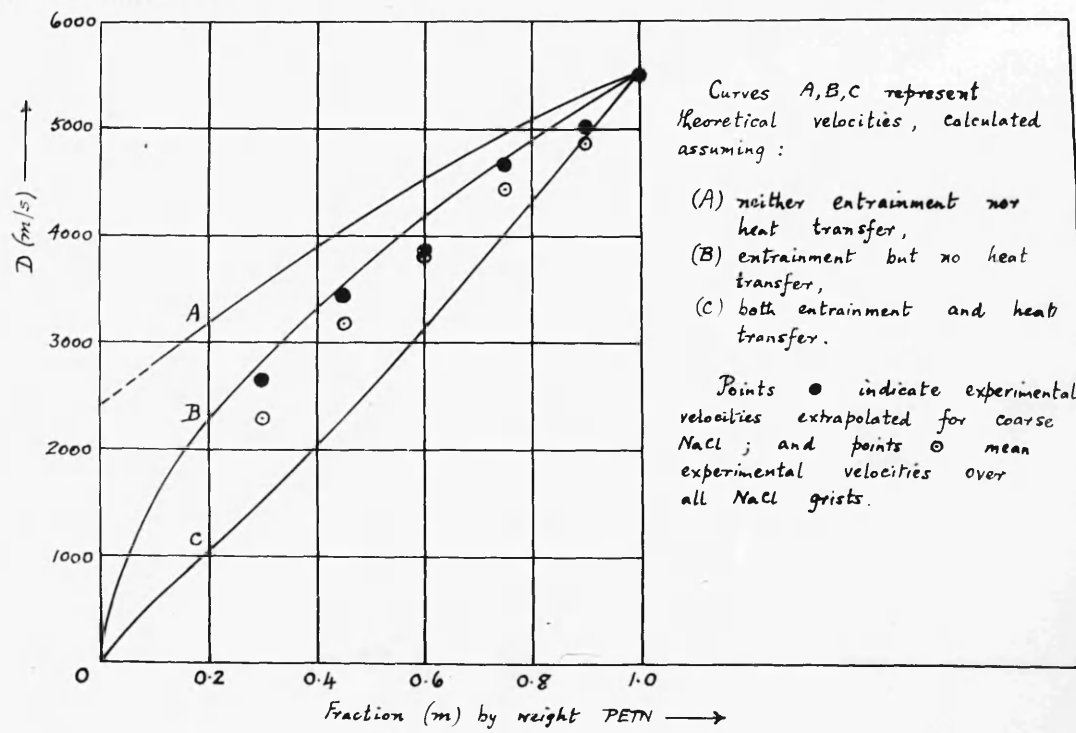


FIG. 18.5:1 PETN/NaCl MIXTURES. $\Delta = 1.00 \text{ g./cm}^3$.

For comparison, Figure 18.5:1 also contains the velocities calculated on the assumptions of § 18.4. The agreement is poor. It might, however, be argued that this is due to the small cartridge diameter used. To dispose of this point, a fresh batch of 30 PETN/70 NaCl containing all grists was prepared, and fired in $1\frac{1}{4}$ ", $2\frac{3}{8}$ " and $2\frac{15}{16}$ " diameters. The velocities at 1.00 g./cm³ were 2270, 2450 and 2400 m./s. respectively, showing that the effect of diameter is small, and the velocity does not approach the value indicated by § 18.4. Agreement with Table 18.5:1, on the other hand, is even closer than before, so that part at least of the small discrepancy remaining in Fig. 18.5:1 is due merely to the small diameter of the cartridges used.

In view of the experimental evidence regarding grist size, it was not strictly necessary to carry out calculations by § 18.2 or § 18.3. However, Figure 18.5:1 contains the values predicted by § 18.2, in order to illustrate the approximately linear variation of D with m, referred to in that section. Agreement with the experimental values is, as expected, very poor.

The above study suggests that inert material may normally be regarded as entrained by the detonation products, but absorbing no heat from them within a significant time.

§ 18.6 Nitroglycerine/kieselguhr mixtures

A further test was made with mixtures of nitroglycerine and kieselguhr. Since the practicable cartridge densities varied sharply with composition, the explosive component being in this case a liquid, the experimental determinations of velocity were carried out first, and calculations then made, by the methods of § 18.1 etc, at the

loading densities actually used.

Experimental: Mixtures containing 70, 60, 50 and 40% nitroglycerine were prepared on a 100 lb. scale in an industrial mixer, and cartridgeed in paper and cardboard tubes $1\frac{1}{16}$, $2\frac{1}{8}$ and $6\frac{1}{4}$ inch diameter, the length being in each case about six times the diameter. The largest tubes, which were used in order to permit a reliable extrapolation to infinite diameter, were filled first, since only moderate pressures can be applied in hand loading to such wide tubes, and it was essential to maintain a constant density at all three diameters for each mixture. An increment occupying about 4" was placed in the tube and pushed in as tightly as possible with a 5"-diameter wooden rod. The density of this increment was calculated from its length, and the remainder of the tube loaded at that density in small increments. The same density was then used in the smaller cartridges. By very careful control of the incremental weight and length, it was possible to reach a high degree of precision in the density. This depended, of course, upon an accurate knowledge of the tube section. The 6" cardboard tubes used were of an exceptionally regular shape and size: they were circular to better than 0.7%, and the variation in sectional area from end to end did not exceed 0.8%. Under such conditions, the density was known to within \pm 0.5%, a precision not in general easy to achieve except in accurately machined metal tubes.

The velocities were measured by the Dautriche method. The means are shown in Table 18.6:1, together with theoretical values

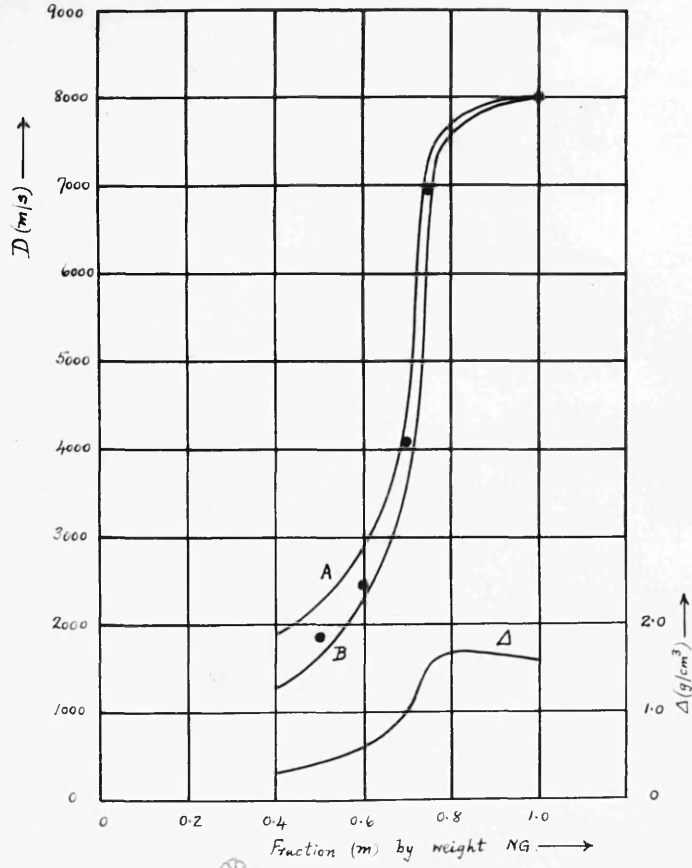


FIG. 18.6:1 Nitroglycerine /Kieselguhr mixtures.

A : Entrainment but no heat transfer.

B : Entrainment and heat transfer.

● : Experimental velocities in large-diameter cartridges.

computed on the alternative assumptions of §§18.1, 18.2. In using the theory of §18.1 it is necessary to know $D_e(\Delta_e)$ for the pure explosive. The fact that nitroglycerine is a liquid makes this difficult to obtain, though it could be done by using emulsions containing small proportions of other material. Since the only information of this kind available related to rather small cartridge diameters, $D_e(\Delta_e)$ was deduced by analogy with PETN, which is of similar constitution. It is found, in fact, that the maximum experimental velocities of most pure explosive compounds can be closely represented down to 0.5 g./cm³ by

$$D_e(\Delta_e) = D_e(1.0) + 3500(\Delta_e^{-1}), \quad (1)$$

and for lower densities a reasonable estimate may be made by extrapolating graphically to the ideal theoretical limit D_i at $\Delta_e = 0$.

The comparison between experiment and theory is best judged from Figure 18.6:1, which includes also results for Arctic Dynamite (75 nitroglycerine/25 kieselguhr) and for pure nitroglycerine. As a consequence of the rapid increase in density with percentage nitroglycerine, the variation of velocity is particularly dramatic. However, it is well reproduced by the theory of §§ 18.1, 18.2. The behaviour at 40 and 50 per cent guhr, (and the failure at higher guhr contents) no doubt reflect an appreciable transfer of heat to the guhr, which is in a very fine state of division.

Table 18.6:1
Nitroglycerine/kieselguhr mixtures

% N/G	Δ (g./cm ³)	D (m./s.) at diameter			Limit m./s.	D calc. (m./s.) §18.1	§18.2
		1 ¹ /16"	2 ¹ /8"	6 ¹ /4"			
70	0.99	2800	3300	3960	4080	4220	3650
60	0.63	2250	2400	2450	2460	2910	2300
50	0.45	1700	1750	1850	1860	2230	1650
40	0.33	Failed	Failed	Failed	-	1750	1200

§ 18.7 Nitroglycerine/NaCl mixtures

Theoretical: Mixtures of nitroglycerine and common salt are of great practical interest, because of their extensive application in [168, 163, 164, 153] the design of coal-mining explosives. The extreme sensitivity of

[66,166]

nitroglycerine makes it possible to obtain stable propagation in bare cartridges of moderate diameter (~ 1 inch) over a very wide range of composition, from pure nitroglycerine down to 2 or 3 percent by weight of the explosive.

According to the theory of §§ 18.1, 18.2, we should expect such extremely diluted mixtures to have unusually low velocities of detonation, and this is found in practice to be the case: stable waves with velocities as low as 600 m./s. have been observed.

The loading densities which are readily obtained in practice vary with percentage salt. When this is low (up to 20%), the powder density is $1.2 - 1.4 \text{ g./cm}^3$; beyond 20%, the mixture is flooded with nitroglycerine(NG) and the density rises rapidly to a maximum of about 1.8 g./cm^3 at 30% NG; thereafter it subsides towards 1.6 g./cm^3 , the density of liquid NG itself. We have made calculations by the methods of §§ 18.1, 18.2 for a wide range of both m and Δ , paying, however, most attention to the region $0 < m < 0.2$, which is of greatest practical interest. The results are best summarised graphically: Fig. 18.7:1 shows the variation of D with m for $\Delta = 1.0, 1.2, 1.3, 1.4 \text{ g./cm}^3$, according to the alternative assumptions of §§ 18.1, 18.2 regarding heat transfer. The most important parts of the curves are, of course, those below $m = 0.2$, since, for higher values of m , Δ rises beyond 1.4; the entire curves, however, are drawn for completeness.

As a check upon the approximate theory of § 18.1, the velocity was also calculated by the general method, adopting the same assumptions

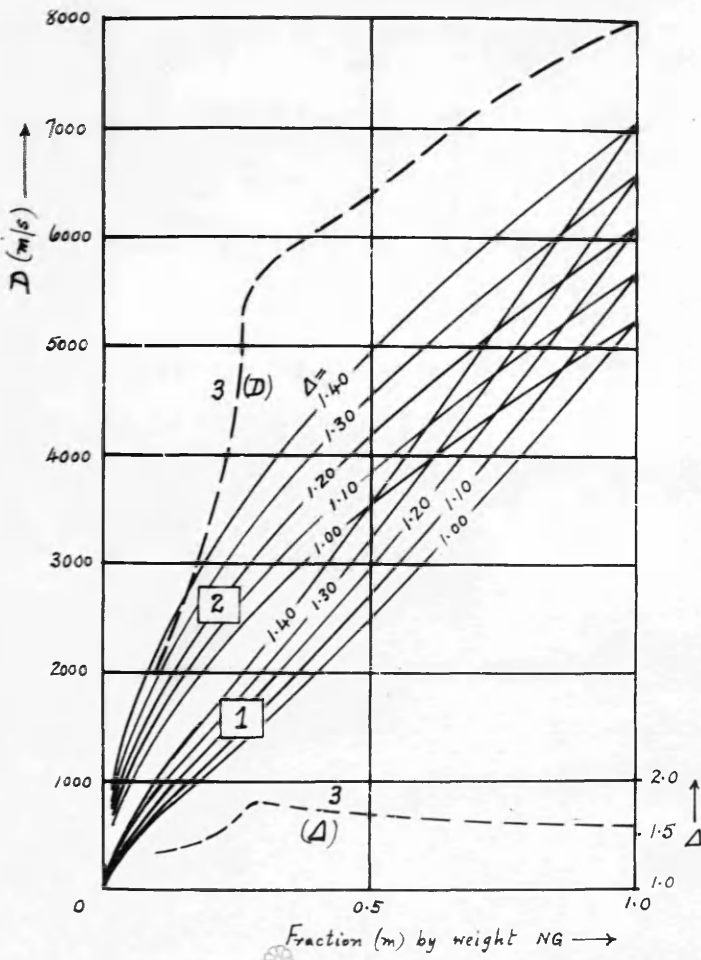


FIG. 18.7:1 NITROGLYCERINE/NaCl MIXTURES.

1: Both entrainment and heat transfer.

2: Entrainment but no heat transfer.

3: As in 2, but at natural densities.

regarding entrainment etc., for a few selected values of m and A .

The results agreed closely with those of Fig. 18.7:1.

Calculations were also made for two nitroglycerine/NaCl mixtures containing small proportions of kieselguhr, which were used in experimental work described below. The velocities are included in Fig. 18.7:3 below.

Experimental: For comparison with the above calculations, a series of velocity measurements was undertaken on mixtures containing 5, 7, 10, 15, 25 and 30% nitroglycerine, gelatinised with appropriate small proportions of nitrocotton. The method of preparing the cartridges and carrying out the measurements was as described in §17 above. As usual, particular care was taken to ensure that the loading density was accurately known and constant for each mixture; and variation between mixtures was in the present case, also reduced to a minimum: for this purpose, minor additions of kieselguhr were made to the 25 and 30% mixtures. Where it was necessary to pass from one sample of NaCl to another, the grist distributions were matched as closely as possible. These precautions should assist to make the results comparable throughout the entire series.

The experimental velocities, measured at the largest diameters by the Dautriche method, checked by an electronic microsecondmeter, and at the smaller sizes by a high-speed camera, are graphed against diameter in Fig. 18.7:2. The curves for 15, 25 and 30% NG are of a rather interesting shape. Up to moderately large diameters (~ 4 inch) the velocity tends in each case towards a limit which lies well beneath the theoretical value based upon thermal insulation of the salt (though above that corresponding to thermal equilibrium).

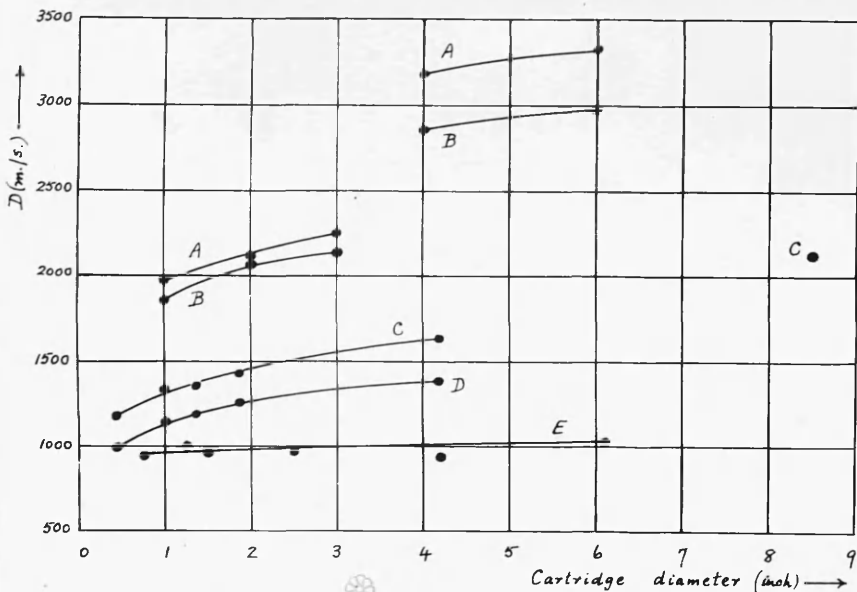


FIG. 18.7:2 NITROGLYCERINE / COMMON SALT MIXTURES.

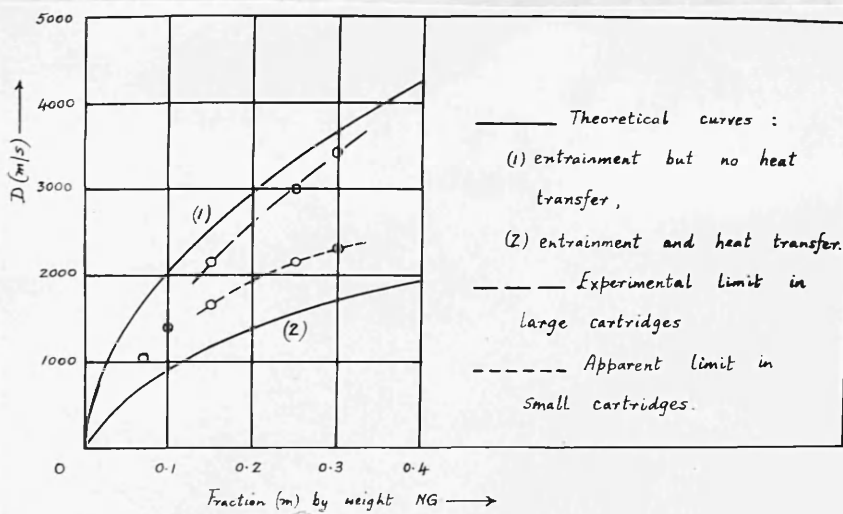


FIG. 18.7:3 NITROGLYCERINE / NaCl MIXTURES.

At the largest diameters, however, considerably higher velocities were recorded, approaching rather well to the upper theoretical limit. This feature is reminiscent of the behaviour of nitroglycerine gelatines described in § 17, and appears to indicate the presence of two velocity levels. Fig. 18.7:3 summarises the results.

§ 18.8 Energy absorbed in compressing inert diluents

In § 15 it was stated that the compressional energy of an inert diluent which absorbed no heat by conduction could be approximately

Δ
 A: NG 30/NaCl 60/gahr 10 1.35
 B: NG 25/NaCl 70/gahr 7 1.35
 C: NG 14.9/NC 0.6/NaCl 85 1.35
 D: NG 9.7/NC 0.3/NaCl 90 1.35
 E: NG 7/NaCl 93 1.33
 (THE 5% MIXTURE
 FAILED TO PROPAGATE IN
 6-INCH DIAMETER.)

assessed by assuming the diluent to have passed through a non-reactive shock to the CJ-pressure p_1 . The energy in question, which is equivalent to a decrement $-\delta Q$, in the heat of reaction Q_r , is then given by

$$\delta Q_r \approx \frac{1}{2} p_1 (1-m) (\varphi_0 - \varphi_r). \quad (1)$$

It may be assumed that D will be nearly proportional to the square-root of the remaining energy. Numerical results for the commercial explosives and a selection of the explosive-inert mixtures considered above are shown in Table 18.8:1. It can be seen that the error in D is in fact unimportant: only in the permitted gelatines does it exceed 1.5%, and in no case is it as large as the experimental uncertainty in D itself.

§ 18.81 Theoretical estimates of heat-transfer to inert diluents

In attempting to estimate theoretically the heat-transfer to an inert diluent within the reaction zone, we meet the following difficulties.

- (a) The reaction time is known only from indirect evidence, and certainly cannot be relied upon to better than an order of magnitude. [82, 57, 39]
- (b) The thermal diffusivity of the diluent is not precisely known, and will not in any case be constant, over the temperature ranges concerned.
- (c) The condition at the surface of a diluent particle cannot be reliably stated, and must frequently involve melting, which invalidates a straightforward application of ordinary diffusion theory.

Table 18.8:1

Effect upon detonation velocity of energy loss in compressing inert diluent

Explosive	m	P_1 ton/in ²	$-3Q_1$ cal/g.	Q_1 cal/g.	% correction to D
2	0.74	243	5.2	510	- 0.51
3	0.88	107	1.16	683	- 0.09
5	0.90	263	2.65	793	- 0.17
6	0.81	227	3.95	739	- 0.27
7	0.65	267	9.3	563	- 0.83
8	0.86	300	4.7	723	- 0.33
9	0.30	190	9.8	367	- 1.34
10	0.84	336	6.5	721	- 0.45
14	0.40	156	5.0	434	- 0.58
15	0.69	140	3.0	583	- 0.26
16	0.70	337	12.2	645	- 0.94
22	0.75	912	32.3	1,130	- 1.43
25	0.69	630	34.3	784	- 2.19
26	0.74	635	29.8	789	- 1.89
39	0.80	275	5.6	635	- 0.44
40	0.85	233	3.1	772	- 0.20
<hr/>					
PETN/NaCl					
	0.01	4	0.014	14.1	- 0.05
	0.02	8	0.043	28.2	- 0.08
	0.05	20	0.207	70.6	- 0.15
	0.1	40	0.65	141	- 0.23
	0.2	80	2.32	282	- 0.41
	0.3	120	4.58	424	- 0.54
	0.5	213	8.9	706	- 0.63
	0.7	320	10.8	988	- 0.55
	0.9	430	6.0	1,271	- 0.24

(d) The diluent may contain a substantial proportion of fine particles, to whose size the method of sieve analysis can only provide an upper limit.

It is clear that precise estimates of heat transfer are out of the question. However, the diffusivity will decrease with rise of temperature, and the presence of a thermal impedance and a region of melting at the surface can only reduce the heat transfer. Thus, if the proportion of "fines" is small, and if we use a low temperature value for the diffusivity, assume temperature continuity at the surface and ignore latent heat, and treat the product gases as a well-stirred fluid, we should arrive at an upper limit to the energy transferred within any given reaction time.

The problem will be further simplified by regarding the diluent as composed of identical spherical particles, plunged at time zero into a finite mass of well-stirred fluid at the CJ-temperature. The solution, [22] which has been given by the writer, expresses the fraction F of the final heat transfer, accomplished within any time t, in terms of dimensionless variables $\tau \equiv kt/a^2$ and $\omega \equiv c_1/c_2$, where k, a, c_1 are the diffusivity, radius and heat capacity of the particles, and c_2 the heat capacity of the fluid. Figure 18.81:1 summarises this solution.

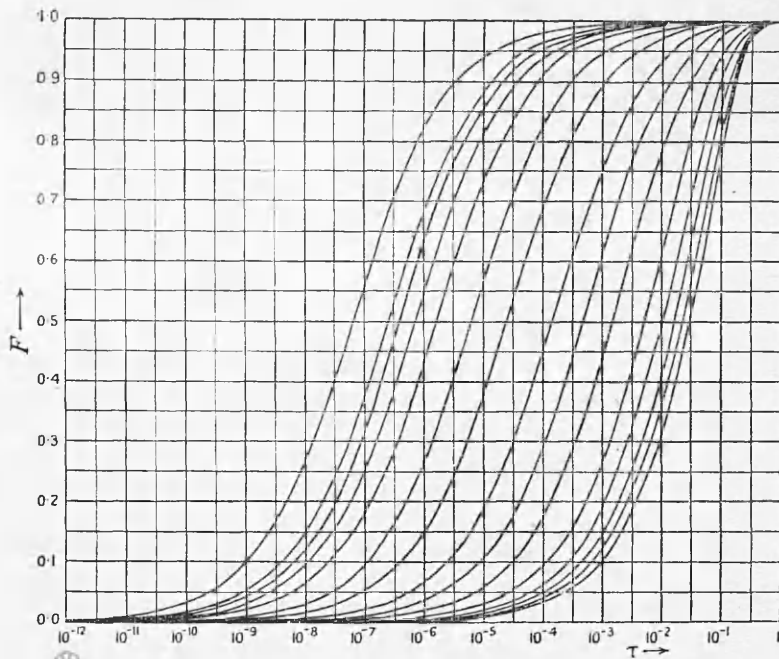


Fig. 18.81:1 Variation of F with τ for various values of w . From left to right the curves correspond to $w = 1000, 500, 400, 300, 200, 100, 50, 20, 10, 5, 2, 1, 0.5, 0.2, 0$.

We shall assume a mean specific heat 0.275 cal./g. for the fluid and 0.375 cal./g. for the diluent. These are of the correct order for typical product gases and for NaCl respectively. Then

$$w = 0.733(1-m)/m. \quad (1)$$

We take $\kappa = 0.025 \text{ cm}^2/\text{sec.}$, and $a = 0.019, 0.010, 0.0055 \text{ cm.}$, corresponding to mean radii of spherical particles in the sieve ranges 30 - 60, 60 - 100, 100 - 200 B.S.S. F may now be read off from Fig. 18.81:1, for each of these radii, in conjunction with times of 1, 5 and 10 $\mu \text{ sec.}$, and for values of $m = 0.9, 0.8, \text{ etc.}$ down to 0.05. The results, which cover the entire practical range, are collected in Table 18.81:1. The proportion of the total heat actually transferred, and the corresponding drop in D are then given by:

$$2 \frac{\delta D}{D} \sim \frac{\delta Q_i}{Q_i} = - \frac{w}{w+1} \cdot F. \quad (2)$$

It can be seen that if $m \geq 0.7$, and if the diluent grist is not

Table 18.81: 1

Fraction (F) of final heat transfer to typical diluent

m	ω	Time			1 u sec.			5 u sec.			10 u sec.			
		B.S.S.	30-60	60-100	100-200	30-60	60-100	100-200	30-60	60-100	100-200	30-60	60-100	100-200
Mean Radius (cm.)		0.019	0.010	0.0055		0.019	0.010	0.0055	0.019	0.010	0.0055			
0.9	0.0814	0.03	0.06	0.10		0.065	0.12	0.22		0.10	0.18		0.32	
0.8	0.183	0.03	0.07	0.11		0.075	0.13	0.23		0.11	0.19		0.33	
0.7	0.314	0.04	0.08	0.12		0.08	0.14	0.25		0.13	0.20		0.36	
0.5	0.733	0.05	0.09	0.16		0.10	0.18	0.30		0.17	0.25		0.43	
0.2	2.93	0.11	0.19	0.30		0.21	0.34	0.51		0.32	0.45		0.52	
0.1	6.60	0.18	0.32	0.48		0.34	0.52	0.70		0.45	0.66		0.80	
0.05	13.9	0.30	0.50	0.66		0.52	0.68	0.82		0.63	0.79		0.87	

appreciably finer than 100 B.S.S., the reduction in velocity cannot exceed about 2.5%. In view of the extreme assumptions made, we may expect it to be much less than this in practice. On the other hand, explosives containing large proportions of diluent, even of relatively coarse grist, may well suffer a major depression of velocity by thermal transfer to the inert component. These conclusions, which are as precise as the present analysis admits, stand in satisfactory agreement with the experimental evidence already reviewed.

§ 18.9 The design of explosives with ultra-low velocities of detonation [F. 164]

It was mentioned in § 18 that the achievement of very low detonation velocities was a problem of practical importance in the design of coal-mining explosives.

The velocity falls, of course, with decrease in loading density. However, not only does this provide no useful solution to the practical problem, since an explosive of extremely low density (even if one could be manufactured) would have correspondingly low power in the borehole, but it does not answer even the theoretical question of realising ultra-low wave velocities: as shown in § 12, D cannot be depressed, by mere reduction in density, below the "ideal" value D_i , which for normal explosives such as nitroglycerine will be of the order of 2,400 m./s.

On the other hand, it appears from § 18.1 that dilution with inert material does provide a method of achieving velocities well below D_i . This can be emphasised by considering equations 18.1 (6,7,8) for $m \ll 1$. Since then Δ_e is small, so also is p_i , and we can replace φ_i by φ_o and D_e by D_i , whereupon

$$\Delta_e = \frac{m\Delta}{1-\Delta\varphi_o}, \quad (1)$$

and so

$$D \doteq D_i \frac{\sqrt{m}}{1 - \Delta\phi_0} . \quad (2)$$

$\Delta\phi_0$ may be given a typical value of 0.6 for lightly pressed powders; then

$$D \doteq 2.5 D_i \sqrt{m} . \quad (3)$$

For example, if $m = 0.01$, $D \doteq D_i/4 \sim 600$ m./s. This conclusion is well borne out in practice, since stable wave velocities of 600-700 m./s. have in fact been recorded with nitroglycerine/diluent mixtures containing a few per cent of the explosive component. [66, 166]

Equation (3) cannot, of course, be expected to apply at indefinitely small values of m . Apart from the fact that ρ_0 will then become important, the probable existence of an activation threshold, disregarded in our treatment, may be expected to define a lower limit of velocity below which stable propagation cannot take place. Questions of "sensitivity" or the conditions under which propagation fails, are, however, outside the scope of this thesis.

In the above discussion, thermal transfer to the diluent has been ignored. Now, it is probable (§§ 18.5, 18.6, 18.7, 18.81) that this transfer can be controlled by suitable choice of grist, and could be made substantial when the proportion of diluent is high; and any such transfer must lead in practice to a reduction in D . Hence, from the standpoint of achieving low velocities, it might seem more natural to consider the most favourable case, that of thermal equilibrium. However, if the diluent is permanently inert, ultra-low velocities can be secured only at the cost of power, and the

resultant explosive, however interesting theoretically, would be useless in blasting practice. In practical applications, therefore, it is necessary to use a diluent which is inert only in what concerns the detonation wave, but is capable of releasing a useful measure of energy at a later stage. But from this point of view, the diluent must evidently be supposed to absorb an insignificant quantity of heat during the primary reaction. The system envisaged above is in line with such assumptions, and there seems no reason to doubt that in small cartridges a two-stage reaction, in which the shock-front is supported only by the first stage, can in fact take place.

CONTINUATION

§19 Structure of the reaction zone in a steady plane detonation wave: introduction

In §9 we have presented the fundamental equations for a steady plane detonation wave in any material, and have described in general terms the structure of the wave. According to this theory the detonation wave is a "reactive shock", that is, a shock wave propagated through the unconsumed explosive, and sustained by the ensuing chemical reaction. In §9.4 the consequences of this view have been further developed, and it has appeared that the pressure, density and translational velocity, after an abrupt rise in the leading shock front, subsequently decline throughout the reaction zone to their values in the CJ-plane; the temperature, however, may be expected to rise continuously, as reaction proceeds in a homogeneous explosive, above the level to which it is suddenly carried in the shock front. The sum of translational and sound velocities must exceed the wave velocity D throughout the reaction zone, and especially at its head, falling to equality with D only in the CJ-plane.

In order to carry out a more detailed analysis of the reaction zone structure, we must return to equations (4) to (6) of §9, which apply at any section in the steady zone. A complete determination would involve the search for time-independent solutions of these equations, together with the chemical kinetic equations and the appropriate equations of state not only for the original explosive and for its final equilibrium products but also for the reacting mixture at every intermediate stage. Without in the first place

attempting this, however, it is possible to simplify the problem if we make the same assumption as in §9.4, namely that the composition is determined by one parameter only in addition to the state variables p and T . For then the distribution of pressure, density and so forth through the steady zone may be evaluated in terms of this single parameter without reference to the reaction kinetics, which are involved only in relating the distribution to time or distance co-ordinates. As was pointed out in §9.4, the assumption proposed is not unreasonable in the case of a condensed explosive. It is less reliable in gases, where the reaction is essentially homogeneous and extremely fast, and several participating processes may have comparable rates. However, since the use of the ideal gas equation permits a simple approximate treatment, we shall indicate the consequences of carrying forward the same simplifying assumption to this case also.

§19.1 Döring's solution for an ideal gaseous explosive

As usual, the subscript o refers to the undisturbed explosive, and the subscript $,$ to the CJ-plane, while unqualified symbols are attached to an arbitrary section within the steady zone. Conditions immediately behind the shock front are distinguished by subscript s . Then, from Table 10:1 we have at once, to a first approximation

$$v_i = \frac{\gamma_i}{\gamma_i + 1} v_o \quad (1)$$

$$p_i = \frac{2Q_i(\gamma_i - 1)}{v_o} = \frac{D^2}{(\gamma_i + 1)v_o} \quad (2)$$

$$T_i = \frac{2Q_i \gamma_i}{(\gamma_i + 1)c_i} = \frac{D^2 \gamma_i}{(\gamma_i - 1)(\gamma_i + 1)^2 c_i} \quad (3)$$

$$W_i = \frac{\sqrt{2Q_i(\gamma_i^2 - 1)}}{\gamma_i + 1} = \frac{D}{\gamma_i + 1} \quad (4)$$

$$a_s = \gamma_s \frac{\sqrt{2\gamma_s(\gamma_s - 1)}}{\gamma_s + 1} = \frac{\gamma_s D}{\gamma_s + 1} \quad (5)$$

and of course,

$$a_s + W_s = D. \quad (6)$$

On the other hand, immediately behind the shock front, where no reaction has taken place, by § 6.23,

$$v_s = \frac{\gamma_s - 1}{\gamma_s + 1} v_0 \quad (7)$$

$$p_s = \frac{2D^2}{(\gamma_s + 1)v_0} \quad (8)$$

$$T_s = \frac{2D^2}{(\gamma_s + 1)^2 c_0} \quad (9)$$

$$W_s = \frac{2D}{\gamma_s + 1} \quad (10)$$

$$a_s = \frac{D}{\gamma_s + 1} \sqrt{2\gamma_s(\gamma_s - 1)}, \quad (11)$$

and it can easily be seen that $a_s + W_s > D$. If we now further assume

$c_0 = c$, $\gamma_0 = \gamma$, $\equiv \gamma$, then

$$2 \frac{v_s}{v_i} = \left(\frac{a_s}{a_i} \right)^2 = \frac{T_s}{T_i} = 2 \frac{\gamma - 1}{\gamma} \quad (12)$$

$$\frac{p_s}{p_i} = \frac{W_s}{W_i} = 2. \quad (13)$$

These equations relate the values of v , p etc, at the two extremities X_s, X_i of the steady zone. The pressure and streaming velocity are just twice as large in the shock front as at the CJ-plane. The temperature is one-third to four-fifths as high. The greatest variation is in the density which, if $\gamma = 1.2$ for example, falls by a ratio of six to one from X_s to X_i . At any intermediate section, where a fraction c of the final release of chemical energy has occurred, the RH-equation may be written, to

the same approximation as before:

$$\frac{Pv}{\gamma-1} - cQ_1 = \frac{1}{2}P(v_o - v). \quad (14)$$

When P , v_o and Q_1 are eliminated from (14) by means of (1, 4) and 9(11) there results

$$\frac{v}{v_i} = \frac{\gamma - \sqrt{1-c}}{\gamma}, \quad (15)$$

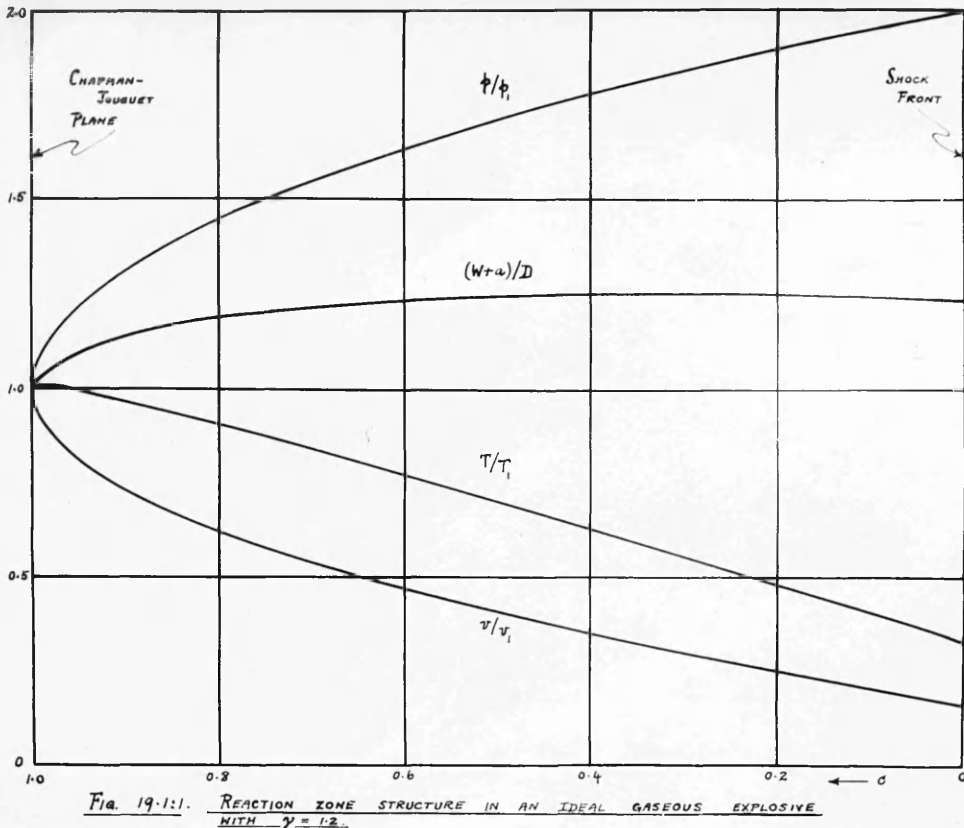
whereupon

$$\frac{W}{W_i} = \frac{P}{P_i} = 1 + \sqrt{1-c}, \quad (16)$$

$$\left(\frac{a}{a_i}\right)^2 = \frac{T}{T_i} = \frac{(\gamma - \sqrt{1-c})(1 + \sqrt{1-c})}{\gamma}. \quad (17)$$

(15)-(17) express the manner of variation of v , P etc. within the steady zone: they were derived by Döring by a more complicated method. It is easy to see that v increases throughout with c , and W, P decrease. T on the whole increases, but reaches a maximum value $(\gamma+1)^2 T_i / 4\gamma$ when $c = (3-\gamma)(\gamma+1)/4$, thereafter declining again slightly to T_i . $W+a$ always exceeds D for $c < 1$, though it may not always change monotonically.

In fact, if $\gamma < (7-\sqrt{17})/2 = 1.44\dots$, $/$ passes through a maximum equal to $\frac{1}{2}(1 + \sqrt{\gamma+1})$ where $2\sqrt{1-c} = \gamma-1 + \sqrt{\gamma+1}$. Figure 19.1:1 illustrates the way in which the pressure, temperature etc. vary with the fraction c for $\gamma = 1.2$.



§ 19.2 Time- and distance-profiles for an ideal gaseous explosive

The above case is naturally much idealised. It would be quite possible to carry out more detailed calculations of the same sort, making due allowance for changes in composition and so forth, for any system whose state can be defined by three variables only: t, T, c .
[52]
 For example, Döring suggests the case of electrolytic gas, assuming that the only participating process is



However, the neglect of reactions involving H, O and OH would certainly have a substantial effect upon the numerical results, which would therefore be no more reliable than those derived from the ideal theory. But if auxiliary reactions are to be taken into account it becomes

S. S.

impossible to determine the wave structure without reference to the kinetic equations themselves. Although such a complete analysis could in principle be made, it would evidently be laborious. On the other hand, if we restrict ourselves to the ideal case, an approximate idea of the nature of the space- and time- distributions may be reached. For this purpose it is necessary to complete the solution 19.1 (15, 16, 17) by evaluating c as a function of time or distance. We use a system of space-coordinates travelling with the wave, the origin being fixed in the shock-front and the positive y -direction towards the reaction products. Since the wave is steady, c , and so also v, ρ etc. are functions of y only. In the moving reference system the material at y has translational velocity $u = D - W$, so that the reaction kinetic equation may be written

$$\left(\frac{dc}{dt} \right) = (D - W) \frac{dc}{dy} = F(\rho, T, c), \quad (1)$$

where F is supposed known, and (dc/dt) represents the usual "massbound" derivative, that is, the rate of change of c for each material element as it moves across the section y . However, if c is taken to represent the fraction consumed from one of the species originally present, in which the reaction is monomolecular then,

$$\frac{1}{\mu} \left(\frac{d\mu}{dt} \right) = -Z e^{-A/RT}, \quad (2)$$

where

$$\mu \equiv (1-c)\rho. \quad (3)$$

Z is an approximately constant frequency factor and A the activation energy per mole. In a constant-volume reaction (2) becomes

$$\left(\frac{dc}{dt} \right) = Z(1-c) e^{-A/RT}, \quad (4)$$

and in such a reaction, proceeding from T_s to T_i ,

$$T_i - T = (T_i - T_s)(1 - e^{-\xi}), \quad (5)$$

so that, by (4)

$$\left(\frac{dT}{dt}\right) = Z(T_i - T)e^{-A/RT}. \quad (6)$$

[71, 57]
The appropriate solution is

$$Zt = Ei(\xi) - Ei(\xi_s) + e^{\xi} [Ei(\xi_s - \xi_i) - Ei(\xi - \xi_i)], \quad (7)$$

where $\xi \equiv A/RT$, etc., and

$$Ei(x) \equiv \int_{-\infty}^x e^y dy / y. \quad (8)$$

According to (7), $T(t)$ approaches T_i along a sigmoid curve, whose point of inflexion is located at T' , where $\left(\frac{dT}{dt^2}\right)_{T=T'} = 0$, that is, where

$$\xi'(\xi' - \xi_i) = \xi_i. \quad (9)$$

If $\xi_i > 4$, (9) leads approximately to

$$\xi' = \xi_i + 1, \quad (10)$$

whereupon the first and last terms on the right of (7) may be neglected at the point of inflexion. To the same approximation, we replace $Ei(x)$ by e^x/x in the other terms, so that

$$Zt' \doteq \frac{\xi_i e^{\xi_s}}{\xi_s (\xi_s - \xi_i)} = \frac{RT_s^2}{A(T_i - T_s)} e^{A/RT_s}. \quad (11)$$

For small values of ξ_i , the inflexion is very sharp, almost the entire course of the reaction being confined within an extremely short

time-interval on either side of $t = t'$. When ξ_s is larger, the acceleration will tend to be rather less abrupt. Examples are shown in Figure 19.2:1

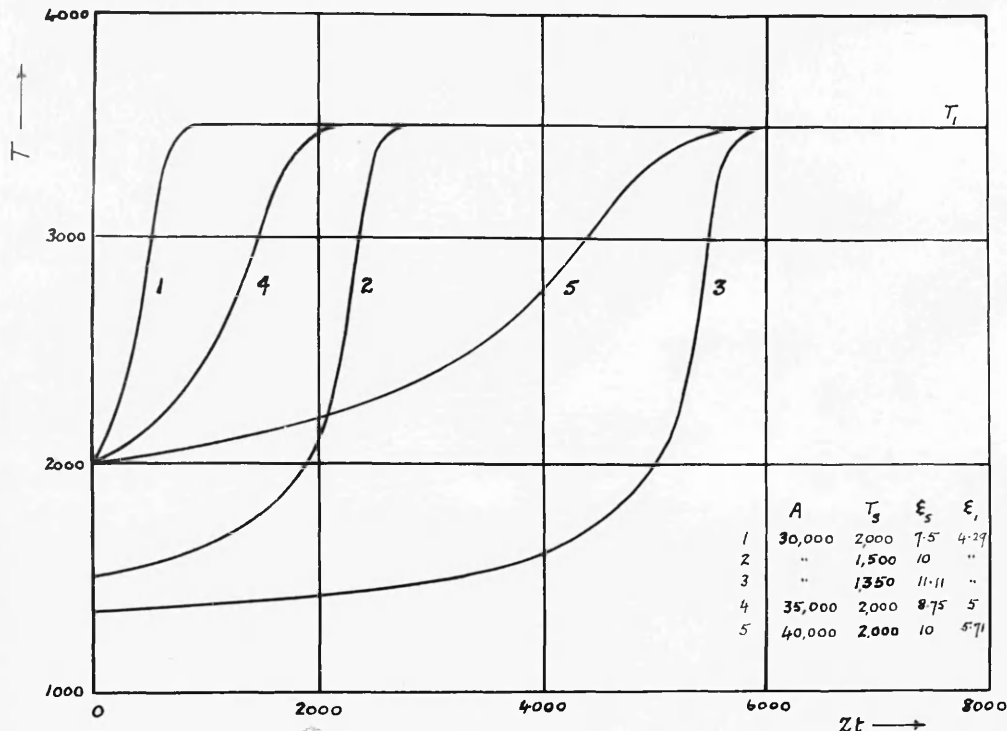


FIG 19.2:1. THE RISE IN TEMPERATURE IN A CONSTANT-VOLUME ADIABATIC THERMAL EXPLOSION.

It is clear from (6) or (7) that a single curve can be used to describe the course of T in all constant-volume adiabatic thermal explosions for which ξ_s and Z have the same values. The initial temperature, as expressed by ξ_s , does not affect the curvature of this curve at any given T , but merely selects the point on it corresponding to $t = 0$. In other words, ξ_s determines only the length [57]

of the induction time t' . When ξ_s is large (T_s small), t' will be relatively long; when ξ_s is small (T_s large), relatively short.

The above considerations refer to a constant-volume reaction, and are not therefore strictly valid for the detonation wave. However, the general nature of the results will remain unaffected. Since T , as represented by 19.1(17), is not far from linear in c , (2) and 19.1(15, 17) lead approximately to

$$\left(\frac{dT}{dt}\right) = BZ(T_i - T)e^{-A/RT}, \quad (12)$$

where B varies only between $\frac{2(\gamma-1)}{2\gamma-1}$ and 1. The progress of the reaction is therefore modified only to a secondary extent by the departure from constant-volume conditions. As an example we have taken $\gamma = 1.2$, $A = 30,000$ cal./mol $T_i = 3,500^{\circ}\text{K}$, and evaluated c by numerical methods as a function of Zt , where t is measured from the instant at which the material element under consideration passes through the shock-front. The pressure, temperature, etc. are then derived immediately from 19.1 (15, 16, 17), and the space-distribution from (1) in the form

$$\frac{Zy}{W_i} = \int_0^c (\gamma - \sqrt{1-c}) \frac{d(Zt)}{dc} dc. \quad (13)$$

The various profiles are shown in Figs. 19.2:2 and 19.2:3. They must be regarded as illustrative only. The presence of an appreciable induction time is a consequence of the particular values of γ , A and T_i used: if A were only 20,000 cal./mol. say, or $\gamma = 1.4$, T_i remaining unchanged, there would be no significant induction period.

The "reaction time" is extremely short: if $Z \sim 10^{14}$, it is of

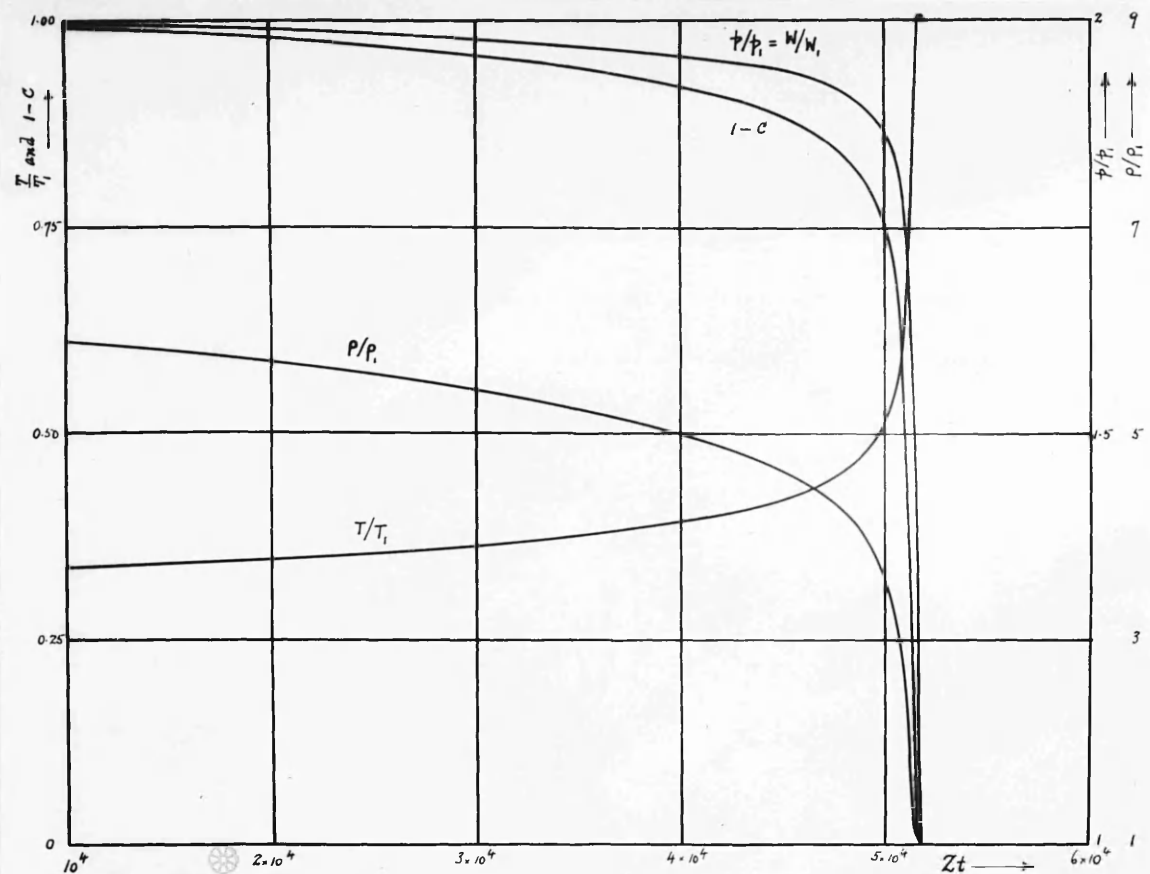


FIG. 19-2:2 REACTION ZONE STRUCTURE : IDEAL GASEOUS EXPLOSIVE.

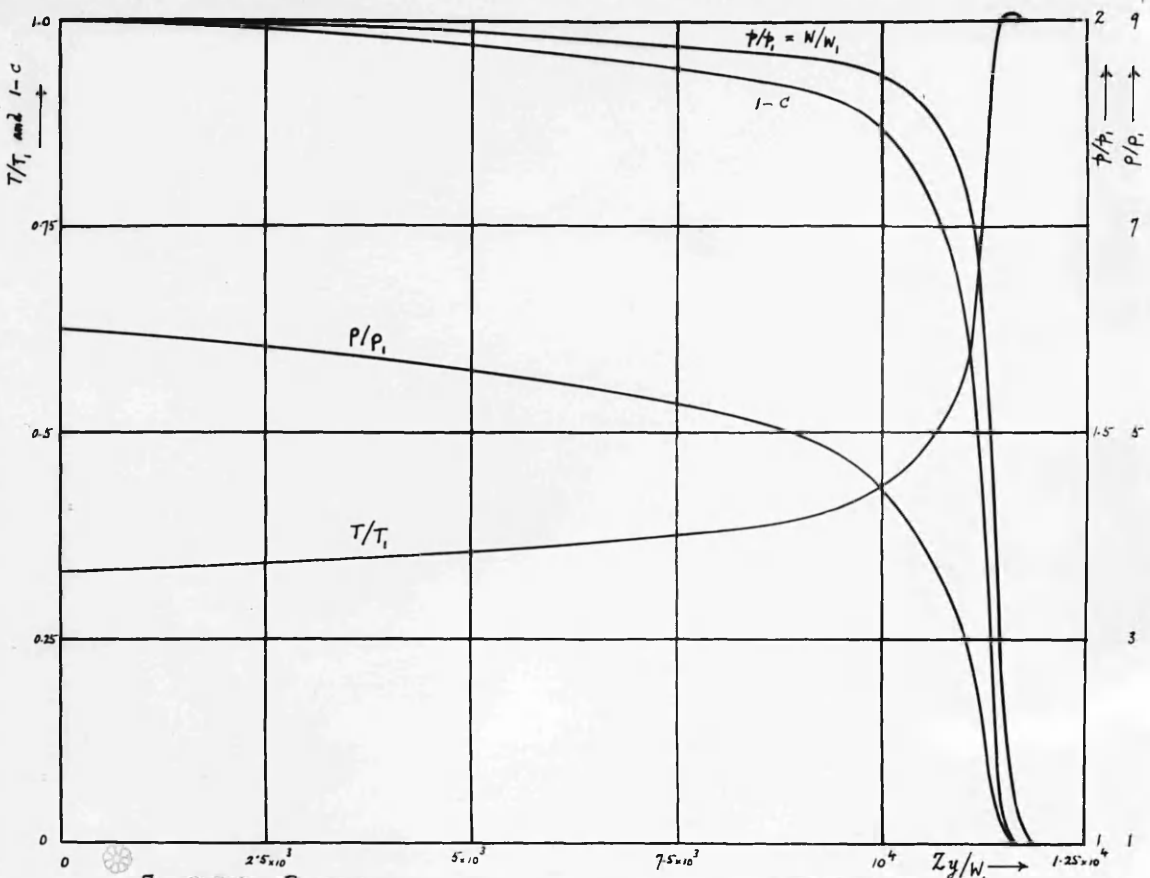


FIG. 19-2:3. REACTION ZONE STRUCTURE : IDEAL GASEOUS EXPLOSIVE.

order 10^{-9} sec. The corresponding reaction zone length $\sim 10^{-5}$ cm. Of course, if Z and A are of the order specified, it is inevitable that the reaction time should be of this order, in view of the very high initial temperature produced in the leading shock. There is no difficulty from a physical standpoint in accepting a reaction time even as short as 10^{-9} sec. since 10^5 vibrations can occur in this time; nor in accepting a reaction zone length of order 10^{-5} cm., since this will contain some 100 mean free paths. For comparison, the thickness of the leading shock is of order 10^{-7} cm. a negligible length on the scale of Fig. 19.2:3. For $Z < 10^{14}$, the reaction time and zone width would be greater, and the shock-thickness relatively even less important.

It may be noted that the zone-width is considerably less than $D \times$ the reaction time. This is because W is high throughout most of the zone; by 9.1(10), if $\gamma_0 = 1.4$, W is almost as large as D immediately behind the shock-front, and Figs. 19.2:2, 3 show that $D-W$ does not become large until we approach the CJ-plane.

§ 19.3 Structure of the reaction-zone in a condensed explosive

Analysis of the reaction-zone structure for a condensed explosive presents much greater difficulties. Even if we simplify the problem by assuming perfect homogeneity at every stage, it is a formidable task to supply an equation of state which will describe the reacting material as it passes continuously from the original liquid or solid explosive to the appropriate equilibrium products. It is not, indeed, difficult to derive equations parallel to 9.1(15, 16, 17) on the basis

170

of the Abel equation with constant covolume, and the resultant
[57] wave structure is, broadly speaking, very similar to that shown in
Fig. 19.1:1. However, most condensed explosives have a granular
structure, and the marked effects of grain size upon the behaviour of
the detonation wave make it appear probable that reaction frequently
consists in surface burning of the grains. Even apparently
homogeneous liquids such as nitroglycerine may decompose heterogeneously
from reaction nuclei provided by minute discontinuities of one kind or
another, for example gas bubbles.^[14] In such cases, the partially reacted
material will consist of solid or liquid fragments burning in a gaseous
atmosphere which is constantly augmented by the products of their
decomposition. The temperatures of the two phases at any stage will
certainly differ, and it is not even certain that they share the same
translational velocity. Compression of the unreacted particles also
requires to be taken into account. Under such circumstances, the
assumption of a homogeneous process is evidently a poor approximation.

We shall rather assume that, at any intermediate stage in the
reaction of a typical element of explosive, part of the element has
been transformed into gaseous products in effective chemical
equilibrium, while the remainder is still in its original condensed
state. It will further be assumed, in conformity with the arguments
of §§ 18.6, 18.7, 18.81, that this unreacted portion, though it may
have absorbed energy by compression, has not been significantly heated
by thermal diffusion from the hot gases. Finally, in keeping with
the assumptions made at the CJ-plane, we shall regard the condensed

and gaseous phases in any section as sharing a common velocity W , so that conservation of mass, momentum and energy may be expressed by the usual simple equations.

At the section corresponding to W , let a fraction c of the explosive have reacted and reached equilibrium, so that a fraction $m = m_0 + c(1-m_0)$ by mass of the element is gaseous, where m_0 is the mass of gas (air) present in unit mass of the undetonated material. Except when C is very small, m is indistinguishable from c , but the use of m allows the equations to be applied up to the shock-front. We also assume, for simplicity, that the composition of the reacted phase is independent of C : this will not of course, in general be true, but the simplification should not seriously affect the results. Then, if accented symbols refer throughout to properties of the gas phase, reckoned per unit mass of that phase, and ε, φ are the internal energy and specific volume of the diluent, the RH-family is

$$m(E' - E'_{NTP}) + (1-m)(\varepsilon - \varepsilon_{NTP}) = cQ_i + \frac{1}{2}(\dot{p} + p_0)(v_0 - v). \quad (1)$$

If we now regard the diluent as having traversed a simple shock from \dot{p}_0 to \dot{p} , then

$$\varepsilon - \varepsilon_{NTP} = \frac{1}{2}(\dot{p} + p_0)(\varphi_0 - \varphi). \quad (2)$$

In view of the relatively small compressibility of liquids and solids, and the assumption of negligible heat transfer, this term will in any case be a minor one, except perhaps at small c , and the above rough formulation simplifies (1), which with the relations

$$v_0 = m_0 v'_0 + (1-m_0) \varphi_0, \quad (3)$$

$$v = m v' + (1-m) \varphi , \quad (4)$$

becomes

$$m(E' - E'_{NTP}) = cQ_1 + \frac{1}{2}(\dot{p} + \dot{p}_0)[m_0 v'_0 - m v' + (m - m_0)\varphi_0] . \quad (5)$$

By means of the equations of state for the gas phase, (5) can now be expressed in terms of \dot{p} and v' , whereupon the intermediate RH-equation relating \dot{p}, v follows from (4), provided $\varphi(\dot{p})$ is known.

(5) can be simplified when $c=0$, or when m is not very small. In the former case, which corresponds to conditions immediately behind the leading non-reactive shock, we set $m=m_0$, whereupon

$$E' - E'_{NTP} = \frac{1}{2}(\dot{p} + \dot{p}_0)(v'_0 - v') . \quad (6)$$

This is identical with the RH-equation for shocks in the gas (air) originally present. If this gas behaves ideally, with constant specific heat ratio γ , then (6) becomes

$$\frac{v'}{v'_0} = \frac{\dot{p}/\dot{p}_0 + \lambda}{\lambda \dot{p}/\dot{p}_0 + 1} , \quad (7)$$

where $\lambda \equiv (\gamma+1)/(\gamma-1)$. When $\dot{p}/\dot{p}_0 \gg 1$, (7) reduces to

$$v' = v'_0 / \lambda . \quad (8)$$

According to the present assumptions, therefore, the gas pockets suffer only a moderate compression in the shock-front, and must therefore reach extremely high temperatures.

Again, when m is not very small, $m \approx c$, and m_0/m is negligible, whence

$$E' - E'_{NTP} = Q_1 + \frac{1}{2c}(\dot{p} + p_0)[v_0 - \varphi_0 - c(v' - \varphi_0)]. \quad (9)$$

In particular, when $c = 1$ and so $v' = v_1$, this becomes

$$E_1 - E'_1 = Q_1 + \frac{1}{2}(\dot{p} + p_0)(v_0 - v_1), \quad (10)$$

which is the usual RH-equation for equilibrium.

When the RH-family of curves has been drawn, by means of (6) and (9), the pressure, density and streaming velocity are obtained as functions of c by intersecting the family with the tangent to the final curve ($c = 1$). The gas phase temperature is determined from \dot{p} , v' and the equation of state. The temperature reached by shock-wave compression, according to (2), in the partially reacted explosive particles can be estimated from \dot{p} , if an equation of state is assumed for the condensed explosive material.

§ 19.4 Application to PETN

The analysis of § 19.3 has been applied to PETN. The equation of state used for the gaseous phase in the reacting material is 13.3(5), i.e.

$$\dot{p}(v' - \alpha) = n'RT, \quad (1)$$

where n' is the number of gaseous moles per gm. of gas, and α is a function of v' defined as in 13.3 (12-15). Subject to this state equation, $E' - E'_{NTP}$ is a function of temperature only, provided either that the product composition is independent of temperature and pressure,

or that the covolume a is independent of composition. The former condition is well fulfilled in explosives of approximate oxygen balance over an adequate range of T, p . The (E', T) -relation is found, in fact, to be closely linear for PETN between 2,000 and 5,500°K, and can be represented over that range by

$$E' - E'_{273} = 0.371T - 279 \text{ cal./g.} \quad (2)$$

The following values indicate the accuracy of fit, which justifies extrapolation to, say, 10,000°K

$T^{\circ}\text{K}$	2,000	2,500	3,000	3,500	4,000	4,500	5,000	5,500
$E' - E'_{273}$ (cal/g)	488	658	834	1,014	1,197	1,387	1,575	1,765
Equation (2)	463	649	831	1,020	1,206	1,391	1,577	1,763

In (2), we eliminate T by means of (1). Then, if ρ_0 is neglected and Q_0 set = 1,412 cal./g. (Table 14.3:3), $\varphi_0 = 0.565 \text{ cm}^3/\text{g}$, the RH-equation 19.3(9) becomes

$$\frac{p}{\rho} (\text{atm.}) = \frac{6.98 \times 10^4}{5.8v' - 5.3\alpha - 0.2825 - \frac{v_0 - 0.2825}{C}} \quad (3)$$

The RH(p, v)-equation follows from (3) and 19.3(4). To estimate φ , the compression was regarded as isothermal, and in the absence of relevant data PETN was assumed to compress like NaCl. Thus (cf. §15.11),

$$\varphi = 0.565 \frac{\frac{p + 2 \times 10^5}{\rho} - 5^5}{1.8p + 2 \times 10^5} \text{ cm}^3/\text{g} \quad (4)$$

where ρ is in atm. This approximation is, of course, crude, but it probably introduces only minor errors.

The calculations were made over the range of c at $\Delta = 0.5$, 0.75 and 1.0 g./cm³. The RH-families are shown in Figs. 19.4:1,2,3. To complete each family, it was still necessary to draw the curve $c=0$, defined by 19.3(6), or by 19.3(7) if the gas (air) originally present can be taken as ideal. However, the theoretical temperatures in the gas-pockets at the shock-front turn out to be so extreme that the ideal gas equation is quite inadequate, and account has even to be taken of dissociation and ionization. For air, we, therefore, use the data of § 6.3, whereupon 19.3(7) is replaced by the pressure-density relation of Fig. 6.3:2. φ follows from (4) and v from 19.3(4) with $m = m_0$. The RH-curves are drawn in Figs. 19.4: 1,2,3.

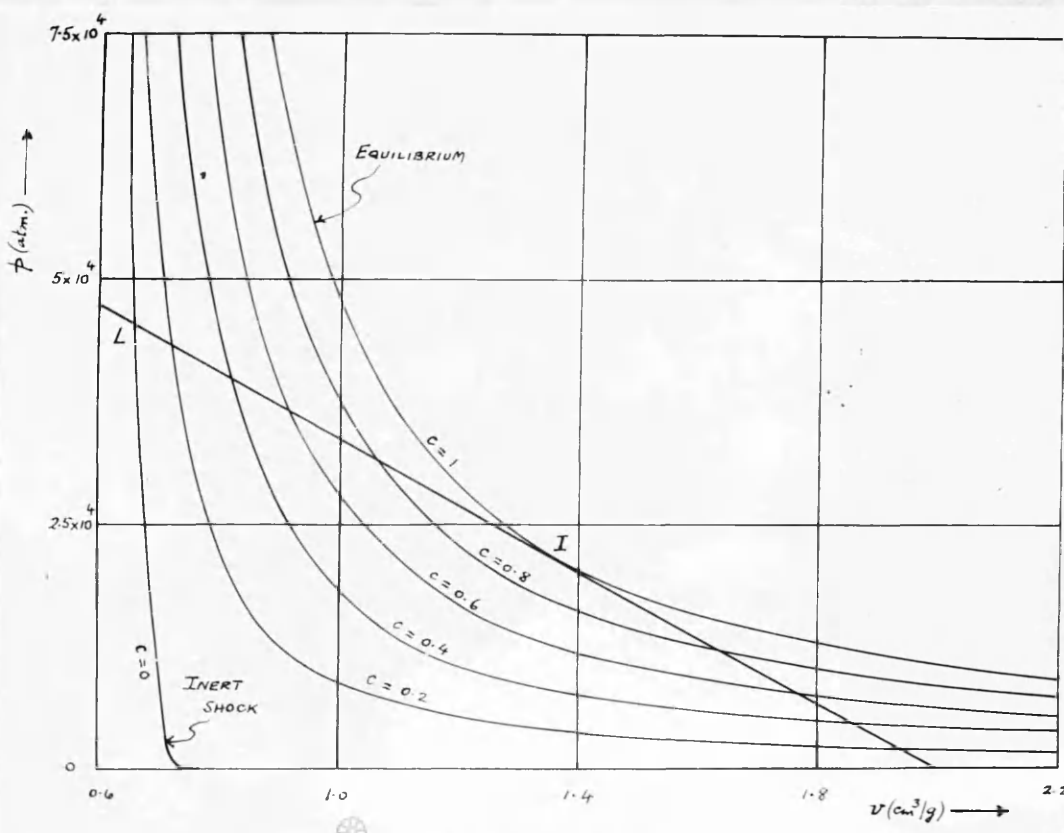
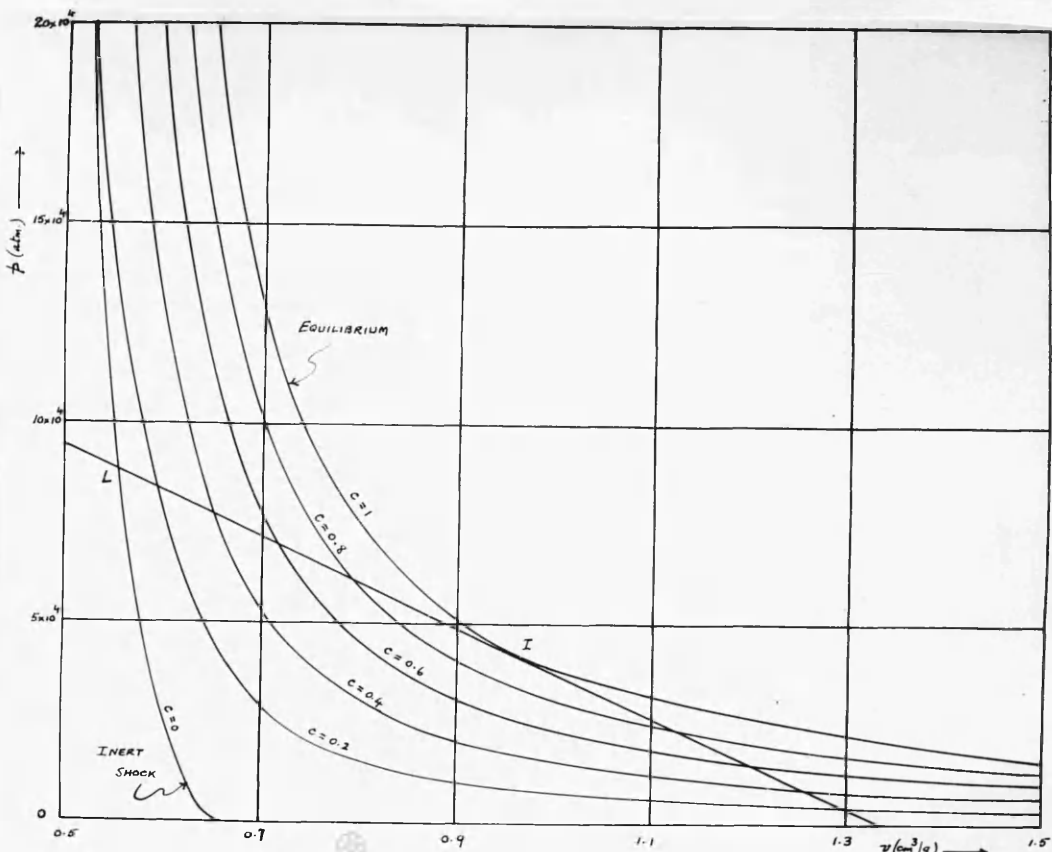
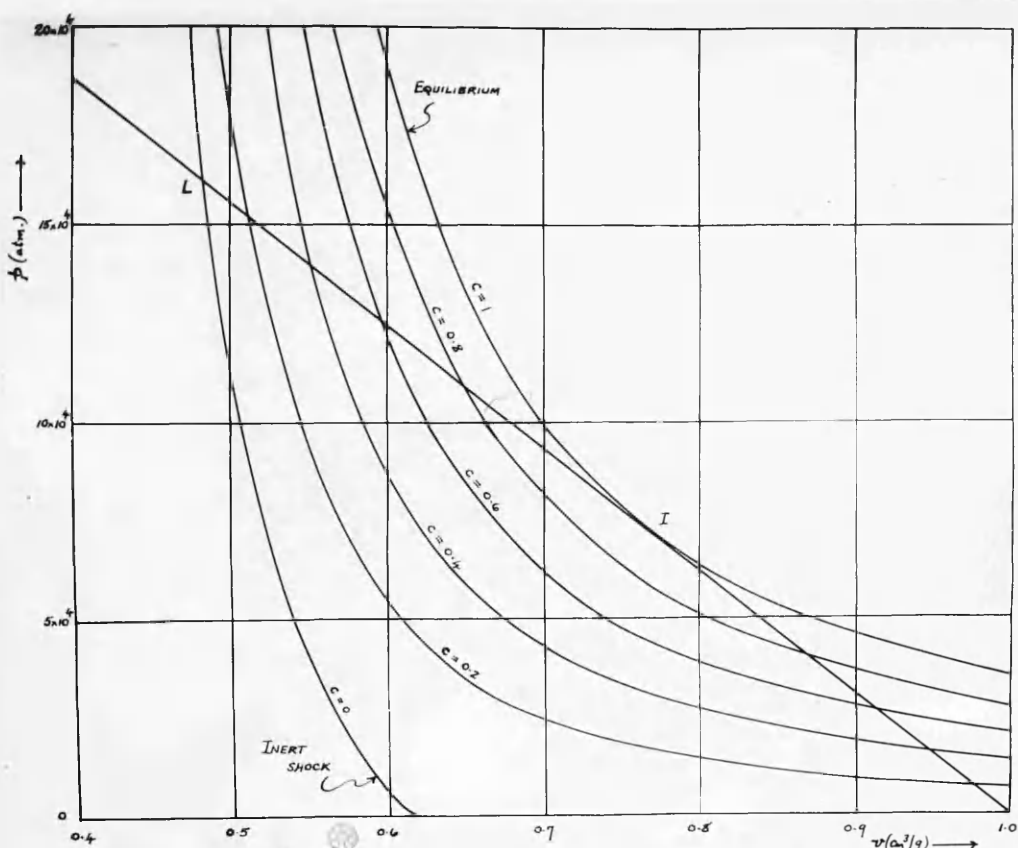


FIG. 19.4:1. RH-DIAGRAM FOR DETONATION IN PETN, $\Delta = 0.5 \text{ g/cm}^3$

FIG. 19.4:2 RH-DIAGRAM FOR DETONATION IN PETN, $\Delta = 0.75 \text{ g/cm}^3$.FIG. 19.4:3. RH-DIAGRAM FOR DETONATION IN PETN, $\Delta = 1.0 \text{ g/cm}^3$.

The intersections of the RH-family with the tangent to $C = 1$ determine ρ, v etc. as functions of C . Fig. 19.4:4 illustrates the course of these functions for $\Delta = 1.0 \text{ g./cm}^3$; the other two loading densities give similar profiles. Numerical values for all three densities are collected in Table 19.4:1. For comparison, the table also includes values calculated from equations 19(15, 16, 17) with $\gamma = 3$, an order of value for the adiabatic index ($-d\log p/d\log v$)_{102,136,83} suggested by various workers. It can be seen that the behaviour of v, ρ and W at the higher loading densities approaches that of the idealised homogeneous material with $\gamma = 3$. The temperature in the gas phase, however, behaves in quite a different manner, falling from an extremely high level in the shock-front to the equilibrium value T , at the CJ-plane. In fact, according to the present theory, the gaseous temperature is determined principally by compression, and only to a minor extent and in the rear of the reaction zone by release of chemical energy.

Conditions in the shock-front have also been calculated for $\Delta = 1.25$ and 1.5 g./cm.^3 , though the rest of the structure has not been analysed in detail for these densities. Table 19.4:2 summarises the shock-front variables over the range of Δ considered, and shows how they compare with the CJ-values.

An estimate of the temperatures produced by compression of the condensed phase can be made by following the line of thought which led to 19.3(2). The temperature of the explosive fragments at any section where the pressure is ρ will then be the shock temperature corresponding to ρ . Of course, we do not have the requisite physical data for PETN to enable such temperatures to be properly calculated. However,

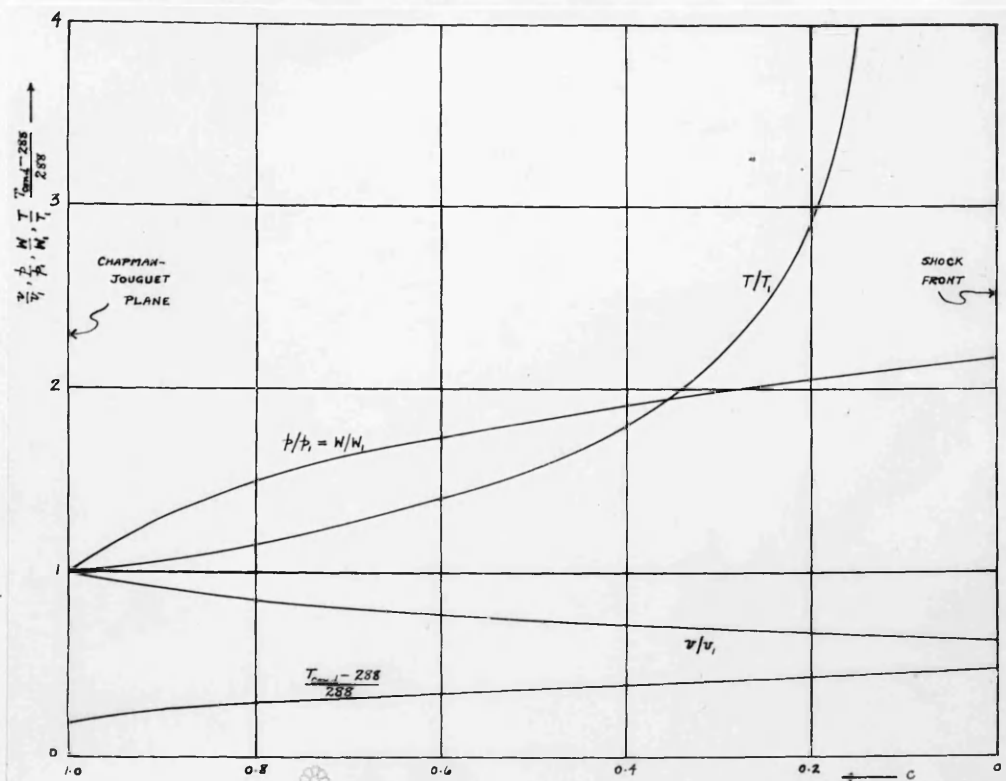


FIG. 19.4:4. REACTION ZONE STRUCTURE IN PETN, $\Delta = 1.0 \text{ g/cm}^3$.

Table 19.4:1

Reaction zone structure in PETN at $\Delta = 0.5, 0.75, 1.0 \text{ g./cm}^3$.

Δ	v/v_I	$p/p_I = w/w_I$	T/T_I	$T_{\text{cond}} - 288(\text{o})$
0	0.5 : 0.75 : 1.00	* : 0.5 : 0.75 : 1.00	* : 0.5 : 0.75 : 1.00	* : 0.5 : 0.75 : 1.00
0.2	0.48 : 0.58 : 0.63 : 0.67 : 0.70 : 0.71 : 0.74 : 0.79 : 0.83 : 0.87 : 0.90 : 0.93 : 0.96 : 0.98 : 1.00	: 2.13 : 2.10 : 2.18 : 2	: 34.6 : 61.6 : 110.7	: 1.333 : 56 : 135 : 332
0.4	0.52 : 0.61 : 0.66 : 0.70 : 0.71 : 0.74 : 0.88 : 1.00 : 1.12 : 1.25 : 1.38 : 1.51 : 1.64 : 1.78 : 1.91 : 2.04	: 2.06 : 1.90	: 2.69 : 2.87	: 2.90 : 1.33 : 51 : 125 : 307
0.6	0.66 : 0.73 : 0.77 : 0.79 : 0.81 : 0.84 : 0.88 : 0.92 : 0.96 : 1.00 : 1.04 : 1.08 : 1.12 : 1.16 : 1.20 : 1.24	: 1.67 : 1.73 : 1.63	: 1.35 : 1.36	: 1.40 : 1.29 : 42 : 98 : 232
0.8	0.76 : 0.83 : 0.84 : 0.85 : 0.88 : 0.91 : 0.95 : 1.00 : 1.04 : 1.08 : 1.12 : 1.16 : 1.20 : 1.24 : 1.28 : 1.32	: 1.50 : 1.45	: 1.12 : 1.15	: 1.15 : 1.23 : 34 : 82 : 190
1.0	1.00 : 1.00 : 1.00 : 1.00 : 1.00 : 1.00 : 1.00 : 1.00 : 1.00 : 1.00 : 1.00 : 1.00 : 1.00 : 1.00 : 1.00	: 1.00 : 1.00	: 1.00 : 1.00	: (23) : (50) : (105)

* Calculated from equations 19(15, 16, 17) with $\gamma = 3$.

The CJ-values are as follows:

Δ	v_I	p_I	T_I	w_I
0.5	1.36	0.97	41,900	1,240
0.75	21,300	73,800 atm.	5,060	1,340 m/s.
1.0	5,000	5,150 K.	5,060	1,340 m/s.

$T_{\text{cond}} - 288(\text{o})$

$0.5 : 0.75 : 1.00$

$0.5 : 0.75$

42

98

232

$51 : 125$

$51 : 125$

307

$135 : 332$

$135 : 332$

332

Table 19.4:2

Conditions at the shock-front (suffix s) and at the CJ-plane
 (suffix $,$) in PETN. ρ denotes overall density and
 ρ' density of gaseous phase alone

Δ (gm./cm ³)	0.5	0.75	1.00	1.25	1.50
D (m./s.)	3,670	4,520	5,560	6,800	8,150
T_s (°K)	173,000	312,000	570,000	850,000	1,160,000
($T_{\text{cond}}s$) (°K)	344	423	620	1,070	1,935
T_c (°K)	11,300	19,000	29,000	50,000	68,000
T_i (°K)	5,000	5,060	5,150	5,220	5,340
p_s (atm.)	45,400	88,000	160,900	275,000	427,000
p_i (atm.)	21,300	41,900	73,800	121,000	188,000
W_s (m./s.)	2,500	2,600	2,920	3,250	3,520
W_i (m./s.)	1,175	1,240	1,340	1,430	1,550
$p_s/p_i = W_s/W_i$	2.13	2.10	2.18	2.77	2.77
p_s'/ρ'_0	8.58	7.30	6.42	7.05	6.95
ρ_s/Δ	3.05	2.40	2.08	1.92	1.77
ρ_i/Δ	1.47	1.38	1.31	1.27	1.23
p_s/ρ_i	2.08	1.74	1.59	1.51	1.44

consistently with equation (4), they may be very roughly assessed by comparison with those already derived for NaCl (§ 6.58). If the NaCl satisfies a state equation

$$p\varphi = a\varphi^{-\ell} - c\varphi^{-1} + eT, \quad (5)$$

where a , b , c , e are constants, and if we assume that the expansion coefficient and compressibility of PETN at NTP are equal to those for NaCl, and that the pressure along the isotherm through NTP is the same function of φ/φ_0 for both substances (all which assumptions are consistent with (4)), then the state equation for PETN is

$$k p\varphi = (ak^{-\ell})\varphi^{-\ell} - (ck^{-1})\varphi^{-1} + eT, \quad (6)$$

where k is the ratio of densities at NTP, that is, $k = 1.77/2.17 = 0.815$. Now, by equations 6.53 (6,8),

$$\begin{aligned} (T-T_0) \frac{e}{\varphi} \left[\frac{1}{G} \frac{\varphi}{\varphi_0} - \frac{1}{2} \left(1 - \frac{\varphi}{\varphi_0} \right) \right] &= \frac{c}{2\varphi_0^2} \left(3 - \frac{\varphi_0}{\varphi} \right) \left(\frac{\varphi_0}{\varphi} - 1 \right) \\ &\quad - \frac{a}{\varphi_0^{\ell+1}} \left[\frac{1}{\ell} - \frac{1}{2} \left(\frac{\varphi_0}{\varphi} - 1 \right) \right] \left(\frac{\varphi_0^\ell}{\varphi} - 1 \right), \end{aligned} \quad (7)$$

where T is the shock temperature corresponding to φ and $G = e/c_v$ is Grüneisen's constant. But if NaCl and PETN are compressed through the same ratio φ/φ_0 , the right side of (7) has, by (6), the same value in each case. So also has e/φ . Consequently,

$$\frac{T_{PETN} - T_0}{T_{NaCl} - T_0} = \frac{\frac{1}{G} - \frac{1}{2} \left(\frac{\varphi_0}{\varphi} - 1 \right)}{\frac{1}{G'} - \frac{1}{2} \left(\frac{\varphi_0}{\varphi} - 1 \right)}, \quad (8)$$

where G refers to NaCl and G' to PETN. Since $G = 3$ and $G'/G = c_v/k c'_v \sim 1/3$, we conclude that $G' \sim 1$. By means of the shock-wave data previously tabulated for NaCl, the compressional heating $T_{cond} - T_0$ of the explosive fragments can be estimated for each

pressure. The results are included in Tables 19.4:1, 2 and Fig. 19.4:4. They cannot be expected to have more than a qualitative significance, but they certainly suggest only a slight compressive heating, except at the highest loading densities.

The enormous shock-front air pocket temperatures shown in Table 19.4:2 must be treated with reserve. In formulating the present theory we have taken account of the heterogeneous nature of the explosive only in one sense. That is to say, the presence of two phases is recognised and allowed for, but the finite size of the unit of each phase - the explosive particle or gas pocket - is disregarded. This means, in effect, that from a hydrodynamic standpoint the material is treated as homogeneous, although satisfying the equation of state prescribed by its actual heterogeneous structure. Such a procedure cannot be expected to give a reliable description of events which take place within distances of the order of the explosive grain size. It is true that such experimental estimates as have been made of the reaction zone length suggest an order of magnitude many times (in the case of mixed explosives very many times) greater than the grain diameter; however these estimates are uncertain.

To remove this shortcoming would require a detailed analysis of the small-scale processes within each explosive grain and the adjoining gas pockets: we cannot attempt this at the moment. Nevertheless, there seems in fact no reason to doubt that the picture presented above is qualitatively correct. In particular,

there are good grounds for believing that extremely high temperatures will arise in the air pockets. Thus, both theory and experiment agree in attributing temperatures of the order of $30,000^{\circ}\text{K}$ to the luminous air waves produced beyond the end of a detonating cartridge (§ 20). It is difficult to avoid the conclusion that air pockets, in which repeated reflexions must occur, will reach considerably higher temperatures. This in turn suggests that a significant part of the light given out by a granular explosive detonated under water (to eliminate external luminous shocks) may arise from compression of the air pockets. Recent experiments which tend to support this view are described in § 195, below. It will also be shown (§ 19.7) that the failure of detonation in loosely packed cartridges under static air pressures of 50 to 100 atm. can be accounted for by the present theory, and indeed might be thought to require some such theory to explain them.

§ 19.5 The source of the light recorded in photographs of detonating explosives

It is now generally recognised that a large part of the light arising from the detonation of a condensed explosive cartridge is due to the system of shock waves produced in the surrounding air. When the air is replaced, for example, by water, the total luminosity is greatly reduced, and may even be entirely suppressed. The high-speed camera records shown in Fig. 19.5:1 of Blasting Gelatine detonating in air and water illustrate this effect.

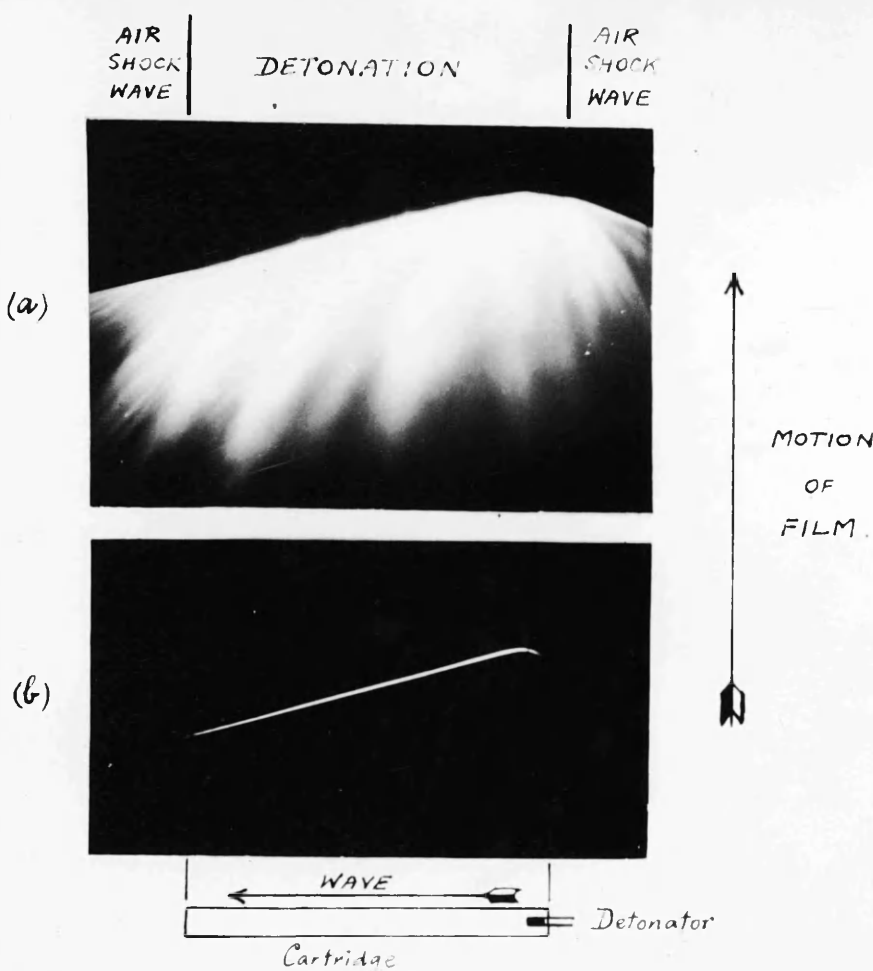


FIG. 19.5:1 . BLASTING GELATINE

DETONATING AT "HIGH VELOCITY" IN

(a) AIR

(b) WATER.

The light still reaching the camera when atmospheric shocks are eliminated, has been rather freely assumed to arise from the chemical reaction; and indeed a measurement of the reaction time has been proposed by several workers in terms of the breadth of high-speed camera traces, such as that shown in Fig. 19.5:1b. Even if the light were due to reaction, however, we should have no guarantee that its duration corresponded to the reaction time: it might well be either longer or shorter; and in fact it appears unsafe to assume

that the light from a granular explosive is necessarily associated with reaction at all. §§ 19.3, 19.4 have shown reason to expect very high temperatures in the air-pockets, before reaction commences, and it is at least possible that the light comes partly (or even entirely) from these.

In order to test this suggestion, composite charges were made by loading common salt (NaCl) and a plastic explosive (cyclotrimethylenetrinitramine plus filler) in alternate layers in a celluloid tube. The successive layers of NaCl were of increasing length. The charges were enclosed in wide water-filled glass tubes and fired in a side-on position in front of the highspeed camera. Fig. 19.5:2 shows a typical record. Contrary to what might at first glance be supposed, the intense streaks of light correspond to the layers of NaCl and not to those of explosive.

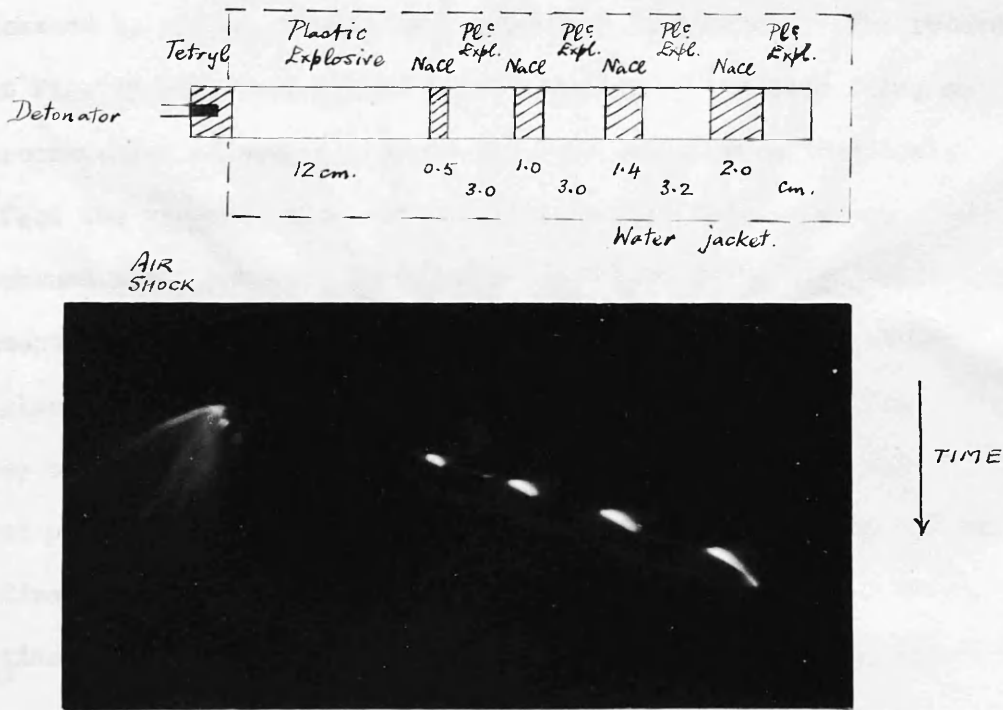


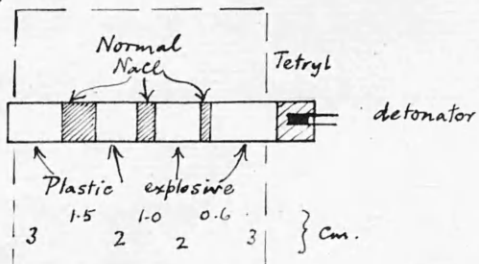
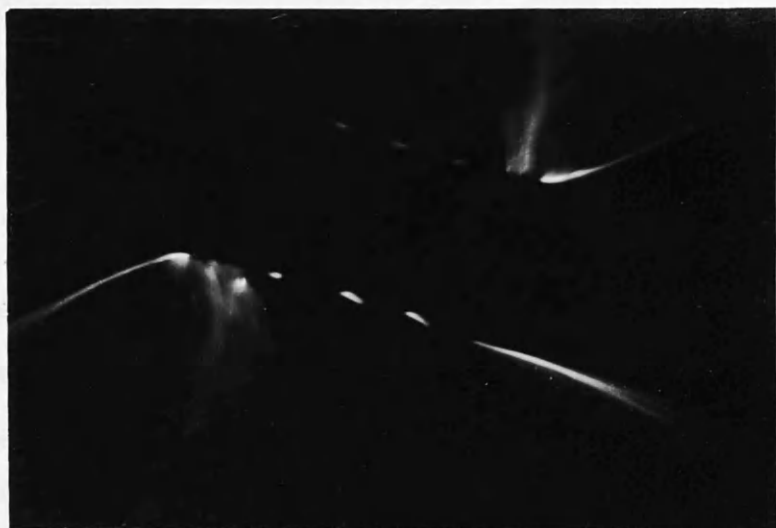
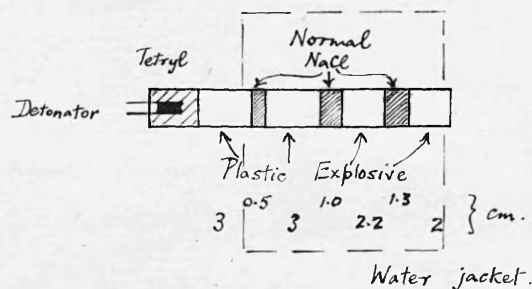
FIG. 19.5:2

This is made clear by reference to the key printed above the record. The streaks fall off in intensity with distance through each layer of NaCl. If we suppose that they represent the passage of a shock through the salt layer, then the velocity of this shock also falls with distance. The layers of explosive give very faint wave-traces, leading (significantly) from the tail of one salt streak to the nose of the next, at high and steady speed; propagation failed beyond 2 cm. of salt. There is no light from the water shock, but the faint parallel line lying beneath the primary wave trace may be due to the impact of this shock on the outer glass tube (perhaps rendered luminous by the presence of air bubbles on the glass); the time-interval involved is of the correct order.

That the light emitted by the salt layers arose within the depth of the salt and not merely on its surface was confirmed by firing two further shots, similar to the above, in one of which the salt was blackened by mixing it with one per cent of lampblack. The records, shown in Fig. 19.5:3, were placed close together on the same film, so that circumstances of emulsion speed and development were identical; and in fact the general level of intensity is the same in each. The blackened salt, however, contributes much less light than the translucent material. Very faint explosive traces and reflexions at the glass tube appear on the negative: these are so indistinct that they have been lost in printing. It will be noted that the explosive picked-up through 1.3 cm. of salt, but failed through 1.5 cm.

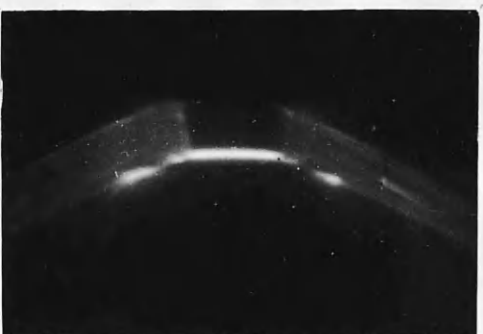
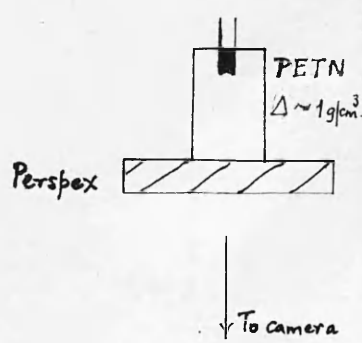
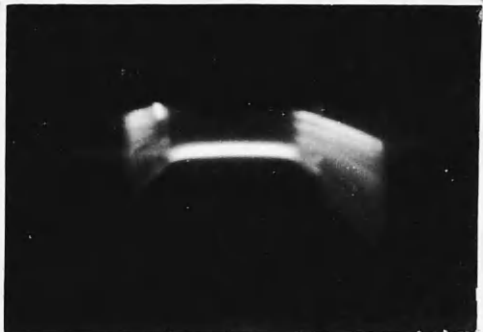
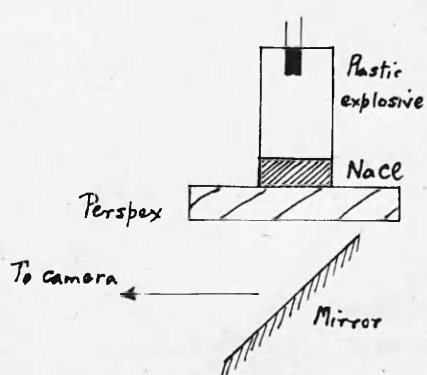
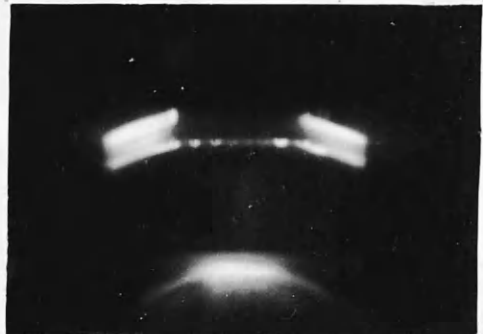
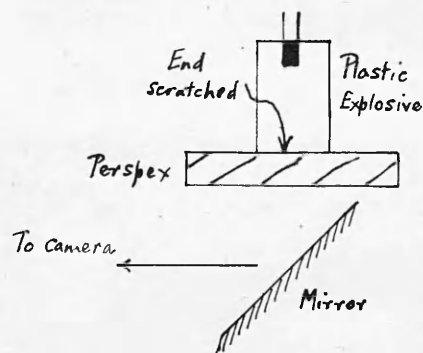
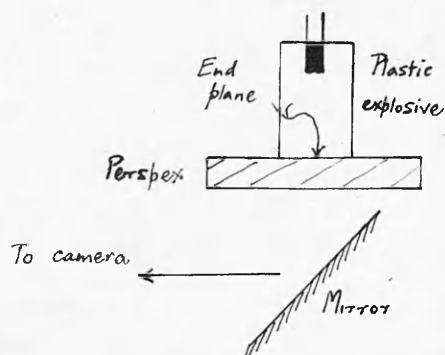
A final demonstration, perhaps even more striking than the above, was provided by firing three cartridges pointed head-on towards the

Water jacket

AIR
SHOCKAIR
SHOCK ↑↑ AIR
SHOCKFIG. 19.5 : 3.

camera*. The end of each cartridge remote from the detonator and nearest to the lens was butted tightly against a small $\frac{1}{2}$ -inch thick block of Perspex. Since only this end surface is viewed by the camera, water confinement is then unnecessary, and the sloping lines in Figures 19.5:4a, b, c represent the lateral air shocks: they are cut short by the limited size of the mirror.* Between these lateral traces is a dark space, where the undetonated layers of explosive obscure the approaching wave. This can become visible only when it reaches (or nears) the end of the charge. Fig. 19.5:4a, which corresponds to a cartridge of the plastic explosive alone, shows practically no light from the detonation wave: the diffuse splash some 20 μ sec. later is due to impact on the mirror. However, when a $\frac{1}{2}$ -inch layer of NaCl is interposed between explosive and Perspex (Fig. 19.5:4c) a most intense band of light is recorded. Fig. 19.5:4b provides interesting confirmation: in this case the explosive was butted directly against the Perspex, but a series of parallel scores were first made on its end surface. These produce bright flashes of light when the wave reaches them.

* In order to avoid damaging the lens, the cartridges were actually fired downwards, and a 45° -mirror used to reflect the light: but this does not affect the argument.



For comparison, Fig. 19.5:4d is a similar record of a cartridge of the granular explosive PETN. This produces a band of light comparable with that arising from the salt in Fig. 19.5:4C.

The significance of these photographs hardly requires emphasis. No appreciable light is emitted by the reaction in the plastic explosive, whose texture almost precludes the presence of air pockets; but copious light is emitted by the non-reactive NaCl, which of course contains abundant air-pockets. When air-spaces are artificially introduced into the plastic explosive, it becomes luminous. Finally, a granular explosive, less brisant than the other, emits intense light.

It would be premature, on the basis of these experiments alone, to suggest that none of the light recorded from detonating condensed explosives is due to the chemical reaction. Instances may be immediately quoted, such as the liquid nitroglycerine, where a (*rather faint*) luminous wave is observed in the (apparent) absence of air bubbles. However, the observations which we have reported make it probable that, after atmospheric shocks have been suppressed, a great part at least of the remaining light from a granular explosive is due to compression of the air pockets between the explosive grains. This confirms the theory of § 19.3, and simultaneously casts doubt on any estimate of reaction time in terms of the duration of luminosity.

§19.6 The mechanism of propagation in condensed explosives

It is possible, as we have seen, to give a reasonably convincing and quantitative theoretical account of the large-scale properties of the stable detonation wave in condensed explosives, and even to attempt an analysis of its structure, without reference either to the mechanism

of reaction or to the means whereby its initiation is transferred from one layer to the next. On these aspects opinion is divided. A view commonly held, with regard at least to granular explosives, is that reaction is initiated by some means on the surface of the explosive grains, and thereafter spreads inward at a rate determined by the temperature and pressure. In detail, the process then resembles the burning of a propellant, although from a macroscopic viewpoint this process must be regarded as taking place within some such wave-structure as is described in §19.3. This heterogeneous theory of a "deflagration within a detonation" has been developed in particular by Eyring and ⁵⁷⁷ coworkers, who show that, if temperature and pressure are assumed constant, the corresponding rate-law is of two-thirds order, and the total reaction time directly proportional to the grain radius. Apart from this quantitative prediction, which finds some experimental support, the fact that increased fineness leads in general to a rise in velocity (cf. §17.3(d)) supports the heterogeneous theory.

With regard to the precise means whereby the explosive grain is initiated, Eyring quotes evidence for the view that initiation commences with "hot-spots" produced by compression or grinding at the points of contact between grains. On this theory, the reaction time will depend, not only on the average grain size, but also on the efficiency of initiation of each grain, as represented by the number of contact points. Such a variation of reaction time with efficiency of initiation may, of course, be postulated in general, whether the mechanism depends on contact effects or not. For example, the two alternative velocities

observed with nitroglycerine gelatines (§17.2) and recently also with hydrogen peroxide-fuel mixtures and granular explosives can be explained if we assume that reaction may be initiated in two different ways, one of which requires a higher energy input than the other but leads to a more rapid reaction. For example, let us suppose that in a detonation wave of low velocity and therefore also low shock pressure, initiation of each explosive element takes place on the surface, either by friction and impact, or by thermal conduction from pockets of gas raised to very high temperatures in the leading shock. The reaction is then heterogeneous, and proceeds at a relatively low rate determined largely by the process of heat diffusion into the explosive element. In moderate cartridge diameter, therefore, we may expect (§17) only a small part of the heat of reaction to be set free in advance of the CJ-plane, and the detonation velocity to be "locked" at a low level. As the cartridge diameter is increased, this low velocity may be expected to rise, and in the absence of any alternative mechanism of initiation, should continue to do so in a smooth manner until at sufficiently large diameters the full hydrodynamic velocity is almost attained. However, considering the processes within the shock zone in more detail, we can presume that small shock waves will pass through the grains, and that the intensity of these "microshocks" will depend naturally upon that of the wave as a whole. It is clear, therefore that, in addition to the localised surface heating produced by impact, friction and contact with hot surrounding gas, each element of explosive will now suffer a more or less homogeneous energy increase due to the passage of these microshocks. If, now, as the cartridge diameter is

increased, the velocity and so the pressure at the wave-front rise to such a level that this homogeneous energy absorption is sufficient to initiate reaction, the decomposition of the element may be expected to complete itself in a relatively much shorter time than before. A small advance beyond the diameter at which this process first becomes operative should then lead to an abrupt shortening of the reaction zone thickness, and a consequent exploitation by the wave of the reaction energy to a much fuller degree than would otherwise have been possible in such diameters. An immediate consequence of this will, of course, be a sudden rise in velocity to a value probably little short of the theoretical limit. It is also clear that, in diameters greater than the critical diameter just defined, only the higher velocity will be stable, the lower value, even if temporarily established by the use, say, of a weak primer, changing spontaneously into the higher as a consequence of the change of the mechanism suggested.

It is not claimed that the above theory of the two-velocity effect is necessarily the correct one; but it does appear to stand in agreement with all presently available evidence, and in particular with the experimental results of §17.2, which have since been found [43] to apply qualitatively also to granular explosives.

With regard to the likelihood of the above mechanisms operating in practice, we have now a certain amount of theoretical evidence. Thus, [39] Ratner concluded that temperatures sufficiently high to ensure rapid reaction should be expected from shock waves travelling in liquid explosives with the high velocity of detonation ($\sim 7,000 - 8,000$ m./s.); but this conclusion would not apply if the velocity were of the order of

2,000 m./s. Again, in granular explosives, our own calculations (§19.4) of the temperatures produced by compression in the explosive grains make it appear rather unlikely that initiation of each grain is effected in this way, except perhaps at the higher loading densities. On the other hand, if the air pockets are in fact raised to transient temperatures (T_s) of the order of 10^4 to 10^6 degrees in the shock-front, they may well serve as reaction nuclei, or "hot spots". Of course, though the temperature of such a nucleus is high, its heat capacity is small, so that a relatively much lower compromise temperature (T_c) will be instantly established at the air-explosive interface. In the case of two solids of known thermal properties independent of temperature, one of which is heated and placed in contact with the other, this compromise temperature is easily evaluated. Reliable calculation is out of the question in our case, but by making the fairest possible assumptions regarding the mean thermal parameters we have deduced for PETN the values of T_c shown in Table 19.4:2.

They are about one-tenth^{went} of T_s , but still very high. Little significance can be attached to their absolute values, which in any case would tend rapidly to fall in consequence of the abrupt cooling of the gas phase by expansion, as indicated in Fig. 19.4:4. But they certainly do not discourage the view that gas pockets may serve as reaction nuclei in low-velocity propagation.

Rather striking experimental evidence on this question has recently been reported by Gurton, who finds that the low velocity in certain explosives is inhibited by subjecting these to hydrostatic air pressures of less than 100 atm. It can be foreseen that pressures of this low

order will have little effect upon the CJ-variables in condensed explosives, where the pressures involved are enormously greater. Neither, we may suspect, will the energy input into the explosive grains themselves in the shock-front be appreciably altered. As Gurton points out, the only part of the system likely to be affected is the gas pockets. In the following section, we present a detailed analysis by which these expectations are confirmed.

§19.7 The effect on the detonation wave of varying the initial hydrostatic pressure

We consider a granular explosive, occupying a fixed cartridge volume, part of which is taken up by the grains of explosive themselves, and the remainder by pockets of air between the grains. (Under the term "air" is included any other gas which may in exceptional cases replace the normal atmosphere). We are concerned with the effect of varying the hydrostatic pressure of this air, without changing the overall cartridge volume: as when the cartridge is enclosed in a porous wrapper and the surrounding atmospheric pressure is either raised or lowered.

Assume, in the first place, that the products of detonation form an ideal gas with constant γ and composition independent of temperature and pressure. The air initially present is supposed also ideal, with the same γ . Then if 1 cm^3 of the undetonated cartridge contains $m\Delta$ gm. of explosive and $(1-m)\Delta$ gm. of air, and Q , is the heat liberated by 1 gm. of explosive, the terminal RH-equation is, when $p_0 \ll p$,

$$\frac{p_0 v_0}{\gamma - 1} = \frac{1}{2} p_0 (v_0 - v_r) + Y, \quad (1)$$

where $v_0 \equiv 1/\alpha$ and $Y \equiv mQ + cT_0$, c being the specific heat

of the products. The CJ-condition is

$$\frac{v_f}{v_o} = \frac{\gamma}{\gamma+1}. \quad (2)$$

Eliminating v_f , we have

$$p_f = 2\Delta Y(\gamma-1). \quad (3)$$

Although we are primarily concerned with granular explosives, the above argument applies to a gaseous detonation if $m = 1$. For such a case, however, $\Delta \propto p_0$ if p_0 is not too high, so that

$$p_f \propto p_0, \quad (4)$$

justifying the neglect of p_0 in (1) and (2). It follows at once that the values of W , and D are independent of p_0 in an ideal gaseous explosive. This conclusion, together with (4), are well confirmed by Manson's detailed calculations for various gases.

Returning to the granular explosive, we can now relate p_f to p_0 . Let the superscript $^\circ$ refer to conditions when $p_0 = 1$ atm. Thus, Δ° is the cartridge density at 1 atm., and $p_0^\circ \equiv 1$. Then, at p_0 atm.,

$$\Delta = m^\circ \Delta^\circ + (1 - \varphi_m^\circ \Delta^\circ) \delta_0, \quad (5)$$

where φ_m is the specific volume of the explosive component alone, and δ_0 the initial density of the gas filler, in each case at p_0 . The explosive is, however, negligibly compressed at any practicable p_0 , so that we may write $\varphi_m = \varphi_m^\circ \equiv \varphi$, say. It will also be assumed

that the air remains ideal up to p_0 , whence

$$\delta_o = p_0 \delta_o^\circ. \quad (6)$$

Finally, if $\Delta^\circ \neq 0.05 \text{ g./cm}^3$, we may set $m^\circ \approx 1$.

Then (3) gives

$$\frac{p_i}{p_0} = 1 + (-\varphi \Delta^\circ) \frac{\delta_o^\circ}{\Delta^\circ} p_0, \quad (7)$$

which is the required relation. It may be expected to apply rather closely to an explosive cartridge at $\Delta^\circ \approx 0.1 \text{ g./cm}^3$ and subjected to pressures not exceeding 100 atm.

As an example, take $\Delta^\circ = 0.06 \text{ g./cm.}^3$, $\varphi = 0.6 \text{ cm.}^3/\text{g.}$ (gun-cotton), $\delta_o^\circ = 1.293 \times 10^{-3} \text{ g./cm.}^3$ (air), $p_0 = 80 \text{ atm.}$ Then $p_i/p_0 = 2.66$. It appears that the effect of raising p_0 by a factor of 80 is to raise p_i by a factor of about $2\frac{1}{2}$ only. It will be noticed that p_0/p_i is still negligible, justifying (1, 2). This will remain true, even when p_0 is very large, for then, by (7),

$$\frac{p_i}{p_0} \sim (-\varphi \Delta^\circ) \frac{\delta_o^\circ}{\Delta^\circ} \cdot p_0^\circ = 30,$$

with the numerical values chosen. (Of course, the solution cannot apply rigorously when p_0 is too large, because of the failure of (6)).

As to D and W, they are still independent of p_0 , to the same approximation.

The above idealised theory was verified by detailed calculations, according to the methods of §13, for a nitrocotton containing 13.45% N₂, and cartridge at 0.06 g./cm³ at N.T.P. Table 19.7:1 shows the results,

at 1 atm. — 100 atm., together with the predictions of the approximate theory, which is quite well confirmed. The conclusions may be summarised as follows:-

In an explosive whose density does not exceed 0.1 g./cm.³, W_i and D are unaffected by varying p_0 between 0 and 100 atm. At gaseous densities, p_i varies in proportion to p_0 ; at 0.1 g./cm.³ much more slowly.

These conclusions give no grounds for expecting p_i to have any marked effect upon the propagation. However, when we transfer attention from the CJ-plane to the shock-front, a very different picture emerges. Since, as we have seen, $p_i \gg p_0$, and since it is clear that $p_s > p_i$, where p_s is the shock-front pressure, the theory of §19 is applicable, according to which

$$\frac{p_s}{p_i} \doteq \frac{W_s}{W_i} \doteq 2. \quad (8)$$

This may be confirmed by a detailed analysis, which we omit here. Consequently, for gaseous explosives, and also for condensed explosives of low density, the shock pressure varies in the same ratio as the CJ-pressure, when p_0 is altered. This means, of course, that p_s/p_0 is independent of p_0 for a gaseous explosive, but depends markedly on p_0 for a granular explosive at 0.1 g./cm.³. In fact, in the latter case, from (7, 8),

$$\frac{p_s}{p_0} \doteq 2p_i^{\circ} \left[\frac{1}{p_0} + (1 - \varphi\Delta^{\circ}) \frac{\delta_0^{\circ}}{\Delta^{\circ}} \right], \quad (9)$$

or, approximately,

$$\frac{p_s}{p_0} / \frac{p_s^{\circ}}{p_0^{\circ}} = \frac{1}{p_0} + (1 - \varphi\Delta^{\circ}) \frac{\delta_0^{\circ}}{\Delta^{\circ}}. \quad (10)$$

Now, according to 19.3(8), if air behaves ideally, the compression ratio of the air pockets in an intense shock-front is approximately $1/\lambda$, irrespective of p_0 . Consequently,

$$T_s/T_o \doteq p_s/\lambda p_0. \quad (11)$$

$$\frac{T_s}{T_o} \doteq \frac{1}{p_0} + (1 - \varphi \Delta^\circ) \frac{\delta_o^\circ}{\Delta^\circ}. \quad (12)$$

With the same numerical values as before, $T_s \sim T_o^\circ / 30$. The shock-front air temperature is thus reduced in a ratio somewhat less than, but of the same order as, that through which p_0 is raised. The air pocket variables at the shock-front, according to the above equations, are included in Table 19.7:1.

In deriving these values, the air has, of course, been treated as an ideal gas with constant ratio of specific heats. We have seen, however, (§ 6.3) that this approximation involves major errors at high shock intensities. The shock-front variables have, therefore, been recalculated for $p_0 = 1$ atm., using the method of § 19.4, and the data of § 6.3. Nitrocotton was assumed to compress like starch, for which an isotherm is available. The amended values of p_s , w_s and T_s are shown in Table 19.7:1; p_s and w_s are almost unchanged, but T_s is greatly reduced. Unfortunately, the data of § 6.3 do not apply when p_0 differs from 1 atm. In order to obtain comparative figures, we have assumed that T_s will be reduced in the same ratio at any higher pressure p_0 as it is at $p_0 = 1$ atm.

Finally, a tentative estimate has been made, as in § 19.6, of the

compromise temperatures T_c produced at the surface of the nitrocotton fibres. These are indicated in the last column of Table 19.7:1.

At high loading densities, $\frac{P}{P_0}$ is no longer proportional to A , and equation (7) can hardly be expected to apply accurately. On the other hand, since δ°/A° is now small, $\frac{P}{P_0}/\frac{P}{P_0}^{\circ}$ approaches unity for moderate values of P_0 , so that the error in (7) is unlikely to be serious. This was confirmed by making detailed calculations for PETN at 0.75 and 1.5 g./cm.³ (at NTP), with $P_0 = 1$ atm. and 80 atm. The CJ-variables are shown in Tables 19.7:2, 3, together with values predicted by (7). The shock-front variables were also estimated, as for the nitrocotton, first with air as an ideal gas with constant γ , and then by means of the accurate shock characteristics of Fuchs et al. Tables 19.7:2, 3 summarise these calculations also.

The above studies appear to provide a satisfactory explanation of the fact (quoted in §19.6) that detonation may be inhibited in granular explosives of moderate or low density by applying an initial hydrostatic air pressure of 50-100 atm. The CJ-variables are relatively little affected by such pressures, unless indeed the cartridge density is extremely low; but the pressure-ratio across the shock-front and the consequent temperature rise in the air pockets depend critically upon P_0 .

In conclusion, it will be appreciated that the high velocity of detonation, if propagated by a "homogeneous" mechanism, should be independent of initial hydrostatic pressure. [67] Gurton finds that this is in fact the case.

Table 19.7:1

Nitrocotton (13.45% N₂) cartridged at 0.06 g./cm.³ and detonated at various air pressures.

A: detailed calculations
 B: idealised theory

Initial		CJ-plane		Shock-front					
		P_0 (atm)	P_1 (atm)	W_1 (m./s.)	D (m./s.)	P_s (atm)	W_s (m./s.)	T_s (°K)	$T_c - T_o$ (°C)
1	A	1,450	1,020	2,390	2,975	2,090	29,700	2040	
	B				2,900	2,040	150,000		
5	A						6,550	894	
	B	1,600	1,020	2,390	3,200	2,040	33,000		
10	A						3,580	631	
	B	1,750	1,020	2,390	3,500	2,040	18,000		
20	A						2,100	454	
	B	2,050	1,020	2,390	4,100	2,040	10,600		
50	A						1,210	321	
	B	2,920	1,020	2,390	5,840	2,040	6,120		
80	A	3,420	910	2,370			989	290	
	B	3,900	1,020	2,390	7,800	2,040	4,990		
100	A						912	272	
	B	4,470	1,020	2,390	8,940	2,040	4,160		

Table 19.7:2

PETN cartridged at 0.75 g./cm³ and detonated at various air pressures.

A: detailed calculations
 B: idealised theory

Initial				CJ-plane				Shock-front			
		$\frac{P_0}{(atm)}$		$\frac{P_1}{(atm)}$		$\frac{W_1}{(m./s.)}$		$\frac{D}{(m./s.)}$		$\frac{P_s}{(atm)}$	
											$\frac{W_s}{(m./s.)}$
											T_s
											$T_c - T_o$
											(°K)
											(°C)
1	A	41,900		1,240		4,520		89,400		2,650	317,000: 18,600
	B							83,800		2,480	3,800,000:
5	A										63,300: 7,700
	B	42,100		1,240		4,520		84,200		2,480	760,000:
10	A										32,000: 5,200
	B	42,300		1,240		4,520		84,600		2,480	384,000:
20	A										16,200: 3,470
	B	42,700		1,240		4,520		85,400		2,480	194,000:
50	A										6,650: 1,920
	B	44,000		1,240		4,520		88,000		2,480	79,800:
80	A	47,600		1,250		4,730					4,280: 1,430
	B	45,200		1,240		4,520		90,400		2,480	51,300:
100	A										3,480: 1,230
	B	46,100		1,240		4,520		92,200		2,480	41,800:

Table 19.7:3

PETN cartridge at 1.5 g./cm.³ and detonated at various air pressures.

- A: detailed calculations
- B: idealised theory

Initial		CJ-plane			Shock-front		
$\frac{P_0}{(atm)}$	$\frac{P_f}{(atm)}$	$\frac{W}{(m_s)}$	$\frac{D}{(m_s)}$	$\frac{P_s}{(atm)}$	$\frac{W_s}{(m_s)}$	T_s (oK)	$T_c - T_0$ (°C)
1 A	188,000	1,550	8,150	426,000	3,510	1,160,000	68,100
B				376,000	3,100	17,107,000	
5 A						232,000	28,830
B	188,100	1,550	8,150	376,200	3,100	3,424,000	
10 A						116,000	19,000
B	188,200	1,550	8,150	376,400	3,100	1,712,000	
20 A						58,100	12,680
B	188,500	1,550	8,150	377,000	3,100	857,600	
50 A						23,400	7,050
B	189,200	1,550	8,150	378,400	3,100	344,400	
80 A	191,100	1,535	8,260			14,700	5,140
B	190,000	1,550	8,150	380,000	3,100	216,100	
100 A						11,800	4,382
B	190,600	1,550	8,150	381,200	3,100	173,300	

§ 20 Normal incidence of a plane detonation wave upon the boundary of an adjoining medium

In § 7 the behaviour of non-reactive shocks at material boundaries was discussed. The general analysis applies also to reactive shock waves, that is, to detonation waves. Thus, when a detonation wave S_1 initiated within a volume of explosive reaches its surface a shock wave S_2 will in all cases proceed into the surrounding medium whether this be gas, liquid or solid. At the same time, a wave S_2 will be reflected into the detonation products; whether this is a shock or rarefaction will depend upon the physical properties of these products and of the environment.

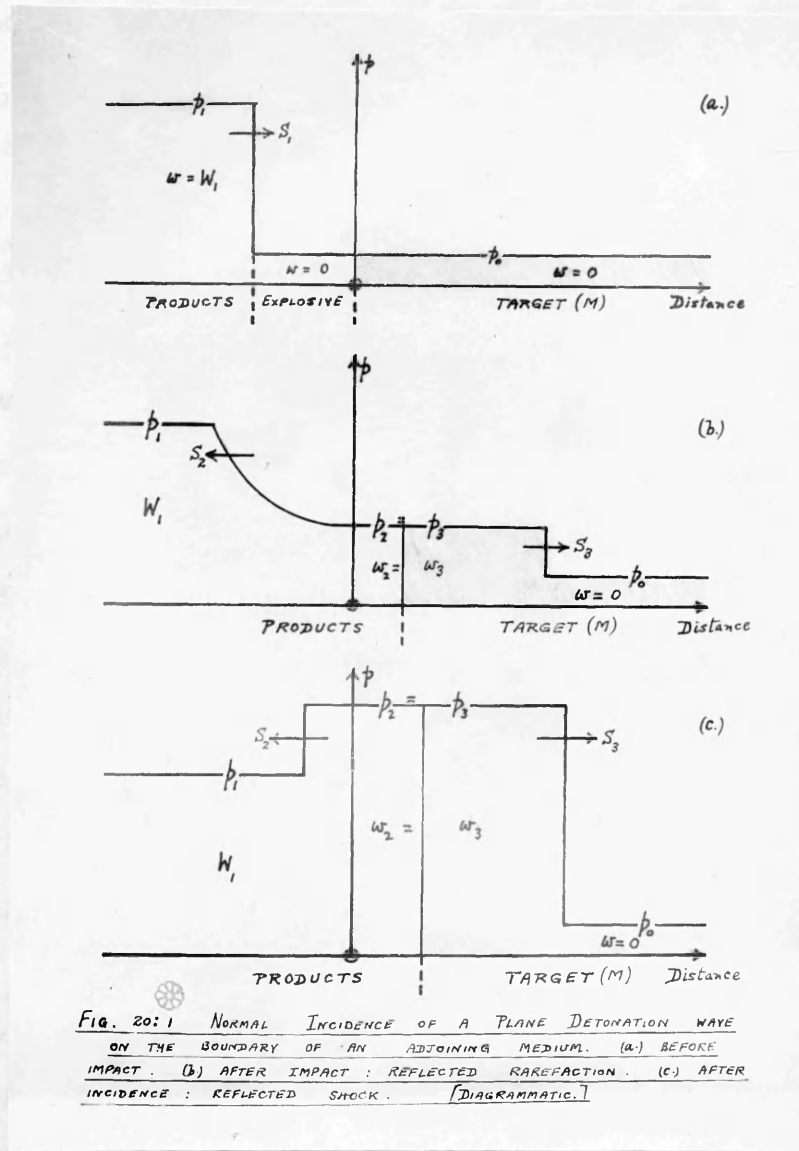
The system of waves arising at the surface of an explosive cartridge is naturally complicated by the cylindrical form and finite dimensions of the cartridge. As detonation proceeds along its length, a lateral shock wave of conical shape, similar to the head wave associated with a bullet in flight, passes outward into the surrounding medium, while a corresponding disturbance spreads through the detonation products. The subsequent three-dimensional non-steady flow will be exceedingly complex. However, if the zone of initiation is assumed to be sufficiently remote for steady conditions to have become established, and if the reaction zone is still regarded as plane, an [74] approximate treatment becomes possible. Again, when the plane detonation front arrives at the extremity of the cartridge, a terminal shock proceeds into the adjoining region. This wave will at first also be plane, and independent of the lateral shock, though subsequently interacting with it. An approximation to the state of affairs at the end of the cartridge may be [94,132] made by disregarding lateral effects and assuming that the detonation wave has itself proceeded so far from the zone of initiation that conditions are uniform throughout the space behind the CJ-plane. Even when this is not true, the theory should apply immediately after arrival of the detonation

wave at the end of the cartridge. In the present section, we shall show how the initial motion is determined for the case of normal plane incidence.

Shortly before arrival at the surface, conditions are as indicated in Figure 20:1a. In the bounding medium and the small strip of undetonated explosive the velocity is zero, and the other variables have values distinguished as usual by suffix \circ . Behind the detonation wave, conditions are again constant and the velocity, pressure, etc. have their CJ-values, represented by suffix 1. We disregard the reaction zone structure and the more extreme conditions temporarily realised within it, which in view of the brief reaction time can have only a transient effect upon the motion.

Figures 20:1b,c represent the position shortly after arrival at the surface.

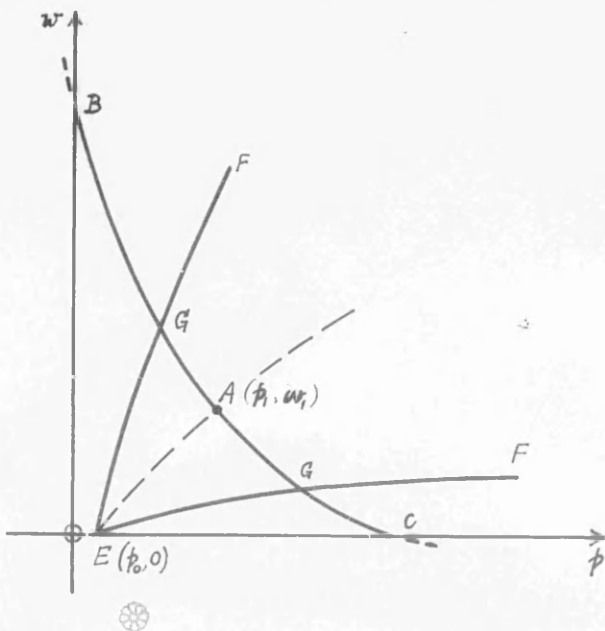
A steady plane shock S_3 has developed in the second medium (M), and a disturbance S_2 which may be either a shock or a rarefaction has returned a little way into the products. Conditions in M behind S_3 are distinguished by suffix 3, and are constant up to the material boundary, which must itself therefore move forward with velocity w_3 . Immediately beyond the boundary, the product variables are represented by suffix 2. In a reflected shock (Fig. 20:1c) these values are maintained up to S_2 , where they change abruptly to the CJ-values. Otherwise (Fig. 20:1b) the values p_2, w_2 etc. persist back to a point which moves with velocity $-a_2 + w_2$; thereafter they change continuously to the CJ-values at the nose of the reflected rarefaction which moves with velocity $-a_2 + w_2$. By 10(33) this is in general negative. Whether the rear of the rarefaction moves backward or forward depends on circumstances: there will in fact be a value of p_2/p_1 for which it remains fixed ($a_2 = w_2$). For example, when the products behave like an ideal gas with constant ratio γ of specific heats, it can be shown (§ 20.01) that the point in question moves



forward if $p_2/p_1 < \left[(3\gamma-1)/\gamma(\gamma+1) \right]^{2\gamma/(\gamma-1)}$. This will certainly happen with condensed explosives in air where $p_2/p_1 \sim 10^{-3}$. In any case, the gradients of pressure etc. in the rarefaction decrease with time. If S_2 is a shock, then $p_2 > p_1$ and $w_2 < W_1$; if a rarefaction, $p_2 < p_1$ and $w_2 > W_1$.

By means of the normal shock wave equations we may now express the fluid variables behind S_3 in terms of any one such variable and the conditions ahead of S_3 . In particular, a relation arises between p_3 and w_3 , involving p_0, v_0 and the equations of state of the second medium. This may be referred to (§7) as the $RH(pw)$ -relation for the transmitted shock. Similarly, the variables behind S_2 and close to the material boundary are expressible, by means either of the shock-wave equations or the Riemann adiabatic wave equations in terms of any one such variable and the conditions ahead of S_2 . In particular, a relation exists between p_2 and w_2 , involving the CJ-values and the state equations for the reaction products. This may be referred to as the $RH(pw)$ -relation or the $R(pw)$ -relation for the reflected wave, according to the nature of this wave. However, continuity at the surface of separation requires that $p_3 = p_2, w_3 = w_2$ (though the remaining variables will change discontinuously across the surface). Two equations are then available to determine p_2 and w_2 , whereupon the problem may be completely solved.

The analysis is best illustrated graphically in the (p, w) -plane.

FIG. 20:2. (ϕ, w) -DIAGRAM FOR NORMALINCIDENCE . BA : REFLECTED RAREFACTIONSAC : REFLECTED SHOCKS . EF, EF' : TRANSMITTEDSHOCKS.

Thus, in Figure 20:2 let $A(\phi_1, w_1)$ represent the constant state behind the detonation wave. Then conditions behind S_2 are defined by some point (ϕ_2, w_2) on the curve BAC of which the part BA above A (where $\phi_2 < \phi_1$, $w_2 > w_1$) represents rarefactions in the products with initial state prescribed by A , while the part AC below A (where $\phi_2 > \phi_1$, $w_2 < w_1$) represents shock waves in the products under the same initial conditions. The composite curve BAC , which may be called the **RHR**-curve through A , although defined by different equations above and below A , is continuous together with its slope and curvature at A ; this follows from the fundamental shock and adiabatic wave equations of Part I. (The **RH**- and **R**-curves have in fact double contact and cross each other at A). On the other hand, conditions (ϕ_3, w_3) behind S_3 are necessarily represented by some point on the curve EF , the **RH**(ϕw)-curve for shocks in the target medium. The solution is

therefore determined by the point of intersection G of the two curves.

It is clear that while S_3 is necessarily a shock (since rarefactions in the target are represented by the adiabatic continuation of FE below the pressure-axis), S_2 may be of either type, according as G lies above or below A .

Evidently the RHR -curve BAC , in conjunction with a series of RH -curves EF for various target materials, is sufficient to solve all problems relating to the normal reflection of plane detonation waves in the selected explosive. The intersection of BAC with the ω -axis represents conditions at a free surface, that is, when the target is a vacuum; its intersection with the p -axis represents conditions at a rigid boundary, that is, when the target is incompressible. Passage from a condensed explosive to a gaseous atmosphere and from a gaseous explosive to a liquid or solid target correspond very approximately to these extreme conditions.

The condition that S_2 should be a shock wave is, so far, of an a posteriori nature; in solving an actual problem, we must base our choice of RH - or R -equation on an assumption regarding the nature of S_2 . If the conclusions contradict this assumption the alternative equation is to be used. However, in practice there is usually very little difficulty, and in doubtful cases it may be expected that p_2 will be close to p_1 , so that the solution may be carried out equally well with either RH - or R -equation, since for points close to A the two overlapping curves are almost coincident. Although the general criterion for shock reflection must be of an a posteriori nature, it can be put in a simple and convenient form if we assume the two intersecting curves to be monotonic. For then the condition that S_2 be a shock is evidently that EF intersect the ordinate through A at a

point lower than A itself, in other words that

$$\omega_3(p_1) < W_1. \quad (1)$$

If $\omega_3(p_1) = W_1$, no reflected wave arises, and S_3 has the same pressure ratio as the detonation wave.

From the fundamental shock and adiabatic wave formulae, the $RHR(pw)$ -equation is

$$\omega_2 - W_1 = \begin{cases} \int_{p_2}^{p_1} dp / a_p, & \text{if } p_2 < p_1 \\ -\sqrt{(p_2 - p_1)(v_1 - v_2)}, & \text{if } p_2 > p_1. \end{cases} \quad (2a)$$

(2a) is to be taken in conjunction with the adiabatic (p, ρ) -relation;
(2b) with the $RH(p, \rho)$ -relation:

$$E_2 - E_1 = \frac{1}{2}(p_2 + p_1)(v_1 - v_2).$$

If the products constitute an ideal gas with constant γ , (2) becomes

$$\omega_2 - W_1 = \frac{2a_1}{\gamma-1} \left[1 - \left(\frac{p_2}{p_1} \right)^{\frac{\gamma-1}{2\gamma}} \right], \quad \text{if } p_2 < p_1 \quad (3a)$$

$$\omega_2 - W_1 = -a_1 \sqrt{\frac{2}{\gamma p_1}} \cdot \frac{p_2 - p_1}{\sqrt{(\gamma+1)p_2 + (\gamma-1)p_1}} \quad \text{if } p_2 > p_1. \quad (3b)$$

At a free surface $p_2 = 0$, whence

$$\omega_2 = W_1 + \frac{2a_1}{\gamma-1} = \frac{3\gamma-1}{\gamma-1} W_1. \quad (4)$$

The subsequent motion is thus identical with that of a compressed gas released from rest into a vacuum, save that a velocity W_1 is superimposed. It can easily be shown that $\omega_2 > 2W_1$. The rarefaction front spreads backward at a speed $a_1 - W_1$, which is necessarily positive. The velocity profile is linear within the wave, whose overall length increases at the constant rate $(\gamma+1)a_1/(\gamma-1)$.

At a rigid boundary, $w_1 = 0$, and so by (3b) and 10(8,31) we deduce

$$\frac{(\pi_{1-1})^2}{\gamma \pi_1^2} = \frac{2(\pi_{2-1})^2}{(\gamma+1)\pi_2 + \gamma-1}, \quad (5)$$

where $\pi_1 \equiv p_1/p_0$, $\pi_2 \equiv p_2/p_1$.

If $\pi_1 \gg 1$, this gives as an upper limit

$$\pi_2 = \frac{\gamma+1 + \sqrt{17\gamma^2 + 2\gamma + 1}}{4\gamma}, \quad (6)$$

which varies only between 2.62 and 2.28. On the other hand, if $\pi_{1-1} \ll 1$,

(5) leads to $\pi_2 \pi_{1-1} \approx 2(\pi_{1-1})$; that is

$$p_2 - p_0 \approx 2(p_1 - p_0), \quad (7)$$

though this case would hardly arise in a real explosive gas. (6) and (7) were given by Pfriem. [132] It is interesting to compare (6) with the corresponding limit for total reflection of a non-reactive gaseous shock, namely (equation 7.12(2))

$$\pi_2 = \frac{3\gamma-1}{\gamma-1}$$

which can rise to very high values when γ is close to 1. The pressures produced on a rigid obstacle by gaseous detonation waves are distinctly less than those produced by non-reactive gaseous shocks of the same intensity. Another useful comparison may be made between the pressure p_2 determined by (5) and the quantity $i \equiv p_1 - p_0 + p_1 W^2$, which was proposed by Rudenberg as a measure of the effect of a shock wave upon a rigid obstacle. By equations 10(34, 35), we have

$$i = p_0(\pi_{1-1})(1 + \frac{\pi_{1-1}}{\gamma \pi_1}). \quad (8)$$

When π_1 is large, therefore,

$$\frac{i}{p_2} \sim \frac{\gamma+1}{2.5\gamma} \sim \begin{cases} 0.8 & \text{if } \gamma = 1 \\ 0.64 & \gamma = 5/3 \\ 0.53 & \gamma = 3 \end{cases} \quad (9)$$

When π_{i-1} is small

$$\frac{i}{p_2 - p_0} \approx 0.5 \quad . \quad (10)$$

It thus appears that Rudenberg's expression, while inexact, provides a useful qualitative measure of the effect.

The velocity D_2 , relative to the detonation products, of the shock reflected from a rigid wall is easily found by means of the fundamental equation 6(8), which applies equally to reactive and non-reactive waves. In fact, since the mass velocity behind the reflected shock is $-W_i$, relative to the fluid ahead, we have

$$-D_2 W_i p_i = p_2 - p_i \quad . \quad (11)$$

Also

$$DW_i \Delta = p_i - p_0 \doteq p_i \quad . \quad (12)$$

Hence $\frac{D_2}{D} = -\frac{\Delta}{p_i}(\pi_{i-1}) = -(1 - \frac{W_i}{D})(\pi_{i-1})$. (13)

Subject to the approximation 10(32,33), this gives

$$\frac{D_2}{D} \doteq -\frac{\gamma}{\gamma+1}(\pi_{i-1}) = -\frac{1}{4}[1 + \sqrt{1+y^2}] \quad , \quad (14)$$

where $y \equiv 4\gamma/(\gamma+1)$. The wave velocity relative to rest is

$d_2 = D_2 + W_i$, and so

$$\frac{d_2}{D} = -\frac{\gamma(\pi_{i-1}-1)}{\gamma+1} = -\frac{1}{4}[y-3+\sqrt{1+y^2}] \doteq \begin{cases} -0.31, & \gamma = 1 \\ -0.35 & 1.1 \\ -0.40 & 1.2 \\ -0.47 & 1.4 \\ -0.79 & 3 \end{cases} \quad (15)$$

The temperature T_2 behind the reflected wave may be determined approximately by setting $\pi_2 = 2.5$. It varies from T_i when $\gamma = 1.0$ to $1.88 T_i$ when $\gamma = 3$.

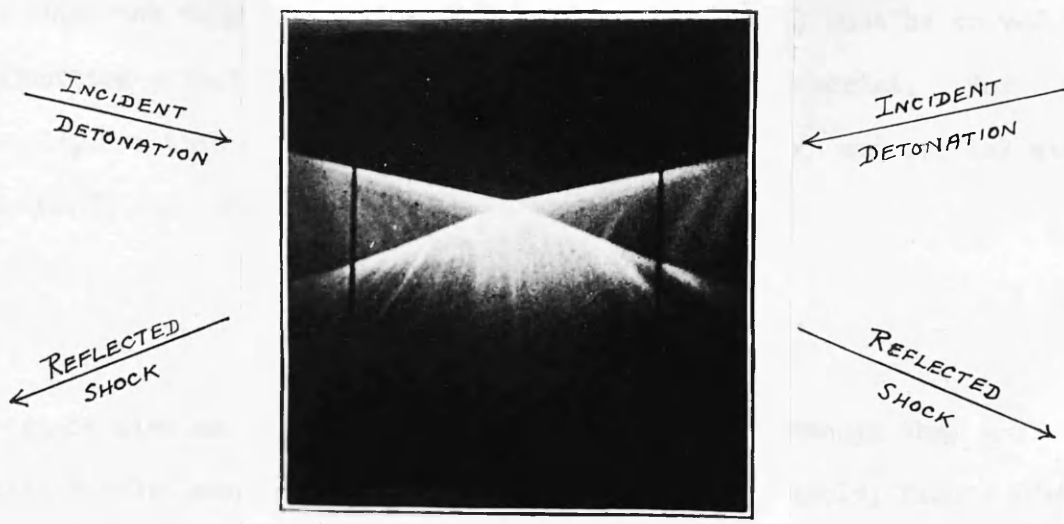


FIG. 20:3. FRONTAL COLLISION OF
TWO DETONATION WAVES IN $C_2N_2 + 2O_2$.

(DIXON, PHIL. TRANS. (A) 200, 315 (1903))

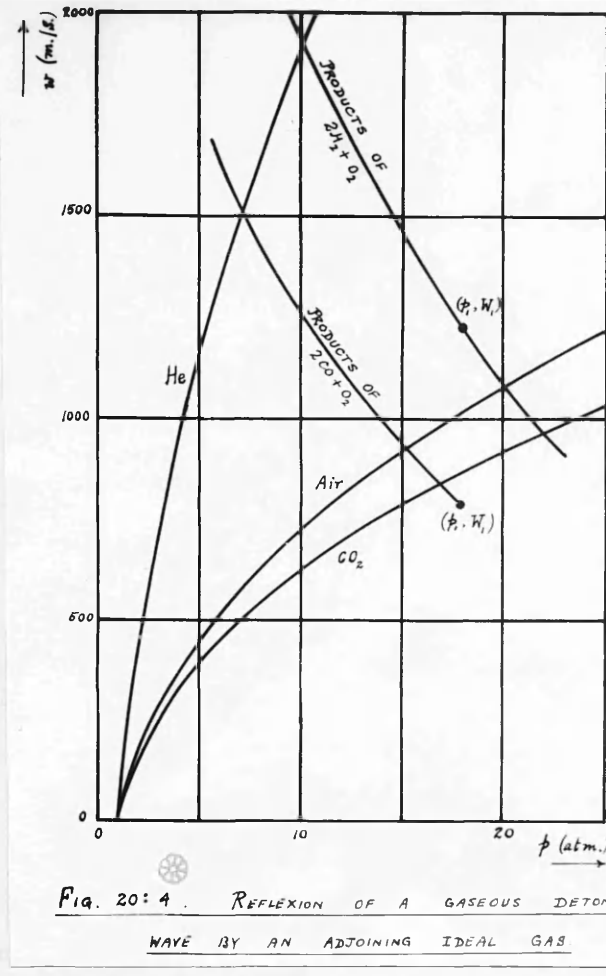
Figure 20:3 shows a classical photograph, by Dixon, of the collision of two detonation waves in $C_2N_2 + 2O_2$: by measurement of the slopes we find $\frac{d_2}{D} \approx -0.45$, close to the point of reflexion.

In gaseous explosives, the detonation pressure p_1 is usually much less than 100 atm. The streaming velocity w_3 behind the shock transmitted into a solid target is therefore very small, 1-2 m./s. at most, so that such targets may be regarded for all practical purposes as rigid, in calculating the properties of the reflected wave. The value of $p_3 = p_2$ thus obtained may then be used to determine the transmitted wave parameters if these are required. When the target is a liquid, its greater compressibility involves a somewhat higher value of w_3 , perhaps as much as 10 m./s., so that the reflected wave is modified to a slightly greater extent. For most purposes, however, the correction will be unimportant.

When the target is neither vacuous nor rigid, (3) must be solved in conjunction with the $RH(pw)$ -relation for the target material. For example, let this be an ideal gas with constant $\gamma = \gamma_0$ and initial state (v_0, p_0, T_0) . Then, by 6.2(4),

$$w_3 = w_2 = \sqrt{2v_0} \cdot \frac{p_2 - p_0}{\sqrt{(\gamma_0 + 1)p_2 + (\gamma_0 - 1)p_0}}. \quad (16)$$

We cannot give an explicit solution of (3) and (16), though they are easily handled numerically or graphically. As an example, Figure 20:4 shows the RHR-curve for electrolytic gas $2\text{H}_2 + \text{O}_2$.



W_1 and p_1 were taken from Lewis and Friauf (see Table 11:1) and γ was assumed constant with the value of 1.236 deduced from Table 11:1 by means of equation 10(36). An approximate curve for $2\text{CO} + \text{O}_2$ is also

drawn ($\gamma \approx 1.212$), together with the RH -curves for shock waves in helium, air and carbon dioxide, regarded as ideal with constant γ .

In the case of $CO + O_2$ all the reflected waves are rarefactions; in the other case, only that produced by a helium target.

The criterion for a reflected shock can be given explicitly.

By (1), (16) and 10(35) it is

$$\rho_0 > 2\Delta \frac{(\gamma+1)\pi_i + \gamma-1}{(\gamma_0+1)\pi_i + \gamma_0-1} \doteq 2\Delta \frac{\gamma+1}{\gamma_0+1}, \quad (17)$$

where Δ is the original density of the explosive gas, and ρ_0 that of the target gas. For example, if $\gamma = 1.2$ and $\gamma_0 = 1.4$, we require $6\rho_0 > 11\Delta$. (17) may again be compared with the corresponding equation for a strong non-reactive incident wave (7.14(3) with π_i large): apart from the factor 2, the equations are identical.

We may also consider the effect of reducing the target pressure (leaving the explosive at 1 atm.). If π_i and $\pi_3 \equiv \pi_i \pi_2 \equiv p_3/p_0$ are both assumed large, but $\pi_2 \ll 1$, π_3 is related to p_0 by the equation

$$a_0 \sqrt{\frac{2\pi_3}{\gamma_0(\gamma_0+1)}} \doteq N_i + \frac{2a_0}{\gamma-1} \left[1 - \left(\frac{p_0 \pi_3}{p_i} \right)^{\frac{\gamma-1}{2\gamma}} \right], \quad (18)$$

in which only π_3 and p_0 vary, and the [bracket] approaches 1 as $p_0 \rightarrow 0$. Thus, although p_3 falls with p_0 , the ratio p_3/p_0 rises towards the maximum

$$\pi \equiv (p_3/p_0)_{\max} \doteq \left(\frac{3\gamma-1}{\gamma^2-1} \cdot D \right)^2 \cdot \frac{\gamma_0(\gamma_0+1)}{2a_0^2}. \quad (19)$$

The corresponding temperature ratio T_3/T_0 is equal to $(\gamma_0-1)\pi/(\gamma_0+1)$, [94] and may evidently reach very high values when p_0 is small. For example, if $D/a_0 = 7$, $\gamma = 1.2$, $\gamma_0 = 1.4$, $(T_3/T_0)_{\max} \sim 500$. The second factor in (19) depends only on the target gas, and shows that, for p_0 small

$$p_3 \propto M_o(\gamma_o + 1), \quad (20)$$

where M_o is the molecular weight of the target. Similarly

$$T_3 \propto M_o(\gamma_o - 1). \quad (21)$$

We shall refer to these equations again below. Taylor has derived similar equations for the expansion of a slab of compressed gas. Table 20:1 illustrates the effect of reducing p_0 in a case where $p_1 = 21$ atm., $W_1/a_0 = 3$, $a_1/a_0 = 3.78$, $\gamma_o = 1.4$, $\gamma = 1.2$. The last line of the Table represents the limit as $p_0 \rightarrow 0$.

Table 20:1

p_0 (atm)	p_3 (atm)	p_3/p_0	T_3/T_o	w_3/a_0	D_3/a_0
1	8	8	2.29	2.18	2.65
10^{-1}	3.3	33	6.47	4.43	5.34
10^{-2}	1.07	107	18.83	7.97	9.60
10^{-3}	0.235	235	40.1	11.9	14.2
0	0	2790	465	40.8	44.0

In condensed explosives, the ideal gas equation cannot be used and an accurate calculation would as usual require to be based upon more complex equations. Such calculations are exemplified below. However, as in estimating the CJ-variables for the steady detonation wave, general guidance can again be obtained by the use of the Abel equation 12(1) with constant covolume(α). The RH(pw)-equation for reflected non-reactive shocks is, by 12(14),

$$w_2 = W_1 - (\pi_2 - 1) \sqrt{\frac{2p_1(v_1 - \alpha)}{(\gamma + 1)\pi_2 + \gamma - 1}}. \quad (22)$$

For adiabatic waves, $p(v - \alpha)^\gamma = \text{const.}$, and so

$$\alpha^2 = \text{const. } \gamma v^2 (v - \alpha)^{-(\gamma + 1)}, \quad (23)$$

whence

$$\frac{dp}{\rho} = \frac{2}{\gamma - 1} d \left[\frac{\alpha(v - \alpha)}{v} \right]. \quad (24)$$

The $R(\rho w)$ -equation for reflected rarefactions is therefore

$$w_2 = W_1 + \frac{2}{\gamma-1} \left[\frac{a_1(v_1-\alpha)}{v_1} - \frac{a_2(v_2-\alpha)}{v_2} \right] \quad (25)$$

$$= W_1 + \frac{2a_1}{\gamma-1} \cdot \frac{v_1-\alpha}{v_1} \left[1 - \left(\frac{p_2}{p_1} \right)^{\frac{\gamma-1}{2\gamma}} \right]. \quad (26)$$

It is to be noted that w_2 is no longer linear in a_2 . At a rigid target $w_2=0$ in (22). If W_1 and $v_1-\alpha$ are now expressed in terms of π_1 , by 12(13,14), equation (5) is recovered. The conclusions deduced from that equation for the case of a gaseous explosive may therefore be expected to remain at least qualitatively valid in the more general case. Again, at a free surface, $p_2=0$ in (26), whereupon

$$w_2 = W_1 + \frac{2a_1}{\gamma-1} \cdot \frac{v_1-\alpha}{v_1} \doteq \frac{3\gamma-1}{\gamma-1} W_1, \quad (27)$$

as before. The velocity of escape is therefore also indicated, to an order of magnitude, by the ideal gas equation. However, (27) seriously overestimates w_2 , in consequence of the very crude approximation involved in the use of a constant α .

It is much more convenient, and at the same time probably more accurate, to assume that the products follow a polytropic equation

$$\rho v^n = \text{const.} \quad (28)$$

Equations of this type with $n \sim 3$ are applicable to the products of typical condensed explosives, and n may in fact be taken to remain approximately constant down to quite low pressures, say a few thousand atmospheres. The error in extending the equation even to zero pressure should not therefore be serious for the present semi-quantitative treatment. Subject to (28), however, the products behave like a perfect gas with ratio n of specific heats, and the theory outlined above can therefore be

taken over without change. Thus, if we set $n = 3$, the velocity of escape into a vacuum is by (4)

$$\omega_2 \sim 4W_1 \sim D. \quad (29)$$

Since a normal gaseous atmosphere approximates to a vacuum from the point of view of a condensed explosive, it appears that the streaming velocity behind the terminal shock sent out into such an atmosphere must be close to the detonation velocity D itself. The atmospheric shock wave velocity will thus somewhat exceed D , a prediction well confirmed in practice.* More detailed guidance is supplied by equation (18).

Neglecting, to a first approximation, the term in $p_0\pi_3/p_1$, we have, with $\gamma = n = 3$,

$$\pi_3 \equiv \frac{p_3}{p_0} \sim \frac{\gamma_0(\gamma_0+1)}{2} \left(\frac{D}{a_0} \right)^2 = \frac{D^2}{2RT_0} M_0(\gamma_0+1), \quad (30)$$

and so also

$$\frac{T_3}{T_0} \sim \frac{\gamma_0(\gamma_0-1)}{2} \left(\frac{D}{a_0} \right)^2 = \frac{D^2}{2RT_0} M_0(\gamma_0-1), \quad (31)$$

as in (20) and (21). (30) and (31) represent limits when $p_0 \rightarrow 0$; the corresponding limit of ω_3 is D while the velocity D_3 of the transmitted shock approaches $(\gamma_0+1)D/2$. For higher pressures, a second approximation to π_3 is

$$\pi_3 = \frac{D^2}{2RT_0} M_0(\gamma_0+1) \left[1 - 3 \left(\frac{p_0\pi_3}{2D^2\Delta} \right)^{\frac{1}{3}} \right]. \quad (32)$$

Table 20:2 shows the effect of p_0 upon the properties of the air wave transmitted from an explosive for which $n = 3$, $D = 7500$ m./s. and $\Delta = 1.5$ gm/cm³, while Table 20:3 allows the behaviour of various atmospheres to be compared. The numerical values cannot, of course, be taken as precise; in particular, the neglect of rise in specific heat with temperature must involve a gross exaggeration of T_3 ; p_3 , ω_3 and D_3 will also be underestimated, since n in fact decreases with p_0 . However, even these idealised calculations are sufficient to show

* e.g. Fig. 19.5:1a.

the order of pressure and temperature in the atmospheric shock, and the manner in which these quantities depend upon D , M_0 , γ_0 and p_0 . It is clear that, while ω_3 and D_3 vary rather little, p_3 and T_3 depend critically upon the nature and pressure of the gas. p_3 is always small by comparison with p_1 , but T_3 as a rule greatly exceeds T_1 . The extremely high theoretical shock wave temperatures suggest in fact that the intense luminosity accompanying detonation of condensed explosives is in large measure due to the attendant air waves. As remarked in §19.5, this has been experimentally confirmed by firing cartridges within a sheath of water, when the light emitted is very much reduced; even intense shocks in water produce only a moderate temperature rise. Moreover, according to (30) and (31) the temperatures reached in gaseous targets increase with γ or M_0 . We should therefore expect a given explosive to produce the most intensely luminous waves in monatomic gases of high molecular weight. Finally, from (32) it appears that the luminosity should be enhanced by reducing the atmospheric pressure, both because the shock temperatures must increase, and also because ionisation will be facilitated by reduction in pressure. Muraour has discussed these consequences of the theory (in numerous papers),^[18] and shown them to be confirmed in practice. Muraour and collaborators have applied the above principles to the successful design of extremely brief and intense light flashes for high speed photography.^[19] For example, it is found that flashes with an intensity of order 5×10^8 candles, but lasting only a few microseconds, can be obtained from small quantities of high-velocity explosive detonating in a suitable atmosphere. As a light source, this arrangement is therefore in the same class with electronic devices such as the "Megalite" or "Sieflash".

Table 20:2

The effect of atmospheric pressure on the terminal air shock wave from a condensed explosive, whose products follow the adiabatic $\rho v^3 = \text{const.}$, $D = 7500 \text{ m./s.}$, $A = 1.5 \text{ cm}^2/\text{cm}^3$, $T_0 = 288^\circ\text{K}$,
(and so $p_1 = 210,000 \text{ atm.}$)

$\frac{p_0}{(atm.)}$	π_3	$\frac{p_3}{(atm.)}$	ω_3 (m./s.)	D_3 (m./s.)	T_3 ($^\circ\text{K}$)
1	635	635	6640	7970	30,800
10^{-1}	727	72.7	7100	8520	35,100
10^{-2}	772	7.72	7320	8780	37,400
10^{-3}	794	0.794	7420	8910	38,300
0	813	0	7500	9000	39,500

Table 20:3

Terminal shock wave transmitted to various gases by the condensed explosive of Table 20:2. $T_0 = 288^\circ\text{K}$, $\frac{p_0}{(atm.)} = 1$

<u>Target gas</u>	M_0 (gm/mol.)	γ_0	$\frac{p_3}{(atm.)}$	ω_3 (m./s.)	D_3 (m./s.)	T_3 ($^\circ\text{K}$)
Hydrogen	2.02	1.41	51.6	7,120	8,560	2,810
Air	28.8	1.40	635	6,640	7,970	30,800
Chlorine	70.92	1.34	1395	6,350	7,420	58,800
Helium	4.00	1.63	109	7,050	9,260	7,800
Neon	20.2	1.642	500	6,720	8,870	35,300
Argon	39.88	1.667	939	6,500	8,650	68,000
Krypton	82.92	1.689	1809	6,240	8,400	134,000
Carbon dioxide	44.0	1.30	897	6,520	7,500	34,000
Methane	16.04	1.310	357	6,800	7,850	14,100
Ethane	30.06	1.220	614	6,630	7,350	17,800
Propane	44.08	1.155	847	6,530	7,050	17,900
Butane	58.10	1.110	1067	6,450	6,800	16,300

Accurate numerical calculations of the transmitted and reflected waves in any particular case involve no further difficulty of principle, but require a knowledge of the equations of state of products and target. [82a] Jones has carried through such calculations for the case of PETN in air, using the state equation for the product gases which he deduced from experimental detonation velocities. His results at two cartridge densities are shown in Table 20:4 for comparison with Table 20:2. Despite the appreciable discrepancies which are of the sort expected, it will be seen that the idealised theory presents a qualitatively correct picture of the process. Initial air shock wave velocities [44] have been accurately measured by Cybulski for PETN at $\Delta = 1.51$ and 1.17 gm/cm^3 . They stand in very fine agreement indeed with predictions based on Jones' theory.

Table 20:4

Properties of the terminal air wave beyond PETN cartridges
at two selected loading densities (H.Jones)

Δ gm/cm^3	D (obs.) (m./s.)	W_1 (m./s.)	p_1 (atm.)	w_3 (m./s.)	p_3 (atm.)	D_3 (m./s.)
1.503	7430	1860	206,000	7,760	850	8,900
0.966	5407	1510	78,200	6,500	600	7,570

The same procedure may be at once applied to liquid targets - or to targets which are solid under normal conditions, provided they are regarded as behaving like liquids under the enormous pressures produced by brisant explosives. To determine conditions on normal incidence, we need only intersect the $RHR(pw)$ -curve for the detonation products with the $RH(pw)$ -curve for the target material. Such target shock curves were collected above in Fig. 7.3:1, and are redrawn in Fig. 20:5, together with RHR -curves for the products of four important blasting explosives, namely, No. 22 of Table 16.1:1, Nos. 25, 37 of Table 16.2:1 and No. 44 of Table 16.3:1.

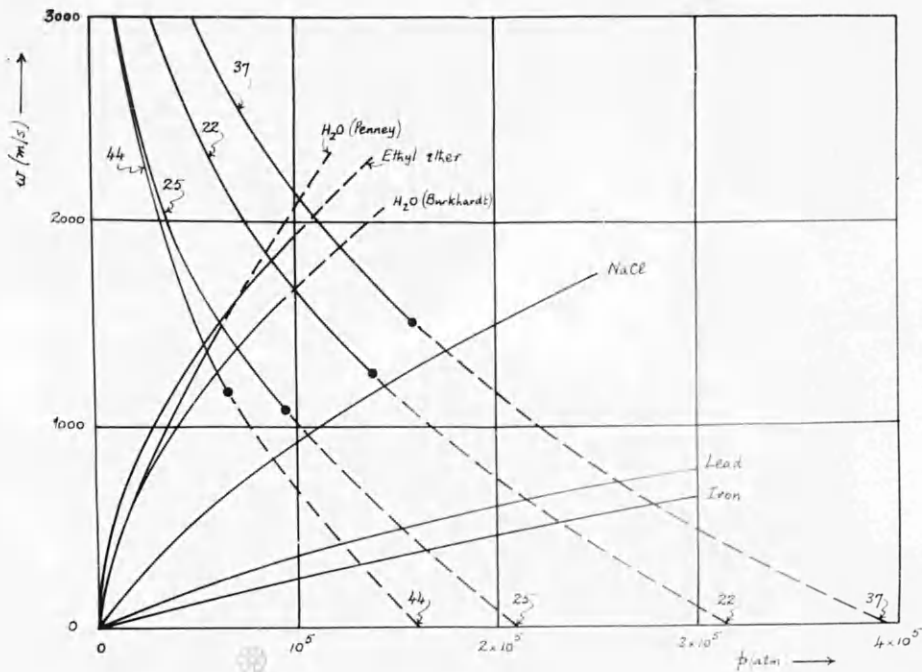


Fig. 20:5. Reflection of detonation waves in four commercial explosives. The RHR-curve. 22, 25, 37, 44 refer to the compositions similarly numbered in Tables 16.1:1, 16.2:1, 16.3:1. The circle on each is the CJ-point.

The method whereby these *RHR*-curves were derived is set out in §§ 20.1, 20.2. The nature of the reflexions and the order of p_3 and w_3 can be read from Fig. 20:5, and the remaining target variables deduced from the shock-wave equations and tables of §§ 6.41, 6.55, 6.56 and 6.58. For example, with explosive No. 37 of Table 16.2:1 (Blasting Gelatine),

<u>Target</u>	p_3 (atm.)	w_3 (m./s.)	D_3 (m./s.)	$T_3 - T_0$ (°C)
Iron	278,000	615	5,590	150
Lead	260,000	725	3,160	1,015
NaCl	173,500	1,370	5,680	1,285
Water*	109,000	2,915	5,450	

* by extrapolation.

It can be seen that even an iron target is far from rigid under such a blow; the values of p_3 corresponding to $w_3 = 0$, which approximate to $2.5p_1$ (in agreement with equation (6)) would be realised only in the frontal collision of two detonation waves. This explains the success of the Dautriche method (§ 17.01).

The possibility of applying reflexion techniques in measuring the CJ-variables has already been discussed in § 7.6.

§ 20.01 Condition for forward movement of the rear of a reflected rarefaction

As stated in § 20, the rear of the rarefaction moves with velocity $w_2 - a_2$. But, by 4(9),

$$w_2 - w_1 = - \frac{2}{\gamma-1} (a_2 - a_1). \quad (1)$$

Using 10(33), we deduce

$$\frac{w_2 - a_2}{a_1} = \frac{3\gamma-1}{\gamma(\gamma-1)} - \frac{\gamma+1}{\gamma-1} \left(\frac{p_2}{p_1} \right)^{\frac{\gamma-1}{2\gamma}}. \quad (2)$$

Consequently,

$$w_2 - a_2 \gtrless 0 \quad \text{as} \quad \frac{p_2}{p_1} \leq \left[\frac{3\gamma-1}{\gamma(\gamma+1)} \right]^{\frac{2\gamma}{\gamma-1}} \quad (3)$$

This critical ratio falls from unity when $\gamma = 1$ through $8/27$ when

$\gamma = 3$ to zero when $\gamma = \infty$.

§ 20.1 Reflected waves in the products of commercial blasting explosives:
products entirely gaseous

The equation of state used is 13.3(5), so that, as in § 19.4, we may write:

$$E - E_1 = \ell(T - T_1) \quad (1)$$

where ℓ is a constant, of the nature of a mean specific heat, for any particular explosive. The RH-equation for reflected shocks is then expressible directly in terms of p, v :

$$p \left\{ \frac{\ell(v-\alpha)}{nR} - \frac{1}{2}(v_v - v) \right\} = \ell T_1 + \frac{1}{2}p_1(v_v - v). \quad (2)$$

By means of (2) and the state equation, we can compute p_2 as a function of v_2 , whereupon the $RH(pw)$ -relation 20(2b) follows at once.

The adiabatic relation, by (1) is

$$\ell dT = -pdv, \quad (3)$$

which, with the state equation, gives after reduction

$$\log_{10} p = -\bar{\gamma} \log_{10} v + \log_{10} \sigma(x) + 0.4343(\bar{\gamma}-1)g(x) + \text{const.}, \quad (4)$$

where

$$\bar{\gamma} \equiv 1 + \frac{nR}{\ell}, \quad (5)$$

and

$$g(x) \equiv \int_0^x \frac{\sigma-1}{x} dx, \quad (6)$$

x and $\sigma(x)$ being defined as in equations 13.3(14,15). (4) can be written

$$pv^{\bar{\gamma}} = \text{const. } \sigma e^{-(\bar{\gamma}-1)g}, \quad (7)$$

which reduces correctly to the familiar ideal adiabatic when v is large, since then $\sigma \rightarrow 1$ and $g \rightarrow 0$. The functions σ and g are shown in Fig. 13.3:2 above.

To determine ω_2 from 20(2a), we require $(\partial p/\partial v)_s$ in terms of v . This can be obtained either by differencing the (v, p) -table or more accurately from

$$(\partial p/\partial v)_s = \frac{p}{v-\alpha} \left(\gamma - \frac{da}{dv} \right), \quad (8)$$

using Fig. 13.3:1. The integration 20(2a) may then be performed numerically. In practice, it was found possible to fit the adiabatic over a wide range by an equation of the form

$$p = Bv^{-b} + C, \quad (9)$$

where B, C, b are constants, most conveniently determined by matching the equation at three points whose values of v form a geometric progression (cf. § 6.52). Subject to (9), the velocity of sound a is

$$a = \sqrt{Bv(p-C)}, \quad (10)$$

and

$$\omega_2 = W_1 + \frac{2}{t-1} (a_1 - a_2), \quad (11)$$

An equation of the same form as for an ideal gas with constant ratio of specific heats.

Explosive 44 (Table 16.3:1)

Equation (9) becomes (atm., $\text{cm}^3/\text{g.}$)

$$p = 22,325 v^{-2.6627} + 1188 \quad (12)$$

and the composite $RHR(p, \omega)$ -curve is drawn in Fig. 20:5.

Explosive 37 (Table 16.2:1)

(9) becomes

$$p = 20,200 v^{-3.39} + 4930 \quad (13)$$

and the RHR -curve is shown in Fig. 20:5.

§ 20.2 Reflected waves in the products of commercial blasting explosives: products partly condensed

The present discussion is limited to cases where non-reactive material is present in the original explosive and survives in the products. As previously (§ 15 etc.), we assume the diluent completely entrained; we shall also assume that it remains cold, not only in the reaction zone, but also during the subsequent shock on rarefaction. This extrapolation of our earlier arguments justifying neglect of thermal transfer can be accepted only if the times involved are short. It is to be regarded, therefore, as focussing attention upon the flow immediately after impact on the target: this should be sufficient to determine at least the initial behaviour.

We might also safely ignore the compressional energy of the condensed phase (§ 18.81), since the pressures involved are never more than $2.5 \frac{p}{\rho}$. However, if accented symbols refer as usual to properties of the gaseous phase, reckoned per unit mass of that phase, and ϵ, φ are the internal energy and specific volume of the diluent, we have for reflected shocks

$$m(E' - E'_1) + (1-m)(\epsilon - \epsilon_1) = \frac{1}{2}(\rho + \rho_1)(v_r - v), \quad (1)$$

and also

$$v = mv' + (1-m)\varphi \quad (2)$$

$$v_r = mv'_r + (1-m)\varphi_r, \quad (3)$$

where m is the proportion by weight of explosive in the original mixture. If we now regard the diluent as having passed through a simple shock from ρ_1 to ρ , then

$$\epsilon - \epsilon_1 = \frac{1}{2}(\rho + \rho_1)(\varphi_r - \varphi). \quad (4)$$

For relatively incompressible diluents, present in moderate proportions, the

term is in any case a minor one, but the use of (4) should remove most of the slight error involved in simply neglecting compressional energy.

(1) then becomes

$$E' - E_1' = \frac{1}{2} (\rho + \rho_1) (\nu' - \nu). \quad (5)$$

We may then apply to the gas phase alone the theory already developed in § 20.1. ν is afterwards obtained from (2), φ being first computed in terms of ρ : for this purpose the isothermal (ρ, φ) -relation will usually be accurate enough, though the shock-relation may be used if available.

The remainder of the (ρ_2, ω_2) -computation is exactly as before.

Reflected rarefactions are similarly dealt with. In this case, the adiabatic becomes

$$m dE' + (1-m) d\varepsilon = -\rho d\nu. \quad (6)$$

By an approximation of the same order as (4), we may identify $d\varepsilon$ with $-\rho d\varphi$, whereupon (6) gives

$$dE' = -\rho d\nu'. \quad (7)$$

After $\nu'(\rho)$ has been determined, ν is calculated by (2), and ω_2 obtained from 20(2a) either by numerical integration or more conveniently by fitting an equation of the form 20.1(9) to the (ρ, ν) -adiabatic, and using 20.1(10,11).

Explosive 22 (Table 16.1:1)

20.1(9) becomes

$$\rho = 11,050 \nu^{-3.97} + 6150 \quad (8)$$

and the RHR -curve is drawn in Fig. 20:5.

Explosive 25 (Table 16.2:1)

20.1(9) is

$$\rho = 8,830 \nu^{-3.62} + 4250 \quad (9)$$

and the RHR -curve is drawn in Fig. 20:5.

§ 20.3 The "brisance" of a detonating explosive

The theory outlined above will evidently be relevant in attempting to account for and to predict the practical effects produced by detonating explosives. These effects have been, as a rule, rather loosely included in the term "brisance" or shattering power. It has been customary to represent this by some convenient parameter which would describe at least qualitatively [96] the effect upon target materials. Thus Kast proposed as an index of brisance the quantity fDA , where $f \equiv \frac{P_0 V T}{273}$, P_0 being 1 atm. and V the "gas volume" (the volume occupied by one gm. of products at NTP); in other words, $f = nRT$. Kast's brisance has the dimensions of pressure x velocity.

[47] Becker considered that a more natural index would be P , itself, which may be written WDA . Taking into account not only the hydrostatic pressure but also the "dynamic" pressure PW^2 , we obtain Rudenberg's expression [144] $WDA/(D-W)$, which approaches the CJ Pitot-pressure, and is thus more appropriate to represent end-brisance. While there is little doubt that such indices are useful guides to performance they are open to criticism in attempting to express the effect upon an external medium without reference to the properties of this medium itself and their reciprocal effect upon the detonation products. A more significant index must refer to the system as a whole, and not merely to the explosive. It thus becomes clear that the brisance of a selected explosive will depend upon its environment, and that the order of brisance of two explosives may even be different with reference to different targets. The obvious parameter to represent brisance in a given case is the pressure P_2 between the reflected and transmitted waves. If it is then desired to assign a characteristic index to each explosive, this may be approximately identified, at least for targets of a particular type, with the value of P_2 corresponding to some standard target of that type. For example, if we are chiefly concerned with attack upon metals, an

appropriate index of relative brisance would be the pressure produced in a selected standard metal. The same index would not necessarily remain appropriate with reference to highly compressible targets.

Let us for instance adopt an iron target as standard. According to Figure 20:5 the $RH(pw)$ -curve for shock waves in iron is almost linear, with equation

$$w \doteq Ap. \quad (1)$$

The slope at (p_1, w_1) of the RHR -curve for reflected waves in the products is, by 20(3b), $-a_1/n p_1$, or approximately $-w_1/p_1$. A first estimate of p_2 is therefore given by

$$Ap_2 \doteq w_1(2 - p_2/p_1), \quad (2)$$

that is,

$$p_2 = \frac{2p_1}{1 + Ap_1/w_1} = \frac{2w_1 D \Delta}{1 + A D \Delta}, \quad (3)$$

where $A \doteq 2.2 \times 10^{-3}$ m./sec.atm. $\doteq 2.17 \times 10^{-5}$ cm³.sec./m.g. for iron.

The theory of transmission at an interface is also relevant to the problem of initiation by a shock or detonation wave emerging from an adjacent medium. We shall return to this question below (§ 20.4). Here it is sufficient to point out that successful initiation under such circumstances will depend, not simply upon the intensity of the shock emerging from the initiator, but rather upon that of the shock produced in the receptor.

§ 20.4 Contact transmission of detonation

When the target material is itself an explosive capable of detonation, the analysis of § 20 requires to be modified. Of course, if reaction in the target medium ("receptor") could be disregarded, we might proceed exactly as before: the RHR(ρw)-curve for waves reflected through the products of detonation in the first explosive (the "primer") would then be intersected with the RH(ρw)-curve for non-reactive shocks in the receptor. For example, if the target were an ideal gas, equation 20(16) would be used; while if the receptor were granular we should proceed from equation 19.3(7), or more generally from 19.3(6). Since, as will be indicated below, neglect of reaction cannot in any case be justified, the idealised equation 19.3(7) is quite accurate enough to illustrate the results of this procedure. Assuming $p_3 \gg p_0$ and $m_0 \ll 1$, we have, from 19.3(3,4,7)

$$\frac{v_3 - \varphi_3}{v_0 - \varphi_0} \doteq \frac{v_3'}{v_0'} \doteq \frac{\gamma_0 - 1}{\gamma_0 + 1}, \quad (1)$$

where all the variables refer to the receptor material. The RH(ρw)-relation is then at once found to be

$$\omega_3 = \sqrt{\frac{p_3}{\gamma_0 + 1} [2v_0 + (\gamma_0 - 1)\varphi_0 - (\gamma_0 + 1)\varphi_3(p)]}. \quad (2)$$

If we disregard the difference between φ_3 and φ_0 , and set $\gamma_0 = 1.4$, (2) becomes

$$\omega_3 = \sqrt{\frac{5}{6}(v_0 - \varphi_0)p_3}. \quad (3)$$

For example, with $v_0 = 1 \text{ cm}^3/\text{g.}$, $\varphi_0 = 0.5 \text{ cm}^3/\text{g.}$, and in units of m./s. and atm.,

$$\omega_3 \doteq 6.5 \sqrt{p_3}. \quad (4)$$

Consideration at once shows, however, that reaction in the receptor must participate in the actual process of transmission. For otherwise we should be obliged to apply the above analysis to the propagation of the detonation wave over any section in a single explosive cartridge — with absurd results, since the RH($\dot{p}\omega$)-curve just derived corresponds to the RH(v,p)-curve $C = 0$ in Fig. 9.4:1, and evidently cannot pass through the CJ-point. We must therefore select a physically more reasonable RH($\dot{p}\omega$)-relation for the transmitted wave. It is clear that, to avoid the objection just raised, the corresponding curve in the (v,p)-plane must pass through the point of tangency I on the final RH(v,p)-curve (Fig. 9.4:1). This suggests at once that the most logical (v,p)-characteristic to choose, when the receptor is "underprimed" (that is, when the initial transmitted wave velocity falls short of the stable value) is the locus of points of contact of the pencil of tangents from A(v_0, p_0) to the family of RH-curves with parameter C. From a physical standpoint, this choice implies that the transmitted wave, though advancing with less than the stable velocity and therefore bound to accelerate, does so in a continuous manner and has a high degree of quasi-stability at the outset.

In the case of an ideal gaseous receptor, we can determine the (v,p)-contact locus, and the relative (\dot{p},ω)-curve, analytically. For, since the CJ-condition applies at every point on this locus (§ 9.4), its equation is no other than 10(9), which in the present notation becomes

$$\frac{p_3 - p_0}{v_0 - v_3} = \frac{\gamma_0 \dot{p}_3}{v_3} , \quad (5)$$

whereupon

$$\omega_3 = (\dot{p}_3 - \dot{p}_0) \sqrt{\frac{v_0}{(\gamma_0 + 1) \dot{p}_3 - \dot{p}_0}} , \quad (6)$$

as in 10(35a). (6) extends from $(\bar{p}_0, 0)$ to the receptor CJ-point, and lies entirely below the corresponding non-reactive RH-curve, since by 10(38) the value of w_3 for any \bar{p}_3 is only $1/\sqrt{2}$ times the value for inert shocks. It follows that the transmitted pressure \bar{p}_3 and velocity D_3 are greater than would be the case if reaction were ignored; while w_3 is less, so that the entry of reaction makes the receptor a more rigid target. These conclusions are precisely what we should expect on physical grounds.

In the case of "overpriming", the RH-curve just derived evidently cannot apply. The simplest choice in this case is the $(\bar{p}\omega)$ -relation corresponding to the upper branch IC (Fig. 9.4:1) of the terminal $\text{RH}(\nu, \bar{p})$ -curve itself. Its equation is found to be ($\bar{p}_3 \gg \bar{p}_0$)

$$w_3 = \sqrt{\frac{v_0}{\gamma_0 + 1}} (2\bar{p}_3 - P) , \quad (7)$$

where P is the CJ-pressure. The slope of (7) at the CJ-point is twice that of (6), so that the composite curve has a discontinuous gradient there; but there is nothing inherently unreasonable in this. In fact, it is probable that the mechanism of build-up from a condition of under-priming is basically different from that of "build-down" after overpriming. (Cf. § 9.4).

For condensed explosive targets, although an analytical treatment is not readily available, the transmitted $\text{RH}(\bar{p}\omega)$ -curve for underpriming may be derived numerically by drawing the pencil of upward tangents to the family of $\text{RH}(\nu, \bar{p})$ -curves, if these have been determined. The $\text{RH}(\bar{p}\omega)$ -curve for overpriming is obtained at once from the terminal $\text{RH}(\nu, \bar{p})$ -curve. As an illustration, this has been done with the curves of Fig. 19.4:2, for PETN at 1.0 g./cm^3 . The composite $\text{RH}(\bar{p}\omega)$ -curve is shown in Fig. 20.4:1, and the post-wave variables for quasi-stable detonation in this explosive are collected in Table 20.4:1.

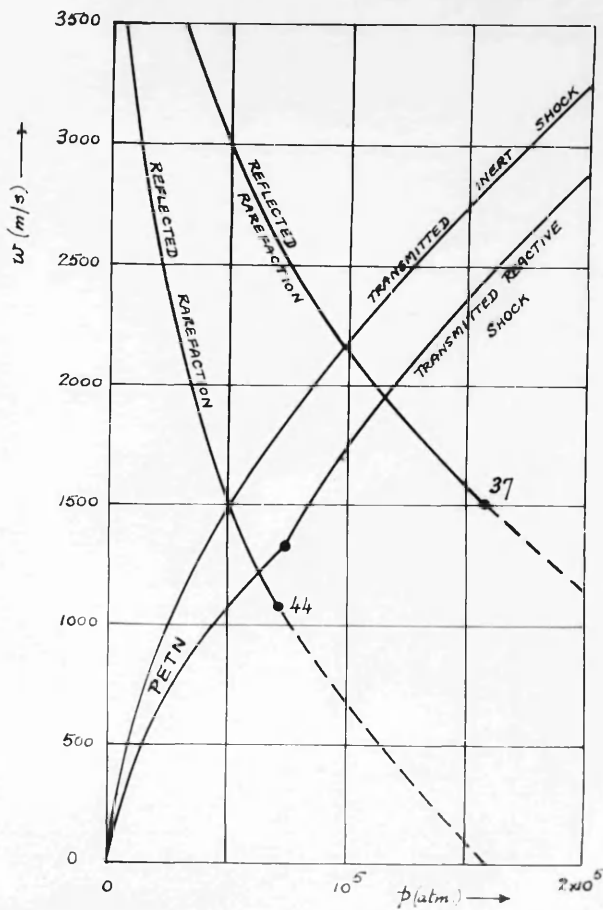


Fig. 20.4:1. PETN PRIMED BY TWO

COMMERCIAL EXPLOSIVES. • : CJ-POINTS.

Table 20.4:1

Quasi-stable detonation waves in PETN, $\Delta = 1.0 \text{ g/cm}^3$.

Class of detonation	c	v_3 $\text{cm}^3/\text{g.}$	P_3 atm.	W_3 m./s.	D_3 m./s.
Under-primed	0.2	0.808	13,000	500	2,620
Under-primed	0.4	0.790	28,000	770	3,660
Under-primed	0.6	0.771	44,000	1,009	4,400
Under-primed	0.8	0.763	59,000	1,188	5,000
(CJ)	1.0	0.760	74,000	1,340	5,560
Over-primed		0.694	100,000	1,760	5,730
Over-primed		0.656	125,000	2,080	6,060
Over-primed	1.0	0.628	150,000	2,370	6,400
Over-primed		0.607	175,000	2,630	6,720

According to the present theory, conditions immediately after normal impact of a detonation wave in a priming explosive (M) upon the surface of PETN cartridged at 1 g./cm³. are determined by the intersection of the RH(ρw)-curve of Fig. 20.4:1 with the appropriate RHR-curve for reflected waves in the products of M. Two such curves have been redrawn from Fig. 20:5, and the transmitted wave variables are shown in Table 20.4:2.

Table 20.4:2

PETN at 1.0 g/cm³. primed by Explosives 37, 44

Primer	Incident wave		Transmitted reactive wave		Transmitted non-reactive wave	
	ρ_1	W_1	D_1	ρ_3	W_3	D_3
atm.	:m./s.	:m./s.	atm.	:m./s.	:m./s.	atm.
No. 37 (Table 16.2:1)	:159,000	:1,500	:7,370	:115,000	:1,960	:5,940
	:	:	:	:	:	:
No. 44 (Table 16.3:1)	:68,000	:1,172	:4,500	:64,000	:1,230	:5,160
	:	:	:	:	:	:

The receptor is considerably overprimed by Explosive 37, and slightly underprimed by Explosive 44. The reflected wave in each case is a rarefaction, very weak with Explosive 44. The condition for no reflected wave is, of course, that the primer CJ-point lie on the receptor RH-curve; while the condition for exactly balanced priming is that the two CJ-points coincide. The latter condition is naturally satisfied at every section in a single explosive cartridge.

For comparison, Fig. 20.4:1 also shows the transmitted RH-curve for non-reactive waves, defined by equation (2) above. The corresponding waves transmitted by Explosives 37, 44 are again summarised in Table 20.4:2. The alternative solutions differ rather widely, and it appears that a crucial experiment could easily arbitrate between them, if this were thought necessary. However, there seems little doubt that the reactive wave theory must be closer to the truth.

§21. References

In each reference, the number first stated represents the source, which can be identified from the key below. The number underlined indicates the volume of the appropriate journal (or, in the case of series of reports, the serial number of the report). This is followed by the page number and date.

- (1) M.N.Alentzev, N.N.Sobolev. 30, 51, 691 (1946); 31, 16, 990 (1946).
- (2) R.Becker. 14, 23, 40, 304 (1917).
- (3) 10, 4, 393 (1921).
- (4) 12, 3, 152, 249 (1922).
- (5) 10, 8, 321 (1922).
- (6) M.Berthelot, P. Vieille. 6, 93, 18 (1881); 94, 101, 822 (1882).
- (7) M.Berthelot. 6, 94, 149 (1882); 96, 672 (1883).
- (8) 21, 6, 556 (1885)
- (9) H.A.Bethe. Quoted in Ref. (60).
- (10) F.R.Bichowsky, F.D.Rossini. Thermochemistry of Chemical Substances. New York (1936).
- (11) L. Boltzmann. 26, 7, 477 (1899)
- (12) M.Born, M.Bradburn. 35, 39, 104 (1943).
- (13) M.Born, R.D.Misra. 35, 36, 466 (1940).
- (14) F.P.Bowden, M.F.R. Mulcahy, R.G.Vines, A.Yoffe. 2, 188, 291 (1947).
- (15) M.Bradburn. 35, 39, 113 (1943).
- (16) P.W.Bridgman. Bibliographies in:
 - (a) The Physics of High Pressure. London (1931).
 - (b) 29, 18, 1 (1946).
- (17) P.W.Bridgman. 20, 48, 309 (1912).
- (18) 19, 3, 597 (1935).
- (19) 19, 5, 964 (1937).

- (20) P.W.Bridgman. 36, 60, 351 (1941).
- (21) 20, 76, 1 (1945).
- (22) 20, 76, 9 (1945).
- (23) 20, 76, 55 (1945).
- (24) K.J.Brimley. 51, 2, 2 (1950).
- (25) S.R.Brinkley. 19, 15, 114 (1947).
- (26) E.J.Burcik, E.H.Eyster, D.M.Yost. 19, 9, 118 (1941).
- (27) P.Caldirola. 19, 14, 738 (1946).
- (28) C.Campbell, W.B.Littler, C.Whitworth. 2, 137, 380 (1932).
- (29) C.Campbell, C.Whitworth, D.W.Woodhead. 37, 59 (1933).
- (30) D.L.Chapman. 3, 47, 90 (1899).
- (31) H.W.Clapham. 45 (1928).
- (32) J.C.Clark. 58, 20, 363 (1949).
- (33) R.H.Cole. Underwater Explosions. Princeton 1948.
- (34) A.Comey, F.B.Holmes. 13, 8, 305 (1913).
- (35) J.H.Cook. 45 (1945).
- (36) 45 (1948).
- (37) M.A.Cook. 19, 15, 518 (1947); 16, 1081 (1948).
- (38) 19, 16, 554, 1165 (1948).
- (39) J.L.Copp, A.R.Ubbelohde. 44, 44, 646, 658 (1948).
- (40) T.P.Cotter, S.J.Jacobs. 41, 5618 (1945). Quoted in Ref. (37).
- (41) R.Courant, K.O.Friedrichs. Supersonic Flow and Shock Waves. New York, 1948.
- (42) L.Crussard. 25, 6, 1 (1907).
- (43) I.G.Cumming. 45 (1949).
- (44) W.B.Cybulska, W.Payman, D.W.Woodhead. 2, 197, 51 (1949).
- (45) Dautriche. 6, 143, 641 (1906).
- (46) Dautriche. 50, 16, 27 (1911)

- (47) D.R.Davies. 4, 61, 105 (1948).
- (48) P. Debye. 11, 39, 789 (1912).
- (49) 38, 14, 259 (1913).
- (50) H.B.Dixon. 1, 184, 97 (1893).
- (51) 1, 200, 315 (1903).
- (52) W.Döring. 11, 43, 421 (1943).
- (53) W.Döring, G.Burkhardt. Beiträge zur Theorie der Detonation.
Berlin-Gatow (1944).
- (54) S.Earnshaw. 1, 150, 133 (1860).
- (55) C.J.Egan, J.D.Kemp. 18, 59, 1264 (1937).
- (56) H.Eyring, J.O.Hirschfelder. 28, 41, 249 (1937).
- (57) H.Eyring, R.E.Powell, G.H.Duffey, R.B.Parlin. 33, 45, 69 (1949).
- (58) J.G.Fox. 52, 200 (1945). (Quoted in Ref. (37)).
- (59) W.Friedrich. 13, 28, 2 etc. (1933).
- (60) K.Fuchs, G.J.Kynch, R. Peierls. 43, 61 (1942).
- (61) R. Furth. 2, 183, 87 (1945).
- (62) P.Gay, W.Lyle. 45 (1946).
- (63) H.P.Greenwald, R.V.Wheeler. 57, 14 (1925).
- (64) E. Grüneisen. 11, 39, 257 (1912).
- (65) E.A.Guggenheim. Modern Thermodynamics by the Methods of Willard Gibbs. London (1933).
- (66) O.A.Gurton. 45 (1945).
- (67) 45 (1949).
- (68) Hamel. 16, 55, 1895 (1910).
- (69) H.Happel. 11, 21, 342 (1906).
- (70) J.B.Henderson, H.R.Hassé. 2, 100, 461 (1921).
- (71) A. Herpin. 6, 223, 276 (1946).
- (72) G. Herzberg. Molecular Spectra and Molecular Structure (1939).

- (73) G.Herzberg, G.R.Walker. 5, 161, 647 (1948).
- (74) R.Hill, D.C.Pack. 2, 191, 524 (1947).
- (75) J.O.Hirschfelder, F.G.McClure, C.F.Curtiss. 46 (1942).
- (76) J.O.Hirschfelder, W.E.Roseveare. 28, 43, 15 (1939).
- (77) J.O.Hirschfelder, D.F.Stevenson, H.Eyring. 19, 2, 896 (1937).
- (78) A. Hugoniot. 7, 3, 477 (1887).
- (79) 8, 57, 3 (1887); 58, 1 (1889).
- (80) E.Jones, D.Mitchell. 5, 161, 98 (1948).
- (81) H. Jones. 46 (1942).
- (82) 2, 189, 415 (1947).
- (82a) 60, p. 590 (1948).
- (83) H. Jones, A.R.Miller. 2, 194, 480 (1948).
- (84) W.Jost. 14, 41, 183 (1935).
- (85) W. Jost. Explosions- und Verbrennungsvorgänge in Gasen. Berlin (1939).
- (86) E. Jouguet. 6, 132, 673 (1901); 134, 1418 (1902);
135, 778 (1902); 138, 1685 (1904).
- (87) 6, 139, 121 (1904).
- (88) 6, 140, 711 (1905).
- (89) 7, 1, 347 (1905); 2, 5 (1906).
- (90) 6, 144, 415 (1907); 149, 1361 (1909); 150, 91 (1910).
- (91) 6, 157, 545 (1913).
- (92) Mécanique des Explosifs. Paris (1917).
- (93) 6, 181, 658 (1925).
- (94) 6, 202, 796, 1225, 1320 (1936); 54, 21, 235 (1947).
- (95) R.A.Joyner. 45 (1914).
- (96) H.Kast. Spreng- und Zundstoffe. Braunschweig 1921.

- (97) H. Kast. 49, 36, 72 (1923).
- (98) F.G.Keyes. 18, 60, 1761 (1938).
- (99) J.B.Khariton, S.B.Ratner. 30, 41, 293 (1943).
- (100) J.E.Kilpatrick, E.J.Prosen, K.S.Pitzer, F.D.Rossini. 32, 36, 559 (1946).
- (101) J.G.Kirkwood, E.Montroll. 41, 676 (1942) (Quoted in Ref. 33).
- (102) L. Landau, K. Staniukovich. 30, 46, 362 (1945).
- (103) H. Langweiler. 12, 19, 271 (1938).
- (104) J.E.Lennard-Jones. 2, 106, 463 (1924).
- (105) J.E.Lennard-Jones, A.F.Devonshire. 2, 163, 53 (1937).
- (106) B.Lewis, G. von Elbe. Combustion, Flames and Explosions of Gases.
Cambridge (1938).
- (107) B.Lewis, J.B.Friauf. 18, 52, 3905 (1930).
- (108) G.N.Lewis, 20, 37, 49 (1901); 24, 38, 205 (1901).
- (109) E.Mach, J. Wosyka. 23, 72, 44 (1875).
- (110) R. Majumdar. 27, 21, 107 (1929).
- (111) E. Mallard, H. le Chatelier. 6, 93, 145 (1881).
- (112) N. Manson. 6, 218, 29 (1944).
- (113) W. Maxwell. 45 (1945).
- (114) L. Medard. 6, 222, 1491 (1946).
- (115) R.D.Misra. 35, 36, 175 (1940).
- (116) D. Mitchell, S. Paterson. 5, 160, 438 (1947).
- (117) G.Morris, H. Thomas. 40, 1, 132 (1947).
- (118) H. Muraour. 9, 47, 3 (1942).
- (119) Muraour, Michel-Levy, Vassy. 55 (1941), p.161.
- (120) P. Naoum. Nitroglycerin und Nitroglycerinsprengstoffe. Berlin 1924.
- (121) A. Noble, F.A.Abel. 1, 165, 49 (1874).
- (122) S.Paterson. 4, 59, 50 (1947).
- (122a) 59, 163, 98 (1947).

- (123) S.Paterson. 6, 224, 891 (1947).
- (124) 3, 39, 76 (1948).
- (125) S.Paterson, P.H.Ford. 45 (1948).
- (126) S.Paterson. 40, 1, 221 (1948).
- (127) 19, 16, 159, 847 (1948).
- (128) 4, 61, 119 (1948).
- (129) W.Payman, W.C.F.Shepherd. 2, 186, 293 (1946).
- (130) W.Payman, N.S.Walls. 37, 123, 420 (1923).
- (131) W.G.Penney, H.K.Dasgupta. 42, 333 (1942).
- (132) H. Pfriem. 17, 12, 244 (1941).
- (133) M.Pier. 14, 15, 536 (1909); 16, 897 (1910).
- (134) K.S.Pitzer. 33, 27, 39 (1940).
- (135) G.I.Pokrovsky, K.P.Staniukovich. 30, 53, 33 (1946).
- (136) L. Prandtl. 39, 3, 241 (1906).
- (137) W.J.M.Rankine. 1, 160, 277 (1870).
- (138) S.B.Ratner. 30, 42, 265 (1944).
- (139) 61, 22, 357 (1947).
- (140) Rayleigh. 2, 84, 247 (1910).
- (141) B.Riemann. 22, 8, 156 (1860).
- (142) F.D.Rossini. 32, 2, 359 (1939).
- (143) J.F.Roth. 13, 34, 193 (1939); 35, 193, 220, 243 (1940).
- (144) R. Rudenberg. 40, 113, 237 (1916).
- (145) H. Schardin. 38, 33, 60 (1932).
- (146) H. Schardin. Probleme der Detonation. Deut. Akad. Luftfahrtforsch. (1941).
- (147) A. Schmidt. 13, 27, 145 etc. (1932).
- (148) 13, 29, 259, 296 (1934).
- (149) 13, 30, 364 (1935); 31, 8 etc. (1936).

- (150) A. Schmidt. 13, 33, 280, 312 (1938).
- (151) E. Schrödinger. 38, 20, 452 (1919).
- (152) R.L.Scorah. 19, 3, 425 (1935).
- (153) W.C.F.Shepherd, H.C.Grimshaw. 48, 109 (1950). In the press.
- (154) W.Siegel. 24, 87, 641 (1914).
- (155) Sprengel. 53, 921, 2642 (1871).
- (156) G.G.Stokes. 3, 33, 349 (1848).
- (157) J.Taffanel, H. Dautriche. 6, 155, 1221 (1912).
- (158) G. Tamman. 11, 37, 975 (1912)
- (159) G.I.Taylor. 2, 84, 371 (1910).
- (160) G.I.Taylor. 46, (1940).
- (161) J.Taylor. 45(1939).
- (162) J. Taylor. 40, 1, 67 (1947).
- (163) 47, 179, 329 (1949)
- (164) 48, 109, 358 (1950).
- (165) J. Taylor, R. Burns. 45 (1940).
- (166) J.Taylor, O.A.Gurton. 48, 109 (1950). In the press.
- (167) J. Taylor, C.R.L.Hall. 28, 51, 593 (1947).
- (168) J. Taylor, J. Hancock. 48, 106, 678 (1947).
- (169) J. Taylor, R.E.Ward. 45 (1940).
- (170) L.H.Thomas. 19, 12, 449 (1944).
- (171) O.M.Todes. 56, 11, 71 (1933).
- (172) V.A.Tsukerman. 30, 40, 267 (1943).
- (173) W. Weibull. 5, 159, 402 (1947).
- (174) J. Whetstone. 45 (1948).
- (175) R. York, E.P.White. 34, 40, 227 (1944).

KEY TO JOURNALS.

The abbreviations are those used by the Chemical Society in their Abstracts

1. Phil. Trans (A)
2. Proc. Roy. Soc. (A)
3. Phil. Mag.
4. Proc. Physical Soc.
5. Nature
6. Compt. rend.
7. J. Math. pures, appl.
8. J. école polyt.
9. Chim. et Ind.
10. Z. Physik
11. Ann. Physik
12. Z. tech. Phys.
13. Z. Schiess. und Spreng.
14. Z. Elektrochem.
15. Akust. Z.
16. Z. Ver. deut. Ing.
17. Forsch. Geb. Ing-wes.
18. J. Amer. Chem. Soc.
19. J. Chem. Physics.
20. Proc. Amer. Acad. Arts Sci.
21. Ann. Chim. et Phys.
22. Abhand. Ges. Wiss. Göttingen
23. Sitzungsber. Akad. Wiss. Wien
24. Z. physikal. Chem.
25. Bull. Soc. Ind. Minerale.
26. Proc. Amsterdam Acad.
27. Bull. Calcutta Math. Soc.
28. J. Phys. Coll. Chem.
29. Rev. Mod. Physics
30. Compt. rend. Acad. Sci. U.R.S.S.
31. J. Exp. Theor. Physics U.S.S.R.
32. J. Res. Nat. Bur. Stand.
33. Chem. Rev.
34. Trans. Amer. Inst. Chem. Eng.
35. Proc. Camb. Phil. Soc.
36. Physical Rev.
37. J.C.S.
38. Physikal Z.
39. Z. Turbinenwes.
40. Research.
41. O.S.R.D. papers (quoted in
Ref's. 33, 37).
42. R.C. papers (Quoted in Ref. 33).
43. M.S. Atomic reports (declassified).
44. Trans. Faraday Soc.
45. Privately published I.C.I. reports.
46. Private communication.
47. Coll. Guardian.
48. Trans. Inst. Min. Eng.
49. Z. angew. Chem.

- 50. Mem. Poudres Salp.
- 51. Trans. Soc. Instr. Tech.
- 52. Nav. Ord. papers (Quoted in Ref. 37).
- 53. U.K. Patent.
- 54. Mém. Artill. franç.
- 55. Rev. d'Optique
- 56. J. Phys. Chem. Russ.
- 57. Safety in Mines Res. Board Papers.
- 58. J. Appl. Physics.
- 59. Engineering.
- 60. Third Symposium on Combustion and Explosion, Wisconsin, 1948.
- 61. Acta Physicochim. U.R.S.S.

*From the PHILOSOPHICAL MAGAZINE, Ser. 7, vol. xxviii. p. 1,
July 1939.*

**THE IGNITION OF INFLAMMABLE GASES BY HOT
MOVING PARTICLES.**

BY

**STEWART PATERSON, M.A., B.Sc.,
METCALFE RESEARCH FELLOW, GLASGOW UNIVERSITY.**

*From the PHILOSOPHICAL MAGAZINE, Ser. 7, vol. xxviii. p. 1,
July 1939.*

The Ignition of Inflammable Gases by Hot Moving Particles.

By STEWART PATERSON, M.A., B.Sc., Metcalfe Research Fellow,
Glasgow University *.

1. *Introductory.*

THAT the igniting power of heated solid particles introduced into an inflammable gas will diminish with increasing speed of motion through the gas can be deduced from the observations of several writers †, but no quantitative determinations of the influence of speed seem as yet to have been published.

In view of the practical importance of this matter, especially in connexion with accidents from explosion in mines, as well as its general interest, it was thought desirable to undertake measurements of the effect

* Communicated by Prof. E. Taylor Jones.

† Wüllner and Lehmann, *Ann. Min. Belg.* vi. p. 9 (1886). Couriot and Meunier, *Ann. Min. Belg.* xiii. p. 91 (1908). White and Price, *J. Chem. Soc.* cxv. pp. 1479, 1501 (1919). Mason and Wheeler, *J. Chem. Soc.* cxxxi. p. 2089 (1922). Burgess and Wheeler, "Safety in Mines Research Board Paper 46," p. 7 (1928); paper 54, p. 10 (1929); paper 62, p. 11 (1930). Coward and Wheeler, *S. M. R. B.* paper 53, p. 19, 23 ff. (1929). Silver, *Phil. Mag.* (7) xxiii. p. 641 (1937).

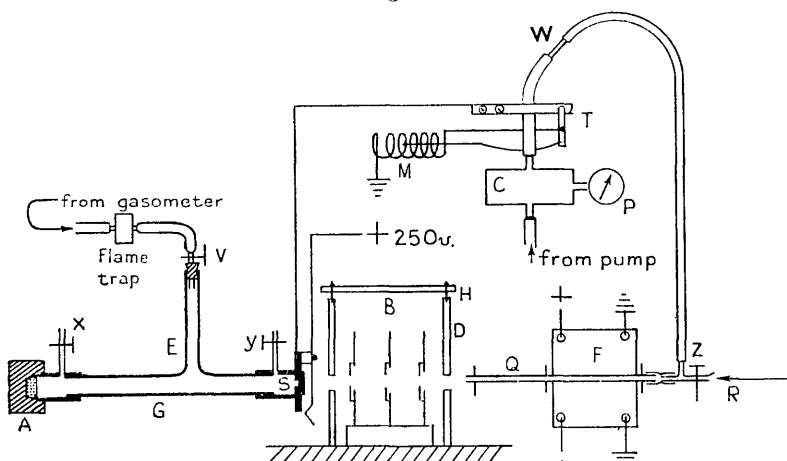
of speed, which, with theoretical observations upon them, are described in the present paper.

2. Experimental Arrangement.

The particles used were small platinum and quartz spheres, and the method consisted, briefly, in heating these pellets in a horizontal tube furnace and shooting them by means of compressed air into a vessel containing explosive gas; the speeds were previously determined with a ballistic pendulum.

Fig. 1 illustrates the arrangement finally adopted as most suitable for the purpose of the experiments.

Fig. 1.



Semi-diagrammatic view of apparatus.

The explosive gas was contained in a horizontal tube G of pyrex glass, 80 cm. long and 4 cm. in diameter. The tube was closed at the end A by a conical cap of wood, which fitted tightly over a conical brass sheath and contained a plug of wet asbestos wool to receive the pellet. The other end bore a brass cap with a circular opening 1 cm. in diameter, which could be closed by the rotary shutter S. The vertical side-tube E served as an indicator of successful ignition by the moving particle: the flame which spread through E could readily be observed, whereas the flame in G, travelling with the ball, was much more rapid.

The pellet under examination was heated in a quartz (fused silica) tube Q, clamped within the furnace F. In order to secure a wide range of speed, and accurate aiming, the quartz tube, whose function is to

direct and accelerate the pellet, must have a bore very little (usually about 10 per cent.) greater than the diameter of the pellet, and as long a "muzzle" as possible. A glance at the calibration curves of fig. 2 will show the relative importance of this muzzle-distance when higher speeds are required. 2-foot tubes were finally employed, corresponding to a muzzle of about 45 cm. The question of cooling in the muzzle has been considered. (Section 5, p. 10.)

Various metals have been used for the furnace-winding—nichrome, molybdenum, kanthal, and platinum. An efficient and economical furnace was finally constructed on the "cascade" principle due to Harker *: its heating element is a platinum-wound alundum tube (12 in. $\times \frac{1}{4}$ in.) protected by a wider coaxial "Kanthal A 1" coil, also mounted on an alundum tube and generously lagged. The furnace consumes about 330 watts at 1300° C. and was used up to that temperature for over 300 hours without injury. It has been taken up to 1500° C.

The quartz tube Q was joined by rubber to a glass "T"-piece, having a tap Z on the horizontal arm. Through this tap the pellet could be introduced into Q and afterwards viewed by an optical (Wanner type) pyrometer, which faced in the direction of the arrow R. Silver † has explained that this type of instrument may be used under our conditions. As a check the pyrometer was compared with a standard thermocouple, and found in perfect agreement over the range used (800° C.–1300° C.). Temperatures given below are therefore direct pyrometer readings. The question of how far these readings correspond to the temperature of the pellet *when it enters the explosive mixture* is considered in Section 5, p. 10.

The compressed air was generated in a reservoir C (equipped with a 60 lb./sq. in. gauge P), and released through Q by the tap T. Consistent speeds were obtained only when the rate of release did not vary, and a spring tap was therefore used: it was simply a strip of spring brass bound down across the pressure lead by a rotary switch. This tap reduced the variation in speed at any given pressure to ± 1 per cent. A ball-valve W prevented excessive loss of air from C.

For simplicity in operation, the shutter S and tap T were electrically connected, by a device somewhat similar to that used by Silver ‡. When S had just completely uncovered the entrance to G, it closed a circuit through the solenoid M, and the attraction of M on a soft iron rod was communicated to the switch of T by a slack chain. To eliminate auxiliary switches, the components of T were themselves placed in the solenoid circuit.

* Harker, Proc. Roy. Soc. (A) lxxvi. p. 235 (1905).

† Silver, loc. cit. p. 640.

* Loc. cit. p. 639.

To filter out the pellet from its propelling air, which was found to disturb ballistic measurements and presumably tended to dilute the explosive mixture, as well as being itself capable of producing ignition *, three baffle-plates B were introduced between S and Q. Experience showed that three plates were sufficient, when placed at least 8 cm. apart, the extreme plates being 10 cm. from S and Q respectively. The accurate aiming † permitted the use of such small apertures that the air which passed through B had a scarcely measurable effect on the pendulum. Each plate was furnished with a device which permitted adjustment of the position (and size) of the aperture to compensate for bends developed in Q by the heating. A shield D was erected over the plates in order to trap the ball if it failed to pass through : the gap indicated at H in fig. 1 is necessary, to allow the puff of air an alternative (and wider) exit.

3. Experimental Procedure.

The pressure gauge on C was first calibrated in terms of speed for a number of convenient muzzles. A ballistic pendulum was used (in place of G), the pellet being caught in a plug of plasticine on the bob and the deflexion recorded by a graduated thread drawn through a smooth hole. Fig. 2 shows a specimen calibration.

As a check this was repeated after each experiment proper. It was done with the furnace cold : variation of speed with temperature is not to be anticipated, in view of the small coefficients of expansion of quartz and platinum.

In ignition experiments the pellet was inserted through tap Z and pushed carefully into the chosen position with a quartz rod. Its temperature and propelling pressure were adjusted to suitable values, and the explosion-vessel filled with gas by displacing the air. Taps X, V, Y, Z were then closed in that order, and S (and thereby T) opened. If an explosion occurred ‡, the condensed water was evaporated from G by a current of air before refilling with gas.

Ignition was recorded by a cross, non-ignition by a circle, on a plane whose coordinates were speed (abscissa) and temperature. When the available ranges of these variables had been covered, the appropriate region of the plane was divided roughly into two parts, one containing crosses only, and corresponding to ignition, the other circles only, corresponding to non-ignition. It was possible to draw a curve separating these regions, and this curve was taken to represent approximately the relation between speed and igniting temperature.

* Experiments on the igniting power of hot air are at present in progress.

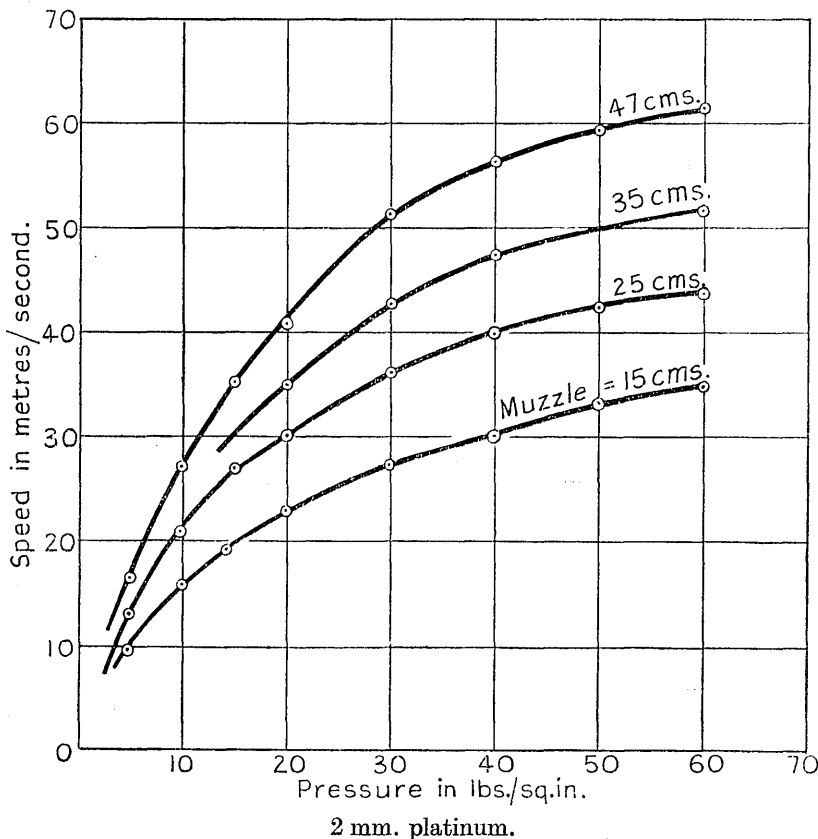
† The "spread" at A did not exceed 1 cm. ; the distance AQ exceeded 1 metre.

‡ There was seldom any ambiguity.

4. Results.

Coal-gas-air mixtures were used throughout, Silver having shown * that methane-air required inconveniently high temperatures. It is hoped that the observations on coal-gas will apply at least qualitatively

Fig. 2.



to other explosive mixtures and in particular to fire-damp. The following analysis of the gas used was kindly supplied by Glasgow Corporation :—

	H ₂ .	CH ₄ .	CO.	N ₂ .	CO ₂ .	C _n H _m .	O ₂ .	Total.
Per cent. .	50.1	18.8	18.4	6.5	3.4	2.3	0.5	100.0

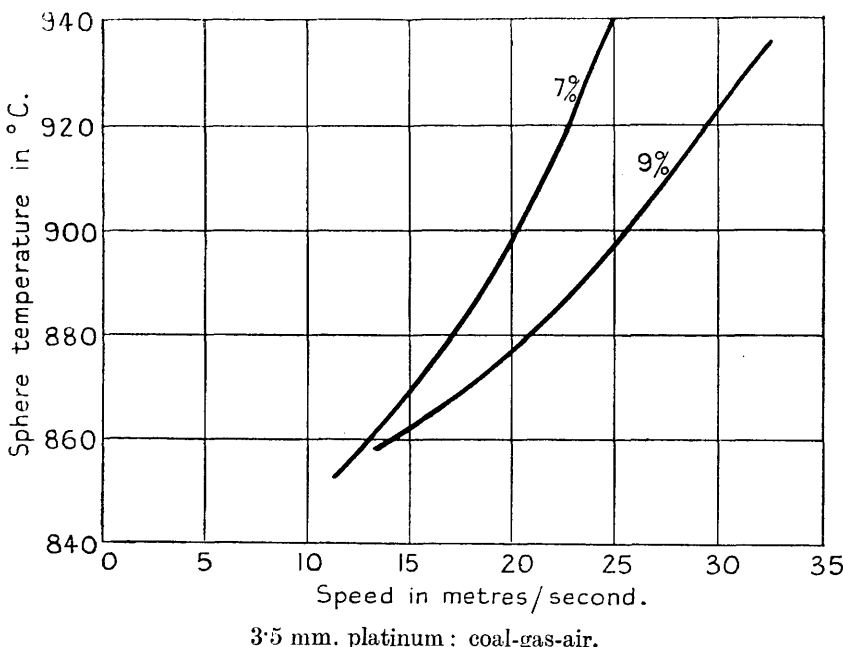
(A). *Platinum Spheres.*—The slope of the characteristic curve was found to decrease as the pellet diameter was increased. For diameters greater than 4 mm. this slope was so small that a temperature range of

* Loc. cit. p. 641.

only some 50° could be covered. As the pyrometer cannot detect differences much less than 10° , the curves were very vague. Our first results apply, therefore, to 3.5 mm. platinum spheres, and are shown in fig. 3.

It is to be understood that the region on the left of any characteristic corresponds to ignition, that on the right to non-ignition. In other words, there is at each temperature a limiting speed, defined by the curve, beyond which ignition is not obtained *. The characteristics are approximately linear, the curve for 9 per cent. coal-gas has a smaller slope than that for 7 per cent., and the "minimum" ignition temperature is about

Fig. 3.



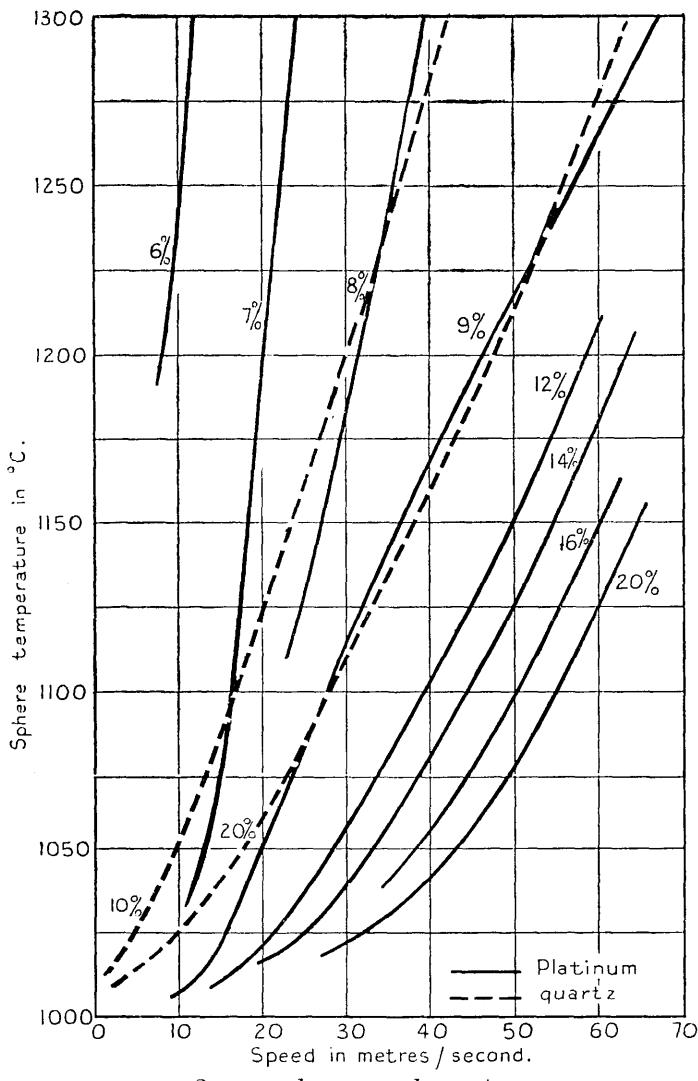
the same for each mixture. The form taken by the curves when both temperature and speed were very high could not be determined, owing to limitations of speed.

2 mm. platinum spheres were next examined ; this proved to be the most convenient size. We have seen that large spheres give flat and there-

* By suitable choice of temperature and speed, ignition can be delayed until the pellet is arrested at the asbestos target, whereupon flame spreads back through G to S. Though this fact is implied in the curves of figs. 3 and 4, it is thought worthy of mention, as a convincing demonstration of the effect of speed upon igniting power.

fore inaccurate characteristics ; in the same way pellets of less than 2 mm. diameter have characteristics which are equally indefinite because they

Fig. 4.



2 mm. spheres: coal-gas-air.

are so steep. The high speeds (over 100 metres/second) available at 60 lb./sq. in. with 1.5 mm. platinum spheres could not, unfortunately, be put to any use. With the 2 mm. pellets, a 9 per cent. mixture was

first examined. The characteristic is shown on fig. 4, together with subsequent results for other mixtures. The 9 per cent. characteristic covers the entire available range of speed (0–64 metres/sec.) and over 300° of temperature (980° C.–1310° C.), and summarizes the results of 290 shots.

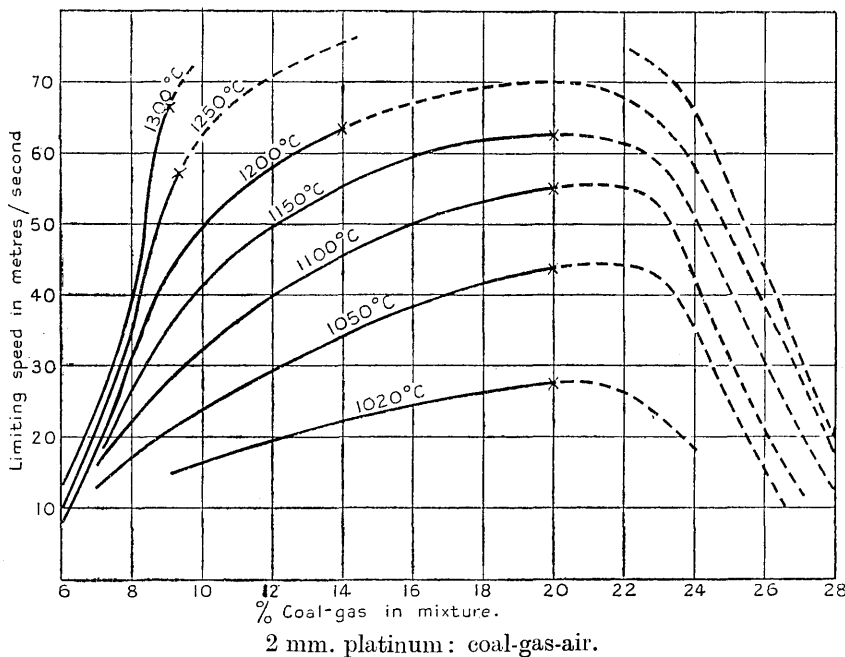
Similar curves were derived for 6, 7, 8, 12, 14, 16, and 20 per cent. coal-gas : the effect of concentration was found to be very marked (fig. 4). The same features, however, can be noted in fig. 4 as in fig. 3 : the curves are all linear except for an initial "tail"—they all rise from approximately the same minimum temperature, and their slope decreases, as the concentration is raised from the lower limit of inflammability (5–6 per cent.) towards its value for maximum flame-speed (about 20 per cent.).

When the limiting speed (that is, the greatest speed which will permit ignition at a given temperature) is graphed, for any chosen temperature, against percentage gas in mixture, a curve is obtained, which rises as concentration increases, but shows a distinct tendency to flatten out at 16–20 per cent. (fig. 5). This prompts one to enquire whether, for greater concentrations, the curve may descend again. 25, 26, 28, 30, and 32 per cent. mixtures were tried, in order to decide the question. A difficulty was, however, foreseen. When the shutter S is opened, diffusion at once smooths out the discontinuity of concentration, so that every mixture from pure air to the gas in G is to be found in this region. Provided we are using a concentration less than 20 per cent., the above results show that the diluted mixtures are all *less* ignitable, and so any ignition can safely be recorded as an ignition of the gas in G. But if the curves of fig. 5 descend beyond 20 per cent., and if G contains a mixture beyond this strength, then some of the diluted mixtures will be, not less, but *more* ignitable. Hence an explosion may take place under conditions which would not ignite the mixture in G. This explosion will, of course, traverse the (richer) gas in the tube (supposed below the upper limit of inflammability—about 32 per cent.), and unless the flame-speed is low, *i. e.*, the mixture well beyond 20 per cent., it will be difficult to say whether the flame is *accompanying* the pellet or merely *following* it. The turbulence and heating produced by the pellet will evidently exaggerate this difficulty by increasing the normal speed of the flame.

That the curves of fig. 5 do descend again was proved quite clearly by explosions in 28 and 30 per cent. mixtures. These were difficult to ignite by *direct action of the pellet*; they behaved in much the same way as 7 and 8 per cent. except that, even when a non-ignition was obviously to be recorded, a green flame started at the shutter, as far as could be judged at the moment of passage of the pellet, and floated along the tube in its wake. Counting this as a non-ignition, 30 per cent. could not be ignited at 10 metres/sec. even at 1300° C. 28, 26, and 25 per cent. mixtures behaved very erratically, as indeed the above argument would

anticipate. It appeared useless to look for *real* characteristics at these concentrations. One point, however, was tested. If the explosions with these rich mixtures are often due (as there is little doubt) to the diluted gas at the shutter, then the characteristic in which *every* sort of ignition is counted as an "ignition" should coincide with that appropriate to the most ignitable mixture, and so will not be very different from the 20 per cent. curve. This was found approximately true. The curves for "shutter-ignition" in 25, 28, 32 per cent. were all more or less the same, and coincided roughly with that for 20 per cent.; they seemed to suggest

Fig. 5.



that 21 per cent. might be (slightly) more ignitable than 20 per cent. In fig. 5 the broken lines indicate what is probably the course of the curves above 20 per cent.; but except near 30 per cent. they are very uncertain.

(B) *Quartz Spheres*.—On account of their fragility and irregular shape these have not been used to the same extent as platinum. It was found, however, that good spheres could easily be made in the carbon arc, and results for 2 mm. quartz are shown (by a broken line) in fig. 4. Very high speeds could be commanded, but were of little use, as the characteristics rose much more steeply than in the case of platinum. It will be noticed that the *minimum* ignition temperatures of the two mixtures

used coincide, just as was found with platinum ; moreover, what is more interesting, these minimum temperatures are the same for the two substances : this agrees with Silver's * result. At high speeds, however, quartz and platinum show marked differences in behaviour.

Note on "Ageing" of Spheres.

It had been noticed throughout the work with 2 mm. platinum spheres (of which five were used) that the older spheres were always more efficient in igniting than the new. A characteristic was sketched for a new pellet and found approximately parallel to the corresponding curve of fig. 4, but displaced upward, except at the lower end, through about 40° . Similar improvements with platinum wires are on record †. It is thought probable that some connexion exists in the present case between the increased igniting power and the conspicuous surface-changes which took place. Before use the platinum spheres were polished and metallic in appearance. After a few ignitions they took on a milky aspect, as though the surface had been ruffled. Through long use their colour changed to dark grey and finally to a grey-black. The surface looked very rough under a low magnification. (The track on a photographic plate of the "aged" sphere was much brighter than that of a new sphere at the same temperature and speed.)

Sufficient work has not been done with quartz to detect such an improvement if it exists ; but the surface undergoes a rapid change, becoming opaque after a few ignitions.

5. Cooling of Spheres.

As was pointed out above, the use of baffle-plates requires that the pellet traverse about 40 cm. of air between heating-tube and explosion-vessel. It is obviously important to know whether any considerable cooling takes place in this interval, and, if so, whether it depends on the speed of transit. The question will first be considered theoretically.

The heat-losses from a sphere moving in a fluid are due to :

- (a) Radiation.
- (b) Conduction-convection.

(a) The radiation loss from a heated surface may be expressed as $\leq e\sigma AT_s^4$, where σ is Stefan's constant $((5 \cdot 6)10^{-12}$ watt/cm. 2 .°K. 4), A the area and T_s the absolute temperature of the surface, and e a factor depending on the surface and also on T_s . The maximum value of e is,

* *Loc. cit.* p. 644 ; fig. 3.

† Thornton, Phil. Mag. (6) xxxviii. p. 615 (1919) ; Shepherd and Wheeler, S. M. R. B. paper 36, p. 19 (1927).

of course, 1, when the surface is perfectly black ; for polished platinum at 1600° K. International Critical Tables give 0.197 *. We shall probably be safe, therefore, in adopting the value $e=0.5$ as an upper limit in our case. The loss per sq. cm. is then $<(2.8)10^{-12}(1573)^4$ watts at the upper limit (1573° K.) of our temperature range,

$$\text{i.e.,} \quad \text{loss/cm.}^2 \text{ sec.} < 4.08 \text{ calories.}$$

For a 2 mm. sphere, therefore,

$$\text{loss} \equiv \frac{dH_R}{dt} < 0.502 \text{ cals./sec.}$$

The speeds used varied from 10^3 to 6.10^3 cm./sec. and the gap was 40 cm., to which must be added a further 30 cm. in the cold muzzle. Thus the time of cooling varied from 0.07 to 0.0117 sec. With the exception of the 6 and 30 per cent. mixtures, however, the minimum speed at 1573° K. was over 2.10^3 cm./sec., and so the time of cooling less than 0.035 sec. Hence the heat-loss (H_R) from radiation was always less than 0.0176 cal., and usually much less than this.

If, now, the surface temperature T_s be identified with that of the sphere as a whole (see below), a loss of 0.0176 cal. will produce a temperature drop $-DT_s = \frac{0.0176}{mc_1}$, m being the mass and c_1 the specific heat of the sphere. For a 2 mm. platinum sphere, $m=0.093$ gm. As to c_1 , Landolt-Börnstein † give, for platinum :

$$0-1000^\circ \text{ C. : } c_1 = 0.0377 \text{ cal./gm. } ^\circ\text{K.}$$

$$0-1177^\circ \text{ C. : } c_1 = 0.0388 \text{ cal./gm. } ^\circ\text{K.}$$

whence c_1 at 1100° C. is approximately 0.045 cal./gm. $^\circ\text{K.}$ International Critical Tables ‡ give

$$c_1 = \frac{1}{(4.2)(195.2)} \cdot [25.89 + (5.23)10^{-3}\theta] \text{ cal./gm. } ^\circ\text{K.}$$

at Centigrade temperature θ : this expression leads to a value of 0.0386 at 1100° C. Adopting 0.04 as a probable least value in our range, we have, finally,

$$-(DT_s)_R \leq 4^\circ.3.$$

(b) The loss by conduction-convection is not so readily estimated. In the first place it must be stated that all the results, experimental and theoretical, which we shall use refer to conditions where a *steady* heat-field has been set up ; however, the consideration that our pellet emerges

* Vol. v. p. 243.

† *Phys. Chem. Tabellen.*

‡ Vol. v. p. 93.

from the heating-tube in a sheath of hot air suggests that the estimates of heat-loss on the assumption of steady flow are not likely to be too small.

The only available data on the convective cooling of spheres refer to diameters of the order of 1 cm. and relatively low temperatures and speeds ; we have recourse, therefore, to the Similarity Principle, in order to render them applicable. Considerations of similarity show * that the heat-loss per second from a sphere of radius a at temperature T_s (absolute) to a fluid at T_∞ , when the state is steady and natural convection relatively small, is

$$\frac{dH_c}{dt} = ak(T_s - T_\infty)\psi(Re, St) \quad \dots \dots \dots \quad (1)$$

k being the thermal conductivity of the fluid, and $\psi(Re, St)$ some unknown function of the Reynolds number (Re) and Stanton number (St) †. k , Re , St must be calculated for the appropriate temperature, which is usually taken as $T = \frac{1}{2}(T_s + T_\infty)$ ‡.

Kinetic theory allows us to write $St = \text{const.}$ for a given gas, and in particular we have $St = 1.35$ § for diatomic gases (e. g., air),

i. e., $k = 1.35 \mu c_p$, and so (1) becomes

$$\frac{dH_c}{dt} = a\mu c_p(T - T_\infty)\phi(Re) \quad \dots \dots \dots \quad (2)$$

ϕ being some unknown function. Boussinesq, with certain simplifying assumptions, derived ϕ theoretically ; he gave ||

$$\frac{dH_c}{dt} = 4\sqrt{2\pi k\rho c_p}Va^3(T_s - T),$$

$$\text{i. e.,} \quad \frac{dH_c}{dt} = [4\sqrt{1.35\pi}]a\mu c_p(T_s - T_\infty)\sqrt{Re}.$$

which implies that

$$\phi(Re) = 8.26\sqrt{Re}.$$

* See Davis, Phil. Mag. (6) xliv. p. 940 (1922).

† $Re \equiv \frac{2Va\rho}{\mu}$; $St \equiv \frac{k}{\mu c_p}$, where $V \equiv$ velocity, $\rho \equiv$ density, $\mu \equiv$ (dynamical) viscosity, and $c_p \equiv$ sp. heat (const. press.), of the fluid.

‡ Nusselt, Zeits. d. Ver. deutsch. Ing. p. 685 (1917); Davis, Phil. Mag. (6) xli. p. 902 (1921).

§ Eucken, Phys. Zeits. xii. p. 1104 (1911); Langmuir, Phys. Rev. xxxiv. p. 404 (1912); Fage and Falkner (Aero. Res. Com. R. and M. no. 1408 (1931)) give $St = 1.30$ as a mean experimental value.

|| Journ. de Math. (6) I, iii. p. 308 (1905), etc. We have written ρc_p for Boussinesq's "C."

Compan * verified this form of ϕ from $Re=2100$ to $Re=8300$, and Mitchell's † results support the same conclusion, though he did not himself accept it, over a range of 1800 to 53,000. Our own values of Re are smaller (190 to 1500), but it is very unlikely that the above form will be departed from at these values: in the case of cylinders, the \sqrt{Re} -law fails, if it fails at all, only when Re becomes very large ‡. We therefore adopt

$$\frac{dH_c}{dt} = Aa\mu c_p(T_s - T_\infty) \sqrt{Re}, \quad \dots \dots \dots \quad (3)$$

A being a constant derivable from Compan or Mitchell. It follows that

$$-\left(\frac{dT_s}{dt}\right)_c = \frac{3A}{4\pi} \cdot \frac{\mu c_p}{a^2 \rho_1 c_1} (T_s - T_\infty) \sqrt{Re},$$

where ρ_1 , c_1 refer to the sphere, at T_s ,

$$i.e., \quad -\left(\frac{dT_s}{dt}\right)_c = \frac{Bc_p}{\rho_1 c_1} \sqrt{\frac{\mu \rho V}{a^3}} \cdot (T_s - T_\infty). \quad \dots \dots \quad (4)$$

For c_p , μ , ρ we have adopted the expressions § ($T \equiv$ absolute temp. = $\frac{1}{2}(T_s + T_\infty)$)

$$c_p = 0.2272(1 + 0.0002 T),$$

$$\mu = \frac{(15)10^{-6}T^{3/2}}{124 + T},$$

$$\rho = (1.293)10^{-3} \left(\frac{273}{T} \right).$$

Both Mitchell and Compan used copper spheres, and their range of temperature was comparatively low and narrow. Under these conditions, $c_p \sqrt{\mu \rho}$ is almost constant, with a mean value of 0.0001138 at $T=360$. c_1 may be taken as 0.1 and ρ_1 is 8.93. Inserting Mitchell's values of $\frac{dT_s}{dt}$ ‖, a , V , and $T_s - T_\infty$, we find $B = 2.72$ (cf. Boussinesq: 2.789). The agreement with Boussinesq is striking, but both estimates are almost certainly exaggerated. The theoretical figure refers to conditions of zero viscosity; but the boundary layer must reduce heat-transfer below Boussinesq's value. Indeed a comparison of his expressions ¶ for the loss from cylinders

* Ann. de Chim. et de Phys. xxvi. p. 545 (1902).

† Edin. Phil. Trans. xl. p. 47 (1901-4).

‡ Davis, Phil. Mag. (6) xli. p. 903 (1921).

§ Langmuir, loc. cit. pp. 404-405.

|| Uncorrected for radiation, which seems relatively small.

¶ Boussinesq, loc. cit. p. 297.

with the experimental data of King * shows an exaggeration of about 65 per cent. Again, Hughes † has recorded a considerable increase in heat-loss when the sphere is suspended (as in Mitchell's experiments) in a relatively narrow pipe. It seems probable, therefore, that B is less than 2.72 ; but if we adopt that figure, then

$$-\left(\frac{dT_s}{dt}\right)_c = \frac{2.72c_p}{\rho_1 c_1} \sqrt{\frac{\mu \rho V}{a^3}} \cdot (T - T_\infty), \dots \quad (4')$$

an equation applicable to all cases of spheres in (unbounded) fluids under steady conditions of forced convection. Let us apply (4') to the 2 mm.

platinum spheres. Since the cooling is small, we write $(\Delta T_s) = \left(\frac{dT_s}{dt}\right)_c \Delta t$;

and $\Delta t = 40/V$ (the *convective* cooling begins only after emergence, cf. p. 11).

$\frac{T_s - T_\infty}{\sqrt{V}}$ had a max. value $10\sqrt{10}$, and appropriate values of a , ρ , μ , c_p ,

c_1 , ρ_1 , are : $a = 0.1$, $\rho = (3.716)10^{-4}$, $\mu = (4.09)10^{-4}$, $c_p = 0.270$, $c_1 = 0.044$, $\rho_1 = 21.37$.

Hence

$$-(\Delta T_s)_c < 12^\circ.2.$$

The maximum radiation drop was $4^\circ.3$. These maxima do not really occur together, so that their sum, i. e., $16^\circ.5$ is greater than the greatest drop to be expected. In the opinion of the writer it is *considerably* greater.

Compan's results can also be used to evaluate the constant B of (4) : the result is 0.448, which is much smaller than Mitchell's figure. The fact that Compan used a wider pipe may partly account for the difference ; at any rate, the value of our convective drop based on his work would be $2^\circ.0$ instead of $12^\circ.2$.

It remains to justify the above assumption of uniform temperature throughout the pellet. We make use of Fourier's ‡ well-known solution for symmetrical heat flow in a solid sphere, when the surface loss is proportional to the excess surface temperature $T_s - T_\infty$. It is

$$\frac{T(r, t) - T_\infty}{T_0 - T} = \frac{2pa}{k_1} \sum_{n=1}^{\infty} \left[\frac{\sin \frac{\epsilon_n r}{a}}{\frac{\epsilon_n r}{a}} \cdot \frac{e^{-\frac{k_1}{\rho_1 c_1} \cdot \frac{\epsilon_n^2 t}{a^2}}}{\epsilon_n \operatorname{cosec} \epsilon_n - \cos \epsilon_n} \right],$$

* King, Phil. Trans. (A) ccxiv. p. 405 (1914).

† Hughes, Proc. Univ. Durham Phil. Soc. viii. p. 189 (1930).

‡ *Théorie Anal. de la Chaleur*, ch. v.

where $T(r, t)$ is temperature of shell, radius r , at time t ; T_0 the (uniform) temperature of sphere when $t=0$; k_1 the thermal conductivity of sphere; $p[T(a, t)-T_\infty]$ the heat loss per unit area per second, and ϵ_n the n th +ve real root of the equation

$$\epsilon \cot \epsilon = 1 - \frac{pa}{k_1}.$$

Now $p=p_c+p_r$ (convection and radiation), where

$$p \equiv \frac{dH_c/dt}{4\pi a^2(T_s - T_\infty)}$$

$$= 0.0003020\sqrt{V} \text{ from (3), (4'),}$$

with a maximum value of 0.02340 at $V=6000$; and

$$p_r \equiv \frac{dH_r/dt}{4\pi a^2(T_s - T_\infty)}$$

$$\doteq \frac{e\sigma(T_s^4 - T_\infty^4)}{T_s - T_\infty}$$

$$\doteq e\sigma T_s^4/(T_s - T_\infty),$$

and while this is not constant we can regard it as being so, with its greatest value, viz., 0.00315 (at $T_s=1573$, $T_\infty=293$)

$$\therefore p \leqq 0.0266.$$

As to k_1 , we have no data for high temperatures, but theoretically k is independent of T for metals. Assuming $k_1=0.17$, we have for ϵ the equation: $\epsilon \cot \epsilon = 1 - 0.0157$; the first two roots are: $\epsilon_1 \doteq 12^\circ 20'$ and $\epsilon_2 \doteq 257^\circ 39'$. The second term of the series is found to be minute compared with the first, even for $t=0$, $r=0$. Consequently,

$$\frac{T - T_\infty}{T_0 - T_\infty} \doteq \frac{2pa}{k_1} \cdot \frac{\sin \frac{\epsilon_1 r}{a}}{\frac{\epsilon_1 r}{a}} \cdot \frac{e^{-\frac{k_1}{\rho_1 c_1} \cdot \frac{\epsilon_1^2 t}{a^2}}}{\epsilon_1 \operatorname{cosec} \epsilon_1 - \cos \epsilon_1}.$$

Hence if T_c is the core-temperature

$$\frac{T_c - T_\infty}{T_s - T_\infty} = \frac{\epsilon_1}{\sin \epsilon_1} \doteq \frac{100}{99.3}.$$

There is thus, in our experiments with 2 mm. platinum spheres (and *a fortiori* with larger sizes) never more, and generally much less, than 1 per cent. drop in surface-temperature as compared with core-temperature.

The above analysis suggests that the cooling during flight is not of such a magnitude as to vitiate our experimental results. In particular it

may be observed that the effect increases with decrease of speed, so that the slower ball is, if anything, *cooler* than the faster ball. There is, therefore, no question of the effect of speed upon ignition being due to cooling.

The theory has been tested in three ways :—

(1) Calorimetric measurements were made by shooting the ball into a small brass vessel, placed beyond the baffles, and connected to a thermocouple. No difference in heat-loss could be detected between a 15 metre/sec. and a 30 metre/sec. ball after traversing the same stretch of air (the apparatus was accurate to $\frac{1}{2}$ per cent.).

(2) Ignition curves were derived in the usual way with the mouth of the heating tube removed to 64 cm. instead of 40 cm. from the explosion tube. The curves coincided with those formerly obtained at 40 cm. This indicates that the heat-loss at 40 cm. was of such a magnitude that (assuming it to be proportional to the distance traversed) an increase of 50 per cent. was unobservable. The original heat-loss, itself, may therefore be taken as negligible.

(3) Direct photographic record was made of the temperature of the pellet surface during flight, by shooting it across the field of a wide angle lens. A series of tracks, on one plate, corresponding to the same speed of flight (indicated by curvature), but different temperatures, allowed the cooling to be estimated. Differences of 20° produced a noticeable change in intensity, and it could be said with conviction that no such cooling occurred.

6. Theoretical.

The factors which may be supposed to affect the ignition of a gas by a hot moving surface are so many, and in some cases so obscure, that a complete theory is probably out of the question. To begin with, the hydrodynamical problem of fluid flow round a sphere, except in the ideal case of zero viscosity and subcritical speeds, is exceedingly complex. It is true that viscosity-effects in gases are small at a distance from solid surfaces ; but they become important in the boundary layer adjoining these surfaces, and it is precisely with such a layer that we are concerned ; moreover, the speeds employed have often been above the critical limit for stream-line flow ; in other words, ignition spreads through a turbulent wake, and the conditions of continued propagation may be thereby complicated. When the hydrodynamical equations are taken in conjunction with the equations of heat transfer, they present a problem which cannot in general be solved exactly. Its solution, however, would be of doubtful value for our purpose, as we may expect the conditions of fluid-flow and heat-transfer to be modified if not transfigured by the chemical reaction. This reaction in turn is far from simple, when initiated, as in our case, by an incandescent surface. How far the ignition is purely

thermal and how far it depends on adsorption at the surface we do not know.

The following theory is a " thermal " one, developed along the lines followed by Silver *, i. e., on the assumption that extinction is due to over-rapid loss of heat to the unburnt gas. The process of ignition is considered to occur in the viscous boundary layer surrounding the sphere : we therefore regard the sphere as at rest in, and at the same temperature as, the immediately adjoining gas, but losing heat at a rate dependent (as indicated in section 5 above) on its real velocity through the distant gas, and proportional to its temperature excess over that gas. This implies a surface temperature gradient which is similarly proportional ; and we further assume with Silver, though this may perhaps be questioned, that the same gradient persists for a small, but finite distance out into the

gas, i. e., that $\frac{\partial^2 T}{\partial n^2} = 0$ at the surface, n being a normal vector.

Let us assume the rate of heat-transfer (total) to be given by equation (3) of section 5, i. e., by

$$\begin{aligned}\frac{dH}{dt} &= A a \mu c_p (T_s - T_\infty) \sqrt{Re} \\ &= \frac{A}{1.35} a k (T_s - T_\infty) \sqrt{\frac{2aV\rho}{\mu}} \dagger.\end{aligned}$$

We assume also spherical symmetry, and therefore adopt a uniform

surface gradient $\frac{\partial T}{\partial n}$ given by :

$$-4\pi a^2 k \frac{\partial T}{\partial n} = \frac{A}{1.35} a k (T_s - T_\infty) \sqrt{\frac{2aV\rho}{\mu}},$$

whence
$$\frac{\partial T}{\partial n} = -C(T_s - T_\infty) \sqrt{\frac{V\rho}{a\mu}} \ddagger,$$

in which $C = \frac{A\sqrt{2}}{(1.35)4\pi}$ is a numerical constant with a probable value of

* Loc. cit. p. 649.

† See page 12.

‡ It is interesting to note that essentially the same expression for $\frac{\partial T}{\partial n}$ is obtained by assuming the temperature to fall uniformly from T_s to T_∞ in the thickness of the boundary layer ; for this thickness is of the order of $\sqrt{\frac{a\mu}{V\rho}}$ (see Prandtl, *Handbuch der Experimentalphysik*, iv. 1, p. 36).

about 0·6 (Boussinesq : 0·8358). This gradient is assumed to hold throughout a shell of thickness δ . The rate of loss of heat from this shell is therefore

$$4\pi(a+\delta)^2Ck\sqrt{\frac{V\rho}{a\mu}}(T_s-T_\infty)-4\pi a^2Ck\sqrt{\frac{V\rho}{a\mu}}(T_s-T_\infty)$$

i. e., $8\pi Ck\delta(T_s-T_\infty)\sqrt{\frac{V\rho a}{\mu}},$

which must be equated to the rate of development of heat through reaction in order to define a critical condition for flame. This heat of reaction is, in Silver's notation, $\int_a^{a+\delta} 4\pi x^2 \beta Q e^{-A/RT(x)} dx$, where $T(x)$ by our assumption is $=T_s - C(T_s - T_\infty) \sqrt{\frac{V\rho}{a\mu}}(x-a)$. In order that the variable part may be relatively small and the integral reduce to $4\pi a^2 \delta \beta Q e^{-A/RT_s}$, we require $\delta C \sqrt{\frac{V\rho}{\mu a}}$ small: in other words, δ must be small compared with the thickness of the boundary layer ($C \approx 1$), which is otherwise evident. Equating these heats,

$$8\pi Ck\sqrt{\rho/\mu}(T_s-T_\infty)V^{1/2}=\beta Qa^{3/2}e^{-A/RT_s} \dots \dots \dots \quad (1)$$

In this equation, $k\sqrt{\rho/\mu}$ will vary little with temperature in our range [$\frac{1}{2}(T_s+T_\infty)=783$ to 933] for any one explosive mixture: for air the variation is only between $(14\cdot38)10^{-5}$ and $(14\cdot27)10^{-5}$; it will vary to a greater extent with the mixture strength, but still not enough to vitiate our (chiefly qualitative) applications of (1). Again, Q is a characteristic of the reaction, which we suppose the same in each case. Hence

$\frac{8\pi k C \sqrt{\rho/\mu}}{Q}$ will be regarded as a single constant D . In the resultant equation, viz.,

$$D(T_s-T_\infty)V^{1/2}=\beta a^{3/2}e^{-A/RT_s}, \dots \dots \dots \quad (2)$$

β depends only on the concentration (for a given reaction), A is regarded as constant, and R is the gas-constant per gram-molecule.

Comparison with Experiments (on Coal-Gas).

(a) If the mixture (β) and V , T_∞ are kept constant, (2) gives

$$a^{3/2} \propto (T_s-T_\infty)e^{A/RT_s}.$$

We suggest, therefore, that $\log \left(\frac{T_s-T_\infty}{a^{3/2}} \right)$ will vary linearly with $1/T_s$.

and that the "gradient" will be $-\frac{A}{R}$. Inserting Silver's results, we find

that this is true, except that, as with Silver's own expression $\log\left(\frac{T_s - T_\infty}{a}\right)$, the gradient seems more nearly $-\frac{2A}{R}$. But the value of A is uncertain.

(b) If T_s , T_∞ , and a are constant, and the mixture (β) variable, then

$$V \propto \beta^2.$$

β consists of two factors, the constant C of the integrated van't Hoff isochore $w = Ce^{-A/RT}$ and a factor f which depends on the concentration of the mixture. While f is unknown unless the kinetics of the reaction are completely specified, it may be taken as varying from zero at a 0 per cent. mixture through a maximum to zero at a 100 per cent. mixture. Since, therefore, $V \propto f^2$ we have qualitative agreement with our experimental curves of fig. 5.

(c) Keep β , a , T_∞ constant, as in the principal series of explosions. Then

$$V \propto \frac{1}{(T_s - T_\infty)^2} e^{-2A/RT_s};$$

writing

$$\frac{RT_s}{2A} \equiv \theta, \quad \frac{RT_\infty}{2A} \equiv \theta_\infty, \quad \text{we}$$

have

$$V \propto \frac{1}{(\theta - \theta_\infty)^2} e^{-1/\theta}.$$

Now

$$\frac{\theta_\infty}{\theta} = \frac{T_\infty}{T_s} \doteq \frac{3}{13} \quad \text{when } T_s = 1300$$

$$\text{and } \doteq \frac{3}{16} \quad \text{when } T_s = 1600.$$

$\therefore \frac{\theta_\infty}{\theta}$ varies only a little, and we may write $V \propto \frac{1}{\theta^2} e^{-1/\theta} \equiv v$ (say). When v is plotted against θ , it gives a curve of the well-known frequency shape, which is linear (approx.), with $\frac{d\theta}{dv}$ positive, between $\theta = 0.1$ and $\theta = 0.4$, i. e., between

$$T_s = \frac{2A}{10R} \quad \text{and} \quad T_s = \frac{8A}{10R}.$$

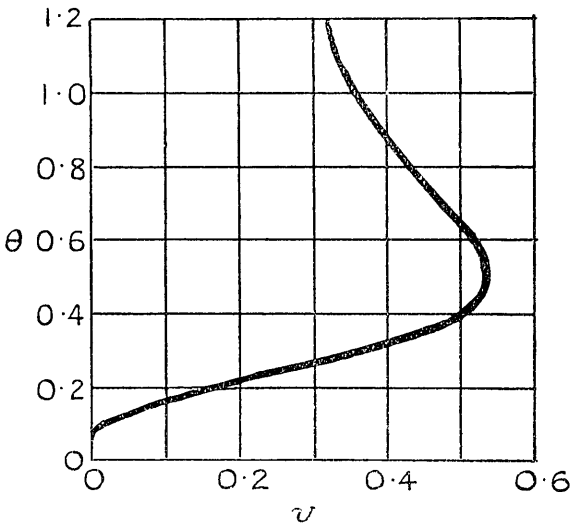
If we take A as 10,000 * and R as 2, the limits become : $T_s = 1000 \text{ } ^\circ\text{K}$. and $T_s = 4000 \text{ } ^\circ\text{K}$. These include our range of temperature. The theory therefore accounts for the linear form and the direction of the characteristics in figs. 3 and 4 ; it must be pointed out, however, that the value of A here assumed, while probably sound, is not that suggested by paragraph (a) above.

As to the *slopes* of the characteristics, they can be obtained from our theory in terms of the current coordinates V and T_s ; for evidently

$$\frac{dV}{dT_s} = \frac{2V}{T_s} \left\{ \frac{A}{RT_s} - 1 - \frac{T_\infty}{T_s} \right\}$$

$$\therefore \frac{2V}{T_s} \left\{ \frac{4700}{T_s} - 1 \right\}$$

Fig. 6.



$$\text{Graph of } v = \frac{1}{\theta^2} e^{-1/\theta}.$$

on the present assumption. The slopes have been calculated from this expression for the points on the curves of fig. 4 where $T_s = 1423$ (except 6 per cent.). They are all of the same order of magnitude as those displayed in fig. 4 ; in most cases the discrepancy is small, but in some it amounts to as much as ± 50 per cent. No systematic variation is apparent. The same remarks apply to fig. 3.

* Cf. Silver, *loc. cit.* p. 652.

(d) β , T_s , T_∞ constant. Then

$$V \propto a^3.$$

This relation is difficult to test, for unless the diameters of our spheres are very nearly equal there is no temperature at which points are known for both characteristics. For example, the 2 mm. platinum curves begin at about 1000°C . and those for 3.5 mm. platinum, owing to limitations of speed, have not been extended above 930°C . By extrapolation we have estimated the limiting speed for a 3.5 mm. sphere at 1020°C . in 7 per cent. coal-gas-air to be about 35 metres per second. The observed value for a 2 mm. sphere is 10 metres per second. These figures suggest rather $V \propto a^2$ than $V \propto a^3$.

(e) Our theory makes no provision for the nature of the surface, nor the material of the sphere. It is therefore probably unable to explain the difference in behaviour of quartz and platinum, and the "ageing" of the platinum spheres.

(f) Finally, keeping β , V , and a constant, let us examine the effect on T_s of varying T_∞ . From (2),

$$\frac{\partial T_s}{\partial T_\infty} = \frac{1}{1 - \frac{A}{R T_s^2} (T_s - T_\infty)}.$$

If $\frac{A}{R} = 5000$, as before, $T_s = 1300$, $T_\infty = 300$, then $\frac{\partial T_s}{\partial T_\infty} = -\frac{1}{2}$. Thus T_∞ ,

T_s should have variations of the same order, but in opposite directions. The explosive mixture was heated to above 200°C . in the hope of detecting this effect, but $(T_s)_{\min}$. for the 2 mm. platinum spheres did not change by an observable amount from its value when T_∞ was the normal room-temperature (20°C .). The question calls for more detailed examination.

In conclusion we may say that, while the above theory accounts for most of the prominent features of ignition by hot particles, it leaves a good deal to be desired in other respects. Improvement is perhaps to be expected when the mechanism of heat-exchange and reaction at the surface are more precisely known, and the temperature distribution around a moving sphere has been completely analysed in the light of contemporary knowledge of boundary layers and turbulent flow. The fact that speed has such a pronounced influence upon ignition precludes any purely surface theory of the effect: the mechanism of transference (whether "thermal" or "chain") must play a part. But the conditions at the surface, though not the only factors, are, in the writer's opinion, of prime importance.

7. Summary.

(1) A survey of the literature of ignition by hot surfaces suggests that the speed of relative motion of gas and surface is a factor determining whether ignition takes place ; it is further surmised that increase of speed results in decrease of igniting power.

(2) An apparatus for examining the effect of speed when the surface is that of a small sphere is then described in detail.

(3) The results obtained with this apparatus are given. They apply to coal-gas-air and may be summarized as follows :—

(a) There is a minimum ignition temperature, for a given size of sphere, below which ignition has not been obtained. This temperature appears independent of the richness of the mixture, of the "age" of the sphere, and of its material, as far as this has been varied (quartz and platinum). It is well above the ignition temperatures by the more usual sources of ignition.

(b) For temperatures above this minimum, ignition is regularly observed, provided that the speed does not exceed a critical value. When this value is exceeded ignition does not take place.

(c) This critical speed is a function of the temperature : it increases as the temperature is increased, according to a roughly linear relation.

(d) The slope of the temperature-critical speed characteristic decreases (*i. e.*, the critical speed for any given temperature increases) as the richness of the mixture is increased from its value at the lower explosive limit. The slope reaches a minimum value at a concentration somewhat in excess of that corresponding to maximum flame-speed ; and subsequently increases as the mixture-strength is further raised towards its upper explosive limit.

(e) The characteristics for fused silica ("quartz") spheres rise more steeply than those for platinum spheres of the same size, but the minimum ignition temperature is the same as before, and shows the same constancy with varying mixture-strength.

(f) The platinum spheres are found to improve their igniting power with use.

(g) The initial temperature of the mixture appears to have no effect (over a range of 200° C.) on the *minimum* igniting temperature of a platinum sphere (2 mm.).

(4) The question of cooling suffered by the spheres before entry into the mixture is examined theoretically and experimentally. The effect is concluded to be negligible in the present experiments.

(5) A theory is given which explains qualitatively the main features of the work ; the points mentioned in (3) (e), (f), (g), above do not find

an explanation in this theory, which is of an excessively simple nature. Suggestions for improvement are made.

The experiments were conducted in the Research Laboratories of the Natural Philosophy Department at Glasgow University, under the supervision of Professor E. Taylor Jones, and I am glad to have this opportunity of expressing my indebtedness to him for constant help and encouragement. I wish also to thank Imperial Chemical Industries, Ltd., who suggested the problem, for permission to publish, and for a personal grant. To Dr. G. Green I am obliged for many valuable references.

(2.)

*From the PHILOSOPHICAL MAGAZINE, Ser. 7, vol. xxx. p. 437,
December 1940.*

**THE IGNITION OF INFLAMMABLE GASES
BY HOT MOVING PARTICLES.—II.**

BY

STEWART PATERSON M.A., B.Sc.

*The Ignition of Inflammable Gases
by Hot Moving Particles.—II.*

By STEWART PATERSON, M.A., B.Sc.,
formerly Metcalfe Research Fellow and Thomson
Experimental Scholar, Glasgow University *.

[Received April 1, 1940.]

IN this paper further experiments are described on the ignition of inflammable gases by hot moving particles.

1. *Introduction.*

Previous work † on the ignition of coal-gas-air, hydrogen-air, and pentane vapour-air mixtures by platinum and quartz spheres had shown the existence of a definite minimum temperature to which any given sphere must be raised before it was capable, under the experimental conditions, of igniting a given mixture. This temperature depended upon the nature and strength of the mixture, and upon the diameter of the sphere. The observation ‡ that it depended also, to a marked degree, upon the speed of relative motion of gas and sphere, increasing apparently without limit as the speed was raised, cast doubt on the original conception § of an "instantaneous ignition temperature" (*i. e.*, one corresponding to infinite speed of flight), and focused attention rather upon low relative speed. Experiments have therefore been made with particles moving more slowly (at 1·2 metre/sec.) than heretofore, and the observed ignition temperatures, which correspond in every case to the above speed, form the subject of this report. They are lower, and in some cases considerably lower, than those previously determined for higher speeds.

2. *Experimental Arrangement.*

Really low and easily controlled and measured speeds might be secured by suspending the chosen sphere at rest, heating it inductively, and

* Communicated by Professor E. Taylor Jones.

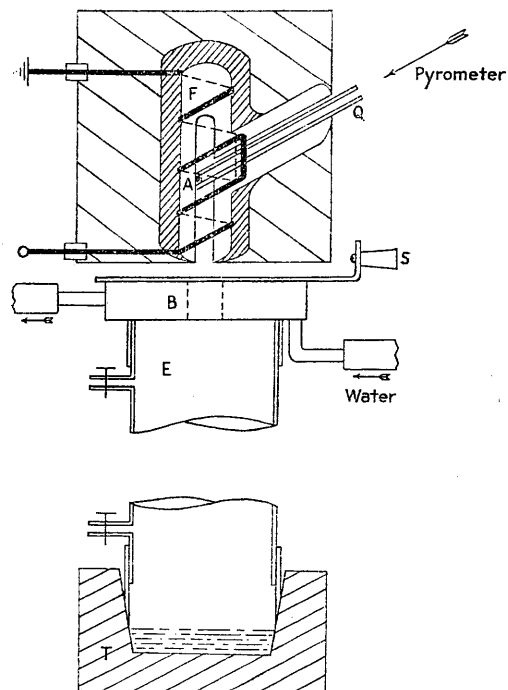
† R. S. Silver, *Phil. Mag.* (7) xxiii. p. 633 (1937). S. Paterson, *ib.* (7) xxviii. p. 1 (1939).

‡ Paterson, *loc. cit.*

§ McDavid, *Journ. Chem. Soc.* exi. p. 1004 (1917); Silver, *loc. cit.*, p. 636.

passing a current of explosive gas over it. Such a method, which recalls the work of various authors on hot wire ignition, has many advantages, but the disadvantages are also pronounced. Apart from obvious problems of suspension and rapid replacement of one sphere by another at the same temperature, inductive heating is restricted to conductors, and the cases of moving gas and moving sphere are equivalent only when elaborate precautions are taken to ensure uniformity of the gas stream.

Fig. 1.



Semi-diagrammatic view of apparatus.

The technique used consisted simply in heating the sphere in a vertical tube furnace and dropping it through a shutter into the explosive mixture ; by abbreviating the drop, one could command speeds as low as 1 metre/sec. Details will be gathered from fig. 1. The furnace F was a small blind T-tube of alundum, wound with "Kanthal Al" strip and lagged with alundum and asbestos wool. (The tube was moulded on a waxed former, and the method of winding is shown in the figure.) The experimental sphere A was supported against the vertical furnace wall within a quartz

tube Q of appropriate bore which passed loosely through the side-arm of the "T." Since this arm inclined at about 20° to the horizon, the sphere automatically took up the required position when inserted in Q, and could then be dropped clear by withdrawing Q a fraction of an inch. This simple method allows constant observation with a pyrometer through Q; and it eliminates speed as a variable factor, since the speed of entry into the gas depends only on the (fixed) distance AB. In all our experiments this distance was 7·3 cm., and the speed of entry therefore 1·2 metre/sec., which probably represents about the lower limit of speed available in the present method, since it does not appear possible to make a high-temperature vertical tube furnace *much* shorter than 10 cm.

The explosion vessel E was a vertical pyrex tube ($3\cdot5 \times 40$ cm.), fitted, as in the former experiments,* with brass sheaths, wooden target T, perforated cover B, and rotary shutter S. Asbestos wool was at first used in T to catch the spheres, but water was ultimately substituted, for reasons to be explained. The cover cap B and shutter S became very hot from their inevitable proximity to the furnace: it was suspected that this caused a lowering of the ignition temperature, and a water-cooled cap was constructed, dependent on natural convection to a large tank: this worked admirably, the shutter never becoming more than slightly warm to the hand.

The experimental procedure is sufficiently obvious: when the chosen sphere had been heated to the required temperature, S was opened and Q slightly withdrawn. After a little practice this could be accomplished very quickly, and it was not thought necessary to "mechanise" the shutter. In the event of ignition occurring (there was never any ambiguity) the condensed water was evaporated from E by a current of air before the next trial.

3. Experimental Results.

As in the previous work, most of the experiments were made with spheres of platinum and quartz, though alumina, porcelain, alundum, slate, titanium oxide, and nickel, as well as several complex slags were also used. Except in the cases of platinum and nickel, these spheres were fashioned in a carbon arc; and only a limited number of substances lend themselves to this treatment. The explosive mixtures were coal-gas-air, hydrogen-air, methane-air, and pentane-air.

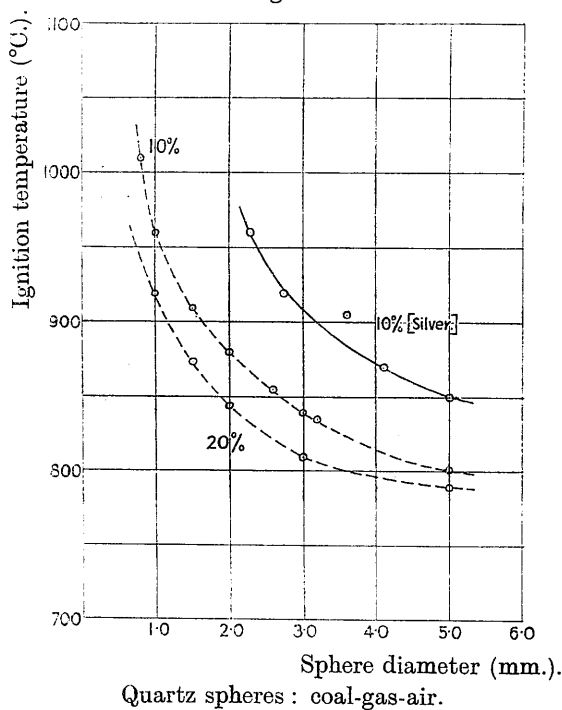
A. Coal-gas-air: variation of ignition temperature with diameter of sphere: quartz spheres.

As soon as it was found that quartz spheres moving through 10 per cent. coal-gas-air at 1·2 metre/sec. gave lower ignition temperatures than those

* Paterson, *loc. cit.*

previously recorded, the relation between these temperatures and the diameters of the spheres was reinvestigated. Fig. 2 enables the results to be compared with those of Silver for the same mixture (10 per cent.) but higher speed (4 metre/sec.). The general shape of the curve is unchanged, but the temperatures are considerably lower; and this fall is greatest for the smaller spheres. As the efficiency of quartz has been found to decrease slightly with use (see par. I of this section), it must be stated that the curve refers to new and highly polished spheres.

Fig. 2.



Quartz spheres : coal-gas-air.

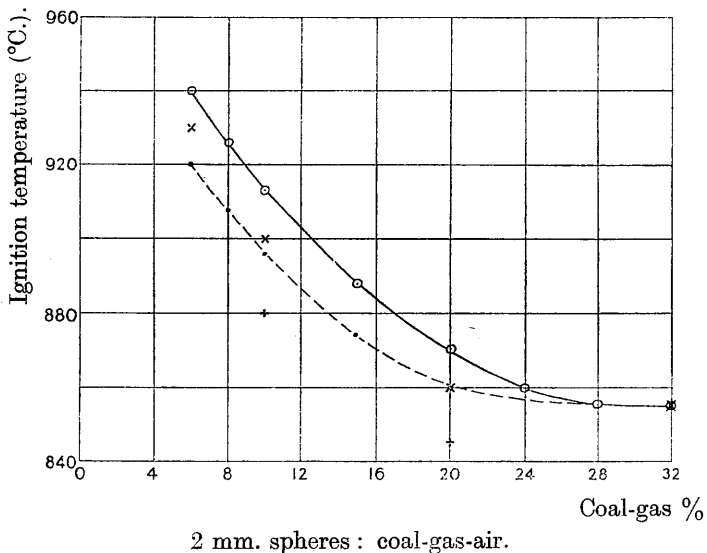
The curve for 20 per cent. coal-gas-air under present conditions is also reproduced in fig. 2. It is similar to the 10 per cent. characteristic, but does not coincide with it. This raises the question of variation with mixture strength.

B. *Coal-gas-air : variation of ignition temperature with percentage gas in mixture : quartz, alundum, and platinum spheres.*

The effect of mixture strength, in the case of 2 mm. spheres, is illustrated in fig. 3. A regular decrease of ignition temperature occurs as the

percentage varies from its lower explosive limit to the value for maximum flame-speed. Thereafter, the decrease is small and may not be significant; but there certainly appears to be no increase (*cf.* the writer, *loc. cit.* p. 8). Reference may here be made to the writer's previous work in which a series of curves * was derived connecting the ignition temperature and speed of platinum and quartz spheres for various strengths of mixture. These curves appeared to converge at low speeds to a single point on the temperature axis; it was suggested, in other words, that the "minimum" ignition temperature did not depend on mixture strength. However, the lowest speeds then used were of the order of 10 metre/sec., and the apparatus was not designed

Fig. 3.



2 mm. spheres : coal-gas-air.

for use even at this level. The curves referred to, instead of "tailing off" at 1000° C., require, in fact, to be extended downwards, and at the low speed now in use a pronounced variation of ignition temperature with mixture strength is still apparent.

In connexion with the curves of fig. 3 two remarks must be made. The platinum curve refers to a sphere which had been used for a long time with the asbestos target (see section 2 above), and was found, in fact, to have acquired a coating of fused asbestos. Under these conditions the sphere behaved with great consistency; but its performance became more

* *Loc. cit.* p. 7, fig. 4.

ERRATUM.

In fig. 3, p. 441, circles refer to platinum, oblique crosses to alundum, points and vertical crosses to quartz. The author is obliged to Mr. Geo. Morris, B.Sc., for drawing this omission to his notice.

erratic when the coating was removed. The behaviour of *clean* platinum spheres has indeed several remarkable features, which will be described later (par. H). The quartz curve was also obtained with an "old" sphere. In this case (as in all others described, except the above) a water target had been substituted for the asbestos, so that no coating was formed; but the igniting power of quartz spheres, as already remarked, decreases slightly (10–20°) with use, before reaching the stable values of fig. 3. Thus, the two isolated points, which represent the lowest ignition temperatures recorded, refer to freshly made spheres. Further details of this effect are again given in par. I.

It is perhaps also worth recording that the ignition temperature of a coal-gas jet, with which the explosion tube was replaced, corresponded with the lowest point on the appropriate curve of fig. 3. There is apparently no particular virtue in the fact that our explosive mixture was normally enclosed in a tube.

C. Hydrogen-air : variation of ignition temperature with sphere diameter : quartz spheres.

Results for 10 per cent. hydrogen-air corresponding to those of fig. 2 are displayed in fig. 4. The relationship between sphere diameter and ignition temperature is of the same general type. Silver's curve * at 4 metre/sec. in a 20 per cent. mixture is again included for comparison. If the ignition temperature varies with mixture strength in the same way as for coal-gas-air—which is probable,—so that a 20 per cent. mixture is more easily ignited than a 10 per cent., the effect of speed must be even greater than fig. 4 would suggest. In view of the violence of explosion in richer hydrogen-air mixtures, however, a percentage-variation curve has not been sought with the present apparatus.

D. Methane-air : quartz and platinum spheres.

In addition to coal-gas-air and hydrogen-air, mixtures of air with methane and pentane vapour were examined by Silver. Methane-air he showed to have very high ignition temperatures: the 8 per cent. mixture could not be ignited by a 6·5 mm. platinum sphere below 1200° C. † The above work on coal-gas and hydrogen gave hope that this figure might be reduced under the present conditions, and a 10 per cent. mixture was chosen in the belief that it would be, if anything, more easily ignited than the 8 per cent. ‡ Failures, however, were recorded up to 1100° C. with a 5·5 mm. platinum sphere, and up to 1115° C. with a 5·2 mm.

* *Loc. cit.* p. 647, fig. 5.

† *Loc. cit.* p. 644.

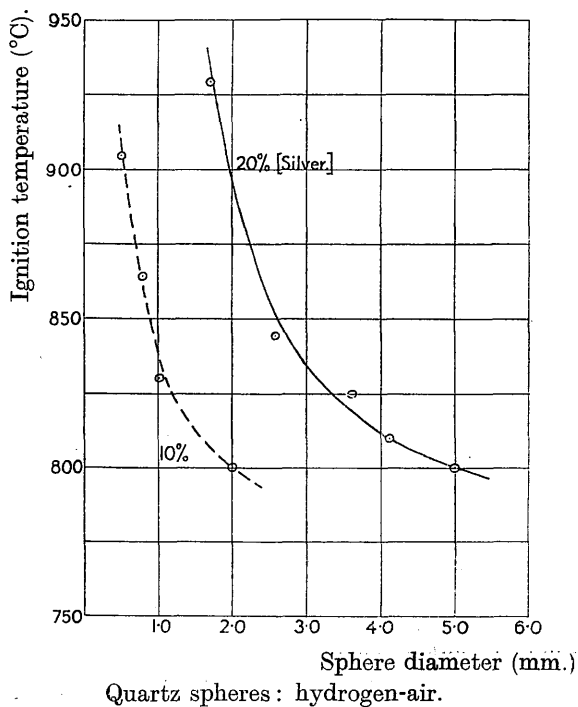
‡ See, however, p. 454.

quartz. The small vertical furnace is relatively inefficient, and 1120°C . represents its safe limit. The actual ignition temperatures were therefore not determined ; but it seems that they are still conspicuously high.

E. Pentane vapour-air : variation of ignition temperature with sphere diameter : platinum spheres.

The relation between ignition temperature and sphere diameter for a 3 per cent. pentane-air mixture is recorded, along with Silver's results at 4 metre/sec., in fig. 5, which recalls figs. 2 and 4 : the new curve is again

Fig. 4.



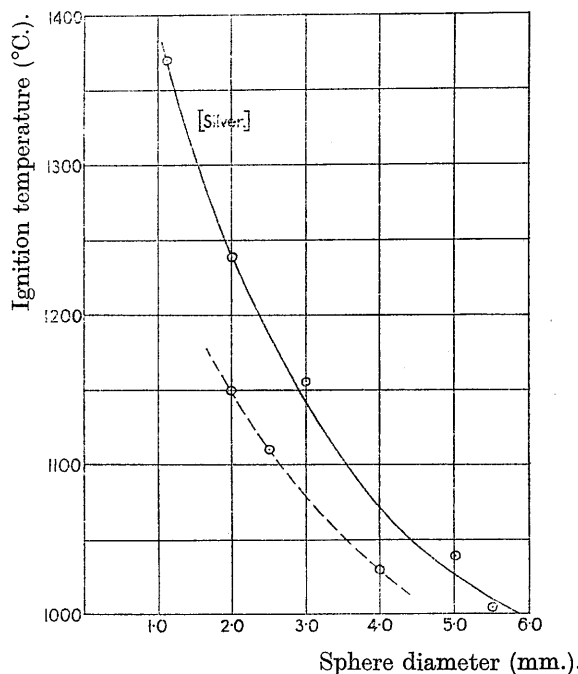
similar to the old but beneath it, and the difference is again greatest for the smaller spheres.

F. Pentane-air : variation of ignition temperature with mixture strength : platinum, quartz, and nickel spheres.

4 mm. spheres were used in this case, in order to work at a temperature suitable for the furnace. Mixtures containing $1\frac{1}{2}$, 2, 3, 4, $4\frac{1}{2}$, 5 per cent. pentane were examined, but no appreciable variation of ignition temperature could be detected. The results are best summarized in a table

(Table I.). It will be seen that the overall variation for any one sphere substance is about 10° , which scarcely exceeds the error of measurement.

Fig. 5.



Platinum spheres : 3% pentane vapour-air.

TABLE I.

Per cent. C_6H_{12} .	4.0 mm. Pt (old).	4.0 mm. Ni.	4.0 mm. quartz.
1½.....	1030° C.	1025° C.	—
2.....	1035	1030	1035° C.
3.....	1030	1020	1020
4.....	1035	1030	1030
4½.....	1030	1030	1030
5.....	1030	1025	—

We must conclude that the ignition temperature under present conditions does not depend upon mixture strength. The effect of sphere substance will be discussed directly.

G. Coal-gas-air, hydrogen-air and pentane-air : effect of sphere substance upon ignition temperature.

Silver's results * for these mixtures referred to spheres of quartz and platinum at 4 metre/sec., and the effect of sphere substance under such conditions was relatively very small. He suggested, however, that this might be due to coincidence.

TABLE II.

Material of sphere.	10 per cent. hydrogen.	10 per cent. coal-gas.
Platinum (old, asbestos-coated)	810° C. (12 per cent.)	915° C.
Platinum (old, clean)	820	915
Platinum (polished)	>875	>1070
Nickel	815	900
Quartz (new) [SiO ₂]	800	880
Alumina [Al ₂ O ₃]	—	880
Alundum	810 (12 per cent.)	900
Porcelain	810	870
Slate	825	895
Titanium oxide [TiO ₂] 2·1 mm.	825	890
Tephroite [2MnO ₄ .SiO ₂]	825	900
Fayalite [2FeO ₄ .SiO ₂] 1·8 mm.	835	860
FeO ₄ .Al ₂ O ₃ 2·1 mm.	825	890
[35MnO ₄ , 25SiO ₂ , 40FeO] 1·9 mm.	830	895

Sphere diameter (unless otherwise stated), 2 mm.

It will be seen from fig. 3 that, although quartz spheres at 1 metre/sec. in coal-gas-air are unquestionably more efficient than asbestos-coated platinum, the agreement is again relatively close ; and it extends to alundum, as the curves show. The pentane results of Table I., which cover the explosive range, cast doubt in this case also on the existence of any important variation with sphere substance.

The question has been examined for 10 per cent. coal-gas-air and 10 per cent. hydrogen-air over a more extensive range of materials. Spheres of approximately 2 mm. diameter were made in the arc from

* *Loc. cit.*

four slags of suitable melting-point and surface-tension : tephroite ($2\text{MnO} \cdot \text{SiO}_2$), fayalite ($2\text{FeO} \cdot \text{SiO}_2$), $\text{FeO} \cdot \text{Al}_2\text{O}_3$, and a ternary mixture containing 35MnO , 25SiO_2 , 40FeO * ; titanium oxide (TiO_2), glazed porcelain, and alumina were also used, and slate gave excellent spheres with a high polish ; a 2 mm. nickel sphere was turned on the lathe ; and results were of course already known for quartz and alundum, and also for platinum with and without asbestos coating. Table II. summarizes the ignition temperatures of 10 per cent. hydrogen-air and 10 per cent. coal-gas-air by this fairly representative collection, and will give some idea of the relative importance or unimportance of sphere substance.

The surfaces were examined microscopically before use, and exhibited wide differences in condition ; some (*e. g.*, alundum) were crystalline, some rough but apparently amorphous, some so highly polished (quartz, porcelain) that it was almost impossible to focus on the surface itself ; the nickel sphere rapidly acquired a thin and adherent oxide film. The significance (if any) of these differences may also be gauged from Table II. It will be seen that platinum forms an exceptional case, and the behaviour of platinum spheres, which is unusually interesting, deserves further mention.

H. "Ageing" of platinum spheres.

It was noticed in previous work † that the igniting power of platinum spheres in coal-gas-air increased with use. This effect reappeared early in the present experiments, but on a more impressive scale. Thus, though an old 2 mm. sphere ("2·0 D") gave consistent ignition at 920°C . in 10 per cent. coal-gas-air, a new specimen (2·0 F) failed repeatedly at temperatures up to 1070°C ., and could probably be taken much higher without effect ; for a larger sphere (2·5 A), also new, failed in each of 28 successive shots at temperatures ranging from 935°C . to 1070°C . After repeated use, however, 2·0 F became as efficient as 2·0 D ; and 2·5 A, as would be expected, surpassed them both.

It was thought at first that an explanation could be found in the action of the asbestos target. As the experiment proceeded, various remarkable colour changes took place in the platinum surface, and it was established beyond doubt that these were due to the target. Asbestos consists of a number of complex silicates, some of which (*e. g.*, crocidolite) are readily fusible ; minute fragments adhere to the glowing platinum surface.

* The ferrous slags became magnetic during treatment, so that they were presumably reduced in the arc.

† Paterson, *loc. cit.* p. 10. Cf. also Thornton, Phil. Mag. (6) xxxviii. p. 624 (1919). White and Price, Journ. Chem. Soc. cxv. p. 1263 (1919). Shepherd and Wheeler, Safety in Mines Research Board Paper, xxxvi. p. 19 (1927).

and spread out upon it when the sphere is replaced in the furnace. As this process results in the formation of a substantial asbestos coat, it will not, perhaps, appear surprising that a new and clean platinum sphere should behave differently from one which has been long in use.

The effect, however, cannot be explained in this way. To begin with, if the improvement is due solely to asbestos deposition, it should disappear when the deposit is removed. The platinum spheres were cleaned easily and thoroughly by washing in hydrofluoric acid, and fresh accretion was prevented by substituting a water target for the asbestos wool. Beyond a loss of consistency, the results with 2·0 D and 2·0 F (in 10 per cent. coal-gas-air) showed little change : the spheres were still capable, on occasion, of producing ignition at as low a temperature as before, and never failed to do so above 950° C. ; there was no suggestion of a return to the 1070° C. level. As a matter of fact, it is now known that changes occur in the platinum surface, and an improvement takes place simultaneously in its igniting power when no asbestos is present and no deposit whatever is formed. The surface, which originally presented the appearance, even under considerable magnification, of a compact and brightly reflecting sheet of metal with a conspicuous "high-light," becomes dull and milky to the eye and reflects very diffusely. When magnified it now shows an extremely fine pitting or etching : the general effect could be described as tinselled. This change is not due either to the sudden cooling when the sphere is dropped, or, as might be suggested, to the reaction at its surface during ignition ; it can be produced simply by heating the sphere for a few hours in a quartz tube at 1000° C. On the other hand, a sphere whose polish has been destroyed in this or any other way, may be restored to the original condition, with its lustre even enhanced, by heating for a similar period *at a bright orange* in the tip of a capillary coal-gas flame ; lower temperatures are, however, ineffective.

It seems possible to correlate these surface changes directly with the changes in igniting power, which, like them, continued to occur after the asbestos deposition had been eliminated. Thus a new and brightly polished sphere (2·0 G) failed to ignite 10 per cent. coal-gas-air at 940° C., 965° C., 985° C., and 1000° C. Three days later, it succeeded at 970° C., and finally at 940° C. ; the surface was now unmistakably tinselled, though still bright. Again, 2·0 F, whose asbestos coat had been removed revealing a tinselled surface, gave consistent ignition (of the same mixture) at 920–940° C. It was heated for some time to a low red in the flame-tip, without, however, recovering its polish ; nor had its igniting power decreased. After two hours at a bright orange, the surface, while rather granular in appearance, was highly lustrous and entirely without pitting. Failures were now recorded at 1000° C., 1000° C., 1060° C., and success only at 1095° C. ; the sphere failed repeatedly at 960° C., but in the end

produced ignition about 990°C . It was found to be still bright and lustrous, but with finer markings in evidence. After a fresh two hours' orange heat in the flame-tip (which removed the markings), $2\cdot0\text{ F}$ gave immediate ignition at 1095°C ., which may be regarded as a probable upper limit for even a "new" sphere; but it failed consistently at $1020^{\circ}\text{C}.$ - 1050°C . It was now steeped at 1020°C . in the furnace for $4\frac{1}{2}$ hours, whereupon it succeeded at once at 1015°C . and 970°C ., and was found to have resumed its familiar tinselling. The entire cycle of ageing and rejuvenation was repeated once more, and could apparently be repeated without limit.

This effect has not been studied so closely in the case of hydrogen-air, but there is no doubt that it exists here too. A new and polished sphere ($2\cdot0\text{ H}$) succeeded in igniting 10 per cent. hydrogen-air at 890°C ., but failed at 850°C . After a very few trials, however, ignition was produced as low as 820°C . At this stage the surface was still apparently polished, but fine division could be seen under the microscope; a successful shot at 935°C . in 10 per cent. coal-gas-air showed that the ageing applied to this mixture also. $2\cdot0\text{ H}$ was now heated for two hours to bright orange in the flame-tip, examined and retested in 10 per cent. coal-gas-air. The surface had lost its tinselling and acquired the "granular" lustrous appearance. It failed at 1015°C . and 1010°C . to ignite the coal-gas mixture, and at 875°C . and 860°C . in 10 per cent. hydrogen-air. Success was then recorded at 890°C ., 860°C ., and later at 820°C ., the original ignition temperature for old spheres.

The effect is well marked in pentane vapour-air. A 3 per cent. mixture was used, and could be ignited very consistently at temperatures above 1030°C . by $4\cdot0\text{ A}$, an old platinum sphere with characteristically tinselled surface. $4\cdot0\text{ B}$, which was new and polished, failed at 1065°C . and 1110°C .; it succeeded at 1155°C ., but failed again twice at 1120°C . Next day, however, ignition was immediately produced at 1040°C ., and the usual tinselling could be detected. ($4\cdot0\text{ B}$ was still somewhat inferior to $4\cdot0\text{ A}$ in 10 per cent. coal-gas-air.) After four hours' intense heating in the flame-tip, $4\cdot0\text{ B}$, whose surface was now lustrous and "fused" in appearance and without a trace of tinselling, failed repeatedly at 1120°C . to ignite the pentane-air mixture. The cycle is therefore complete.

Failure was also recorded up to 1040°C . in 10 per cent. coal-gas-air; this may be compared with the figure of 840°C . for "old" spheres, again exemplifying the effect in coal-gas.

I. "Ageing" of quartz spheres.

Changes in igniting power of the kind described appear to be peculiar to platinum: no improvement with use was detected in any of the other

materials. Thus, a 2 mm. alundum sphere, which ignited 10 per cent. coal-gas-air at 905° C. on its first trial, still failed consistently at 900° C. after its fiftieth. The surface change, which seemed to amount chiefly to roughening of the crystal faces by fracture, had had no effect upon performance. In the case of quartz, which was perhaps the most consistent and efficient igniting substance examined, not only could no improvement be detected, but a definite though slight deterioration took place. Fresh quartz spheres of 2 mm. diameter may be relied upon, under present conditions, to ignite 10 per cent. coal-gas-air at 880° C.; after prolonged use they can be trusted not to do so, and will perhaps fail at 895° C. or 900° C. This seems, however, to be the limit of the effect.

A simultaneous microscopic change occurs in the quartz surface, which loses its almost perfect initial polish and is gradually fractured and roughened until it ends by resembling sandpaper.

4. Discussion.

Since this paper is intended to record the above observations rather than to explain them, they have been described as far as possible without comment. Theoretical approach to the problems of initiation and propagation of flame is difficult, and the suggestions which follow must therefore be regarded as more than usually tentative.

An approximate thermal theory of ignition by heated spheres was put forward by Silver *, and found to agree, as far as could be judged, with his experiments on diameter-temperature variation. The modifications introduced later † to allow for speed of motion did not affect this agreement. It is interesting to see how far the present results, to which the modified theory is directly applicable, may be correlated with those of Silver.

According to the modified theory, a linear relation should exist between

$Y \equiv \log_e \left[\frac{T_s - T_\infty}{a^{3/2}} \right]$ and $X \equiv 1/T_s$, where T_s and a denote temperature and radius of the sphere, and T_∞ initial temperature of the explosive gas; in fact,

$$Y = f(V) - \frac{E}{2} \cdot X, \quad \dots \dots \dots \quad (1)$$

V being the speed of motion and E an activation energy. The results contained in figs. 2, 4, 5 do satisfy a linear relation of this type; and they determine values of E , which, while consistently higher, are in very reasonable agreement (Table III.) with those derived from Silver's work on the

* *Loc. cit.* p. 648.

† Paterson, *loc. cit.* p. 16.

same combustible gases. Moreover, the activation energies for 10 per cent. and 20 per cent. coal-gas-air coincide, as presumably they ought to do ; and the displacements parallel to Y of the (X, Y) curves constructed from Silver's and the present figures respectively agree, not only in sign but also in order of magnitude, with those predicted by (1). For, since $f(V)$ is of the form : Const. $- \frac{1}{2} \log_e V$, and the ratio of speeds used by Silver and the writer was ≈ 4 , the (constant) difference in ordinate of the two curves for a single explosive mixture should be of the order of one unit ; which, in fact, it is.

So far, then, as concerns our present results, and those of Silver at comparable speeds, the theory is satisfactory. It was further shown * to be capable of explaining the writer's experimental relation between speed and ignition temperature for a number of coal-gas-air mixtures. Unfortunately, however, the value of E required was much smaller

TABLE III.

Explosive mixture.	Sphere.	E (Silver).	E (Paterson).
10 per cent coal-gas-air . . .	2·0 mm. quartz.	35,000	41,000
20 per cent. coal-gas-air . . .	2·0 mm. quartz.	—	41,000
10 per cent. hydrogen-air . . .	2·0 mm. quartz.	—	49,000
20 per cent. hydrogen-air . . .	2·0 mm. quartz.	39,000	—
3 per cent. pentane-air . . .	2·0 mm. platinum.	33,000	35,000

$$\text{Values of } E \text{ (cal.) derived from : } \log_e \frac{T_s - T_\infty}{a^{3/2}} = f(v) - \frac{1}{2} E/T_s.$$

(about 10,000 cal.) than those of Table III. This difficulty was noticed at the time. It might, perhaps, be explained in terms of the asbestos coating, which must have existed in the speed-temperature experiments ; but we have seen that asbestos-coated, and indeed all except new or "rejuvenated" platinum surfaces, behave at low speeds very much like quartz. Now the quartz results of fig. 3 required an activation energy of 41,000 cal. It is, therefore, reasonable to expect that the present method would lead to a similarly high value for coated platinum.

Three major criticisms of the theory can be made. It regards ignition as determined by a balance of conduction and reaction in the boundary layer, though conduction alone must provide a balance when there is no reaction ; it focuses attention on the sphere surface and ignores the hot

* Paterson, *loc. cit.*

wake, whereas one might easily argue that the relative importance lies in just the opposite quarter ; and it neglects the agency of diffusion of active particles compared with that of heat transfer. Now the tendency of recent research has been to lay greater and greater stress on diffusion of active particles and to suggest that it may even outweigh thermal conduction in controlling flame.

It is possible, following Landau *, to develop an alternative theory in which both diffusion of chain-carriers and conduction of heat are taken into account, and in which the hot wake, regarded as a cylindrical source of each, is considered to be responsible for ignition. This theory does not, apparently, succeed, any more than the former, in reconciling all our experimental facts ; but if ignition does originate in the hot wake, there is ample reason for failure ; for the wake behind a sphere changes its character completely within a very moderate range of Reynolds number. According to Möller †, who examined photographically the wake behind a sphere of radius r moving through fluid in a vessel of cross-section $4l^2$, "perfectly smooth laminar flow occurs (when $r/l=1/20$) up to $Re=300$ ‡. If Re is gradually increased to 450, the laminar flow, though it still persists, is disturbed, at first occasionally and later regularly, by the formation of eddies. Beyond $Re=450$ ($r/l=1/20$), these eddies commence to detach themselves as vortex rings. They separate unsymmetrically, and so give the impression of being linked in a kind of vortex chain. Above $Re=1000$ ($r/l=1/8$) there appear from time to time discrete eddies, which, as Re is further increased, progressively supersede the chain vortices, until at about $Re=1500$ the fluid contains only discrete eddies forming a "vortex street." The vortex street does not prove stable : the vortices soon unite in cloudy balls, which again show a definite periodicity." Now the results described in this paper refer to values of Re not greater than 30 ; those of Silver to the range 30–150 ; while in the speed-temperature work Re varied between 190 and 1500. If the hot wake plays a determining rôle in ignition, this rôle will almost certainly change its character with that of the wake ; and it will not then be surprising that a theory which presupposes a simple cylindrical wake should fail to reconcile experiments made under such widely divergent conditions of flow.

The resultant ignition criterion, which is derived in the Appendix, is of the same general form, viz.,

$$T_s^x V^y \leq A a^z e^{-E'/T_s} \dots \dots \dots \quad (2)$$

* Chem. Rev. xxi. p. 245 (1937) ; J. Chem. Phys. vii. p. 112 (1939).

† Phys. ZS. xxxix. p. 57 (1938).

‡ $Re \equiv 2Vr/\nu$ (Reynolds number), where ν is the kinematic viscosity.

as its predecessor, though the small positive numbers x, y, z have different values. These values depend to a considerable extent on the assumptions made ; our present criterion runs

$$T_s^{10} V^3 \leq A a^7 e^{-E'/T_s} \dots \dots \dots \quad (3)$$

A is, of course, independent of T_s , V , a ; and E' is a sum of various activation energies. Without discussing this somewhat precarious theory at greater length, we may remark that it is capable of explaining Silver's and the writer's diameter-temperature results to the extent that our original theory explained them. With one reservation *, however, as much can be said of any theory which leads to the form (2). Values of E' derived from (3) for the diameter-temperature work are shown in Table IV. ; the coal-gas-air speed-temperature experiments, as before, require a relatively smaller figure, around 30,000 cal. This is not surprising, for it seems improbable that the derivation of (3) should hold beyond $Re \approx 400$: the wake changes too profoundly. We need not assume, of course, that the wake is unimportant at higher Reynolds numbers; nevertheless, its influence, which was supposed to arise from quiescence and a high concentration of heat and initial centres, may be thought likely to decrease as it becomes turbulent and scattered. In this case the sphere surface may be directly responsible for ignition, and some such theory as was previously put forward, modified to take account of chain-carrier diffusion, will be appropriate.

TABLE IV.

Explosive mixture.	Sphere.	E' (Silver).	E' (Paterson).
10 per cent. coal-gas-air . .	2.0 mm. quartz.	87,500	98,000
20 per cent. coal-gas-air . .	2.0 mm. quartz.	—	97,500
10 per cent. hydrogen-air . .	2.0 mm. quartz.	—	120,000
20 per cent. hydrogen-air . .	2.0 mm. quartz.	105,000	—
3 per cent. pentane-air . .	2.0 mm. platinum.	78,000	86,000

$$\text{Values of } E' \text{ (cal.) derived from } \log_e \frac{T_s^{10}}{a^7} = \phi(V) - E'/T_s.$$

In connexion with the effect of sphere substance upon ignition, and the "ageing" of platinum and quartz spheres, it is necessary to explain why every substance used, including platinum, gave roughly the same

* The Y-displacement explanation (p. 450) will apply only if $x/y \approx 2$; this is fulfilled by (3).

minimum ignition temperature, but in the case of platinum ignition could be prevented, even at a temperature several hundreds of degrees higher, by suitable pre-treatment of the sphere. It is true that the surface roughening which was observed to accompany improvement with the platinum spheres implies a larger increase in surface reaction than in heat transfer, and therefore, according to our original theory, a fall of ignition temperature. But simple explanations in terms of roughness or smoothness do not appear possible, since quartz spheres which became as rough as the platinum (and were originally far smoother) showed no improvement—in fact, a slight deterioration. Again, artificial roughening was found to have no effect upon the ignition temperature.

The factor in Landau's theory which may be supposed to express the effect of sphere substance and surface condition is the active particle density n_0 . It can readily be verified from the Appendix, if it is not obvious *a priori*, that an isothermal increase in n_0 must reduce the ignition temperature, and *vice versa*. Now, apart from changes in the activation energy E_2 of the surface reaction, n_0 will evidently depend upon the freedom with which active products of that reaction are allowed to escape from the surface, in other words, upon the degree of adsorption of such products on the surface itself. If, then, we assume that the rate of reaction was approximately equal for all the surfaces used, and that adsorption was, except for platinum, negligible, we can understand why the ignition temperature did not vary widely with sphere substance. On this view, the unusual behaviour of new or "rejuvenated" platinum must be taken to indicate a high degree of adsorption of active particles; and the process of "ageing," during which the platinum ignition temperature fell to the level common to other substances, must be interpreted as a slow poisoning of the adsorptive surface. This poisoning can apparently be hastened by moderate heating in a quartz tube, and removed by continued exposure at bright orange to a coal-gas-air flame; it coincides with a small-scale fracture or tinselling of the surface.

These suggestions seem to fall in line with the well-known exceptional catalytic and adsorptive properties of platinum*. In particular, it may be claimed that they offer a simpler and more convincing explanation of the improvement in igniting power than that put forward by Thornton and others †, according to which fresh platinum would fail to cause ignition because the reaction on its surface was too rapid to be capable of spreading. The exact nature of the chain-carriers which are adsorbed

* See, *e.g.*, Mellor, 'Inorganic Chemistry,' vol. xvi.

† Thornton, Phil. Mag. (6) xxxviii. p. 618 (1919). White and Price, J. Chem. Soc. cxv. p. 1257 (1919). Mason and Wheeler, *ib.* cxxxi. p. 2083 (1922); cxxv. p. 1869 (1924). Coward and Guest, J. Amer. Chem. Soc. xlvi. p. 2479 (1927).

is uncertain ; however, the fact that the surface becomes so rough, and that it can be aged by heating in an air-filled silica tube, and rejuvenated by intense heating in a coal-gas-air flame (during which the temperature attained appears greatly increased by surface combustion) may suggest that they include oxygen atoms *.

One further point requires comment,—the variation of ignition temperature with percentage combustible gas in mixture. Here, very little can be said. The records of such variation, when ignition was produced by passage through hot tubes †, or into hot vessels ‡, by sudden compression §, by various kinds of electric discharge ||, and by hot wires, &c. ¶, do not lead to any general conclusion. In some cases ignition occurred most readily with the weakest mixture, in others with the strongest, in others again there was a minimum ignition temperature at an intermediate strength. Our observations on coal-gas-air and pentane-air have already been described, but it does not seem easy to put any interesting construction upon them at the moment.

5. Summary.

1. Further experiments are described on the ignition of gases by hot moving spheres. A dropping technique enabled lower speeds (1·2 metre/sec.) to be used than heretofore.

2. The results are as follows :—

(a) Ignition temperatures of 10 per cent. and 20 per cent. coal-gas-air and 10 per cent. hydrogen-air by quartz spheres, and of 3 per cent. pentane vapour-air by platinum spheres vary with sphere diameter in a manner similar to that previously recorded. The actual temperatures are, however, lower, especially for the smaller sizes of sphere.

* Cf. Hall, J. Amer. Chem. Soc. xxii. p. 494 (1900). Roberts, Phil. Mag. (6) xxv. p. 270 (1913).

† Mitscherlich, ZS. Anorg. Chem. cxxi. p. 65 (1922), &c.

‡ Mason and Wheeler, J. Chem. Soc. cxxi. p. 2081 (1922); cxxv. p. 1871 ff. (1924). Mardles, Trans. Far. Soc. xxvii. p. 681 (1931). Naylor and Wheeler, J. Chem. Soc. p. 2460 ff. (1931); p. 1240 (1933); &c.

§ Falk, J. Amer. Chem. Soc. xxviii. p. 1527 (1906); xxix. p. 1548 ff. (1907). Dixon, J. Chem. Soc. xcvi. p. 661 (1910). Dixon and Crofts, ib. cv. p. 2036 (1914). Dixon, Harwood and Higgins, Trans. Far. Soc. xxii. p. 267 (1926).

|| Coward, Cooper, and Jacobs, J. Chem. Soc. cv. p. 1069 (1914). Thornton, Proc. Roy. Soc. (A) xc. p. 272 (1914); xci. p. 17 (1914); xcii. pp. 9, 381 (1915). Wheeler, J. Chem. Soc. cxvii. p. 903 (1920). Coward and Meiter, J. Amer. Chem. Soc. xl ix. p. 396 (1927), &c.

¶ Thornton, Phil. Mag. (6) xxxviii. p. 624 (1919). Coward and Guest, J. Amer. Chem. Soc. xl ix. p. 2479 (1927).

(b) In the case of coal-gas-air, a continuous decrease of ignition temperature occurs as the mixture strength is raised from its lower to upper explosive limit. This applies to spheres of alundum, quartz, and asbestos-coated platinum. No variation with mixture strength of the ignition temperature of pentane-air by platinum, quartz, or nickel spheres could be observed.

(c) The high level of the ignition temperature of methane-air was confirmed ; but detailed records are still lacking.

(d) The effect of sphere substance on the ignition temperatures of 10 per cent. coal-gas-air and 10 per cent. hydrogen-air was examined for an extensive range of materials ; except in the case of platinum, this effect appears to be of secondary importance.

(e) The ignition temperatures of coal-gas-air, hydrogen-air, and pentane-air mixtures by fresh platinum spheres are very much higher than by most other substances ; platinum, however, improves with use, until this difference has practically disappeared. Its surface becomes simultaneously "tinselled." This process of "ageing" may be accelerated by soaking at red heat in a quartz tube ; conversely, the sphere is "rejuvenated" and its tinselling removed by prolonged exposure at a bright orange to a coal-gas-air flame.

(f) Comparable changes do not take place with the other substances used ; in particular, a slight deterioration is observed in quartz.

3. As far as can be judged, the theory already offered is capable of correlating the results summarized in 2 (a) with work by Silver at somewhat greater speeds. Difficulties connected with its simultaneous application to the writer's experiments at high speeds lead to the formulation of an alternative theory, based on Landau's analysis and expressly restricted to low Reynolds numbers. It is shown that this theory is also capable of the above correlation, as well as offering a reasonable account of 2 (d), (e), (f). Simultaneous application to high-speed work is now, of course, out of the question, and for such work a parallel theory, perhaps of the previous type, would be required.

I wish again to thank Professor E. Taylor Jones for constant encouragement and advice ; also Messrs. Imperial Chemical Industries, Ltd., who extended my research grant and gave permission to publish. The experimental work was done in the Research Laboratories of the Natural Philosophy Department at Glasgow University, and I am greatly indebted to Mr. William Reid for many helpful suggestions both in these and in the previous experiments.

APPENDIX.

*Application of Landau's Theory * to ignition by Hot Wakes.*

We regard the heat which has passed from the sphere by conduction into its boundary layer † as canalized in a narrow cylindrical wake of indefinite length but constant radius r_0 . The cylindrical wake is thereby raised to a mean temperature T_1 . It is also supposed to be enriched with active particles, the product of surface reaction within the boundary layer: these are present in concentration n_0 . The cylindrical wake therefore constitutes a source of the type proposed by Landau. The active particles now diffuse outwards; each generates Q units of heat in unit time, and they increase in number at a rate proportional to their density; while the temperature is determined through conduction of heat and its generation by the active particles. Under these conditions, it can be shown by a linear transformation ‡ that Landau's mathematical statement of the problem must lead to non-dimensional solutions for relative temperature and concentration of the form

$$\left(\frac{n}{n_0}, \frac{T - T_\infty}{T_1 - T_\infty} \right) = f_{1,2} \left[\frac{r}{r_0}, \frac{D}{r_0^2} t ; \frac{\alpha r_0^2}{D} ; \frac{\kappa}{D} ; \frac{Q r_0^2 n_0}{k(T_1 - T_\infty)} \right], \quad . \quad (1)$$

where r_0 is the radius of the source, α , D the branching and diffusion coefficients of the active particles, and k , κ the thermal and thermometric conductivities of the gas; $f_{1,2}$ being definite, absolute functions. It follows that Landau's ignition criterion, viz., that the axial temperature shall never fall, will define a critical relation of the form

$$\frac{k(T_1 - T_\infty)}{Q r_0^2 n_0} = \phi \left[\frac{\alpha r_0^2}{D} ; \frac{\kappa}{D} \right] \quad . \quad . \quad . \quad . \quad . \quad (2)$$

in which ϕ is a third absolute function.

Landau's analysis, which assumes further that $D = \kappa$, leads, in fact, to a relation between the dimensionless quantities $\frac{k(T_1 - T_\infty)}{Q r_0^2 r_0}$ and $\frac{\alpha r_0^2}{D}$, which may be written, over a wide range,

$$\frac{k(T_1 - T_\infty)}{Q r_0^2 n_0} \leq K \frac{\alpha r_0^2}{D}, \quad . \quad . \quad . \quad . \quad . \quad (3)$$

K being an absolute constant.

Neglecting factors which do not vary with a , V , T_s , we may reasonably replace $Q\alpha$ by an expression of the type $T_1^{-1} e^{-E_i/RT_1}$, and if we suppose

* *Loc. cit.*

† Thermal and hydrodynamical boundary layers may be assumed to coincide, since Prandtl's number ≈ 1 for gases.

‡ Cf., e. g., Davis, Phil. Mag. (6) xliv. p. 920 (1922), for method.

the rate of creation of active particles by the surface to be independent of the speed of motion V , n_0 will take some such form as $\frac{a^2}{Vr_0^2} T_s^{-\frac{1}{2}} e^{-E_s/RT_s}$.

The main difficulty is to identify r_0 and T_1 . From our initial assumption that all the heat transferred by convection is employed in raising a cylindrical wake of radius r_0 to a mean temperature T_1 , we can deduce, when T_∞ is negligible, that

$$r_0^2 T_1 \simeq a^2 T_s R e^{-\frac{1}{2}} \dots \dots \dots \quad (4)$$

If this picture is completed by making all the gas contained in the boundary layer flow into the same cylinder, and if the temperature and velocity profiles within the layer are assumed linear and coincident (which is legitimate), it can also be shown that

$$r_0^2 T_s \simeq a^2 T_1 R e^{-\frac{1}{2}} \dots \dots \dots \quad (5)$$

Consequently,

$$T_1 \simeq T_s, \dots \dots \dots \quad (6)$$

and

$$r_0 \simeq a R e^{-\frac{1}{2}} \dots \dots \dots \quad (7)$$

Inserting (6) and (7) in (3), and substituting for $Qn_0\alpha$ the forms proposed above, we obtain a limiting relation which, when due allowance is made for the temperature variation of k , D , and ν , reduces to

$$T_s^{10} V^3 = A a^7 e^{-E_s/T_s} \dots \dots \dots \quad (8)$$

A is a constant, independent of a , V , T_s .

(3.)

*From the PHILOSOPHICAL MAGAZINE, Ser. 7, vol. xxxii. p. 384,
November 1941.*

**THE CONDUCTION OF HEAT IN A MEDIUM
GENERATING HEAT.**

BY

**STEWART PATERSON, M.A., B.Sc.,
LATE METCALFE FELLOW, GLASGOW UNIVERSITY.**

The Conduction of Heat in a Medium Generating Heat.

By STEWART PATERSON, M.A., B.Sc.,
late Metcalfe Fellow, Glasgow University *.

Introduction.

THE problem of thermal conduction is frequently complicated in practice by local generation or absorption of heat. This happens, for example, when heat energy is dissipated throughout the medium by the passage of electric current, or when it is generated or absorbed in a change of state such as fusion or chemical reaction. Certain particular cases have been discussed †, in which the rate of generation did not depend explicitly on the temperature, and the classical method of sources provides the basis for a more general treatment, under the same conditions; but when large temperature differences occur and when the rate of generation depends markedly upon temperature, as in most problems of chemical physics where heat conduction plays a part, such assumptions evidently cannot be made. It is still possible, however, to derive explicit solutions of a very general kind when the rate of generation is a linear function of temperature, provided the medium behaves as a solid with constant thermometric conductivity. Since these conditions may be taken as a first approximation to the truth in many cases of practical interest, the corresponding solutions will perhaps be useful.

PART I.—INFINITE SOLID.

The conduction of heat in an infinite homogeneous isotropic solid, in which heat is being generated or absorbed, may be represented as a rule by the equations :

$$\frac{\partial \theta}{\partial t} = \kappa \nabla^2 \theta + G(x, y, z, t; \theta), \quad t > 0, \quad \left. \begin{array}{l} \text{all } x, y, z, \\ \theta \rightarrow \phi(x, y, z), \text{ when } t \rightarrow 0, \end{array} \right\}$$

where κ is the thermometric conductivity, θ the temperature at the point (x, y, z) at time t , and G some specified function of the independent

* Communicated by Prof. E. Taylor Jones.

† *E.g.*, Awbery, Phil. Mag. (7) iv. p. 629 (1927); Orstrand, Wash. Acad. Sci. J. xxii. p. 530 (1932).

variables x, y, z, t and also of θ . $\phi(x, y, z)$ represents the initial temperature, supposed given, and ∇^2 the Laplacian operator $\frac{\partial^2}{\partial x^2} + \frac{\partial^2}{\partial y^2} + \frac{\partial^2}{\partial z^2}$.

We shall solve these equations in the case where

$$G(x, y, z, t; \theta) \equiv f(x, y, z, t) + g(t) \cdot \theta.$$

Consider first the equations :

$$\left. \begin{array}{l} \frac{\partial \theta}{\partial t} = \kappa \nabla^2 \theta + f(x, y, z, t), \quad t > 0, \\ \theta \rightarrow \phi(x, y, z), \quad t \rightarrow 0, \end{array} \right\} \text{all } x, y, z. \quad \dots \quad (1)$$

The solution, which may be obtained by the method of sources, or otherwise, is :

$$\theta = \frac{1}{(4\pi\kappa t)^{3/2}} \int_{-\infty}^{\infty} \int_{-\infty}^{\infty} \int_{-\infty}^{\infty} \phi(\alpha, \beta, \gamma) e^{-\frac{\Sigma(x-\alpha)^2}{4\kappa t}} d\alpha d\beta d\gamma \\ + \int_0^t \frac{1}{[4\pi\kappa(t-\tau)]^{3/2}} \int_{-\infty}^{\infty} \int_{-\infty}^{\infty} \int_{-\infty}^{\infty} f(\alpha, \beta, \gamma, \tau) e^{-\frac{\Sigma(x-\alpha)^2}{4\kappa(t-\tau)}} d\tau d\alpha d\beta d\gamma. \quad (2)$$

The first term, which will be denoted by θ_1 , represents the solution when there is no generation of heat.

Turning now to the proposed equations, viz.,

$$\left. \begin{array}{l} \frac{\partial \theta}{\partial t} = \kappa \nabla^2 \theta + f(x, y, z, t) + g(t) \cdot \theta, \quad t > 0, \\ \theta \rightarrow \phi(x, y, z), \quad t \rightarrow 0, \end{array} \right\} \text{all } x, y, z, \quad \dots \quad (3)$$

$$\text{set } \theta = v(x, y, z, t) \cdot e^{\int_0^t g(\tau) d\tau}.$$

Then v must satisfy

$$\left. \begin{array}{l} \frac{\partial v}{\partial t} = \kappa \nabla^2 v + f(x, y, z, t) e^{-\int_0^t g(\tau) d\tau}, \quad t > 0, \\ v \rightarrow \phi, \quad t \rightarrow 0, \end{array} \right\} \text{all } x, y, z, \quad \dots \quad (4)$$

and it can readily be seen that, if it does so, θ will satisfy (3).

But the solution of (4), by (2) above, is

$$v = \theta_1 + \int_0^t \frac{e^{-\int_0^\tau g(\tau) d\tau}}{[4\pi\kappa(t-\tau)]^{3/2}} \int_{-\infty}^{\infty} \int_{-\infty}^{\infty} \int_{-\infty}^{\infty} f(\alpha, \beta, \gamma, \tau) e^{-\frac{\Sigma(x-\alpha)^2}{4\kappa(t-\tau)}} d\alpha d\beta d\gamma. \quad (5)$$

Hence the solution of (3) is

$$\theta = e^{\int_0^t g(\tau) d\tau} \left\{ \begin{array}{l} \frac{1}{(4\pi\kappa t)^{3/2}} \int_{-\infty}^{\infty} \int_{-\infty}^{\infty} \int_{-\infty}^{\infty} \phi(\alpha, \beta, \gamma) e^{-\frac{\Sigma(x-\alpha)^2}{4\kappa t}} d\alpha d\beta d\gamma \\ + \int_0^t \frac{e^{-\int_0^\tau g(\tau) d\tau}}{[4\pi\kappa(t-\tau)]^{3/2}} \int_{-\infty}^{\infty} \int_{-\infty}^{\infty} \int_{-\infty}^{\infty} f(\alpha, \beta, \gamma, \tau) e^{-\frac{\Sigma(x-\alpha)^2}{4\kappa(t-\tau)}} d\tau d\alpha d\beta d\gamma. \end{array} \right\}. \quad (6)$$

The corresponding solutions for flow of heat in two and one dimensions can readily be deduced from (6). They contain one, or two, less space integrations and one, or two, less powers of $\frac{1}{(4\pi\kappa t)^{1/2}}$ and $\frac{1}{[4\pi\kappa(t-\tau)]^{1/2}}$.

The solution for the case of spherical symmetry can also be deduced from (6). It is formally simpler, however, to derive it, by a well-known method, from the solution for a semi-infinite solid whose bounding plane is maintained at zero temperature. This will be done in the sequel. The solution is

$$\theta = \frac{e^{\int_0^t g(\tau) d\tau}}{r} \left\{ \frac{1}{(4\pi\kappa t)^{1/2}} \int_0^\infty \rho \phi(\rho) \left[e^{-\frac{(r-\rho)^2}{4\kappa t}} - e^{-\frac{(r+\rho)^2}{4\kappa t}} \right] d\rho \right. \\ \left. + \int_0^t \frac{e^{-\int_0^\tau g(\tau) d\tau}}{[4\pi\kappa(t-\tau)]^{1/2}} \int_0^\infty \rho f(\rho, \tau) \left[e^{-\frac{(r-\rho)^2}{4\kappa(t-\tau)}} - e^{-\frac{(r+\rho)^2}{4\kappa(t-\tau)}} \right] d\tau d\rho. \right\}, \quad . . . (7)$$

$\phi(r)$ and $f(r, t)$ corresponding to the $\phi(x, y, z)$ and $f(x, y, z, t)$ of equations (3).

Various interesting results can be deduced for particular cases from (6) and (7). Thus, if f and g are constant in space and time, the solutions are

$$\theta = \frac{f}{g} (e^{gt} - 1) + \frac{e^{gt}}{(4\pi\kappa t)^{3/2}} \int_{-\infty}^\infty \int_{-\infty}^\infty \int_{-\infty}^\infty \phi(\alpha, \beta, \gamma) e^{-\frac{\Sigma(\alpha-\alpha)^2}{4\kappa t}} d\alpha d\beta d\gamma, \quad . . . (8)$$

and $\theta = \frac{f}{g} (e^{gt} - 1) + \frac{e^{gt}}{r(4\pi\kappa t)^{1/2}} \int_0^\infty \rho \phi(\rho) \left[e^{-\frac{(r-\rho)^2}{4\kappa t}} - e^{-\frac{(r+\rho)^2}{4\kappa t}} \right] d\rho. \quad . . . (9)$

PART II.—SEMI-INFINITE SOLID.

When the solid is in any way bounded, in addition to the equations (3), which will now apply only over a limited range of the space co-ordinates, we shall have a surface condition. When, as in most practical cases, this condition can be expressed by the vanishing of a linear function of the temperature and normal temperature gradient at the surface, the general problem can be reduced, by the method of Part I., to the corresponding general problem without generation of heat. For, if (R) denote the range of x, y, z comprised by the solid, and n the normal vector drawn inward from a point on the bounding surface, the equations will then be of the form :

$$\left. \begin{aligned} \frac{\partial \theta}{\partial t} &= \kappa \nabla^2 \theta + f(x, y, z, t) + g(t) \cdot \theta, \quad t > 0, \text{ in } (R), \\ \theta &\rightarrow \phi(x, y, z), \quad t \rightarrow 0, \text{ in } (R), \\ \psi_1(x, y, z, t) \frac{\partial \theta}{\partial n} - \psi_2(x, y, z, t) \theta + \psi_3(x, y, z, t) &\rightarrow 0, \quad n \rightarrow 0, \quad t > 0 \end{aligned} \right\}. \quad . . . (10)$$

The term $g(t)\theta$ can be removed by the substitution $\theta = ve^{\int_0^t g(\tau)d\tau}$, without otherwise altering the form of the equations. We therefore consider :

$$\left. \begin{array}{l} \frac{\partial v}{\partial t} = \kappa \nabla^2 v + f'(x, y, z, t), \quad t > 0, \text{ in (R),} \\ v \rightarrow \phi, \quad t \rightarrow 0, \text{ in (R),} \\ \psi_1 \frac{\partial v}{\partial n} - \psi_2 v + \psi_3' \rightarrow 0, \quad n \rightarrow 0, \quad t > 0 \end{array} \right\}, \quad \dots \quad (11)$$

where

$$f' \equiv f \cdot e^{-\int_0^t g(\tau)d\tau}, \quad \psi_3' \equiv \psi_3 \cdot e^{-\int_0^t g(\tau)d\tau}.$$

Now, if

$$\left. \begin{array}{l} \frac{\partial \theta_1}{\partial t} = \kappa \nabla^2 \theta_1, \quad t > 0, \text{ in (R),} \\ \theta_1 \rightarrow \phi, \quad t \rightarrow 0, \text{ in (R),} \\ \psi_1 \frac{\partial \theta_1}{\partial n} - \psi_2 \theta_1 + \psi_3' \rightarrow 0, \quad n \rightarrow 0, \quad t > 0 \end{array} \right\}, \quad \dots \quad (12)$$

and $w(x, y, z, t, \lambda)$ satisfies

$$\left. \begin{array}{l} \frac{\partial w}{\partial t} = \kappa \nabla^2 w, \quad t > 0, \text{ in (R),} \\ w \rightarrow f'(x, y, z, \lambda), \quad t \rightarrow 0, \text{ in (R),} \\ \psi_1 \frac{\partial w}{\partial n} - \psi_2 w \rightarrow 0, \quad n \rightarrow 0, \quad t > 0 \end{array} \right\}, \quad \dots \quad (13)$$

the solution of (11) is $v = \theta_1 + \int_0^t w(x, y, z, t-\tau, \tau) d\tau$; for this satisfies the first two equations of (11), as can be verified, and $\psi_1 \frac{\partial v}{\partial n} - \psi_2 v + \psi_3'$

$$\begin{aligned} &= \psi_1 \frac{\partial \theta_1}{\partial n} + \psi_1 \int_0^t \frac{\partial}{\partial n} w(x, y, z, t-\tau, \tau) d\tau - \psi_2 \theta_1 \\ &\quad - \psi_2 \int_0^t w(x, y, z, t-\tau, \tau) d\tau + \psi_3' \\ &= \left(\psi_1 \frac{\partial \theta_1}{\partial n} - \psi_2 \theta_1 + \psi_3' \right) + \int_0^t \left(\psi_1 \frac{\partial w}{\partial n} - \psi_2 w \right) d\tau \rightarrow 0 \text{ as } n \rightarrow 0, \quad t > 0. \end{aligned}$$

Since (13) are of the form (12), we have therefore reduced the general solution of (10) to that of (12), *i.e.*, of the corresponding *general* problem without generation of heat.

The three cases commonly discussed are those in which

- (a) the surface temperature is prescribed,
- (b) there is no heat loss through the surface, and
- (c) there is a heat loss by radiation into a medium at temperature $\psi(x, y, z, t)$.

The first case corresponds to $\psi_1(x, y, z, t) \equiv 0$, the second to

$$\psi_2(x, y, z, t) \equiv 0 \equiv \psi_3(x, y, z, t),$$

the third to $\frac{\psi_2(x, y, z, t)}{\psi_1(x, y, z, t)} = \frac{\psi_3(z, y, x, t)}{\psi_1(x, y, z, t)\psi(x, y, z, t)} = h$,

hk being the heat-transfer coefficient of the surface, where k is the thermal conductivity of the solid. The appropriate forms of (12) and (13) are obvious. We conclude with solutions for these three cases in the semi-infinite solids defined by $x > 0$ and $r > a$.

(a) Prescribed surface temperature : (1) $x > 0$.

The equations (10) become

$$\left. \begin{array}{l} \frac{\partial \theta}{\partial t} = \kappa \nabla^2 \theta + f(x, y, z, t) + g(t)\theta, \quad t > 0, \quad x > 0, \\ \theta \rightarrow \phi(x, y, z), \quad t \rightarrow 0, \quad x > 0, \\ \theta \rightarrow \psi(y, z, t), \quad x \rightarrow 0+, \quad t > 0 \end{array} \right\} \text{all } y, z, \dots \quad (14)$$

and the solution is therefore $\theta = e^{\int_0^t g(\tau) d\tau} \left[\theta_1 + \int_0^t w(x, y, z, t-\tau, \tau) d\tau \right]$, where

$$\left. \begin{array}{l} \frac{\partial \theta_1}{\partial t} = \kappa \nabla^2 \theta_1, \quad t > 0, \quad x > 0, \\ \theta_1 \rightarrow \phi, \quad t \rightarrow 0, \quad x > 0, \\ \theta_1 \rightarrow \psi e^{-\int_0^t g(\tau) d\tau}, \quad x \rightarrow 0+, \quad t > 0 \end{array} \right\} \text{all } y, z, \dots \quad (15)$$

and

$$\left. \begin{array}{l} \frac{\partial}{\partial t} w(x, y, z, t, \lambda) = \kappa \nabla^2 w, \quad t > 0, \quad x > 0, \\ w \rightarrow f(x, y, z, \lambda) e^{-\int_0^\lambda g(\tau) d\tau}, \quad t \rightarrow 0, \quad x > 0, \\ w \rightarrow 0, \quad x \rightarrow 0+, \quad t > 0 \end{array} \right\} \text{all } y, z, \dots \quad (16)$$

From the known solutions of these equations we deduce

$$\begin{aligned} \theta = & \frac{e^{\int_0^t g(\tau) d\tau}}{(4\pi\kappa)^{3/2}} \left\{ \int_0^t \frac{e^{-\int_0^\tau g(\tau) d\tau}}{(t-\tau)^{3/2}} \int_0^\infty \int_{-\infty}^\infty \int_{-\infty}^\infty f(\alpha, \beta, \gamma, \tau) e^{-\frac{\Sigma(x-a)^2}{4\kappa(t-\tau)}} \left[1 - e^{-\frac{\alpha x}{\kappa(t-\tau)}} \right] \right. \\ & \times d\tau d\alpha d\beta dy \\ & + \frac{1}{t^{3/2}} \int_0^\infty \int_{-\infty}^\infty \int_{-\infty}^\infty \phi(\alpha, \beta, \gamma) e^{-\frac{\Sigma(x-a)^2}{4\kappa t}} \left[1 - e^{-\frac{\alpha x}{\kappa t}} \right] d\alpha d\beta dy \\ & \left. + x \int_0^t \frac{e^{-\int_0^\tau g(\tau) d\tau}}{(t-\tau)^{5/2}} \int_{-\infty}^\infty \int_{-\infty}^\infty \psi(\beta, \gamma, \tau) e^{-\frac{x^2 + (y-\beta)^2 + (z-\gamma)^2}{4\kappa(t-\tau)}} d\tau d\beta dy \right\}. \quad (17) \end{aligned}$$

The corresponding solutions for flow in two and one dimensions can, as before, be readily deduced from the general solution.

(2) $r > a$.

The equations are :

$$\left. \begin{aligned} \frac{\partial \theta}{\partial t} &= \kappa \frac{1}{r} \frac{\partial^2}{\partial r^2} (r\theta) + f(r, t) + g(t)\theta, \quad t > 0, \quad r > a, \\ \theta &\rightarrow \phi(r), \quad t \rightarrow 0, \quad r > a, \\ \theta &\rightarrow \psi(t), \quad r \rightarrow a+, \quad t > 0. \end{aligned} \right\}. \quad (18)$$

Substituting $r\theta = u$, $r = a + x$, we have

$$\frac{\partial u}{\partial t} = \kappa \frac{\partial^2 u}{\partial x^2} + (a+x)f(a+x, t) + g(t)u, \quad t > 0, \quad x > 0,$$

$$u \rightarrow (a+x)\phi(a+x), \quad t \rightarrow 0, \quad x > 0,$$

$$u \rightarrow a\psi(t), \quad x \rightarrow 0+, \quad t > 0,$$

the solution of which can be obtained from (17). Reverting to the original variables, we get

$$\begin{aligned} \theta &= \frac{e^{\int_0^t g(\tau) d\tau}}{r(4\pi\kappa)^{1/2}} \left\{ \int_0^t \frac{e^{-\int_0^\tau g(\tau) d\tau}}{(t-\tau)^{1/2}} \int_a^\infty \rho f(\rho, \tau) \left[e^{-\frac{(r-\rho)^2}{4\kappa(t-\tau)}} - e^{-\frac{(r-2a+\rho)^2}{4\kappa(t-\tau)}} \right] d\tau d\rho \right. \\ &\quad \left. + \frac{1}{t^{1/2}} \int_a^\infty \rho \phi(\rho) \left[e^{-\frac{(r-\rho)^2}{4\kappa t}} - e^{-\frac{(r-2a+\rho)^2}{4\kappa t}} \right] d\rho + a(r-a) \int_0^t \frac{e^{\int_0^\tau g(\tau) d\tau - \frac{(r-a)^2}{4\kappa(t-\tau)}} \psi(\tau)}{(t-\tau)^{3/2}} d\tau \right\} \end{aligned} \quad (19)$$

The solution for an *infinite* solid with spherical symmetry of flow can also be deduced from (17). In this case, the equations are

$$\left. \begin{aligned} \frac{\partial \theta}{\partial t} &= \kappa \frac{1}{r} \frac{\partial^2}{\partial r^2} (r\theta) + f(r, t) + g(t)\theta, \quad t > 0, \quad r > 0, \\ \theta &\rightarrow \phi(r), \quad t \rightarrow 0, \quad r > 0 \end{aligned} \right\}, \quad (20)$$

which reduce, with $r\theta = u$, to

$$\frac{\partial u}{\partial t} = \kappa \frac{\partial^2 u}{\partial r^2} + rf(r, t) + g(t)u, \quad t > 0, \quad r > 0,$$

$$u \rightarrow r\phi(r), \quad t \rightarrow 0, \quad r > 0,$$

$$u \rightarrow 0, \quad r \rightarrow 0+, \quad t > 0.$$

The solution of this can be written down from (17), and leads to the expression for θ given in (7) above.

(b) No surface loss : (1) $x > 0$.

Equations (10) are now :

$$\left. \begin{aligned} \frac{\partial \theta}{\partial t} &= \kappa \nabla^2 \theta + f(x, y, z, t) + g(t)\theta, \quad t > 0, \quad x > 0, \\ \theta &\rightarrow \phi(x, y, z), \quad t \rightarrow 0, \quad x > 0, \\ \frac{\partial \theta}{\partial x} &\rightarrow 0, \quad x \rightarrow 0+, \quad t > 0. \end{aligned} \right\} \text{all } y, z. \quad . . . \quad (21)$$

(12) and (13) take similar form, but without the heat generation terms. Their solutions can be written down by the familiar method of extending the solid with symmetrical temperature field beyond $x = 0$; and the value of θ is found to be

$$\theta = \frac{e^{\int_0^t g(\tau) d\tau}}{(4\pi\kappa)^{3/2}} \left\{ \int_0^t \frac{e^{-\int_0^\tau g(\tau) d\tau}}{(t-\tau)^{3/2}} \int_0^\infty \int_{-\infty}^\infty \int_{-\infty}^\infty f(\alpha, \beta, \gamma, \tau) e^{-\frac{\Sigma(x-a)^2}{4\kappa(t-\tau)}} \left[1 + e^{-\frac{\alpha x}{\kappa(t-\tau)}} \right] \times d\tau d\alpha d\beta d\gamma \right. \\ \left. + \frac{1}{t^{3/2}} \int_0^\infty \int_{-\infty}^\infty \int_{-\infty}^\infty \phi(\alpha, \beta, \gamma) e^{-\frac{\Sigma(x-a)^2}{4\kappa t}} \left[1 + e^{-\frac{\alpha x}{\kappa t}} \right] d\alpha d\beta d\gamma \right\}. \quad . . . \quad (22)$$

Solutions for two- and one-dimensional flow follow as before.

(2) $r > a$.

(10) becomes

$$\left. \begin{aligned} \frac{\partial \theta}{\partial t} &= \kappa \frac{1}{r} \frac{\partial^2}{\partial r^2} (r\theta) + f(r, t) + g(t)\theta, \quad t > 0, \quad r > a, \\ \theta &\rightarrow \phi(r), \quad t \rightarrow 0, \quad r > a, \\ \frac{\partial \theta}{\partial r} &\rightarrow 0, \quad r \rightarrow a+, \quad t > 0 \end{aligned} \right\}, \quad . . . \quad (23)$$

which transforms, with $r\theta = u$, $r = a + x$, into

$$\left. \begin{aligned} \frac{\partial u}{\partial t} &= \kappa \frac{\partial^2 u}{\partial x^2} + (a+x)f(a+x, t) + g(t)u, \quad t > 0, \quad x > 0, \\ u &\rightarrow (a+x)\phi(a+x), \quad t \rightarrow 0, \quad x > 0, \\ \frac{\partial u}{\partial x} - \frac{u}{a} &\rightarrow 0, \quad x \rightarrow 0+, \quad t > 0. \end{aligned} \right\}. \quad . . . \quad (24)$$

The solution of equations (24), which represent linear flow with radiation into a medium at zero temperature, can be obtained from case (c), equation (27) below. In terms of the original variables θ, r it is :

$$\theta = \frac{e^{\int_0^t g(\tau) d\tau}}{r(4\pi\kappa)^{1/2}} \left\{ \frac{1}{t^{1/2}} \int_a^\infty \rho \phi(\rho) \left[\left(e^{-\frac{(r-\rho)^2}{4\kappa t}} + e^{-\frac{(r-2a+\rho)^2}{4\kappa t}} \right) - \frac{2}{a} \int_0^\infty e^{-\frac{\xi}{a} - \frac{(r+\rho+\xi-2a)^2}{4\kappa t}} d\xi \right] d\rho \right\}$$

$$+ \int_0^t e^{-\int_0^\tau g(\tau) d\tau} \int_a^\infty \rho f(\rho, \tau) \left[\left(e^{-\frac{(r-\rho)^2}{4K(t-\tau)}} + e^{-\frac{(r-2a+\rho)^2}{4K(t-\tau)}} \right) - \frac{2}{a} \int_0^\infty e^{-\frac{\xi}{a}} e^{-\frac{(r+\rho+\xi-2a)^2}{4K(t-\tau)}} d\xi \right] \times d\tau d\rho \} . . . (25)$$

(c) *Radiation into medium at prescribed temperature*: (1) $x > 0$.

Equations (10) become in this case

$$\begin{aligned} * \quad \frac{\partial \theta}{\partial t} &= \kappa \nabla^2 \theta + f(x, y, z, t) + g(t)\theta, \quad t > 0, \quad x > 0, \\ \theta &\rightarrow \phi(x, y, z), \quad t \rightarrow 0, \quad x > 0, \quad \text{all } y, z, \\ \frac{\partial \theta}{\partial x} - h[\theta - \psi(y, z, t)] &\rightarrow 0, \quad x \rightarrow 0+, \quad t > 0 \end{aligned} \quad | \quad (26)$$

and equations (11), (12), (13) can be written down at once. The solution of (12), and hence also of (13), can be obtained by means of the appropriate Green's function *, and the solution of (26) finally derived in the form :

$$\begin{aligned} \theta = & \frac{e^{\int_0^t g(\tau) d\tau}}{(4\pi K)^{3/2}} \left\{ \int_0^t e^{-\int_0^\tau g(\tau) d\tau} \int_0^\infty \int_{-\infty}^\infty \int_{-\infty}^\infty f(\alpha, \beta, \gamma, \tau) \left[e^{-\frac{\Sigma(x-a)^2}{4K(t-\tau)}} \left(1 + e^{-\frac{ax}{K(t-\tau)}} \right) \right. \right. \\ & \left. \left. - 2h \int_0^\infty e^{-h\xi - \frac{(x+a+\xi)^2 + (y-\beta)^2 + (z-\gamma)^2}{4K(t-\tau)}} d\xi \right] d\tau d\alpha d\beta d\gamma \right. \\ & + \frac{1}{t^{3/2}} \int_0^\infty \int_{-\infty}^\infty \int_{-\infty}^\infty \phi(\alpha, \beta, \gamma) \left[e^{-\frac{\Sigma(x-a)^2}{4Kt}} \left(1 + e^{-\frac{ax}{Kt}} \right) \right. \\ & \left. \left. - 2h \int_0^\infty e^{-h\xi - \frac{(x+a+\xi)^2 + (y-\beta)^2 + (z-\gamma)^2}{4Kt}} d\xi \right] d\alpha d\beta d\gamma \right. \\ & \left. + h \int_0^t e^{-\int_0^\tau g(\tau) d\tau} \int_{-\infty}^\infty \int_{-\infty}^\infty \int_0^\infty \psi(\beta, \gamma, \tau) (x+\xi) e^{-h\xi - \frac{(x+\xi)^2 + (y-\beta)^2 + (z-\gamma)^2}{4K(t-\tau)}} \right. \\ & \left. \times d\tau d\beta d\gamma d\xi \right\} . . . (27) \end{aligned}$$

Two- and one-dimensional solutions follow easily.

(2) $r > a$.

Equations (10) are now :

$$\begin{aligned} \frac{\partial \theta}{\partial t} = & \kappa \frac{1}{r} \frac{\partial^2}{\partial r^2} (r\theta) + f(r, t) + g(t)\theta, \quad t > 0, \quad r > a, \\ \theta &\rightarrow \phi(r), \quad t \rightarrow 0, \quad r > a, \\ \frac{\partial \theta}{\partial r} - h[\theta - \psi(t)] &\rightarrow 0, \quad r \rightarrow a+, \quad t > 0 \end{aligned} \quad | \quad . . . (28)$$

* See Carslaw, 'Conduction of Heat in Solids,' 2nd ed., p. 184, for this function.

which become, with $r\theta=u$, $r=a+x$,

$$\frac{\partial u}{\partial t} = \kappa \frac{\partial^2 u}{\partial x^2} + (a+x)f(a+x, t) + g(t)u, \quad t > 0, \quad x > 0,$$

$$u \rightarrow (a+x)\phi(a+x), \quad t \rightarrow 0, \quad x > 0,$$

$$\frac{\partial u}{\partial x} - \left(h + \frac{1}{a} \right) \left[u - \frac{ha}{h + \frac{1}{a}} \psi(t) \right] \rightarrow 0, \quad x \rightarrow 0+, \quad t > 0.$$

The solution of these equations, obtained from (27), leads to the following value of θ :

$$\begin{aligned} \theta = & \frac{e^{\int_0^t g(\tau) d\tau}}{r(4\pi\kappa)^{1/2}} \left\{ \int_0^t \frac{e^{-\int_0^\tau g(\tau) d\tau}}{(t-\tau)^{1/2}} \int_a^\infty \rho f(\rho, \tau) \left[\left(e^{-\frac{(r-\rho)^2}{4\kappa(t-\tau)}} + e^{-\frac{(r-2a+\rho)^2}{4\kappa(t-\tau)}} \right) \right. \right. \\ & \quad \left. \left. - 2 \left(h + \frac{1}{a} \right) \int_0^\infty e^{-(h+\frac{1}{a})\xi} e^{-\frac{(r+\rho+\xi-2a)^2}{4\kappa(t-\tau)}} d\xi \right] d\tau d\rho \right. \\ & + \frac{1}{t^{1/2}} \int_a^\infty \rho \phi(\rho) \left[\left(e^{-\frac{(r-\rho)^2}{4\kappa t}} + e^{-\frac{(r-2a+\rho)^2}{4\kappa t}} \right) \right. \\ & \quad \left. \left. - 2 \left(h + \frac{1}{a} \right) \int_0^\infty e^{-(h+\frac{1}{a})\xi} e^{-\frac{(r+\rho+\xi-2a)^2}{4\kappa t}} d\xi \right] d\rho \right. \\ & \left. + ah \int_0^t \frac{e^{-\int_0^\tau g(\tau) d\tau}}{(t-\tau)^{3/2}} \psi(\tau) \int_0^\infty (r+\xi-a) e^{-(h+\frac{1}{a})\xi} e^{-\frac{(r+\xi-a)^2}{4\kappa(t-\tau)}} d\tau d\xi \right\}. \quad (29) \end{aligned}$$

THE HEATING OR COOLING OF A SOLID SPHERE IN A WELL-STIRRED FLUID

By S. PATERSON,
Imperial Chemical Industries Ltd., Explosives Division

MS. received 26 August 1946

ABSTRACT. A solid sphere of uniform initial temperature is heated or cooled in a finite mass of fluid, well stirred and externally insulated. Temperature continuity is assumed at the surface. Solutions are presented suitable for all values of time, radius and conductivity, and of the ratio of heat capacities of sphere and fluid. Numerical results are given, and certain mathematical relations noted.

§ 1. SERIES SOLUTION

ASOLID sphere of radius a , diffusivity κ , heat capacity c_1 and temperature zero is plunged at time $t=0$ into a mass of fluid of heat capacity c_2 at temperature T_0 . The surface temperature of the sphere is assumed equal at all subsequent times to that of the fluid, which is so well stirred or of such high conductivity that its temperature is always uniform throughout. The outer boundary of the fluid is impervious to heat.

Then the temperature T at a distance R from the centre of the sphere is determined by

$$\left. \begin{array}{l} \frac{\partial}{\partial t}(RT) = \kappa \frac{\partial^2}{\partial R^2}(RT), \quad R < a, \quad t > 0, \\ T = 0, \quad R < a, \quad t = 0, \\ T = T', \quad R = a, \quad t > 0, \\ T' = T_0, \quad t = 0, \\ \frac{3\kappa c_1}{a} \frac{\partial T}{\partial R} = -c_2 \frac{dT'}{dt}, \quad R = a, \quad t > 0, \end{array} \right\} \dots\dots(1)$$

where $T'(t)$ is the temperature of the fluid.

For convenience, let $R/a \equiv r$, $\kappa t/a^2 \equiv \tau$, $RT/aT_0 \equiv u$, $T'/T_0 \equiv u'$; also $c_1/c_2 \equiv w$. Then the equations are

$$\left. \begin{array}{ll} \frac{\partial u}{\partial \tau} = \frac{\partial^2 u}{\partial r^2}, & r < 1, \quad \tau > 0, \\ u = u', & r = 1, \quad \tau > 0, \\ u' = 1, & \tau = 0, \\ u = 0, & r < 1, \quad \tau = 0, \\ u = 0, & r = 0, \quad \text{all } \tau, \\ 3w \left(\frac{\partial u}{\partial r} - \frac{u}{r} \right) + \frac{du'}{d\tau} = 0, & r = 1, \quad \tau > 0. \end{array} \right\} \dots\dots(2)$$

If $p \equiv -s^2$ is the Heaviside operator $\partial/\partial\tau$, these equations transform into

$$\left. \begin{array}{ll} \frac{\partial^2 u}{\partial r^2} = -s^2 u, & u = 0, \quad r = 0, \\ 3w \left(\frac{\partial u}{\partial r} - \frac{u}{r} \right) - s^2(u - 1) = 0, & r = 1. \end{array} \right\} \dots\dots(3)$$

The solution is readily found to be

$$\begin{aligned} u &= \frac{s^2 \sin rs}{3w(\sin s - s \cos s) + s^2 \sin s} \\ &\equiv f(s)/F(s), \text{ say.} \end{aligned} \quad \dots \dots (4)$$

The poles s_n of u are the roots of

$$s \cot s = 1 + s^2/3w, \quad \dots \dots (5)$$

and apart from a simple pole at zero consist of real and distinct pairs, positive and negative. The solution (4) therefore transforms into

$$\begin{aligned} u &= \mathcal{L}_{s \rightarrow 0} \frac{f(s)}{F(s)} + 2 \sum_{n=1}^{\infty} \frac{f(s_n)}{s_n F'(s_n)} e^{-s_n^2 \tau}. \\ \text{Hence} \quad u &= \frac{r}{w+1} + 2 \sum_1^{\infty} \frac{\sin rs_n}{\sin s_n} \cdot \frac{e^{-s_n^2 \tau}}{3(w+1) + s_n^2/3w}, \end{aligned} \quad \dots \dots (6)$$

where s_n is the n th positive non-zero root of (5). The corresponding fluid temperature is

$$u' = (u)_{\tau=1} = \frac{1}{w+1} + 2 \sum_1^{\infty} \frac{e^{-s_n^2 \tau}}{3(w+1) + s_n^2/3w}. \quad \dots \dots (7)$$

The above formal solution can be justified by verifying that (6) and (7) do in fact satisfy (2).

When $\tau = \infty$, $u = u' r = r/(w+1)$, as is required. The fraction F of the final heat transfer which has taken place by time t is therefore

$$F = \frac{1 - u'}{1 - 1/(w+1)}, \quad \dots \dots (8)$$

that is,

$$F = 1 - \frac{2}{3w} \sum_1^{\infty} \frac{e^{-s_n^2 \tau}}{1 + s_n^2/9w(1+w)}, \quad \dots \dots (9)$$

(5), (6) and (7) correspond, for the present condition of uniform initial temperature, to the general series solution given by Peddie (1901). When the fluid has infinite heat capacity, that is, when the surface temperature of the sphere is maintained at T_0 , they reduce to

$$u = r + \frac{2}{\pi} \sum_1^{\infty} (-1)^n \frac{\sin n\pi r}{n} e^{-n^2 \pi^2 \tau}, \quad \dots \dots (10)$$

$$u' = 1,$$

which is a familiar case. (9) then becomes

$$F = 1 - \frac{6}{\pi^2} \sum_1^{\infty} \frac{e^{-n^2 \pi^2 \tau}}{n^2}. \quad \dots \dots (11)$$

The n th root s_n of (5) can be seen from a graph of the functions $\tan s$ and $s/(1 + s^2/3w)$ to lie between $n\pi$ and $(n + \frac{1}{2})\pi$. For $n < (\sqrt{3w}/\pi) - \frac{1}{2}$, s_n approaches $(n + \frac{1}{2})\pi$ as n is increased, thereafter returning towards $n\pi$; thus, if w is small, s_n approaches $n\pi$ from the outset. s_n can be calculated without difficulty by

successive approximation. If n/w is sufficiently large, the following expansion is also useful:

$$s_n = n\pi + \frac{3w}{n\pi} - \frac{9w^2(w+2)}{(n\pi)^3} + \dots \quad \dots \dots (12)$$

The first three roots, which are more than we shall require, are presented in table 1 for a wide range of w .

Table 1. The first three positive roots of $s \cot s = 1 + s^2/3w$

w	s_1	s_2	s_3	w	s_1	s_2	s_3
∞	4.712	7.854	10.996	5.0	4.236	7.296	10.329
1000	4.492	7.722	10.899	2.0	3.972	6.938	9.940
500	4.490	7.720	10.895	1.0	3.726	6.681	9.714
400	4.487	7.719	10.893	0.5	3.506	6.502	9.576
300	4.486	7.716	10.890	0.2	3.312	6.376	9.487
200	4.485	7.713	10.885	0.1	3.233	6.330	9.454
100	4.479	7.702	10.866	0.05	3.188	6.307	9.439
50	4.464	7.674	10.830	0.02	3.161	6.293	9.430
20	4.421	7.601	10.759	0.01	3.152	6.290	9.426
10	4.352	7.490	10.573	0.0	3.142	6.283	9.425

The series in (6), (7), etc. no doubt always converge. The rapidity of convergence, however, varies markedly with τ . Thus in (7), if $\tau \geq 1$, the exponent $-s_n^2\tau$ increases numerically by a factor of at least $(2n+1)\pi^2$, and the entire series is negligible, so that $u=r/(w+1)$, $u'=1/(w+1)$ and $F=1$, irrespective of w ; but when $\tau < 1$, the speed of convergence falls off very quickly, at least two terms being required for $\tau=0.1$, eleven for $\tau=0.01$ and over one hundred for $\tau=0.001$. Since for certain purposes it may be necessary to consider values of τ as low as, say, 10^{-10} , the series solution evidently cannot be regarded in practice as covering more than a fraction of the range.

§ 2. ALTERNATIVE SOLUTIONS

We return to (4), substitute $-q^2$ for s^2 , and expand in powers of e^{-q} . This gives

$$u = \frac{q^2}{q^2 + 3wq - 3w} \{ e^{-(1-r)q} - e^{-(1+r)q} + Qe^{-(3-r)q} - Qe^{-(3+r)q} + \dots \} \quad \dots \dots (13)$$

and

$$u' = \frac{q^2}{q^2 + 3wq - 3w} \{ 1 + (Q-1)e^{-2q} + Q(Q-1)e^{-4q} + \dots \}, \quad \dots \dots (14)$$

where

$$Q = \frac{q^2 - 3wq - 3w}{q^2 + 3wq - 3w}. \quad \dots \dots (15)$$

Since e^{-2q} transforms into $1 - \text{erf } 1/\sqrt{\tau}$, we may expect that the bracketed terms beyond the first two in (13) and the first in (14) will be negligible when $1 - \text{erf } 1/\sqrt{\tau}$ is small, say $< 0.1\%$ for $\tau \leq 0.1$. Then (13) and (14) should be suitable for calculation precisely in the range in which (6) and (7) are unsuitable.

In order to obtain an approximation for sufficiently small τ , we may expand $q^2/(q^2 + 3wq - 3w)$ in descending powers of q , and interpret operators of the type $q^{-n}e^{-4q}$ in terms of Hartree's repeated error function integrals (Hartree, 1939). Thus, if $P \equiv 3w$,

$$\frac{q^2 e^{-(1+r)q}}{q^2 + Pq - P} = \Phi_0\left(\frac{1+r}{2\sqrt{\tau}}\right) - P(2\sqrt{\tau})\Phi_1\left(\frac{1+r}{2\sqrt{\tau}}\right) + (P+P^2)(2\sqrt{\tau})^2\Phi_2\left(\frac{1+r}{2\sqrt{\tau}}\right) - \dots, \quad \dots \dots \quad (16)$$

where

$$\Phi_n(x) \equiv \int_x^\infty \Phi_{n-1}(\xi) d\xi$$

and

$$\Phi_0(x) \equiv 1 - \operatorname{erf} x.$$

When $r=1$, the terms in $1+r$ are relatively small, and the first approximation to u' is

$$u' = 1 - P \cdot 2\sqrt{\tau/\pi} + (P+P^2)\tau - \dots \quad \dots \dots \quad (17)$$

For sufficiently small $w\sqrt{\tau}$, say $< 10^{-2}$, these expansions are useful, particularly (16), when $r \ll 1$, but they do not cover the required range. We shall therefore derive alternative expressions.

The terms in $e^{-(1\pm r)q}$ from (13) transform into

$$\mp \frac{1}{\pi i} \int_M \frac{e^{\mu^2\tau - (1\pm r)\mu} \mu d\mu}{(\mu - \alpha)(\mu - \beta)},$$

respectively, where α, β are the roots of $\mu^2 + 3w\mu - 3w = 0$, and M is a path in the μ -plane from $\infty e^{-i\pi/4}$ to $\infty e^{i\pi/4}$ passing a finite distance to the right of $|\alpha|$ and $|\beta|$. The terms therefore yield

$$u \simeq \frac{1}{\alpha - \beta} \{ \alpha [E_{1-r}(\alpha) - E_{1+r}(\alpha)] - \beta [E_{1-r}(\beta) - E_{1+r}(\beta)] \}, \quad \dots \dots \quad (18)$$

where

$$\left. \begin{aligned} E_y(x) &\equiv \frac{1}{\pi i} \int_M \frac{e^{\mu^2\tau - y\mu} d\mu}{\mu - x} \\ &= e^{x^2\tau - xy} \left[1 - \operatorname{erf} \left(\frac{y}{2\sqrt{\tau}} - x\sqrt{\tau} \right) \right] \\ &= e^{-y^2/4\tau} G \left(\frac{y}{2\sqrt{\tau}} - x\sqrt{\tau} \right), \end{aligned} \right\} \quad \dots \dots \quad (19)$$

where

$$G(z) \equiv e^{z^2} (1 - \operatorname{erf} z).$$

(18) and (19) give a first approximation to u . It can be further simplified for particular ranges of r or w . Thus, if r is small, (18) becomes

$$u \simeq \frac{2r}{\alpha - \beta} \left\{ \alpha^2 E_1(\alpha) - \beta^2 E_1(\beta) + \frac{\alpha - \beta}{\sqrt{\pi\tau}} e^{-1/4\tau} \right\}. \quad \dots \dots \quad (20)$$

The relative temperature u/r at the centre is obtained at once from (20). Again, if r is nearly 1, the first bracketed term in (13) will, for small τ , be large compared with the second, so that

$$u \simeq \frac{1}{\alpha - \beta} \{ \alpha E_{1-r}(\alpha) - \beta E_{1-r}(\beta) \}. \quad \dots \dots (21)$$

A first approximation to the fluid temperature is obtained from the first term of (13), or by setting $r=1$ in (21). Thus

$$u' \simeq \frac{1}{\alpha - \beta} \{ \alpha E_0(\alpha) - \beta E_0(\beta) \}. \quad \dots \dots (22)$$

Finally, when $w=0$,

$$\begin{aligned} u &\simeq E_{1-r}(0) - E_{1+r}(0) \\ &= \operatorname{erf} \frac{1+r}{2\sqrt{\tau}} - \operatorname{erf} \frac{1-r}{2\sqrt{\tau}}, \end{aligned} \quad \dots \dots (23)$$

$$\begin{aligned} F &= \frac{3(q \cosh q - \sinh q)}{q^2 \sinh q} \\ &= -3\tau + 6\sqrt{\tau/\pi} + 12\sqrt{\tau} \sum_{n=1}^{\infty} \Phi_1 \left(\frac{n}{\sqrt{\tau}} \right). \end{aligned} \quad \dots \dots (24)$$

(23) and (24) correspond to (10) and (11). (24) converges very rapidly indeed for $\tau \leq 0.1$, giving $F = 6\sqrt{\tau/\pi} - 3\tau$ to better than 1 in 30,000, while for $\tau \geq 0.1$ two terms at most are required of the series in (11).

No matter how small $1-r$ is, short of being absolutely zero, the expressions given by (18), (21) and (23) tend to zero with τ , as required. On the other hand, (22), which is of course continuous with (21) for $\tau > 0$, tends to unity as τ approaches zero. The solutions thus correctly reproduce the required continuity for $\tau > 0$ and discontinuity at $\tau = 0$. It is not the least advantage of the operational method, as remarked by Jaeger (1945), that this is made possible in cases like the present without any special analytical device.

It is of interest to confirm that the second term in (14) is in fact negligible. This term transforms into

$$-\frac{6w}{\pi i} \int_M \frac{e^{\mu^2 \tau - 2\mu} \mu^2 d\mu}{(\mu - \alpha)^2 (\mu - \beta)^2}.$$

We may resolve the integrand into partial fractions, and integrate the terms in $(\mu - \alpha)^{-2}$ and $(\mu - \beta)^{-2}$ by parts. There results

$$\begin{aligned} &+ \frac{12w}{(\alpha - \beta)^3} \left\{ [\alpha\beta - \alpha^2(\alpha - \beta)(\alpha\tau - 1)] E_2(\alpha) - [\alpha\beta + \beta^2(\alpha - \beta)(\beta\tau - 1)] E_2(\beta) \right. \\ &\quad \left. - (\alpha - \beta)(\alpha^2 + \beta^2) \sqrt{\frac{\tau}{\pi}} e^{-\frac{1}{\tau}} \right\}. \quad \dots \dots (25) \end{aligned}$$

Let $\alpha \equiv \frac{1}{2}(-3w + \sqrt{9w^2 + 12w})$ and $\beta \equiv \frac{1}{2}(-3w - \sqrt{9w^2 + 12w})$. Clearly $0 < \alpha < 1$ and $\beta < 0$. Values of α and β for a wide range of w are shown in table 2. If, then, $\tau < 0.1$, $1/\sqrt{\tau} - \alpha\sqrt{\tau}$ and $1/\sqrt{\tau} - \beta\sqrt{\tau}$ are of the order of 3, or greater. Hence, using the asymptotic series for erf , we have

$$\left. \begin{aligned} E_2(\alpha) &\sim e^{-1/\tau} / \sqrt{\pi} (1/\sqrt{\tau} - \alpha\sqrt{\tau}), \\ E_2(\beta) &\sim e^{-1/\tau} / \sqrt{\pi} (1/\sqrt{\tau} - \beta\sqrt{\tau}). \end{aligned} \right\} \quad \dots \dots (26)$$

Table 2. The roots α, β of $x^2 + 3wx - 3w = 0$

w	α	β	w	α	β
1000	0.9997	-3001	5.00	0.9410	-15.94
500	0.9993	-1501	2.00	0.8730	-6.873
400	0.9992	-1201	1.00	0.7913	-3.791
300	0.9989	-901.0	0.50	0.6861	-2.186
200	0.9983	-601.0	0.20	0.5307	-1.131
100	0.9967	-301.0	0.10	0.4179	-0.7179
50	0.9934	-151.0	0.05	0.3195	-0.4695
20	0.9839	-60.98	0.02	0.2168	-0.2768
10	0.9693	-30.97	0.01	0.1583	-0.1883

The factor $e^{-1/\tau}$ already guarantees that the term in $E_2(\alpha)$ in (23) is negligible; and the same can at once be shown to be true of the remaining two terms in virtue of the cancellation of the potentially large β^3 .

Thus, for $\tau \leq 0.1$, u' is given to a close approximation by (22), that is by

$$u' \approx \frac{1}{\alpha - \beta} \{ \alpha e^{\alpha^2 \tau} (1 + \operatorname{erf} \alpha \sqrt{\tau}) - \beta e^{\beta^2 \tau} (1 + \operatorname{erf} \beta \sqrt{\tau}) \}, \quad \dots \dots (27)$$

and F follows from (8).

By an argument precisely similar to the above, it can be shown that for $\tau \leq 0.1$ the terms in (13) beyond the first two are also negligible. So also, of course, is the second itself if τ is near to 1.

§ 3. NUMERICAL RESULTS

u' and F have been computed for $w=1000$ to $w=0$ and $\tau=10^{-12}$ to $\tau=1$. (27) was used for $\tau \leq 0.1$, and (7) for $\tau \geq 0.1$. A comparison between the two types of solution is thus provided at $\tau=0.1$. It will be seen from table 3 that the agreement is close, considering that only four-figure tables were used. The course of F is shown in figure 1. Here an additional check was made at $w=0, \tau=0.1$ and 0.01 , (11) yielding $F=0.7705, 0.3084$ and (24) $F=0.7705, 0.3085$. Finally, as an illustration, the temperature field was calculated for $w=1, \tau=10^{-4}, 10^{-2}, 10^{-1}$ by (18) and for $\tau=0.1, 1$ by (6). Very close agreement was found at $\tau=0.1$. The distribution is shown in figure 2. Except at the centre u/r rises temporarily above its final value.

§ 4. APPENDIX

Several interesting relations emerge from the above. Thus, from (9), since $F \rightarrow 0$ as $\tau \rightarrow 0$,

$$\sum_{n=1}^{\infty} \frac{1}{s_n^2 + 9w(1+w)} = \frac{1}{6(1+w)}, \quad \dots \dots (28)$$

s_n being the n th positive non-zero root of (5). $\Sigma 1/n^2 = \pi^2/6$ is of course a special case, given by (11).

Again, from (11) and (24),

$$\sum_{n=1}^{\infty} \frac{e^{-n^2 \pi^2 \tau}}{n^2} = \frac{\pi^2}{6} \left\{ 1 + 3\tau - 6\sqrt{\frac{\tau}{\pi}} - 12\sqrt{\tau} \sum_{n=1}^{\infty} \Phi_1 \left(\frac{n}{\sqrt{\tau}} \right) \right\}. \quad \dots \dots (29)$$

Table 3. $u' \equiv T'/T_0$ for various values of $w \equiv c_1/c_2$ and $\tau \equiv \kappa t/\alpha^2$

w	τ	Calculated from Equation (27)						Calculated from Equation (7)					
		10^{-12}	10^{-11}	10^{-10}	10^{-9}	10^{-8}	10^{-7}	10^{-6}	10^{-5}	10^{-4}	10^{-3}	10^{-2}	10^{-1}
1000.00	0.997	0.989	0.967	0.901	0.735	0.442	0.178	0.060	0.019	0.006	0.002	0.001	0.000
500.00	0.995	0.983	0.949	0.851	0.629	0.322	0.117	0.038	0.012	0.005	0.002	0.002	0.002
400.00	0.996	0.987	0.959	0.878	0.683	0.370	0.145	0.048	0.016	0.006	0.003	0.003	0.002
300.00	0.990	0.969	0.906	0.746	0.457	0.188	0.063	0.021	0.008	0.004	0.004	0.004	0.003
200.00	0.993	0.979	0.936	0.818	0.568	0.272	0.093	0.031	0.011	0.005	0.005	0.005	0.005
100.00	0.997	0.988	0.967	0.901	0.735	0.443	0.182	0.062	0.022	0.011	0.011	0.010	0.010
50.00	0.995	0.984	0.949	0.852	0.630	0.325	0.122	0.044	0.021	0.021	0.021	0.020	0.020
20.00	0.993	0.979	0.936	0.818	0.571	0.276	0.108	0.052	0.052	0.052	0.052	0.048	0.048
10.00	0.996	0.990	0.967	0.902	0.737	0.451	0.203	0.100	0.100	0.100	0.100	0.091	0.091
5.00	0.995	0.983	0.949	0.852	0.638	0.351	0.185	0.185	0.185	0.185	0.185	0.167	0.167
2.00	0.994	0.980	0.937	0.822	0.596	0.369	0.200	0.100	0.100	0.100	0.100	0.333	0.333
1.00	0.997	0.989	0.967	0.904	0.755	0.548	0.369	0.200	0.200	0.200	0.200	0.500	0.500
0.50		0.995	0.983	0.950	0.864	0.714	0.548	0.369	0.369	0.369	0.369	0.667	0.667
0.20			0.994	0.980	0.941	0.864	0.714	0.548	0.548	0.548	0.548	0.833	0.833
0.10			0.997	0.990	0.970	0.928	0.770	0.617	0.617	0.617	0.617	0.909	0.909
0.05			0.995	0.985	0.963	0.928	0.770	0.617	0.617	0.617	0.617	0.952	0.952
0.02			0.994	0.985	0.975	0.928	0.770	0.617	0.617	0.617	0.617	0.980	0.980
0.01			0.997	0.992	0.985	0.928	0.770	0.617	0.617	0.617	0.617	0.990	0.990

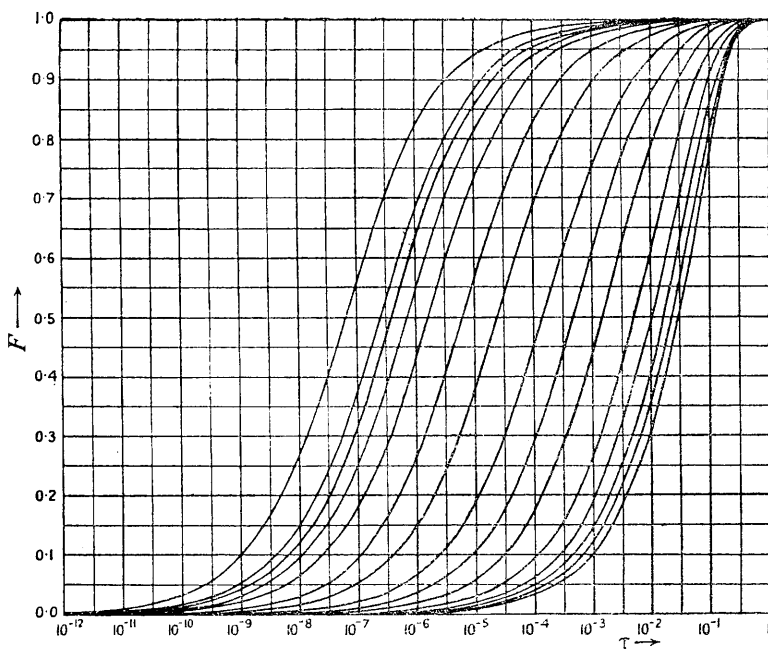


Figure 1. Variation of F with τ for various values of w . From left to right the curves correspond to $w=1000, 500, 400, 300, 200, 100, 50, 20, 10, 5, 0.5, 0.2, 0$.

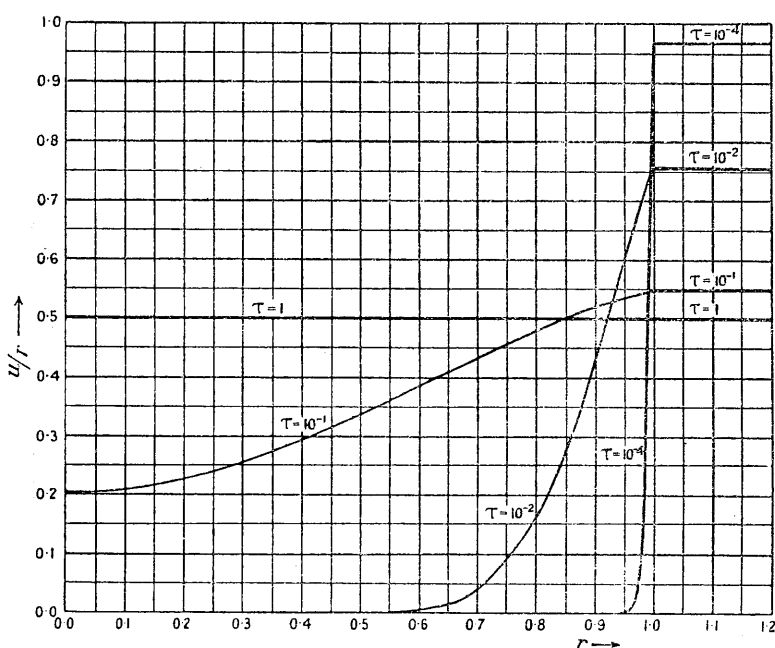


Figure 2. Variation of u/r with r for $w=1$ and various values of τ .

This yields, very closely, for $0 < x \leq 1$,

$$\sum_1^{\infty} \frac{e^{-n^2x}}{n^2} \approx \frac{\pi^2}{6} - \sqrt{\pi x} + \frac{x}{2} \quad \dots \dots (30)$$

and

$$\sum_1^{\infty} \Phi_1(nx) \approx \frac{1}{4x} - \frac{1}{2\sqrt{\pi}} + \frac{x}{12}. \quad \dots \dots (31)$$

By differentiating (29) and (30) with regard to x , or integrating from x to ∞ a series of useful formulae can be derived. For example,

$$\sum_1^{\infty} e^{-n^2x} = \frac{1}{2} \left(\sqrt{\frac{\pi}{x}} - 1 \right) + \sqrt{\frac{\pi}{x}} \sum_1^{\infty} e^{-n^2\pi^2/x} \quad \dots \dots (32)$$

and

$$\sum_1^{\infty} \frac{e^{-n^2x}}{n^4} = \frac{\pi^4}{90} - \frac{\pi^2 x}{6} + \frac{2\sqrt{\pi}}{3} x^{3/2} - \frac{x^2}{4} + \pi(2\sqrt{x})^3 \sum_1^{\infty} \Phi_3 \left(\frac{n\pi}{\sqrt{x}} \right), \quad \dots \dots (33)$$

the series terms on the right of (32) and (33) being negligible for $0 < x \leq 1$. (32) is a particular case of "Poisson's Identity".

REFERENCES

- HARTREE, D. R., 1936. *Mem. Manch. Lit. Phil. Soc.*, **80**, 85.
- JAEGER, J. C., 1945. *Proc. Camb. Phil. Soc.*, **41**, 43.
- PEDDIE, W., 1901. *Proc. Edin. Math. Soc.*, **19**, 34.

CONDUCTION OF HEAT FROM LOCAL SOURCES

IN A MEDIUM GENERATING OR ABSORBING HEAT.

Conduction of heat from local sources in a
medium generating or absorbing heat.

ABSTRACT

An infinite or semi-infinite medium, in which heat is generated or absorbed at a rate proportional to the temperature, is placed at temperature zero in contact with a perfect conductor of finite heat capacity at a higher temperature. Expressions are derived for the subsequent behaviour in linear and spherical cases, and applications suggested.

(2)

If $\bar{u} \equiv \mathcal{L}(u) \equiv \int_0^\infty u e^{-pt} d\tau$ denotes the Laplace transform of u , these equations transform into

$$\begin{aligned}\frac{d^2 \bar{u}}{dx^2} &= (p - H) \bar{u}, \\ \omega \frac{d\bar{u}}{dx} &= p\bar{u} - 1, \quad x = 0,\end{aligned}\tag{3}$$

whose solution, finite at $x = \infty$, is

$$\bar{u} = \frac{e^{-\alpha x}}{p + \alpha \omega},\tag{4}$$

where

$$\alpha \equiv \sqrt{p - H}.\tag{5}$$

u is then determined by the inverse transform

$$u = \mathcal{L}^{-1}(\bar{u}) = \frac{1}{2\pi i} \int_L e^{pt - \alpha x} \frac{dp}{p + \alpha \omega},\tag{6}$$

where L passes from $\mathcal{I}(p) = -\infty$ to $\mathcal{I}(p) = +\infty$ and to the right of the zeros of $p + \alpha \omega$.

The substitution

$$p + \omega \alpha \equiv \lambda\tag{7}$$

enables/

(3)

enables us to write

$$u = e^{\frac{w}{2}(x+w\tau)} [J - K], \quad (8)$$

where

$$J \equiv \frac{1}{2\pi i} \int_M e^{\lambda\tau - (x+w\tau)\sqrt{\lambda + \frac{w^2}{4} - H}} \frac{d\lambda}{\lambda}, \quad (9)$$

$$K \equiv \frac{1}{2\pi i} \int_M e^{\lambda\tau - (x+w\tau)\sqrt{\lambda + \frac{w^2}{4} - H}} \frac{d\lambda}{\lambda\sqrt{\lambda + \frac{w^2}{4} - H}}, \quad (10)$$

and M is the corresponding contour. We may denote $x+w\tau$ by y and $\frac{w^2}{4} - H$ by g^2 . Then by the superposition thereon, $J = \int_0^\tau \varphi(s) ds$ and $K = \int_0^\tau \psi(s) ds$, where

$$\begin{aligned} \varphi(s) &= \frac{1}{2\pi i} \int_M e^{\lambda s - y\sqrt{\lambda + g^2}} d\lambda \\ &= \frac{e^{-gs}}{2\pi i} \int_M e^{\lambda s - y\sqrt{\lambda}} d\lambda \\ &= \frac{y}{2\sqrt{\pi s^3}} \cdot e^{-gs - y^2/4s} \end{aligned} \quad (11)$$

and similarly

$$\begin{aligned} \psi(s) &= \frac{we^{-gs}}{4\pi i} \int_M e^{\lambda s - y\sqrt{\lambda}} \frac{d\lambda}{\sqrt{\lambda}} \\ &= \frac{w}{2\sqrt{\pi s}} \cdot e^{-gs - y^2/4s} \end{aligned} \quad (12)$$

Hence, finally, from (8), (11), (12),

$$u = \frac{ey^{1/2}}{2\sqrt{\pi}} \int_0^\tau \left(\frac{y}{s^{3/2}} - \frac{w}{s^{1/2}} \right) e^{-gs - y^2/4s} ds. \quad (13)$$

It /

It can be confirmed by the direct substitution that (13) satisfies the conditions of the problem.

An alternative form of the solution, which is more convenient if $\beta^2 > 0$, can be obtained, either from (13) by using two relations given by Horenstein,^{*} or more directly from the transform (4).

For, if $\beta \equiv \mu^2 + H$, (6) becomes

$$u = \frac{1}{\pi i} \int_M \exp\left\{(\mu^2 + H)\tau - \mu x\right\} \frac{\mu d\mu}{\mu^2 + \omega\mu + H}. \quad (14)$$

By resolving into partial fractions, we easily deduce

$$\begin{aligned} u = \frac{1}{2g} \left[\left(g - \frac{\omega}{2} \right) e^{-y(g - \frac{\omega}{2})} \operatorname{erfc}\left(\frac{y}{2\sqrt{\tau}} - g\sqrt{\tau}\right) \right. \\ \left. + \left(g + \frac{\omega}{2} \right) e^{y(g + \frac{\omega}{2})} \operatorname{erfc}\left(\frac{y}{2\sqrt{\tau}} + g\sqrt{\tau}\right) \right] \end{aligned} \quad (15)$$

When there is no generation of heat, $g = \omega/2$, and (15) reduces to

$$u = e^{\omega y} \operatorname{erfc}\left(\frac{y + \omega\tau}{2\sqrt{\tau}}\right) \quad (16)$$

The same expression can be derived with rather more trouble from (13), or of course directly from (4) with $\alpha = \sqrt{\beta}$.

A series solution suitable for large values of $x/2\sqrt{\tau}$ can be obtained as follows. By (4),

$$u = e^{H\tau} \cdot v \quad (17)$$

where

$$\bar{v} = \frac{e^{-x\sqrt{\beta}}}{\beta + \omega\sqrt{\beta} + H} \quad (18)$$

Writing q for $\sqrt{\beta}$, and expanding in negative powers of q , we have

* Quart. Appl. Maths. 3, 183 (1945). See also S. Paterson, ib. 4, 305 (1946).

(5)

$$\bar{v} = \frac{e^{-xq}}{q^2} (1 + B_1 q^{-1} + B_2 q^{-2} + \dots), \quad (19)$$

where

$$B_1 = -\omega$$

$$B_2 = \omega^2 - H$$

$$B_3 = 2H\omega - \omega^3$$

$$B_4 = \omega^4 - 3H\omega^2 + H^2$$

(20)

etc.

Hence,

$$u = e^{H\tau} \left[\operatorname{erfc} \frac{x}{2\sqrt{\tau}} + \sum_{n=1}^{\infty} B_n (2\sqrt{\tau})^n \cdot i^n \operatorname{erfc} \left(\frac{x}{2\sqrt{\tau}} \right) \right], \quad (21)$$

if, in Hartree's notation,^{*}

$$i^n \operatorname{erfc}(z) \equiv \int_z^{\infty} i^{n-1} \operatorname{erfc}(z) dz,$$

and $i^0 \operatorname{erfc}(z) \equiv \operatorname{erfc}(z)$ Since, when z is large,

$$i^n \operatorname{erfc}(z) \sim \frac{2}{\sqrt{\pi}} (2z)^{-(n+1)} \cdot e^{-z^2},$$

the series (21) converges rapidly for $\frac{x}{2\sqrt{\tau}} \gg 1$. When $x=0$, (21) reduces to

$$u' = e^{H\tau} \left[1 + \sum_{n=1}^{\infty} B_n \frac{\tau^{n/2}}{T(\frac{n}{2}+1)} \right] \quad (22)$$

$$= e^{H\tau} \left[1 - 2\omega \sqrt{\frac{\tau}{\pi}} + (\omega^2 - H)\tau + \dots \right].$$

(22)/

(22) converges rapidly for small τ .

In what follows, we shall assume $T_0 > 0$, $H > 0$.

Then it is clear from (22) that the surface temperature commences by falling, irrespective of the value of H . From physical considerations, however, it must subsequently rise again, in consequence of the generation of heat, if $H > 0$. Although it appears difficult to define the turning-point in general terms, the behaviour may be illustrated by a special case, corresponding to $\omega^2 = 4H$. For then $g=0$ and the surface temperature is therefore, by (15),

$$u(0) = e^{2\xi^2} \left\{ (1+2\xi^2) \operatorname{erfc} \xi - \frac{2\xi}{\sqrt{\pi}} e^{-\xi^2} \right\}, \quad (23)$$

where

$$\xi \equiv \frac{\omega}{2} \sqrt{\tau}$$

The turning-point is defined by

$$0 = \frac{du(0)}{d\xi} = 4e^{2\xi^2} (1+2\xi^2) \left\{ 2\xi \operatorname{erfc} \xi - \frac{1}{\sqrt{\pi}} e^{-\xi^2} \right\}, \quad (24)$$

which has a single root ~ 0.435 .

As an example, let us suppose a cold explosive gas to be brought in contact with a hot metallic foil. Heat will be generated in the gas according to an Arrhenius function of temperature, which we may represent very roughly by the linear equation

$$\left(\frac{\partial T}{\partial t} \right)_{\text{react.}} = GT, \quad (25)$$

if G is defined by

$$GT_0 = Ae^{-E/RT_0}, \quad (26)$$

where /

(7)

where $A \sim 10^{12} \text{ }^{\circ}\text{K/sec}$. Provided the condition $\omega^2 = 4H$ is satisfied, we may then expect the surface temperature to commence rising after a time t_c defined by $\xi \sim 0.4$, that is, by

$$Gt_c \sim 0.2 \quad (27)$$

By (26), this reduces to

$$t_c \sim 0.2 \times 10^{-12} T_0 e^{E/RT_0} \quad (28)$$

Assuming $E \sim 40,000 \text{ cal/mole}$, we have the following variation of t_c , which may be identified with the lag time for ignition.

$T_0 (\text{ }^{\circ}\text{K})$	5000	4000	3000	2000	1000	700	500
$t_c (\text{sec})$	10^{-7}	2×10^{-7}	5×10^{-7}	10^{-5}	10^{-1}	10^3	10^7

It is clear that ignition in any normal sense requires a foil temperature of the order of $900 \text{ }^{\circ}\text{K}$, which is a physically reasonable level. Since G must evidently be ~ 1 , the condition $\omega^2 = 4H$ implies $\omega \sim \frac{2}{\sqrt{k}} \sim 1$, which corresponds to a foil thickness of the order of 10^{-3} cm . Although this example is a rather crude one, it does illustrate the possibility of a useful application of the present analysis. No doubt this would be more profitable in the case of condensed explosive, where convective effects are absent.

(2) Spherical case.

If R denotes a radial co-ordinate, we suppose the region $R > a$, with thermal constants k, κ , to be initially at zero temperature. The region $R < a$ is filled with a perfect conductor initially at temperature T_0 . Conditions being otherwise as before, we have

$$\frac{\partial T}{\partial t} = \kappa \frac{1}{R} \frac{\partial^2 (RT)}{\partial R^2} + GT, \quad R > a, t > 0,$$

$$T = 0, \quad R > a, \quad t = 0,$$

$$T = T', \quad R = a, \quad t > 0,$$

$$k \frac{\partial T}{\partial R} = c' \frac{dT'}{dt}, \quad R = a, \quad t > 0,$$

$$T' = T_0, \quad t = 0,$$

where c' is the heat capacity of the perfect conductor per unit area of the interface.

For convenience, set $R-a \equiv x, \kappa t \equiv \tau, RT/aT_0 \equiv u, T'/T_0 \equiv u'$, $G/k \equiv H$ and $k/c' \equiv \omega$. Then

$$\begin{aligned} \frac{\partial u}{\partial \tau} &= \frac{\partial^2 u}{\partial x^2} + Hu, \\ u &= 0, \quad \tau = 0; \quad u = u', \quad x = 0, \\ \omega \left(\frac{\partial u}{\partial x} - \frac{u}{a} \right) &= \frac{du'}{d\tau}, \quad x = 0, \\ u' &= 1, \quad \tau = 0 \end{aligned} \tag{30}$$

In the same manner as before, we find

$$\bar{u} = \frac{e^{-\alpha x}}{p + \frac{\omega}{a} + \alpha \omega}, \tag{31}$$

so that

$$u = \frac{1}{2\pi i} \int_L \frac{e^{p\tau - \alpha x}}{p + \frac{\omega}{a} + \alpha \omega} dp. \tag{32}$$

If

If now $\phi + \frac{\omega}{a} \equiv P$, and $H + \frac{\omega}{a} \equiv K$, (32) becomes

$$\frac{RT}{aT_0} \equiv u = \frac{e^{-\omega\tau}}{2\pi i} \int_L \frac{e^{P\tau - \beta x}}{P + \beta\omega} dP, \quad (33)$$

where

$$\beta \equiv \sqrt{\phi - K}. \quad (34)$$

Comparison with (5), (6) shows that T/T_0 is then obtained from the linear solution by multiplying by $aR^{-1}e^{-\omega\tau/a}$ and replacing x by $R-a$ and H by $H+\omega/a$. Thus, if we set $Z \equiv R-a+\omega\tau$, $h^2 \equiv \frac{\omega^2}{4}-H-\frac{\omega}{a}$, (13) yields :

$$\frac{T}{T_0} = \frac{a}{R} \cdot \frac{e^{\omega(\frac{Z}{2}-\frac{Z}{a})}}{2\sqrt{\pi}} \int_0^\tau \left(\frac{Z}{s^{3/2}} - \frac{\omega}{s^{1/2}} \right) e^{-h^2 s - Z^2/4s} ds, \quad (35)$$

and it can be verified by substitution in (29) that this satisfies the conditions of the problem.

Relations corresponding to (15), (16), (21) (22) can be written down in the same way. For example, by (15),

$$T/T_0 = \frac{a}{R} e^{-\frac{\omega\tau}{a}} \cdot \frac{1}{2h} \left\{ \left(h - \frac{\omega}{2} \right) e^{-Z(h-\frac{\omega}{2})} \operatorname{erfc}\left(\frac{Z}{2\sqrt{\tau}} - h\sqrt{\tau}\right) \right. \\ \left. + \left(h + \frac{\omega}{2} \right) e^{Z(h+\frac{\omega}{2})} \operatorname{erfc}\left(\frac{Z}{2\sqrt{\tau}} + h\sqrt{\tau}\right) \right\}, \quad (36)$$

provided $h^2 \equiv \frac{\omega^2}{4}-H-\frac{\omega}{a} > 0$. Otherwise, (35) may be used.

(36) includes, when $H=0$, the interesting case of a perfectly conducting sphere heated or cooled in an infinite medium. The solution, curiously enough, does not seem to have been given previously.

Again, for large $(R-a)/2\sqrt{\tau}$, (21) becomes

$$\frac{T}{T_0} = \frac{a}{R} \cdot e^{(H+\frac{w}{a})\tau} \left[\operatorname{erfc} \frac{R-a}{2\sqrt{\tau}} + \sum_1^{\infty} B_n (2\sqrt{\tau})^n i^n \operatorname{erfc} \frac{R-a}{2\sqrt{\tau}} \right], \quad (37)$$

where B_n is defined by (20) with H replaced by $H+w/a$.

Similarly, by (22),

$$\frac{T'}{T_0} = e^{(H+\frac{w}{a})\tau} \left[1 - 2w\sqrt{\frac{T}{\pi}} + (w^2 - \frac{w}{a} + H)\tau + \dots \right] \quad (38)$$

The remarks concerning the variation of T' in the linear case apply equally to the spherical problem. We may illustrate the behaviour of T' by a special case, corresponding now to $h=0$, that is, to $w^2/4 - w/a = H$. From (36), by letting h approach zero, we deduce,

$$\frac{T'}{T_0} = e^{(1-\frac{4}{aw})\xi^2} \left[(1+2\xi^2) e^{\xi^2} \operatorname{erfc} \xi - \frac{2\xi}{\sqrt{\pi}} \right], \quad (39)$$

where, as before, $\xi = w\sqrt{\tau}/2$. As would be expected, (39) reduces to (23) when the radius $a \rightarrow \infty$.

Since $aw = \frac{3cp}{c'p'}$, where c, p are the specific heat and density of the medium ($R > a$) and c', p' corresponding quantities for the source ($R < a$), and since we require $aw > 4$, (39) cannot apply to any solid sphere in a gas; for such systems, $aw \sim 10^{-2}$. However, it is possible for aw to exceed 4 in the case of a liquid or solid external medium. For example, aluminium spheres in nitroglycerine would give $aw \sim 5$. If we take this value for illustration, (39) has a minimum at $\xi_c \sim 3$, so that $w \sim 6/\sqrt{\tau_c}$. Adopting a typical value of $0.01 \text{ cm}^2/\text{sec}$ for κ , and requiring that $t_c \neq 1/\text{sec}$ for explosion,

explosion, we conclude $\omega \sim 60 \text{ cm}^{-1}$, whereupon $a \sim \frac{1}{12} \text{ cm.}$. Then $H \sim 180$, and so $G \equiv \kappa H \sim 1.8$. However, for nitroglycerine, $G \sim 10^{17} T_0^{-1} e^{-20,000/T_0}$ by equation (26). Hence, finally, $T_0 \sim 600^\circ\text{K}$. The analysis therefore suggests that an aluminium sphere of radius 1mm. will ignite nitroglycerine if raised to a temperature of about 300°C . The result is perfectly reasonable, since nitroglycerine in bulk ignites at about 200°C .

(6)

ON CERTAIN TYPES OF SOLUTION

OF THE EQUATION OF HEAT CONDUCTION.

On certain types of solution of the equation of heat conduction

Let $f(x, y, z, t)$ satisfy the equation

$$f_t = \nabla^2 f \equiv f_{xx} + f_{yy} + f_{zz} \quad (1)$$

For certain purposes, particularly in connection with the propagation of a boundary of fusion, etc., it is of interest to discover solutions of (1) which permit the equation:

$$f = \text{constant} \quad (2)$$

to be solved explicitly in the form:

$$g(x, y, z) = h(t). \quad (3)$$

This suggests the examination of solutions of the type

$$f = f(\zeta), \quad (4)$$

where $\zeta \equiv \varphi(x, y, z)\psi(t)$, (5)

and f, φ, ψ are functions to be determined. To save repetition, Roman capitals denote arbitrary constants throughout.

$$(1) \text{ Linear system } f = f(x, t) = f[\zeta(x, t)] ; \quad f_t = f_{xx}. \quad$$

(a) Let $\zeta \equiv x^m t^n$. Then, by (1)

$$nx^2 f'(\zeta) = m(m-1)tf'(\zeta) + m^2 x^m t^{n+1} f''(\zeta). \quad (6)$$

That is

$$\frac{f''}{f'} = \frac{nx^{2+\frac{m}{n}} - m(m-1)\zeta^{\frac{1}{n}}}{m^2 \zeta^{1+\frac{1}{n}}}. \quad (7)$$

Consequently $n=0$ or $m=-2n$.

If $m=-2n \neq 0$, we may without loss of generality take $n=-\frac{1}{2}$, whereupon $m=1$ and

$$\frac{f''}{f'} = -\zeta^{\frac{1}{2}}. \quad (8)$$

$$\text{Then } f' = Ae^{-\zeta^{\frac{1}{2}}}, \quad (9)$$

and so

$$f(\zeta) = B \operatorname{erf}(\zeta/2) + C. \quad (10)$$

$n=0$ yields the trivial case

$$f(\zeta) = A\zeta^{\frac{1}{n}} + B = Ax + B, \quad (11)$$

which may be regarded as a limiting form of (10).

The only solutions of (1) of the form $f(x^m t^n)$

are therefore

$$f = \text{Berf}\left(\frac{x}{2\sqrt{t}}\right) + C, \quad (12)$$

$$f = Ax + B. \quad (13)$$

(b) To generalise, let now $\zeta = \varphi(x)\psi(t)$.

Here $f_t = \varphi\dot{\psi}f'$ and $f_{xx} = \ddot{\varphi}\psi f' + \dot{\varphi}^2\psi^2 f''$,

where the dot signifies differentiation with respect to x or t . Consequently, by (1)

$$\frac{f''}{f'} = \frac{\varphi\dot{\psi} - \psi\ddot{\varphi}}{\dot{\varphi}^2\psi^2}. \quad (14)$$

If we denote f''/f' by $\theta(\zeta)$, then

$$\theta_x = \theta'\psi\dot{\varphi}, \quad \theta_t = \theta'\varphi\dot{\psi}.$$

Consequently

$$\varphi\dot{\psi}\theta_x = \psi\dot{\varphi}\theta_t, \quad (15)$$

and from (14) and (15), after some reduction, we have

$$\frac{2\varphi\ddot{\varphi}}{\dot{\varphi}^2} \cdot \frac{\dot{\psi}}{\psi} = \left(\frac{3\dot{\psi}}{\psi} - \frac{\ddot{\psi}}{\dot{\psi}}\right) + \left(\frac{2\ddot{\varphi}^2}{\dot{\varphi}^2} - \frac{\ddot{\varphi}}{\dot{\varphi}} - \frac{\ddot{\varphi}}{\varphi}\right), \quad (16)$$

which is of the form: $f_1(x)f_2(t) = f_3(t) + f_4(x)$.

It follows that either f_1 or f_2 is a constant. That is,

$$\varphi\ddot{\varphi} = B\dot{\varphi}^2 \quad \text{or} \quad \dot{\psi} = A^2\psi. \quad (17)$$

In the former case,

$$\varphi\ddot{\varphi} + \dot{\varphi}\ddot{\varphi} = 2B\dot{\varphi}\ddot{\varphi} = 2\varphi\ddot{\varphi}^2/\dot{\varphi},$$

so that $f_4(x) \equiv 0$. Also

$$\dot{\varphi} = C\varphi^B, \quad \varphi^{-B} = (-B)(Cx+D), \quad (18)$$

and we lose no generality in setting $B=0$, so that

$$\varphi = Cx+D. \quad (19)$$

$$\text{Then } 3\dot{\psi}/\psi = \ddot{\psi}/\dot{\psi}, \quad (20)$$

$$\text{whence } \dot{\psi} = -E\psi^3, \quad \psi = 1/2\sqrt{Et+F}, \quad (21)$$

and we may, without loss, take $E=2C^2$.

Finally, by (14), (18) and (21),

$$f''/f' = -\frac{E\zeta}{C^2} = -2\zeta, \quad (22)$$

which leads to

$$f(\zeta) = \text{Perf}(\zeta) + Q. \quad (23)$$

Thus, when $\varphi\ddot{\varphi}/\dot{\varphi}^2 = \text{constant}$, the only solution is

$$f = \text{Perf}\left(\frac{x+R}{2\sqrt{t+s}}\right) + Q. \quad (24)$$

$$f = Px + Q \quad (25)$$

is again a trivial limiting case.

$$\text{If } \dot{\psi} = A^2\psi, \quad f_3(t) = 2A^2 \quad \text{and} \quad \psi = Be^{A^2t}. \quad (26)$$

Also, by (14)

$$f''/f' = \frac{A^2\varphi - \ddot{\varphi}}{\dot{\varphi}^2} \cdot \frac{\varphi}{\zeta}, \quad (27)$$

so that

$$\ddot{\varphi} - A^2\varphi = C\dot{\varphi}^2/\varphi.$$

The term $C\dot{\varphi}^2/\varphi$ can be removed by setting $\varphi = \Phi^{\frac{1}{1-C}}$, so that we may take $C = 0$, giving

$$\varphi = De^{Ax} + Ee^{-Ax}. \quad (28)$$

Then by (27)

$$f''/f' = 0, \quad (29)$$

which implies

$$f = F\zeta + G. \quad (30)$$

Collecting (26), (28) and (30), we conclude that when $\dot{\psi}/\psi = \text{constant}$, the only solution is

$$f = e^{A^2t}[Pe^{Ax} + Qe^{-Ax}] + R. \quad (31)$$

A may be imaginary, in which case P and Q are complex.

The only solutions $f[\varphi(x)\psi(t)]$ of $f_t = f_{xx}$ are therefore: (24), (25) and (31).

$$(2) \text{ Cylindrical system} \quad f = f(r, t) = f[\zeta(r, t)] ; \quad f_t = f_{rr} + \frac{1}{r} f_r .$$

$$\text{Let} \quad \zeta \equiv \varphi(r) \psi(t) .$$

$$\text{Then} \quad \theta(\zeta) \equiv f''/f' = \frac{\varphi\ddot{\psi} - \dot{\varphi}\psi - \frac{1}{r}\dot{\varphi}\psi}{\dot{\varphi}^2\psi^2} , \quad (32)$$

and (15) leads to

$$\frac{2\varphi\ddot{\psi}}{\dot{\varphi}^2} \cdot \frac{\dot{\psi}}{\psi} = \left(\frac{3\dot{\psi}}{\psi} - \frac{\ddot{\psi}}{\dot{\psi}} \right) + \left(\frac{2\dot{\varphi}^2}{\dot{\varphi}^2} - \frac{\ddot{\varphi}}{\dot{\varphi}} - \frac{\dot{\varphi}}{\varphi} + \frac{1}{r^2} + \frac{1}{r}\frac{\ddot{\varphi}}{\dot{\varphi}} - \frac{1}{r}\frac{\dot{\varphi}}{\varphi} \right) , \quad (33)$$

$$\text{whence} \quad \varphi\ddot{\psi} = B\dot{\varphi}^2 \quad \text{or} \quad \dot{\psi} = -A^2\psi .$$

$$\text{In the former case,} \quad \dot{\varphi} = C\varphi^B , \quad \varphi^{1-B} = C(1-B)(t+D) ,$$

$$\text{and we may take} \quad B = 0 , \quad C = 1 , \quad \text{whereupon}$$

$$\ddot{\varphi} = 0 , \quad \dot{\varphi} = 1 , \quad \varphi = r+D . \quad (34)$$

Then, by (33)

$$0 = \left(\frac{3\dot{\psi}}{\psi} - \frac{\ddot{\psi}}{\dot{\psi}} \right) + \frac{1}{r^2} - \frac{1}{r(r+D)} ,$$

$$\text{so that} \quad D = 0 , \quad \text{giving} \quad \varphi = r . \quad \text{Also}$$

$$\psi\ddot{\psi} = 3\dot{\psi}^2 , \quad \dot{\psi} = -E\psi^3 , \quad \psi = 1/\sqrt{2E(t+R)} .$$

$$\text{We may take} \quad E = 2 , \quad \text{whence}$$

$$\zeta = \frac{r}{2\sqrt{t+R}} . \quad (35)$$

Finally, by (32),

$$f''/f' = -2\zeta - \frac{1}{\zeta} , \quad (36)$$

which leads to

$$f = P Ei\left(\frac{-r^2}{4(t+R)}\right) + Q . \quad (37)$$

$$\text{Again, if} \quad \dot{\psi} = -A^2\psi , \quad \psi = Be^{-A^2t} , \quad \text{and}$$

$$f''/f' = -\frac{\varphi}{\zeta} \cdot \frac{A^2\varphi + \ddot{\varphi} + \dot{\varphi}/r}{\dot{\varphi}^2} , \quad (38)$$

so that

$$\ddot{\varphi} + \frac{1}{r}\dot{\varphi} + A^2\varphi = C\dot{\varphi}^2/\varphi . \quad (39)$$

The term, $c\dot{\varphi}^2/\varphi$ can be removed by substituting $\varphi \equiv \varphi^{\frac{1}{1-c}}$, so that we may without loss take $c = 0$. The solution of (39) is then

$$\varphi = D J_0(Ar) + E Y_0(Ar), \quad (40)$$

where J_0 and Y_0 are zero-order Bessel functions of first and second kinds respectively.

Finally, by (38),

$$f''/f' = 0,$$

so that

$$f = G\zeta + R. \quad (41)$$

Collecting the results,

$$f = e^{-At^2} [P J_0(Ar) + Q Y_0(Ar)] + R. \quad (42)$$

A may again be imaginary, with P, Q complex.

When $A = 0$, we have the trivial limiting case

$$f = P \ln r + Q. \quad (43)$$

(37), (42) and (43) represent the only solutions $f[\varphi(r)\psi(t)]$ of $f_t = f_{rr} + \frac{1}{r}f_r$.

(3) Spherical system $f = f(r, t) = f[\zeta(r, t)]$; $f_t = f_{rr} + \frac{2}{r}f_r$.

As before, let $\zeta \equiv \varphi(r)\psi(t)$. The cylindrical solution applies, except that $1/r$ must be replaced by $2/r$ in (32) and (33). (35) follows as before, but (36) becomes

$$f''/f' = -2\zeta - \frac{2}{\zeta}, \quad (44)$$

which leads to

$$f = P \left[\frac{\sqrt{t+R}}{r} e^{-\frac{r^2}{4(t+R)}} + \frac{\sqrt{\pi}}{2} \operatorname{erf} \frac{r}{2\sqrt{t+R}} \right] + Q. \quad (45)$$

Again, if $\dot{\varphi} = A^2\psi$, (39) becomes

$$\ddot{\varphi} + \frac{2}{r}\dot{\varphi} - A^2\varphi = c\dot{\varphi}^2/\varphi, \quad (46)$$

and the term $c\dot{\varphi}^2/\varphi$ may be removed as before, so that we take $c = 0$, whereupon

$$\varphi = [D e^{Ar} + E e^{-Ar}] / r. \quad (47)$$

(41) still applies, and so

$$f = \frac{e^{At}}{r} [Pe^{Ar} + Qe^{-Ar}] + R. \quad (48)$$

A may again be imaginary, with complex P, Q .

When $A = 0$, we have the trivial limiting case

$$f = \frac{P}{r} + Q. \quad (49)$$

(45), (48) and (49) are the only solutions

$$f [\phi(r)\psi(t)] \quad \text{of} \quad f_t = f_{rr} + \frac{2}{r} f_r.$$

(7.)

PROPAGATION OF A BOUNDARY OF FUSION.

PROPAGATION OF A BOUNDARY OF FUSION.

General Theory

We consider a volume of material, divided into two regions 1 and 2, each of density ρ , by a moving surface S . On S a change of phase occurs, at a definite temperature (which we may take to be zero) and with absorption or liberation of a latent heat per unit mass. If θ_1, k_1, K_1 are the temperature, thermal conductivity and diffusivity of phase 1, and θ_2, k_2, K_2 corresponding quantities for phase 2, the surface S is the isothermal

$$\theta_1(x, y, z, t) = 0 = \theta_2(x, y, z, t) \quad (1)$$

and the boundary condition on this surface is

$$k_1/\text{grad } \theta_1 - k_2/\text{grad } \theta_2 = \pm L\rho/\text{grad } \theta_1 = \pm L\rho/\text{grad } \theta_2 \quad (2)$$

Subscripts denote partial differentiation.

The condition for a simple solution is thus seen at once to be that θ_1, θ_2 separately satisfy

$$\frac{\text{grad}^2 \theta}{\theta_t} = \text{const. when } \theta = 0 \quad (3)$$

For example, in the one-dimensional cases of linear, axially symmetrical or spherically symmetrical flow, we require

$$\frac{\theta^2}{\theta_t} = \text{const. when } \theta = 0 \quad (4)$$

where/

(2)

where τ is the appropriate space co-ordinate.

In addition, θ_1, θ_2 must, of course satisfy

$$(\theta_1)_t = K_1 \nabla^2 \theta_1; \quad (\theta_2)_t = K_2 \nabla^2 \theta_2, \quad (5)$$

which for the above one-dimensional cases become

$$(\theta_1)_t = K_1 \left[(\theta_1)_{\tau\tau} + \frac{n(\theta_1)_\tau}{\tau} \right]; \quad K_2 \left[(\theta_2)_{\tau\tau} + \frac{n(\theta_2)_\tau}{\tau} \right] \quad (6)$$

where $n = 0, 1, 2$ in the three cases, respectively.

Particular solutions

We consider solutions of the form

$$\theta = \omega(\zeta) \quad (7)$$

$$\text{where } \zeta = \Phi(\tau) \psi(t) \quad (8)$$

It has been shown elsewhere that the only such solutions are:-

$$\left\{ \begin{array}{l} \theta = A\tau + F \left(\frac{\tau + B}{2\sqrt{K(t+C)}} \right) + D \\ \theta = e^{A^2 K t} \left[B e^{A\tau} + C e^{-A\tau} \right] + D \end{array} \right. \quad (9)$$

$$\text{Linear case} \quad \left\{ \begin{array}{l} \theta = A\tau + B \end{array} \right. \quad (10)$$

$$\left\{ \begin{array}{l} \theta = AEi \left(\frac{-\tau^2}{4K(t+B)} \right) + C \end{array} \right. \quad (12)$$

$$\text{Axially symmetrical case} \quad \left\{ \begin{array}{l} \theta = e^{-A^2 K t} \left[B J_0(A\tau) + C Y_0(A\tau) \right] + D \\ \theta = A \ln \tau + B. \end{array} \right. \quad (13)$$

(14)

* See additional paper (6)

$$(5)$$

Spherically $\left\{ \begin{array}{l} \theta = A \left[\frac{\sqrt{K(c+B)}}{r} e^{-\frac{4K(c+B)}{r^2}} - \frac{\sqrt{\pi}}{2} e^{+fc} \left(\frac{r}{2\sqrt{K(c+B)}} \right) \right] + C \\ \text{symmetrical} \quad \theta = \frac{e^{A^2 K t}}{r} \left[B e^{A r} + C e^{-A r} \right] + D \\ \text{case} \quad \theta = \frac{A}{r} + B \end{array} \right. \quad (15)$

of these we must discard the trivial solutions (11), (14) and (17); and also (12) and (16), which cannot be made to satisfy (4). (4) is, however, satisfied by (9), (12) and (15), and also by (10), if either B or C is zero.

Solution (10), which was mentioned by Stefan⁽¹⁾, defines a boundary of fusion moving with constant speed. It is of restricted interest. For example, consider the solution

$$\left. \begin{array}{l} \theta_1 = B \left[e^{-A(r-AK,t)} - 1 \right], \quad r \geq AK,t \\ \theta_2 = C \left[e^{\frac{K_1}{K_2} A(AK,t-r)} - 1 \right], \quad 0 \leq r \leq AK,t. \end{array} \right. \quad (18)$$

This describes the behaviour of a semi-infinite solid, whose initial temperature is $\theta_1 = B(e^{-At} - 1)$, and whose surface temperature at $r=0$ is $\theta_2 = C(e^{\frac{K_1}{K_2} At} - 1)$. However, B and C must, by (2), satisfy

$$k_2 C / k_1 - k_1 B / K_1 = L_P \quad (19)$$

(9), (12) and (15) define boundaries of fusion whose position varies linearly with the square root of the time, measured from an appropriate zero. Solutions based on (9) are, in fact, well-known,⁽²⁾ and correspond to problems of some importance. (12) and (15) also yield solutions of practical interest, which do not appear to have been studied.

(4)

1) Propagation of a Boundary of Fusion from a line source of heat

Let Q units of heat be generated per unit time, per unit length of the line $x=0$, in an infinite fusible solid, whose initial temperature is $- \Theta$, referred to the melting point as zero. A cylindrical boundary of fusion, $x = R(t)$ say, then advances into the solid. Let suffices 1, 2 refer to the solid and liquid phases respectively. We assume a solution:

$$\theta_1 = -AEi\left(-x^2/4K_1 t\right) - B \quad (20)$$

$$\theta_2 = -CEi\left(-x^2/4K_2 t\right) - D \quad (21)$$

whereupon

$$R(t) = \alpha \sqrt{t} \quad (22)$$

say, α a constant to be determined.

Then

$$AEi\left(-\alpha^2/4K_1 t\right) + B = 0 \quad (23)$$

$$CEi\left(-\alpha^2/4K_2 t\right) + D = 0 \quad (24)$$

When $t=0$, $R=0$, and $\theta_1 = -B$. Hence

$$B = \Theta \quad (25)$$

Also,

$$\frac{\partial \theta_1}{\partial x} = -\frac{2A}{x} e^{-x^2/4K_1 t}; \quad \frac{\partial \theta_2}{\partial x} = -\frac{2C}{x} e^{-x^2/4K_2 t} \quad (26)$$

Thus/

$$(26)$$

(5)

Thus $\lim_{\alpha \rightarrow 0} \left[-2\pi k_2 + \frac{\partial \theta_2}{\partial \alpha} \right] = 4\pi k_2 C$, so that

$$C = \frac{Q}{4\pi k_2}$$

(27)

Again, by (2), (22) and (26),

$$k_2 C e^{-\alpha^2/4K_2} - k_1 A e^{-\alpha^2/4K_1} = \frac{L \rho \alpha^2}{4} \quad (28)$$

where L, ρ are the latent heat and density of the material. (23), (24), (25), (27) and (28) determine A, B, C, D and α . Eliminating A, B, C, D , we have, for α :

$$\frac{Q}{4\pi} e^{-\alpha^2/4K_2} + \frac{k_1 @ e^{-\alpha^2/4K_1}}{Ei(-\alpha^2/4K_1)} = \frac{L \rho \alpha^2}{4} \quad (29)$$

The left side of (29) decreases monotonically from $Q/4\pi$ when $\alpha = 0$ to $-\infty$ when $\alpha = \infty$. Hence the equation has always one, and only one, real positive root. In terms of the root, the solution is:

$$\begin{aligned} \theta_2 &= \frac{Q}{4\pi k_2} \left[Ei(-\alpha^2/4K_2) - Ei(-\alpha^2/4K_2 t) \right], \quad 0 < t < \alpha \sqrt{t} \\ \theta_1 &= -@ \left[1 - \frac{Ei(-\alpha^2/4K_1 t)}{Ei(-\alpha^2/4K_1)} \right], \quad t > \alpha \sqrt{t} \end{aligned} \quad (30)$$

As an example, consider an ice-water system, for which
 Water: $k_2 = 0.00144 \text{ Cal/cm.sec.}^0 \text{ K.}$, $K_2 = 0.00144 \text{ cm}^2/\text{sec.}$
 Ice: $k_1 = 0.0053 \text{ Cal/cm.sec.}^0 \text{ K.}$, $K_1 = 0.0155 \text{ cm}^2/\text{sec.}$
 and $L \rho (\text{ice}) = 73.6 \text{ Cal/cm}^3$.

Suppose/

Suppose that $-B = -2$, and $Q = 2.00 \text{ Cal/cm.sec.}$, which represents approximately the heat supplied by a very thin wire, of resistance 1Ω , carrying a current of 1 amp. Then (39) yields

$$\alpha = 0.06637 \text{ cm/sec}^{\frac{1}{2}}.$$

$$\text{and } A = 1.681^\circ, B = 2^\circ, C = 131.7^\circ, D = 43.73^\circ.$$

The corresponding temperature profiles are shown in Table 1.

Table 1

α/\sqrt{t} (Cm/sec $^{\frac{1}{2}}$)	θ_2 ($^{\circ}\text{C}$)	θ_1 ($^{\circ}\text{C}$)
0.024	196.6	
0.3394	117.6	
0.4158	75.56	
0.4799	48.78	
0.5367	30.00	
0.5879	16.12	
0.6351	5.51	
0.6637	0	0
0.9248		-0.8196
1.128		-1.2362
1.302		-1.4780
1.456		-1.6312
1.783		-1.8319
2.059		-1.9178
2.302		-1.9581
2.523		-1.9781
2.724		-1.9883
2.905		-1.9936

In practice, since θ_2 rises indefinitely, a boundary of vaporisation must follow the boundary of fusion. The theory could be extended to cover this if the effect of pressure on the boiling point and latent heat were ignored. Although this is not legitimate in the case described, the solution will be included for its general interest. If suffix 3 refers to the vapour state, we assume in addition to (20), (21):

$$\theta_3 = -FEi\left(-\frac{\alpha^2}{4K_3}e\right) - C \quad (31)$$

Then the boundaries of vaporisation and fusion are $\tau_{12}\sqrt{e}$, $\tau_{23}\sqrt{e}$, say, whereupon (23) and (24) apply, and also:

$$CEi\left(-\frac{\alpha^2}{4K_2}e\right) + D = -\nabla \quad (32)$$

$$FEi\left(-\frac{\alpha^2}{4K_3}e\right) + G = -\nabla \quad (33)$$

where ∇ is the boiling point, referred to the melting point as zero. (25) holds as before, while F and K_3 must be substituted for C and K_2 in (27.). (28.) is replaced by two similar equations, involving L_{12} and L_{23} . We have thus eight relations to determine $A, B, C, D, F, G, \alpha_{12}, \alpha_{23}$. Elimination of the six coefficients leads to the following simultaneous

equations for α_{12}, α_{23} :

$$\frac{Q}{4\pi} e^{-\frac{\alpha^2_{23}}{4K_3}} - \frac{\frac{R_2 \nabla e}{4K_2}}{Ei\left(-\frac{\alpha^2_{12}}{4K_2}\right) - Ei\left(-\frac{\alpha^2_{23}}{4K_2}\right)} = \frac{L_{23} P}{4} \alpha_{23}^2 \quad (34)$$

$$\frac{\frac{R_2 \nabla e}{4K_2}}{Ei\left(-\frac{\alpha^2_{12}}{4K_2}\right) - Ei\left(-\frac{\alpha^2_{23}}{4K_2}\right)} + \frac{\frac{k_1 \Theta e}{4K_1}}{Ei\left(-\frac{\alpha^2_{12}}{4K_1}\right)} = \frac{L_{12} P}{4} \alpha_{12}^2 \quad (35)$$

These /

These could be solved cyclically in a numerical case. This has not been carried out for the system ice-water-steam, in view of the physically unreal assumptions:

Propagation from a point source.

Let Q units of heat be generated per unit time at $r = 0$, the conditions being otherwise as before. A spherical boundary $r = R(t)$ proceeds outward. We assume the solution:

$$\theta_1 = A \left[\frac{\sqrt{K_1 t}}{r} e^{-r^2/4K_1 t} - \frac{\sqrt{\pi}}{2} e^{+fc} \frac{r}{2\sqrt{K_1 t}} \right] - B \quad (36)$$

$$\theta_2 = C \left[\frac{\sqrt{K_2 t}}{r} e^{-r^2/4K_2 t} - \frac{\sqrt{\pi}}{2} e^{+fc} \frac{r}{2\sqrt{K_2 t}} \right] - D \quad (37)$$

Then

$$R(t) = \alpha \sqrt{t} \quad (38)$$

say, and

$$A \left[\frac{\sqrt{K_1}}{\alpha} e^{-\alpha^2/4K_1} - \frac{\sqrt{\pi}}{2} e^{+fc} \frac{\alpha}{2\sqrt{K_1}} \right] = B \quad (39)$$

$$C \left[\frac{\sqrt{K_2}}{\alpha} e^{-\alpha^2/4K_2} - \frac{\sqrt{\pi}}{2} e^{+fc} \frac{\alpha}{2\sqrt{K_2}} \right] = D \quad (40)$$

Also, as before,

$$B = 0, \quad (41)$$

while

$$\frac{\partial \theta_1}{\partial r} = - \frac{A \sqrt{K_1 t}}{r^2} e^{-r^2/4K_1 t}; \quad \frac{\partial \theta_2}{\partial r} = - \frac{C \sqrt{K_2 t}}{r^2} e^{-r^2/4K_2 t} \quad (42)$$

Thus,

(3)

$$\text{Thus } \lim_{t \rightarrow 0} \mathcal{L} \left[-4\pi k_2 x^2 \frac{\partial \theta_2}{\partial r} \right] = 4\pi k_2 \sqrt{k_2 t} \cdot C, \text{ so that}$$

$Q = q\sqrt{t}$, say, q constant, and

$$C = q / 4\pi k_2 \sqrt{k_2}$$

(15)

From (2), (39), (40), (42), (43), we obtain the following equation for α :

$$\frac{q}{4\pi} e^{-\alpha^2/4k_2} = \frac{k_1 \alpha \textcircled{H}}{1 - \frac{\alpha}{2\sqrt{\frac{\pi}{k_1}}} e^{\alpha^2/4k_1} e^{i\phi_c} \left(\frac{\alpha}{2\sqrt{k_1}} \right)} = \frac{i\rho \alpha^3}{2} \quad (44)$$

The left side again decreases monotonically from $q/4\pi$ to $-\infty$ as α increases from 0 to ∞ . Hence (44) has always one and only one real positive root. We have therefore derived a solution for propagation from a point source whose strength increases as \sqrt{t} .

The solution may be readily extended to cover the case in which two (or more) surfaces of phase - change arise. The analysis is similar to that indicated above for the cylindrical system.

Appendix.

Proof that the functions in (29) and (44) decrease monotonically for $\alpha > 0$.

Consider $f(\alpha) \equiv e^\alpha Ei(-\alpha)$

$$\frac{df}{d\alpha} = e^\alpha \left[Ei(-\alpha) + e^{-\alpha}/\alpha \right] \equiv e^\alpha g(\alpha) \text{ say.}$$

Then

$$\frac{dg}{d\alpha} = -e^{-\alpha}/\alpha^2 < 0$$

But when $\alpha = +\infty$, $g = 0$. Hence $g > 0$, and $\frac{dg}{d\alpha} > 0$. It/

It follows at once that the function on the left of (29) decreases monotonically. Its value is $\frac{Q}{4\pi}$ at 0 and $-\infty$ at ∞ .

Again, let $f(\alpha) = \frac{1}{\alpha} - \sqrt{\pi} e^{-\alpha^2} erfc(\alpha)$

$$\begin{aligned} \frac{df}{d\alpha} &= -\alpha e^{-\alpha^2} \left[2\sqrt{\pi} erfc(\alpha) - \frac{2}{\alpha} e^{-\alpha^2} + \frac{1}{\alpha^3} e^{-\alpha^2} \right] \\ &\equiv -\alpha e^{-\alpha^2} g(\alpha), \text{ say} \end{aligned}$$

$$\text{Then } \frac{dg}{d\alpha} = -3e^{-\alpha^2/\alpha^4} < 0. \quad \text{But } g(\infty) = 0$$

Hence $g > 0$ and so $\frac{df}{d\alpha} < 0$. It follows at once that the function on the left of (44) decreases monotonically. Its value is $\frac{Q}{4\pi}$ at 0 and $-\infty$ at ∞ .

References.

- (1) Stefan, Wied. Ann. 41, 725(1890); 42, 269(1891).
- (2) Carslaw and Jaeger. Conduction of Heat in Solids. Oxford 1947, pp. 71, 227.

(8.)

RAPIDLY CONVERGENT SERIES FOR

$$\sum_{n=1}^{\infty} n^{2r} e^{-nx}, \quad t \text{ INTEGRAL AND } 0 < x \leq 1.$$

RAPIDLY CONVERGENT SERIES FOR $\sum_{n=1}^{\infty} n^{2r} e^{-n^2 x}$, r
INTEGRAL AND $0 < x \leq 1$.

Consider the series

$$S_{2r}(x) \equiv \sum_{n=1}^{\infty} n^{2r} e^{-n^2 x}, \quad (1)$$

where r is zero or a positive or negative integer. $S_{2r}(x)$ is a convergent series of positive terms for all x, r . The convergence is rapid if x is large, but may become very slow when x is small. It is the object of this note to derive alternative series for $S_{2r}(x)$, which shall converge rapidly for small x .

Let $\bar{S}_{2r}(p) \equiv \int_0^\infty e^{-px} S_{2r}(x) dx$ be the Laplace transform of $S_{2r}(x)$. Then, in particular,

$$\bar{S}_0 = \sum_1^{\infty} \int_0^\infty e^{-(p+n^2)x} dx = \sum_1^{\infty} \frac{1}{p+n^2}, \quad (2)$$

since the terms are all positive and the resultant series converges.

Writing $p \equiv q^2$, we have, then,

$$\bar{S}_0 = \frac{\pi}{2q} \coth(\pi q) - \frac{1}{2q^2} \quad (3)$$

$$= -\frac{1}{2q^2} + \frac{\pi}{2q} + \pi \sum_{m=1}^{\infty} \frac{e^{-2m\pi q}}{q}. \quad (4)$$

The inverse transforms of the terms in (4) are familiar, leading at once to

$$S_0(x) \equiv \sum_1^{\infty} e^{-n^2 x} = -\frac{1}{2} + \frac{1}{2} \sqrt{\frac{\pi}{x}} + \sqrt{\frac{\pi}{x}} \sum_1^{\infty} e^{-n^2 \pi^2 / x}. \quad (5)$$

(5) is a special case of Poisson's Identity. Its rate of convergence is extremely rapid when x is small. Thus, for $0 < x \leq 1$, the series terms on the right are negligible, and

$$\sum_1^{\infty} e^{-n^2 x} \doteq \frac{1}{2} (\sqrt{\frac{\pi}{x}} - 1), \quad (6)$$

to better than 1 part in 10,000. (6) may be written

$$\sum_{r=1}^{\infty} y^{-r^2} = \frac{1}{2} \left(\sqrt{\pi / \ln \frac{1}{y}} - 1 \right), \quad 1 > y \geq e^{-1}, \quad (7)$$

whence

$$\lim_{y \rightarrow 1^-} (1-y)^{\frac{1}{2}} \sum_{r=1}^{\infty} y^{-r^2} = \frac{\sqrt{\pi}}{2}. \quad (8)*$$

Let, now,

$$\Phi_{-r}(z) \equiv \frac{2}{\sqrt{\pi}} \int_z^{\infty} \int_z^{\infty} \cdots \int_z^{\infty} e^{-z^2} (dz)^{r+1}, \quad r \geq -1,$$

so that

$$\Phi_1(z) \equiv \frac{2}{\sqrt{\pi}} e^{-z^2},$$

and

$$\Phi_0(z) \equiv \frac{2}{\sqrt{\pi}} \int_z^{\infty} e^{-z^2} dz \equiv 1 - \text{erf}(z) \equiv \text{erfc}(z).$$

Then, (5) can be written

$$S_o(x) = \frac{1}{2} \left(\sqrt{\frac{\pi}{x}} - 1 \right) + \frac{\pi}{2\sqrt{x}} \sum_{r=1}^{\infty} \Phi_r \left(\frac{n\pi}{\sqrt{x}} \right). \quad (9)$$

†

However, the following recurrence formula can be established by induction

$$2r \Phi_{-r}(z) = -2z \Phi_{-(r-1)}(z) + \Phi_{-(r-2)}(z), \quad (10)$$

whereupon

$$\begin{aligned} (2\sqrt{x})^{r-2} \Phi_{-(r-2)}(n\pi/\sqrt{x}) &= 2^r \left\{ \frac{r}{2} x^{\frac{r}{2}-1} \Phi_{-r}(n\pi/\sqrt{x}) + \frac{n\pi}{2} x^{\frac{r}{2}-\frac{3}{2}} \Phi_{-(r-1)}(n\pi/\sqrt{x}) \right\} \\ &= \frac{d}{dx} (2\sqrt{x})^r \Phi_{-r}(n\pi/\sqrt{x}). \end{aligned} \quad (11)$$

Thus, for example,

$$\frac{1}{2\sqrt{x}} \Phi_1 \left(\frac{n\pi}{\sqrt{x}} \right) = \frac{d}{dx} 2\sqrt{x} \Phi_{-1} \left(\frac{n\pi}{\sqrt{x}} \right). \quad (12)$$

Then integration of (9) from x to ∞ , which is legitimate, since all the terms are positive, and the resultant series convergent, gives

$$S_{-2}(x) = \frac{\pi^2}{6} - \sqrt{\pi x} + \frac{x}{2} - \pi(2\sqrt{x}) \sum_{r=1}^{\infty} \Phi_{-r} \left(\frac{n\pi}{\sqrt{x}} \right). \quad (13)$$

A second integration leads to

$$S_{-4}(x) = \frac{\pi^4}{90} - \frac{\pi^2 x}{6} + \frac{2\sqrt{\pi} x^{3/2}}{3} - \frac{x^2}{4} + \pi(2\sqrt{x}) \sum_{r=1}^{\infty} \Phi_{-r} \left(\frac{n\pi}{\sqrt{x}} \right), \quad (14)$$

and in general ($r \geq 0$)

$$\begin{aligned} S_{-2r}(x) &= 2^{2r-1} \pi^{2r} \left[\frac{B_r}{2r!} - \frac{B_{2r-1} x^{r-\frac{1}{2}}}{4\pi^2 (2r-2)!} + \dots + (-1)^{r-1} \frac{B_r x^{r-1}}{(4\pi^2)^{r-1} (2r-1)!} \right] \\ &\quad + (-1)^r \sqrt{\pi} \frac{2^{2r-1} (x)^{r-\frac{1}{2}}}{(2r)!} + (-1)^{r-1} \frac{x^r}{2r!} \\ &\quad + (-1)^{r+1} \pi (2\sqrt{x})^{2r-1} \sum_{n=1}^{\infty} \Phi_{-(2r-n)} \left(\frac{n\pi}{\sqrt{x}} \right), \quad (15) \end{aligned}$$

where B_r is the r^{th} Bernoulli number.

For example, take $r = 2$, and $x = 1$. Then

$S_{-4}(1) \doteq e^{-1} + e^{-4}/16 = 0.3690$ to four places, while the right side of (14) is

$$\begin{aligned} 1.0823 - 1.6449 + 1.1816 - 0.2500 + 8\pi \sum_{n=1}^{\infty} \Phi_{-3} (n\pi) \\ = 0.3690 + 8\pi \sum_{n=1}^{\infty} \Phi_{-3}. \end{aligned}$$

Thus, even when $x = 1$ the Φ -series is negligible. The advantage of (14) is realised, of course, only for smaller values of x .

The importance of $\pi (2\sqrt{x})^{2r-1} \sum \Phi_{-(2r-n)}$ can be judged by expanding

$\Phi_{-(2r-n)}(\pi/\sqrt{x})$ in descending powers of $\frac{\pi}{\sqrt{x}}$: the first term is then $\frac{2}{\sqrt{\pi}} e^{-\pi^2/x} / 2^{2r} (\pi^2/x)^r$,

so that $\pi (2\sqrt{x})^{2r-1} \sum \Phi$ is of the order of

$$(x/\pi)^{2r-\frac{1}{2}} \cdot e^{-\pi^2/x}$$

which is always negligible for $0 < x \leq 1$.

(9) may also be differentiated repeatedly with respect to x . Let

$$(-1)^{r-1} \Phi_r(x) \equiv \frac{2}{\sqrt{\pi}} \frac{d^{r-1}}{dx^{r-1}} e^{-x^2}, \quad r \geq 1.$$

Then, by (11), for $r \geq 1$,

$$\frac{1}{(2\sqrt{x})^r} \Phi_r \left(\frac{n\pi}{\sqrt{x}} \right) = \frac{d}{dx} \left[\frac{1}{(2\sqrt{x})^{r-2}} \cdot \Phi_{r-2} \left(\frac{n\pi}{\sqrt{x}} \right) \right], \quad (16)$$

and finally

$$\frac{1}{(2\sqrt{x})^{2r+1}} \Phi_{2r+1} \left(\frac{n\pi}{\sqrt{x}} \right) = \frac{d^r}{dx^r} \left[\frac{1}{2\sqrt{x}} \cdot \Phi_1 \left(\frac{n\pi}{\sqrt{x}} \right) \right]. \quad (17)$$

Hence ($r \geq 1$)

$$S_{2r} = \frac{(2r\sqrt{\pi})}{12r(2\sqrt{x})^{2r+1}} + \frac{(-1)^r \cdot 2\sqrt{\pi}}{(2\sqrt{x})^{2r+1}} \sum_{n=1}^{\infty} \left[\frac{d^{2r}}{dz^{2r}} e^{-z^2} \right]_{z=\frac{n\pi}{\sqrt{x}}} , \quad (18)$$

which may be written:

$$S_{2r} = \frac{\sqrt{\pi}}{2^r \cdot 2^{r+\frac{1}{2}}} \left[\frac{12r}{12 \cdot 2^{r+1}} + (-1)^r \sum_{n=1}^{\infty} e^{-\frac{n^2\pi^2}{2x}} D_{2r}(n\pi\sqrt{\frac{2}{x}}) \right] \quad (19)$$

where D is Weber's parabolic cylinder function.

Since the first term in the asymptotic expansion of $D_{2r}(z)$ is $\tilde{e}^{z^2/4} z^{2r}$, the ratio of the series in (19) to the remaining term is of order

$$\frac{24r}{12r} \cdot \left(\frac{4\pi^2}{x}\right)^r \cdot e^{-\pi^2/x} .$$

This is of the order of 10^{-4} or smaller, provided

$$(\pi^2/x)^r e^{-\pi^2/x} \leq e^{-\pi^2} , \quad (20)$$

which is equivalent to

$$r \leq \pi^2 \left(\frac{1}{x} - 1\right) / \ln \frac{\pi^2}{x} . \quad (21)$$

Evaluating (21) for r in terms of x , we conclude that

$$S_{2r} = \frac{\sqrt{\pi} (2r)}{12r (4x)^{r+\frac{1}{2}}} , \quad r \geq 1 , \quad (22)$$

to better than 1 in 10,000, provided

$$x \leq 0.7 \quad 0.62 \quad 0.52 \quad 0.45 \quad 0.38 \quad 0.32 \quad 0.28$$

$$\text{when } r = 1 \quad 2 \quad 3 \quad 4 \quad 5 \quad 6 \quad 7$$

$$x \leq 0.25 \quad 0.22 \quad 0.20 \quad 0.18 \quad 0.16 \quad 0.15$$

$$\text{when } r = 8 \quad 9 \quad 10 \quad 11 \quad 12 \quad 13 , \quad \text{etc.}$$

Since we have neglected the factor $2^{2r+1}/12r$, which decreases with rising r , the range is actually somewhat wider for the larger values of r .

Example: $r = 4$, $x = 0.4$.

$$\sum_{n=1}^{\infty} n^4 e^{-0.4n^2} \doteq 359.2 \quad \text{from the first 6 terms}$$

$$S_{\infty}(0.4) \doteq 359.2 \quad \text{from (22)}$$

By writing y for $\pi\sqrt{x}$ in the above relations, we obtain a corresponding set of approximate expressions for $\sum_{n=1}^{\infty} \frac{\Phi}{2r+1}(ny)$, $r = 0, \pm 1, \pm 2, \dots$, when

$y \geq 10$. For example, from (13),

$$\sum_{r=1}^{\infty} \Phi_{-1}(ny) \doteq \frac{y}{12} - \frac{1}{2\sqrt{y}} + \frac{1}{4y} , \quad (23)$$

and from (18),

$$\sum_{r=1}^{\infty} \Phi_{2r+1}(ny) \doteq (-1)^{r+1} \frac{(2r)}{\sqrt{\pi} Lx} , \quad r \geq 1 , \quad (24)$$

which is independent of y (≥ 10), and for $r=1$ gives

$$\sum_{z=1}^{\infty} e^{-\frac{n^2 z^2}{4}} D_z(nz) \doteq \frac{1}{2} , \quad z > 14 . \quad (25)$$

* Bromwich. Theory of Infinite Series. 2nd Ed. p. 150.

† Hartree. Mem. Proc. Manchester Lit. Phil. Soc. 80, 85 (1936).

(9.)

SERIES EXPANSION

OF A CLASS OF INTEGRALS.

SERIES EXPANSION OF A CLASS OF INTEGRALS.

(1)
It was shown by Weber that, if $\mu > 0$, and $f(x, y, z)$ satisfies the equation

$$\nabla^2 f \equiv \frac{\partial^2 f}{\partial x^2} + \frac{\partial^2 f}{\partial y^2} + \frac{\partial^2 f}{\partial z^2} = \lambda f, \quad (1)$$

then

$$I \equiv \int_{-\infty}^{\infty} \int_{-\infty}^{\infty} \int_{-\infty}^{\infty} f(\alpha, \beta, \gamma) e^{-\frac{(x-\alpha)^2 + (y-\beta)^2 + (z-\gamma)^2}{4\mu}} d\alpha d\beta d\gamma$$

$$is = 8(\pi\mu)^{3/2} e^{\lambda\mu} f(x, y, z). \quad (2)$$

In the present note, we derive a more general expression for the integral I , applicable when (1) is not satisfied.

Linear Case.

$$I \equiv \int_{-\infty}^{\infty} f(\alpha) e^{-\frac{(x-\alpha)^2}{4\mu}} d\alpha. \quad (3)$$

Substitute $\alpha = x + \xi\sqrt{4\mu}$ and expand the integrand in powers of ξ , integrating term by term. Then, since for $r=0, 1, 2, \dots$

$$\int_{-\infty}^{\infty} \xi^{2r} e^{-\xi^2} d\xi = \frac{(2r)\sqrt{\pi}}{2^{2r} r!}; \quad \int_{-\infty}^{\infty} \xi^{2r+1} e^{-\xi^2} d\xi = 0, \quad (4)$$

we have

$$I = 2\sqrt{\pi\mu} \sum_{r=0}^{n-1} \frac{\mu^r}{r!} f^{(2r)}(\alpha) + R_n, \quad (5)$$

where/

(2)

where

$$R_{2n} \equiv \sqrt{\pi} \frac{(4\mu)^n}{[2n]} \int_{-\infty}^{\infty} \xi^{2n} f^{(2n)}(x + p \cdot 2\sqrt{\mu} \cdot \xi) e^{-\xi^2} d\xi, \quad (6)$$

and $0 < p < 1$. Hence, provided $R_{2n} \rightarrow 0$ as $n \rightarrow \infty$,

$$I = 2\sqrt{\pi\mu} \sum_{n=0}^{\infty} \frac{\mu^n}{[n]} f^{(2n)}(x). \quad (7)$$

In particular, if $f''(x) = \lambda f(x)$, then $f^{(2n)}(x) = \lambda^n f(x)$, and so

$$I = 2\sqrt{\pi\mu} e^{\lambda\mu} f(x), \quad (8)$$

the linear case of Weber's theorem. As another example, suppose f satisfies the diffusion equation:-

$$f_{xx}(x,t) = \lambda f_t(x,t). \quad (9)$$

Then,

$$\frac{\partial^{2n} f}{\partial x^{2n}} = \lambda^n \frac{\partial^n f}{\partial t^n}, \quad (10)$$

and so, by (7),

$$\int_{-\infty}^{\infty} f(x,t) e^{-\frac{(x-\alpha)^2}{4\mu}} d\alpha = 2\sqrt{\pi\mu} f(x, t + \lambda\mu), \quad (11)$$

which is a familiar result. Again, let f satisfy the wave equation:-

$$f_{xx} = \lambda^2 f_{tt}, \quad (12)$$

so that

$$\frac{\partial^{2n} f}{\partial x^{2n}} = \lambda^{2n} \frac{\partial^{2n} f}{\partial t^{2n}}. \quad (13)$$

Then/

(3)

Then

$$\int_{-\infty}^{\infty} f(x,t) e^{-\frac{(x-\alpha)^2}{4\mu}} d\alpha = 2\sqrt{\pi\mu} \sum_{n=0}^{\infty} \frac{\mu^n \lambda^{2n}}{n!} \frac{\partial^{2n} f(x,t)}{\partial t^{2n}} \quad (14)$$

$$= \frac{1}{\lambda} \int_{-\infty}^{\infty} f(x,\tau) e^{-\frac{(t-\tau)^2}{4\mu\lambda^2}} d\tau. \quad (15)$$

(15) may be exhibited in a more symmetrical form, without any real loss in generality, by setting $\lambda = 1 = \mu$, whereupon

$$\int_{-\infty}^{\infty} f(x,t) e^{-\frac{(x-\alpha)^2}{4}} d\alpha = \int_{-\infty}^{\infty} f(x,\tau) e^{-\frac{(t-\tau)^2}{4}} d\tau. \quad (16)$$

(16) can be readily verified from the fact that, when $\lambda = 1$, f must have the form

$$f(x,t) = \varphi(x+t) + \psi(x-t).$$

If $f(x)$ is a repeated derivative or integral of the error function, (7) may be summed, leading to a useful series of results. Thus, define

$$\bar{\Phi}_o(x) \equiv \text{erfc}(x) \equiv \frac{2}{\sqrt{\pi}} \int_x^{\infty} e^{-x^2} dx \quad (17)$$

$$\begin{aligned} \bar{\Phi}_r(x) &\equiv (-i)^r \frac{d^r}{dx^r} \bar{\Phi}_o(x) && r = \\ \bar{\Phi}_{-r}(x) &\equiv \left(\int_x^{\infty} \right)^r \bar{\Phi}_o(x) (dx)^r && 1, 2, 3, \dots \end{aligned} \quad (18)$$

Then, if $s = 0, \pm 1, \pm 2, \dots$, and $\bar{\Psi}_s(x) \equiv \left(\frac{x}{2}\right)^s \bar{\Phi}_s(x)$, it may be verified that

$$\bar{\Psi}_{s+2}(x) = \frac{d}{dx} \bar{\Psi}_s(x), \quad (19)$$

where/

(4)

where $Z = x^{-2}$. Hence,

$$\Psi_{s+2n}(x) = \frac{d^n}{dz^n} \Psi_s(x) . \quad (20)$$

From (18) and (20) we then deduce

$$\frac{d^{2n}}{dx^{2n}} \Phi_s(x) = \left(\frac{2}{x}\right)^{s+2n} \frac{d^n}{dz^n} \Psi_s(x) . \quad (21)$$

Then, by (7),

$$\int_{-\infty}^{\infty} \Phi_s(x) e^{-\frac{(x-\alpha)^2}{4\mu}} d\alpha = 2\sqrt{\pi\mu} \left(\frac{2}{x}\right)^s \sum_{n=0}^{\infty} \frac{(4\mu x)^n}{(n)} \frac{d^n}{dz^n} \Psi_s(x) ,$$

which is a Taylor series, yielding

$$\int_{-\infty}^{\infty} \Phi_s(x) e^{-\frac{(x-\alpha)^2}{4\mu}} d\alpha = \frac{2\sqrt{\pi\mu}}{(1+4\mu)^{s/2}} \cdot \Phi_s\left(\frac{x}{\sqrt{1+4\mu}}\right) , \quad (22)$$

where $s = 0, \pm 1, \pm 2, \dots$.

(7) is also particularly convenient if f is a polynomial.

Conditions for validity of (7)

The above treatment is purely formal. It is legitimate, provided

(a) I exists, and

(b) $R_{2n} \rightarrow 0$, as $n \rightarrow \infty$.

The convergence of the series Σ in (7) does not necessarily guarantee that $R_{2n} \rightarrow 0$; although in general this may be safely assumed. Of course, if Σ is uniformly convergent for all x , it converges to I . But this condition is not necessary, as is shown by the example $f(x) = e^{kx}$ for which it does not hold, although $R_{2n} \rightarrow 0$. The following theorem covers many cases of the above type.

If/

(5)

If $f^{(2n)}(y) < A^{2n}(C + Be^{qy^2})$ for all y and $n > m$, where A, B, C, q are independent of y and n , and $q < \frac{1}{4\mu}$, then $R_{2n} \rightarrow 0$. The proof is somewhat tedious but straightforward.

General Case.

Let $f(\rho)$ be any scalar point function, and let $d\rho$ be an element of space at the point ρ . Then if z is any fixed point,

$$I \equiv \int f(\rho) e^{-\frac{(z-\rho)^2}{4\mu}} d\rho = 8(4\mu)^{3/2} \sum_0^\infty \frac{\mu^n}{(2n)!} \nabla^{2n} f(z), \quad (23)$$

where the integral is taken throughout the whole of space. (23) generalises Weber's result, and may be proved formally as follows. In terms of rectangular Cartesians, the integral I is

$$I \equiv \int_{-\infty}^{\infty} \int_{-\infty}^{\infty} \int_{-\infty}^{\infty} f(x, \beta, \gamma) e^{-\frac{\Sigma(x-\alpha)^2}{4\mu}} d\alpha d\beta d\gamma.$$

If we substitute $\alpha \equiv x + \xi \sqrt{4\mu}$, $\beta \equiv y + \eta \sqrt{4\mu}$, $\gamma \equiv z + \zeta \sqrt{4\mu}$, and expand the integrand in powers of ξ, η, ζ , we obtain

$$I = (4\mu)^{3/2} \sum_0^\infty I_{2n}, \quad (24)$$

where

$$I_{2n} \equiv \frac{(4\mu)^n}{(2n)!} \int_{-\infty}^{\infty} \int_{-\infty}^{\infty} \int_{-\infty}^{\infty} e^{-\Sigma \xi^2} \left(\xi \frac{\partial}{\partial x} + \eta \frac{\partial}{\partial y} + \zeta \frac{\partial}{\partial z} \right)^{2n} f(x, y, z) d\xi d\eta d\zeta, \quad (25)$$

all odd powers of $(\Sigma \xi \frac{\partial}{\partial x})$ being discarded at once in virtue of equation (4).

$(\Sigma \xi \frac{\partial}{\partial x})^{2n} f$ may now be expanded, retaining only terms containing even/

(6)

even powers of ξ , η and ζ . The coefficient of $\xi^{2p} \eta^{2q} \zeta^{2r}$ is

$$\frac{\ln}{12p 12q 12r} \cdot \frac{\partial^{2n} f}{\partial x^{2p} \partial y^{2q} \partial z^{2r}} ,$$

and the corresponding integral is, by (4),

$$\iiint_{-\infty}^{\infty} e^{-\Sigma \xi^2} \xi^{2p} \eta^{2q} \zeta^{2r} d\xi d\eta d\zeta = \pi^{\frac{3}{2}} \frac{12p 12q 12r}{2^{2n} 12p 12q 12r} . \quad (26)$$

Consequently,

$$\begin{aligned} I_{2n} &= \frac{\pi^{\frac{3}{2}\mu^n}}{\ln} \sum_{p,q,r} \frac{\ln}{12p 12q 12r} \cdot \frac{\partial^{2n} f}{\partial x^{2p} \partial y^{2q} \partial z^{2r}} \\ &= \frac{\pi^{\frac{3}{2}\mu^n}}{\ln} \nabla^{2n} f(x, y, z) , \end{aligned} \quad (27)$$

and (23) follows at once.

If $\nabla^2 f = \lambda f$, (23) shows that

$$I = 8(\pi\mu)^{\frac{3}{2}} e^{\lambda\mu} f(x, y, z) , \quad (28)$$

which is Weber's result (2). Again, if $\nabla^2 f = \lambda \partial f / \partial t$,

$$I = 8(\pi\mu)^{\frac{3}{2}} f(x, y, z, t + \lambda\mu) , \quad (29)$$

while, if $\nabla^2 f = \lambda^2 \partial^2 f / \partial t^2$,

$$I = 8(\pi\mu)^{\frac{3}{2}} \sum_0^{\infty} \frac{\mu^n \lambda^{2n}}{\ln} \frac{\partial^{2n} f}{\partial t^{2n}} = \frac{4\pi\mu}{\lambda} \int_{-\infty}^{\infty} f(x, y, z, \tau) e^{-\frac{(t-\tau)^2}{4\mu\lambda^2}} d\tau , \quad (30)$$

a relation which is somewhat less obvious than (15). No generality is lost by setting $\lambda = 1 = \mu$, whereupon

$$\iiint_{-\infty}^{\infty} f(x, y, z, t) e^{-\Sigma(x-\alpha)^2} d\alpha d\beta d\gamma = 4\pi \int_{-\infty}^{\infty} f(x, y, z, \tau) e^{-(t-\tau)^2} d\tau . \quad (31)$$

Conditions/

(7)

Conditions for validity of (23).

(23) will in all normal cases hold, if the series converges; but a rigorous proof in any particular instance must depend upon examination of R_{z_n} . It may be proved that a sufficient condition is

$$\left| \frac{\partial^m f}{\partial x^a \partial y^b \partial z^c} \right| < A^m (\beta + C e^{q^m x^2})$$

for all x, y, z and $m > n$, where $q < 1/4\mu$ and A, β, C, q are independent of n, a, b, c .

REFERENCE

- (1) Crelle's J. 49.

One dimensional Flow behind a Steady Plane Detonation

ACCORDING to the accepted theory of plane detonation, the equilibrium reaction products have a well defined initial forward velocity W_1 which together with their acoustic velocity a_1 and the velocity D of the wave itself satisfy the Chapman-Jouguet (CJ) relation

$$W_1 + a_1 = D \quad \dots(1)$$

Considerations of momentum show¹ that the products must subsequently decelerate. The steady reaction zone is therefore followed by a rarefaction which will become less steep with time. The structure of this rarefaction has been analysed by TAYLOR² and PFRIEM³. If detonation is initiated at $x = 0$, $t = 0$, and moves with constant velocity D , the flow is defined by

$$x = (W + a)t \quad \dots(2)$$

$$\text{where } W_1 - W = \int_{\varrho}^{\varrho_1} a \frac{d\varrho}{\varrho} \quad \dots(3)$$

and ϱ is the density corresponding to W . Equation 3 is to be supplemented by the adiabatic relation. In particular, if this has the form

$$p = \text{constant} \times \varrho^\gamma \quad \dots(4)$$

equation 2 becomes

$$\frac{W}{W_1} = 1 - \frac{2D}{(\gamma + 1)W_1} \left(1 - \frac{x}{Dt} \right) \quad \dots(5)$$

In the present note we are concerned with the motion of a typical material element, in other words with the 'Lagrangian' solution. This is defined by

$$\frac{dW}{dt} = \frac{\partial W}{\partial t} + W \frac{\partial W}{\partial x} \quad \dots(6)$$

which by equation 5 reduces to

$$t \frac{dW}{dt} = \frac{\gamma - 1}{\gamma + 1} (W_1 - W) - \frac{2a_1}{\gamma + 1} \quad \dots(7)$$

Integration of equation 7 gives

$$\frac{dx}{dt} = W = W_1 - \frac{2a_1}{\gamma - 1} \left[1 - \left(\frac{t_0}{t} \right)^{\gamma - 1} \right] \quad \dots(8)$$

where t_0 is the instant at which the chosen element traverses the CJ plane. A second integration yields

$$\frac{x}{Dt_0} = \left(1 - \frac{\gamma - 1}{\gamma + 1} \frac{a_1}{D} \right) \frac{t}{t_0} + \frac{\gamma - 1}{\gamma + 1} \frac{a_1}{D} \left(\frac{t}{t_0} \right)^{2/\gamma + 1} \quad \dots(9)$$

which is the required particle path. According to equations 8 and 9, the particle decelerates and reverses its direction of motion at (x', t') where

$$\frac{t'}{t_0} = \left(1 - \frac{\gamma - 1}{2} \frac{W_1}{a_1}\right)^{-\frac{(\gamma+1)}{\gamma-1}} \quad \dots \quad (10)$$

$$\frac{x'}{Dt_0} = \frac{a_1}{D} \left(1 - \frac{\gamma - 1}{2} \frac{W_1}{a_1}\right)^{-2/\gamma-1} \quad \dots \quad (11)$$

The locus of turning-points in the (x, t) plane is thus a straight line

$$\frac{x'}{Dt} = 1 - \frac{\gamma + 1}{2D} W_1 \quad \dots \quad (12)$$

as is otherwise obvious from equation 5.

If we use the well known approximations

$$W_1 \doteq \frac{D}{\gamma + 1} \doteq \frac{a_1}{\gamma} \quad \dots \quad (13)$$

and write $\nu \equiv (\gamma - 1)/(\gamma + 1)$, these results become

$$\nu \frac{W}{W_1} \doteq (1 + \nu) \left(\frac{t}{t_0}\right)^{-\nu} - 1 \quad \dots \quad (14)$$

$$2\nu \frac{x}{Dt_0} \doteq (1 + \nu) \left(\frac{t}{t_0}\right)^{1-\nu} - (1 - \nu) \frac{t}{t_0} \quad \dots \quad (15)$$

$$\frac{2x'}{Dt_0} \doteq \frac{t'}{t_0} \doteq (1 + \nu)^{\frac{1}{\nu}} \quad \dots \quad (16)$$

which in turn for almost isothermal conditions ($\nu \sim 0$) approach

$$\frac{W}{W_1} = 1 - \ln \frac{t}{t_0} \quad \dots \quad (17)$$

$$\frac{2x}{Dt_0} = \frac{t}{t_0} \left(2 - \ln \frac{t}{t_0}\right) \quad \dots \quad (18)$$

$$\frac{2x'}{Dt_0} = \frac{t'}{t_0} = e = 2.718 \dots \quad \dots \quad (19)$$

If motion is prevented at $x = 0$, for example by enclosing the explosive in a tube rigidly sealed at the plane of initiation, the particle remains at rest after reaching x' . If the tube is open, equations 8 and 9 continue to apply while the particle returns through its initial position Dt_0 and ultimately passes out at the open end.

Wave speed photographs of detonating gases frequently contain, in addition to the straight edge which indicates the steady velocity of the wave front, a

family of curved lines corresponding to much lower velocities and generally taken to define the movement of the luminous products⁴. An unusually fine example, due to BONE and FRASER⁵, is reproduced in Figure 1a. The locus of turning-points on the curved paths is, in fact, a straight line of which the slope is one half that of the wave trace as predicted by equation 16. The comparison can, however, be carried further by using equation 15 and assigning a value to γ : Figure 1b was drawn in this way with $\gamma = 1.2$ (a probable value). The theory is well confirmed, since the two figures may be almost exactly superimposed.

S. PATERSON

*Imperial Chemical Industries Ltd
Nobel Division, Research Dept
Stevenston, Ayrshire*

(Received December 1949)

REFERENCES

- ¹ LANGWEILER, H. *Z. tech. Phys.* 19 (1938) 271
- ² TAYLOR, G. I. Unpublished paper, 1941
Proc. roy. Soc. A 200 (1950) 235
- ³ PFRIEM, H. *Forsch. IngWes.* 12 (1941) 143
- ⁴ LEWIS, B. and FRAUENFELD, J. B. *J. Amer. chem. Soc.* 52 (1930) 3905
- ⁵ BONE, W. A. and FRASER, R. P. *Phil. Trans. roy. Soc., Lond. A* 230 (1931) Plate 17, No. 18

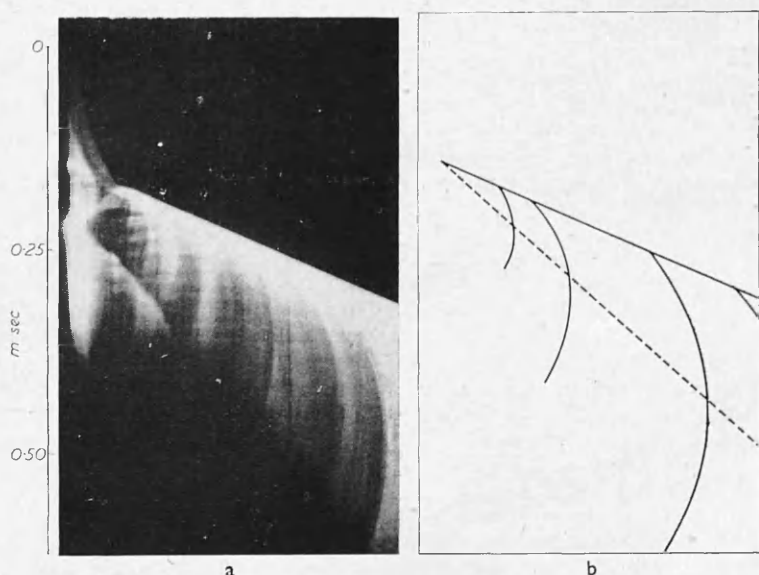


Figure 1. Flow behind a steady plane detonation in a gaseous explosive. a Moving-film photograph by BONE and FRASER⁵ of initiation of detonation in $C_2H_2 + O_2$. (By permission of Royal Society) b Theoretical trace, according to equation 15 with $\nu = t/t_0$ when $\gamma = 1.2$

Reprinted from QUARTERLY OF APPLIED MATHEMATICS
Vol. IV, No. 3, October, 1946

ON CERTAIN INTEGRALS IN THE THEORY OF HEAT CONDUCTION*

By STEWART PATERSON (*I.C.I. (Explosives) Limited, Stevenston, Scotland*)

In a recent note¹ W. Horenstein evaluates the integrals

$$\phi \equiv \int_0^t x^{-3/2} \exp\left(-\frac{a^2}{x} - b^2 x\right) dx, \quad (1)$$

$$\psi \equiv \int_0^t x^{-1/2} \exp\left(-\frac{a^2}{x} - b^2 x\right) dx, \quad (2)$$

in terms of the tabulated exponential and error functions. The evaluation of the more general integral, viz.

$$\int_k^t \exp(-s^2 - n^2/s^2) ds$$

from which ϕ and ψ are easily derived, was given by Riemann.²

Integrals of the above type arise in the solution by classical methods of various heat conduction problems. It is the purpose of this note to point out that treatment of many such problems by the Heaviside "operational" or equivalent Laplace transform method leads directly and naturally to the required solution in tabulated functions.

Thus, to take a simple case, the classical solution of

$$\frac{\partial \theta}{\partial t} = \frac{1}{4} \frac{\partial^2 \theta}{\partial a^2} - b^2 \theta; \quad \theta \rightarrow 0, t \rightarrow 0, \theta \rightarrow 1, a \rightarrow 0 +, \quad (3)$$

* Received Nov. 24, 1945.

¹ W. Horenstein, Quart. Appl. Math. 3, 183-184 (1945).

² B. Riemann, *Partielle Differentialgleichungen*, 2nd ed., 1876, p. 173.

(where θ is a function of a and t) will be

$$\theta = a\pi^{-1/2}\phi.$$

If, however,

$$\bar{\theta}(a, p) \equiv \int_0^\infty e^{-pt}\theta(a, t)dt,$$

equations (3) transform into

$$\frac{\partial^2 \bar{\theta}}{\partial a^2} = 4(p + b^2)\bar{\theta}; \quad \bar{\theta} \rightarrow \frac{1}{p}, \quad a \rightarrow 0 + \quad (4)$$

which lead at once to

$$\bar{\theta} = p^{-1} \exp [-2a\sqrt{(p + b^2)}]. \quad (5)$$

The inversion theorem for the Laplace transform then gives

$$\theta = \frac{1}{2\pi i} \int_{\gamma-i\infty}^{\gamma+i\infty} \lambda^{-1} \exp [\lambda t - 2a\sqrt{(\lambda + b^2)}] d\lambda, \quad (6)$$

along the usual contour.

By a series of obvious and natural steps,³ it is easy to show that this is equal to

$$\begin{aligned} & \frac{e^{2ab}}{4\pi i} \int_{\gamma'-i\infty}^{\gamma'+i\infty} \lambda^{-1} \exp [\lambda t - 2(a + bt)\sqrt{\lambda}] d\lambda + \frac{e^{-2ab}}{4\pi i} \int_{\gamma''-i\infty}^{\gamma''+i\infty} \lambda^{-1} \exp [\lambda t - 2(a - bt)\sqrt{\lambda}] d\lambda, \\ &= \frac{e^{2ab}}{2} \left[1 - \operatorname{erf} \left(\frac{a}{\sqrt{t}} + b\sqrt{t} \right) \right] + \frac{e^{-2ab}}{2} \left[1 - \operatorname{erf} \left(\frac{a}{\sqrt{t}} - b\sqrt{t} \right) \right], \end{aligned}$$

and it can be verified that this satisfies (3).

³ H. Jeffreys, *Operational methods in mathematical physics*, Cambridge, 1931, p. 70.